Analysis of Organosilicone Surfactants and their Degradation Products

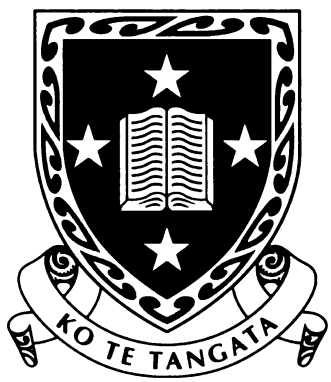

The University of Waikato

Te Whare Wānanga o Waikato

A thesis submitted in partial fulfilment
of the requirements for the
Degree of Doctor of Philosophy in Chemistry
at the University of Waikato by:

Lea S. Bonnington

2000

ALMUSTAFA, the chosen and the beloved, who was a dawn unto his own day, had waited twelve years in the city of Orphalese for his ship that was to return and bear him back to the isle of his birth.

And in the twelfth year, on the seventh day of Ielool, the month of reaping, he climbed the hill without the city walls and looked seaward; and he beheld his ship coming with the mist.

Then the gates of his heart were flung open, and his joy flew far over the sea. And he closed his eyes and prayed in the silences of his soul.

But as he descended the hill, a sadness came upon him, and he thought in his heart:

How shall I go in peace and without sorrow? Nay, not without a wound in the spirit shall I leave this city.

Long were the days of pain I have spent within its walls, and long were the nights of aloneness; and who can depart from his pain and his aloneness without regret?

Too many fragments of the spirit have I scattered in these streets, and too many are the children of my longing that walk naked among these hills, and I cannot withdraw from them without a burden and an ache.

It is not a garment I cast off this day, but a skin that I tear with my hands.

Nor is it a thought I leave behind me, but a heart made sweet with hunger and with thirst.

Kahlil Gibran

The Prophet

ABSTRACT

In this work the analysis of the organosilicone surfactant Silwet L-77 and components thereof is described. The commercial product Silwet L-77 was demonstrated to comprise of ~70% M_2D-C_3-O-$(EO)_n$-CH_3 (**1**),* ~5% M_2D-C_3-O-$(EO)_n$-H (**2**) and ~25% polar constituents. M_2D-C_3-O-$(EO)_n$-CH_3 oligomers were obtained by reversed-phase chromatography of Silwet L-77, and by synthetic procedures. Pure oligomers (n = 3, 6 and 9) were synthesised by reaction of the corresponding allyl-capped oligoethoxylate monomethyl ether M_2D^H over a Pt catalyst. The allyl-capped ethoxylate monomethyl ethers were synthesised by reaction of allyl chloride with the corresponding ethoxylate monomethyl ethers (n = 3, 6 and 9). The longer chained oligoethylene glycols (n = 6 and 9) were prepared by etherification of smaller oligomers. Preparation of the organosilicone compounds M_2D-C_3-O-EO-$COCH_3$ and M_2D-C_3-OH were also investigated.

Atmospheric pressure ionisation mass spectrometry (API/MS) is demonstrated to be a valid and informative method for the characterisation and quantitation of the organosilicone surfactants. Consistently reproducible quantitative results were achieved using an online HPLC separation system. Atmospheric pressure chemical ionisation (APcI) was used to enable high sample throughput, and the resulting HPLC/APcI/MS data obtained were improved both in reproducibility and sensitivity over conventional HPLC methods.

The uptake mechanisms of agrochemical formulations and the role that surfactants play in this process are not well understood. The quantitative API/MS method developed and the use of synthesised Silwet L-77 components (**1**) enabled investigation of Silwet L-77 uptake into plant foliage (*Chenopodium album*). The influence of Silwet L-77 and constituents thereof on herbicide uptake was addressed, and dosage, spread, surfactant structure, solvation and solubility were implicated as important for uptake enhancement.

Aspects of Silwet L-77 degradation were also addressed, for which API/MS methods were shown to be valid and informative. The well-established instability of Silwet L-77 to acid and alkaline conditions was characterised in more detail, with products, mechanisms and relative rates presented. Certain limitations of the API/MS method (i.e. product overlap, analyte suppression) required the use of

* M_2D- = $[Si(CH_3)_3$-$O]_2$-$Si(CH_3)$- ; C_3 = $(CH_2)_3$; EO = CH_2CH_2O

additional methods to supplement the results obtained (LC/MS, GC/MS and NMR).

The range of products formed in the degradation of Silwet L-77 were numerous as a result of the ability of the siloxane moiety to rearrange into a variety of lengths and structures, and compounded by the large number of components comprising the Silwet L-77 formulation. Unequivocal assignment of degradation product structure was thus complicated. Mass recovery following degradation was reduced in all experiments indicating the loss of volatile siloxane compounds. This was confirmed by headspace analysis. An increase in overall water-solubility for the degradation products over the parent surfactant was also observed. Rates and products appeared to be dependent on the conditions used, and were especially influenced by the solution pH.

The use of fourier transform ion cyclotron resonance mass spectrometry (FTICR/MS) enabled the tentative assignment of four major products in the water-soluble fraction of degraded Silwet L-77. These were $CH_3O(EO)_nH$ (**20**), [**1**-$SiCH_3$+H] (**21**), cyclic tetramer [**28**; R^1, R^2, R^3, R^4 = C_3-O-$(EO)_n$-CH_3] and linear dimer [**24**; R^1, R^2 = TMS; R^3, R^4 = $(EO)_n$-CH_3].

Analysis of the degradation of purified M_2D-C_3-O-$(EO)_n$-Me (ave. n ~ 7.5) samples by electrospray mass spectrometry (ESI/MS), FTICR/MS and HPLC/ESI/MS indicated $CH_3O(EO)_nH$ (**20**), [**1**-$SiCH_3$+H] (**21**) and [**1**-$2SiCH_3$+2H] (**22**) as common degradation products. The linear dimer **24**, [R^1 = H, R^2 = TMS; R^3, R^4 = $(EO)_n$-CH_3] was also indicated. The results also demonstrated that the $HO(EO)_nH$, M_2D-C_3-O-$(EO)_n$-H (**2**) and $(M^R)_2D$-O-$(EO)_n$-$CH_2CH{=}CH_2$ (**9**, **10**, **11**; R = H or CH_3) compounds observed in the Silwet L-77 degradation mixture were synthetic by-products rather than degradation products.

The degradation of single M_2D-C_3-O-$(EO)_n$-R oligomers confirmed the $CH_3O(EO)_nH$ (**20**), [**1**-$SiCH_3$+H] (**21**) and [**1**-$2SiCH_3$+2H] (**22**) as degradation products, and also indicated a range of linear and cyclic products both with and without the EO chains and terminal TMS groups intact. In general, the more silylated analogues of a structural series partitioned preferentially into the heptane-soluble fraction, and higher EO content derivatives were more commonly observed in the water-soluble fraction. Typically the products formed followed that for expected silanol stabilities, with longer EO chain products more stable as

low condensation polymers and silanols, and short EO chains more commonly observed in cyclic products.

The GC/MS analysis of the heptane-soluble fraction of acid-degraded Silwet L-77 enabled the tentative assignment of the cyclic trimer, **27** [R^1, R^2, R^3 = -C_3-OH] product. ^1H and ^{13}C NMR data also indicated this structure. ^1H NMR of the water-soluble fraction showed proton integration values indicative of the [**1**-2$SiCH_3$+2H] (**22**) structure. After 2 years, the terminal M^R groups were no longer detectable and extensive condensation had occurred, as determined by ^{29}Si NMR.

The results demonstrated the rapid degradation of Silwet L-77 and derivatives thereof under extremes of pH and the highly complex nature of the products which are formed. API/MS was a valid and informative method for the study of the products formed, especially the high resolution FTICR/MS technique.

Investigation into the stability of Silwet L-77 solutions on typical soil substrates indicated that there is little chance of surfactant persistence in aqueous soil environments. Reduced recovery was considered to be a result of degradation and/or strong sorption processes. Losses were most significant on substrates exhibiting extreme supernatant pH values (montmorillonite, halloysite). Reduced recoveries were also higher with higher clay content. Studies on clays indicated that supernatant pH, potential for intercalation and surface charges are important factors in the recovery process. In the case of the montmorillonite and illite clays, recoveries may be more significantly affected by sorption, as strong surfactant-substrate interactions were observed immediately following application.

The results obtained support previous observations that Silwet L-77 is relatively benign in the natural environment. Primary degradation is rapid and ultimate degradation to naturally occurring compounds i.e. CO_2, H_2O and $Si(OH)_4$, can be predicted according to the structures of the observed intermediates. However covalent bonding of degradation products to substrates was observed which may result in some environmental accumulation. In land applications this could cause aggregation of silicate minerals and/or affect the sorption capacity of the soil. An increase in sorption capacity could have positive or detrimental effects. The concentrations required for biotoxicity for Silwet L-77 and degradation products thereof are in large excess of any likely input by agricultural practices. Phytotoxicity was also low and this appeared to be a result of the dilution effects caused by high spreading.

ACKNOWLEDGEMENTS

First and foremost, I would like to thank my chief supervisor Dr. William Henderson who, along with providing significant scientific input, has been exceedingly supportive and encouraging throughout the course of this work. Thank you also to my second supervisor, Dr. Jerzy Zabkiewicz (Forest Research) for the very numerous and helpful contributions. Financial assistance from Forest Research (PGSF), NZFUW and NZVCC is gratefully acknowledged.

I would like to extend my appreciation to the staff at PPC (Forest Research), Alison Forster, Robin Gaskin, Linda Lester, Zhiqian Liu, Rachel Murray and Kevin Steele, for their guidance, advice and assistance. Many thanks to the staff of the School of Science and Technology (U.O.W.), in particular Kerry Allen, Amu Apreti, Heidi Eschmann, Pat Gread, Wendy Jackson, Peter Jarman, Jacqui MacKensie, Jannine Sims and Ralph Thomson, for technical assistance, support and patience. The invaluable discussions provided by Dr. Nick Kim, Dr. Lyndsay Main, Dr. Chris McLay, Dr. Brain Nicholson and Dr. Alistair Wilkins (University of Waikato) are gratefully acknowledged. Thank you also to Cameron Evans, Dr. Nick Kim and Penelope Lind for kindly proof reading sections of this thesis.

I am indebted to Dr. Craig Gribble (Waikato Polytechnic), Dr. Denis Lauren (HortResearch) and Chris Monk (U.O.W.) for kindly providing equipment, for patience in my tardy return thereof, and for useful discussions. Thank you to Dr. Keith Fisher, Dr. Gary Willett, Adriana Dinca and Rui Zhang of the University of New South Wales for enabling access to their equipment, technical guidance and also for their kindness. Dr. George Policello of Witco Corporation was extremely generous with samples, time and advice, for which I am very grateful. A special thank you to Dr. J. Scott McIndoe, whose fountain of knowledge on organosilicone synthetic chemistry provided the turning point for this thesis.

It would also be appropriate to acknowledge Mr Smith of Selwyn College who first taught me the fascination of chemistry, and to thank him for his infectious enthusiasm.

Thank you to my family and friends - in particular the people of Sanbukai - for their patience, friendship and support. A special thank you to Terry Hill for his inspirational guidance which has impacted on all aspects of my life.

Finally, last but not least, to my dearest mother Margaret Bonnington, thank you for your unfailing love and encouragement, for always believing in me and for teaching me to do the same.

TABLE OF CONTENTS

CHAPTER 4

The Development of API/MS Methods for the Quantitation of Organosilicone Surfactants

CHAPTER 6

A Study of the Degradation of Silwet L-77

LIST OF FIGURES

LIST OF TABLES

LIST OF SCHEMES

ABBREVIATIONS

a.m.u. = atomic mass units

APcI = atmospheric pressure chemical ionisation

API = atmospheric pressure ionisation

BPI = base peak intensity

CD = coefficient of variation ([Standard deviation/mean]*100/1)

$C_6(EO)_3$ = triethylene glycol monohexyl ether

CI = chemical ionisation

CID = collision induced dissociation (aka CAD = collision activated decomposition)

EI = electron ionisation

EO = ethoxylate (CH_2CH_2O)

ESI = electrospray ionisation

FTICR = fourier transform ion cyclotron resonance

GC = gas chromatography

HPLC = high performance liquid chromatography

IEI = internal electron ionisation

LC = liquid chromatography

LOD = limit of detection

LSD = light scattering (mass) detection

MCA = multi-channel acquisition

M, D, T and Q = $R_3SiO_{0.5}$, $R_2SiO_{(0.5)2}$, $RSiO_{(0.5)3}$, and $SiO_{(0.5)4}$, respectively

MS = mass spectrometry

$(MS)^n$ = tandem mass spectrometry

m/z = mass to charge ratio

NMR = nuclear magnetic resonance

PDMS = polydimethylsiloxanes

PEG = polyethylene glycol [$HO\text{-}(CH_2CH_2O)_n\text{-}H$]

ppb = parts per billion

ppm = parts per million

RP C_{18} = reversed-phase silica gel (modified with a octadecyl hydrocarbon)

SD = standard deviation

SIR = selected ion recording (aka SIM = selected ion monitoring)

S/N = signal/noise

SORI = sustained off-line resonance irradiation

TIC = total ion current

TMS = $Si(CH_3)_3$

Please note:

All numbered compounds appear in the fold out section at the rear of this thesis. For simplicity, the organosilicone constituents of Silwet L-77, $[Si(CH_3)_3\text{-}O]_2\text{-}Si(CH_3)\text{-}CH_2CH_2CH_2\text{-}O\text{-}(CH_2CH_2O)_n\text{-}CH_3$ (**1**), have been abbreviated to $M_2D\text{-}C_3\text{-}O\text{-}(EO)_n\text{-}CH_3$. Likewise the term $M_2D\text{-}C_3\text{-}O\text{-}(EO)_n\text{-}H$ has been used to describe the Silwet L-408 surfactants, $[Si(CH_3)_3\text{-}O]_2\text{-}Si(CH_3)\text{-}CH_2CH_2CH_2\text{-}O\text{-}(CH_2CH_2O)_n\text{-}H$ (**2**). M_2D^H refers to $[Si(CH_3)_3\text{-}O\text{-}]_2\text{-}SiH(CH_3)$ (**3**) and $M_2D\text{-}C_3\text{-}O\text{-}EO\text{-}H$ to $[Si(CH_3)_3\text{-}O]_2\text{-}Si(CH_3)\text{-}CH_2CH_2CH_2\text{-}OCH_2CH_2\text{-}OH$. The M and D nomenclature of siloxanes is described in Chapter 2. The term *flow injection* has been used to describe API/MS analysis of single pulse injections of sample in the absence of any online separation.

CHAPTER 1

Atmospheric Pressure Ionisation Mass Spectrometry

1.1 INTRODUCTION

Mass spectrometers provide information on the molecular weight of compounds, and since the development of the first instrument in 1912 there have been tremendous advancements in the capabilities and applications of the technique.[1] All mass spectrometric methods involve ionisation then subsequent separation of the ions according to their mass-to-charge ratio. The efficiency by which the analyte of interest can be ionised determines the effectiveness of the mass spectral analysis. Once an analyte is in an ionised form in the gas phase it can be detected by the mass spectrometer.

Conventional ionisation techniques include electron impact (EI) and gas-phase chemical ionisation (CI), which limited mass spectral analysis to robust and volatile analytes. However the development of numerous other ionisation techniques, such as fast atom bombardment (FAB), secondary ion (SI), particle-beam, matrix assisted laser desorption (MALDI) and thermospray (TS), has further extended the range of compounds amenable to mass spectral analysis.

1.2 ATMOSPHERIC PRESSURE IONISATION/MASS SPECTROMETRY

A further recent development in mass spectral techniques is atmospheric pressure ionisation/mass spectrometry (API/MS). API/MS includes two ionisation techniques - namely electrospray ionisation (ESI) and atmospheric pressure chemical ionisation (APcI). The pioneering research of API/MS, specifically ESI/MS, was conducted by Dole and his colleagues,[2,3] although the technique was later refined by Yamashita and Fenn.[4a-c] Both techniques are considered soft ionisation methods, with little if any, extra internal energy imparted to the ions. The fundamental difference between the two methods lies in the order in which ionisation and evaporation occur. Under electrospray ionisation, the evaporation of the solvent occurs subsequent to the ionisation of the analyte. In atmospheric pressure chemical ionisation, the analyte solution is first transferred into the gas phase, and then ionised by ion-molecule reactions (CI). The mild conditions with which these methods enable ionisation of analyte molecules has rendered API/MS

one of the most popular analytical methods available. For example, comparison of the ion source temperature of a classical EI mass spectrometer (100 - 300°C) with that of an API mass spectrometer (ambient), highlights one of the factors that renders API/MS such a popular technique.[5]

1.2.1 Electrospray ionisation (ESI)

Electrospray ionisation is a process whereby ions are emitted, in the form of charged liquid droplets, directly into the gas medium from the bulk solution.[5] The solution containing the analyte of interest is passed through a high voltage capillary (3 - 6 kV), and then sprayed into a chamber at atmospheric pressure. Ions are transferred into the gas phase following evaporation of the solvent from the charged liquid droplets formed. A schematic diagram of typical ESI/MS hardware is shown in Figure 1.1.

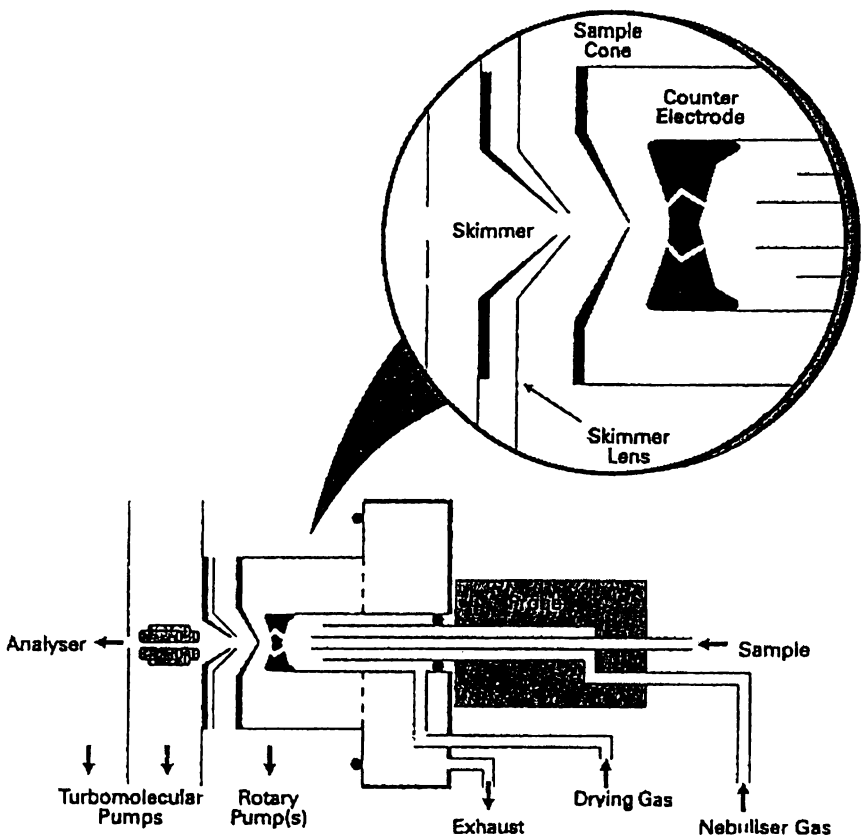

Figure 1.1. Schematic diagram of an electrospray ion source coupled to a mass analyser*

* Source: VG Platform Users Guide, Fisons Instruments, Issue 3, 1994

The ESI mechanism involves three major processes, (i) the production of charged droplets, (ii) the production of smaller, highly charged droplets, and (iii) the transfer of ions into the gas-phase (Figure 1.2).

The first step results from an ion separation process, also known as electrophoretic charging. An external electric field induces a partial separation of the positive and negative electrolyte ions in the solution. The predominant charge of the bulk solution depends on the polarity of the induced potential.[6] A charge redistribution of the bulk solution occurs as the like-charged ions move away from the charged capillary and the oppositely-charged ions migrate toward it, until the imposed field is essentially removed. It is this ion separation which renders ionisation by API/MS techniques to be defined as relatively "soft" as compared with other methods, as other forms of ionisation are consequently suppressed.[7]

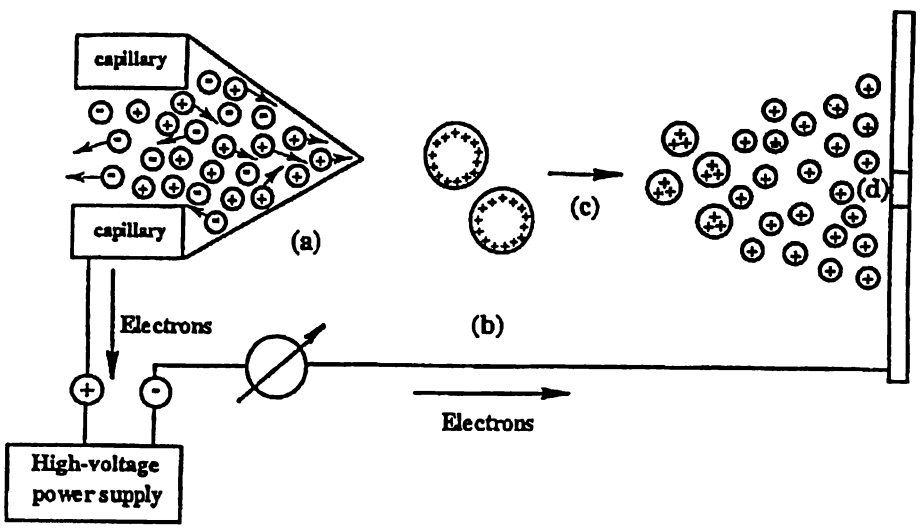

Figure 1.2. Production of gas-phase ions by electrospray ionisation*

The resulting excess charge at the solution surface leads to the destabilisation of the surface such that it is drawn out downfield. A liquid cone, referred to as a Taylor cone, is formed at the capillary tip as a result of competing forces between the electric field and the surface tension of the liquid (Figure 1.2, a).[8] At some distance downstream the liquid filament becomes unstable and small charged droplets are produced from the tip of the liquid cone (Figure 1.2, b).[9] An excess of ions of the same charge as the capillary potential, will be contained in the droplets and the droplet surface will be enriched with these ions.[7] Droplet formation

* Source: C. Depree, MSc Thesis, University of Waikato, 1995

requires an energy source sufficient enough to overcome the surface energy of the bulk liquid, and in conventional ESI/MS this is provided by an electrostatic potential. Variations on ESI/MS also utilise heat and pneumatic nebulisation.[5,10]

In the second step of the process, solvent molecules from the charged droplets then evaporate and the droplet becomes increasingly smaller. As evaporation continues, a critical point, where the charge-to-volume ratio is such that the droplets become electrohydrodynamically unstable,[6] is reached. At this point the repulsive forces between the like-charges (Coulombic forces) exceeds the droplet cohesive forces. This is known as the Rayleigh limit, where the droplets explode, producing a number of smaller droplets (Figure 1.2, c).[11] The fission that occurs is termed uneven, as a large droplet of about 98% of the mass, and about twenty much smaller monodisperse offspring droplets are formed. The smaller droplets, with radii of approximately one-tenth of the parent droplet, carry off only about 2% of the mass, but also remove about 15% of the charge of the initial droplet. The resulting droplets undergo further successive evaporation-fission processes generating smaller and smaller "parent" and "offspring" droplets, until at some point the solvated ions are transferred into the gas phase (Figure 1.2, d). The gas-phase ions are thought to ultimately result from the offspring droplets,[7] although the mechanism of the gas-phase transfer is not well understood. Two principal hypotheses exist for the mechanism, understanding of which is precluded by the inability to observe the fission of the offspring droplets due to their small size (~10 nm). These are described as the charged residue model (CRM) and the ion desorption model (IDM), and experts differ on the relevance of the available experimental evidence to either proposals.[12,13] The charged residue model (also termed the single ion in droplet theory)[7] proposes that the gas-phase ions simply result from solvent evaporation from very small droplets ($r \approx 1$ nm) containing only one ion.[14] According to the ion desorption model, direct evaporation of single ions clustered with several solvent molecules can occur from very small and highly charged droplets ($r \approx 8$ nm) near the Rayleigh limit.[15,16] The declustering of such ions would occur in the dry interface gas, and in the collision-induced dissociation (CID) stage in the vacuum region, where the pressure is low and the ions are accelerated by the imposed field.[17] In any case, the predictions for the two mechanisms for practical purposes are quite similar, and once in the

gas phase the ions can be detected by the mass spectrometer. Detection methods are discussed in more detail in Section 1.5.

1.2.2 Atmospheric pressure chemical ionisation (APcI)

In APcI, the solution containing the analyte is passed through a heated capillary such that the sample is transferred into the sampling source in the gas phase. A schematic diagram of the APcI/MS hardware is shown in Figure 1.3.

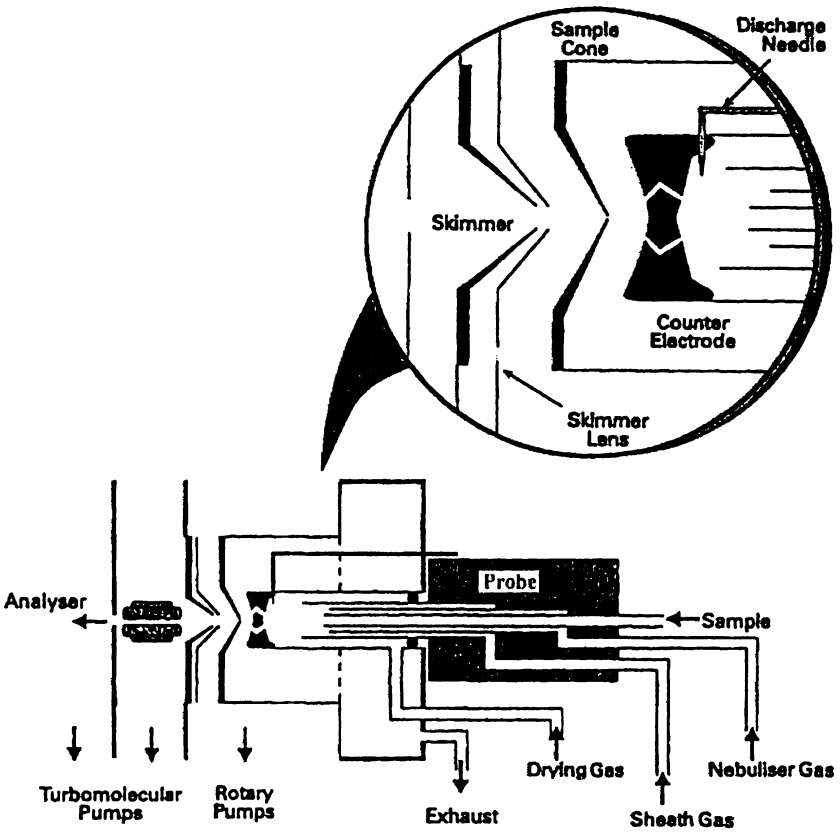

Figure 1.3. Schematic diagram of an APcI ion source coupled to a mass analyser*

The nebulising and make-up gases are introduced coaxially to the heated sample inlet, and the sample and solvent are thus transferred into the source in the gas phase. This section of the MS interface is thus also termed a heated pneumatic nebuliser interface.[18,19] A corona discharge needle, held at a high voltage (3 - 6 kV) provides a source of ionising electrons which react with solvent molecules to produce reactive intermediate ions, i.e. H_3O^+, $CH_3OH_2^+$, $CH_3OH_2^+ \cdot (H_2O)_n \cdot (CH_3OH)_m$, CH_3CNH^+, etc.[20] These intermediate ions then

* Source: VG Platform Users Guide, Fisons Instruments, Issue 3, 1994

further react with analyte molecules by CI, to give pseudo-molecular ions that can be detected by mass spectrometric methods.[5]

As the gases are transferred into the low pressure regions of the spectrometer, rapid gas expansion with concomitant cooling occurs.[21] This provides the opportunity for collisions between the highly reactive monomer ions formed by this ionisation technique and other gaseous molecules in close proximity.[19,22] As a result of this, ion-solvent cluster ions may form. Heating of the ion source region,[23] the introduction of a dry (counter-current) curtain gas between the ion source and the vacuum expansion region[19] and the application of an electric field in the same region all reduce formation of these.[8,20]

1.2.3 Ion separation and detection methods

Most commonly, API sources are connected to quadrupole mass analysers, however magnetic sector, time-of-flight (TOF), ion trap (IT) and Fourier transform ion cyclotron resonance (FTICR) mass analysers are also amenable.[24,25] Ion separation by all these methods is achieved with the use of magnetic and/or electric fields.

A quadrupole mass filter comprises of four parallel rods arranged in two pairs, where opposite electrodes carry identical charges. A dc voltage and a superimposed radio-frequency (rf) potential are applied to each pair, opposite in sign and phase respectively to that of the other pair of electrodes. Ions travel parallel to the poles (z direction) at constant velocity, but acquire oscillations in the x and y directions due to the dc voltage and rf potentials applied. Measurement of this oscillation enables determination of the mass-to-charge ratio of the ion.[26] The voltages are varied, maintaining the rf/dc voltage ratio, to obtain separation of the ions according to mass. At any point in the scan only one mass can pass through the quadrupole system, hence the term mass filter.[27]

Magnetic sectors separate ions according to their mass-to-charge ratio by measuring the radius of their circular orbits in a uniform magnetic field.[28] Time-of-flight mass analysers use the different velocities adopted by ions of different mass after acceleration through a potential gradient[27] in the form of a pulsed ion beam.[26] Ion traps use static electric and magnetic fields to cause oscillations in ion movements parallel to the direction of the applied voltage. The frequency of these oscillations can be used to determine the mass-to-charge ratio of the ions.[28]

The mechanism of FTICR/MS mass-to-charge determination involves excitation of ions in a static magnetic field. This causes a proportional increase in the circular ICR orbital motion of the ion, which induces an oscillating difference in charge between two opposing detection electrodes. A current is thus produced, which can be translated to a voltage difference. Amplification of the voltage difference yields an ion decay signal which can be digitised and Fourier transformed to give a frequency domain signal. Mass-to-charge information is consequently produced by mathematical conversion of the frequency values.[29]

The application of FTICR/MS to the mass analysis of API- generated ions is becoming increasingly popular.[1a,30a-f] FTICR/MS as an analytical technique is extremely attractive, as it utilises frequency to determine the mass-to-charge ratio of an ion. Frequency can be measured more accurately than any other physical property, and therefore FTICR/MS offers extremely high resolution mass measurement. FTICR/MS can routinely provide MW data to four-decimal place accuracy. Furthermore, the instrument can be operated in tandem mass spectrometry mode ($[MS]^n$)* through ion trapping, enabling the analysis of single ions within complex mixtures. Ions are selected in ICR/MS by ejection of all others. This is achieved by application of suitable excitation pulses with the appropriate frequencies and amplitudes.[31] In this mode, gas-phase reactions can also be studied, which can yield further information regarding structure and reactivity. The selected ion can be excited and caused to fragment/react with collision gases introduced via a pulsed valve, and the resulting fragments/products observed in a MS spectrum. Sustained off-resonance irradiation (SORI) has proven an efficient method for collision-induced dissociation (CID)* by improving sensitivity and resolution (by maintaining the ion at the centre of the ICR cell) and enabling dissociation of multiply-charged ions.[32] In SORI-CID a low-amplitude r.f. excitation at a frequency slightly offline from the ion's cyclotron frequency is used. The phase of this excitation frequency is alternated, causing the cyclotron orbit of the ion to repeatedly expand and contract. By maintaining a low excitation amplitude the ion remains close to the centre of the cell. Low energy collisions with an introduced gas then cause gradual activation of the ion which subsequently leads to the dissociation.

---

* $[MS]^n$: *n* stages of mass analysis employed to selectively study sequential fragmentation of ions

The main methods of ion detection by mass spectrometry are by photographic plate, Faraday cup, electron multiplier and scintillation counting, the most common of which is the electron multiplier. In the photographic plate, ions contact with an earthed metal plate. The consequent neutralisation of the ions generates a flow of current through a connected resistor, which can be measured to determine ion abundance. The Faraday cup is a metal cup analogue of the photographic plate, which is more efficient, but less sensitive. In the electron multiplier, ions contact with the first of a series of electrodes (~10). The first electrode then releases a shower of electrons to the second electrode and so forth, causing a cascade of electrons, whereby amplifying the signal to the order of 10^6. The scintillation counter, or Daly detector, measures scintillations produced by ions hitting a phosphor screen. The signals are then amplified and detected by a photomultiplier.

1.2.4 Applications of API/MS

API/MS methods can be applied to compounds ranging from biomolecules to inorganic metal complexes. The phenomenon of multiple charging enables the analysis of high MW molecules (>100,000 Da) within the range of a standard linear quadrupole mass spectrometer, thus eliminating the need for special mass spectrometers equipped to detect high molecular mass species. The analysis of very polar, intractable compounds, previously inaccessible by conventional mass spectrometric techniques, is also made possible by API/MS, by virtue of the solvent-phase sample introduction method.[33] Furthermore, due to the soft nature of the ionisation process, non-ionic compounds can also often be detected. Complexation of non-ionic compounds with ions present in the solvent matrix enables the formation of detectable pseudo-molecular ions. Any polar neutral molecules capable of H-bonding will form adducts with H^+, NH_4^+ or alkali metal ions by these methods,[34] and thus can potentially be detected by API/MS. Polyethyleneglycols (PEGS) exhibit a strong affinity for alkali metal cations[35a-e] and thus are well characterised by API/MS methods.[36a-e] This is especially relevant to the analysis of nonionic surfactants by API/MS, many of which contain

---

* aka CAD = Collisionally activated decomposition

polyethylene groups as the hydrophilic moiety. Conversely, non-polar substances are generally not ionised by API methods. Detection of some such compounds has however, been observed as a result of electrochemical oxidation/reduction reactions. This can be induced and/or enhanced with the use of acids and other charge transfer reagents, and in general should be more successful with APcI-type ionisation.[34,37]

The potential applications of the API/MS technique to the analysis of environmental samples are numerous as a consequence of the ease of sample preparation, high sensitivity and selectivity and the ability to perform online LC separation. Relatively little sample preparation is required, which is advantageous both in the reduced loss of the sample, and also in the reduced time required for sample manipulation. Furthermore, the high sensitivity of the technique enables the analysis of very dilute solutions, i.e. where the sample concentration is in the order of parts-per-billion.

API methods have become one of the most popular ionisation techniques for the online coupling of liquid phase separation methods with mass spectrometry. Conventional ESI/MS operates at extremely low flow-rates (1-10 μL min^{-1}) rendering it impractical for use in large-scale environmental analyses. Where a sheath gas assists nebulisation the technique has also been described as pneumatically assisted ESI/MS[38] and ionspray,[8,9,39] although inconsistencies exist with the use of the ionspray/electrospray terminology.[10] The use of higher source temperatures and drying gas flow rates to facilitate evaporation enables even higher flow–rates to be adopted. This variation on ESI/MS is termed megaflow ESI/MS[21] or high-flow pneumatically assisted ESI/MS.[40,41] ESI/MS at reduced flow rates (of the order of nL min^{-1}), especially for the use in capillary electrophoresis, has also been reported and these techniques have been dubbed "microelectrospray", "nanoelectrospray", and "picoelectrospray".[42] APcI methods conventionally operate at high solvent flow rates (1 mL min^{-1}) and thus are well suited to online-LC methods.

1.2.5 Quantitation by API/MS

Several methods have been developed for the quantitation of analytes by API/MS.[7,43-46] Online-HPLC methods are somewhat established for practical

applications, whilst direct infusion methods require extensive data manipulation. In this section the principles governing the models used for direct infusion quantitation will be discussed.

The capillary current, I, resulting from the charged droplets leaving the capillary (Figure 2) provides a quantitative measure of the electrolyte ions produced by the spray. Comparison of this current, I, with the mass spectrometrically detected analyte ion intensity, I_{A+}, has shown that these two parameters are not closely related.[7] However, within a certain range the capillary current, I, shows a linear response to external changes. Over the same range, the analyte ion intensity, I_{A+}, is also shown to respond linearly, although the gradients of the two linear responses are quite different. Variables that do not influence f, the fraction of droplet charge that is converted to gas-phase charge, significantly lead to good correlations between the capillary current and the observed total gas-phase ion current.[7]

In order to understand the mechanisms of ESI/MS pertaining to quantitation, it is necessary to first consider a single analyte system. Analyte ion intensity (A) is affected by the presence of other electrolytes. Even in a single analyte system the solution involved is not a single electrolyte system in reality, because of impurity ions present in the solvent matrix. The impurities (B) are at constant concentration, and at low concentrations of A ($<10^{-5}$ M), carry the capillary current. The sum of the mass analysed total ion intensities $I_{total} \approx I_A + I_B$, is also constant in this range, because it is dominated by I_B.

At higher concentrations of A ($>10^{-5}$ M) the total electrolyte concentration increases, and therefore so does the capillary current, although the increase in current I is small relative to the concentration change - a factor of 2-4 for a change in concentration by a factor of 100. The I_{total} responds to concentration change in a similar manner, and thus I and I_{total} are approximately proportional in this concentration range. Due to this weak dependence of I on the total concentration, at $[A^+] > 10^{-5}$ M the intensity of I_B will decrease. The current I is proportional to the droplet charge, so the droplet charge is thus also only weakly affected by concentration change. However, within the droplet the A^+ and B^+ ions will be competing in the conversion to gas phase ions. In the case of nonionic species they will also be competing for the available charge. Thus an increase in $[A^+]$

should lead to a decrease of I_B. On the basis of these considerations the following relationship between analyte ion intensity and concentration (Equation 1.1) has been proposed.[43] The equation for I_B is analogous.

$$I_A = fpI\frac{k_A[A^+]}{k_A[A^+]+k_B[B^+]} \tag{1.1}$$

where: I_A is the mass spectrometrically detected ion intensity of A^+, corrected for the mass dependent transmission of the mass analyser

$[A^+]$ and $[B^+]$ are the electrolyte concentrations in the solutions analysed

f is the fraction of droplet charge that is converted to gas-phase charge

p is the ion sampling efficiency of the MS

k_X is the ratio of gas-phase ions X^+ relative to the solution concentration

For quantitative determinations only the value of the k_A/k_B ratio is required, which can be determined by derivatisation of Equation 1.1. When $[A^+] = [B^+]$, Equation 1.1 can be simplified to give Equation 1.2, and thus the value of k_A/k_B.

$$\frac{I_A}{I_B} = \frac{k_A}{k_B} \tag{1.2}$$

The value of fp can be determined by measuring I, I_A and I_B and using a further derivatisation of Equation 1.1, Equation 1.3.

$$fp = \frac{I_A + I_B}{I} \tag{1.3}$$

Equation 1.1 thus predicts a proportional dependence of f on the relative concentrations of ions in the droplets. A constant sensitivity is predicted for analyte concentrations < 10^{-5} M. Above this a decreasing sensitivity is predicted. It also predicts that the presence of electrolytes other than the analyte always leads to a decrease in the analyte sensitivity.

When considering a sample containing two analytes, A and B, the system becomes a three electrolyte system due to the solvent impurities, C. Equation 1.1 can be extended to include the additional analyte, as shown (Equation 1.4).

$$I_A = fpI\frac{k_A[A^+]}{k_A[A^+]+k_B[B^+]+k_C[C^+]} \tag{1.4}$$

However, over the 10^{-8} – 10^{-3} M concentration range, a single value for the k_A/k_B ratio will not satisfy Equation 1.1, unless $k_A \approx k_B$. When $k_A > k_B$ a lower k_A/k_B ratio is observed at lower concentrations. At low concentrations k is said to be dependent on surface activities only. The higher k_A/k_B at higher concentrations has been attributed to A^+ having a higher ion evaporation rate (Iribarne rate constant)[†] and/or higher surface activity. Differences in surface activity will affect quantitation by this method, as the ratio of the surface charges N_A/N_B will not be proportional to the concentration ratio, [A]/[B], as is assumed by Equation 1.1.[43]

When an internal standard is to be used in quantitative API/MS this should have the same surface activity and the same ion evaporation coefficient as the analyte. Only in this case will Equation 1.5 hold. Furthermore the concentration of the analyte and the internal standard should be in the same low (10^{-8}-10^{-6} M) or high (10^{-5}-10^{-3} M) concentration range.[43]

$$\frac{I_A}{I_B} = \frac{[A^+]}{[B^+]} \tag{1.5}$$

An additional predictive model for quantifying analytes in the presence of matrix ions has been proposed, based on the concept that the surface excess charge state is a separate phase to that of the interior of the droplet. The final equation obtained has the same form as Equation 1.4, except that the k constants represent equilibrium constants for the phase distribution reaction, rather than ion evaporation rate constants, and I is the concentration of excess charge.[44]

[†] The Iribarne rate constant is a measure of the ion evaporation rate or desolvation energy. The logic follows that an electrolyte that more readily evaporates from the solvated charged droplet will give a higher mass spectrometrically detected ion intensity.

Guilhaus *et.al.* extended Equation 1.4 to enable the application of the model to multiple component mixtures, as shown in Equation 1.6.[45]

$$I_{XI^+} = fpI\frac{k_i'[X_i^+]}{\left(\sum_{i=1}^{n} k_i'[X_i^+]\right)+C} \tag{1.6}$$

Results obtained using Equation 1.6, and those obtained with a simplified version, Equation 1.7, were compared with known concentrations. Results obtained using Equation 1.7 were skewed to a higher concentration, in most cases, with more normally distributed results obtained with Equation 1.6.

$$[A^+] = \frac{I_{A^+} \times k_B'[B^+]}{I_{B^+} \times k_A'} \tag{1.7}$$

As indicated, accurate quantitative determinations by direct infusion API/MS methods require each ion in the sample mixture to be monitored. The oligomeric nature of surfactant solutions renders this approach very laborious and thus unsuitable for routine analysis. However it is possible that, if the response factors of analogous oligomers can be assumed to be equal due to structural similarities, the total surfactant concentration may be determined from data of only a few components. A model, as shown in Equation 1.8, has been proposed that fits a known surfactant distribution to the concentrations of selected measured components and thereby determines a scaling factor to yield total surfactant concentration.[46]

$$\hat{Y} = \sum_{j=1}^{J} \hat{y}_j = \hat{\beta} \tag{1.8}$$

Where : $\hat{Y}$ is the predicted total concentration of all components

J is the total number of components in the mixture

$\hat{y}_j$ is the predicted concentration of each component

$\hat{\beta}$ is the least-squares estimate for β, the (unknown) proportionality constant given by Equation 1.9.

$$\hat{\beta} = \sum_{i=1}^{I} y_i \Big/ \sum_{i=1}^{I} x_i \tag{1.9}$$

Where : y_i is the measured concentration of component i

x_i is the weight fraction of component i in the known ("theoretical") distribution

I are the discrete measured components

The method was applied to the analysis of alkyl ethoxysulfate anionic surfactants, and the observed and calculated values obtained were within experimental error for the solutions (laboratory prepared) investigated. The method found to be especially useful in cases where high sensitivity selected ion mode (SIR) analysis was required, i.e. when results were below the limit of detection for total ion mode analysis. Under SIR only a limited number of the components can be selected, and thus this model can provide information regarding all analogues of an oligomeric mixture.

1.3 THESIS OUTLINE

The objective of the research described in this thesis was to apply the API/MS method to the qualitative and quantitative analysis of the organosilicone surfactant Silwet L-77 and closely related derivatives. Other methods have also been incorporated to validate and supplement results obtained.

In this chapter mass spectrometric techniques, in particular API/MS, are reviewed. In Chapter 2 compound preparation is described, along with a review of general siloxane chemistry. Chapter 3 describes the qualitative characterisation of Silwet L-77 by API/MS methods, whilst in Chapter 4 this is extended to quantitative investigations. In Chapter 5 the quantitative methods developed are applied to studies of plant uptake of Silwet L-77 formulations. Chapter 6 presents results pertaining to Silwet L-77 degradation whilst in Chapter 7, environmental aspects of Silwet L-77 degradation are addressed.

1.4 REFERENCES

[1] *a.* A.L. Burlingame, R.K. Boyd, S.J. Gaskell, *Anal. Chem.*, 1998, **70**, 647R-716R; *b. ibid*, 1996, **68**, 599R-651R; *c. ibid*, 1994, **66**, 634R-683R; *d.* A.L. Burlingame, T.A. Baillie, D.H. Russell, *Anal. Chem.*, 1992, **64**, 467R-502R; *e.* A.L. Burlingame, D. Maltby, D.H. Russell, P.T. Holland, *Anal. Chem.*, 1988, **60**, 294R-342R; *f.* other articles in this series (*Anal. Chem.*, 1990, **62**, 268R-303R; 1986, **58**, 165R-211R; 1984, **56**, 417R-467R; 1982, **54**, 363R-409R; 1980, **52**, 214R-258R; 1978, **50**, 346R-384R; 1976, **48**, 368R-403R; 1974, **46**, 248R-287R)

[2] M. Dole, L.L. Mack, R.L. Hines, R.C. Mobley, L.D. Ferguson, M.B. Alice, *J. Chem. Phys.*, 1968, **49**, 2240-2247

[3] L.L. Mack, P. Kralik, A. Rheude, M. Dole, *J. Chem. Phys.*, 1970, **52**, 4977-4986

[4] *a.* M. Yamashita, J.B. Fenn, *J. Phys. Chem.*, 1984, **88**, 4451-4459; *b.* M. Yamashita, J.B. Fenn, *J. Phys. Chem.*, 1984, **88**, 4671-4675; *c.* C.M. Whitehouse, M. Yamashita, J.B. Fenn, R.N. Dreyer, *Anal. Chem.*, 1985, **57**, 675-679

[5] E.C. Huang, T. Wachs, J.J. Conboy, J.D. Henion, *Anal. Chem.*, 1990, **62**, 713A-725A

[6] M.G. Ikonomou, A.T. Blades, P. Kebarle, *Anal. Chem.*, 1991, **63**, 1989-1998

[7] P. Kebarle, L. Tang, *Anal. Chem.*, 1993, **65**, 972A-987A

[8] J.B. French, N.M. Reid, J.A. Buckley, *U. S. Patent*, 1977, 4 121 099

[9] G.I. Taylor, *Proc. R. Soc. A*, 1964, A280, 383

[10] A.L. Burlingame, R.K. Boyd, S.J. Gaskell, *Anal. Chem.*, 1994, **66**, 634R-683R

[11] J.W.S. Rayleigh, *Philos. Mag.*, 1882, **14**, 31, 184

[12] J.B. Fenn, J. Rosell, T. Nohmi, S. Shen, F.J. Banks, Jr, *Biochemical and Biotechnological Applications of Electrospray Ionisation Mass Spectrometry*, ed. A.P. Synder, ACS Symposium series 619, ACS, Washington DC, 1996, 60-80

[13] P. Kebarle, Y. Ho, *Electrospray Ionisation Mass Spectrometry. Fundamentals, Instrumentation and Applications*, Ed. R.B. Cole, Wiley, New York, 1997, 3-63

[14] M.G. Ikonomou, A.T. Blades, P. Kebarle, *Anal. Chem.*, 1990, **62**, 957-967

[15] J.V. Iribarne, B.A. Thomson, *J. Chem. Phys.*, 1976, **64**, 2287-2294

[16] B.A. Thomson, J.V. Iribarne, *J. Chem. Phys.*, 1979, **71**, 4451-4463

[17] A.T. Blades, P. Jayaweera, M.G. Ikonomou, P. Kebarle, *J. Chem. Phys.*, 1990, **92**, 5900-5906

[18] W.M.A. Niessen, A.P. Tinke, *J. Chromatogr. A*, 1995, **703**, 37-57

[19] T.R. Covey, E.D. Lee, A.P. Bruins, J.D. Henion, *Anal. Chem.*, 1986, **58**, 1451A-1460A

[20] A.P. Bruins, *Trends Anal. Chem.*, 1994, **13**, 81-90

[21] VG Platform Users Guide, Fisons Instruments, Issue 3, ©Fisons PLC, September 1994

[22] R.K. Mitchum, W.A. Korfmacher, *Anal. Chem.*, 1983, **55**, 1485A-1499A

[23] W.E. Wentworth, C.F. Batten, D.E. Desai, *J. Chromatogr.*, 1987, **390**, 249-260

[24] J.A. Loo, C.G. Edmonds, R.R. Ogorzalek Loo, H.R. Udseth, R.D. Smith, *Topics in Mass Spectrometry - Experimental Mass Spectrometry*, Ed. D.H. Russell, Plenum, NY, Vol. 1, 1994

[25] S.A. Hofstadler, R. Bakhtiar, R.D. Smith, *J. Chem. Ed.*, 1996, **73**, A82-A88

[26] S.R. Shrader, *Introductory Mass Spectrometry*, Allyn and Bacon Inc., Boston, 1971

[27] M.E. Rose, R.A.W. Johnstone, *Mass spectrometry for chemists and biochemists*, Cambridge University Press, Cambridge, 1982

[28] P.A. Tipler, *Physics – For Scientists and Engineers*, Worth Publishers, Vol. 2, 3rd Ed., 1991

[29] A.G. Marshall, P.B. Grosshans, *Anal. Chem.*, 1991, **63**, 215A-229A

[30] *a.* S.A. Hofstadler, D.A. Laude, Jr., *Anal. Chem.*, 1992, **64**, 569-572; *b.* E.R. Williams, *Trends Anal. Chem.*, 1994, **13**, 247-251; *c.* M.W. Senko, C.L. Hendrickson, L. Pasa-Tolic, J.A. Marto, F.M. White, S. Guan, A.G. Marshall, *Rapid Commun. Mass Spectrom.*, 1996, **10**, 1824-1828; *d.* I.J. Amster, *J. Mass Spectrom.*, 1996, **31**, 1325-1337; *e.* M.V. Gorshkov, L. Pasa-Tolic, J.E. Bruce, G.A. Anderson, R.D. Smith, *Anal. Chem.*, 1997, **69**, 1307-1314; *f.* K.D. Henry, J.P. Quinn, F.W. McLafferty, *J. Am. Chem. Soc.*, 1991, **113**, 5447-5449

[31] E. de Hoffmann, *J. Mass Spectrom.*, 1996, **31**, 129-137

[32] I. J. Amster, , *J. Mass Spectrom.*, 1996, **31**, 1325-1337

[33] G. Schmelzeisen-Redeker, L. Butfering, F.W. Rollgen, *Int. J. Mass Spectrom. Ion Processes*, 1989, **90**, 139-150

[34] T. Covey, *Biochemical and Biotechnological Applications of Electrospray Ionisation Mass Spectrometry*, Ed. A.P. Synder, ACS Symposium series 619, ACS, Washington DC, 1996, 21-59

[35] *a.* C.J. Pederson, *J. Am. Chem. Soc.*, 1967, **89**, 7017-7034; *b.* T. Okada, *Anal. Chem.*, 1990, **62**, 327-331; *c.* L.L. Chan, K.H. Wong, J. Smid, *J. Am. Chem. Soc.*, 1970, **92**, 1955–1963; *d.* G.W. Gokel, D.M. Goli, R.A. Schultz, *J. Org. Chem.*, 1983, **48**, 2837-3842; *e.* H.K. Frendsdorff, *J. Am. Chem. Soc.*, 1971, **93**, 600-604

[36] *a.* S.F. Wong, C.K. Meng, J.B. Fenn, *J. Phys. Chem.*, 1988, **92**, 546-550; *b.* T. Nohmi, J.B. Fenn, *J. Am. Chem. Soc.*, 1992, **114**, 3241-3246; *c.* H. Lin, G.J. Gonyea, S.K. Chowdhury, *J. Mass Spectrom.*, 1995, **30**, 381-383; *d.* K. Wang, X. Han, R.W. Gross, G.W. Gokel, *J. Chem. Soc., Chem. Commun.*, 1995, 641-642; *e.* R. Colton, S. Mitchell, J.C. Traeger, *Inorg. Chim. Acta*, 1995, **231**, 87-93

[37] R.B van Breemen, *Anal. Chem.*, 1995, **67**, 2004-2009

[38] A.P. Bruins, *Trends Anal. Chem.*, 1994, **13**, 37-43

[39] R.D. Voyksner, *Environ. Sci. Technol.*, 1994, **28**, 118A-127A

[40] S. Chiron, S. Papilloud, W. Haerdi, D. Barcelo, *Anal. Chem.*, 1995, **67**, 1637-1643

[41] C. Molina, M. Honing, D. Barcelo, *Anal. Chem.*, 1994, **66**, 4444-4449

[42] A.L. Burlingame, R.K. Boyd, S.J. Gaskell, *Anal. Chem.*, 1996, **68**, 612R-613R

[43] P. Kebarle, L. Tang, *Anal. Chem.*, 1993, **65**, 3654-3668

[44] C.G. Enke, *Anal. Chem.*, 1997, **69**, 4885-4893

[45] D.S. Selby, M. Guilhaus, J. Murby, R.J. Wells, *J. Mass Spectrom.*, 1998, **33**, 1232-1236

[46] D.D. Popenoe, S.J. Morris, III, P.S. Horn, K.T. Norwood, *Anal. Chem.*, 1994, **66**, 1620-1629

CHAPTER 2

Silwet L-77 Purification and Siloxane Synthesis

2.1 INTRODUCTION

2.1.1 Siloxane Chemistry

The siloxanes are a group of polymers represented in a wide range of applications and are thus of great commercial importance. The most common siloxanes of industrial use are the polydimethylsiloxanes (PDMS), linear polymers containing $-O-Si(Me)_2-$ as the repeating unit. The thermal stability, good UV resistance, chemical and biological inertness and low surface tension are among the favourable characteristics inherent to the siloxane polymers.[1] Substitution of the methyl groups on the siloxane backbone leads to products of varied structure and activities. The low surface tension characteristic of the polysiloxanes is determined by the organic side groups.[2]

Si bonds tetravalently through sp^3 hybrid orbitals thus adopting a tetrahedral structure. The Si atom acts as an electron acceptor in dative $d_\pi - p_\pi$ bonding rendering the oxygen atoms less basic. The Si-O bond is relatively polar (52% ionic) in character and the average bond energy is high (452 kJ mol^{-1}).[3] A wide variation in the Si–O–Si bond angle, ranging from 100 to 180°,[2] is observed (as a result of the dative back bonding). The Si–O bond length is relatively long (~1.65 Å)[4] and is attributed to the large orbital radii.[5] The hydrophobic nature of the polysiloxanes, despite the presence of the polar Si–O bonds, is inferred by the relatively long Si–O and Si–C bonds which reduce the steric interactions between substituents on neighbouring Si atoms. Consequently freedom of rotation around the Si–O and Si–C bonds is observed. Steric interaction is further reduced by distortion in the Si–O–Si bond angle. A screening of the polar backbone by the hydrophobic substituents thus occurs, lowering the polarity, and therefore the surface tension of the molecule.[1]

2.1.1.1 Nomenclature

The nomenclature adopted to define siloxane compounds uses the letters M, D, T and Q to represent $R_3SiO_{0.5}$, $R_2SiO_{(0.5)2}$, $RSiO_{(0.5)3}$, and $SiO_{(0.5)4}$, respectively. The notation thus refers to the number of oxygen atoms bonded to the silicon (mono-, di-, tri-, and quaternary). The nomenclature usually assumes R = Me, and

substitution of methyl groups is indicated by a superscript suffix, e.g. D^{Ph} represents the unit $Me(Ph)SiO_{(0.5)2}$.

2.1.1.2 Preparation

Industrially, the polysiloxanes are manufactured stepwise via the diorganodichlorosilanes, which are produced by reaction of elemental silicon with methyl chloride (Equation 2.1). This reaction is known as the Müller-Rochow Process[6,7] and employs the use of a copper catalyst and temperatures of around 300°C.

$$MeCl_{(g)} + Si_{(s)} \rightarrow Me_3SiCl_{(g)} + Me_2SiCl_{2(g)} + MeSiCl_{3(g)} \quad (2.1)$$

The product mixture is purified by fractional distillation, and the diorganodichlorosilane, comprising approximately 80% of the product mixture, is used to synthesise PDMS. The mono- and trichloro- products are also however intermediates of siloxane synthesis.

Hydrolysis of the dichlorosilane yields cyclic and linear siloxane intermediates via the reactive disilanol (Equation 2.2). The molecular weight distribution of the final product is controlled by the amount of H_2O present.

$$Me_2SiCl_{2(l)} + H_2O_{(l)} \rightarrow \text{“}Me_2Si(OH)_2\text{”} \downarrow$$

$$[Me_2SiO]_{m(l)} + HO(Me_2SiO)_nH_{(l)} + HCl_{(g)} \ (m, n \approx 3\text{-}15) \quad (2.2)$$

The reactivity of SiR_xCl_{4-x} with water is thought to be due to the ability of Si to expand its coordination number beyond four, thereby enabling addition of OH to the Si atom. A pentavalent transition state is thus formed, the formation of which is the rate-determining step (Equation 2.3).[3]

$$\begin{array}{c} H-O\cdots SiR_3 \\ | \quad | \\ H \quad Cl \end{array} \quad (2.3)$$

The silanol product is formed, with HCl generated as the byproduct. The reactivity of the silanols is such that, under the industrial conditions used,

condensation of the monomers occurs rapidly to yield the cyclic and linear siloxane intermediates (Equation 2.2). The mechanism for the condensation of silanols is thought to proceed through a six-membered activated transition complex involving two molecules of silanol and one water/alcohol molecule.

The cyclic siloxanes produced are polymerised and end-blocked to yield the desired linear polymers by the reaction shown in Equation 2.4.

$$x(Me_2SiO)_{n(l)} + (Me_3Si)_2O_{(l)} \rightleftharpoons Me_3Si\text{–}O\text{–}[SiMe_2O]_{xn}\text{–}SiMe_{3(l)} \qquad (2.4)$$

The energy of the Si–O bond is approximately the same in the linear and cyclic siloxanes and the reactions are therefore controlled through entropy changes. In the condensation of silanols with different groups on the silicon atoms, a thermodynamic equilibrium is established between different structures as the result of the cleavage and rearrangement of siloxane bonds. The catalysts that facilitate the establishment of such equilibria are called equilibrating catalysts.[4]

Mineral acids catalyse the condensation of silanols and are used in the synthesis of a number of disiloxanes, cyclosiloxanes and polysiloxanes. Organic acids are also used, especially in the condensation of $R_2Si(OH)H$, $R_3Si(OH)$ and $HO(R_2SiO)_nH$ compounds. Alkali metal hydroxides and quaternary ammonium bases are also active condensation catalysts. Quantitatively, a combination of BF_3, CH_3CO_2H and pyridine is used to condense silanols. In this catalytic system no cleavage of the Si-O-Si bonds occurs and catalysts of this type are thus known as non-equilibrating catalysts.

Reactions of siloxanes with alcohols are also well known, the reactions proceeding to the thermodynamically more stable mixture (Equation 2.5).[4]

$$RSiOSiR' + R''OH \rightleftharpoons RSiOH + R''OSiR' \qquad (2.5)$$

2.1.1.3 Other Organofunctional Siloxanes

Mixed methyldichlorosilanes ($MeRSiCl_2$) are made from $MeHSiCl_2$ and the appropriate alkene via hydrosilylation. The silanol is then produced by hydrolysis of the diorganodichlorosilane. Ring opening polymerisation of the cyclics formed

is achieved by acid or base catalysts, and molecular weight is controlled by the use of end-blocking hexaalkyldisiloxanes.[1]

Chloroalkyl functionalised silanes, i.e. $R_3Si–(CH_2)_x–Cl$, act as common precursors for further organofunctional silanes. The propyl radical is one of the most prevalent linking groups used, due to its solvolytic and thermal stability, and relative ease of preparation. Attachment of the substituent at the α-C position is synthetically difficult and often less practical, whilst high reactivity is often observed when the substituent is attached to the β-C atom. This is due to the stabilisation of the carbenium ion by Si–C hyperconjugation, polarisation and inductive effects.[1]

2.1.1.4 Hydrosilylation

The addition of silanes across an unsaturated group, such as a C=C bond, can be catalysed by a number of methods including photochemically, with free radicals, by $AlCl_3$, and by various transition metal complexes. The catalysts are the same as those used in hydrogenation, although many more exist, including the early and late transition metals such as Co, Ni, Zr, Ru(II), Rh(I), Pd, Pt, and the lanthanides. The Pt group catalysts are dominant and include Speier's catalyst and the Karstedt catalyst.

Hexachloroplatinic acid in isopropylalcohol (Speier's catalyst)[8] is the most commonly used hydrosilylation catalyst. Its popularity is secured in its broad applicability and effectiveness at low concentrations. The generally accepted mechanism is known as the Chalk-Harrod mechanism,[9] shown in Scheme 2.1. The first step involves the attachment of an olefin to Pt in the zero oxidation state. This is followed by oxidative addition of the silane, yielding Pt(II). Rearrangement and ligand substitution yields a Pt(II) complex with a saturated alkyl substituent. Finally reductive elimination yields the product and the recycled catalyst.[1]

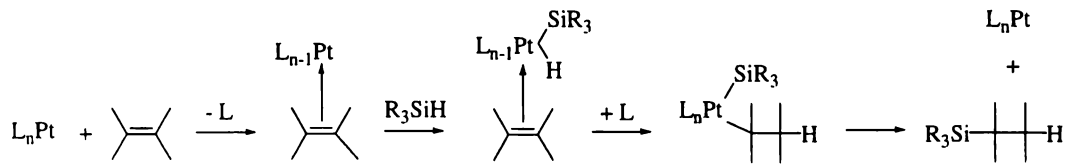

Scheme 2.1. The Chalk-Harrod mechanism for hexachloroplatinic acid catalysed hydrosilylation

Initial bonding of the olefinic ligand to the Pt can occur through either unsaturated carbon, depending on the substituents on the alkene, and consequently isomeric products can be formed.

More recently it has been proposed that insertion into the Pt–Si bond can occur (Scheme 2.2), c.f. into the Pt–H bond as for the Chalk-Harrod mechanism.[10]

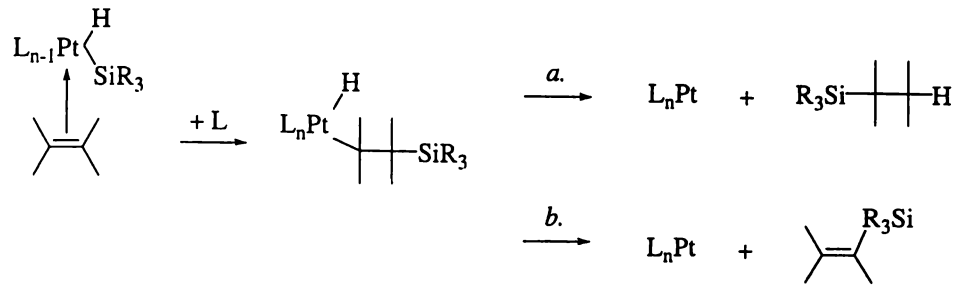

Scheme 2.2. Proposed mechanism for hydrosilylation with insertion into the M–Si bond

Reductive elimination (*a.*) from the intermediate yields the conventional products for which the Chalk-Harrod mechanism fits. However products resulting from *β*–elimination (*b.*) were also isolated, supporting the Pt–Si insertion mechanism.

2.1.2 Siloxane Characterisation

The molecular weight distribution and average molecular weight of polysiloxanes is most commonly determined by size exclusion chromatography (SEC). Other methods of analysis include ^{29}Si NMR, FT-IR, supercritical fluid chromatography (SFC),[21] direct exposure probe (DEP) analysis,[21] inductively coupled plasma (ICP) analysis,[19,20] thermogravimetric analysis (TGA),[11] pyrolysis,[12] differential scanning calorimetry (DSC)[11] and UV spectroscopy.[13]

NMR using the ^{29}Si (I=½) nucleus is an especially valuable analytical technique by which reliable quantitative information can be obtained. The chemical shift range for ^{29}Si nuclei is large (125 ppm) and the M, D, T and Q units are well separated. The more neighbouring O atoms on a silicon atom the higher the field at which that Si will resonate. In general R_3SiO type compounds are observed at δ_{Si} +44 to –44 ppm, averaging at around 12 ppm, whilst R_2SiO_2 type compounds resonate between δ_{Si} +14 and –74 ppm, with the average observation at around –20 ppm. $RSiO_3$ δ_{Si} are observed at –37 to –99 ppm, averaging at around –54 ppm, and SiO_4 compounds give Si resonances between

–71 to –114 ppm.[14] Furthermore, the Si nucleus is highly sensitive and can be influenced by substitution at up to 6 bonds away.

In general, MD^RM ($R \neq H$) compounds show chemical shifts at δ_{Si} 0 - 10 and –15 - –25 for the M and D silicon atoms, respectively.[15] Cyclics (D_n) resonate at lower frequencies than the linear siloxane analogues (M_2D_n), and shifts to higher field are observed with increasing n for the D Si resonances in linear (MD_nM) and cyclic (D_n) siloxanes.[16] A slight decrease is observed for the corresponding M δ_{Si} (MD_nM siloxanes).[17] Silanols also show distinctive chemical shifts, with M^{OH} and D^{OH} resonances observed at δ_{Si} –10 - –15 and δ_{Si} –55 - –65, respectively.[18]

DEP methods have been shown to be appropriate for qualitative screening purposes, but do not provide useful quantitative information.[21] ICP can also be coupled with HPLC and SEC (also referred to as GPC, or gel permeation chromatography) methods to yield further structural information.[19,20] Mass spectrometric methods are also useful and are discussed in the following section.

Quantitation of silanols and silane diols can be achieved by titration with Fischer reagent, as shown in Equation 2.6.[4]

$$R_3SiOH + I_2 + SO_2 + 2CH_3OH \rightarrow R_3SiOCH_3 + 2HI + CH_3HSO_4 \quad (2.6)$$

This titration takes advantage of the well-known reaction (Equation 2.7) between trialkylsilanols and alcohols to give the siloxane derivative and a molecule of water. This is thought to proceed through a six-membered activated transition complex involving two molecules of the alcohol and one of the silanol.

$$R_3SiOH + R'OH \rightleftharpoons R_3SiOR' + H_2O \quad (2.7)$$

2.1.2.1 MS of siloxanes

Many of the afore-mentioned methods of analysis (ICP, SFC, pyrolysis) can be coupled with detection by gas chromatography/mass spectrometry (GC/MS). SFC/MS has been successfully applied to the analysis of cyclic siloxanes in silicone oils where SEC and ^{29}Si NMR methods were demonstrated to be inadequate.[21] Some silanol compounds, i.e. $M^{OH}{}_2D_8$, have also been successfully analysed by SFC, where detection was by CI/MS with a soft ionisation media (NH_3).[21]

The application of direct pyrolysis-mass spectrometry (DP-MS) to the characterisation of polymers is becoming increasingly accepted. Information pertaining to structure, isomeric differentiation, copolymer composition and sequence, structures of intermediates, identification of volatile additives and thermal decomposition processes can be obtained.[22] Volatile components of siloxane mixtures, present either as analytes, impurities, or degradation products can also be analysed directly by GC/MS.

Chemical ionisation (CI) is often more informative than conventional electron impact (EI) methods for MS characterisation of siloxanes. Molecular ions of PDMS polymers (linear and cyclic) are generally not observed by EI, with the highest mass detected usually that resulting from cleavage of a methyl group.[22] These structures form stabilised oxonium ions due to the $d_\pi - p_\pi$ back bonding between the Si and O atoms. EI is informative for siloxanes containing only a few silicon atoms, however it does not provide information pertaining to the complete molecule as the chain length increases. Information regarding the repeat units contained within a polymer can however still be obtained.[21] EI spectra will also not distinguish between cyclic siloxanes and linear silanols, for which the same ions are observed - resulting from cyclisation of the linear diols following methyl and water loss.[21]

The MS analysis of intact siloxane polymers has been achieved with CI,[21] MALDI[21] and SI[23] ionisation techniques. These methods are especially of interest as they offer useful information in the high-mass range. By these methods, cation-adducts of the parent molecules are observed, enabling average MW and distribution to be determined. However, some difficulties still exist in the application of MALDI methods to the determination of molecular mass distribution, as certain instrument parameters result in mass discrimination at low molar mass ranges (<1000 a.m.u.).[24,25] MALDI methods do however offer information regarding structure, i.e. are capable of distinguishing between cyclic and linear components, not afforded by stand-alone SEC or SFC (FID detection) methods. The combination of MALDI and SEC[26] or SFC[27] techniques thus provides complementary information, thereby minimising the limitations of the individual methods. MALDI/MS following HPLC has also been reported,[27] however the difference in the sample phase for these techniques (solid vs liquid) precludes online coupling.

Ion separation methods following ionisation can be by conventional quadrupole mass filter, or with more recent developments including Fourier transform, Fourier transform ion cyclotron resonance and time-of-flight, thus further extending the capabilities of the MS methods.[23]

2.1.2.2 API/MS and siloxanes

Siloxanes generally show only very weak, if any, H-bonding capacity. This is because the dative $d_\pi - p_\pi$ nature of the Si–O bond reduces the electron density on the O atom, rendering it less basic than usual. As a consequence, nonionic siloxane compounds are not readily observed by API/MS methods, although sensitivity should be improved with APcI over ESI.

API-MS/MS has been used to analyse the products of photo-oxidation of the volatile methyl-silicon compounds $(CH_3)_3Si(OH)$ and $(CH_3)_2Si(OH)_2$, although the MS conditions used were not specified.[28] The reactions were initiated by OH-radicals and Cl atoms. The spectrum of $(CH_3)_2Si(OH)_2$ in Cl_2 and air, in the absence of irradiation, showed a small pseudo-parent ion, $[(CH_3)_2Si(OH)_2 + H]^+$, and ions corresponding to the characteristic condensation products, $[(CH_3)_2Si(OH)]_2$-O, $[(CH_3)_2Si(OH)$-O-$]_2$-$Si(CH_3)_2$ and the cyclic siloxane, $[(CH_3)_2SiO]_3$. Ions corresponding to water adducts, and homo- and hetero-dimers of these peaks were also observed. With irradiation, ions corresponding to $(CH_3)_2Si(OH)_2$, $CH_3Si(OH)_3$ and $CH_3Si(OH)_2$-OCHO were observed, with much fewer condensation product ions detected. The spectrum of $(CH_3)_3Si(OH)$ in Cl_2 and air in the absence of irradiation showed the peaks due to the pseudo-parent ion, $[(CH_3)_3Si(OH) + H]^+$ and corresponding water cluster ions. An analogous ion series resulting from a synthetic impurity, $(CH_3)_3SiOCH_3$ was also observed. With irradiation, peaks corresponding to $(CH_3)_2Si(OH)_2$ and $CH_3Si(OH)_3$, the corresponding formate esters, $(CH_3)_2Si(OH)$-OCHO, $CH_3Si(OH)_2$-OCHO, and water clusters thereof, were detected.

APcI/MS studies on linear PDMS and cyclic siloxanes yielded an ion at *m/z* 237, which was assigned to $[\text{hexamethylcyclotrisiloxane} + CH_3]^+$.[29] ESI/MS has been described as a useful technique for characterising silatranes,[30] and tetraalkoxysilanes.[31] $[M + H]^+$, $[M + NH_4]^+$ and $[M + Na]^+$ type product ions were observed, despite the reduced basicity displayed by siloxane oxygen atoms and silatrane-type amines. The compounds analysed also contained ether and amine moieties providing more likely sites for ion formation. As discussed

previously, the ionisation of polyether-type compounds by ESI/MS is well known. Furthermore, other studies have shown the chelating effect of polyether chains to be unaffected by the introduction of a Si atom at the beginning of the chain.[32] The acid-catalysed hydrolysis of the polymeric tetraalkoxysilatranes was also observed by ESI/MS.[31]

ESI/MS has been used in the structural elucidation of the fluorine end-blocked polydiphenylsiloxanes, $Me_3Si[OSi(CH_2CH_2CF_3)CH_3]_xOSiMe_3$ where $x = 6 - 13$.[33] Ammonium acetate was added to the aqueous solvent such that $[M + NH_4]^+$ type molecular ions were observed with high efficiency. The reaction of $Ph_2Si(OH)_2$ with HF was also investigated, from which several condensation products were characterised.

2.1.2.3 Isotopic abundances

Most elements occur naturally as mixtures of various isotopes - atoms of the same element that differ in the number of neutrons in the nucleus. The chemical properties of different isotopes are considered to be identical due to the unvarying numbers of electrons. The masses and isotopic abundances of the elements of interest in this study are summarised in Table 2.1.

Table 2.1. Average and exact isotopic masses of selected elements[34]

Element	Isotope	Exact Mass	Abundance (%)	Relative Abundance (%)	Average Mass
Hydrogen	^{1}H	1.00782504	99.985	100.0000	
	^{2}H	2.01410179	0.015	0.0150	1.00794
Carbon	^{12}C	12.0000000	98.90	100.0000	
	^{13}C	13.0033548	1.10	1.1122	12.0110
Nitrogen	^{14}N	14.0030740	99.63	100.0000	
	^{15}N	15.0001090	0.37	0.3673	14.0067
Oxygen	^{16}O	15.9949146	99.76	100.0000	
	^{17}O	16.9991306	0.04	0.0381	
	^{18}O	17.9991594	0.20	0.2005	15.9994
Sodium	^{23}Na	22.9897697	100.000	100.0000	22.9898
Silicon	^{28}Si	27.9769284	92.21	100.0000	
	^{29}Si	28.9764964	4.67	5.0634	
	^{30}Si	29.9737717	3.10	3.3612	28.0855
Potassium	^{39}K	38.9637079	93.2581	100.0000	
	^{40}K	39.9639988	0.0117	0.0130	
	^{41}K	40.9618254	6.7302	7.2170	39.0983

According to the natural abundances of the isotopes an averaged mass for an element can be calculated. Low resolution mass spectrometry will often give peaks corresponding to the average mass, however exact masses for each isotope are required for high resolution mass spectral determinations.

In the mass spectrum, the base peak (molecular ion, P)* is given a value of 100, and all other peaks are given values relative to this peak height. By multiplying the relative abundance of each isotope by the number of atoms of that element in the molecule, the probability of observing that ion in the spectrum can be determined. Silicon with three isotopes of detectable abundances can produce a distinctive isotope pattern that may aid structural assignment. The $(P + 1)^+$ ion is as for typical carbon-containing ions of similar mass, but the $(P + 2)^+$ and $(P + 3)^+$ ions are often more significant.[35]

2.1.3 Uses of Siloxanes

The commercially important siloxanes can be classified into several categories according to their physical attributes, namely the silicone fluids, greases, rubbers and resins. Siloxanes have varied properties - they can be hydrophilic or hydrophobic, inert or active, as determined by the organofunctional substituents - and as a result their applications are numerous and varied. Their many applications include use as insulators, thermal conductors, lubricants, coating materials, adhesives, profoamers, antifoams, water repellents, paints, sealants, cosmetics and pharmaceuticals, in fields as varied as the textile industry to medicine.

2.1.4 Siloxanes as Surfactants†

The substitution of a polar moiety onto the hydrophobic siloxane backbone results in the generation of a surface-active molecule which, depending on the nature of the substituent, is capable of a variety of applications. Due to the tertiary structure adopted, the siloxane backbone behaves much like a purely organic moiety. The limiting surface area of the molecule is thus controlled by the substituents on the Si atom, and is independent of the size of the siloxane backbone.[1] Examples of the hydrophilic substituents used include amines,

---

* Where the molecular ion, P = ion composing of the most abundant isotopes of all the elements

† A contraction of the term, surface-active compounds. A material which adsorbs onto surfaces or interfaces of a system and alters to a marked degree the free energies of those surfaces/interfaces

carboxylates, sulfates, thiols and polyethylene glycols. Typically silicon glycols are produced in a two-phase (polar/non-polar) system by nucleophilic displacement of the halogen atom of a chloropropylsiloxane in the presence of phase transfer catalysts such as quaternary ammonium or phosphonium salts.[1]

Silicone surfactants are used in textile, concrete and thermoplastic production processes and are also often added to non-aqueous paints due to their ability to also function in organic media. Applications include use as emulsifiers, dispersants, wetters, adhesives, lubricants and release agents.[36]

Organosilicone surfactants can be classified according to the position of substitution of the hydrophilic (A) moiety. Insertion into the siloxane polymer itself leads to monofunctional, i.e. $(TMS)_3O\text{-}Si(Me)A\text{-}O(TMS)_3$, and polyfunctional linear, i.e. $(TMS)_3O\text{-}[Si(Me)A\text{-}O]_n\text{-}[Si(Me)_2O]_m\text{-}O(TMS)_3$, type surfactants. Substitution at the ends of the siloxane polymer yields surfactants classified as difunctional, i.e. $A\text{-}[Si(Me)_2O]_n\text{-}Si(Me)_2A$ and polyfunctional branched, i.e. $A\text{-}[Si(Me)_2O]_x\text{-}[Si(Me)RO]_y\text{-}[Si(Me)_2O]_z\text{-}Si(Me)_2A$.[36] Silwet L-77, the surfactant of interest in this study, fits into the monofunctional category. Alkylsilicones have polyfunctional linear type structures with hydrophobic alkyl substituents, i.e. $A = (CH_2)_nCH_3$. These have been reported as effective adjuvants in oil-based agrochemical formulations as they display surface-active properties in non-aqueous media.[37]

2.1.4.1 Organosilicone Adjuvants

Surfactants are commonly used in agrochemical formulations as adjuvants* to improve physico-chemical characteristics of the solution and to increase the uptake of active ingredients.[38] The efficacy of organosilicone surfactants in agrochemical formulations was first reported in 1973,[39] and since then their use has become increasingly widespread.[38,40] The first organosilicone adjuvant was commercialised in 1985 (Silwet L-77), and several others have since reached the market.[40] In particular, the Silwet organosilicone surfactants have received considerable attention, the general structure for which is shown below. As is the case with most adjuvants, efficacy is dependent on the plant type, herbicide used and environmental conditions.

* Nonionic wetting agent

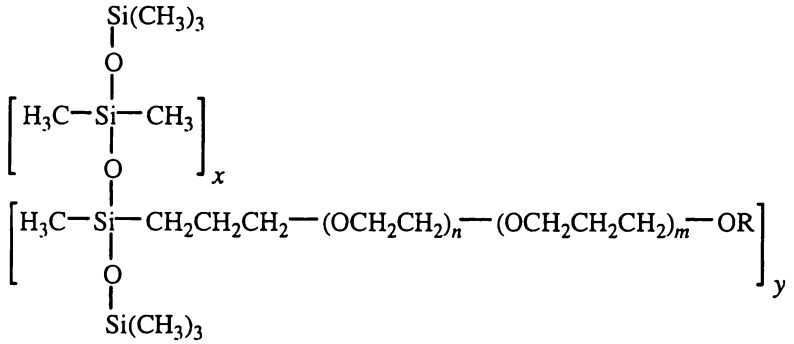

Silwet surfactant general structure

Trisiloxane based spreading agents (x = 0) enhance spray coverage and, in many cases, increase the uptake of agrochemicals. The uptake is closely related to the spreading ability[41] and reduction of surface tension of these surfactants.[42] The low surface tension is one of the most significant differences of organosilicone surfactants compared to conventional surfactants. This is associated with the comparatively compact hydrophobic moiety.[43] It has been shown previously that Silwet L-77 can be absorbed quite rapidly into plant foliage and that the uptake can be by both stomatal infiltration and cuticular absorption.[42,44a-c] Stomatal infiltration requires a reduction in the surface tension of the applied solution to < 30 mN m^{-1},[45] and is a well established uptake mechanism of trisiloxane surfactants.[38,40]

2.1.4.2 Silwet L-77

The organosilicone surfactant of interest in this study is known as Silwet L-77 (Compound **1**), a trisiloxane methyl-capped ethoxylate surfactant of the general formula $[(CH_3)_3SiO]_2$-$(CH_3)Si$-$(CH_2)_3$-$(OCH_2CH_2)_n$-OCH_3.

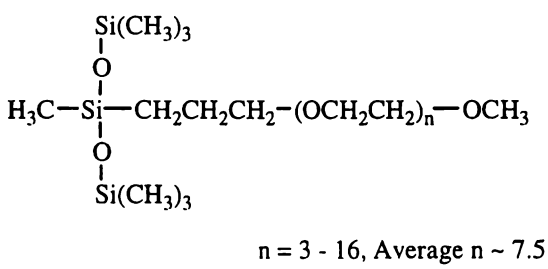

n = 3 - 16, Average n ~ 7.5

Compound 1. Silwet L-77

The commercial formulation of Silwet L-77 is a mixture of the trisiloxy polyethoxylate monomethyl ethers (**1**, n = 3 - 16), hereafter described as M_2D-C_3-

$O\text{-}(EO)_n\text{-}Me$. In addition, the commercial formulation also contains some un-capped trisiloxane ethoxylate surfactants (Silwet L-408 structures, Compound **2**, hereafter described as $M_2D\text{-}C_3\text{-}O\text{-}(EO)_n\text{-}H$) and some more polar polyethoxylate ether constituents.

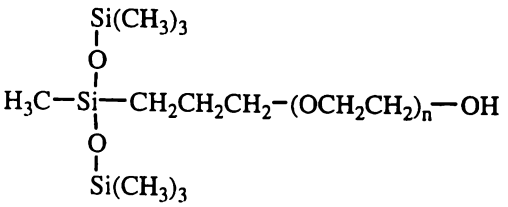

n = 3 - 16, Average n ~ 7.5

Compound 2. Silwet L-408

Commercially, trisiloxane ethoxylates, such as Silwet L-77 surfactant are manufactured by the hydrosilylation of 1,1,1,3,5,5,5-heptamethyltrisiloxane with an allyloxypolyethyleneoxide (average EO content ~ 7.5), in the presence of a platinum catalyst, according to the procedure described by Bailey and Synder.[46] In the case of Silwet L-77 the polyether is methyl capped prior to the hydrosilylation.[47]

2.1.4.3 Other Si-containing Surfactants

Whilst the hydrolytic and pH instability (see Chapter 6) of many of the siloxane surfactants, including Silwet L-77, is favourable for environmental reasons, this property can limit use of the materials in certain agrochemical formulations.[38] Several reports have addressed variations in structure in order to improve their stabilities. Nonionic trimethylsilylalkyl polyether silane surfactants, of the type $(CH_3)_3Si\text{-}(CH_2)_x\text{-}O\text{-}(CH_2CH_2O)_y\text{-}H$, have been synthesised that show much higher stabilities than the siloxane analogues.[48] Results also show comparable efficacy of these compounds as adjuvants. Ionic analogues exhibiting surfactant properties and improved pH/hydrolytic stabilities have also been described.[49,50] Two other silane surfactants, $[(CH_3)_3Si(CH_2)]_2\text{-}Si(Me)\text{-}X$, where X = 3-glycidyloxypropyl, and $-(CH_2)_3\text{-}O\text{-}CH_2\text{-}CH(OH)\text{-}CH_2SO_3Na$, have also been reported as exhibiting good alkali and acid resistance.[51]

Variation on the alkyl spacer group and hydrophobic moeities of trisiloxane surfactants has also been attempted, in an attempt to improve the stability of the Si-O-Si substructure, with limited success.[49] A M_2D^R trisiloxy surfactant, where

R consisted of propoxylate (PO) and ethoxylate (EO) substituents attached to a propyl linker group, i.e. $[(CH_3)_3SiO]_2$-$(CH_3)Si$-$(CH_2)_3$-O-$(PO)_{1.5}$-$(EO)_8$-$(PO)_{1.5}$-H, has been described which reportedly demonstrated hydrolytic stability.[52] Stability at acidic pH over 24 hours was also reported for two silicone polyether copolymers (Silwet L-7001* and Silwet L-7602†) over Silwet L-77 and other organosilicone surfactants [Silwet L-7607,‡ Sylgard 309§ and an experimental surfactant (Q2-5152)].[53]

2.1.5 Chapter Objectives

The objective of the research described in this chapter was to obtain purified samples and individual components of the Silwet L-77 surfactant. This would provide model compounds to be used for the study of Silwet L-77 degradation processes and uptake mechanisms into plant foliage. This was achieved by separation of the commercial Silwet L-77 mixture, and by synthetic methods. The Silwet L-77 mixture was purified by preparative RP C_{18} HPLC to remove the starting reagents and synthetic by-products, and individual M_2D-C_3-O-$(EO)_n$-Me oligomers were also obtained by this method. Pure oligomers of M_2D-C_3-O-$(EO)_n$-Me (n = 3, 6 and 9) were synthesised from pure ethoxylate monomethyl ether starting reagents. The longer chained oligoethylene glycols (n = 6 and 9) were not commercially available and were therefore produced by condensation of smaller oligomers. Methods for the synthesis of M_2D-C_3-O-EO-$COCH_3$ and M_2D-C_3-OH were also investigated.

---

* MW ~ 20 000, with a large number of pendant polyether chains. Polyether chains are 40:60 EO:PO based and are methyl capped.

† MW ~ 3 000, with all polyether chains EO based and methyl capped.

‡ MW ~ 1 100, M_2D_2-type structure with two methyl capped $(EO)_n$ chains, Ave. n ~ 7.5

§ M_2D-C_3-O-$(EO)_n$-$COCH_3$, Ave. n ~ 7.5

2.2 MATERIALS AND METHODS

HPLC CONDITIONS

Preparative HPLC conditions

Three Waters Delta-Pak C_{18} 25 x 100 mm Radial-Pak columns in series were used with detection by refractive index (RI). The elution solvents and flow-rates were as specified.

Analytical HPLC conditions - detection by light scattering mass detection

A Phenomenex RP C_{18} 4.6 x 150 mm analytical column (3 μm particle size) was used with an elution solvent of 30:70 H_2O/CH_3CN (0.5 mL min^{-1}). A tube temperature setting of 100°C and gas flow rate setting of 2.4 L min^{-1} was adopted for the light scattering mass detector.

Semi-preparative HPLC conditions

Semi-preparative RP C_{18} HPLC was conducted using a Beckman Ultrasphere ODS C_{18} column (1 x 25 cm, 5 μm) equipped with a solvent splitter. For detection by light scattering mass detector, an elution solvent of 65:35 CH_3CN/H_2O at a flow rate of 3 mL min^{-1} was used, with 0.5 mL min^{-1} going to the detector and 2.5 mL to fraction collection. A tube temperature setting of 100°C and gas flow rate setting of 2.4 L min^{-1} was adopted for the detector. For detection by ESI/MS a flow rate of 3 mL min^{-1} was adopted with 0.05 mL min^{-1} going to the detector and 2.95 mL to fraction collection. The elution solvents were as specified, and the MS conditions were as described in Appendix II. Fractions were concentrated by a combination of rotary evaporation, vacuum and freeze drying methods.

Analytical HPLC/APcI/MS conditions

A Waters Nova-Pak C_{18} 100 x 8 mm (4 μm) Radial-Pak column equipped with a guard column assembly was used. The elution solvents and flow-rates were as specified. Instrument conditions were as specified in Appendix II, excluding the scan time for which a setting of 4 seconds was adopted.

2.2.1 Separation of Silwet L-77

2.2.1.1 Purification of Silwet L-77 by preparative HPLC separation

A purified sample of the M_2D-C_3-O-$(EO)_n$-Me components of Silwet L-77 (50 mg, 500 μL injection aliquots) was obtained by preparative RP C_{18} HPLC using an elution solvent of 15:85 H_2O/CH_3CN at a flow-rate of 10 mL min^{-1}.

2.2.1.2 Separation of individual oligomers from commercial Silwet L-77

Silwet L-77 (115 mg) was first purified by RP C_{18} gravity elution column chromatography (5 cm x 3 cm i.d.) with a gradient elution of 50% MeOH (H_2O) through to 100% MeOH, in 5% increments, using 50 mL of each elution solvent (Scheme 2.3). Each fraction was analysed by analytical RP C_{18} HPLC with detection by light scattering mass detection.

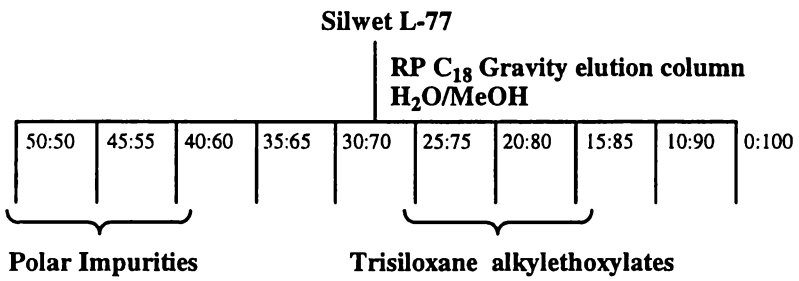

Scheme 2.3. RP C_{18} separation of commercial Silwet L-77

The fractions containing the trisiloxy alkylethoxylate components (M_2D-C_3-O-$(EO)_n$-H and M_2D-C_3-O-$(EO)_n$-Me) were then further separated by semi-preparative RP C_{18} HPLC with light scattering mass detection. Aliquots (250 μL) of the gravity elution column fractions were directly injected without further work-up. The fractions were analysed by ESI/MS to assign structures and then combined accordingly.

2.2.1.3 Determination of Silwet L-77 percentage composition

The percentage composition of the M_2D-C_3-O-$(EO)_n$-Me surfactants (**1**) within the commercial Silwet L-77 formulation was determined by HPLC with detection by two different methods. Analysis was conducted by: *a.* preparative HPLC (85% $MeOH/H_2O$, 10 mL min^{-1}) with detection by refractive index (RI); and *b.* analytical HPLC (10:90 H_2O/CH_3OH; 0.3 mL min^{-1}) with detection by light scattering mass detection (tube temperature, 80°C; gas flow, 1 L min^{-1}). A single concentration (0.5 g, 2 mL) was analysed by preparative HPLC, whilst a series of concentrations (0.025, 0.05, 0.075, 0.1 mg; 100 μL injection aliquots) were

analysed by analytical HPLC. The results of these determinations were used to prepare a solution of the commercial formulation at a concentration corrected for the impurities {2.87 g L^{-1}, n[M_2D-C_3-O-$(EO)_n$-Me] = 3.2 x 10^{-3} mol L^{-1}}. This solution, and a purified sample prepared at a molar equivalent (2.00 g L^{-1}) were analysed by analytical HPLC (light scattering mass detection) with Triton X-45 as the internal standard and the responses compared.

2.2.2 Synthesis of M_2D-C_3-OR siloxanes

Pure M_2D-C_3-O-$(EO)_n$-Me (n = 3, 6 and 9) oligomers (refer to Compound **1**) were synthesised by reaction of the corresponding allyl capped oligoethoxylate monomethyl ether with bis(trimethylsiloxymethylsilane) {M_2D^H, $[(CH_3)_3Si\text{-}O\text{-}]_2$-$SiH(CH_3)$} over a Pt catalyst. The allyl-capped ethoxylate monomethyl ethers were synthesised by reaction of allyl chloride with the corresponding ethoxylate monomethyl ethers (n = 3, 6 and 9). The longer chained oligoethylene glycols (n = 6 and 9) were not commercially available and were therefore produced by combinations of smaller oligomers following a modified method from Krespan,[54] involving etherifications and chlorinations. A variation on the method for the longer chain (n = 9) oligomer was also conducted based on the synthesis by Wagner *et al.*,[55] in an attempt to increase the reaction yield (2.2.2.3.B). This reaction sequence involved the combination of monochloro triethylene glycol monoallyl ether with hexaethylene monomethyl glycol.

2.2.2.1 Synthesis of M_2D-C_3-O-$(EO)_3$-Me

The procedure adopted for the synthesis of M_2D-C_3-O-$(EO)_3$-Me is shown in Scheme 2.4.

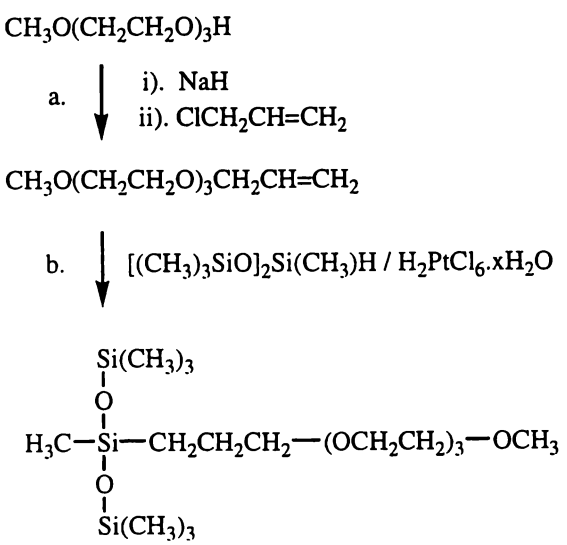

Scheme 2.4. Reaction sequence yielding M_2D-C_3-O-$(EO)_3$-Me

Step a.

A 3 molar equivalent of NaH (4.39 g, 0.18 mol) was ground with a pestle and mortar and added quickly to a solution of $CH_3O(CH_2CH_2O)_3H$ (10.02 g, 0.06 mol) in THF (40 mL) under nitrogen with stirring, following a cycle of three degassings. The solution effervesced ($H_{2(g)}$) and refluxed under the heat of its own reaction indicating the generation of the desired alkoxide ion. The mixture was degassed and then refluxed under nitrogen with stirring for 3 hours. The colourless solution changed to a yellow colour after 5 minutes, then to a tan-colour in ten minutes. A 1.5 mole equivalent (5 mL, 0.09 mol) of distilled $ClCH_2CH{=}CH_2$ was then added and the reflux continued for a further 2.5 hours. ESI/MS analysis of the reaction mixture (cream-coloured cloudy solution) confirmed formation of the alkylethoxylate ($[M + Na]^+$, *m/z* 227), and indicated the reaction had gone to completion as no peaks attributable to $CH_3O(CH_2CH_2O)_3H$ ($[M + Na]^+$, *m/z* 187) were observed. The solution was allowed to cool then filtered via a sintered glass filter, washing through with ether. The filtrate was then concentrated by rotary evaporation and vacuum to give a pale yellow coloured oil (10.65 g, 85% yield).

Step b.

A solution of $CH_3O(CH_2CH_2O)_3CH_2CH{=}CH_2$ (*Step a.*, 10.65 g) in THF (30 mL) was degassed three times then stirred under nitrogen in an ice bath. A catalytic amount of $H_2PtCl_6.xH_2O$ (1 mL, 0.1 mol L^{-1}) in THF was added and the solution degassed. A one mole equivalent of M_2D^H (11.62 g, 0.05 mol) was added in THF (10 mL) followed by a cycle of three degassings. The icebath was removed and the solution refluxed for 3.5 hours, yielding a dark brown-coloured clear solution. ESI/MS analysis showed the ion corresponding to the $CH_3O(CH_2CH_2O)_3CH_2CH{=}CH_2$ starting reagent to be approximately 12% of that of the product. The reflux was terminated and the solution allowed to cool. The mixture was filtered via a Whatman glass microfiber filter, washing with THF, and then concentrated by rotary evaporation and vacuum. The product mixture (21.29 g) was then purified by SiO_2 column chromatography (100 g) with a heptane to EtOAc to CH_3CN solvent gradient elution profile. The M_2D-C_3-O-$(EO)_3$-Me product (pale yellow clear liquid) was eluted with 85 - 60 % heptane (EtOAc) at a yield of 18.06 g. The percentage yield for this reaction (*Step b.*) was 81%, giving an overall synthetic yield of M_2D-C_3-O-$(EO)_3$-Me of 69%.

A portion of the product was further purified by semi-preparative RP C_{18} HPLC with 90:10 MeOH/H_2O as the elution solvent. Purity of the resulting fraction was checked by analytical RP C_{18} HPLC eluting with 85:25 MeCN/H_2O at a flow rate of 1 mL min^{-1}, and by GC/MS.

2.2.2.2 Synthesis of M_2D-C_3-O-$(EO)_6$-Me

The method used for preparation of the HO-$(EO)_6$-Me ethoxylate monomethyl ether is shown in Scheme 2.5. A small variation on the procedure used in Section 2.2.2.1 (Scheme 2.4, *Step a.*) for alkylation of the ethoxylate monomethyl ether was adopted, in that NaOH rather than NaH was used, NaOH being preferred for safety reasons. The hydrosilylation was performed as in Section 2.2.2.1 (Scheme 2.4, *Step b.*).

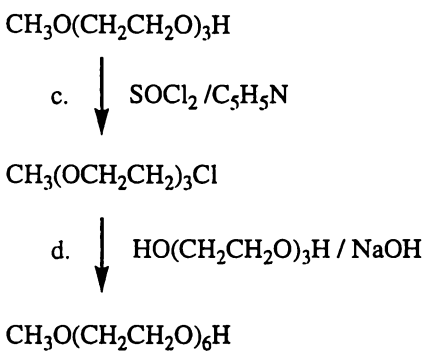

Scheme 2.5. Reaction sequence yielding the $(EO)_6$ ethoxylate monomethyl ether

Step c.

A catalytic amount of pyridine (7 drops) was added to 10 mL of $CH_3O(CH_2CH_2O)_3H$ (10.26 g, 0.06 mol) following a cycle of three degassings. The solution was then degassed, cooled with an icebath, and a 3 mole equivalent of $SOCl_2$ (14 mL, 0.19 mol) added dropwise over 15 minutes under nitrogen with stirring. The icebath was removed and the solution was then refluxed (nitrogen, stirring) for 4 hours to give a red-coloured clear solution and white crystals. ESI/MS analysis of the solution confirmed the reaction had gone to completion with the $[CH_3(OCH_2CH_2)_3Cl + H]^+$ ion (*m/z* 183) dominating the spectrum and no ion corresponding to the starting glycol observed. The solution was allowed to cool, then concentrated by vacuum. It was assumed that all the $CH_3O(CH_2CH_2O)_3H$ was converted to $CH_3(OCH_2CH_2)_3Cl$ in the subsequent calculations.

Step d.

A solution of $HO(CH_2CH_2O)_3H$ (17 mL, 0.12 mol) and NaOH pellets (4.94 g, 0.12 mol) was degassed and heated to 130°C. The external heat source was then removed and the $CH_3(OCH_2CH_2)_3Cl$ (*Step c.*, 0.06 mol) added dropwise over 15 minutes under nitrogen with stirring. A small volume of THF (5 mL) was used to wash in the residual $CH_3(OCH_2CH_2)_3Cl$. The external heat source was reapplied and the mixture was then allowed to react under nitrogen with stirring for 10 hours. ESI/MS analysis confirmed the reaction had gone to completion with no evidence of the limiting reagent [$CH_3(OCH_2CH_2)_3Cl$] in the spectrum. A $CH_3O(CH_2CH_2O)_6H$: $CH_3O(CH_2CH_2O)_9CH_3$ (product: by-product) ratio of 1: 0.3 was indicated. The solution was allowed to cool then filtered via a sintered glass suction filter, washing through with isopropanol (50 mL). The filtrate was then concentrated by rotary evaporation and vacuum to give a dark brown viscous product mixture.

The product mixture was purified via repetitive 5 g applications on an Al_2O_3 (90 g) column. Three column volumes (150 mL) of each of three solvents (A, 80:20 petroleum spirits /EtOAc; B, 100% EtOAc; and C, 95% EtOH) were used as the elution solvents. The fractions were analysed by ESI/MS and combined accordingly. The $CH_3O(CH_2CH_2O)_9CH_3$ by-product eluted first with Solvent A, the desired $CH_3O(CH_2CH_2O)_6H$ product eluted Solvent A to B, and the excess starting reagent $HO(CH_2CH_2O)_3H$ eluted with Solvent C. The fractions were combined to give yields of 12.45 g, 6.02 g (0.02 mol, 33 %) and 5.33 g, respectively.

The second fraction (6.02 g) was further purified by preparative RP C_{18} HPLC with an elution solvent of 60:40 H_2O/MeOH at a flow rate of 8 mL min^{-1}. The $CH_3O(CH_2CH_2O)_6H$ (pale yellow liquid, 5.77 g, 0.02 mol, 32 %) eluted at 19 - 24 minutes, as confirmed by ESI/MS analysis.

Step a.

A solution of $CH_3O(CH_2CH_2O)_6H$ (*Step d.*, 1.30 g, 0.004 mol) with NaOH (0.34 g, 0.008 mol) in THF (15 mL) was degassed three times then heated to reflux under nitrogen with stirring. $ClCH_2CH{=}CH_2$ (0.5 mL, 0.009 mol) in THF (10 mL) was then added and the reflux continued. At 6.5 hours the $[CH_3O(CH_2CH_2O)_6CH_2CH{=}CH_2 + NH_4]^+$ ion (*m/z* 354) dominated the ESI/MS spectrum, with the ion attributable to the glycol starting material negligible. The

solution was allowed to cool then filtered via a sintered glass filter, washing through with isopropanol (40 mL). The filtrate was then concentrated by rotary evaporation and vacuum to yield 2.36 g of impure product as a yellow oil.

Step b.

The $CH_3O(CH_2CH_2O)_6CH_2CH{=}CH_2$ (*Step a.*) was reacted with M_2D^H (1.57 g, 0.007 mol) in the presence of $H_2PtCl_6.xH_2O$ (1 mL, 0.1 mol L^{-1}) as for Section 2.2.2.1. The solution was cooled, filtered and concentrated after 9 hours reflux with the ESI/MS spectrum showing a product: starting material ratio of 1: 0.2. The product mixture (3.04 g) in 0.25 g aliquots was then purified via a RP C_{18} gravity column (25 g) with a 50:50 H_2O/MeOH to 100% MeOH gradient elution. The desired M_2D-C_3-O-$(EO)_6$-Me product (0.19 g) was eluted with 20:80 H_2O/MeOH. This fraction was further purified by preparative RP C_{18} HPLC using an elution solvent of 15:85 H_2O/MeOH at a flow-rate of 8 mL min^{-1}. This yielded 0.63 g (0.0015 mol, 37%) of pure product, eluting over 38 - 62 minutes, as confirmed by ESI/MS analysis. Some product (0.07 g, 4 %) was also obtained over 62 - 76 minutes coeluting with the by-product M_2D-C_3-O-$(EO)_3$-Me. A portion of the product was further purified by semi-preparative RP C_{18} HPLC with 70:30 CH_3CN/H_2O as the elution solvent. Purity of the resulting fraction was checked by analytical RP C_{18} HPLC (75:25 MeCN/H_2O, 1 mL min^{-1}) and GC/MS.

2.2.2.3.A Synthesis of M_2D-C_3-O-$(EO)_9$-Me - Method A

The method used for preparation of the HO-$(EO)_9$-Me ethoxylate monomethyl ether is shown in Scheme 2.6. The procedure used in Section 2.2.2.2 for alkylation of the ethoxylate monomethyl ether (*Step a.*) was adopted. The hydrosilylation was performed as for Section 2.2.2.1 (*Step b.*)

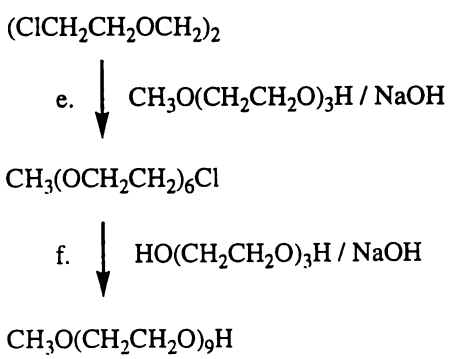

Scheme 2.6. Reaction sequence yielding the $(EO)_9$ ethoxylate monomethyl ether

Step e.

A solution of $(ClCH_2CH_2OCH_2)_2$ (20 mL, 0.13 mol) and NaOH (5.17 g, 0.13 mol) was degassed twice then heated to 110°C under nitrogen with stirring. A molar equivalent of $CH_3O(CH_2CH_2O)_3H$ (20.48 mL, 0.13 mol) was added dropwise over 1.5 hours and the resulting solution left to react for a further 3 hours (110°C, nitrogen, stirring). ESI/MS analysis of the reaction mixture revealed a ratio of ~ 0.8: 1: 0.4 for $CH_3(OCH_2CH_2)_6Cl$: $CH_3O(CH_2CH_2O)_9CH_3$: $CH_3O(CH_2CH_2O)_3H$ (product: by-product: starting material). The external heat source was removed and once cooled, the solution was filtered via a Whatman glass microfibre filter washing through with ether (40 mL) and the filtrate concentrated by rotary evaporation and vacuum. The $CH_3(OCH_2CH_2)_6Cl$ product was then purified by vacuum distillation to give 3.28 g (0.01 mol) of a colourless oil (bpt 142°C, 2 mm/Hg) at a yield of 17%.

Step f.

A solution of $HO(CH_2CH_2O)_3H$ (2.2 mL, 0.02 mol) and NaOH (0.89 g, 0.02 mol) in THF (10 mL) was prepared. Under reflux with nitrogen and stirring, the $CH_3(OCH_2CH_2)_6Cl$ (*Step e.*, 3.28 g, 0.01 mol) in THF (15 mL) was added dropwise over 2 hours. The residual $CH_3(OCH_2CH_2)_6Cl$ from the pressure equalising dropping funnel was washed in with three 5 mL aliquots of distilled THF and the mixture was then allowed to react under reflux. The progress of the reaction was monitored by ESI/MS and terminated at 19 hours. With application of heat the solution changed to a pale yellow, then to a tan coloured clear solution. The product mixture consisted of a yellow-coloured clear supernatant and a white crystalline material. The ESI/MS spectrum of the supernatant at 19 hours showed a $HO(CH_2CH_2O)_3H$ (*m/z* 173): $CH_3(OCH_2CH_2)_6Cl$ (*m/z* 332): $CH_3O(CH_2CH_2O)_9H$ (*m/z* 446): $CH_3O(CH_2CH_2O)_9CH_3$ (*m/z* 460) ratio (starting material: starting material: product: by-product) of 0.3: 0.1: 0.8: 1 although the dominant peak in the spectrum was an unassignable ammonium adduct at *m/z* 372.

The solution was allowed to cool, then concentrated by vacuum. A solvent extraction between ether (60 mL) and water (20 mL) was performed with the ether layer washed with a further 5 mL water after partitioning. Both fractions were concentrated by rotary evaporation and vacuum and the water-soluble fraction was then filtered via a Whatman glass microfibre gravity filter, washing

through with isopropanol (50 mL). The ether fraction (0.57 g) was obtained as a pale yellow oil consisting predominantly of the dimethylether by-products. The water-soluble fraction (6.17 g) was an orange coloured oil composed of the excess $HO(CH_2CH_2O)_3H$ starting reagent and the desired $CH_3O(CH_2CH_2O)_9H$ product.

The water-soluble fraction was purified via two repetitive applications on an Al_2O_3 (100 g) column. A solvent gradient of 100% heptane –> 100% EtOAc –> 100% EtOH –> 100% MeOH was used. The fractions were analysed by ESI/MS and combined accordingly. The dimethylether by-products $CH_3O(CH_2CH_2O)_9CH_3$ and $CH_3O(CH_2CH_2O)_{15}CH_3$ eluted over 50: 50 heptane/EtOAc to 100% EtOAc, the desired $CH_3O(CH_2CH_2O)_9H$ product eluted with 20:80 heptane/EtOAc to 85:15 EtOAc/EtOH and the excess starting reagent $HO(CH_2CH_2O)_3H$ eluted with EtOH. The fractions were combined to give yields of 1.34 g, 2.01 g and 1.60 g, respectively, with the second fraction consisting predominantly of the desired $CH_3O(CH_2CH_2O)_9H$ product. This fraction was further purified by preparative RP C_{18} HPLC with an elution solvent of 60:40 H_2O/MeOH at a flow-rate of 8 mL min^{-1}. The $CH_3O(CH_2CH_2O)_9H$ (0.47 g, 0.001 mol, 11 %) eluted at 26 - 35 minutes as confirmed by ESI/MS analysis.

Step a.

The $CH_3O(CH_2CH_2O)_9H$ (*Step f.*, 0.47 g, 0.001 mol) was reacted with $ClCH_2CH{=}CH_2$ (0.18 mL, 0.003 mol) in the presence of crushed NaOH pellets as for Section 2.2.2.2. The reaction progress was monitored by ESI/MS analysis at selected time intervals thereafter. At 4 hours, a product: reactant ratio of only 0.15: 1 was observed so additional $ClCH_2CH{=}CH_2$ (0.3 mL, 0.005 mol) and NaOH (0.26 g, 0.006 mol) was added. With this addition a change from colourless to yellow was observed for the solution. Analysis after 20 hours showed a product: reactant ratio of 1: 0.25, at which point further $ClCH_2CH{=}CH_2$ (0.18 mL, 0.003 mol) and NaOH (0.21 g, 0.005 mol) were added. The reflux was concluded after an additional 4 hours, totalling 24 hours. The ESI/MS spectrum showed the peak assignable to the reactant to be approximately 7% that of the product. The product mixture was filtered and concentrated as previously to give 2.32 g of a yellow oil-like solid. The concentrated filtrate was then applied to a reversed phase RP C_{18} (29 g) column after dissolving in 5 mL of water and eluted with 3 column volumes of water (105 mL) and 2 column volumes (70 mL) of

MeOH. The MeOH eluted fraction was concentrated by rotary evaporation and vacuum to give 0.70 g (0.0015 mol) of impure product as a yellow viscous oil.

Step b.

$CH_3O(CH_2CH_2O)_9CH_2CH=CH_2$ (*Step a.*, 0.70 g, 0.001 mol) was reacted with M_2D^H (0.37 g, 0.0017 mol) in the presence of $H_2PtCl_6.xH_2O$ (1 mL, 0.1 mol L^{-1}) as for Section 2.2.2.1. The reflux was terminated after 9 hours (product: starting material ratio of 1: 0.2 by ESI/MS) and the solution cooled and concentrated. The product mixture was then purified via a 29 g RP C_{18} reversed phase open column prepared with 50: 50 H_2O/MeOH. The first fraction was eluted with 2 column volumes (60 mL) of 40: 60 H_2O/MeOH (105 mL) and the second fraction was eluted with 4 column volumes (120 mL) of 10: 90 H_2O/MeOH. The 10: 90 H_2O/MeOH eluted fraction containing the desired M_2D-C_3-O-$(EO)_9$-Me product was concentrated by rotary evaporation and vacuum to give 0.61 g of a yellow oil. This fraction was further purified by preparative RP C_{18} HPLC with an elution solvent of 15: 85 H_2O/MeOH at a flow-rate of 8 mL min^{-1}. The purified product (52 mg, 7.5 x 10^{-6} mol, 0.8%) eluted at 59 - 78 minutes as confirmed by ESI/MS analysis.

2.2.2.3.B Synthesis of M_2D-C_3-O-$(EO)_9$-Me - Method B

A second synthesis of M_2D-C_3-O-$(EO)_9$-Me was conducted, adopting a variation in the synthesis of the alkylethoxylate as shown in Scheme 2.7.

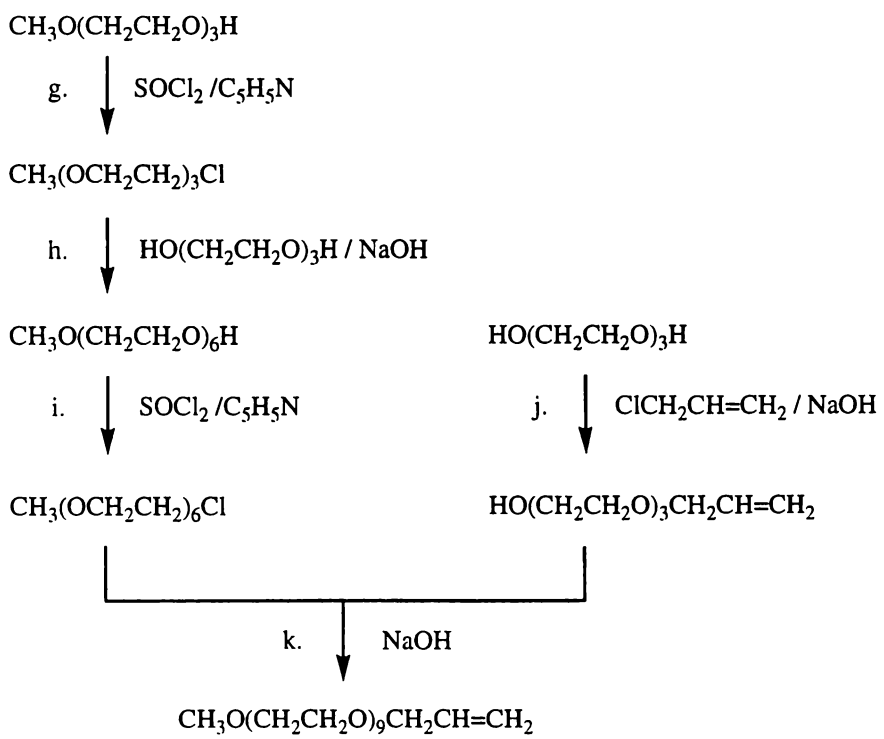

Scheme 2.7. Second reaction sequence adopted to yield C_3-O-$(EO)_9$-Me

Step g.

A catalytic amount of pyridine (8 drops) was added to 10 mL of $CH_3O(CH_2CH_2O)_3H$ (10.26 g, 0.06 mol) followed by a cycle of three degassings. The solution was then cooled with an ice bath and $SOCl_2$ (23 mL, 0.32 mol) added dropwise over 10 minutes under nitrogen with stirring. The ice bath was removed and the solution was allowed to reflux (nitrogen, stirring) for 5 hours. ESI/MS analysis was used to confirm the reaction had gone to completion. Once cooled, the solution was concentrated by vacuum to give a red clear solution with some colourless crystals precipitated.

Step h.

A solution of NaOH (3.01 g, 0.08 mol) dissolved in $HO(CH_2CH_2O)_3H$ (17 mL, 0.12 mol) was heated to 120°C under nitrogen and stirring. $CH_3(OCH_2CH_2)_3Cl$ (*Step g.*, 0.06 mol) was added dropwise over 1.5 hours and the mixture stirred and heated for a further 4 hours to give a dark brown solution. The solution was allowed to cool, filtered via a Whatman glass microfibre gravity filter, washing through with isopropanol (100 mL), and concentrated by rotary evaporation and vacuum.

Step i.

A catalytic amount of pyridine (5 drops) was added to the unpurified $CH_3O(CH_2CH_2O)_6H$ mixture (*Step h.*) followed by a cycle of two degassings. The solution was then cooled with an ice bath and $SOCl_2$ (13 mL, 0.18 mol) added dropwise over 25 minutes under nitrogen with stirring. The ice bath was removed, 20 mL of THF added and the solution refluxed for 5 hours (nitrogen, stirring). Once cooled, the solution was concentrated by vacuum and purified by vacuum distillation. A fraction (8.39 g) containing both the $CH_3(OCH_2CH_2)_6Cl$ and the by-product $CH_3O(CH_2CH_2O)_9CH_3$ was obtained at 157-160°C (2 mm/Hg). This fraction was purified on a SiO_2 column (75 g) eluting with heptane through to EtOAc. The $CH_3(OCH_2CH_2)_6Cl$ was eluted with 30:70 heptane/EtOAc at a yield of 5.57 g (0.018 mol, 30%).

Step j.

A solution of $HO(CH_2CH_2O)_3H$ (2.01 g, 0.013 mol) and NaOH (0.56 g, 0.014 mol) in THF (15 mL) was prepared under nitrogen with stirring, following a cycle of three degassings. To the refluxing solution, $ClCH_2CH{=}CH_2$ (0.75 mL, 0.014 mol) was added dropwise over 15 minutes and the reflux continued. The reaction

mixture was analysed by ESI/MS at 2.5, 7 and 14.5 hours and it was observed that the ion attributable to the $HO(CH_2CH_2O)_3H$ starting material was still significant (~25%), and had not changed over the 7 – 14 hour reflux period. Further $ClCH_2CH=CH_2$ (0.75 mL, 0.014 mol) was therefore added and the solution allowed to react for a further 8 hours, to give a reactant: product ratio of 0.15: 1. With an additional 3 hour reflux this was unchanged thus the reaction was concluded, totalling 25 hours of reflux. The solution was allowed to cool, concentrated by vacuum, then filtered via a sintered glass filter, washing through with ether (50 mL) and isopropanol (20 mL). The filtrate was concentrated by rotary evaporation and vacuum to give 2.35 g of a yellow-coloured clear viscous oil. This was then purified on an Al_2O_3 column (100 g) with a solvent gradient of 50: 50 heptane/EtOAc through to EtOAc and EtOH. The desired $HO(CH_2CH_2O)_3CH_2CH=CH_2$ (1.64 g, 0.009 mol, 66%) was eluted in the 30: 70 heptane/EtOAc to 100% EtOAc fractions as determined by ESI/MS analysis.

Step k.

A solution of the $HO(CH_2CH_2O)_3CH_2CH=CH_2$ (*Step j*, 1.64 g, 0.009 mol) and NaOH (0.42 g, 0.01 mol) in THF (10 mL) was prepared under nitrogen with stirring, following a cycle of three degassings. $CH_3(OCH_2CH_2)_6Cl$ (*Step i*, 2.71 g, 0.009 mol) in THF was added dropwise over 5 minutes and the solution refluxed for 9 hours. ESI/MS analysis of the reaction mixture showed both starting materials were still present. Additional NaOH (0.17 g, 0.04 mol) was added and the solution refluxed for a further 15 hours (totalling 24 hours of reflux time). The ESI/MS spectrum showed a $HO(CH_2CH_2O)_3CH_2CH=CH_2$: $CH_3(OCH_2CH_2)_6Cl$: $CH_3O(CH_2CH_2O)_9CH_2CH=CH_2$ 1 (starting material: starting material: product) ratio of 0.2: 0.1: 1. The solution was allowed to cool, concentrated by rotary evaporation, then filtered via a sintered glass filter, washing through with ether (50 mL). The filtrate was then concentrated by rotary evaporation and vacuum to give 4.32 g of a yellow-coloured clear solid. The product mixture was purified by Al_2O_3 column chromatography (100 g) using a solvent gradient of heptane through to EtOAc. The product, $CH_3O(CH_2CH_2O)_9CH_2CH=CH_2$, (2.06 g, 0.004 mol, 51%) was eluted with 100% EtOAc.

Step b.

The $CH_3O(CH_2CH_2O)_9CH_2CH{=}CH_2$ (*Step k.*, 2.06 g, 0.004 mol) was reacted with M_2D^H (0.98 g, 0.004 mol) in the presence of $H_2PtCl_6.xH_2O$ (1 mL, 0.1 mol L^{-1}) as for Section 2.2.2.1. The ESI/MS spectrum of the solution after 16 hours reflux showed the ion assignable to the $CH_3O(CH_2CH_2O)_9CH_2CH{=}CH_2$ starting material (*m/z* 488, $[M + NH_4]^+$) to be less than 10% that of the product (*m/z* 708, $[M + NH_4]^+$). The solution was allowed to cool, filtered via a Whatman glass microfiber filter washing through with THF, and then concentrated by rotary evaporation and vacuum. The product mixture (1.88 g) was then purified by Al_2O_3 column chromatography (100 g) using a solvent gradient of petroleum spirits through to EtOAc. The desired M_2D-C_3-O-$(EO)_9$-Me product (0.57 g, 0.0008 mol, 21%) was eluted in the 85% - 40% petroleum spirits fractions. The product was further purified by preparative RP C_{18} HPLC using an elution solvent of 15:85 H_2O/MeOH at a flow-rate of 8 mL min^{-1}. The product (0.24 g, 0.0004 mol, 9%) eluted at 62 - 78 minutes as confirmed by ESI/MS analysis.

2.2.2.4 Synthesis of M_2D-C_3-OH

The procedure adopted for the synthesis of M_2D-C_3-OH (Compound **4**) is shown in Scheme 2.8. The hydrosilylation method used was as for the previous syntheses.

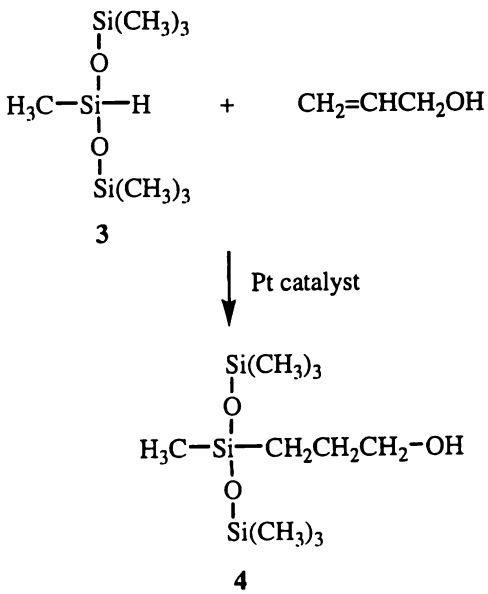

Scheme 2.8. Reaction sequence adopted for the synthesis of M_2D-C_3-OH (4)

A solution of $HOCH_2CH{=}CH_2$ (0.85 g, 0.015 mol) in THF (10 mL) was degassed three times then stirred under nitrogen in an ice bath. A catalytic amount of $H_2PtCl_6.xH_2O$ (0.5 mL, 0.1 mol L^{-1}) in THF was added and the solution degassed. M_2D^H (3.26 g, 0.015 mol) was added in THF (10 mL) and the solution degassed. The icebath was then removed and the solution was refluxed for 10 hours under nitrogen with stirring.

The solution, once cooled, was filtered via a Whatman glass microfiber filter washing through with THF, and then concentrated by rotary evaporation (50°C) and vacuum to give 4.2 g of product mixture (100%). The product mixture was analysed by ESI/MS and GC/MS. For comparison, the M_2D^H starting material was also analysed by these methods, however it was found to be undetectable by ESI/MS.

2.2.2.5 Synthesis of M_2D-C_3-O-EO-$COCH_3$ (5)

Two methods of synthesis of M_2D-C_3-O-EO-$COCH_3$ were attempted, varying only in the addition order of the reactants (Scheme 2.9). The synthesis was conducted in order to develop methodology appropriate for the synthesis of radiolabelled versions of organosilicone surfactants. The procedures, with appropriate scaling, potentially should be applicable to the reagents Silwet L-408 and ^{14}C-CH_3COCl, to yield a radiolabelled version of Sylgard 309. The radiolabelled synthesis was not attempted in this work.

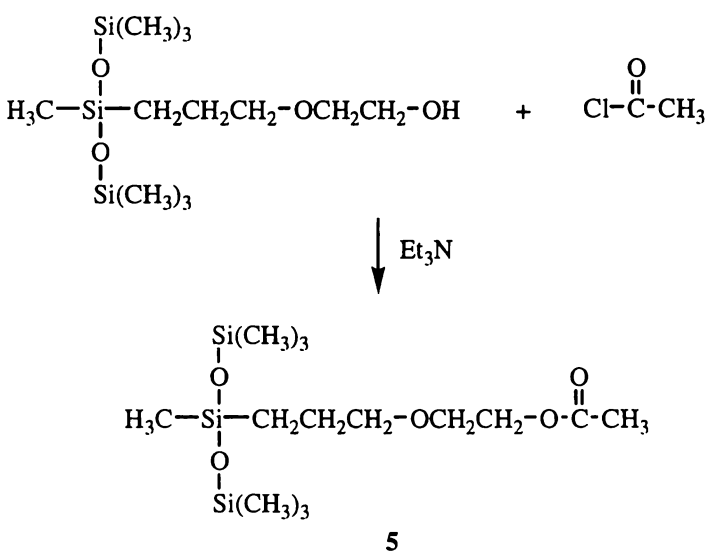

5

Scheme 2.9. Reaction sequence adopted for the synthesis of M_2D-C_3-O-EO-$COCH_3$ (5)

2.2.2.5.A Base addition prior to acetyl chloride addition

A solution of M_2D-C_3-O-EO-H (1.00 g, 0.003 mol) in ether (20 mL) was degassed three times then stirred under nitrogen. A 2 molar equivalent of Et_3N (1 mL, 0.006 mol) was added dropwise with stirring in an icebath, followed by a 2.2 molar equivalent of CH_3COCl (0.5 mL, 0.007 mol). The solution was stirred for 4 hours under nitrogen, with analysis by ESI/MS at 0.5 and 3 hours. The solution was filtered, washing through with ether (10 mL), and then concentrated by rotary evaporation (30°C) and vacuum to give 0.86 g of product mixture (76%).

2.2.2.5.B Base addition following acetyl chloride addition

A solution of M_2D-C_3-O-EO-H (1.00 g, 0.003 mol) in ether (20 mL) was degassed three times then stirred under nitrogen. A 2.2 molar equivalent of CH_3COCl (0.5 mL, 0.007 mol) was added and the solution degassed. Et_3N (1 mL, 0.006 mol) was then added dropwise to the solution in an icebath (with stirring). The icebath was removed and the solution then stirred for 24 hours under nitrogen. The solution was filtered, washing through with ether (20 mL), and then concentrated by rotary evaporation (30°C) and vacuum to give 1.08 g of product mixture (96%). The solution was analysed by ESI/MS at 1 and 24 hours.

2.3 RESULTS AND DISCUSSION

2.3.1 Separation of Silwet L-77

2.3.1.1 Purification of Silwet L-77 by preparative HPLC separation

The chromatogram of Silwet L-77 by preparative RP C_{18} HPLC is shown in Figure 2.1. The two broad peaks eluting over 31 - 37 and 37 - 54 minutes were assigned to the M_2D-C_3-O-$(EO)_n$-H (**2**) and M_2D-C_3-O-$(EO)_n$-Me (**1**) structures respectively, as determined by ESI/MS spectra and RP C_{18} HPLC/ESI/MS chromatograms of fractions.

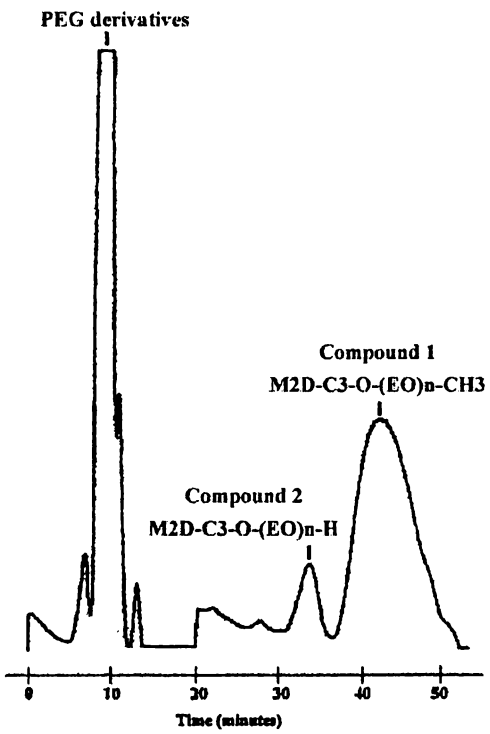

Figure 2.1. Preparative RP C_{18} HPLC chromatogram of commercial Silwet L-77

Separation of the M_2D-C_3-O-$(EO)_n$-H (**2**) and M_2D-C_3-O-$(EO)_n$-Me (**1**) structures was achieved, as determined by ESI/MS spectra and HPLC/ESI/MS chromatograms of fractions. The chromatogram of the M_2D-C_3-O-$(EO)_n$-Me (**1**) fraction is shown in Figure 2.2 below. The M_2D-C_3-O-$(EO)_n$-Me (**1**) oligomers are observed eluting after 43 minutes.

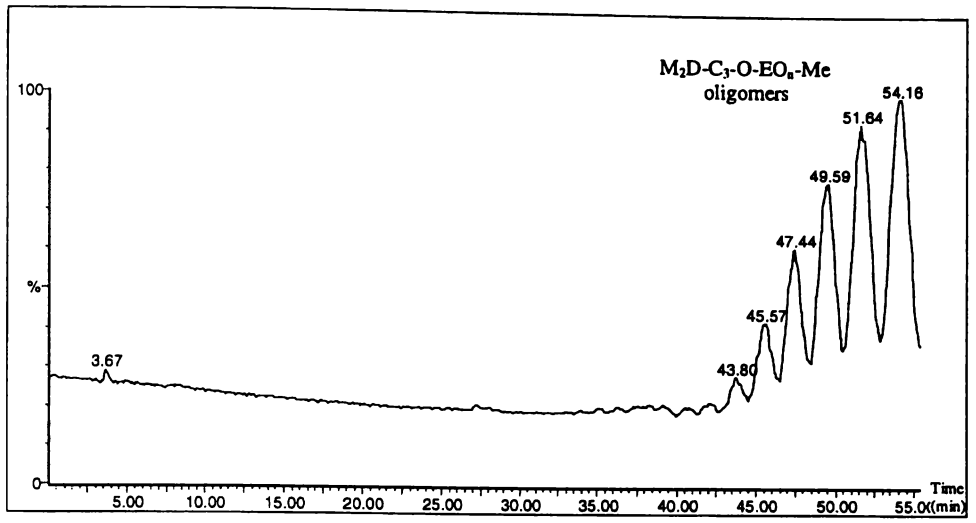

Figure 2.2. RP C_{18} HPLC/ESI/MS chromatogram of M_2D-C_3-O-$(EO)_n$-Me purified from Silwet L-77

For comparison, a reversed-phase HPLC/ESI/MS chromatogram of a sample of freshly prepared Silwet L-77 is shown in Figure 2.3 below. The M_2D-C_3-$(EO)_n$-Me (**1**) oligomers are those peaks eluting between 43 and 83 minutes. The polyethoxylate monomethyl ether and un-capped polyethoxylate diols are eluted early in the chromatogram (3-15 minutes) whilst the M_2D-C_3-O-$(EO)_n$-H (**2**) surfactants are observed between 25-45 minutes.

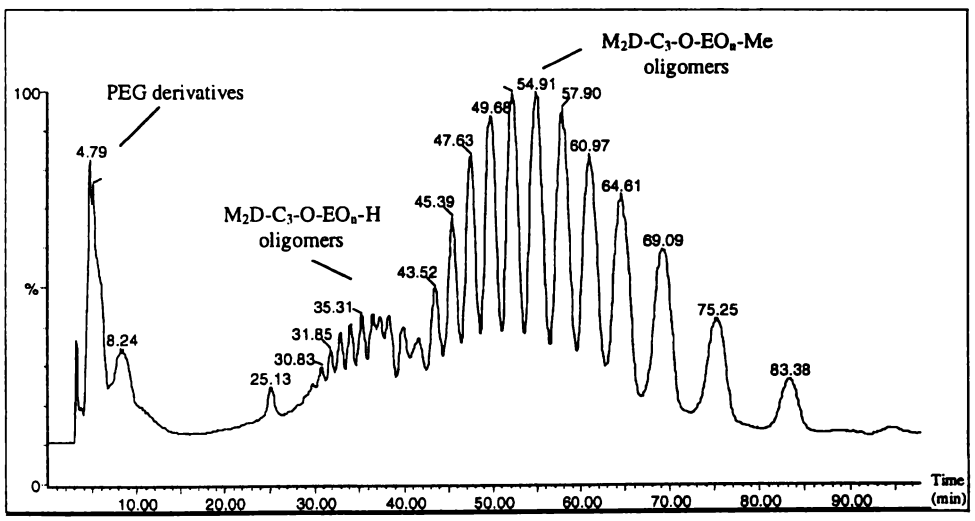

Figure 2.3. RP C_{18} HPLC/ESI/MS (30:70 H_2O/CH_3CN) of commercial Silwet L-77

2.3.1.2 Separation of individual oligomers from commercial Silwet L-77

The analytical RP C_{18} HPLC chromatograms of Silwet L-77 purified via a gravity elution RP C_{18} column with a gradient elution of 50% MeOH (H_2O)

through to 100% MeOH are shown in Figure 2.4 below. The M_2D-C_3-O-$(EO)_n$-R components are observed in the 75%, 80% and 85% MeOH fractions.

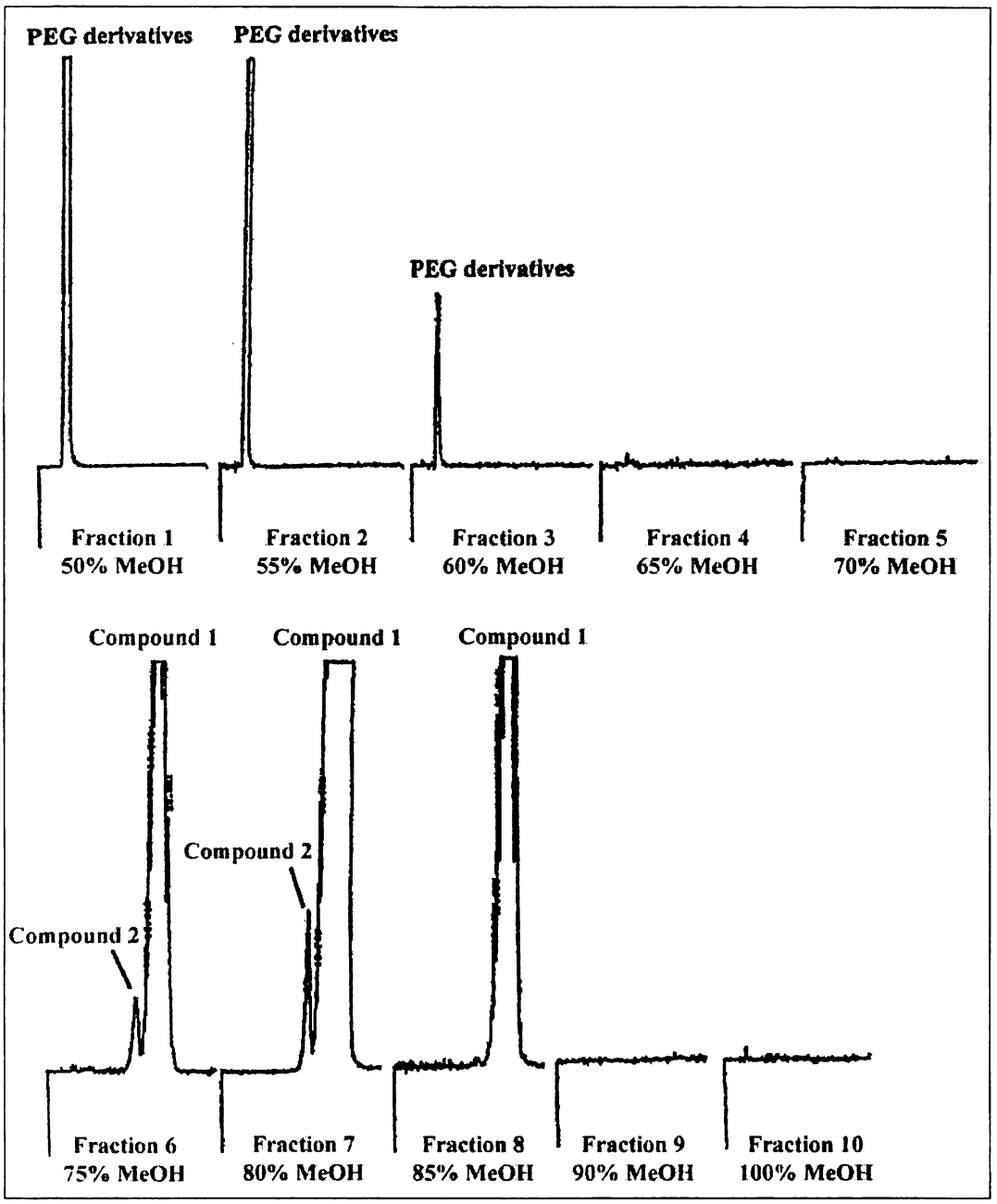

Figure 2.4. HPLC Profiles of fractions from Silwet L-77 separation by RP C_{18} chromatography

Some polar material was eluted with 50 - 60% MeOH from the open column whilst the trisiloxane alkylethoxylates along with other products eluted with 75 - 85% MeOH (retention time of 4 and 18 minutes respectively under the analytical HPLC conditions). Separation of the 75, 80 and 85% MeOH open column fractions by semi-preparative HPLC yielded some early eluting material (3, 6 and 8 minutes) and two oligomer series at 22 – 30 and 30 - 50 minutes.

The M_2D-C_3-O-$(EO)_n$-Me (**1**) oligomers were eluted as resolved peaks over 30 - 50 minutes, from which pure oligomers of n = 6 – 15 were obtained. The purity of selected oligomers, as determined by HPLC/APcI/MS, is presented in Table 2.2.

Table 2.2. Purity of M_2D-C_3-O-$(EO)_n$-Me (1) oligomers isolated by HPLC

M_2D-C_3-O-$(EO)_n$-Me	n = 5	n = 7	n = 11	n = 13+14	n = 15
%Purity	83	77	83	52+41	>99
%Contribution of n = x + 1 oligomer	5	-	-	5	-
%Contribution of n = x - 1 oligomer	12	23	17	2	-

Analysis by ESI/MS (Figure 2.5) showed the resolved peaks eluted at 22 – 30 minutes to be due to M_2D-C_3-O-$(EO)_n$-H (**2**) structures. High resolution data by FTICR/MS confirmed the M_2D-C_3-O-$(EO)_n$-H (**2**) assignment with the calculated mass* and observed mass for the *m/z* 567 peak (M_2D-C_3-O-$(EO)_6$-H oligomer) giving identical values (*m/z* 567.2873). All the other oligomers were within 0.0003 a.m.u. agreement.

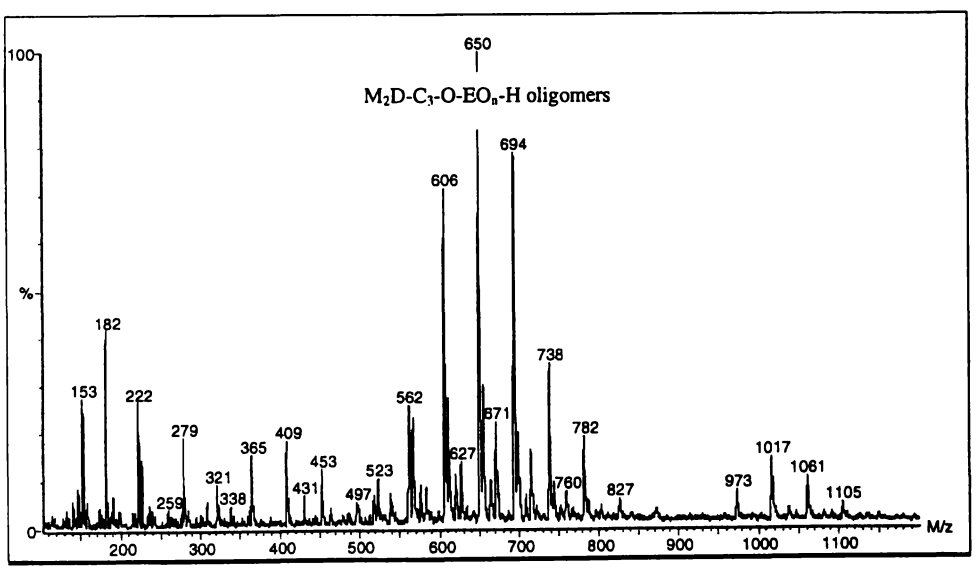

Figure 2.5. ESI/MS spectrum of the combined fractions eluted at 22 – 30 minutes from the Silwet L-77 formulation

This assignment was further confirmed by analysis by HPLC/ESI/MS and comparison with the chromatogram of commercial Silwet L-408 where retention times and spectra were identical (Figure 2.6).

* Most abundant isotopes used for calculated masses

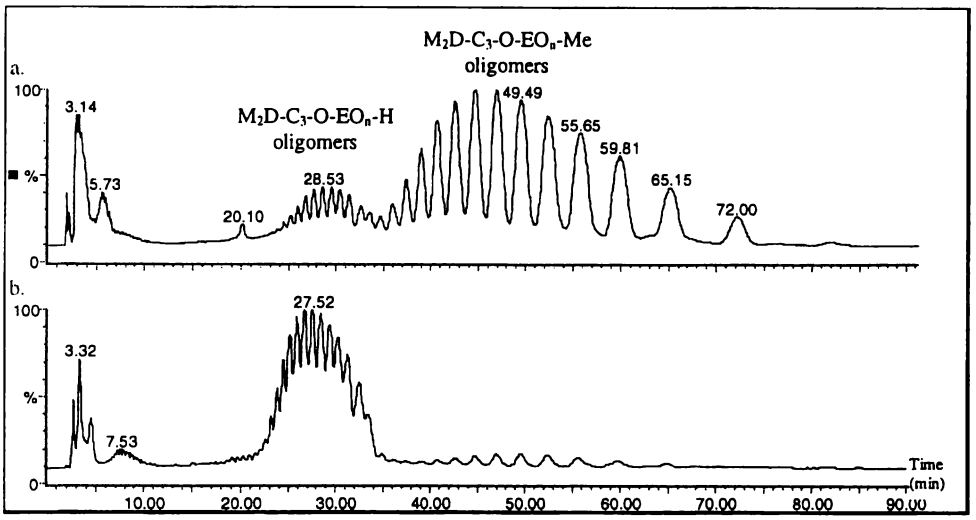

Figure 2.6. RP C_{18} HPLC/ESI/MS chromatograms of *a.* Silwet L-77 and *b.* Silwet L-408

A higher molecular weight series (*m/z* 934, 978, 1022, 1066, 1109 and 1154) was also evident in the ESI/MS and FTICR/MS spectra of this fraction (not shown) for which three plausible structures can be assigned. The linear dimer (Compound **6**, n_{TOTAL} = 11 - 16; $n_{/EO\ chain\#}$ = 5.5 - 8) matches as does the cyclic trimer (Compound **7**, n_{TOTAL} = 12 – 17; $n_{/EO\ chain\#}$ = 6 – 8.5) and the cyclic tetramer (Compound **8**, n_{TOTAL} = 9 - 14; $n_{/EO\ chain\#}$ = 3 – 4.6).

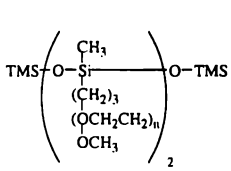

6

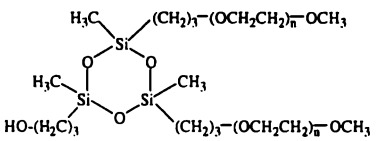

7

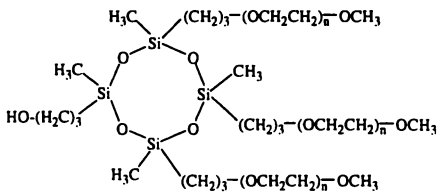

8

The linear dimer (**6**) gives the best agreement between calculated and observed masses and also has likely ethoxylate chain lengths (Table 2.3). It is possible that this linear dimer is a synthetic by-product as it is also a commercially available product (Silwet L-7607).

Table 2.3. High molecular weight series in HPLC fraction eluted over 22 – 30 minutes

MW (observed)	Possible structures	n_{TOTAL}	$n_{/EO\ chain\#}$	Molecular Formula	MW (calculated)[a]	Δm/M (ppm)
1109.6291[b]	**6**	15	7.5	$Si_4C_{46}H_{102}O_{20}Na$	1109.5940	32
	7	16	8	$Si_3C_{46}H_{98}O_{22}Na$	1109.7058	-69
	8	13	4.3	$Si_4C_{45}H_{98}O_{21}Na$	1109.5576	64

[a] Most abundant isotope of each element used; [b] Ion Series = *m/z* 934, 978, 1022, 1066, 1109, 1154 (Na^+ adducts)

Analysis of the polar material in the Silwet L-77 formulation by ESI/MS (Figure 2.7) revealed two NH_4^+ adduct series at *m/z* 400, 444, 488, 532, 576, 620, 664, 708 and *m/z* 562, 606, 650, 694, 738, 782, 826, 871, 915, 959, 1003, 1047, 1091,1135.

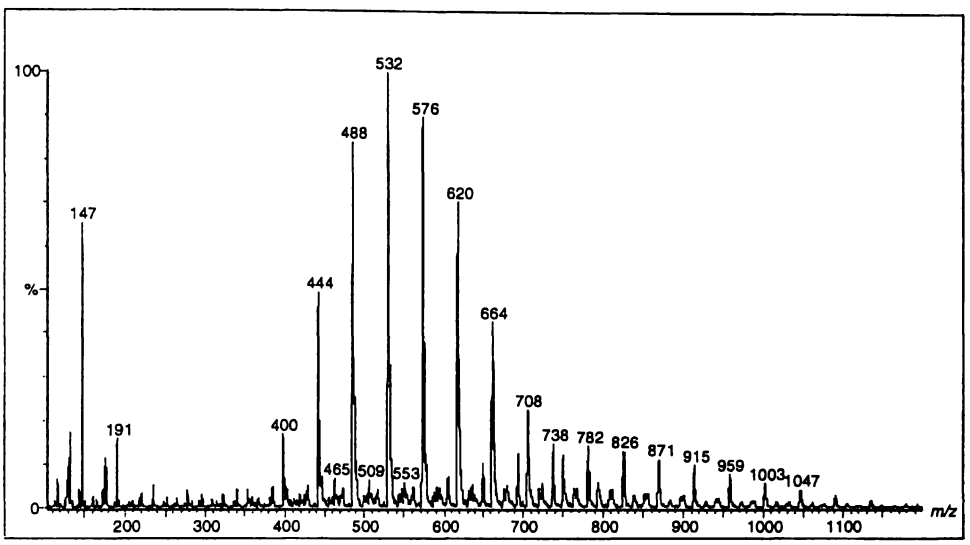

Figure 2.7. ESI/MS spectrum of polar constituents in the Silwet L-77 formulation

The former series corresponds to molecular weights for the cyclic trimer **7**, however this is not a plausible structure as the ions observed would required EO contents of n = 0 - 7. These molecular weights also match $M_2D\text{-}C_3\text{-}O\text{-}(EO)_n\text{-}Me$ (n = 2 – 9), however the short retention times rule this out as a viable assignment.

The adducts observed correspond to molecular weights of 382, 426, 470, 514, 558, 602, 646 and 690 a.m.u. In an attempt to find the molecular weight of the backbone structure 44 a.m.u. was consecutively subtracted to give possible molecular weights of 338, 294, 250, 206, 162, 118, 74 or 30, for the n = 0 structure.

Because no derivatives of $M_2D\text{-}C_3\text{-}O\text{-}(EO)_n\text{-}Me$ with molecular masses matching this series could be found, potential by-products of the synthetic procedure were addressed. In the synthesis of Silwet L-77, $CH_3O(EO)_nH$ is alkylated with $XCH_2CH{=}CH_2$ (X = undisclosed halogen) to give $CH_3O(EO)_nCH_2CH{=}CH_2$. The presence of $HO(EO)_nH$ in the $CH_3O(EO)_nH$ starting material however, will result in the concomitant production of $HO(EO)_nCH_2CH{=}CH_2$. Neither structures of $RO(EO)_nCH_2CH{=}CH_2$, R = CH_3 or H, were found to match the required molecular mass, however further derivatives of $HO(EO)_nCH_2CH{=}CH_2$ can be proposed.

As documented in the literature, hydrosilylation of olefins possessing an alcohol group in the structure is often complicated by side reactions between the hydroxyl group and the Si atom, resulting in the formation of Si-O-C linkages.[56] In the case of M_2D^H and $HO(EO)_nCH_2CH{=}CH_2$ this would give rise to Compound **9**, hereafter denoted as $M_2D\text{-}O\text{-}(EO)_n\text{-}CH_2CH{=}CH_2$.

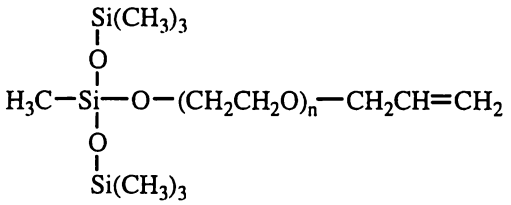

9

The molecular weight of **9** for n = 0 is 278 a.m.u, which does not correspond with any of the molecular weights sought. However examination of the structure indicates the compound would be of too low a polarity to be eluted at the observed retention times. Compound **9** is less polar than $M_2D\text{-}C_3\text{-}O\text{-}(EO)_n\text{-}CH_3$, and so would be retained longer on the RP C_{18} support, i.e. at > 30 minutes. This is significantly different to the observed retention times of ~ 5 minutes. Hydrolysis of the terminal TMS groups would increase the polarity of **9**, as was found for the corresponding analogues of $M_2D\text{-}C_3\text{-}O\text{-}(EO)_n\text{-}CH_3$ (Compounds **21** and **22**), discussed in more detail in Chapter 6. This would yield the structures, **10** and **11**, which have molecular weights of 206 and 134, respectively. The abbreviations $MD(M^{OH})\text{-}O\text{-}(EO)_n\text{-}CH_2CH{=}CH_2$ and $(M^{OH})_2D\text{-}O\text{-}(EO)_n\text{-}CH_2CH{=}CH_2$, respectively, will be used to describe **10** and **11** hereafter.

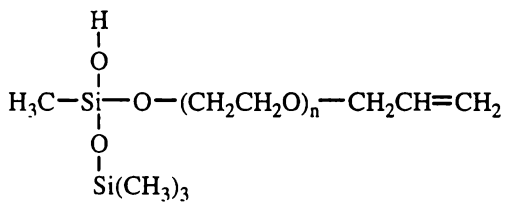

10

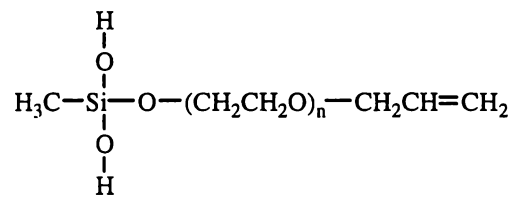

11

The molecular mass of structure **10** matches with the desired molecular weights, and the observed ions correspond to plausible EO content (n = 4 – 11). Furthermore the oligomeric distribution is as expected for the starting materials used. The dominant ion was observed at *m/z* 532, which corresponds to the n = 7

oligomer of **10**. Comparison of the calculated molecular mass of **10** (*m/z* 581, n = 8) with the high resolution FTICR/MS data is presented in Table 2.4. Olefinic resonances* were also observed in the ^{1}H NMR spectrum of the isolated fraction, further supporting this assignment.

Table 2.4. FTICR/MS results of polar fractions from Silwet L-77

MW (observed)	Possible structures	n_{TOTAL}	$n_{/EO\ chain\#}$	MF	MW (calculated)	Δm/M (ppm)
407.2282 [a]	$CH_3O(EO)_nH$	8	8	$C_{17}H_{36}O_9Na$	407.2257	6
581.3475 [b]	**7**	4	2	$Si_3C_{22}H_{50}O_{10}Na$	581.2601	150
	10	8	8	$Si_2C_{23}H_{50}O_{11}Na$	581.2789	118
787.4748 [c]	**12**	8	8	$Si_4C_{31}H_{72}O_{13}Na$	787.3948	102
	13	9	9	$Si_3C_{31}H_{68}O_{15}Na$	787.3764	125

[a] Ion Series *m/z* 407, 451, 495, 539, 583 (Na^+ adducts); [b] Ion Series *m/z* 449, 493, 537, 581, 625, 669, 713, 757, 801, 845 (Na^+ adducts); [c] Ion Series *m/z* 567, 611, 655, 699, 743, 787, 831, 875, 919, 963, 1007, 1051, 1095, 1139 (Na^+ adducts)

The higher molecular weight ion series in the spectrum of the polar constituents (Figure 2.7), corresponds to both the linear dimer **12** (n = 3 – 16) and the cyclic trimer **13** (n = 4 – 17). The Na^+ adducts of this series were also observed by FTICR/MS, comparative calculations of which are shown in Table 2.4 (*m/z* 787). The calculated mass for the linear dimer is in better agreement with the observed mass.

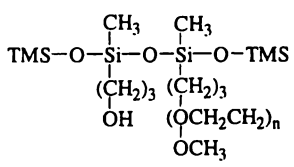

12

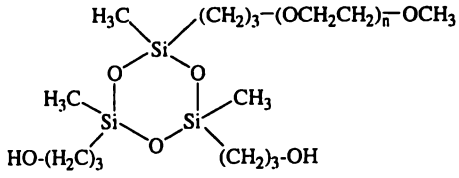

13

Analysis by FTICR/MS also revealed another Δ *m/z* = 44 series at *m/z* 407, 451, 495, 539 and 583 which can be assigned to the free monomethyl polyethoxylates, $CH_3O(EO)_nH$, (n = 8 - 12 Na^+ adducts), for which mass difference calculations are well within agreement (Table 2.4, *m/z* 407).

This was further confirmed by comparison of the HPLC/ESI/MS chromatogram (60:40 H_2O/MeOH) with those of commercially available

* ^{1}H NMR olefinic resonances (D_2O) δ_H: 6.2 ppm, d.d; 6.0 ppm, m.

$CH_3O(EO)_nH$ (not shown) and $CH_3O(EO)_3H$ (Figure 2.8). Identical retention times and spectra confirmed the $CH_3O(EO)_nH$ assignment.

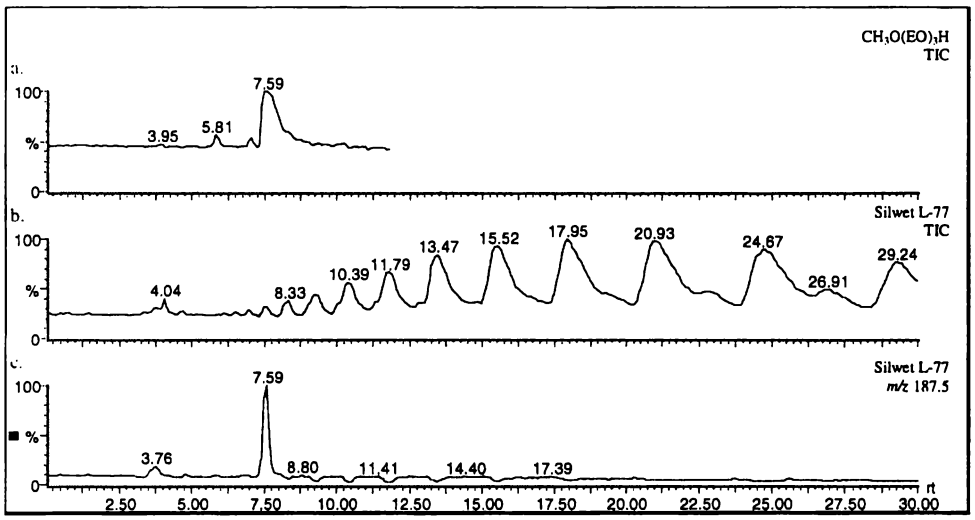

Figure 2.8. RP C_{18} HPLC/ESI/MS chromatograms of *a.* $CH_3O(EO)_3H$, *b.* Silwet L-77 and *c.* the extracted chromatogram of $CH_3O(EO)_3H$ (m/z 187) from the *b.* trace.

The above HPLC/ESI/MS chromatogram (Figure 2.8.b) also revealed the presence of the uncapped-polyethylene glycol, $HO(EO)_nH$, series (observed as the right hand side shoulder peaks), and was confirmed by comparison of the corresponding spectra.

2.3.1.3 Determination of Silwet L-77 percentage composition

Integration of a preparative HPLC chromatogram of Silwet L-77 (detection by RI) indicated the surfactants (Compounds **1** [M_2D-C_3-O-$(EO)_n$-Me] and **2** [M_2D-C_3-O-$(EO)_n$-H]) constituted 75% of the mixture, according to the relative peak intensities. A series of concentrations of Silwet L-77 were also analysed by analytical HPLC with light scattering mass detection. Integration of the resulting chromatograms gave 23.2-25.5%, 4.0-5.6% and 68.9-72.8% percentage compositions for the early eluting polar fractions, M_2D-C_3-O-$(EO)_n$-H structures (**2**) and M_2D-C_3-O-$(EO)_n$-Me structures (**1**), respectively.

An averaged value of 70% for the M_2D-C_3-O-$(EO)_n$-Me composition of Silwet L-77 was thus used to prepare a 3.2×10^{-3} mol L^{-1} M_2D-C_3-O-$(EO)_n$-Me solution from of Silwet L-77 (2.86 g L^{-1}). The response of a diluted sample of this solution by analytical HPLC (light scattering mass detection), was compared with that of a

purified M_2D-C_3-O-$(EO)_n$-Me sample* (2.00 g L^{-1}) and the absolute response values were found to be well within experimental error. A range of concentrations from each solution were consequently prepared (7.69 x 10^{-8} – 2.15 x 10^{-6} mol L^{-1}) and analysed by analytical HPLC. The absolute and relative responses (Triton X-45® [TX-45] as the internal standard) of the M_2D-C_3-O-$(EO)_n$-Me peak were very comparable for the two solutions as shown in Figures 2.9 and 2.10.

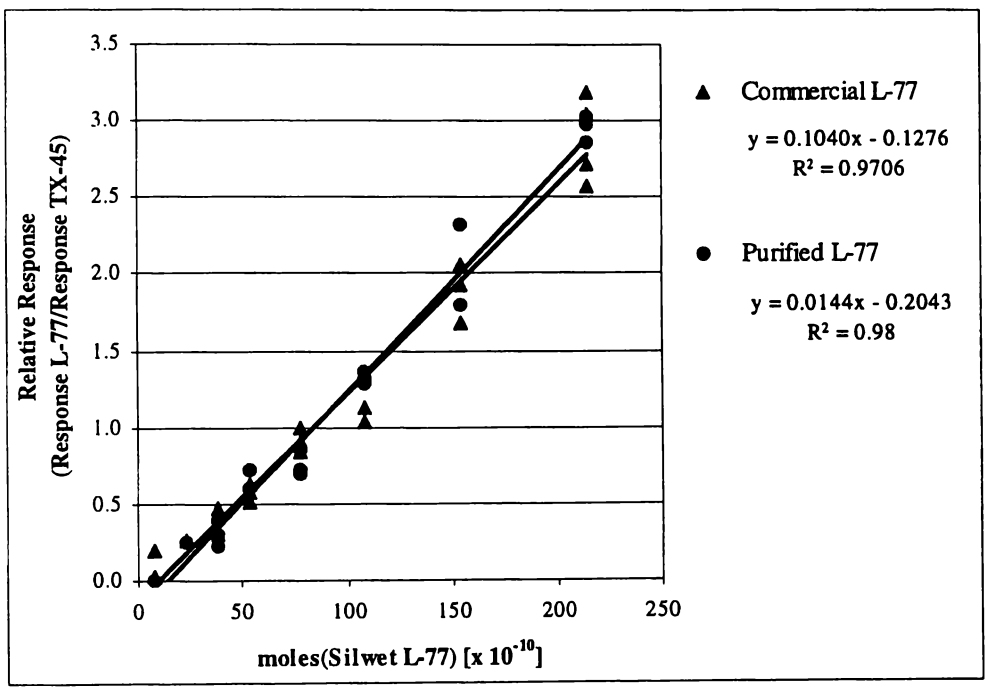

Figure 2.9. Comparison of relative HPLC responses of standard solutions of commercial Silwet L-77 (2.87 g L^{-1}) and a purified M_2D-C_3-O-$(EO)_n$-Me sample (2.00 g L^{-1}) with Triton X-45 as the internal standard

* Section 2.3.1.1

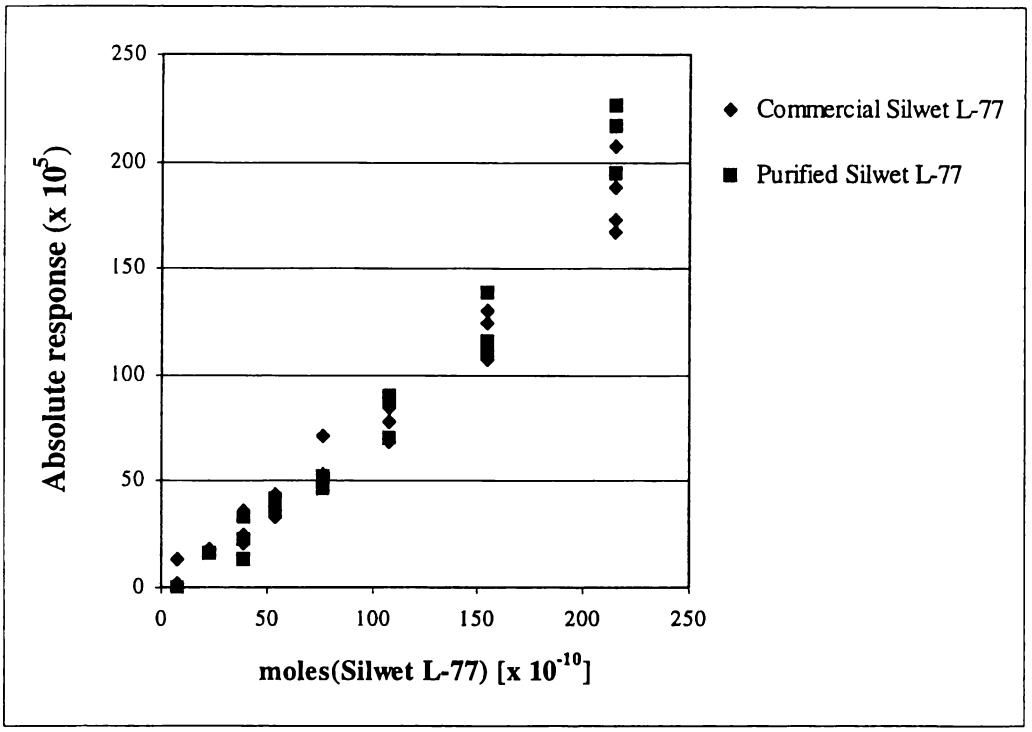

Figure 2.10. Comparison of absolute HPLC responses of standard solutions of commercial Silwet L-77 (2.87 g L^{-1}) and a purified M_2D-C_3-O-$(EO)_n$-Me sample (2.00 g L^{-1}).

The ratio of the absolute (Purified L-77/Commercial Silwet L-77) and relative (Purified [L-77/TX-45]/Commercial [L-77/TX-45]) responses for the two solutions over all the concentrations was also highly reproducible, averaging 1.0 ± 0.2 and 1.0 ± 0.3, respectively (Appendix A.IV.1). This data demonstrates that M_2D-C_3-O-$(EO)_n$-Me oligomers comprise ~ 70% of the Silwet L-77 formulation.

2.3.2. Synthesis of M_2D-C_3-O-R siloxanes

HPLC separation of M_2D-C_3-O-$(EO)_n$-Me oligomers proved to be a highly laborious process yielding only small amounts of the compounds. Synthetic procedures were thus investigated in order to obtain larger quantities.

In the synthesis of the pure trisiloxane alkylethoxylates used in this work, allyl capped oligoethoxylate monomethyl ethers were produced by reaction of allyl chloride with isolated oligomers of oligoethoxylate monomethyl ethers. Reaction of this intermediate with bis(trimethylsiloxymethylsilane), M_2D^H, using a Pt catalyst yielded the desired trisiloxane alkylethoxylates of various $(EO)_n$ (n = 3, 6 and 9) oligomers (Scheme 2.10).

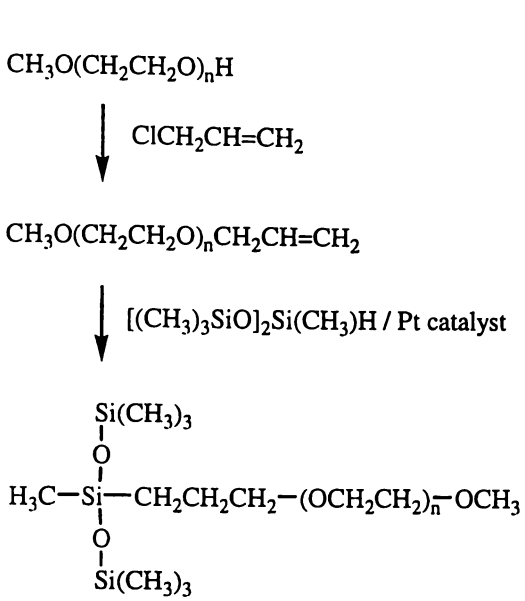

Scheme 2.10. Reaction sequence adopted to yield trisiloxane alkylethoxylate oligomers

2.3.2.1 Synthesis of M_2D-C_3-O-$(EO)_3$-Me

M_2D-C_3-O-$(EO)_3$-Me (refer to Compound **1**) was synthesised by reaction of the allyl capped triethoxylate monomethyl ether with M_2D^H over a Pt catalyst (Scheme 2.4). The allyl capped ethoxylate monomethyl ether was prepared by reaction of allyl chloride with the commercially available triethoxylate monomethyl ether.

The alkoxide ion of $CH_3O(CH_2CH_2O)_3H$, generated by reaction with NaH, was reacted with $ClCH_2CH=CH_2$ to give $CH_3O(CH_2CH_2O)_3CH_2CH=CH_2$ as a yellow oil at a yield of 85%. The hydrosilylation of the $CH_3O(CH_2CH_2O)_3CH_2CH=CH_2$ with M_2D^H was then achieved with the catalyst $H_2PtCl_6.xH_2O$ under reflux (THF). The M_2D-C_3-O-$(EO)_3$-Me product was purified via normal phase SiO_2 separation at a percentage yield of 81% for the hydrosilylation reaction, giving an overall synthetic yield of 69%.

The analytical RP C_{18} HPLC/APcI/MS chromatogram of the M_2D-C_3-O-$(EO)_3$-Me product, following purification by semi-preparative RP C_{18} HPLC, confirmed greater than 95% purity, with a small contribution from an unidentified polar product. The GC/MS chromatogram (0 - 35 minutes) showed a single peak eluting at 19.5 minutes. The corresponding spectrum showed a pattern characteristic of siloxanes, with the highest mass ion occurring at *m/z* 411, assigned to $[M_2D\text{-}C_3\text{-O-}(EO)_3\text{-Me} - CH_3]^+$.

2.3.2.2 Synthesis of M_2D-C_3-O-$(EO)_6$-Me

M_2D-C_3-O-$(EO)_6$-Me (refer to Compound **1**) was synthesised by chlorination, etherification and hydrosilylation methods. The n = 6 oligoethylene glycol is not commercially available and was therefore prepared by chlorination of triethoxylate monomethyl ether, followed by etherification with triethylene glycol (Scheme 2.5), using a modified method from Krespan.[54]

The chlorination of $CH_3O(CH_2CH_2O)_3H$ with $SOCl_2$ to form $CH_3(OCH_2CH_2)_3Cl$ was achieved by catalysis with pyridine under reflux. The $CH_3(OCH_2CH_2)_3Cl$ was then etherified with $HO(CH_2CH_2O)_3H$ in the presence of NaOH at 130°C. The $CH_3O(CH_2CH_2O)_6H$ product was purified via column chromatography using Al_2O_3 and preparative RP C_{18} HPLC methods. The $CH_3O(CH_2CH_2O)_6H$ was then allylated with $ClCH_2CH{=}CH_2$ under reflux (THF), in the presence of base (NaOH) to give $CH_3O(CH_2CH_2O)_6CH_2CH{=}CH_2$. $H_2PtCl_6.xH_2O$ catalysed hydrosilylation (THF reflux) of the $CH_3O(CH_2CH_2O)_6CH_2CH{=}CH_2$ with M_2D^H yielded M_2D-C_3-O-$(EO)_6$-Me which was purified via RP C_{18} gravity elution chromatography and preparative RP C_{18} HPLC. The synthetic yield for the reaction sequence was 37%

The analytical RP C_{18} HPLC/APcI/MS chromatogram of the M_2D-C_3-O-$(EO)_6$-Me product, following purification by semi-preparative RP C_{18} HPLC, showed 96% purity, with a 4% contribution from M_2D-C_3-O-$(EO)_5$-Me. A single peak (26.5 minutes) was observed in the GC/MS chromatogram (0 - 55 minutes), which showed a characteristic siloxane spectrum.

Whilst the methods employed here for the synthesis of M_2D-C_3-O-$(EO)_n$-Me oligomers of were successful, some improvements to the methodology can be envisaged. It is proposed that purification of the synthetic mixtures by distillation methods may increase yields and purity, and also reduce the cost and waste associated with the organic solvents used in chromatography. A vacuum of sufficiently low pressure was not accessible for this work, and consequently distillation was not possible as excessively high temperatures were required. However this method has been used successfully elsewhere.[55]

Furthermore, it is proposed that following a synthetic procedure where the reaction intermediates are of lower polarity, i.e. by introduction of the $CH_2CH{=}CH_2$ moiety early in the procedure as performed by Wagner *et al.*,[55]

would also further simplify purification. Accordingly, a revised method for the synthesis of the M_2D-C_3-O-$(EO)_6$-Me oligomer is proposed in Scheme 2.11.

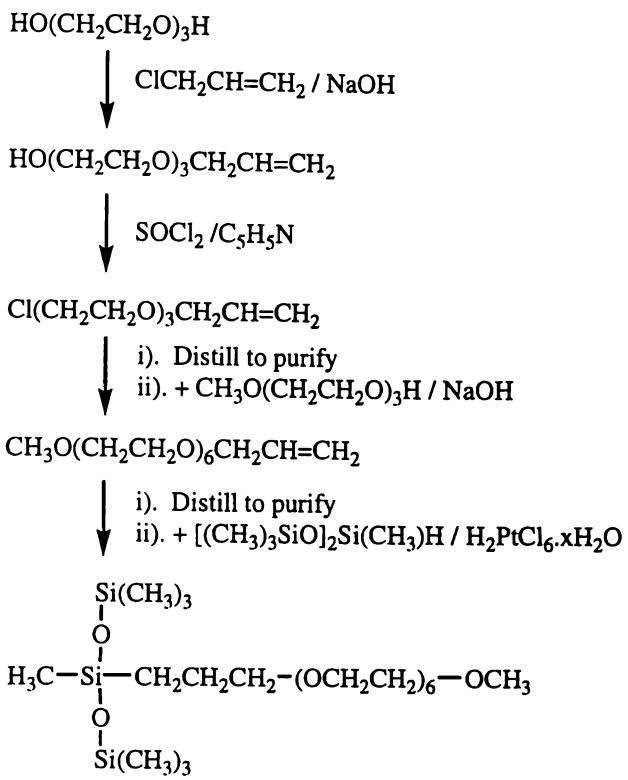

Scheme 2.11. Revised sequence recommended for the synthesis of M_2D-C_3-O-$(EO)_6$-Me

Following this method, rather than that used in Scheme 2.5, should simplify the synthesis and also lead to higher yields.

2.3.2.3.A Synthesis of M_2D-C_3-O-$(EO)_9$-Me – Method A

M_2D-C_3-O-$(EO)_9$-Me (refer to Compound **1**) was synthesised by the hydrosilylation and etherification methods used in Section 2.3.2.1. The allyl-capped ethoxylate monomethyl ether was synthesised by reaction of allyl chloride with the corresponding nonaethoxylate monomethyl ether. The n = 9 oligoethylene glycol was produced by combinations of smaller n = 3 oligomers (Scheme 2.6), using a modified method from Krespan.[54]

$CH_3(OCH_2CH_2)_6Cl$ was formed by condensation of $(ClCH_2CH_2OCH_2)_2$ and $CH_3O(CH_2CH_2O)_3H$ under basic conditions (NaOH) with external heating (110°C). The $CH_3(OCH_2CH_2)_6Cl$ product was purified by vacuum distillation at a

yield of 17%. The $CH_3(OCH_2CH_2)_6Cl$ was then etherified with $HO(CH_2CH_2O)_3H$ under reflux in THF with NaOH. An ether/water solvent extraction was performed on the product mixture and the $CH_3O(CH_2CH_2O)_9H$ product was purified by Al_2O_3 and preparative RP C_{18} HPLC chromatographic methods from the water-soluble fraction. Allylation of the $CH_3O(CH_2CH_2O)_9H$ with $ClCH_2CH=CH_2$ was achieved by refluxing with NaOH (THF). The product mixture was purified via RP C_{18} gravity elution chromatography. The hydrosilylation of the $CH_3O(CH_2CH_2O)_9CH_2CH=CH_2$ with M_2D^H was catalysed by $H_2PtCl_6.xH_2O$ under reflux (THF). The M_2D-C_3-O-$(EO)_9$-Me product was purified via RP C_{18} gravity elution and preparative RP C_{18} HPLC methods.

The analytical RP C_{18} HPLC/APcI/MS chromatogram following purification by semi-preparative RP C_{18} HPLC, showed 90% purity for the final product, with a 6% and 4% contribution from the $(EO)_8$ and $(EO)_7$ oligomers, respectively. The GC/MS chromatogram (0 - 65 minutes) showed a single peak with a characteristic siloxane spectrum eluting at 45.5 minutes. The yield for the synthesis was very low at 0.8%.

2.3.2.3.B Synthesis of M_2D-C_3-O-$(EO)_9$-Me – Method B

M_2D-C_3-O-$(EO)_9$-Me (refer to Compound **1**) was synthesised by hydrosilylation of the allyl capped nonaethoxylate monomethyl ether. The allyl-capped ethoxylate monomethyl ether was synthesised by the combination of monochloro triethylene glycol monoallyl ether with hexaethylene monomethyl glycol (Scheme 2.7), based on the synthesis by Wagner *et al.*[55] The monochloro triethylene glycol monoallyl ether was produced by combination of triethylene glycol with allyl chloride. The hexaethylene glycol was synthesised by etherification of chlorinated triethylene monomethyl ether with triethylene glycol.

The chlorination of $CH_3O(CH_2CH_2O)_3H$ with $SOCl_2$ to yield $CH_3(OCH_2CH_2)_3Cl$ was catalysed by pyridine under reflux. The $CH_3(OCH_2CH_2)_3Cl$ was then added to a heated solution (120°C) of $HO(CH_2CH_2O)_3H$ and NaOH to yield $CH_3O(CH_2CH_2O)_6H$. The chlorination of the $CH_3O(CH_2CH_2O)_6H$ mixture with $SOCl_2$ was catalysed by pyridine under reflux, to give $CH_3(OCH_2CH_2)_6Cl$ which was purified by vacuum distillation and normal phase SiO_2 gravity elution chromatography.

$HO(CH_2CH_2O)_3H$ was allylated with $ClCH_2CH{=}CH_2$ in the presence of NaOH under reflux (THF) and the product $[HO(CH_2CH_2O)_3CH_2CH{=}CH_2]$ purified by Al_2O_3 gravity elution chromatography. The $HO(CH_2CH_2O)_3CH_2CH{=}CH_2$ was then etherified with $CH_3(OCH_2CH_2)_6Cl$ using NaOH under reflux (THF) to give $HO(CH_2CH_2O)_9CH_2CH{=}CH_2$ which was purified on an Al_2O_3 column. The desired M_2D-C_3-O-$(EO)_9$-Me was synthesised by $H_2PtCl_6.xH_2O$ catalysed hydrosilylation of $HO(CH_2CH_2O)_9CH_2CH{=}CH_2$ with M_2D^H (THF reflux). The product mixture was purified by Al_2O_3 gravity elution chromatographic and preparative RP C_{18} HPLC methods. The M_2D-C_3-O-$(EO)_9$-Me product was obtained at 9 % yield.

2.3.2.4 Synthesis of M_2D-C_3-OH (4)

The hydrosilylation method used for the previous syntheses was applied to allyl alcohol and M_2D^H (**3**) in an attempt to synthesise M_2D-C_3-OH (Scheme 2.8). This compound was desired as it is a possible degradation product of Silwet L-77. Derivatives of this compound are presented as degradation products in later sections, as determined by ESI/MS, and thus it was important to establish the ability of this compound to be ionised by ESI/MS methods.

The ESI/MS spectrum of the product mixture revealed a large number of peaks. With the addition of HCO_2H an ion at *m/z* 281 was observed in the 60V spectrum which can be tentatively assigned to $[\mathbf{4} + H^+]^+$, although a large number of other peaks were also evident (Figure 2.11).

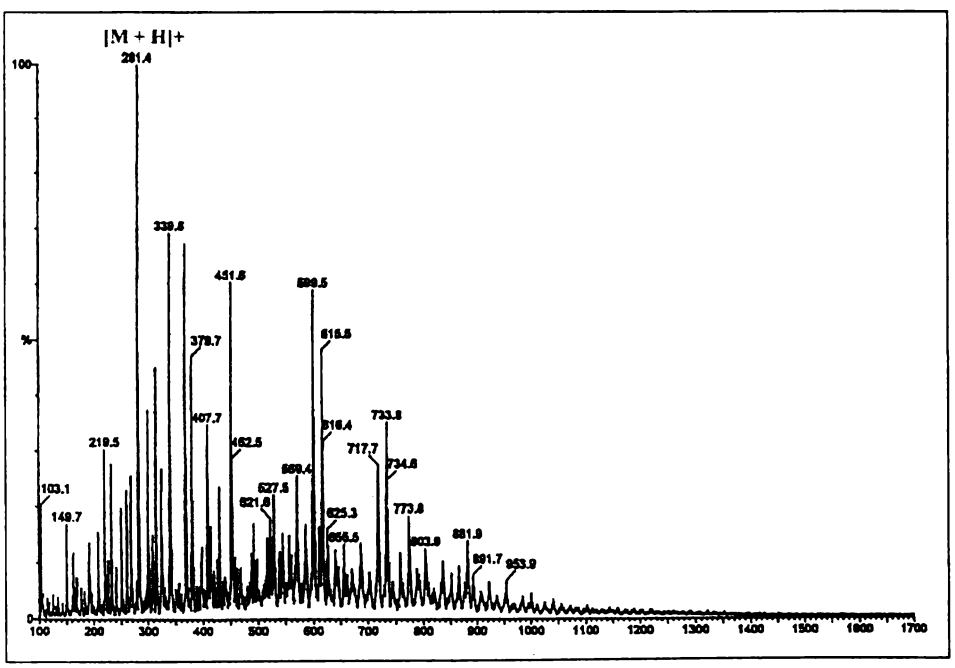

Figure 2.11. ESI/MS spectrum of the (M_2D^H + $CH_2{=}CHCH_2OH$) product mixture

A large number of peaks were also observed in the GC/MS chromatogram of the product mixture (Figure 2.12.a). The peaks observed at 3.2 and 4.5 minutes in the chromatogram of the starting material were also observed, although the siloxane compound eluting at 4.7 minutes in the starting material was no longer evident. The spectrum of the peak observed at 8.7 minutes revealed signals at *m/z* 221, 207, 191, 133, 103 and 73, and is tentatively assigned to **4**. These fragment ions can be assigned to $[\mathbf{4} - CH_2CH_2CH_2OH]^+$, $[\mathbf{4} - TMS]^+$, $[\mathbf{4} - OTMS]^+$, $[\mathbf{4} - 2TMS - H]^+$, $[\mathbf{4} - 2TMS - CH_2OH]^+$ and $[TMS]^+$, respectively (Figure 2.12.b).

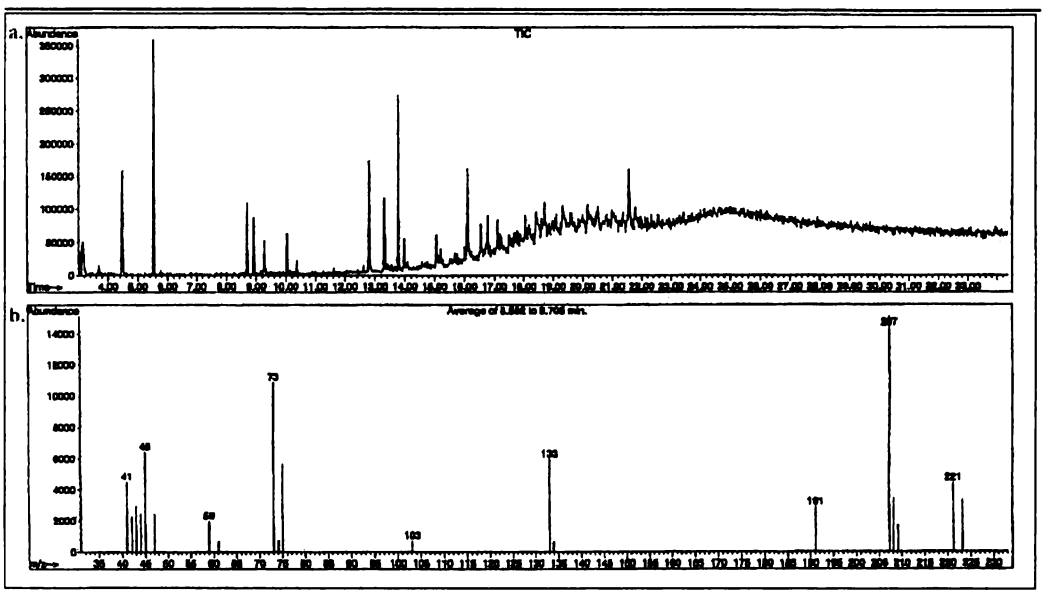

Figure 2.12. (M_2D^H + CH_2=$CHCH_2OH$) product mixture *a.* GC/MS chromatogram and *b.* spectrum of peak at 8.7 minutes

The other peaks in the chromatogram were unassigned although it was observed that the mass spectra were distinctive of siloxanes.

As discussed in Section 2.3.1.2, hydrosilylation of alkenes with alcohol groups in the structure can lead to side reactions between the hydroxyl group and the Si atom. Si-O-C linkages, which result from such unwanted side reactions, can lead to intermolecular cross-linking. Protection of the hydroxyl group, or use of the more reactive alkyne can be used to prevent this from occurring.[56]

Reaction of M_2D^H with the hydroxyl of $HOCH_2CH=CH_2$, as used in this experiment, would yield $[Si(CH_3)_3\text{-}O\text{-}]_2\text{-}Si(CH_3)\text{-}OCH_2CH=CH_2$, of molecular mass 278 a.m.u. Further reaction of this molecule with another molecule of M_2D^H would yield $[Si(CH_3)_3\text{-}O\text{-}]_2\text{-}Si(CH_3)\text{-}OCH_2CH_2CH_2O\text{-}Si(CH_3)[Si(CH_3)_3\text{-}O\text{-}]_2$, of

molecular mass 500 a.m.u. No corresponding molecular ion or adducts for either of these species were observed in the GC/MS or ESI/MS spectra, and thus these side reactions cannot be used to explain the complicated product mixture obtained.

The complicated product mixture prompted analysis of the M_2D^H (**3**) starting material. The GC/MS chromatogram revealed three peaks, eluting at 3.2, 4.5 and 4.7 minutes (Figure 2.13.a.). The first peak (3.2 minutes) gave a spectrum corresponding to the solvent toluene, the source of which was not investigated. The two later peaks gave spectra characteristic of siloxane compounds. Both spectra show ions at *m/z* 73 and 207. Assuming the *m/z* 207 ion is the $[M - CH_3]^+$ ion, characteristic of siloxanes, then the molecular mass of both compounds would be 222, the molecular mass of M_2D^H. Isomers of M_2D^H can be predicted by addressing the synthetic procedure used to generate such compounds.

M_2D^H is produced by condensation of $HOSiMe_3$ and $(HO)_2SiHMe$ (Equation 2.10) formed from the hydrolysis of $ClSiMe_3$ and Cl_2SiHMe, respectively (Equations 2.8 and 2.9).

$$ClSiMe_3 + H_2O \rightarrow HOSiMe_3 + HCl \quad (2.8)$$

$$Cl_2SiHMe + H_2O \rightarrow (HO)_2SiHMe + HCl \quad (2.9)$$

$$2[HOSiMe_3] + (HO)_2SiHMe \rightarrow M_2D^H + 2H_2O \quad (2.10)$$

These chlorosilane starting materials would be expected to contain analogous compounds with varying proportions of Me and Cl substituents, i.e. Cl_2SiMe_2 and $ClSiHMe_2$, according to the nature of the production process. These compounds will also undergo hydrolysis (Equations 2.11 and 2.12), and subsequent condensation of the products with $HOSiMe_3$ will yield M^HDM of molecular mass 222 (Equation 2.13).

$$Cl_2SiMe_2 + H_2O \rightarrow (HO)_2SiMe_2 + HCl \quad (2.11)$$

$$ClSiHMe_2 + H_2O \rightarrow HOSiHMe_2 + HCl \quad (2.12)$$

$$HOSiHMe_2 + (HO)_2SiHMe + HOSiMe_3 \rightarrow M^HDM + 2H_2O \quad (2.13)$$

Other condensation possibilities exist, i.e. $(M^H)_2D$, M_2D, $(M^H)_2D^H$ however the absence of corresponding peaks in the chromatogram indicate these by-products

have been removed in the purification process. It is likely that the similar nature of M_2D^H and M^HDM complicates purification, and thus both are observed in the M_2D^H product mixture.

The structures, although sharing the same molecular weight, give different retention times and EI/MS spectra, although these could not be assigned conclusively. The mass spectrum of the peak eluting at 4.5 minutes showed ions at *m/z* 73, 133, 191 and 207, whilst the peak eluting at 4.7 minutes (Figure 2.13.*b.*) showed ions at *m/z* 73, 193 and 207. The two differences in the two spectra are the ions at *m/z* 133, 191 and 193. The ions observed at *m/z* 73, 133 and 207 are assignable to $[SiMe_3]^+$, $[M - OTMS]^+$ and $[M - CH_3]^+$ respectively, and can be predicted for both M_2D^H and M^HDM. However, the *m/z* 133 ion was only observed in the spectrum from the 4.5 minute peak.

The *m/z* 193 fragment ion equates to the loss of CH_2CH_3 from the M = 222 a.m.u. parent molecule. A mechanism for the generation of this ion is proposed in Scheme 2.12

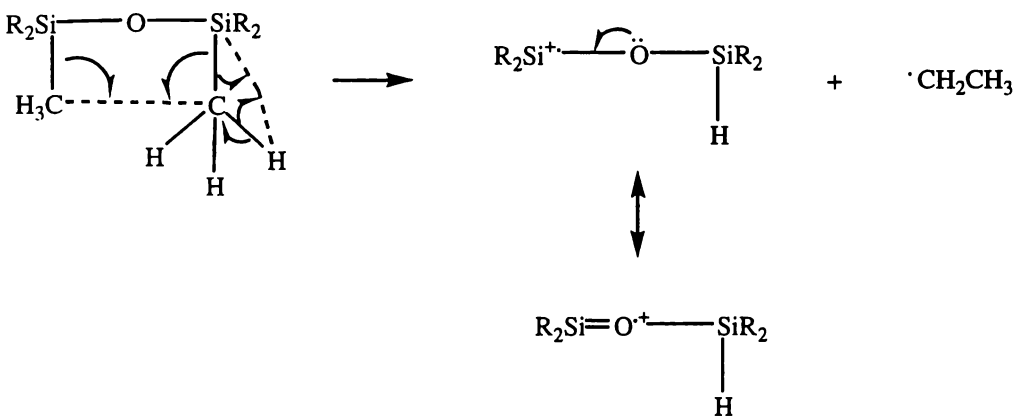

Scheme 2.12. Proposed mechanism for the generation of *m/z* 193 fragment ion from M^RD^RM

This mechanism can be applied to both M_2D^H and M^HDM, however the resulting ion (*m/z* 193) was only observed in spectrum from the 4.7 minute peak. No plausible fragmentation could be proposed to aid assignment of the *m/z* 191 ion.

Comparison with NIST Mass Spectral Library[†] results for M_2D^H showed a spectrum with fragment ions at *m/z* 73, 133, 207 and 221.* The small ion at *m/z* 221 corresponds to $[M - H]^+$. Reference spectra for M^HDM were not available.

[†] National Institute of Standards and Technology (NIST) Mass Spectral Search Program, Version 1.6d, 1998

From these results the M_2D^H (3) structure could not be unequivocally assigned, although results did demonstrate that the starting material contained two isomers of the compound.

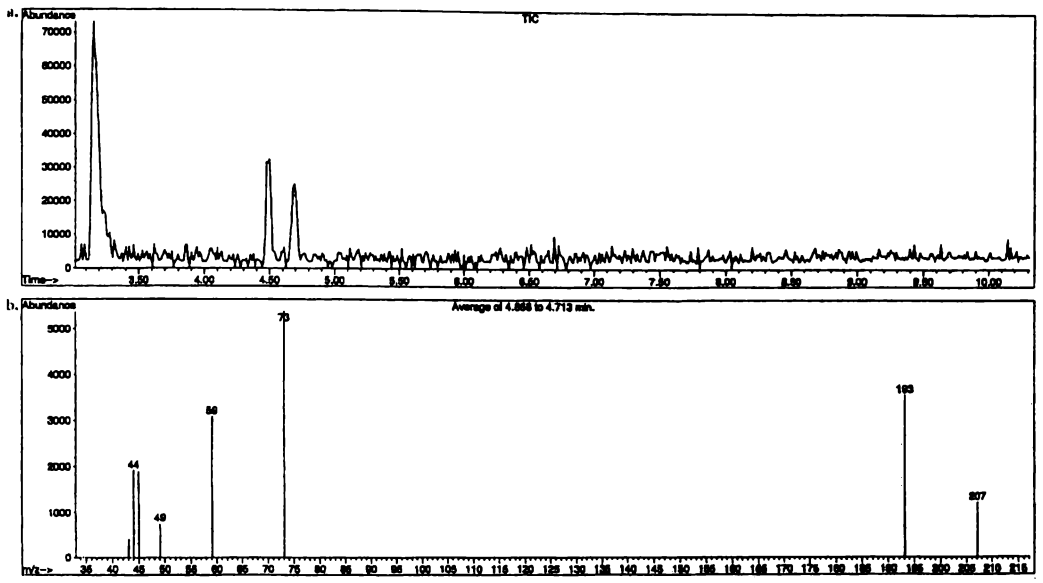

Figure 2.13. ***a.*** **GC/MS chromatogram and** ***b.*** **spectrum at 4.7 minutes of the M_2D^H starting material (3)**

2.3.2.5 Synthesis of M_2D-C_3-O-EO-$COCH_3$ (5)

M_2D-C_3-O-EO-$COCH_3$ was obtained by the reaction of M_2D-C_3-O-EO-H and acetyl chloride, in the presence of Et_3N base (Scheme 2.9). Addition of the base after the addition of the acetyl chloride gave a much higher mass yield (2.3.2.5.A, 76%, 4 hours; 2.3.2.5.B, 96%, 24 hours), although this reaction was left for longer. Due to the instability of the siloxanes to extremes of pH, a lower yield might have been expected from the longer reaction. An excess of base was used in both cases indicating that the product was relatively stable to Et_3N at these concentrations. An important influence on the stability of the product may be the absence of water, preventing hydrolysis from occurring, and the use of Et_3N which is a relatively weak organic base as compared with the stronger OH^- base which would catalyse hydrolysis.

GC/MS analysis showed the purity of the product mixtures to be very comparable (2.3.2.5.A, 96% purity, Figure 2.14.a; 2.3.2.5.B, 97% purity, Figure 2.15.a). The product was eluted at 15.7 min, with the largest ion in the

---

* NIST MS #: 104190, Seq. #: M84726

corresponding EI/MS spectrum (Figure 2.15.b) at *m/z* 323, corresponding to loss of the acetyl group from the M_2D-C_3-O-EO-$COCH_3$ (**5**) product (i.e. [**5** - $COCH_3$]$^+$). The EI/MS spectrum showed additional fragment ions at *m/z*, 221, 207, 191, 177, 161, 147, 133, 119 and 117. The *m/z* 221 ion corresponding to [**5** – (C_3-O-EO-$COCH_3$)]$^+$ and the *m/z* 207 ion to either of the rearranged products [**5** – (C_3-O-EO-$COCH_3$) – CH_3 + H]$^+$ or [**5** – (EO-$COCH_3$) – TMS + H]$^+$. The *m/z* 191 ion can be formed by loss of O from the latter *m/z* 207 species, to give [**5** – (EO-$COCH_3$) – OTMS + H]$^+$, thus supporting the [**5** – (EO-$COCH_3$) – TMS + H]$^+$ assignment for the *m/z* 207 ion. Subsequent loss of a methylene group by rearrangement of a methyl group will yield the *m/z* 177 [**5** – (EO-$COCH_3$) – OTMS – CH_2 + H]$^+$ ion, and further loss of O will yield [**5** – (O-EO-$COCH_3$) – OTMS – CH_2 + H]$^+$ (*m/z* 161). Confirmation of the propyl group is observed by successive loss of methylene groups from the *m/z* 161 ion yielding *m/z* 147 [**5** – (CH_2O-EO-$COCH_3$) – OTMS – CH_2 + H]$^+$, *m/z* 133 [**5** – (CH_2CH_2O-EO-$COCH_3$) – OTMS – CH_2 + H]$^+$ and *m/z* 119 [**5** – ($CH_2CH_2CH_2$O-EO-$COCH_3$) – OTMS – CH_2 + H]$^+$ species. The ion at *m/z* 133 also corresponds to the [**5** – (EO-$COCH_3$) – 2TMS]$^+$ structure. The ion at *m/z* 117 corresponds to loss of O from the *m/z* 133 ion and is possible for either assignment. Additional ions were observed at *m/z*, 281, 265, 87 and 73. The *m/z* 73 is the characteristic [TMS]$^+$ ion, and the ions at *m/z* 281, 265 and 87 are unassigned.

A minor impurity, eluting at 15.3 minutes was observed in the GC chromatograms of both 2.3.2.5 product mixtures. The MS spectrum is shown in Figure 2.14.*b.* and shows characteristic siloxane ion fragments. An additional impurity, with a spectrum characteristic of a siloxane compound, eluted at 18.7 minutes in the GC chromatogram of the 2.3.2.5.A product mixture, although was absent in the corresponding 2.3.2.5.B GC analysis.

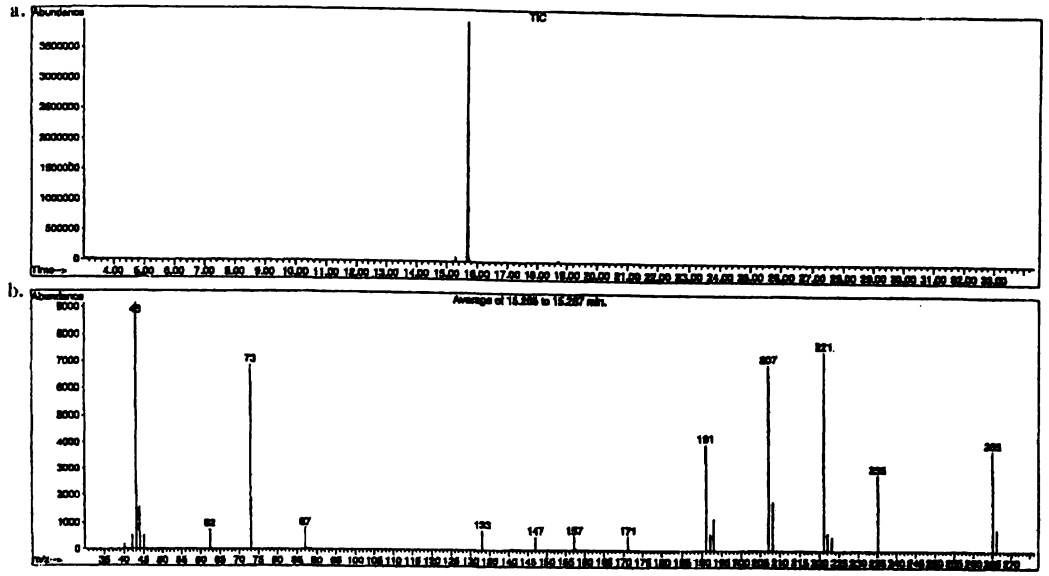

Figure 2.14. *a.* **GC/MS chromatogram of 2.3.2.5.A product mixture** *b.* **GC/MS spectrum of common impurity in 2.3.2.5 product mixture (elution time 15.3 minutes)**

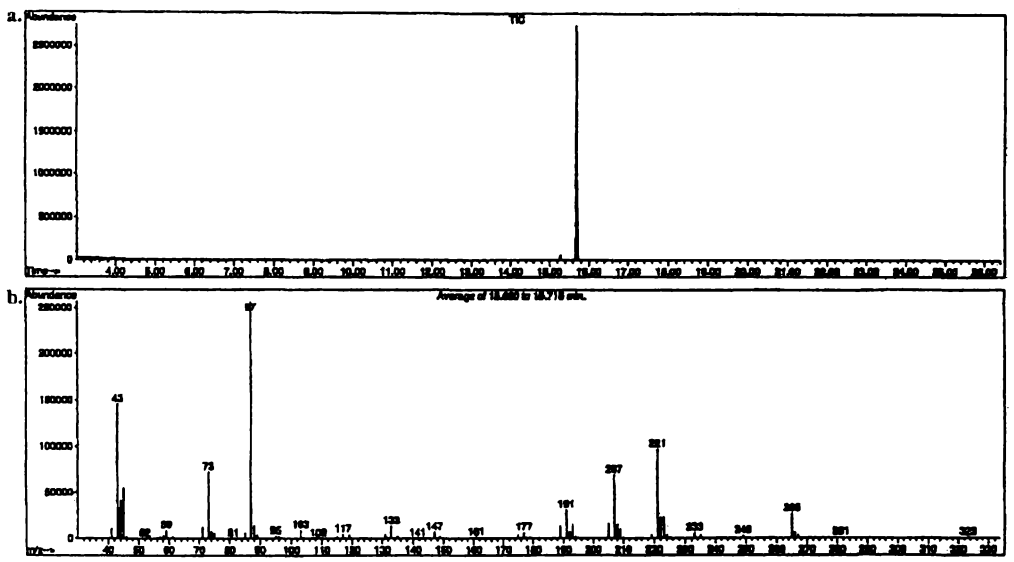

Figure 2.15. *a.* **GC/MS chromatogram of 2.3.2.5.B product mixture** *b.* **GC/MS spectrum of M_2D-C_3-O-EO-$COCH_3$ in 2.3.2.5 product mixture (elution time 15.7 minutes)**

Overall, according to the GC/MS results, addition of the base after the addition of the acetyl chloride (2.3.2.5.B) gave the most favourable results, with higher yield and purity, and less by-products obtained. In contrast to the GC/MS results, analysis by ESI/MS showed a cleaner spectrum for the 2.3.2.5.A preparation, with all impurities at less than 10% (BPI). The major impurity (*m/z* 618) in the 2.3.2.5.B product mixture was at 35% intensity.

2.5 CONCLUSION

The commercial product Silwet L-77 was demonstrated to comprise of ~70% M_2D-C_3-O-$(EO)_n$-Me, ~5% M_2D-C_3-O-$(EO)_n$-H and ~25% polar constituents, in addition to a small proportion of the tetrasiloxane linear dimer, **6**. The polar material in the Silwet L-77 formulation is determined to comprise of $MD(M^{OH})$-O-$(EO)_n$-$CH_2CH{=}CH_2$, the tetrasiloxane linear dimer, **12**, the free monomethyl polyethoxylates, $CH_3O(EO)_nH$, and uncapped-polyethylene glycol, $HO(EO)_nH$.

M_2D-C_3-O-$(EO)_n$-Me oligomers were successfully isolated by RP C_{18} chromatography of Silwet L-77, however this proved to be a highly laborious process yielding only small amounts of the compounds. Synthetic procedures were investigated and were found to be a more efficient method for obtaining these compounds. Pure M_2D-C_3-O-$(EO)_n$-Me oligomers (n = 3, 6 and 9) were synthesised by reaction of the corresponding allyl-capped oligoethoxylate monomethyl ether with M_2D^H over a Pt catalyst. The allyl-capped ethoxylate monomethyl ethers were synthesised by reaction of allyl chloride with the corresponding ethoxylate monomethyl ethers (n = 3, 6 and 9). The longer chained oligoethylene glycols (n = 6 and 9) were prepared by etherification of smaller oligomers. Synthesis of M_2D-C_3-O-EO-$COCH_3$ was achieved by acetylation of M_2D-C_3-O-EO-H, and preliminary investigations into the preparation of M_2D-C_3-OH are also described.

2.6 REFERENCES

[1] T.C. Kendrick, B. Parbhoo, J.W. White, *The Silicon – Heteroatom Bond*, Eds. S. Patai, Z. Rappoport, John Wiley and Sons Ltd, 1991, Chapter 3, 67-150

[2] C.A. Pearce, *Silicon Chemistry and Applications*, The Chemical Society, 1972

[3] L.H. Sommer, *Stereochemistry, Mechanism and Silicon*, McGraw-Hill Inc., 1965

[4] M.G. Voronkov, V.P. Milesshkevich, Y.A. Yuzhelevskii, *The Siloxane Bond: Physical Properties and Chemical Transformations*, Consultants Bureau, New York, 1978

[5] R. Janoschek, *Organosilicon Chemistry: From Molecules to Materials*, Eds. N. Auner, J. Weis, VCH, 1994, 81-86

[6] R. Müller, *D. R. (Germany) Patent*, 1942, 5348

[7] E.G. Rochow, *U.S. Patent*, 1941, 2380995

[8] J.L. Speier, J.A. Webster, G.H. Barnes, *J. Am. Chem. Soc.*, 1957, **79**, 974

[9] A.J. Chalk, J.F. Harrod, *J. Am. Chem. Soc.*, 1965, **87**, 16-21

[10] A.M. Lapointe, F.C. Rix, M. Brookhart, *J. Am. Chem. Soc.*, 1997, **119**, 906-917

[11] H.D. Zhu, S.W. Kantor, W.J. MacKnight, *Macromol.*, 1998, **31**, 850-856

[12] R.A. Mantz, P.F. Jones, K.P. Chaffee, J.D. Lichtenhan, J.W. Gilman, I.M. Ismail, M.J. Burmeister, *Chem. Mater.*, 1996, **8**, 1250-1259

[13] K. Kabeta, K. Shuto, S. Sugi, T. Imai, *Polymer*,1996, **37**, 4327-4331

[14] H. Marsmann, *NMR – Basic Principles and Progress*, Ed. P. Diehl, E. Fluck, R. Kosfeld, 1981, Springer-Verlag, Berlin, Vol. 17: Oxygen-17 and Silicon-29, 65-235

[15] R.K. Harris, J.D. Kennedy, W. McFarlane, *NMR and the Periodic Table*, Ed. R.K. Harris, B.E. Main, Academic Press, 1978, Chapter 10, 309-377

[16] E. A. Williams, *Annual Reports on NMR Spectroscopy*, Academic Press, London, 1983, Vol. 15, 235-289

[17] G. Engelhardt, H. Jancke, M. Magi, T. Pehk, E. Lippmaa, *J. Organometal. Chem.*, 1971, **28**, 293-300

[18] R.B. Taylor, B. Parbhoo, D.M. Fillmore, *The Analytical Chemistry of Silicones*, Ed. A. Lee Smith, John Wiley and Sons Ltd, 1991, Chapter 12, 347-419

[19] J.C. Carpenter, J.A. Cella, S.B. Dorn, *Environ. Sci. Technol.*, 1995, **29**, 864-868

[20] N.J. Fendinger, D.C. McAvoy, W.S. Eckhoff, B.B. Price, *Environ. Sci. Technol.*, 1997, **31**, 1555-1563

[21] U. Just, F. Mellor, F. Keidel, *J. Chromatog. A.*, 1994, **683**, 105-113

[22] A. Ballistreri, D. Garozzo, G. Montaudo, *Macromol.*, 1984, **17**, 1312-1315

[23] H. Zhuang, J.A. Gardella, D.M. Hercules, *Macromol.*, 1997, **30**, 1153-1157

[24] X. Tang, P.A. Dreifuss, A. Vertes, *Rapid Commun. Mass Spectrom.*, 1995, **9**, 1141-1147

[25] A.M. Belu, J.M. DeSimone, R.W. Linton, G.W. Lange, R.M. Friedman, *J. Am. Soc Mass Spectrom.*, 1996, **7**, 11-24

[26] G. Montaudo, M.S. Montaudo, C. Puglisi, F. Samperi, *Int. J. Poly. Anal. Charact.*, 1997, **3**, 177-192

[27] U. Just, R.P. Krüger, *Organosilicon Chemistry II: From Molecules to Materials*, Eds. N. Auner, J. Weis, VCH, 1996, 625-632

[28] E.C. Tuazon, S.M. Aschmann, R. Atkinson, *Environ. Sci. Tech.*, 2000, **34**, 1970-1976

[29] I. Kudaka, Y. Katsuno, Y. Furukawa, A. Okamoto, K. Hiraoka, *J. Mass Spectrom. Soc. Jpn.*, 1997, **45**, 591-602

[30] T. Kemmitt, W. Henderson, *J. Chem. Soc., Perkin Trans. 1*, 1997, 729-739

[31] T. Kemmitt, W. Henderson, *Aust. J. Chem.*, 1998, **51**, 1031-1035

[32] U. Siemeling, *Polyhedron*, 1997, **16**, 1513-1516

[33] L.K. Frevel, W. Lee, R.E. Tecklenburg, *J. Am. Soc. Mass Spectrom.*, 1999, **10**, 231-240

[34] *a.* J. Barker, *Mass Spectrometry, ACOL*, 2nd Ed., Wiley, UK, 1999; *b.* Bruker Almanac 1994

[35] R.M. Smith, *Understanding Mass Spectra*, Tech. Ed. K.L. Busch, Wiley, NY, 1999

[36] G.L.F.Schmidt, *Industrial Applications of Surfactants*, Ed. D.R. Karsa, The Royal Society of Chemistry, London, 1987, 24-32

[37] G.A. Policello, P.J.G. Stevens, R.E. Gaskin, B.H. Rohitha, G.F. McLaren, *Proc. 4th Int. Symp. Adj. for Agrochem.*, 1995, FRI Bulletin No. 193, 303-307

[38] M. Knoche, *Weed. Res.*, 1994, **34**, 221-239

[39] L.L. Jansen, *Weed Sci.*, 1973, 21, 130-135

[40] P.J.G. Stevens, *Pestic. Sci*, 1993, **38**, 103-122

[41] G.A. Policello, P.J. Stevens, W.A. Forster, G.J. Murphy, *Pesticide Formulations and Application Systems*, Eds. F.R. Hall, P.D. Berger, H.M. Collins, ASTM publishers, 1995, Vol. 14, p 313-317

[42] R.E. Gaskin, *Proc. 4th Int. Symp. on Adjuvants for Agrochemicals*, NZ FRI Bulletin No. 193, Ed. R.E. Gaskin, Melbourne, 1995, 243-248

[43] J. Sun, C.L. Foy, *Proc. 4th Int. Symp. on Adjuvants for Agrochemicals*, NZ FRI Bulletin No. 193, Ed. R.E. Gaskin, Melbourne, 1995, 225-230

[44] *a.* F.C. Roggenbuck, D. Penner, R.F. Burow, B. Thomas, *Pestic. Sci.*, 1993, **37**, 121-125; *b.* F.C. Roggenbuck, L. Rowe, D. Penner, L. Petroff, R. Burow, *Weed Technol.*, 1990, **4**, 576-580; *c.* J.A. Zabkiewicz, W.A. Forster, K.D. Steele, Z.Q. Liu, *Proc. 4th Int. Symp. on Adjuvants for Agrochemicals* , NZ FRI Bulletin No. 193, Ed. R.E. Gaskin, 1995, 219-224

[45] J. Schönherr, M.J. Bukovac, *Plant Physiol.*, 1972, **49**, 813-819

[46] D.L. Bailey, N.Y. Snyder, *U.S. Patent*, 1967, 3 299 112

[47] Personal correspondence, George Policello, 28/4/00, Witco Corporation, Organosilicones Group, Tarrytown, NY.

[48] K.D. Klein, S. Wilkowski, J. Selby, *Proc. 4th Int. Symp. Adj. for Agrochem.*, 1995, FRI Bulletin No. 193, 27-31

[49] K.D. Klein, W. Knott, G. Koerner, *Organosilicon Chemistry II: From Molecules to Materials*, Eds. N. Auner, J. Weis, VCH, 1996, 613-618

[50] K.D. Klein, D. Schaefer, P. Lersch, *Tenside Surf. Det.*, 1994, **31**, 115-119

[51] A.R.L. Colas, F.A.D. Renauld, G.C. Sawicki, *GB Patent*, 1988, 8 819 567

[52] G. Feldmann-Krane, W. Hoehner, D. Schaefer, S.S. Dietmar, *DE Patent*, 1993, 4 317 605

[53] M. Knoche, H. Tamura, M.J. Bukovac, *J. Agric. Food Chem.*, 1991, **39**, 202-206

[54] C. G. Krespan, *J. Org. Chem.*, 1974, **39**, 2351-2355.

[55] R. Wagner, Y. Wu, G. Czichocki, H.V. Berlepsch, B. Weiland, F. Rexin, L. Perepelittchenko, *Appl. Organometal. Chem.*, 1999, **13**, 611-620.

[56] C.J. Herzig, *Organosilicon Chemistry: From Molecules to Materials*, Eds. N. Auner, J. Weis, VCH, 1994, p 253-260

CHAPTER 3

Characterisation of Organosilicone Surfactants by API/MS

3.1 INTRODUCTION

As a technique for agrochemical analyses, API/MS is extremely attractive, with relatively little sample preparation required, and detection possible to very low levels. It is also potentially possible to analyse both the active ingredient and the surfactant from the same sample, eliminating the need for radio-tracers and parallel trials, and further enhancing its applicability to environmental samples.

The application of API/MS methods to the analysis of pesticides and herbicides in environmental samples has become widely accepted, with many reports by APcI/MS,[1a-h] standard ESI/MS[2a-c] and high-flow pneumatically assisted ESI/MS[3a-d] methods.

API/MS methods, especially those combined with online separation techniques are advantageous over conventional techniques for the analysis of surfactants in many respects. The conventional techniques for analysis of these compounds, such as potentiometric or colorimetric methods, GC/MS and HPLC, are often laborious, and are of lower sensitivity. Potentiometric and colorimetric methods are further disadvantaged in that they are non-selective, and prone to interferences. GC/MS is often hindered by low analyte volatility, and UV detection by the lack of chromophores in many of these compounds, rendering sample derivatisation necessary for analysis by these methods. The conventional methods for HPLC detection are also disadvantaged in their non-specificity. Analysis by API/MS offers increased sensitivity and selectivity and a minimisation of the sample preparation required, through removal of the need for sample derivatisation prior to detection.

3.1.1 Analysis of surfactants by API/MS

Surface active compounds give very high responses with ESI. Surface activity influences the ability of a compound to be detected by API/MS as it has been observed that the species found in the offspring droplets, and thus those ultimately transferred into the gas phase for detection, are those that reside on the surface of the parent droplet (Section 1.2.1).[4,5]

API/MS methods have been successively applied to the analysis of ionic and non-ionic surfactants. The detection of non-ionic surfactants by API/MS is achieved by virtue of the ability of these compounds to complex with low level inorganic cations (e.g. H^+, NH_4^+, Na^+ and K^+) inherently present in the solvent matrix. Several qualitative[6a-d] and quantitative[7a-d] ESI/MS and qualitative[6c,8,9] and quantitative[10a-c] APcI/MS studies have been reported. A comprehensive review of the applications of LC-MS to the analysis of surfactants in water samples has also recently been published.[11]

3.1.2 Collision induced dissociation (CID)

The use of collision induced dissociation to provide structurally informative fragments by API/MS has been described.[7b] This can be achieved by increasing the potential between the sample and skimmer cones in appropriate MS instruments, thereby yielding spectra resembling those obtained with $(MS)^n$ techniques. CID fragmentation has been observed for some surfactants by API/MS, but only for protonated species and only for branched alcohol ethoxylates.[6b,12] Similar results were obtained for PEGs analysed by FAB-MS/MS.[13] Under the low CID conditions (~ 50 eV) employed, fragmentation was readily observed for protonated adducts, but little fragmentation was observed for Na^+ or K^+ attachment ions. The CID in these cases mainly yielded the free cation. Under high energy CID conditions (~ 20 000 eV) however, fragmentation was observed for both $[M + H]^+$ and $[M + X]^+$, X = Na^+ and K^+ ions, with linear and cyclic PEG derivatives.[14] The use of xenon as the collision gas was also reported to increase the CID efficiency of $[M + Na]^+$ ions.[13]

3.1.3 Chapter objectives

The objective of this chapter was to fully characterise the organosilicone surfactant, Silwet L-77 by various API/MS methods. The requirements were to establish and optimise standard operating conditions for the analysis of Silwet L-77 by:

1. Standard ESI/MS
2. Megaflow ESI/MS
3. APcI/MS
4. ESI and APcI coupled with FTICR/MS detection

Standard ESI/MS was used to determine the validity of API/MS methods to the analysis of the compound. Investigations were then extended to megaflow ESI/MS and APcI/MS methods, which operate at flow-rates more appropriate to routine analyses. FTICR was applied to samples of Silwet L-77 with the aim of obtaining the further structural information from high resolution data, CID, gas-phase reactions and internal electron impact (IEI) methods.

3.2 MATERIALS AND METHODS

Sample preparation

A preparation solvent of 1:1 MeOH/H_2O was used for all solutions, unless otherwise stated. This preparation solvent was selected on the basis that it is the solvent used to wash-off leaf-applied samples, and thus would be compatible with application samples to be subsequently analysed (See Chapter 5). Stock solutions (1000 ppm w/v) of the surfactants were prepared by dilution of 0.1 g in 0.1 L with 1:1 MeOH/H_2O. Further solutions were prepared by serial dilution. All solutions were prepared fresh daily. $CH_3CO_2NH_4$ solutions were prepared at 1 mM concentration. The optimisation of operating parameters was performed with Silwet L-77 at a concentration of 1 ppm for the ESI/MS methods, and at 10 ppm for APcI/MS, unless otherwise stated.

API/MS analysis

All sample injections were single pulse injections of 10 µL. Optimal operating parameters were established in either MCA (multi-channel acquisition) or continuum modes. In the MCA mode, a number of scans are acquired and the final spectrum obtained is the average of these. The BPI (base peak intensity), i.e. the intensity (peak height) of the largest peak, can be used to determine ideal operating conditions. In the continuum mode, a plot of total ion current over time is obtained. Quantitative information can be obtained from integration of the peak area in the resulting "chromatogram". For megaflow ESI/MS determinations, the optimal values for scan time and inter-scan time were established using the peak heights in MCA mode. All other optimal conditions were established by the peak area method. In the APcI/MS determinations, data obtained in MCA mode were

the averaged result of five scans, whilst in the other modes varying scan numbers were acquired, with consistency within each determination ensured.

Total Ion Current (TIC) measurements were scanned over the range of *m/z* 350 – 1000 and *m/z* 300 – 1000 for the ESI/MS and APcI/MS methods, respectively. For Selected Ion (SIR) measurements (a.k.a. SIM), the adducts to be selected were first determined by analysis of full scan spectra taken in MCA mode. Either all the possible adducts, i.e. the NH_4^+, Na^+ and K^+ adducts, or selected adducts (where extreme dominance was observed) of the oligomer of interest were selected. An excess of salt was added where indicated, to minimise formation of other adducts. In the megaflow ESI/MS determinations, an excess of ammonium acetate salt was added to control adduct formation, and thus for selected ion measurements, only the NH_4^+ adducts were selected.

The optimised parameter values were adopted for all subsequent measurements, once established, unless otherwise stated.

3.2.1 Standard ESI/MS

The default operating conditions initially adopted for each experiment were as outlined in Table 3.1 below.

Table 3.1. Default operating conditions for standard ESI/MS analysis

Parameter	Value
Mode	Positive
Cone Voltage	60V
Scan Time (*m/z* 300-1000)	5.0 seconds
Inter-Scan Time	0.1 seconds
Dwell Time	1.0 second
Inter-Channel Delay	0.01 seconds
Span	1 a.m.u.
Source Temperature	60°C
Drying Gas Flow Rate	250 L h^{-1}
Nebulizing Gas Flow Rate	15 L h^{-1}
Capillary/Corona Voltage	3.5 kV
Skimmer Lens Offset	5 V
High Voltage (HV) Lens*	0.5 kV
Resolution	12.0
Multiplier	650
Ion Energy	2.0 V
Ion Energy Ramp	0
Cone Voltage Ramp	0
Prep. Solvent Composition	1:1 MeOH/H_2O
Elution Solvent Composition	2:1 MeOH/H_2O
Solvent Flow-Rate	0.02 mL min^{-1}

* also referred to as the counter electrode

3.2.2 Megaflow ESI/MS

The initial operating conditions adopted for each experiment were the optimal values established for standard ESI/MS (Table 3.12).

3.2.3 APcI/MS

The initial operating conditions adopted for each parameter are listed in Table 3.2.

Table 3.2. Initial operating conditions for APcI/MS analysis

Parameter	MCA (TIC)	SIR Continuum
Cone Voltage - 10 ppm	40 V	-
Scan Time (*m/z* 300-1000)	2.0 seconds	N/A
Inter-Scan Time	0.1 seconds	N/A
Dwell Time (2 Channels)	N/A	0.30 seconds
Inter-Channel Delay (2 Channels)	N/A	0.05 seconds
Span (2 Channels)	N/A	1 a.m.u.
Probe Temperature	400 °C	-
Source Temperature	150 °C	-
Drying Gas Flow Rate	-	225 L h^{-1}
Sheath Gas Flow Rate	-	75 L h^{-1}
Corona Voltage	3.2 kV	-
Skimmer Lens Offset	6.0 V	-
HV Lens	0.0 kV	-
Multiplier	650	-
Ion Energy	2.0 V	-
Elution Solvent Composition	-	2:1 MeOH/H_2O
Solvent Flow-Rate	-	1 mL min^{-1}

3.2.4 FTICR/MS

3.2.4.1 Sustained offline resonance irradiation CID of M_2D-C_3-O-$(EO)_n$-Me

Sustained offline resonance irradiation (SORI) CID of M_2D-C_3-O-$(EO)_n$-Me oligomers, isolated from the Silwet L-77 mixture in the MS, was investigated. The ions at *m/z* 625 [M_2D-C_3-O-$(EO)_7$-Me, Na^+ adduct], *m/z* 581 [M_2D-C_3-O-$(EO)_6$-Me, Na^+ adduct] and *m/z* 801 [M_2D-C_3-O-$(EO)_{11}$-Me, Na^+ adduct] were selected and CID with air and argon investigated. SORI-CID of the *m/z* 581 ion was investigated by two methods, varying in the order of activation and gas introduction in order to confirm the observed results. Following ejection of all ions other than the ion at *m/z* 581 from the source, the ion was activated and then the gas (air and argon) introduced. In the second method the collision gas was introduced prior to activation of the ion.

3.2.4.2 Internal electron ionisation (IEI) analysis of Silwet L-77

Silwet L-77 (gas phase) was introduced to the source via the leak inlet by applying a vacuum of 2.0 x 10^{-9} mBar to the liquid sample. An internal ionisation energy of 70 eV was applied to the sample in the source. Two IEI spectra were acquired.

3.3 RESULTS AND DISCUSSION

The effect of various parameters, including instrument settings and sample, solvent and matrix composition, on the resulting response of Silwet L-77 by the API/MS methods was investigated. Ideal conditions for analysis by standard ESI/MS, megaflow ESI/MS and APcI/MS were determined and are summarised in Tables 3.3, 3.13 and 3.14, respectively. Ideal settings are defined as those which gave highest responses and/or lowest standard deviations.

The degree to which variations in each parameter affected the relative response obtained is also discussed. A parameter is defined as having a high effect on response when the values within that experiment show maximal variation in intensity of greater than 25%. An intermediate effect on the response is defined as a variation of 10 % - 25 %, and a low effect on the response is defined as a variation of less than 10 %.

The ideal values established are tabulated at the end of each section. Only those parameters for which some discussion was required to rationalise the results obtained are included separately.

3.3.1 Standard ESI/MS method development

Of the instrument settings investigated, the parameters which had the most significant effect on response included ion mode, capillary voltage, cone voltage, source temperature, drying gas flow-rate and the multiplier setting. Skimmer lens offset, HV lens, resolution, scan time, dwell time, and span settings had an intermediate effect on the response, whilst inter-scan time, inter-channel delay and ion energy settings showed low influence.

INSTRUMENT SETTINGS

3.3.1.1 Positive vs negative ion mode

Analysis of Silwet L-77 in positive ion mode gave good response down to concentrations of 10 ppb. The ability of polyethers to chelate NH_4^+ and alkali-metal cations enables the analysis of polyether-containing nonionic surfactants, such as Silwet L-77, by API/MS methods. Ionisation in the negative ion mode was negligible at all concentrations analysed, as Silwet L-77 has no sites capable of adducting with anions, nor has any moieties capable of cleavage to yield anionic species.

3.3.1.2 Total ion current (TIC) mode vs selected ion recording (SIR) mode

Sensitivity and selectivity was much improved with SIR-mode acquisitions over TIC measurements. This is consistent with other literature results, for which a sensitivity of 5 times greater was reported for the SIR mode analysis as compared with the TIC mode using corresponding extracted ion chromatograms.[7c] The potential for Silwet L-77 oligomers to form a number of adducts however, may complicate ion selection in SIR-mode acquisitions. Higher responses were observed with larger number of ions selected, but in general a concomitant increase in standard deviation was also observed. In practical terms, i.e. for routine analyses, SIR mode acquisitions are also favourable as the data file size is also appreciably less. The effect of matrix interference is also reduced by analysis in the SIR mode although information regarding the entire sample composition is lost.

3.3.1.3 Cone voltage (CV)

The ideal cone voltages for Silwet L-77 are relatively high, at 40 V and over for all concentrations and methods investigated, indicating a high stability for the adduct complexes.

I. By base peak intensity (BPI) in multi-channel acquisition (MCA) mode

A small mass discrimination with changing CV is observed in analysis by API/MS, such that in general smaller molecules ionise better with lower cone voltages. In the analysis of Silwet L-77, an increase in CV lead to an increase in the MW of the ion showing the largest BPI as demonstrated in Figure 3.1.

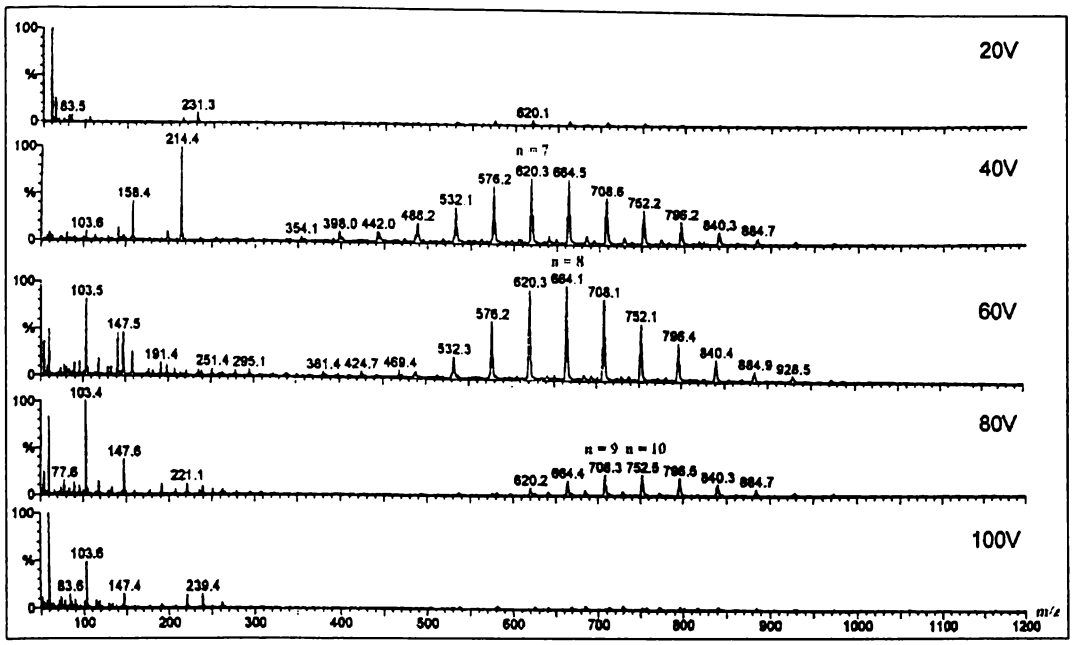

Figure 3.1. ESI/MS spectra of Silwet L-77 at varying cone voltages (20, 40, 60, 80 and 100 V)

The ideal cone voltage generally decreased with increasing concentration (Table 3.3). It was noted however that, the ideal cone voltage was always observed however, at a value for which the $(EO)_7$ oligomer was dominant. In the Silwet L-77 mixture, this oligomer is of highest concentration, so it follows that a CV that enhances this oligomer most will lead to the highest BPI.

Table 3.3. Ideal cone voltages for different concentrations of Silwet L-77 by peak height

[Silwet L-77] (ppm)	Ideal Cone Voltage
0.1	60V
1.0	60V
10.0	50V
100.0	40V

II. By peak area in TIC continuum mode at constant concentration (1 ppm)

In continuum mode the largest responses were observed at a cone voltage of 50V, in both full scan mode and selected ion recordings (Table 3.4). This is in contrast to the 60V value obtained in the previous investigation by BPI.

Table 3.4. Ideal cone voltages for different concentrations of Silwet L-77 by peak area

Cone Voltage	50V	60V	70V	80V	60V-80V[a]	50V	60V	70V	80V
Mode	TIC [b]	TIC	TIC	TIC	TIC	SIR [c]	SIR	SIR	SIR
Absolute Response [d]	8.3	7.7	6.9	4. 4	5.8	3.9	3.1	3.49	1.8
SD	0.2	0.3	0.4	0.1	0.2	0.2	0.1	0.02	0.1
CV	2.6%	4.1%	6.6%	2.6%	4.3%	4.3%	3.7%	0.6%	6.5%
Relative Response	1.00	0.92	0.83	0.52	0.69	1.00	0.79	0.89	0.47

[a] Cone ramp; [b] *m/z* range of 350 – 1000; [c] Four channels (ions) selected, corresponding to the NH_4^+ and K^+ adducts of the $(EO)_n$, n = 7 & 8 oligomers; [d] Average of four analyses, TIC values x 10^7, SIR values x 10^5

III. By peak area in TIC continuum mode for a concentration series

Four concentrations (0.1, 1, 10, 100 ppm) of surfactant were injected successively, each in duplicate. Cone voltages of 40, 50, 60 and 90 V, and a cone ramp of 40 – 60 V were investigated.

Cone voltage settings of 90 V and 40 V gave the lowest sensitivities. Highest sensitivity was observed with the cone voltage settings of 50 V and the 40 – 60 V cone ramp. Linearity was best with a cone voltage of 60 V, although the gradient of the regression fit was small.

IV. Collision Induced Dissociation

Increasing the cone voltage did not yield any fragment ions for Silwet L-77 by API/MS. It has been reported that, in general, structurally significant ions are not generated by CID when the parent ion of interest is an alkali-cation adduct, as compared with a proton adduct.[12] CID fragmentation has only been reported for branched, or secondary, alcohol ethoxylate (SAE) surfactants, non-ionic surfactants where the polyethoxylate chain is attached to a secondary carbon.[6b,12] In the first study, the fragmentation was achieved at 30 V, whilst the parent $[M + H]^+$ adduct ions were observed at 20 V.[12] In the second study, the $[M + H]^+$ parent adduct ions were observed at 40 V, with fragments observed at 55 V and 85 V.[6b] These CV values are low as compared with those used to analyse the Silwet L-77, and intact M_2D-C_3-O-$(EO)_n$-Me molecules are still observed at the fragmentation cone voltages mentioned. The authors reported that CID of primary alcohol ethoxylates (PAE) and nonylphenol ethoxylates (NPE) under these same conditions (55 V and 85 V) was also not achieved.[6b]

The fragments observed in the first study are ions produced by bond cleavage,[12] of the type produced by EI, and thus appear to be real CID products. The reported products of the CID in the second study were of the type $[HO(CH_2CH_2O)_xH + H]^+$ i.e. were protonated adducts of neutral PEG compounds,[6b] which are somewhat inconsistent with expected structures for CID. Although not addressed by the authors it is possible that these are synthetic by-products within the formulation, rather than products of CID. The change in cone voltage may simply have altered the ratio of ionised components reaching the detector, as determined by the relative basicity of the nonionic compounds present. In support of the assignment by the authors these analytes might however therefore have also been expected under the same conditions for the PAE and NPE samples also analysed – and no such ions were observed. Furthermore the products of the CID of SAE were analogous to those obtained from photocatalytic (TiO_2) decomposition. Two explanations for the preferential observation of CID of SAE are the stabilisation of the resulting (cation/radical) fragments by the secondary carbon and an observed preference for protonation at the oxygen adjacent to the secondary carbon, as determined by modelling calculations.[6b]

The authors reporting the successful CID of SAE also reported a concomitant increase in the relative intensities of the $[M + Na]^+$ and $[M + K]^+$ ions, which was interpreted as suggesting a lower susceptibility to fragmentation for these ions. Alternatively, this could simply be a result of a stronger affinity for alkali-metal cations over protons, causing a change in the relative ratios of the pseudo-molecular ions. At higher cone voltages, more intense cation adducts are observed, with a concomitant reduction in the proton adducts. An increase in the ion molecular collisions may be causing a dissociation of the less stable adduct complexes, thereby precluding detection of $[M + H]^+$ species. Signal weakening for fragment ions was observed with increases in the relative proportions of the $[M + NH_4]^+$, $[M + Na]^+$ and $[M + K]^+$ adducts, as a result of decreasing acid concentration,[12] confirming resistance of cationised molecules to CID.

The CID of Silwet L-408 was thus also investigated, as $[M + H]^+$ adducts of parent ions, although minor, were observed. The ability of Silwet L-408 to form H^+ adducts is attributed to the basic -OH terminal group, also present in NPEs and AEs. The use of acidified solvents to reduce the formation of adducts with other ions in the solvent matrix is common practice. However in the case of Silwet L-

408 the $[M + H]^+$ adduct is still relatively weak, even with addition of acid. The $[M + H]^+$ adducts of Silwet L-408 were only detectable up to 40 V, whilst the $[M + Na]^+$ and $[M + K]^+$ adducts were stable up to 80 V and 120 V, respectively. No detectable fragments were observed with increasing cone voltage.

The effect on the spectrum of Silwet L-408 with varying skimmer lens offset (-50 V to 50 V) was also investigated, but no fragment ions were detected.

3.3.1.4 Source Temperature

A source temperature setting of 130 °C gave the highest absolute response, for both 1:1 (Table 3.5) and 2:1 MeOH/H_2O (Table 3.6) as the elution solvent. This source temperature setting also gave the lowest standard deviation with 2:1 MeOH/H_2O as the elution solvent, although not for 1:1 MeOH/H_2O. However the data may not be directly comparable as the modes of analysis were different for these two experiments (TIC and SIR respectively).

Table 3.5. Average relative response over a range of source temperatures with 1:1 MeOH/H_2O as the eluting solvent

Temperature (°C)	40	50	60	70	80	90	100	110	120	130	140
Relative Response*	0.44	0.45	0.71	0.71	0.76	0.75	0.82	0.85	0.96	1.0	0.92
CV	1.3%	3.8%	1.4%	3.1%	1.8%	2.8%	0.9%	1.8%	2.0%	3.4%	6.0%

* Average of three injections; TIC mode; *m/z* range of 350 - 1000

A large increase in absolute response (60%) was observed on increasing the source temperature from 50 °C to 60 °C with 1:1 MeOH/H_2O. Improvements in absolute responses thereafter were of the magnitude of approximately 10% with every 10 °C increase, with both solvent systems.

Table 3.6. Average relative response over a range of source temperatures with 2:1 MeOH/H_2O as the eluting solvent

Temperature (°C)	60	80	100	120	130	140
Relative Response*	0.34	0.43	0.62	0.79	1.00	0.93
CV	3.9%	6.3%	3.9%	2.9%	1.6%	1.8%

* Average of three injections; SIR mode; Four channels (ions) selected, corresponding to the NH_4^+ adducts of the $(EO)_n$, n = 6, 7, 8 & 9 oligomers.

3.3.1.5 Drying gas flow rate

A drying gas flow rate of 200 L h^{-1} gave the highest response for the values investigated (Table 3.7).

Table 3.7. Average absolute response over a range of drying gas flow rates

Flow rate (L h^{-1})	100	150	200	250	300	350	400
Absolute Response (x 10^5)*	64.6	65.48	66.0	63.923	62.129	58.0	52.5
SD (x 10^5)	0.3	0.07	0.4	0.005	0.009	0.5	0.4
CV	0.5%	0.1%	0.7%	0.008%	0.01%	0.9%	0.8%

* Average of two injections

3.3.1.6 Chemical composition of capillary

No retention/separation within the capillary was observed, elution time being independent of analyte or capillary composition for the two modified silica capillaries investigated.† Variation in peak shapes in previous investigations can be attributed to solvent mixing problems incurred when the composition of the sample preparation solvent differs significantly from that of the elution solvent, causing inconsistent flow of the sample through the system.

SAMPLE

3.3.1.7 Major adduct variation

Silwet L-77 oligomers form adducts with the inorganic ions, NH_4^+, Na^+, and K^+, inherently present at low levels in analytical solvents (Figure 3.2). $[M + H]^+$ adducts are not observed even with the addition of acidic media. In the absence of any added salts the distribution of adducts formed is variable. In general, however, the lower molecular weight surfactant oligomers show a preference for the sodium adduct, whilst the higher oligomers show an increase in preference for the potassium adduct. This is consistent with results from various investigations into the metal-ion complexing abilities of polyether derivatives.

† Standard fused silica capillary and a modified capillary electrophoresis capillary (SGE Australia Pty Ltd, Ringwood Victoria, Australia, Product No. 062832)

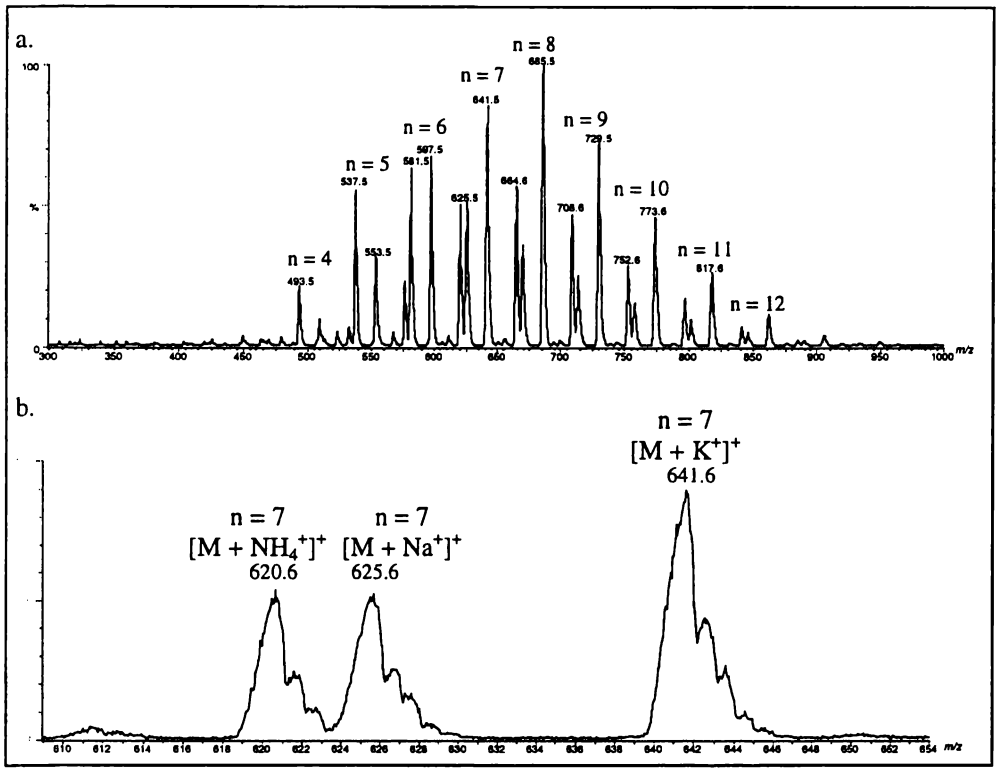

Figure 3.2. ESI/MS spectrum of Silwet L-77, a. over *m/z* 300 – 1000, and b. expanded over the range of the M_2D-C_3-O-$(EO)_7$-CH_3 oligomer

In studies of PEG compounds it was found that more than seven EO units were necessary to bind the K^+ ion in phase transfer experiments,[15] and specific complexations of $(EO)_6$ with Na^+ ions and $(EO)_7$ with K^+ ions were demonstrated.[16] Interactions between $(EO)_8$ and $(EO)_7$ PEGs were observed with the K^+ ion and between $(EO)_7$ and $(EO)_6$ with the Na^+ ion.[17] It was also found that at least five EO units were required for the complexation of PEGs with a K^+ cation-exchange resin.[18] Studies with small chain PEG compounds (n = 1 – 4) showed binding to Na^+ was stronger than to K^+ ions.[19]

It has been reported that, in general, crown ether ligands complex most strongly with metal cations of ionic radii best matching the cavity formed by the polyether ring.[20] The crown ether 18-crown-6 $[(EO)_6]$ shows selectivity among monovalent cations for the K^+ ion,[21] but also binds Na^+ much more strongly than any other crown ether,[22] consistent with the expected fit of each cation in the particular ligand cavity. The Na^+ binding constants have in fact been shown to maximise for $(EO)_6$ over the n = 4 – 13 EO range. The change in selectivity order for Na^+ and K^+ ions with increasing crown ether ring size has been demonstrated, with $Na^+ > K^+$ for $(EO)_4$, $Na^+ \approx K^+$ for $(EO)_5$, $Na^+ < K^+$ for $(EO)_6$ and $Na^+ \ll K^+$ for $(EO)_7$.[23] ESI/MS studies on $(EO)_4$ and $(EO)_6$ crown ethers with various metal cations also

showed that size relationships were dominating influences on complex formation.[24]

3.3.1.8 Multiple charging

Multiply charged species of Silwet L-77 are not observed, even with extremely low cone voltages. This is consistent with results obtained with a basic model designed to predict the maximum number of charges a PEG oligomer can retain.[25,26] It was concluded that one sodium ion is attached per 17 EO units,[6a] and thus only single charging is expected for the Silwet L-77 oligomeric mixture [$(EO)_n$, $n \approx 3 - 16$].

3.3.1.9 Ideal concentration

Silwet L-77 at a concentration of 1 ppm (10 ng, 10 μL injection aliquot) was adopted as the ideal concentration. At this concentration, the signal/noise ratio was such that the effect of background interference was negligible, and also the concentration was low enough that sample elution times were short with minimal tailing observed.

SOLVENT

3.3.1.10 Flow rate

Higher peak area responses were observed with slower solvent flow rates. This phenomenon is well documented in the literature, and is a result of increased efficiency of the ionisation process at lower liquid flows.[27]

In these investigations, analysis time and standard deviation are also important factors and thus a flow rate of 0.02 mL min^{-1} was selected as optimal. This value gave the lowest standard deviation and one of the highest absolute responses for both 1:1 MeOH/H_2O (Figure 3.3, Table 3.8) and 2:1 MeOH/H_2O (Table 3.9) as the elution solvent.

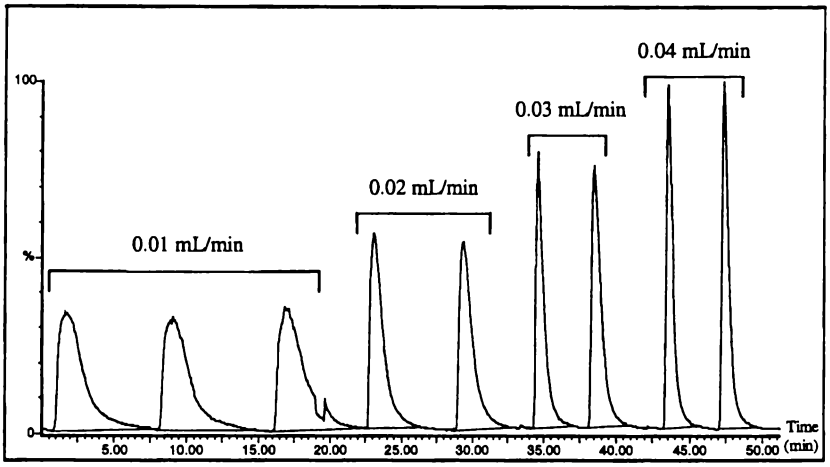

Figure 3.3. Continuum profile of multiple injections of Silwet L-77 with increasing solvent flow-rate (1:1 MeOH/H_2O as the elution solvent)

Table 3.8. Response of Silwet L-77 with the varying solvent flow-rates with 1:1 MeOH/H_2O as the elution solvent

Flow Rate (mL min^{-1})	0.01	0.02	0.03	0.04
Average Response*	107787	91403	88403	85993
SD	5867	284	1641	127
CV	5.4%	0.3%	1.9%	0.2%

* Average of two injections; SIR mode; Four channels (ions) selected, corresponding to the NH_4^+ and K^+ adducts of the $(EO)_n$, n = 7 & 8 oligomers

Table 3.9. Response of Silwet L-77 with the varying solvent flow-rates with 2:1 MeOH/H_2O as the elution solvent

Flow rate (mL min^{-1})	0.01	0.02	0.03	0.04	0.05
Average Response*	6287863	6020860	5418283	5210515	4928475
SD	164109	42712	28931	136702	80707
CV	2.6%	0.7%	0.5%	2.6%	1.6%

* Average of two injections; SIR mode; Four channels (ions) selected, corresponding to the NH_4^+ adducts of the $(EO)_n$, n = 6, 7, 8 & 9 oligomers

Over a concentration series the effect of varying the flow rate between 0.01 mL min^{-1} and 0.02 mL min^{-1} on the absolute response was relatively minimal with the slower flow rate giving a slightly higher response (106 %) overall. The faster flow rate, however, significantly hastened elution times (163 %), and is therefore preferable for multiple analyses (Table 3.10).

Table 3.10. Response of Silwet L-77 with varying concentrations at 0.01 and 0.02 mL min^{-1} solvent flow-rates

Flow rate	0.01 mL min^{-1}		0.02 mL min^{-1}	
[Silwet L-77] (ppm)	Time taken to elute peak (minutes)	Relative Response	Time taken to elute peak (minutes)	Relative Response
0.1	1.61	1.2	1.06	1.0
1.0	6.09	9.4	3.41	9.2
10.0	10.43	63	6.35	63
100.0	15.03	222	9.73	210

*SIR mode; Two channels (ions) selected, corresponding to the Na^+ adducts of the $(EO)_n$, n = 7 & 8 oligomers.

3.3.1.11 Elution solvent composition

The response of a range of Silwet L-77 solutions with varying elution solvents is shown in Figure 3.4. An elution solvent of 2:1 MeOH/H_2O gave the best overall response, yielding responses of 150% that obtained with the preparation solvent, 1:1 MeOH/H_2O. Higher responses were obtained for the 0.5, 1, and 2.5 ppm solutions with 100% MeOH as the elution solvent, however the increase in the response levelled off at the higher concentration. Furthermore 100% MeOH as the elution solvent gave severe tailing, and very irregular peak shapes.

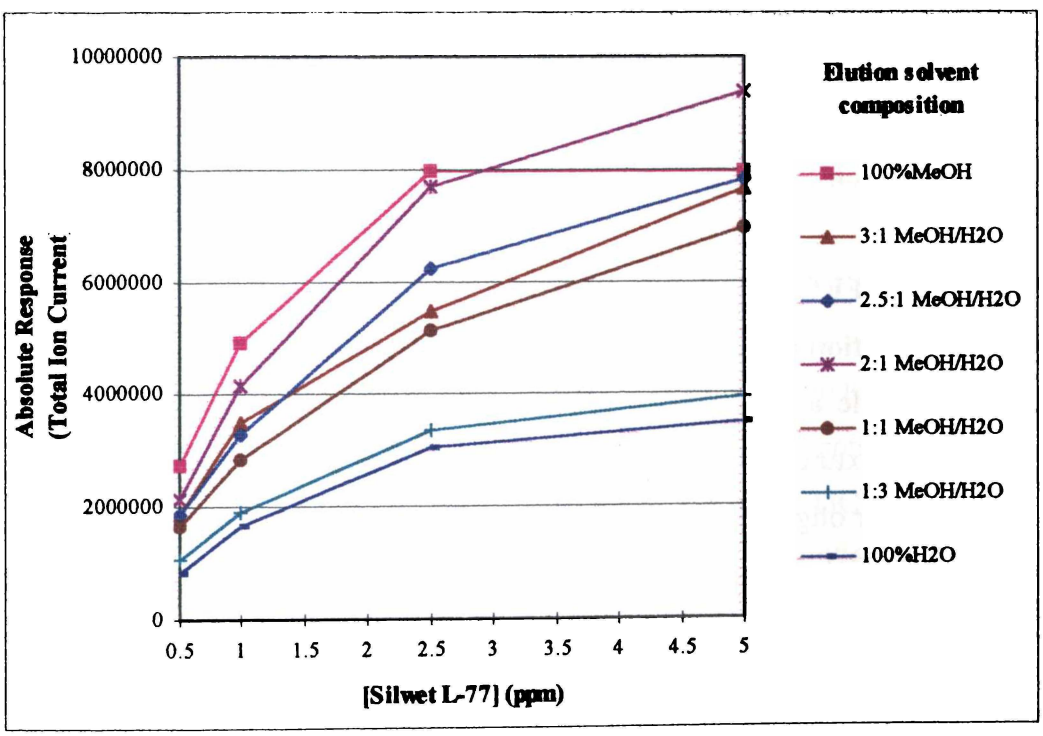

Figure 3.4. Response of Silwet L-77 over a concentration range for various elution solvents*

* Average of two injections; SIR mode; Four channels (ions) selected [$(EO)_n$, n = 7 & 8 oligomers, Na^+ and K^+ adducts]

The smoothest peak shapes were obtained with elution solvents closest in composition to the preparation solvent (1:1 MeOH/H_2O). When the elution solvent was of a higher proportion of organic solvent than the preparation solvent "pre-spikes" were observed. Conversely, when the proportion of aqueous solvent was higher, "post-spikes" were observed.

Differences in retention time with varying elution solvents were also observed. With a preparation solvent of 100% H_2O, the retention times were longer for 100% organic solvents, intermediate for solvent mixtures and shortest for 100% H_2O. Elution time was shortest when the preparation and elution solvents were the same.

Severe tailing of peaks was observed with single solvents, as compared with water/organic solvent composites. The sensitivity with 100% H_2O as the elution solvent was considerably reduced, and the cause of this is well documented for the ESI/MS ionisation process.[4] The relatively high surface tension of H_2O complicates the formation of the Taylor cone, and the use of water can also lead to electric discharge which degrades the performance of ESI/MS.

3.3.1.12 Preparation solvent composition

The total ion current and therefore sensitivity was much higher when solutions were prepared with organic/aqueous solvent mixtures as compared with 100% aqueous solutions.

MATRIX EFFECTS

3.3.1.13 Addition of salt solutions to simplify spectra

The multiple adduct formation observed under ESI/MS for the Silwet L-77 oligomeric mixture results in a highly complicated spectrum. Simplification to one adduct per oligomer is preferred, and often necessary for quantification. The addition of salt solutions to simplify spectra was thus investigated, and it was found that at a thousand-fold molar excess of cation to surfactant, the corresponding cation adduct dominates the spectrum, for any of the NH_4^+, Na^+, or K^+ salt solutions investigated. However over long periods of instrument use, as required for quantitative studies, the use of most salt solutions will have a detrimental effect on the response, through detector saturation and precipitation on

the sampling orifice.[7c] At higher salt concentrations, salt clusters will also form, affecting analyte response, as demonstrated in Figure 3.5.c.

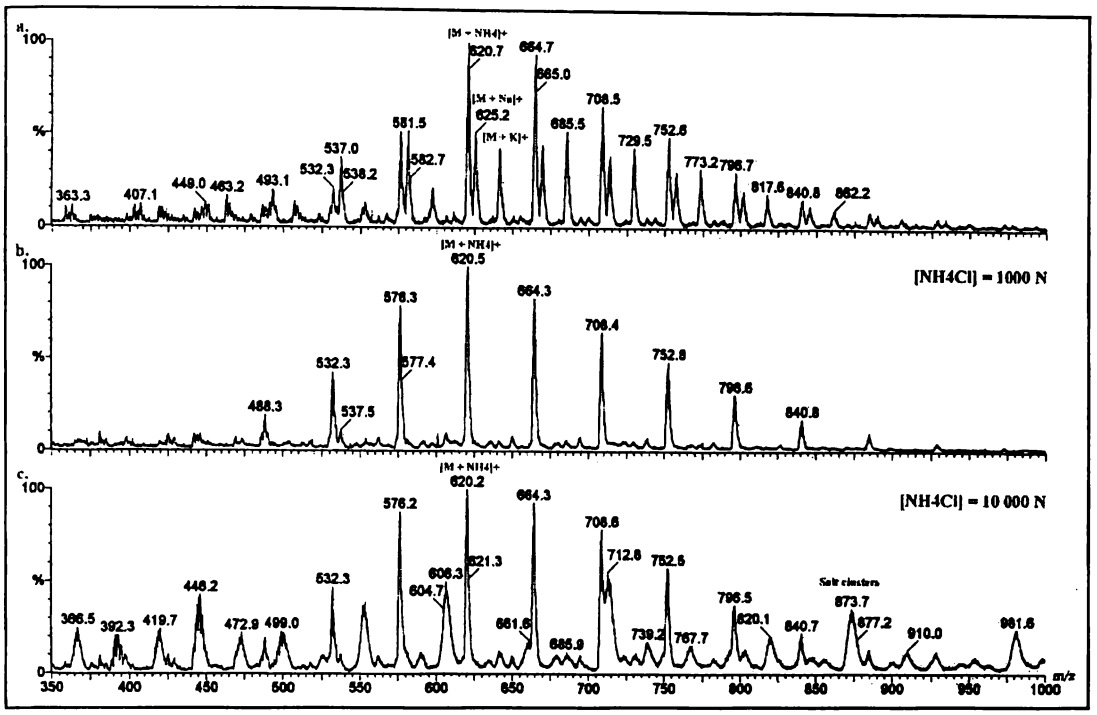

Figure 3.5. ESI/MS spectrum of Silwet L-77 *a.* alone, *b.* with a 1000-fold molar excess of NH_4OH, and *c.* with a 10000-fold molar excess of NH_4OH.

3.3.1.14 Addition of $CH_3CO_2NH_4$

$CH_3CO_2NH_4$ was investigated as a potential salt additive for controlling adduct formation, as its relative volatility should minimise the negative aspects of salt addition in ESI/MS.[28]

I. Ideal Salt Concentration

The highest absolute response in both the TIC and SIR* modes was observed with a 1000-fold molar excess of $CH_3CO_2NH_4$ to surfactant (1 ppm Silwet L-77, 1 mM $CH_3CO_2NH_4$). Extracted ion chromatograms from the TIC mode analysis, corresponding to the n = 6, n = 7, and n = 8 oligomers (*m/z* 576, 620, and 664, NH_4^+ adducts) showed similar trends. Significant increases in absolute response were observed with increasing salt concentration, with levelling off at a 1:1000 molar ratio of surfactant: salt.

* SIR conditions: n = 7 and 8 oligomers, NH_4^+, Na^+, and K^+ adducts selected

Extracted ion chromatograms from the SIR chromatogram show the increase in the intensity of the NH_4^+ adducts, and decrease in the intensity of the other adducts with increasing concentrations of $CH_3CO_2NH_4$.

The highest sensitivity for 0.1 ppm Silwet L-77 was also achieved with 1mM $CH_3CO_2NH_4$ in both TIC and SIR modes equating to a surfactant: salt ratio of 1N: 10 000N.

II. Ideal cone voltage

The highest base peak intensity was observed at a cone voltage of 40 V (*m/z* 620 ion, n = 7 oligomer, NH_4^+adduct). At this cone voltage the spectrum is simplified to the NH_4^+ adducts. Adduct preference varied with cone voltage, with the K^+ adducts dominating at higher cone voltages, despite the presence of $CH_3CO_2NH_4$. Causes of this phenomenon have been discussed in Section 3.3.1.7.

3.3.1.15 Other monovalent cations

Solutions of Silwet L-77 (0.5 ppm) with HCO_2H, NH_4Cl, LiCl, NaCl, KCl, RbCl and CsCl (0.5 ppm and 50 ppm) were analysed to determine the effect on adduct formation and ion intensity. Complexes of all these cations with crown ether derivatives are known.[24] The NH_4^+, Na^+ and K^+ adduct ions were the only adducts of Silwet L-77 observed in all cases. Variation in the major adduct was observed depending on the oligomer. The Silwet L-77 peak areas were unaffected by the presence of the added salt solutions at the concentrations investigated, in both TIC mode and in SIR mode (all possible adducts selected). The concentration of the salts added also had no effect on the resulting peak area. The analysis of the salt solutions alone* as a control experiment showed minimal interference by the ion currents corresponding to the salts.

The addition of H^+ ions enhanced the $[M + Na]^+$ adducts relative to the $[M + NH_4]^+$ and $[M + K]^+$ adducts. This phenomenon has also been reported in the analysis of other nonionic surfactants (NPEs and AEs) with the addition of trifluoroacetic acid.[29]

---

* TIC mode, *m/z* 200 - 1000

3.3.1.16 Multivalent cations

Spectra were measured in the presence of a variety of multivalent salt solutions [$MgCl_2$, $CaCl_2$, $CaSO_4$, $Sr(NO_3)_2$, $BaCl_2$, $CrCl_3$, $NiCl_2$, $CuCl_2$, $ZnBr_2$], as complexes of most of these adducts with crown ether derivatives have been observed.[24] However no adducts of Silwet L-77, other than the aforementioned NH_4^+, Na^+ and K^+ adducts, were observed.

3.3.1.17 Anion variation

The relative response of Silwet L-77 (positive ion mode) was not affected by anion variation for a range of sodium salt solutions (NaF, NaCl, NaBr, NaI, NaOH and $NaNO_3$).

3.3.1.18 Presence of active ingredient

In the presence of glyphosate IPA the response of Silwet L-77 was 90% of that in its absence (Table 3.11). Further experiments are required to confirm and rationalise this, although it can be speculated that ionisation competition with the IPA cation suppressed the Silwet L-77 response.

Table 3.11. Absolute response of Silwet L-77 in the presence and absence of glyphosate IPA

	Silwet L-77 alone	Silwet L-77 + Glyphosate IPA
Average Absolute Response (x 10^7)*	2.7	2.47
SD (x 10^7)	0.1	0.06
CV	4.0%	2.2%

* Average of three replicates

This indicates that glyphosate IPA in the appropriate amounts should also be added to standard solutions used in the quantitative analyses of surfactants in agrochemical formulations.

3.3.1.19 Summary of ideal conditions for standard ESI/MS

The optimised operating conditions established are summarised in Table 3.12.

Table 3.12. Optimised operating conditions for standard ESI/MS analysis

Parameter	MCA	TIC Continuum	SIR Continuum
Mode	Positive	Positive	Positive
Cone Voltage - 0.1 ppm	60 V [a]	-	-
- 1.0 ppm	60 V [a]	50 V [a]	50 V [ac]
- 10.0 ppm	50 V [a]	-	-
- 100.0 ppm	40 V [a]	-	-
Scan Time (*m/z* 350-1000)	-	3.0 seconds [a]	N/A
Inter-Scan Time	-	0.1 seconds [c]	N/A
Dwell Time - 2 Channels	N/A	N/A	1.5 second [a]
- 4 Channels	N/A	N/A	1.0 second [c]
- 5 Channels	N/A	N/A	1.0 second [a]
Inter-Channel Delay (2&4 Channels)	N/A	N/A	0.05 seconds [a]
Span - 2 Channels	N/A	N/A	0.75 a.m.u. [ac]
- 4 Channels	N/A	N/A	1 a.m.u. [ac]
Source Temperature	-	130°C [a]	130 °C [ac]
Drying Gas Flow Rate	-	-	200 L h^{-1} [a]
Nebulizing Gas Flow Rate	15 L h^{-1}	15 L h^{-1}	15 L h^{-1}
Probe Capillary Voltage	-	-	4.2 kV [a]
Skimmer Lens Offset	-	-	6 V [a]
HV Lens	-	-	0.22 kV [a]
Resolution	10.2 [a]	-	-
Multiplier	1000 [ae]	1000 [ae]	-
Ion Energy	5.0 V [a]	-	-
Ion Energy Ramp	0	0	0
Cone Voltage Ramp	0	0	0
Prep. Solvent Composition	1:1 MeOH/H_2O [ND]	1:1 MeOH/H_2O [ND]	1:1 MeOH/H_2O [ND]
Elution Solvent Composition	2:1 MeOH/H_2O [ND]	2:1 MeOH/H_2O [ND]	2:1 MeOH/H_2O [d]
Solvent Flow-Rate	0.02 mL min^{-1} [ND]	0.02 mL min^{-1} [ND]	0.02 mL min^{-1} [ac]

[a] Highest response; [b] Minimum possible setting; [c] Lowest standard deviation; [d] Best combination of high response and low standard deviation; [e] Maximum possible setting; [ND] Not determined

3.3.2 Megaflow ESI/MS method development

Among the instrument settings investigated, the parameters that showed the most significant effect on response (variation in intensity of greater than 25%) were scan time and solvent flow-rate. Inter-scan time and drying gas flow rate had

an intermediate effect on the response (variation of 10% - 25%) whilst dwell time showed intermediate to low influence. Inter-channel delay, span and source temperature showed low influence (variation of less than 10%), for the values investigated.

3.3.2.1 Inter-channel delay (SIR)

For both four and two selected channels, the optimal inter-channel delay time was 0.05 seconds. With four selected channels, a higher absolute response was observed for shorter inter-channel delay times for the values examined. Essentially the same values for absolute response and standard deviation were obtained for inter-channel delay times of 0.02 and 0.05 seconds. Consequently an inter-channel delay of 0.05 seconds was selected as optimal, as longer change over intervals are preferable wherever possible to prevent overloading of the computer. For two selected channels, the highest absolute response and lowest standard deviation was obtained for an inter-channel delay time of 0.05 seconds.

3.3.2.2 Major adduct variation

As in standard ESI/MS, adducts with NH_4^+, Na^+, and K^+ ions were observed under megaflow ESI/MS. In the absence of any added salts the distribution of these adducts was variable. The addition of $CH_3CO_2NH_4$ was also found to simplify spectra favourably.

3.3.2.3 Flow rate

A flow rate of 0.3 mL min^{-1} was selected as the optimal value for routine analysis. The flow rate setting of 0.1 mL min^{-1} gave the highest response and lowest standard deviation, however at this flow rate the 10 µL sample injection eluted over a considerable time interval (2 minutes). Furthermore, a higher flow rate was required to provide adequate pump back-pressure. The flow rate of 0.3 mL min^{-1} also gave a low standard deviation, although the response was 65% of that obtained with 0.1 mL min^{-1} solvent elution. However the loss in response was offset by improvements to the elution time (reduced to 1 minute) and peak shape.

3.3.2.4 Summary of ideal conditions for megaflow ESI/MS

The optimised control settings for megaflow ESI/MS are given in Table 3.13 below.

Table 3.13. Optimised operating conditions for megaflow ESI/MS

Parameter	TIC Continuum	SIR Continuum
Scan Time (*m/z* 350-1000)	1.55 seconds [ab]	N/A
Inter-Scan Time	0.1 seconds [a]	N/A
Dwell Time - 2 Channels	N/A	0.25 seconds [cd]
- 4 Channels	N/A	0.75 seconds [ac]
Inter-Channel Delay (2 & 4 Channels)	N/A	0.05 seconds [ac]
Span - 2 Channels	N/A	0.50 a.m.u. [d]
- 4 Channels	N/A	0.75 a.m.u. [a]
Source Temperature	-	180°C [ac]
Drying Gas Flow Rate	-	300 L h^{-1} [a]
Solvent Flow-Rate	0.3 mL min^{-1}	0.3 mL min^{-1}

a. Highest response; *b.* Minimum possible setting; *c.* Lowest standard deviation; *d.* Best combination of high response and low standard deviation

3.3.3 APcI/MS method development

Among the instrument settings investigated, the instrument parameters which displayed the most significant effect on response were scan time, inter-scan time, probe and source temperatures, drying and sheath gas flow rates, corona voltage, multiplier, ion energy and elution solvent composition. Variation in cone voltage, span, skimmer lens offset, HV lens, and solvent flow-rate had an intermediate effect on the response whilst dwell time and inter-channel delay showed low influence, for the values investigated.

3.3.3.1 Flow rate

A flow rate of 1.75 mL min^{-1} gave the highest absolute response for the values investigated, however due to the high pump back pressures observed at this flow rate a lower flow rate was required. A solvent flow rate of 1.25 mL min^{-1} also gave a high absolute response combined with a low standard deviation, and thus this value was selected as the ideal under these operating conditions. High back-pressure later, however, forced the selection of 1 mL min^{-1} as the solvent flow rate of choice.

3.3.3.2 Adduct Formation

In the absence of any added salts the spectra were dominated by the Na^+ adducts, although the NH_4^+ and K^+ adducts were present at lower intensities. Addition of $CH_3CO_2NH_4$ did not simplify the adduct formation to $[M + NH_4]^+$ species as observed previously, rather only complicated the observed adduct formation, with the Na^+ adducts and NH_4^+ adducts both present at high intensities. This is not favourable in actual application of the technique as the risk of peak overlap, with either impurities or the internal standard in the matrix, is increased when an increase in sample adducts is observed. Best results for APcI/MS analysis were thus obtained without the addition of salt solutions.

3.3.2.4 Summary of ideal conditions for APcI/MS

The optimised control settings for APcI/MS are presented in Table 3.14.

Table 3.14. Optimised operating conditions for APcI/MS*

Parameter	MCA (TIC)	SIR Continuum
Cone Voltage - 10 ppm	60 V [a]	-
Scan Time (*m/z* 300-1000)	1.65 seconds [ab]	N/A
Inter-Scan Time	0.1 seconds [ab]	N/A
Dwell Time (2 Channels)	N/A	0.15 seconds [ac]
Inter-Channel Delay (2 Channels)	N/A	0.07 seconds [a]
Span (2 Channels)	N/A	0.5 a.m.u. [ac]
Probe Temperature	300 °C [a]	-
Source Temperature	180 °C [a]	-
Drying Gas Flow Rate	-	100 L h^{-1} [c]
Sheath Gas Flow Rate	-	250 L h^{-1} [ae]
Corona Voltage	1.6 kV [a]	-
Skimmer Lens Offset	3.0 V [a]	-
HV Lens	0.2 V [a]	-
Multiplier	1000 [ab]	-
Ion Energy	2.4 V [a]	-
Solvent Flow-Rate	-	1 mL min^{-1}

a. Highest response; *b.* Minimum possible setting; *c.* Lowest standard deviation; *d.* Best combination of high response and low standard deviation; *e.* Maximum possible setting; * A default resolution setting of 12 was used

3.3.4 FTICR/MS

3.3.4.1 Silwet L-77 and M_2D-C_3-O-$(EO)_6$-Me

In the analysis of Silwet L-77 by FTICR/ESI/MS only the Na^+ adducts were observed.* The ions detected spanned the n = 4 – 14 oligomers with the n = 9 oligomer dominating the spectrum. The spectrum of the M_2D-C_3-O-$(EO)_6$-Me† solution also showed only the sodium adduct (*m/z* 581). $[M + H]^+$, $[M + NH_4]^+$ and $[M + K]^+$ adducts, in addition to the $[M + Na]^+$ adducts were observed however, for other compounds analysed (M_2D-C_3-O-EO-H, 2-deoxy-D-glucose).

3.3.4.2 Sustained offline resonance irradiation CID of M_2D-C_3-O-$(EO)_n$-Me

It was hoped that information pertaining to structure and stability could be obtained from CID of Silwet L-77 by FTICR/MS. However no fragmentation was observed when the isolated ion at *m/z* 625 (M_2D-C_3-O-$(EO)_7$-Me, Na^+ adduct) was activated in the presence of either air or argon. An investigation into related literature subsequent to these experiments has confirmed similar results have been obtained elsewhere when the parent ion of interest is an alkali-cation adduct, as compared with a proton adduct.[12]

It was consequently proposed that either: i. the cation provided stabilisation for the structure, preventing dissociation; ii. CID causes only the loss of the cation adduct from the Silwet L-77 molecule; or iii. fragmentation was occurring, but the products generated were neutral through loss of the cation adduct, and were thus rendering them undetectable by these methods. These points could be investigated by: i. analysing a smaller oligomer which should be bound less strongly to the cation; ii. ejecting all ions prior to activation then monitoring the generation of free Na^+ ions; and iii. use of a larger oligomer, which is proposed to be less likely to lose the adducting cation due to stronger interactions between the cation and the longer ethoxylate chain.

In order to investigate the points (i) and (ii) postulated above, CID of M_2D-C_3-O-$(EO)_6$-Me was conducted. No fragmentation was observed for the ion (*m/z* 581, Na^+ adduct) with either gas introduction then activation, nor activation then gas introduction. All ions excluding the *m/z* 581 ion were ejected, and it was ensured

---

* All samples were prepared with 0.1 mg mL^{-1} of NaI added to facilitate ionisation

† Obtained by HPLC separation of commercial Silwet L-77

that no ions at *m/z* 23 (free Na^+ ions) were present. Subsequent CID of the isolated *m/z* 581 ion yielded a strong peak at *m/z* 23 confirming the loss of the Na^+ ion, and also accounting for the absence of detectable fragments.

The third postulate was investigated by CID of M_2D-C_3-O-$(EO)_{11}$-Me, however no fragment ions were observed from this oligomer (*m/z* 801, Na^+ adduct).

3.3.4.3 Internal electron ionisation (IEI) analysis of Silwet L-77

The IEI spectrum of Silwet L-77 yielded a large number of fragment ions. A high intensity ion at *m/z* 295 (295.1460 and 295.1832 in duplicate measurements) was observed which can be assigned to $[\mathbf{14}]^+$ or $[CH_3O(EO)_6]^+$.

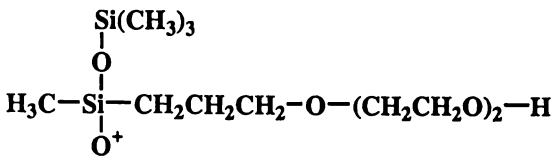

14

The $[CH_3O(EO)_6]^+$ structure is more likely, as **14** is derived from M_2D-C_3-O-$(EO)_2$-H, which is not expected in any significant amount in the Silwet L-77 formulation, due to the low $(EO)_n$ content.[30] Mass difference calculations, as shown in Table 3.15, did not provide any conclusive confirmation of the correct structure due to the relatively large variation (0.04 a.m.u.) between the duplicate spectra.

Table 3.15. Product ions of IEI of Silwet L-77

MW (observed)*	Possible structures	MF	MW (calculated)	Δm/M (ppm)
295.1460	• $[CH_3O(CH_2CH_2O)_6]^+$	$C_{13}H_{27}O_7$	295.1757	100
	• $[\mathbf{14}]^+$	$Si_2C_{11}H_{27}O_5$	295.1397	21
295.1832	• $[CH_3O(CH_2CH_2O)_6]^+$	$C_{13}H_{27}O_7$	295.1757	25
	• $[\mathbf{14}]^+$	$Si_2C_{11}H_{27}O_5$	295.1397	147

* Duplicate spectra

The ion fragmentation pattern observed also supports the $[CH_3O(CH_2CH_2O)_6]^+$ assignment, with peaks observed at *m/z* 295, 279, 265, 251, 235, 221, 207, 191,

177, 163, 147 and 133. These peaks correspond to the sequential loss of O-, CH_2- and CH_2- units from the $[CH_3O(CH_2CH_2O)_6]^+$ structure as shown in Table 3.16.

Table 3.16. Ions in IEI spectrum of Silwet L-77 and proposed assignments

Ion	Possible structure
295	$[CH_3O(CH_2CH_2O)_6]^+$
279	$[CH_3O(CH_2CH_2O)_5CH_2CH_2]^+$
265	$[CH_3O(CH_2CH_2O)_5CH_2]^+$
251	$[CH_3O(CH_2CH_2O)_5]^+$
235	$[CH_3O(CH_2CH_2O)_4CH_2CH_2]^+$
221	$[CH_3O(CH_2CH_2O)_4CH_2]^+$
207	$[CH_3O(CH_2CH_2O)_4]^+$
191	$[CH_3O(CH_2CH_2O)_3CH_2CH_2]^+$
177	$[CH_3O(CH_2CH_2O)_3CH_2]^+$
163	$[CH_3O(CH_2CH_2O)_3]^+$
147	$[CH_3O(CH_2CH_2O)_2CH_2CH_2]^+$
133	$[CH_3O(CH_2CH_2O)_2CH_2]^+$

Other peaks were observed at *m/z* 73, 75 and 103 and are assigned to the structures $[Si(CH_3)_3]^+$, $[CH_3OCH_2CH_2O]^+$ and $[CH_3OCH_2CH_2OCH_2CH_2]^+$, respectively. Peaks at *m/z* 311 and 353 have molecular weights corresponding to the linear dimer (**15**) and the cyclic trimer (**16**), respectively. However, these assignments are not considered to be likely as condensation products would not usually be expected under EI conditions. Furthermore, the $(EO)_n$ content of **15** is not feasible in terms of the starting material EO content.

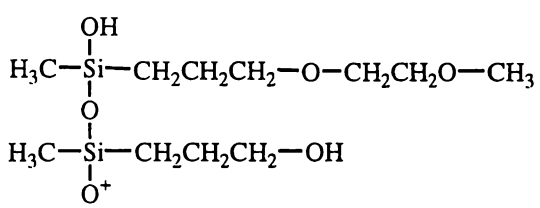

15

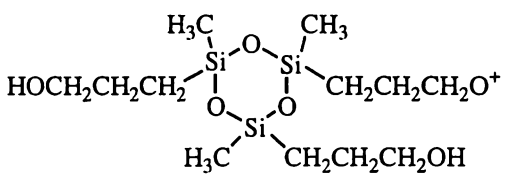

16

Minor peaks which have not been assigned, were also observed at *m/z* 86, 91, 105, 117, 131, 149, 281, 311, 590, 660, 772, 1055 and 1121.

3.4 CONCLUSION

These results demonstrate API/MS techniques are applicable methods for the analysis of Silwet L-77. The nonionic surfactant is detectable by API/MS methods by virtue of the ability of the polyether moeity to chelate NH_4^+ and alkali-metal cations. Complicated adduct formation was minimised by the use of volatile ammonium salts in ESI/MS, although was not beneficial by APcI/MS.

Ideal operating parameters, i.e. those that gave highest response and/or reproducibility, were established for standard ESI/MS, megaflow ESI/MS and APcI/MS methods, and are summarised in Tables 3.12, 3.13 and 3.14, respectively. The parameters which had the most significant effect on response by standard ESI/MS included ion mode, capillary voltage, cone voltage, source temperature, drying gas flow-rate and the multiplier setting. Among the instrument settings investigated for megaflow ESI/MS, scan time and solvent flow-rate showed the most significant effect. By APcI/MS, the response was influenced most by scan time, inter-scan time, probe and source temperatures, drying and sheath gas flow rates, corona voltage, multiplier, ion energy and elution solvent composition.

No structurally significant ions were generated by CID, consistent with results obtained elsewhere for cation-adducts, and information obtained from IEI of Silwet L-77 was also limited.

3.5 REFERENCES

[1] *a.* S. Lacorte, D. Barcelo, *Anal. Chem.*, 1996, **68**, 2464-2470; *b.* M. Castillo, R. Domingues, M.F. Alpendurada, D. Barcelo, *Anal. Chim. Acta*, 1997, **353**, 133-142; *c.* K.A. Barnes, R.J. Fussell, J.R. Startin, M.K. Pegg, S.A. Thorpe, S.L. Reynolds, *Rapid Commun. Mass Spectrom.*, 1997, **11**, 117-123; *d.* A.C. Hogenboom, J. Slobodnik, J.J. Vreuls, J.A. Rontree, B.L.M. van Baar, W.M.A. Niessen, U.A.Th. Brinkman, *Chromatographia*, 1996, **42**, 506-514 ; *e.* K.A. Barnes, R.J. Fussell, J.R. Startin, S.A. Thorpe, S.L. Reynolds,, *Rapid Commun. Mass Spectrom.*, 1995, **9**, 1441-1445; *f.* I. Ferrer, M. Hennion, D. Barcelo, *Anal. Chem.*, 1997, **69**, 4508-4514; *g.* N.H. Spliid, B. Køppen, *Chemosphere*, 1998, **37**, 1307-1316; *h.* D. Puig, I. Silgoner, M. Grasserbauer, D. Barcelo, *Anal. Chem.*, 1997, **69**, 2756-2761

[2] *a.* C. Crescenzi, A. Di Corcia, S. Marchese. R. Samperi, *Anal. Chem.*, 1995, **67**, 1968-1975; *b.* A. Lagana, G. Fago, A. Marino, *Anal. Chem.*, 1998, **70**, 121-130; *c.* R.W. Reiser, A.J. Fogiel, *Rapid Commun. Mass Spectrom.*, 1994, **8**, 252-257

[3] *a.* S. Chiron, S. Papilloud, W. Haerdi, D. Barcelo, *Anal. Chem.*, 1995, **67**, 1637-1643; *b.* C. Molina, M. Honing, D. Barcelo, *Anal. Chem.*, 1994, **66**, 4444-4449; *c.* R.J. Vreeken, P. Speksnijder, I. Bobeldijk-Pastorova, T.H.M. Noij, *J. Chromatogr. A.*, 1998, **794**, 187-199; *d.* L.Y.T. Li, D.A. Campbell, P.K. Bennett, J. Henion, *Anal. Chem.*, 1996, **68**, 3397-3404

[4] P. Kebarle, L. Tang, *Anal. Chem.*, 1993, **65**, 972A-987A

[5] K. Tang, A. Gomez, *Phys. Fluids*, 1994, **6**, 2317-2332

[6] *a.* K.B. Sherrard, P.J. Marriott, R.G. Amiet, R. Colton, M.J. McCormick, G.C. Smith, *Environ. Sci. Tech.*, 1995, **29**, 2235-2242; *b.* K.B. Sherrard, P.J. Marriott, M.J. McCormick, R. Colton, G. Smith, *Anal. Chem.*, 1994, **66**, 3394-3399; *c.* H. Fr. Schröder, *J. Chromatogr. A*, 1997, **777**, 127-139; *d.* M. Bokern, M. Nimtz, H. H. Harms, *J. Agric. Food Chem.*, 1996, **44**, 1123-1127

[7] *a.* C. Crescenzi, A. Di Corcia, R. Samperi, A. Marcomini, *Anal. Chem.*, 1995, **67**, 1797-1804; *b.* A. Di Corcia, *J. Chromatogr. A.*, 1998, **794**, 165-185; *c.* D.Y. Shang, M.G. Ikonomou, R.W. Macdonald, *J. Chromatogr. A.*, 1999, **849**, 467-482; *d.* D.D. Popenoe, S.J. Morris, III, P.S. Horn, K.T. Norwood, *Anal. Chem.*, 1994, **66**, 1620-1629

[8] S. Pattanaargsorn, P. Sangvanich, A. Petsom, S. Roeengsumran, *Analyst*, 1995, **120**, 1573-1576

[9] M. Castillo, D. Barcelo, *Anal. Chem.*, 1999, **71**, 3769-3776

[10] *a.* K.A. Evans, S.T. Dubey, L. Kravetz, S.W. Evetts, I. Dzidic, C.C. Dooyema, *J. Amer. Oil Chem. Soc.*, 1997, **74**, 765-773; *b.* M. Castillo, C.M. Alonso, J. Riu, D. Barcelo, *Environ. Sci. Tech.*, 1999, **33**, 1300-1306; *c.* S.D. Scullion, M.R. Clench, M. Cooke, A.E. Ashcroft, *J. Chromatogr. A.*, 1996, **733**, 207-216

[11] H.F. Schröder, F. Ventura, *Sample Handling and Trace Analysis of Pollutants: Techniques, Applications and Quality Assurance, Techniques and Instrumentation in Analytical Chemistry (TIAC)*, Vol. 21, Ed. D. Barcelo, Elsevier, 2000

[12] A. Di Corcia, C. Crescenzi, A. Marcomini, R. Samperi, *Environ. Sci. Tech.*, 1998, **32**, 711-718

[13] R.P. Lattimer, H. Muenster, H. Budzikiewicz, *Int. J. Mass Spectrom. Ion Processes*, 1989, **90**, 119-129

[14] T.L. Selby, C. Wesdemiotis, R.P. Lattimer, *J. Am. Mass Spectrom.*, 1994, **5**, 1081-1092

[15] S. Yanagida, K. Takahashi, M. Okahara, *Bull. Chem. Soc. Jpn.*, 1977, **50**, 1386-1390

[16] S. Yanagida, K. Takahashi, M. Okahara, *Bull. Chem. Soc. Jpn.*, 1978, **51**, 3111-3120

[17] S. Yanagida, K. Takahashi, M. Okahara, *Bull. Chem. Soc. Jpn.*, 1978, **51**, 1294-1299

[18] T. Okada, , *Anal.Chem.*, 1990, **62**, 327-331

[19] N.S. Poonia, S.K. Sarad, A. Jayakumar, G.Chandrakumar, *J. Inorg. Nucl, Chem.*, 1979, **41**, 1759-1763

[20] C.J. Pederson, *J. Am. Chem. Soc.*, 1967, **89**, 7017-7036

[21] J.D. Lamb, R.M. Izatt, C.S. Swain, J.J. Christensen, *J. Am. Chem. Soc.*, 1980, **102**, 475-479

[22] D.M. Dishong, G.W. Gokel, *J. Org. Chem.*, 1982, **47**, 147-148

[23] H.K. Frensdorff, *J. Am. Chem. Soc.*, 1971, **93**, 600-603

[24] R. Colton, S. Mitchell, J.C. Traeger, *Inorg. Chim. Acta*, 1995, **231**, 87-93

[25] J.B. Fenn, M. Mann, C.K. Meng, S.F. Wong, C.M. Whitehouse, *Science*, 1989, **246**, 64-71

[26] T. Nohmi, J.B. Fenn, *Anal.Chem.*, 1992, **114**, 3241-3246

[27] A.P. Bruins, *J. Chromatogr. A.*, 1998, **794**, 345-357

[28] C.K. Lim, T.J. Peters, *J. Chromatogr. A.*, 1984, **316**, 397-406

[29] C. Crescenzi, A. Di Corcia, R. Samperi, A. Marcomini, *Anal. Chem.*, 1995, **67**, 1797-1804

[30] George Pollicello, Witco, *personal communication* 8/11/99

CHAPTER 4

The Development of API/MS Methods for the Quantitation of Organosilicone Surfactants

4.1 INTRODUCTION

Quantitation of mixtures by API/MS is complicated by competition for ionisation. Several quantitative models have been proposed (refer to Section 1.2.5), however the applicability of these methods to surfactants is complicated due to the nature of the ionisation process. Differences in surface activity will affect the quantitative models as compounds showing higher surface-activity are ionised preferentially. The nature and consequences of this process are discussed further in the following section.

According to the models proposed by Kebarle *et al.*[1] and Guilhaus *et al.*,[2] quantitation by flow injection API/MS requires a knowledge of the response factors of all components of the mixture being analysed. If the background matrix (unmeasured species) varies significantly between samples, the relative ionisation efficiencies for the different analytes will be altered thereby affecting the requirements for accurate quantitation.[3]

4.1.1 Suppression of analyte response in the presence of surfactants

Surface-active compounds give very high responses with ESI. These compounds can also suppress the ionisation of other less surface-active molecules through a shielding of the charged droplet exterior.[4] This is especially relevant in applications of capillary electrophoresis (CE) ESI/MS where surfactants are used to simulate a stationary phase or promote separation. The surfactants reduce the ESI/MS response of the analytes of interest by affecting the electrospray efficiency, dominating ionisation and/or contamination of the ion source. Several approaches have been adopted to overcome these negative influences, with some methods aimed at simply reducing the surfactant influence, i.e. the use of higher molecular weight surfactants[5,6] and the use of APcI in place of the ESI interface. Other methods eliminate the introduction of the surfactant into the ESI/MS altogether. These methods include the use of semipermeable membranes, partial filling micellar electrokinetic chromatography (MEKC),[6] MEKC with anodically migrating micelles, and coupling to capillary zone electrophoresis (CZE).[7]

Investigation into the mechanism of signal suppression by the anionic surfactant sodium dodecyl sulfate (SDS), $CH_3(CH_2)_{11}OSO_3^-Na^+$, has indicated that Coulombic interaction, surface activity and surfactant charge are influential parameters.[8] High concentrations of anions at the liquid-vapour interface in positive mode ESI, resulting from their high surface activity, will destabilise the Taylor cone, resulting in reduced spray efficiency. Furthermore, the subsequent transfer of the positively-charged analytes from the droplets into the gas phase will be compromised due to Coulombic interaction with the oppositely-charged surfactant ions, favouring surfactant-analyte adduction rather than analyte-cation adduct formation. The detection of cationic polypeptides by CE-ESI/MS with the use of cationic and non-ionic surfactants, but not the anionic surfactant SDS, supports this hypothesis.[8,9] However, cationic compounds have been successfully analysed with the high molecular weight polymeric anionic surfactant BBMA* (MW 40 000),[5,6] in contrast to this theory, suggesting other factors are also important.

Addition of a nonionic surfactant to a SDS-containing system also enabled ESI/MS detection of cationic species. It was shown that the nonionic surfactant significantly reduced the surface concentration of the anionic surfactant,[8] presumably through competition effects. It follows that fewer anionic surfactant ions will be transferred to the offspring droplets, by virtue of their formation process. Consequently, production of gas-phase ions of the analyte will be enhanced as a result of reduced Coulombic interactions.

Because it appears that species found in the offspring droplets are those that reside on the surface of the parent droplet,[1,10] it follows that the surface activity will influence the quenching ability of matrix ions. Studies of solutions containing surfactants have shown offspring-droplets consist of a non-proportionally high amount of the surfactant molecules.[8] Comparatively, polymeric surfactants have low surface activities, and as a consequence the offspring droplets generated should contain less polymeric surfactant molecules (BBMA) than their more surface-active anionic counterparts (SDS). The ability of the surfactant to be detected by ESI/MS may also affect the analyte response, noting that BBMA is not detectable and SDS shows strong ionisation.[5]

* Butyl acrylate- butyl methacrylate- methacrylic acid copolymer (sodium salt)

As compared with low molecular weight surfactants, polymeric surfactants have no cmc (critical micelle concentration) and consequently induce the formation of micelles at a much lower concentration. The highest BBMA solution used above (2% w/v)[5] corresponds to a 0.5 mM concentration, as compared with the 1.25 mM (0.04% w/v) SDS solution used.[8] A decrease in signal intensity was observed with an increase in BBMA concentration in the afore-mentioned study.

4.1.2 Quantitation of surfactants

The use of online LC techniques is commonly used in quantitative API/MS, the advantage of which is two-fold. Analyte separation aids in compound identification and also eliminates the problem of ionisation competition. All of the quantitative studies on surfactants thus far reported have incorporated online LC separation prior to the mass spectrometric determination.[11a-g] All of these studies have also however, involved the analysis of environmental samples with complex matrices, often of undetermined composition. Whether this is still essential in mixtures of known composition has not been determined. Due to the competitive nature of ionisation and the dominance of ionisation by surface-active compounds it is possible that mixtures containing these compounds cannot readily be analysed by the flow injection quantitative method.[12]

4.1.3 Chapter Objectives

In this chapter the extension of the API/MS qualitative methods developed in Chapter 3 to quantitation of Silwet L-77 is described. The requirements were to establish and optimise conditions for the quantitation of the surfactant and provide reliable methods for routine analysis by API/MS methods. This was investigated by low and high flow-rate ESI/MS, APcI/MS and HPLC/APcI/MS methods. At standard ESI/MS flow-rates (20 $\mu L\ min^{-1}$), each sample injection requires over 5 minutes to elute. Such long analysis times for each sample render the application of the technique impractical, in the flow injection form, for large-scale environmental analyses. The desire to apply the technology to large sample numbers required the optimisation of the technique to operate at the higher flow rates. The use of a solvent splitter should also enable the application of standard ESI/MS to quantitative studies, although this was not investigated here. Difficulties encountered with flow injection methods led to the investigation of HPLC/APcI/MS methods.

4.2. MATERIALS AND METHODS

The materials and methods used were as for Chapter 3, unless otherwise stated. All response values are determined by integration of peak areas obtained from plots of ion current over time for single pulse injections. For the internal standard determinations, relative responses were calculated from extracted ion chromatograms obtained from the parent chromatogram.

The internal standards used were Agral-90, Agral-100, $C_6(EO)_3$, PEG-400, PPG-425 and Triton X-45. All of these formulations, excluding $C_6(EO)_3$, are oligomeric mixtures of varying EO content. $C_6(EO)_3$ is a short-chain alcohol ethoxylate surfactant (CH_3-$[CH_2]_5$-$O[CH_2CH_2O]_3$-H), of monomeric (n = 3) EO distribution. Agral-90, is a nonylphenyl ethoxylate with mean molar EO = 9, containing ~ 10% isopropyalcohol. Agral-100 was prepared by concentration under vacuum of the commercial Agral-90 product. PEG-400 is a polyethylene glycol (HO-$[CH_2CH_2O]_n$-H) of average molecular weight ~ 400 and PPG-425 is a polypropylene glycol (HO-$[CH_2CH_2CH_2O]_n$-H) of average molecular weight ~ 425. Triton X-45, is an octylphenyl ethoxylate with mean molar EO = 5.

Triton X-45 was used in methods incorporating online HPLC separation as this is an accepted internal standard in the established HPLC-LSD method.[13] Triton X-45 could not be used as an internal standard for Silwet L-77 by flow injection methods as the cation-adducts of Triton X-45 overlap with the corresponding adducts of Silwet L-77 (See A.III). Careful monitoring of adduct formation in flow injection API/MS was required when using Agral as the internal standard, as the Na^+ adducts of Agral overlap with the K^+ adducts of Silwet L-77. Agral-90 could not be used as an internal standard for the online HPLC method as retention times were too similar to those of Silwet L-77 under the conditions used.

4.2.1. Standard ESI/MS method development

4.2.1.1 EXTERNAL STANDARD METHOD

4.2.1.1.1 Limits of detection

Pure solvent and Silwet L-77 solutions at concentrations of 1, 10 and 100 ppb and 1 ppm were analysed in duplicate in both the TIC and SIR modes. For TIC measurements a *m/z* range of 300 – 1000 was used, whilst for SIR the ions

corresponding to the NH_4^+, Na^+ and K^+ adducts of the $(EO)_7$ and $(EO)_8$ oligomers of Silwet L-77 were selected.

4.2.1.1.2 Reproducibility

Multiple injections (seven or ten) of Silwet L-77 at a concentration of 1 ppm were analysed by TIC and SIR in the continuum mode. The response on different days and with different mass ranges (TIC) and adducts (SIR) selected was determined, and the effect of ammonium acetate addition was also investigated.

4.2.1.1.3 Response over a range of Silwet L-77 concentrations

Silwet L-77 solutions of concentrations 0.5, 1.0, 2.0, 4.0, 5.0, 8.0 and 10.0 ppm, prepared in 1mM $CH_3CO_2NH_4$, were analysed in SIR mode. The NH_4^+ adducts of the $(EO)_6$, $(EO)_7$, $(EO)_8$ and $(EO)_9$ oligomers were selected. Because the K^+ adducts were minor but still present, an SIR measurement selecting the NH_4^+ and K^+ adducts of the $(EO)_7$ and $(EO)_8$ oligomers was also acquired to investigate the effect of including minor adducts in quantitative studies.

4.2.1.2 INTERNAL STANDARD METHOD

4.2.1.2.1 PEG-400 as the internal standard

4.2.1.2.1.1 Response factor reproducibility

A mixture of Silwet L-77 and PEG-400 solutions, prepared at concentrations of 2.5 ppm each in 1mM $CH_3CO_2NH_4$, was injected multiple times. The injections were analysed by SIR in the continuum mode. Measurements adopting the ideal cone voltages for each ion (Silwet L-77, 60V; PEG-400, 80V), and with the cone voltage set at 30V for both selected ions were acquired. The ideal cone voltages were determined by comparison of the base peak intensities obtained from MCA spectra taken at various CV settings. For the constant cone voltage measurement 30V was selected, as the spectra of the two compounds of interest were simplified to single adduct formation at this value, although sensitivity was reduced.

4.2.1.2.1.2 Response over a range of Silwet L-77 concentrations

Silwet L-77 solutions at concentrations of 0.5, 1.0, 2.0, 4.0, 5.0, 6.0, 8.0, and 10.0 ppm were prepared, and a 1:1 (v/v) mixture of each with a 5 ppm solution of

PEG-400 was analysed in duplicate by selected ion monitoring. Cone voltage settings were as for the preceding section.

4.2.1.2.2 Agral-90 as the internal standard

4.2.1.2.2.1 Response factor reproducibility

Response factor reproducibility at two concentrations (0.5 ppm and 2.5 ppm) was investigated. A 1:1 (v/v) mixture of the surfactant and internal standard solutions at equal concentrations were injected multiple times. Analysis was by SIR in the continuum mode, at a cone voltage setting of 40V for both selected ions. Reproducibility with elution solvents of 1:1 MeOH/H_2O (0.5 ppm and 2.5 ppm) and 2:1 MeOH/H_2O (2.5 ppm) was investigated.

4.2.1.2.2.2 Response over a range of Silwet L-77 concentrations

Silwet L-77 solutions at concentrations of 0.5, 1.0, 2.0, 4.0, 5.0, 6.0, 8.0, and 10.0 ppm were prepared and a 1:1 (v/v) mixture of each with a 5 ppm solution of Agral-90 was analysed in duplicate by selected ion monitoring. Cone voltage settings and elution solvent compositions were as for Section 2.1.4.1.

4.2.1.2.3 PPG-425 as the internal standard

4.2.1.2.3.1 Response factor reproducibility

Response factor reproducibility at two concentrations (0.5 ppm and 2.5 ppm) was investigated. A 1:1 (v/v) mixture of the surfactant and internal standard solutions at equal concentrations were injected multiple (10) times. The solutions were analysed by SIR in continuum mode. Cone voltage was set at 60V for both selected ions.

4.2.1.2.3.2 Response over a range of Silwet L-77 concentrations

Silwet L-77 solutions at concentrations of 0.5, 1.0, 2.0, 4.0, 5.0, 6.0, 8.0, and 10.0 ppm were prepared, and a 1:1 (v/v) mixture of each with a 5 ppm solution of PPG-425 was analysed in duplicate by selected ion monitoring. A cone voltage of 60V was adopted. The experiment was duplicated to confirm the results obtained.

4.2.2 Megaflow ESI/MS method development

The optimal operating conditions established in Chapter 3 (Table 3.13), excluding the span for which the setting of 1 a.m.u. was adopted, were used unless otherwise stated. All solutions were prepared in 1mM $CH_3CO_2NH_4$.

4.2.2.1 EXTERNAL STANDARD METHOD

4.2.2.1.1 Lower limit of detection

Pure solvent and Silwet L-77 solutions at concentrations of 0.0001, 0.00025, 0.0005, 0.001, 0.01, 0.1 ppm were analysed in replicate (five) by SIR in the continuum mode. Domination of the NH_4^+ adducts was not achieved even in the presence of added ammonium acetate with the K^+ adducts too significant to ignore. Consequently, the NH_4^+ and K^+ adducts of the $(EO)_8$ and $(EO)_9$ oligomers of Silwet L-77 were selected.

4.2.2.1.2 Upper limit of detection

Silwet L-77 solutions at concentrations of 1, 10, 20, 50, 100, 200 and 500 ppm were analysed in replicate (five) by SIR in the continuum mode. The NH_4^+ and K^+ adducts of the $(EO)_8$ and $(EO)_9$ oligomers of Silwet L-77 were selected.

4.2.2.1.3 Reproducibility

Multiple injections (seven) of Silwet L-77 at a concentration of 1 ppm, were analysed by SIR in the continuum mode. Three variations on the ions selected were investigated:

(1) The NH_4^+ and K^+ adducts of the $(EO)_8$ oligomer were selected

(2) The NH_4^+ adducts of the $(EO)_8$ and $(EO)_9$ oligomers were selected

(3) The NH_4^+ and K^+ adducts of the $(EO)_8$ and $(EO)_9$ oligomers were selected.

4.2.2.1.4 Response over a range of Silwet L-77 concentrations

Silwet L-77 solutions of concentrations 0.1, 0.5, 1.0, 2.5, 5.0 and 10.0 ppm were analysed in SIR mode, with the NH_4^+ adducts of the $(EO)_6$, $(EO)_7$, $(EO)_8$ and $(EO)_9$ oligomers selected.

4.2.2.2 INTERNAL STANDARD METHOD

4.2.2.2.1 Agral-100 as the internal standard

The solutions were analysed by SIR in the continuum mode with the NH_4^+ adducts of the $(EO)_7$ oligomer of Silwet L-77 and the $(EO)_8$ oligomer of Agral-90 selected. A cone voltage setting of 40V for both selected ions and a dwell time of 0.50 seconds were selected.

4.2.2.2.1.1 Response factor reproducibility

A 1:1 (v/v) mixture of the surfactant and internal standard solutions at equivalent concentrations (2.5 ppm) was injected multiple (6) times.

4.2.2.2.1.2 Response over a range of Silwet L-77 concentrations

Mixtures (1:1 v/v) of Silwet L-77 solutions, at concentrations of 0.5, 1.0, 2.0, 4.0, 5.0, 6.0, 8.0 and 10 ppm, with Agral-100 (5 ppm) were prepared. Each solution was analysed in duplicate. Linearity with solvent flow-rates of 0.3 mL min^{-1} and 0.2 mL $min^{-1}$was tested.

4.2.2.2.2 $C_6(EO)_3$ as the internal standard

Standard solutions of Silwet L-77 at concentrations of 0.1, 0.25, 0.5, 0.75, 1.0 and 1.5 ppm were prepared, and mixed with an equivalent volume of 1 ppm $C_6(EO)_3$. Each solution was analysed in triplicate in TIC mode, and the response obtained from the extracted ion chromatograms. The sum of the NH_4^+, Na^+ and K^+ adducts of the $(EO)_7$ Silwet L-77 oligomer and the sum of the H^+, NH_4^+, Na^+ and K^+ adducts of $C_6(EO)_3$ were used to generate the standard curve data.

4.2.3 APcI/MS method development

The optimal operating conditions established in Chapter 3 (Table 3.14) were adopted.

4.2.3.1 EXTERNAL STANDARD METHOD

4.2.3.1.1 Lower limit of detection

Pure solvent and Silwet L-77 solutions at concentrations of 0.001, 0.0025, 0.005, 0.0075, 0.01, 0.1, 1.0, and 10.0 ppm were analysed in triplicate by SIR in

the continuum mode. The Na^+ adduct of the $(EO)_6$ oligomer of Silwet L-77 was selected.

4.2.3.1.2 Upper limit of detection

Silwet L-77 solutions at concentrations of 10, 20, 50, 100, 200, 500, 1000 and 2000 ppm were analysed in triplicate by SIR in the continuum mode. Single injections of concentrations of 5000 and 10000 ppm were also analysed. The Na^+ adducts of the $(EO)_6$ and $(EO)_7$ oligomers of Silwet L-77 were selected.

4.2.3.1.3 Reproducibility

Multiple injections (seven) of Silwet L-77 at a concentration of 1 ppm were analysed by SIR in the continuum mode, with the Na^+ adducts of the $(EO)_6$ and $(EO)_7$ oligomers of Silwet L-77 selected.

4.2.3.1.4 Response over a range of Silwet L-77 concentrations

Silwet L-77 solutions at concentrations of 0.5, 1.0, 2.5, 5, 8 and 10 ppm were analysed in duplicate by SIR in the continuum mode. The Na^+ adducts of $(EO)_6$ and $(EO)_7$ oligomers of Silwet L-77 were selected.

4.2.3.2 INTERNAL STANDARD METHOD

4.2.3.2.1 Agral-90 as the internal standard

The solutions were analysed by SIR in the continuum mode with the Na^+ adducts of the $(EO)_6$ oligomer of Silwet L-77, and the $(EO)_7$ oligomer of Agral-90 selected.

4.2.3.2.1.1 Response factor reproducibility

A 1:1 mixture of the surfactant and internal standard (Agral 90) solutions (2.5 ppm) was injected multiple times (seven).

4.2.3.2.1.2 Response over a range of Silwet L-77 concentrations

Silwet L-77 solutions at concentrations of 0.25, 0.5, 1.25, 2.5, 4.0 and 5 ppm, containing Agral-90 at a concentration of 2.5 ppm were prepared in 1 mM $CH_3CO_2NH_4$. Each solution was analysed in duplicate.

4.2.3.2.2 $C_6(EO)_3$ as the internal standard

Standard solutions of Silwet L-77 at concentrations of 1.0, 2.5, 5.0, 7.5, 10.0, 15.0 and 20.0 ppm were prepared, and mixed with an equivalent volume of 10 ppm $C_6(EO)_3$. Each solution was analysed in duplicate by SIR mode, with the Na^+ adducts selected [Silwet L-77 $(EO)_6$ oligomer].

4.2.4 HPLC/APcI/MS method development

A solution of Silwet L-77 (70% M_2D-C_3-O-$(EO)_n$-Me) was prepared at a concentration of 2.86 g L^{-1} in water, equating to a 0.2 % (w/v) surfactant solution, as determined previously (see Section 2.3.1.3). A stock solution of Triton X-45 (0.05 g L^{-1}, 50 ppm), prepared with 40:60 H_2O/MeOH, was used as the internal standard solution.

The standard solutions were prepared by dispensing 1, 3, 5, 7, 10, 14, 20 and 28 droplets (0.24 µL) of the Silwet L-77 stock solution. Aliquots of the internal standard (5 µg in 100 µL) were added and the resulting solutions made up to 10 mL. This yielded Silwet L-77 solutions of concentrations 0.07, 0.21, 0.34, 0.48, 0.69, 0.97, 1.38 and 1.93 ng μL^{-1}, containing 0.5 ng μL^{-1} of the internal standard each, which were used to determine the response ratios by HPLC/APcI/MS. The same solutions were analysed by HPLC with light scattering mass detection, for comparison of the two methods. Chromatographic conditions for both detection methods were selected such that all the Silwet L-77 oligomers were coeluted.

4.2.5 APPLICATION TO FOLIAGE RESIDUE SAMPLES

4.2.5.1 *Chenopodium album* study by flow injection API/MS

All methods used are described in Chapter 5 (Section 5.3.3).

4.2.5.2 Citrus study by flow injection API/MS

Treatments and extractions

A Silwet L-77 solution at 2 g L^{-1} concentration was prepared in water. Droplets (0.24 µL, 20 droplets/leaf) were applied onto the upper surface of a single citrus leaf using a micro-syringe, to give a dose of 9.6 µg surfactant on each leaf. Each treatment contained 5 replicates (1 leaf/replicate). Identical treatments were performed on leaves stripped of their epicuticular wax, by way of cellulose acetate stripping. All plants were kept under constant growing conditions for the

uptake period. At intervals of 2.5, 10, 30 and 240 min after application, the treated leaves were excised and the residue collected by washing off with H_2O/MeOH (1:1 v/v; 2 x 4 mL) and the solution made up to 10 mL with methanol. Agral-90 (5 μg, 100 μL) was added to 5 mL of the washoff (to provide a 1 ppm internal standard solution) for the HPLC analysis. The remaining 5 mL of the solution was used for API/MS analysis, and was either directly analysed, or mixed with internal standard. Solutions requiring internal standard were prepared by taking aliquots and mixing (1:1 v/v) with 1 ppm $C_6(EO)_3$.

Preparation of the standard solutions

Solutions of Silwet L-77 (0.25, 0.5, 0.75, 1.0, 1.5, 2 ng μL^{-1}) containing the Agral-90 internal standard (1 ng μL^{-1}) were used to generate the relative response ratio curves for HPLC analysis. The solutions were prepared by serial dilution of a 0.1 g L^{-1} stock solution of Silwet L-77 with a 1 ng μL^{-1} internal standard solution. Silwet L-77 solutions at concentrations of 0.1, 0.25, 0.5, 0.75, 1.0, and 2.5 ng μL^{-1} were prepared in MeOH/H_2O (60:40) as standard solutions for API/MS. The solutions containing internal standard were prepared as 1:1 (v/v) mixtures of the Silwet L-77 solutions with 1 ppm $C_6(EO)_3$.

Response with Silwet L-77:Agral-90 ratio constant

Silwet L-77 and Agral 90 solutions at concentrations of 0.01, 0.1, 0.5, 1, 2.5, 5.0 and 10 ppm were prepared. Mixtures (1:1 [v/v]) of the equal concentrations were analysed by TIC in triplicate.

4.2.5.3 *Chenopodium album* study by HPLC/APcI/MS

The methods used were as described in Chapter 5, Section 5.3.4.

4.3 RESULTS AND DISCUSSION

4.3.1 Standard ESI/MS method development

4.3.1.1 EXTERNAL STANDARD METHOD

4.3.1.1.1 Limits of detection

The lower limit of detection for convenient quantitation with low standard deviation is of the order of 0.1 ppm for TIC mode analysis (Table 4.1) and 0.01 ppm for SIR mode acquisitions (Table 4.2).

Table 4.1. Determination of lower limit of detection by TIC mode analysis

Silwet L-77 concentration (ppm)	1	0.1	0.01	0.001
Average absolute response (x 10^8)*	1.08	0.31	0.07	0.07
SD (x 10^8)	0.03	0.02	0.01	0.02
CV	3%	8%	17%	26%
Signal/Noise (S/N) ratio**	15	4	1	1

* Average of 2 injections; ** Average response of 2 blank injections = 0.07 x 10^8; *m/z* 300 - 1000

The SIR determinations show much higher sensitivity and S/N ratios, and in general lower standard deviations for equivalent concentrations, as compared with the TIC acquisitions.

Table 4.2. Determination of lower limit of detection by SIR mode analysis

Silwet L-77 concentration (ppm)	1	0.1	0.01	0.001
Average absolute response (x 10^5)*	4.83	0.71	0.083	0.044
SD (x 10^5)	0.38	0.04	0.006	0.006
CV	8%	6%	8%	13%
Signal/Noise (S/N) ratio**	121	18	2	1

* Average of 2 injections; ** Average response of 2 blank injections = 0.04 x 10^5; Six channels (ions) selected, corresponding to the NH_4^+, Na^+, K^+ adducts of the $(EO)_n$, n = 7 & 8 oligomers.

Silwet L-77 solutions down to concentrations of 0.01 ppm (0.1 ng) can be detected (Figure 4.1). However, for quantitation the margin of error at this concentration is significantly high for both TIC and SIR mode acquisitions.

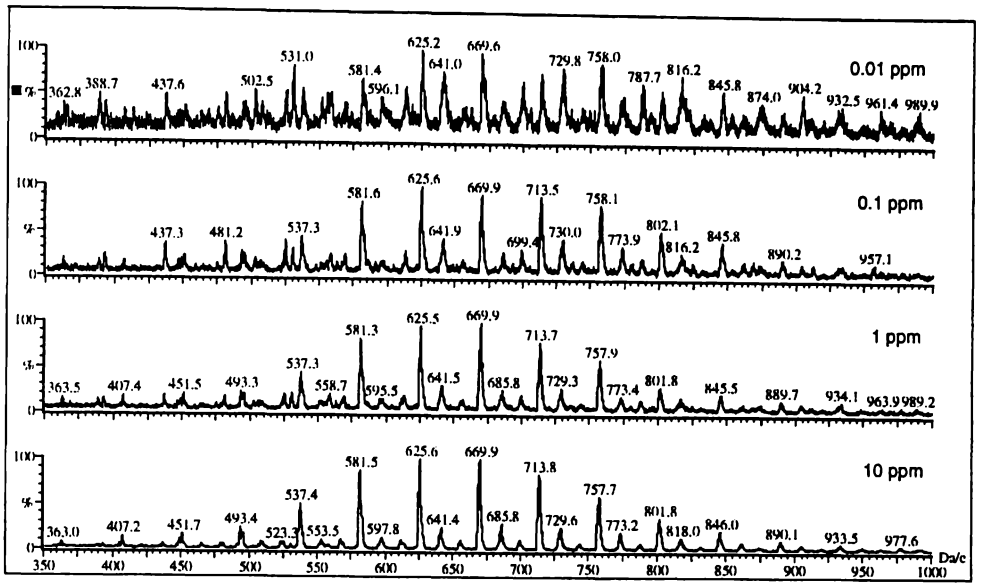

Figure 4.1. ESI/MS spectra obtained for Silwet L-77 solutions of varying concentrations

The upper limit on operating concentration is selected as 100 ppm, for convenience, as at this concentration contamination of the source is significant, and the compounds are found to linger considerably in the system following analysis.

4.3.1.1.2 Reproducibility

The absolute response was found to be very variable between acquisitions taken on different days, indicating a need for the use of an internal standard in quantitative studies. Other authors have also documented the need of internal standards to minimise the influence of fluctuations in detector sensitivity.[14]

The sensitivity and reproducibility was found to be improved in SIR mode (Table 4.4) as compared with TIC mode (Table 4.3), consistent with literature observations.[15]

Table 4.3. Reproducibility as determined by TIC mode analysis

Day	0	12	16	29
m/z range	350-1000	400-1000	300-1000	350-1000
Average Response (x 10^8)	2.0 *	2.5 *	1.08**	0.70 **
SD (x 10^8)	0.3	0.3	0.03	0.07
CV	15%	14%	3%	9%
Blank Average (x 10^8) ***				0.15
Signal/Noise (S/N) ratio				5

* Average of 7 injections; ** Average of 10 injections; *** Average of 2 injections

Standard deviation in the SIR mode was further improved when minor adducts were not included in the determinations, although inclusion of minor peaks did yield a slight increase in response, as expected. This has also been observed in other investigations, where it was found that selecting only the most intense ion resulted in an increase in the S/N ratio, although absolute response values were decreased.[16]

Table 4.4. Reproducibility as determined by SIR mode analysis

Day	0	12	16	16	29	30
Adducts selected*	all [a]	all [a]	all [a]	NH_4^+, K^+	NH_4^+, K^+	NH_4^+, K^+
Average Response (x 10^5)	8.0 [b]	8.5 [b]	4.8 [b]	4.4 [c]	3.12 [c]	1.7 [c]
SD (x 10^5)	0.5	0.8	0.4	0.2	0.09	0.1
CV	6.5%	8.9%	8.0%	3.5%	2.8%	5.7%
Blank Average (x 10^5) [d]	-	-	-	-	0.02	-
S/N ratio	-	-	-	-	143	-

* $(EO)_7$ and $(EO)_8$ oligomers; [a] all adducts = NH_4^+, Na^+ and K^+; [b]Average of 7 injections; [c] Average of 10 injections; [d] Average of 2 injections

It follows that suppression of small adducts, by the addition of a salt solution, should thus result in higher sensitivity and lower error values, and reproducibility in the presence of ammonium acetate was therefore investigated. With addition of the salt, the area contributed by the NH_4^+ adducts of Silwet L-77 is significantly more than the other adducts. The standard deviation of the response in the presence of ammonium acetate was much improved over that in its absence, and the standard deviation was also improved with omission of the minor K^+ adducts (Table 4.5). This is consistent with other studies where better S/N ratios were found when only the most intense ion was selected.[16]

Table 4.5. Reproducibility in the presence of $CH_3CO_2NH_4$, as determined by SIR mode analysis

$(EO)_n$ oligomers selected [a]	6, 7, 8 and 9	7 and 8
Adducts selected	NH_4^+ [b]	NH_4^+ and K^+ [c]
Average absolute response (x 10^5) [d]	29.0	22.4
SD (x 10^5)	0.2	0.2
CV	0.7%	0.9%

[a] M_2D-C_3-O-$(EO)_n$-CH_3, [b] Dominant adduct; [c] All adducts observed; [d] Average of two replicates

4.3.1.1.3 Response over a range of Silwet L-77 concentrations

Because of the inherent problem of ionisation competition between analytes in mixtures, the quantitation of Silwet L-77 without an internal standard present was investigated. Assuming linearity can be achieved, then this may be a possible method for quantitation. The absence of an internal standard however will mean any losses in workup and fluctuations in detector response will not be accounted for. Standard solutions will also need to be analysed regularly, to account for any losses in sensitivity over time.

The response was determined in SIR mode, and the effect of selecting all adducts and only the major adduct was investigated (Table 4.6, Figure 4.2). The response with four ammonium adducts selected was higher than that of four ammonium and potassium adducts, as was to be expected, as the ammonium adducts were dominant through the addition of the ammonium acetate salt. Standard deviations of the two measurements were comparable.

Table 4.6. Response of Silwet L-77 over a concentration range, as determined by SIR mode analysis

Adducts selected	NH_4^+ and K^+ [a]			NH_4^+ [b]		
[Silwet L-77] (ppm) [c]	Average Response (x 10^6) [d]	SD	CV	Average Response (x 10^6) [d]	SD	CV
0.5	1.14	0.00	0.1%	1.66	0.03	1.7%
1.0	2.24	0.02	0.9%	2.90	0.02	0.7%
2.0	3.39	0.04	1.2%	4.87	0.01	0.2%
4.0	6.28	0.02	0.3%	8.26	0.13	1.6%
5.0	7.52	0.00	0.0%	9.85	0.07	0.7%
6.0	-	-	-	11.49	0.07	0.6%
8.0	9.73	0.10	1.0%	12.99	0.03	0.2%
10.0	10.82	0.65	6.0%	15.23	0.23	1.5%

[a] SIR mode; $(EO)_n$, n = 7 and 8 oligomers selected; [b] SIR mode; $(EO)_n$, n = 6, 7, 8 and 9 oligomers selected; [c] Silwet L-77 solutions prepared in 1mM $CH_3CO_2NH_4$; [d] Average of two replicates

The plot of the absolute response as a function of concentration (Figure 4.2) show curvilinear responses for both measurements, which correlate well (R^2 > 0.99) with power least-squares fit regressions.

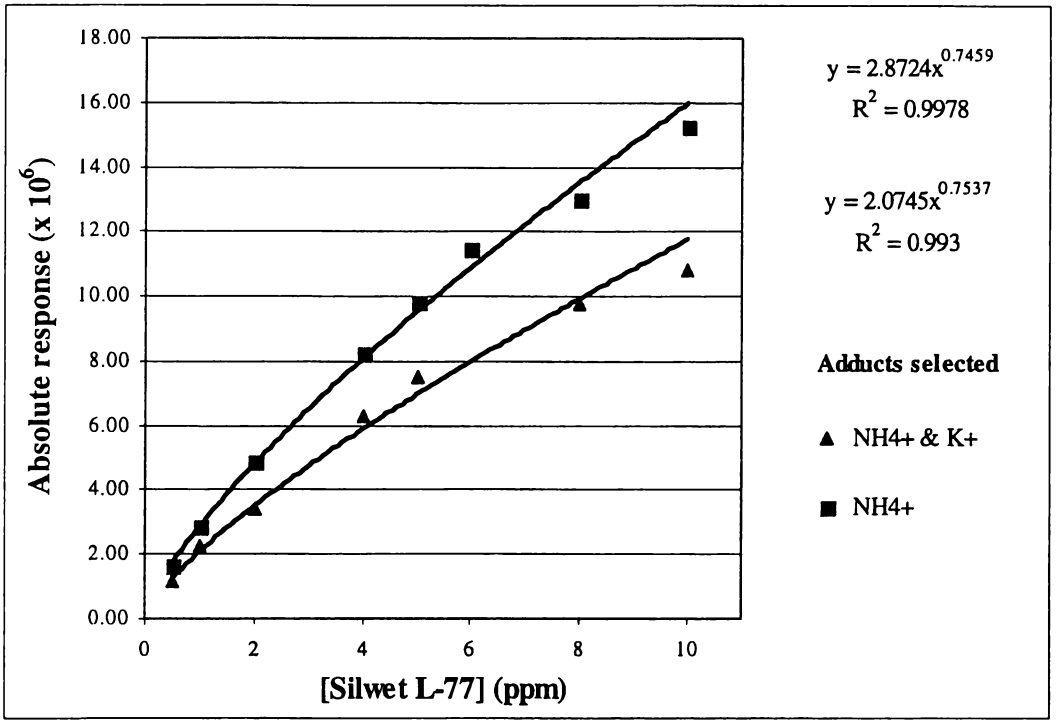

Figure 4.2. Response of Silwet L-77 over a concentration range (SIR mode analysis)

4.3.1.2 INTERNAL STANDARD METHOD

A number of internal standards for use in the quantitative analysis of Silwet L-77 were investigated. Internal standards are essential in quantitative analyses in order to correct for any handling or recovery losses and detector fluctuations.

In order for linearity to be achieved by flow injection ESI/MS, internal standards with similar physical properties, including surface activity, are required.[17] The selection of an appropriate internal standard for Silwet L-77 analysis is further complicated by the fact that most nonionic surfactant formulations are oligomeric mixtures, so difficulties arise in locating a compound with similar surface activity, whilst still maintaining peak separation.

The low molecular weight compounds, PEG-400 and PPG-425 were investigated due to their minimal peak overlap with Silwet L-77, although in practice their reduced surface-activity may preclude their use. The use of the surfactant Agral-90 as a potential internal standard was also examined, although adduct formation needed to be carefully controlled in order to avoid peak overlap.

4.3.1.2.1 PEG-400 as the internal standard

As outlined previously (Section 3.3.1.14), the addition of 1 mM ammonium acetate greatly simplifies the spectrum of Silwet L-77. Ammonium acetate also

simplifies the adduct formation of PEG-400, a polyethylene-glycol oligomeric mixture (average molecular weight ≈ 400 $gmol^{-1}$), with the major peaks of both compounds well resolved. The use of PEG-400 as an internal standard for the analysis of Silwet L-77 was thus investigated. The ideal cone voltages for Silwet L-77 and PEG-400 were different, and thus measurements using the individual ideal cone voltages and a constant cone voltage for both compounds were acquired.

4.3.1.2.1.1 Response factor reproducibility

A much lower standard deviation was observed for data obtained using a constant cone voltage (Table 4.7). The absolute responses are not directly comparable as data were acquired on different days.

Table 4.7. Response factor reproducibility with varying cone voltages

Cone Voltage	80V		60V		30V		30V	
Response ($x 10^5$)	TIC	PEG-400[a]	Silwet L-77[b]	Silwet L-77/ PEG-400	TIC	PEG-400[c]	Silwet L-77[b]	Silwet L-77/ PEG-400
Average	3.89	1.36	2.57	0.52*	76	47.5	28.8	0.606
SD	0.04	0.05	0.04	0.02	1	0.8	0.4	0.009
CV	1.1%	3.9%	1.5%	3.0%	1.6%	1.8%	1.6%	1.5%

* Average of 8 injections; ** Average of 6 injections; [Silwet L-77] = [PEG-400] = 2.5 ppm; [a] $(EO)_{10}$ oligomer, K^+ adduct; [b] $(EO)_7$ oligomer, NH_4^+ adduct; [c] $(EO)_9$ oligomer, NH_4^+ adduct

4.3.1.2.1.2 Response over a range of Silwet L-77 concentrations

Linearity in relative response with varying concentration of Silwet L-77, using PEG-400 as the internal standard was achieved when a constant cone voltage (30V) was adopted. A non-linear response was obtained when different cone voltages for the two compounds being analysed were adopted. A similar non-linear response was obtained in an analogous study conducted on Triton X-45, with Jeffamine M-600 as the internal standard, indicating that a constant cone voltage setting is preferable for quantitative analyses.

The phenomenon of signal suppression observed in the presence of other analytes is demonstrated in Figure 4.3. The internal standard (PEG-400) concentration was constant throughout, however a reduction in the response is observed (middle trace) as the Silwet L-77 concentration was increased (top trace).

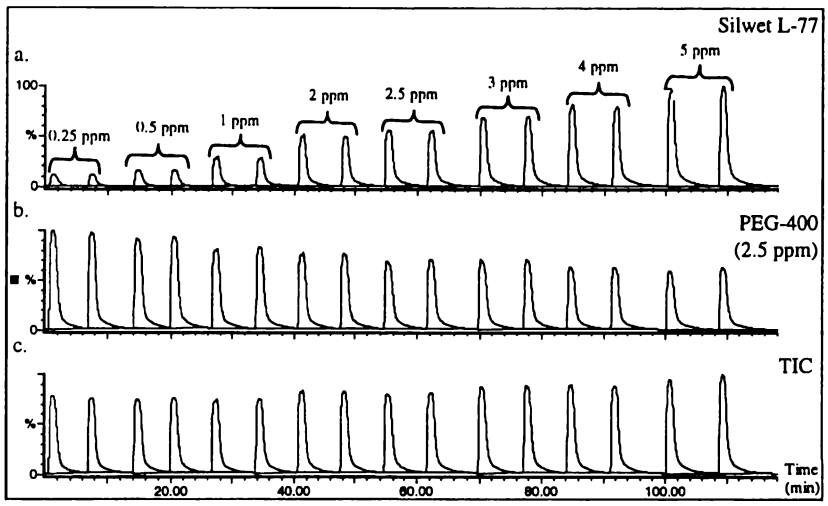

Figure 4.3. Response with increasing concentration of Silwet L-77 and constant PEG-400 concentration with extracted ion chromatograms for *a.* Silwet L-77 and *b.* PEG-400*

A linear response with respect to concentration was obtained for Silwet L-77 with PEG-400 as the internal standard (Figure 4.4). However due to the lower surface-active nature of PEG-400 relative to Silwet L-77, this compound may not be an appropriate internal standard for the quantitation of Silwet L-77 (as discussed in Chapter 1).

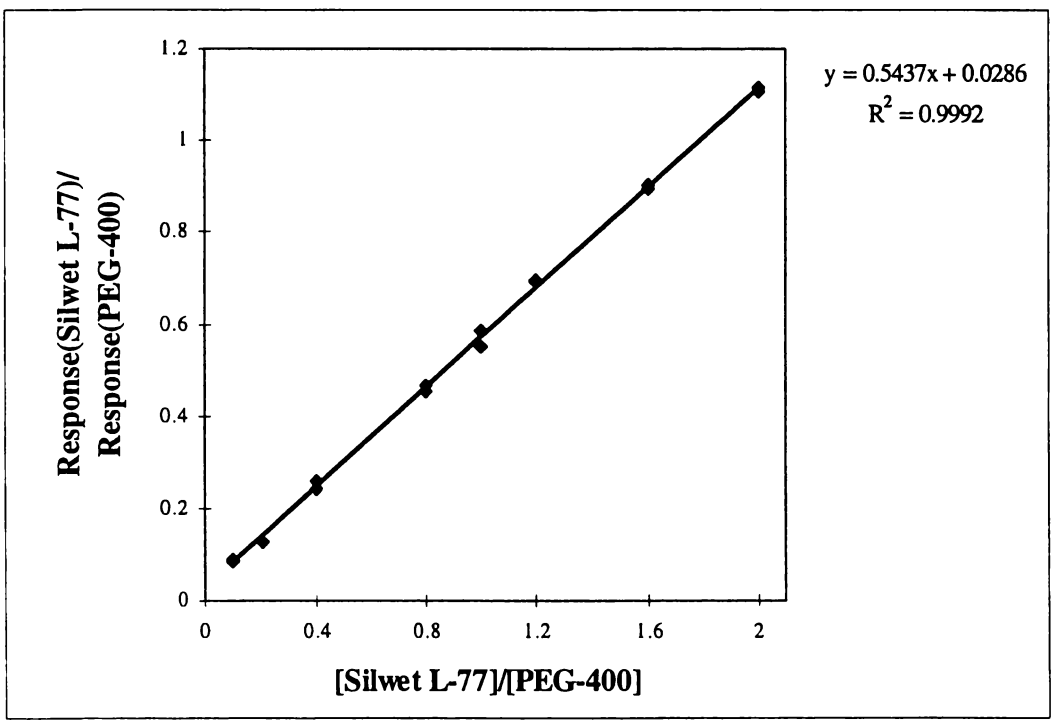

Figure 4.4. Relative response of Silwet L-77 as a function of concentration with PEG-400 as the internal standard (SIR, cone voltage = 30V, [PEG-400] = 2.5 ppm)

* CV = 30V, SIR mode, 2 channels selected, *a.* Silwet L-77: *m/z* 620, $(EO)_7$ oligomer, NH_4^+ adduct; *b.* PEG-400, *m/z* 432, $(EO)_{10}$ oligomer, K^+ adduct

4.3.1.2.2 Agral-90 as the internal standard

Addition of $CH_3CO_2NH_4$ enabled the use of Agral-90 as an internal standard for Silwet L-77, as the NH_4^+ adducts of the two compounds were adequately different in mass. Careful monitoring of the adduct formation was required as the Na^+ adducts of Agral-90 overlap with the K^+ adducts of Silwet L-77.

4.3.1.2.2.1 Response factor reproducibility

The standard deviation of the relative response factors was less than the standard deviations obtained for the absolute responses, for all solvents and concentrations investigated. The standard deviations were also significantly less with the higher concentration investigated (Tables 4.8 and 4.9).

Table 4.8. Response factor reproducibility with surfactant concentrations of 0.5 ppm

Elution solvent	1:1 MeOH/H_2O			
	TIC	Agral-90[a]	Silwet L-77[b]	Silwet L-77/Agral-90
Average Response (x 10^5)[c]	7.3	3.6	3.6	0.98
SD	0.6	0.2	0.3	0.02
CV	7.6%	6.8%	8.8%	2.3%

[a] $(EO)_8$ oligomer, NH_4^+ adduct; [b] $(EO)_7$ oligomer, NH_4^+ adduct; [c] Average of 6 injections

Table 4.9. Response factor reproducibility with surfactant concentrations of 2.5 ppm

Elution solvent	1:1 MeOH/H_2O				2:1 MeOH/H_2O			
	TIC	Agral-90[a]	Silwet L-77[b]	(Silwet L-77/ Agral-90)	TIC	Agral-90[a]	Silwet L-77[b]	Silwet L-77/ Agral-90
Average Response[*]	2.79	1.35	1.43	1.060[**]	6.4	3.00	3.40	1.132[***]
SD	0.09	0.04	0.04	0.006	0.1	0.08	0.06	0.008
CV	3.2%	3.2%	3.1%	0.6%	2.3%	2.6%	1.9%	0.7%

[*] x 10^6; [**] Average of 10 injections; [***] Average of 6 injections; [a] $(EO)_8$ oligomer, NH_4^+ adduct; [b] $(EO)_7$ oligomer, NH_4^+ adduct

4.3.1.2.2.2 Response over a range of Silwet L-77 concentrations

Linearity in the relative response of Silwet L-77 over the 0.25 – 5 ppm concentration range, with Agral-90 as the internal standard, was achieved with both 1:1 and 2:1 MeOH/H_2O as the elution solvent (Figure 4.5). The best lines of

fit showed linear regressions of greater than 0.99 agreement for both solvent systems investigated.

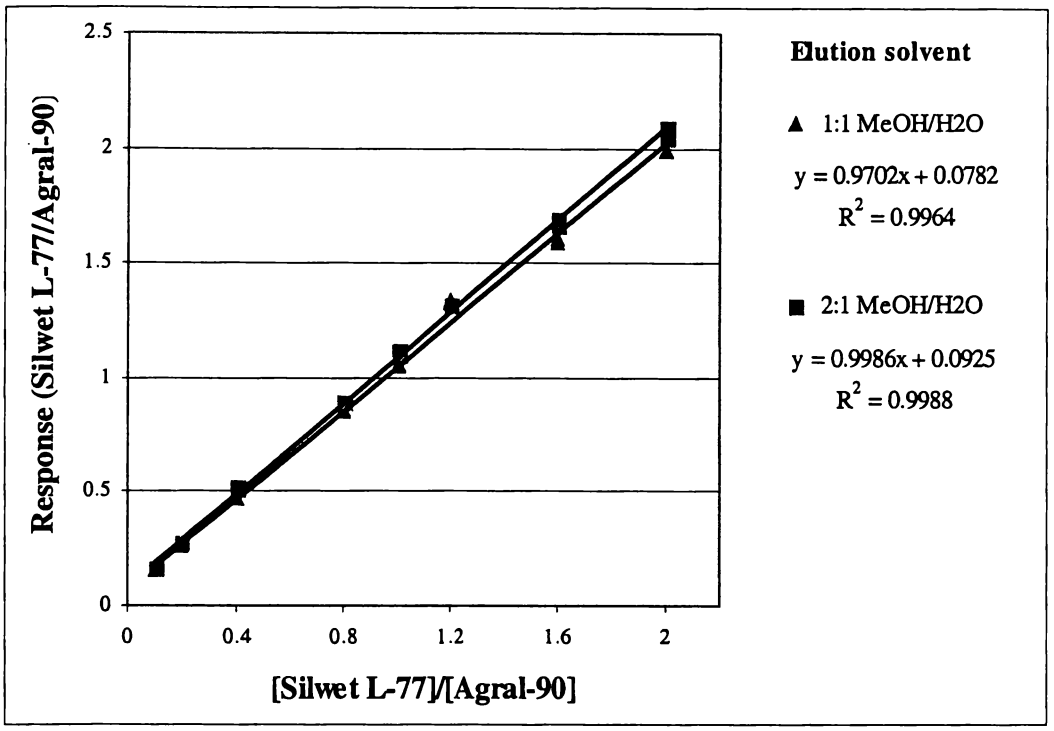

Figure 4.5. Relative response of Silwet L-77 as a function of concentration with Agral-90 as the internal standard (SIR, [Agral-90] = 2.5 ppm)

4.3.1.2.3 PPG-425 as the internal standard

4.3.1.2.3.1 Response factor reproducibility

The standard deviations in the response factors obtained with PPG-425 as the internal standard were higher than for both other internal standards previously investigated (Tables 4.10 and 4.11). Despite the addition of $CH_3CO_2NH_4$, the intensity of the K^+ adducts was significant, and thus was also included in the calculations. The effect of including the K^+ adducts on the resulting standard deviation was variable. The standard deviation of the relative response factors was less than the standard deviations obtained for the absolute responses in both cases.

Table 4.10. Response factor reproducibility with surfactant concentrations of 0.5 ppm

Response (x 10^5)	TIC	PPG-425[a]	Silwet L-77[b] NH_4^+ adduct	Silwet L-77[c]/ PPG-425	Silwet L-77[b] K^+ adduct	Σ (Silwet L-77 adducts)[d]	Silwet L-77 [e]/ PPG-425
Average*	5.6	3.4	1.8	0.52	0.38	2.2	0.62
SD	0.4	0.2	0.1	0.02	0.08	0.2	0.03
CV	6.6%	5.9%	6.3%	3.9%	19.7%	8.1%	4.7%

* Average of 10 injections; [a] $(EO)_6$ oligomer, Na^+ adduct; [b] $(EO)_8$ oligomer; [c] NH_4^+ adduct; [d] NH_4^+ and K^+ adducts; [e] Σ (Silwet L-77 NH_4^+ and K^+ adducts)

Table 4.11. Response factor reproducibility with surfactant concentrations of 2.5 ppm

Response (x 10^5)	TIC	PPG-425[a]	Silwet L-77[b] NH_4^+ adduct	Silwet L-77[c]/ PPG-425	Silwet L-77[b] K^+ adduct	Σ (Silwet L-77 adducts)[d]	Silwet L-77[e]/ PPG-425
Average*	19	11.6	5.2	0.45	2.8	8.0	0.70
SD	1	0.6	0.3	0.02	0.3	0.5	0.02
CV	5.8%	5.5%	6.3%	5.2%	9.5%	6.5%	3.3%

* Average of 10 injections; [a] $(EO)_6$ oligomer, Na^+ adduct; [b] $(EO)_8$ oligomer; [c] NH_4^+ adduct; [d] NH_4^+ and K^+ adducts; [e] Σ (Silwet L-77 NH_4^+ and K^+ adducts)

4.3.1.2.3.2 Response over a range of Silwet L-77 concentrations

Linearity in the relative response of Silwet L-77 was not obtained with PPG-425 as the internal standard. This is most likely due to the different physico-chemical properties of the two compounds. As discussed in Chapter 1, in order for the equation $I_A / I_B = [A]^+ / [B]^+$ to be valid, A and B must have similar surface activities and ion evaporation coefficients.[17] Although not experimentally determined, the structural differences in these two compounds indicate a much lower surface activity for PPG-425 relative to Silwet L-77. The ion evaporation coefficients may also differ.

4.3.1.2.4 Summary of internal standard determinations

In general, the standard deviation of the relative response factors was less than the standard deviations obtained for the corresponding absolute responses, and were also significantly less with higher concentration. For all the internal standards investigated, the response ratios obtained for the two concentrations examined were not within experimental error. This inconsistency in the response ratio may provide difficulties in quantitation. As discussed in Chapter 1 (Section 1.2.5), the value of the k_A/k_B ratio is required for quantitative determinations (where A^+ is the analyte and B^+ is the internal standard). This can be obtained with the equation $k_A/k_B = I_A/I_B$ when $[A^+] = [B^+]$. It follows that if the I_A/I_B ratio is not constant over the concentrations investigated, as observed here, the equations presented to determine $[A^+]$ will not be applicable.

4.3.2 Megaflow ESI/MS method development

4.3.2.1 EXTERNAL STANDARD METHOD

4.3.2.1.1 Lower limit of detection

The lower limit of detection for Silwet L-77 by megaflow ESI/MS is determined to be 0.0005 ppm, or 0.5 ppb, for which a signal to noise ratio of greater than 2 was obtained (Table 4.12).

Table 4.12. Response of Silwet L-77 over a range of low concentrations by megaflow ESI/MS

[Silwet L-77] (ppm)	Average Response*	SD	CV	S/N
0	8169	1350	16%	-
0.0001	6960	454	6%	0.8
0.00025	11861	686	6%	1.4
0.0005	16502	868	5%	2.4
0.001	59234	3849	6%	7.2
0.01	88176	9471	11%	10.8
0.1	508734	15303	3%	62.3

* Average of five injections, SIR, n = 8 + 9 $(EO)_n$ oligomers, NH_4^+ and K^+ adducts

4.3.2.1.2 Upper limit of detection

The response of Silwet L-77 over a range of high concentrations is presented in Table 4.13. A levelling off in the response and increase in standard deviation was observed for the 500 ppm solution.

Table 4.13. Response of Silwet L-77 over a range of high concentrations by megaflow ESI/MS

[Silwet L-77] (ppm)	Average Response (x 10^7)*	SD (x 10^7)	CV
1	4.2	0.2	4%
10	17.3	0.5	3%
20	22.0	0.4	2%
50	28.2	1.5	5%
100	36.3	1.5	4%
200	37.9	1.2	3%
500	37.6	1.8	5%

* Average of five injections

A plot of the results is shown in Figure 4.6. A logarithmic increase with concentration is observed. The best logarithmic least-squares fit (R^2 = 0.9088) was obtained with inclusion of all the values. Using power and linear least-squares fit regressions gave $R^2 > 0.99$ only with the values up to the 20 ppm and 1 ppm, respectively. The upper limit of detection for Silwet L-77 is determined to be 100 ppm, for which power regression of the data gave a correlation coefficient of 0.98.

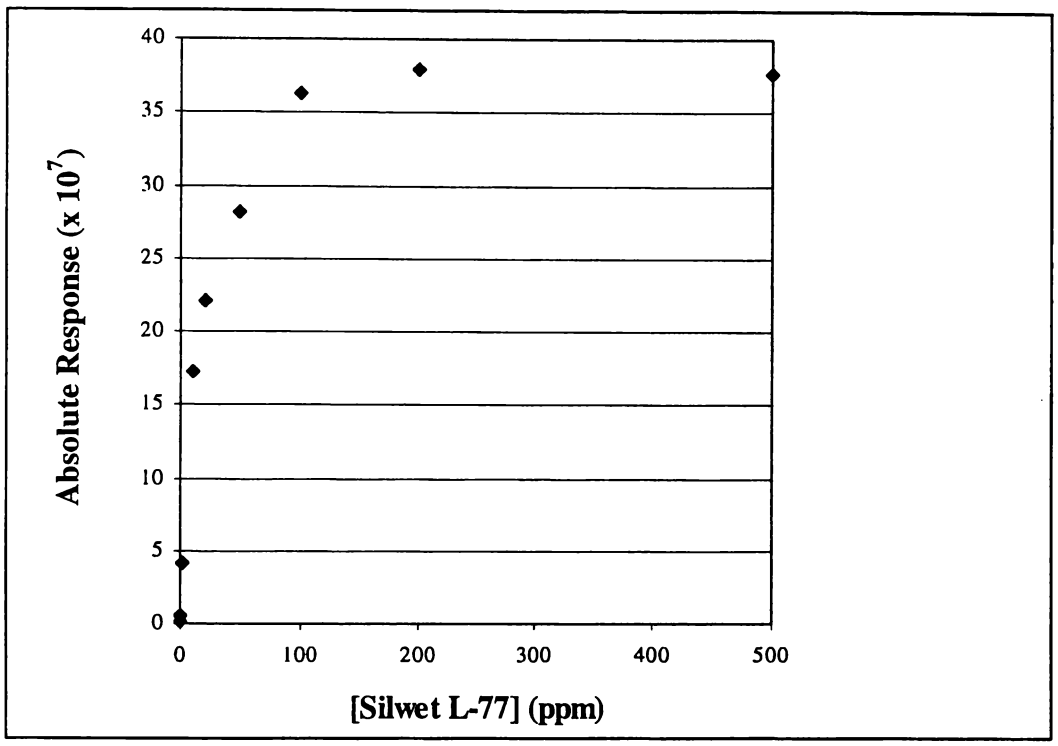

Figure 4.6. Response of Silwet L-77 over a range of high concentrations (megaflow ESI/MS)

4.3.2.1.3 Reproducibility

The highest response was observed when all of the adducts of the $(EO)_8$ and $(EO)_9$ oligomers were selected (Table 4.14). However, this setting also gave the largest standard deviation. Selection of the dominant adducts only (NH_4^+) gave a lower overall response, but also afforded a significant decrease in the standard deviation.

Table 4.14. Response reproducibility of Silwet L-77 at constant concentration

Oligomers	$(EO)_8$	$(EO)_8 + (EO)_9$	$(EO)_8 + (EO)_9$
Adducts	NH_4^+, K^+	NH_4^+	NH_4^+, K^+
Average *	1788836	2637584	3320883
SD	39694	41079	203808
CV	2.2%	1.6%	6.1%

* Average of 7 replicates

4.3.2.1.4 Response over a range of Silwet L-77 concentrations

The trace obtained for multiple injections of increasing concentrations of Silwet L-77 is shown in Figure 4.7. The plot of the absolute response as a function of concentration (Figure 4.8) shows a curvilinear response which correlates well with a power regression ($R^2 > 0.99$).

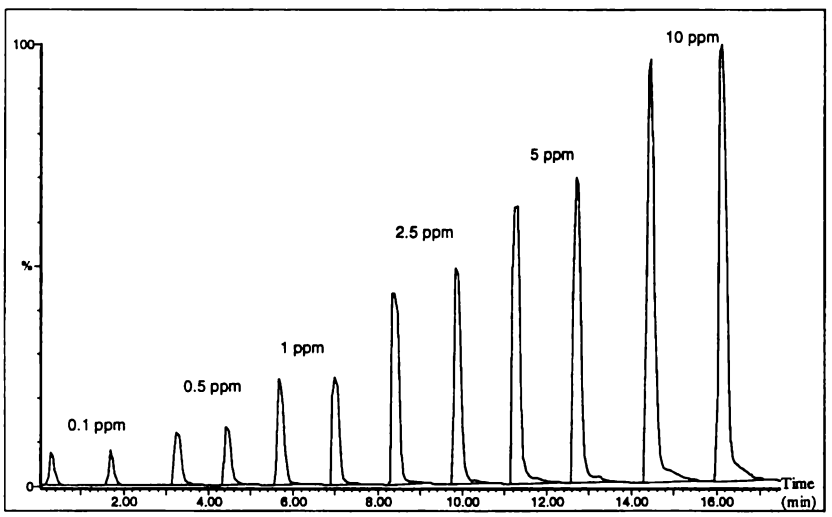

Figure 4.7. Trace of Silwet L-77 response with successive injections of increasing concentration

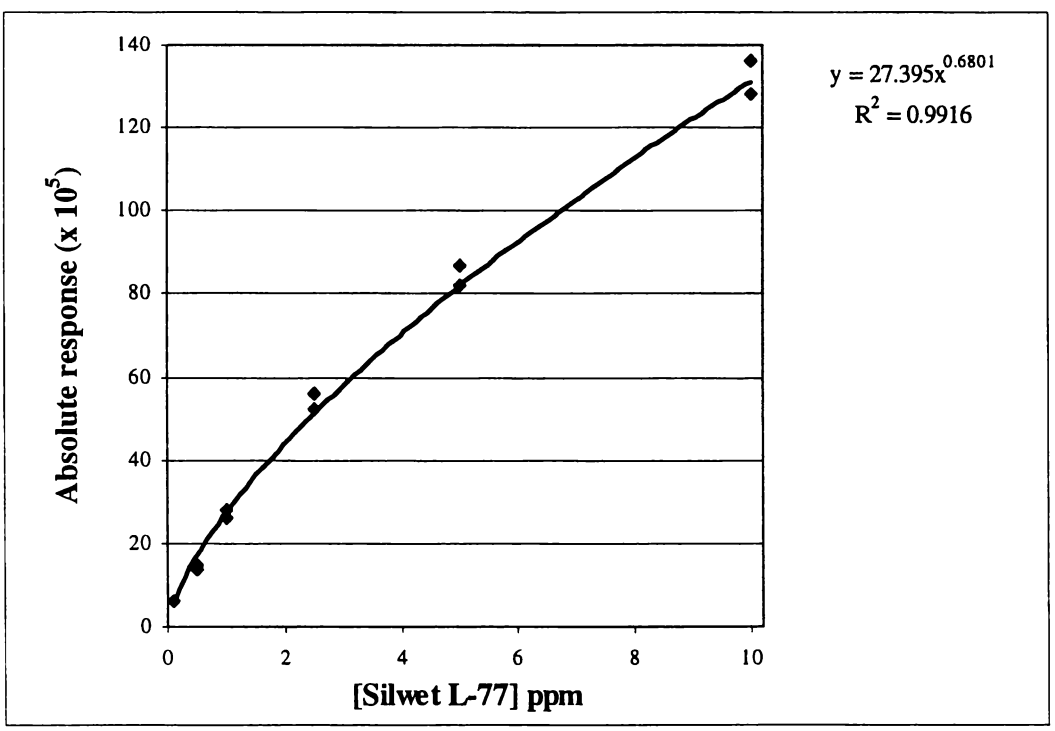

Figure 4.8. Response of Silwet L-77 over a range of concentrations (megaflow ESI/MS)

4.3.2.2 INTERNAL STANDARD METHOD

Agral-90 gave the best results for quantitation by standard ESI/MS and thus was investigated as a possible internal standard for megaflow ESI/MS. As discussed previously, difficulties were encountered in maintaining peak separation when using commercial surfactant formulations as internal standards for Silwet L-77 due to the large number of peaks in the resulting spectrum. The single oligomer surfactant molecule, $C_6(EO)_3$, was thus also investigated as a possible internal standard. The low molecular weight of this compound (234 $gmol^{-1}$) prevents overlap with Silwet L-77 peaks.

4.3.2.2.1 Agral-90 as the internal standard

4.3.2.2.1.1 Response factor reproducibility

The absolute and relative responses of Silwet L-77 with Agral-90 as the internal standard are presented in Table 4.15. The standard deviation of the relative response factor was less than the standard deviations obtained for the absolute responses.

Table 4.15. Response factor reproducibility of Silwet L-77 with Agral-90 as the internal standard

Response ($\times 10^6$)	TIC	Agral-90[a]	Silwet L-77[b]	Silwet L-77/ Agral-90
Average*	4.04	1.75	2.26	1.29
SD	0.08	0.04	0.06	0.02
CV	2.1%	2.5%	2.9%	1.2%

* Average of 6 replicates; [a] $(EO)_8$ oligomer, NH_4^+ adduct; [b] $(EO)_7$ oligomer, NH_4^+ adduct

4.3.2.2.1.2 Response over a range of Silwet L-77 concentrations

A linear relationship between response and concentration was achieved for Silwet L-77, using Agral-90 as the internal standard, with solvent flow-rates of both 0.3 (Table 4.16) and 0.2 mL min^{-1} (not shown for brevity). The best lines of fit of both sets of data show very good linearity ($R^2 > 0.99$) over the concentration range investigated (Figure 4.9).

Table 4.16. Response of Silwet L-77 over a range of concentrations with Agral-90 as the internal standard*

[Silwet L-77] (ppm)	[Silwet L-77]/ [Agral-90]	Response TIC (x 10^6)	Response Agral-90[a] (x 10^6)	Response Silwet L-77[b] (x 10^6)	Response (Silwet L-77/ Agral-90)	SD	CV
0.25	0.1	2.36	2.02	0.34	0.166	0.002	1.0%
0.5	0.2	2.65	2.04	0.58	0.283	0.001	0.3%
1.0	0.4	2.84	1.84	1.00	0.544	0.004	0.8%
2.0	0.8	3.13	1.56	1.57	1.005	0.003	0.3%
2.5	1.0	3.56	1.56	1.99	1.275	0.004	0.3%
3.0	1.2	3.86	1.45	2.31	1.591	0.029	1.8%
4.0	1.6	4.37	1.44	2.90	2.009	0.001	0.04%
5.0	2.0	4.67	1.30	3.35	2.568	0.028	1.1%

* Average of 2 replicates, Solvent flow-rate of 0.3 mL min^{-1}; [a] $(EO)_8$ oligomer, NH_4^+ adduct; [b] $(EO)_7$ oligomer, NH_4^+ adduct

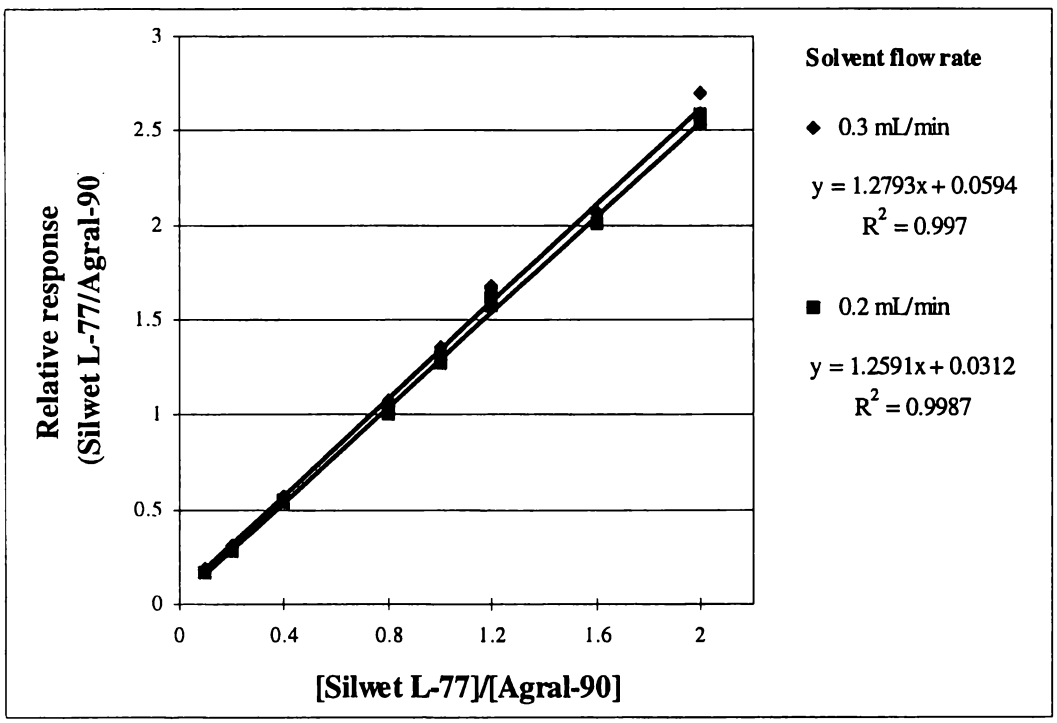

Figure 4.9. Relative response of Silwet L-77 over a range of concentrations with Agral-90 as the internal standard

4.3.2.2.2 $C_6(EO)_3$ as the internal standard

$C_6(EO)_3$ is potentially advantageous as an internal standard as it has a surfactant-type structure, yet is a single oligomer of low molecular weight and thus overlap with Silwet L-77 peaks is avoided.

The relative response data plotted as a function of concentration of Silwet L-77, although not linear, correlated well with a power regression curve (Figure

4.10). The correlation coefficient (R^2 = 0.987) was not as high as that obtained with Agral-90 as the internal standard (R^2 = 0.997).

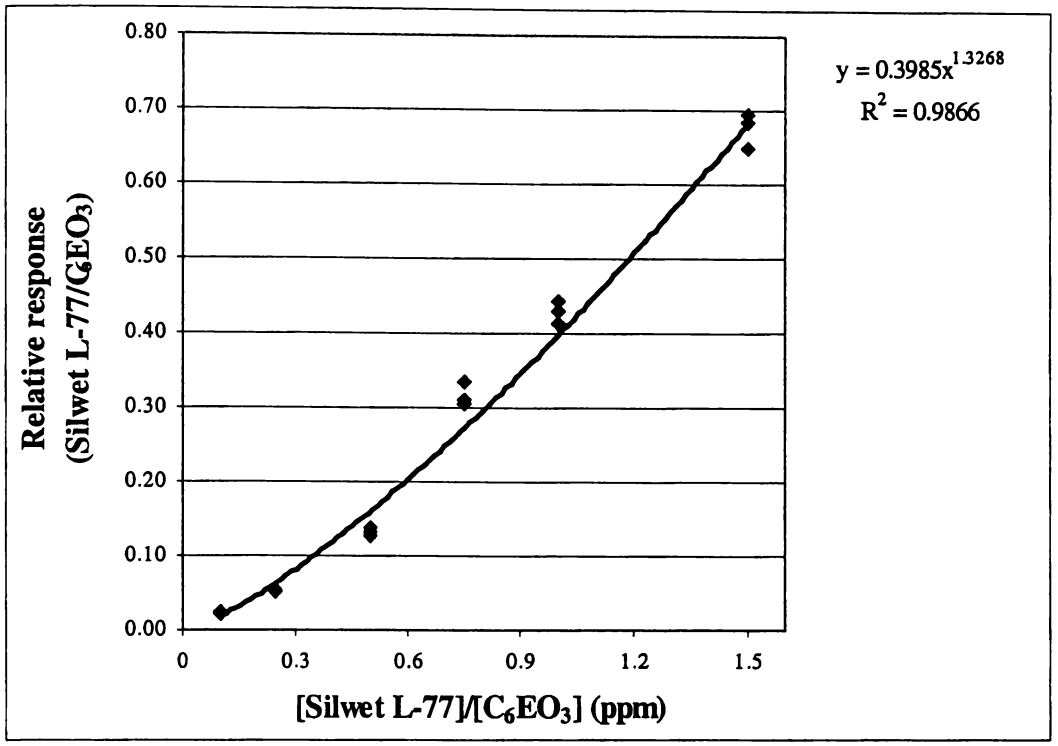

Figure 4.10. Relative response of Silwet L-77 over a range of concentrations with $C_6(EO)_3$ as the internal standard

The non-linear response with increasing Silwet L-77 concentration may be a result of differing ionisation efficiencies for $C_6(EO)_3$ and Silwet L-77. The low EO content of $C_6(EO)_3$ is likely to adversely influence the ionisation capacity of the molecule in the presence of Silwet L-77 (Ave. n ≈ 7.5) and may preclude their combination in quantitative analytical work.

4.3.3 APcI/MS method development

4.3.3.1 EXTERNAL STANDARD METHOD

4.3.3.1.1 Lower limit of detection

The lower limit of detection for Silwet L-77 by APcI/MS was determined to be 0.01 ppm, for which a signal to noise ratio of greater than 3 was obtained (Table 4.17).

Table 4.17. Response of Silwet L-77 over a range of low concentrations by APcI/MS

[Silwet L-77] (ppm)	Absolute Response	SD	CV	Signal /Noise Ratio
0	1148	325	28.3%	1
0.0010	1246	110	8.9%	1
0.0025	1261	175	13.9%	1
0.0050	1217	209	17.2%	1
0.0075	2127	255	12.0%	2
0.01	3488	417	12.0%	3
0.1	13369	359	2.7%	12
1	56839	4017	7.1%	50
10	216847	3124	1.4%	189

4.3.3.1.2 Upper limit of detection

The upper limit of detection was not reached over the concentration range investigated (up to 10000 ppm). An increase in response was observed with all increases in concentration (Table 4.18, Figure 4.11). Sample elution times became excessively long at the higher concentrations rendering analyses at these concentrations impractical, although not impossible. Elution times for the initial peaks (10 ppm) were less than half a minute, but exceeded ten minutes for the higher concentrations (5000 and 10000 ppm).

Table 4.18. Response of Silwet L-77 over a range of high concentrations by APcI/MS

[Silwet L-77] (ppm)	Average Response*	SD	CV
10	8005849	327946	4.1%
20	11210091	479749	4.3%
50	14430620	891306	6.2%
100	22309088	1757845	7.9%
200	29572597	2224079	7.5%
500	62696257	11467694	18.3%
1000	104639589	6364418	6.1%
2000	186799120	11248658	6.0%
5000	360905024**	-	-
10000	518629632**	-	-

* Average of three injections; ** one injection only

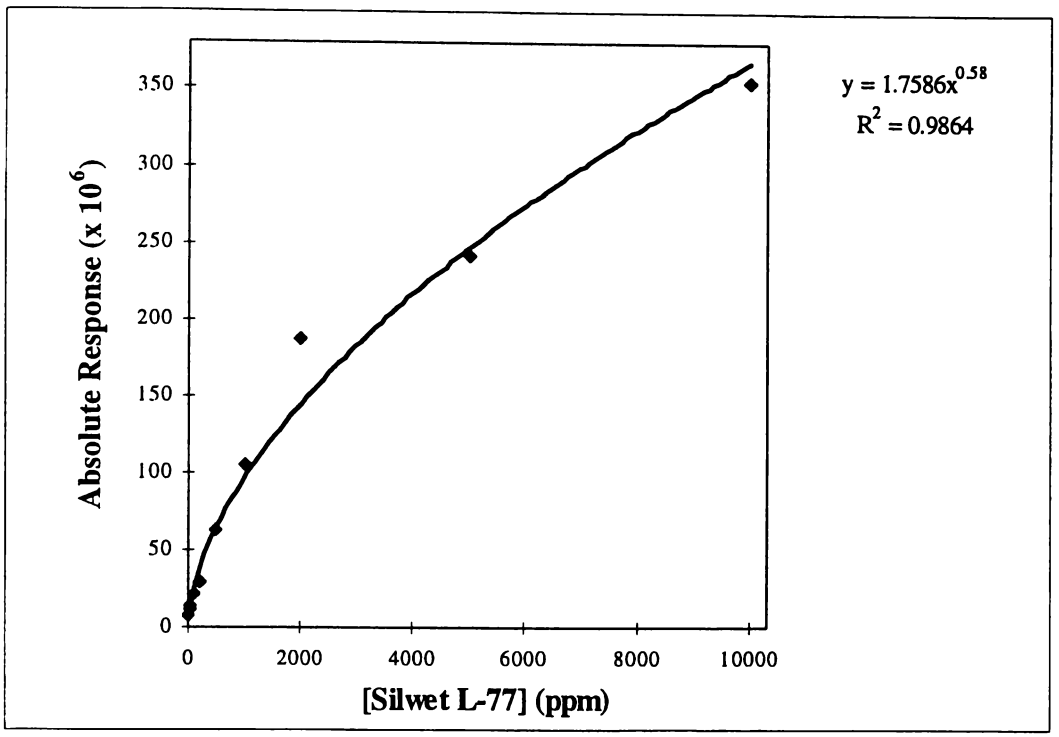

Figure 4.11. Response of Silwet L-77 over a range of high concentrations by APcI/MS

4.3.3.1.3 Reproducibility

The standard deviation obtained by APcI/MS was significant, as compared with that obtained with megaflow ESI/MS. Even in the presence of added ammonium acetate the Na^+ adducts dominated the APcI/MS spectrum, and thus these were selected for the reproducibility determinations. The use of ammonium acetate did not simplify, but rather complicated, adduct formation, and this may account for the large standard deviations obtained (Table 4.19).

Table 4.19. Response reproducibility of Silwet L-77 at constant concentration by APcI/MS

Adduct selected	Na^+
$(EO)_n$ oligomer/s selected	6 and 7
Average Response*	5404250
SD	278357
CV	5.2%

* Average of 7 injections

Because the Na^+ adducts tend to dominate the APcI/MS spectra it is possible that the addition of CH_3CO_2Na will improve the reproducibility by this method. This method has been adopted in other quantitative studies, although due to the non-volatile nature of the salt, system cleaning was required at regular intervals.[15]

The observation that Na^+ adducts dominate in the presence of added H^+ ions previously discussed, also implies that addition of a volatile acid to the mobile phase may improve quantitation. This method has been used in the analysis of NPEO and AEO surfactants in environmental waters,[14] however due to pH instability this is not a viable approach for Silwet L-77.

4.3.3.1.4 Response over a range of Silwet L-77 concentrations

A linear response was obtained for Silwet L-77 over the concentration range investigated, although the standard deviations in some cases were quite significant (Figure 4.12). The best regression coefficient (R^2 = 0.983) was obtained with a linear least-squares fit regression.

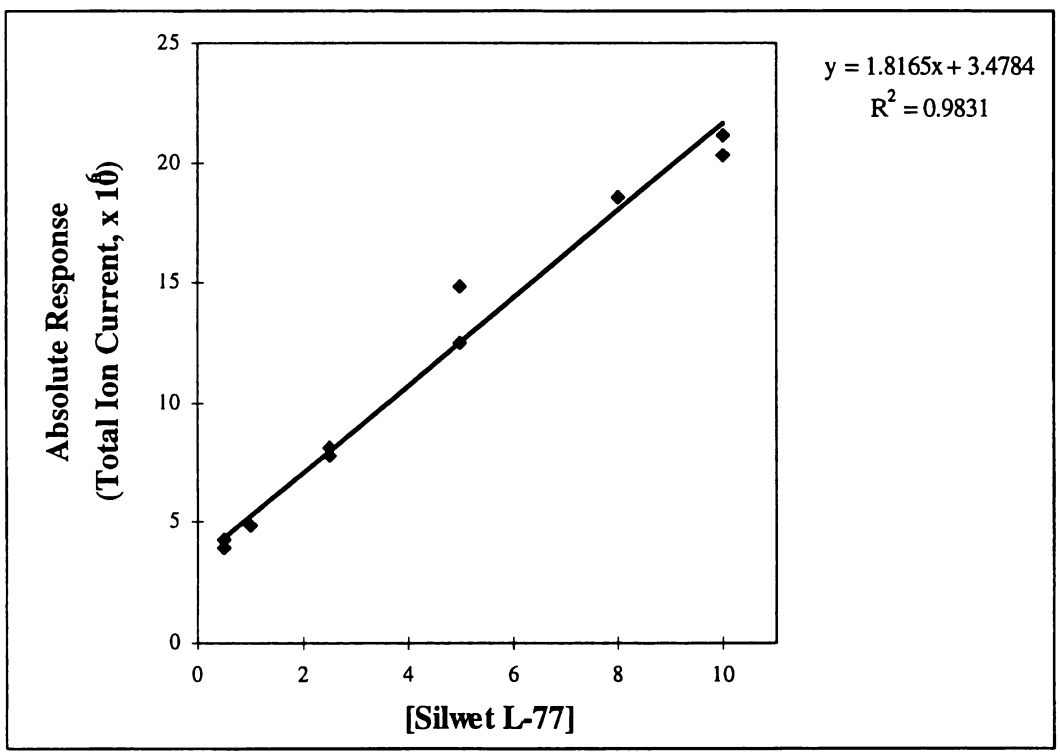

Figure 4.12. Response of Silwet L-77 over a range of concentrations by APcI/MS

4.3.3.2 INTERNAL STANDARD METHOD

The nonylphenol ethoxylate oligomeric mixture, Agral-100, and the single oligomer surfactant molecule, $C_6(EO)_3$ were investigated as possible internal standards for APcI/MS.

4.3.3.2.1 Agral-100 as the internal standard

Agral-100 was used in place of Agral-90, in order to remove all unnecessary components from the analyte mixture. It was hoped this would improve the quantitation, although no direct evidence for this was obtained.

4.3.3.2.1.1 Response factor reproducibility

The standard deviations obtained were quite significant for both the absolute responses and the relative response (Table 4.20).

Table 4.20. Response factor reproducibility of Silwet L-77 with Agral-100 as the internal standard*

	TIC	Agral-100[a]	Silwet L-77[b]	Silwet L-77/ Agral-100
Average response** (x 10^6)	9.0	4.7	4.3	0.92
SD	0.4	0.3	0.4	0.09
CV	4.9%	6.0%	8.7%	10.4%

* 2.5 ppm; ** Average of 7 replicates; [a] $(EO)_7$ oligomer, Na^+ adduct; [b] $(EO)_6$ oligomer, Na^+ adduct

4.3.3.2.1.2 Response over a range of Silwet L-77 concentrations

A linear response was obtained for Silwet L-77 over the concentration range investigated (Table 4.21). The plot of the data gave a linear regression of $y = 0.8481x + 0.1127$, with an R^2 of 0.997. In general, the standard deviation of the relative response factors was less than the standard deviations obtained for the corresponding absolute responses, and was also less at higher concentration. The correlation coefficient was equal to that obtained by megaflow ESI/MS with Agral-90 as the internal standard.

Table 4.21. Response of Silwet L-77 over a range of concentrations with Agral-100 as the internal standard*

[Silwet L-77] (ppm)	[Silwet L-77]/ [Agral-100][a]	Response TIC (x 10^6)	Response Agral-100[a] (x 10^6)	Response Silwet L-77 (x 10^6)	Response (Silwet L-77/ Agral-100)	SD	SD (%)
0.25	0.1	6.7	5.6	1.0	0.19	0.01	7%
0.5	0.2	7.5	5.9	1.6	0.275	0.007	3%
1.25	0.5	8.4	5.4	3.0	0.55	0.02	4%
2.5	1.0	8.8	4.4	4.4	0.995	0.005	1%
4.0	1.6	10.3	4.2	6.0	1.44	0.05	4%
5.0	2.0	11.0	4.1	7.4	1.82	0.07	4%

*Average of two injections; [a] [Agral-100] = 2.5 ppm;

4.3.3.2.2 $C_6(EO)_3$ as the internal standard

A linear response was obtained for Silwet L-77 over the concentration range investigated (Figure 4.13). In general, the standard deviation of the relative response factors was less than the standard deviations obtained for the corresponding absolute responses. The linearity and correlation to the best fit regression was improved as compared to that obtained by megaflow ESI/MS.

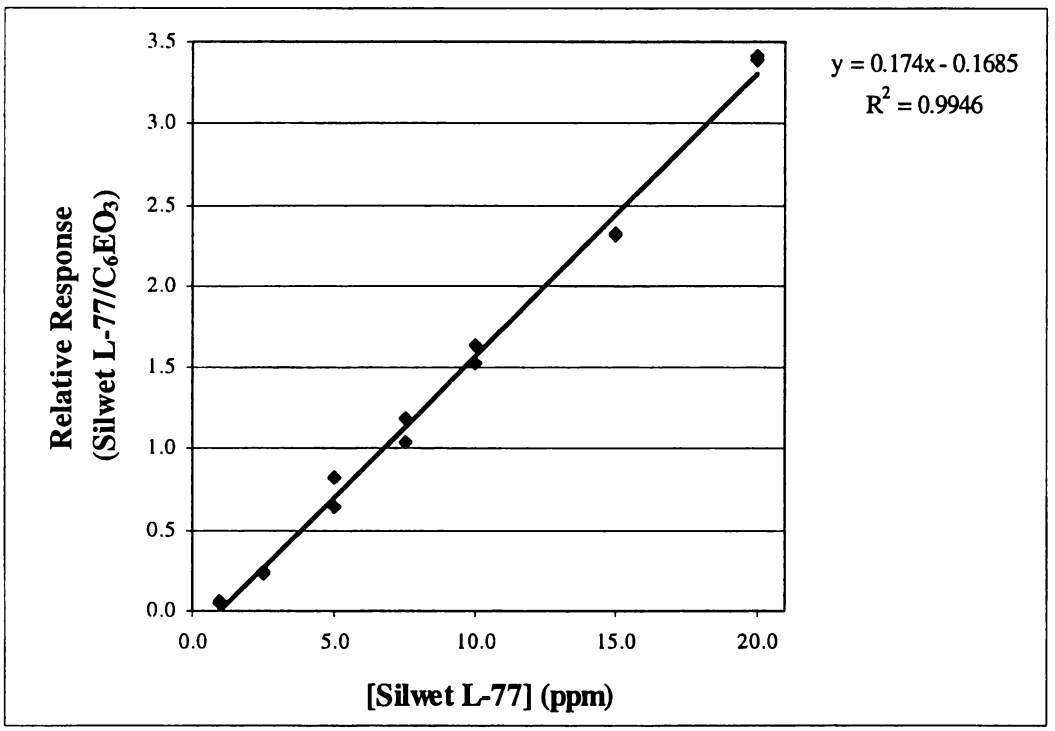

Figure 4.13. Relative response of Silwet L-77 over a range of concentrations with $C_6(EO)_3$ as the internal standard (APcI/MS)

4.3.4 HPLC/APcI/MS method development

Utilisation of an online HPLC column to separate out components of a mixture avoids ion overlap and also removes the problem of ionisation competition, an inherent problem of the analysis of mixtures by API/MS techniques. The adverse effect of impurities interfering with response is also reduced with the use of a separation system prior to detection.

Conditions such that all the Silwet L-77 oligomers were coeluted were selected. This simplifies quantitation, enhances the detection levels, and reduces analysis time. Furthermore, because analysis is in the total ion mode the need to control adduct formation is also removed. The adverse effect of response suppression observed for mixtures does not seem to apply to oligomers of the same surfactant. Presumably this is because compounds of the same structure

exhibit similar response factors. This method has also been successfully adopted elsewhere.[14] It is possible to obtain information on individual oligomers by subsequent extraction of the required ion chromatograms, although care should be taken in the interpretation of such data. It has been noted that although the overall response does not appear to be adversely affected, the ionisation competition inherent to API/MS of mixtures will still be active, and therefore a depression of short chain oligomers by long chain analogues will probably result. This will yield a distorted oligomer distribution with the extracted ion chromatograms as compared with that obtained with separation of each oligomer prior to detection.[18] This was demonstrated by plotting the response vs $(EO)_n$ obtained from separately injected solutions of a range of alcohol ethoxylate oligomers. An exponential increase in response for the $(EO)_1$ to $(EO)_6$ oligomers was observed with a less significant increase for the $(EO)_6$ to $(EO)_8$ oligomers. When the same compounds were injected simultaneously a general decrease in the response was observed for all compounds, and the decrease was much more pronounced for the smaller oligomers. The absolute decreases were comparable for all oligomers, but due to lower responses for lower oligomers, the effect of the decrease was proportionately larger.[14]

The relative response curve for Silwet L-77 with Triton X-45 as the internal standard under HPLC/APcI/MS is shown in Figure 4.14. The lowest concentration measured (0.07 ppm, 0.7 ng injection aliquot) was well within the range of detection for the APcI/MS method (Table 4.23). This was below the limit of detection by conventional HPLC (light scattering mass detection) even with a fifty-fold higher injection volume (500 μL). This demonstrates the improved detection limits possible with this analytical method.

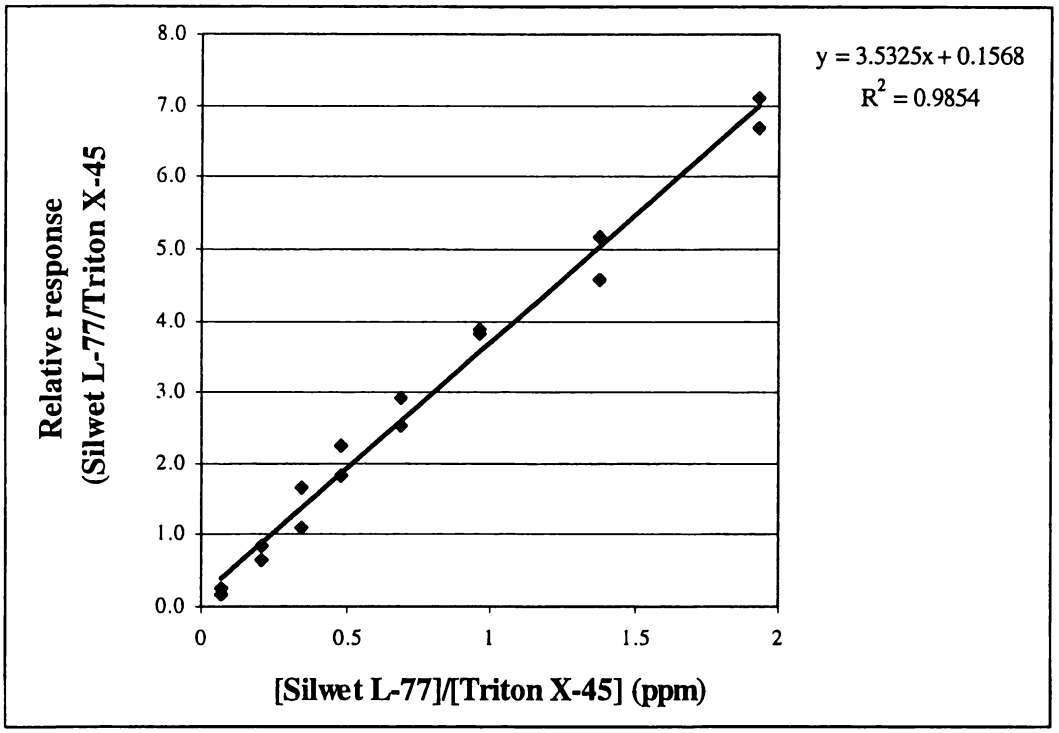

Figure 4.14. Standard curve results for Silwet L-77 with Triton X-45 as the internal standard as determined by HPLC/APcI/MS

The data are presented in Table 4.22, along with the results from parallel analysis by HPLC (light scattering mass detection) for comparison. The HPLC data do not correlate nearly as well to the least-squares fit trendline (power regression, R^2 = 0.9219) as compared with the results obtained by HPLC/APcI/MS (linear regression, R^2 = 0.9854).

Table 4.22. Relative response of Silwet L-77, with Triton X-45 as the internal standard, as determined by HPLC and HPLC/APcI/MS

	HPLC			HPLC/APcI/MS		
[Silwet L-77] (ppm)	Average Response* (Silwet L-77/ Triton X-45)	SD	CV	Average Response* (Silwet L-77/ Triton X-45)	SD	CV
0.07	0.11	0.11	102%	0.21	0.07	31%
0.21	ND**	ND	ND	0.74	0.13	17%
0.34	0.40	0.08	21%	1.37	0.40	29%
0.48	0.57	0.06	10%	2.04	0.31	15%
0.69	0.91	0.08	9%	2.73	0.27	10%
0.97	1.18	0.17	15%	3.85	0.03	1%
1.38	1.89	0.19	10%	4.87	0.41	9%
1.93	2.88	0.28	10%	6.89	0.31	4%

* Average of two injections; ** ND = Not detected

4.3.5 Summary of API/MS quantitative methods

The results obtained in this section validate the application of standard ESI/MS, megaflow ESI/MS and APcI/MS in theory to the quantification of Silwet L-77. The low levels, of the order of parts per billion, at which the surfactant can be measured, and the linear response with respect to concentration, illustrate the potential of this technique in the analysis of low-level environmental samples. Application of the technology to routine analysis of large numbers of samples however, may favour the use of the higher flow methods. The use of a solvent splitter should enable the application of standard ESI/MS to quantitative studies, although sensitivity by this method will be compromised as a result of smaller sample delivery to the detector.

The data obtained for response as a function of concentration, with and without internal standards present, correlated to least-squares fit trendlines with high regression coefficients for all methods investigated. Without the use of internal standards the response was curvilinear, and thus correlated better with power regressions. In practice however, internal standards are considered essential in quantitative analyses in order to correct for handling or recovery losses and detector fluctuations.

Megaflow ES/MS was found to be the most sensitive of the API/MS methods investigated, whilst analysis of higher concentrations could be achieved by APcI/MS. The lower limit of detection (S/N > 2) for standard ESI/MS and APcI/MS was found to be 0.01 ppm, whilst for megaflow ESI/MS it was fifty-fold lower at 0.0005 ppm. The upper limit of detection was greatest for APcI/MS, exceeding 10 000 ppm, whilst for megaflow ES/MS it was 200 ppm. Analysis over a wide range of concentrations (10^6) was possible for both megaflow ES/MS and APcI/MS, APcI/MS showing the larger range of the two. Both methods could comfortably analyse between 0.01 and 100 ppm, with megaflow ES/MS also capable of analysing samples less concentrated than these, and APcI/MS able to analyse more concentrated samples. The linear dynamic range for HPLC/APcI/MS was not determined. However linearity was observed with standards down to 0.07 ppm (lowest concentration analysed). Parallel analysis of the standards by HPLC (light scattering mass detection) demonstrated the

improvements to the detection limit and reproducibility obtainable with the HPLC/APcI/MS method.

4.3.6 APPLICATION TO FOLIAGE RESIDUE SAMPLES

In this section the high flow rate methods developed previously are applied to foliage residue samples in order to validate the use of the methods for routine quantitative analyses. Plant wash-off samples and standards were analysed by the API/MS analytical methods developed and the results verified by parallel determinations with established HPLC methods. The focus of this section is solely the API/MS analytical methods and thus the plant treatments and results are discussed in more detail elsewhere (See Chapter 5).

4.3.6.1 *Chenopodium album* study by flow injection API/MS

Silwet L-77 was applied to *C. album* plants and the wash-off solutions analysed by flow injection API/MS methods. Megaflow ESI/MS did not yield good results, as complicated adduct formation was observed, even with the addition of salts. This resulted in peak overlap with the internal standard, also an oligomeric mixture showing extensive adduct formation. In plant extracts and residue wash-offs it is impossible to control the cations present, and addition of $CH_3CO_2NH_4$ in the hope of swamping the spectra with one adduct proved to be ineffective. In APcI/MS mode the spectra were simplified to the Na^+ adducts of Silwet L-77.

Standard solutions using Agral-90 as the internal standard were prepared (as described in Chapter 5) and were measured at the beginning, middle and end of the analyses of the washoff samples (i.e. every 2 hours). The equation, $I_A / I_B = [A]^+ / [B]^+$ (Refer to Section 1.2.5),[17] was used to determine the concentration of Silwet L-77 ($[A]^+$) from the relative response ratio. The best regression coefficients were obtained using the power least-squares fit trend-line for all the standard curves. The regression coefficients became sequentially lower over the course of the analysis period (~6 hours). The percentage uptake values for the surfactant from the washoff samples were calculated using all three least-squares fit equations (obtained at the beginning, middle and end of the analysis) and are presented in Table 4.23. A relatively large variation in the values was obtained

depending on the equation used. The values shown in bold correspond to the standard curve obtained nearest in time to the washoff samples.

Table 4.23. Comparison of %Uptake of Silwet L-77 into *Chenopodium album* as determined by HPLC and APcI/MS[a]

[Silwet L-77] ($g\ L^{-1}$)	Time (minutes)	Silwet L-77 [HPLC]	Silwet L-77 [APcI/MS][b]	Silwet L-77 [APcI/MS][c]	Silwet L-77 [APcI/MS][d]
Least-squares fit[e]		$y = 0.0009x^{1.0498}$	$y = 2.0258x^{0.7334}$	$y = 2.373x^{0.7503}$	$y = 1.7283x^{0.7640}$
R^2		0.9249	0.9943	0.9896	0.9607
		%Uptake (SD)[f]	%Uptake (SD)	%Uptake (SD)	%Uptake (SD)
1	10	58 (13)	57 (11)	**64 (9)**	45 (13)
	30	49 (16)	66 (12)	**72 (10)**	56 (14)
	240	ND[g]	77 (5)	**80 (4)**	69 (6)
2	10	65 (8)	**70 (5)**	75 (4)	61 (6)
	30	67 (6)	**70 (5)**	75 (4)	61 (6)
	240	94 (26)	**84 (4)**	86 (3)	79 (5)
5	10	36 (6)	58 (8)	66 (6)	**49 (9)**
	30	56 (9)	72 (9)	77 (7)	**65 (11)**
	240	86 (17)	89 (2)	91 (2)	**85 (3)**

[a] SIR, 2 channels selected [$(EO)_6$ oligomers of Silwet L-77 and Agral-90]; [b] Data generated with standard curve obtained at the beginning of the analysis; [c] Data generated with standard curve obtained at the middle of the analysis; [d] Data generated with standard curve obtained at the end of the analysis; [e] y = relative response (Silwet L-77/Agral-90), x = [Silwet L-77]/[Agral-90]; [f] SD = Standard deviation; [g] ND = Not detectable

The variation in the standard curve data with time indicates that standard curves should be acquired regularly (i.e. at least every two hours) throughout quantitative analyses, and the sample data should be analysed with the closest corresponding standard curve data.

The APcI/MS and HPLC data were within replicate standard deviation for all but one of the values (0.1%, 30 minutes). In general, lower standard deviations are observed for the APcI/MS data, and in all cases the regression coefficients are better with APcI/MS. Furthermore the APcI/MS method demonstrated a much lower limit of detection, where some solutions (0.1%, 240 minutes) were of too low a concentration to be detected by the HPLC method.

A 50% uptake of the 0.1% surfactant solution corresponded to a ~0.5 ppm (480 ng mL^{-1}) solution. This equated to injection aliquots of 5 ng and 240 ng for APcI/MS and HPLC, respectively. This is well within the detection range of the

APcI/MS method, which is capable of detecting individual oligomers from samples containing 1 ng (0.1 ppm) or less of surfactant. This injection aliquot for HPLC (250 ng) however equated to the lower operational concentration limit for Silwet L-77, even with the detection enhancement achieved by coelution of the total surfactant content.[13] This makes the MS method potentially at least two thousand times more sensitive than the HPLC method. Good spectrum integrity was obtained for L-77 down to 10 ppb (0.1 ng) but at this concentration the standard deviation between replicate injections became large and is not recommended for routine quantitative analysis.

Overall, APcI/MS appears to be the preferred method of analysis over megaflow ESI/MS, for both accuracy and convenience. The effect of the matrix on the response is less significant, and due to the higher operational flow-rates the time required for sample analysis is much less.

Operationally, the MS analytical technique is much more convenient than the established HPLC methods. Little sample preparation is required and each MS analysis takes less than a minute, thereby speeding up sample throughput. Lower concentrations can be analysed, leading to fewer leaves treated, and removing the need to concentrate solutions, so greater sensitivity is possible and hence lower levels can be analysed.

Against that is the need to carefully select the analytical mode required, depending on analyte structure, and to obtain operational conditions that provide reproducible and linear responses to increasing mass or concentration. Multiple pseudo-parent ions must be identified and the conditions adjusted such that there is effectively only one dominant ion. Other ions present in the matrix impart a considerable influence on response of the analyte and in cases where this cannot be controlled will provide difficulties in flow injection analysis.

4.3.6.2 Citrus study by flow injection API/MS

The flow injection API/MS methods used in Section 4.3.2.1.1 were applied to citrus leaf washoff samples without success. Analysis of the samples by APcI/MS and megaflow ESI/MS with and without internal standard present, was attempted. Plots of relative response as a function of relative concentration gave least-squares fit regressions with high coefficients in all cases. However washoff results were

not in agreement with results from the parallel HPLC method, and often gave values in excess of 100% recovery (Appendix A.IV.2).

In Chapter 1 an equation (1.1) enabling quantitation by flow injection API/MS was given. The k_A / k_B ratio is required, and can be determined using the relationship, k_A / k_B = I_A / I_B. It was noted that although the k_A / k_B ratio is not constant over a wide concentration range, it should be constant at high (>10^{-5} $molL^{-1}$) or low (<10^{-5} $molL^{-1}$) concentrations. The $I_{Silwet\ L\text{-}77}$ / $I_{Agral\ 90}$ ratios over a large concentration range are shown in Table 4.24 and Figure 4.15. The ratio is highly variable and thus indicates that the use of Equation 1.1 for the quantitation of Silwet L-77 and Agral-90 mixtures may not be possible.

Table 4.24. Relative response of Silwet L-77, with Agral-90 as the internal standard, over a range of concentrations (Silwet L-77: Agral-90 concentration ratio constant)

[Surfactant] (ppm)	[Surfactant] (mol L^{-1})	Average relative response * (Silwet L-77/Agral-90)
0.005	1.0 x 10^{-8}	1.39
0.05	1.0 x 10^{-7}	0.63
0.25	5.0 x 10^{-7}	0.49
0.5	1.0 x 10^{-6}	1.28
1.25	2.5 x 10^{-6}	1.14
2.5	5.0 x 10^{-6}	0.88
5	1.0 x 10^{-5}	1.20

*Average of three injections; Background response = 1.14

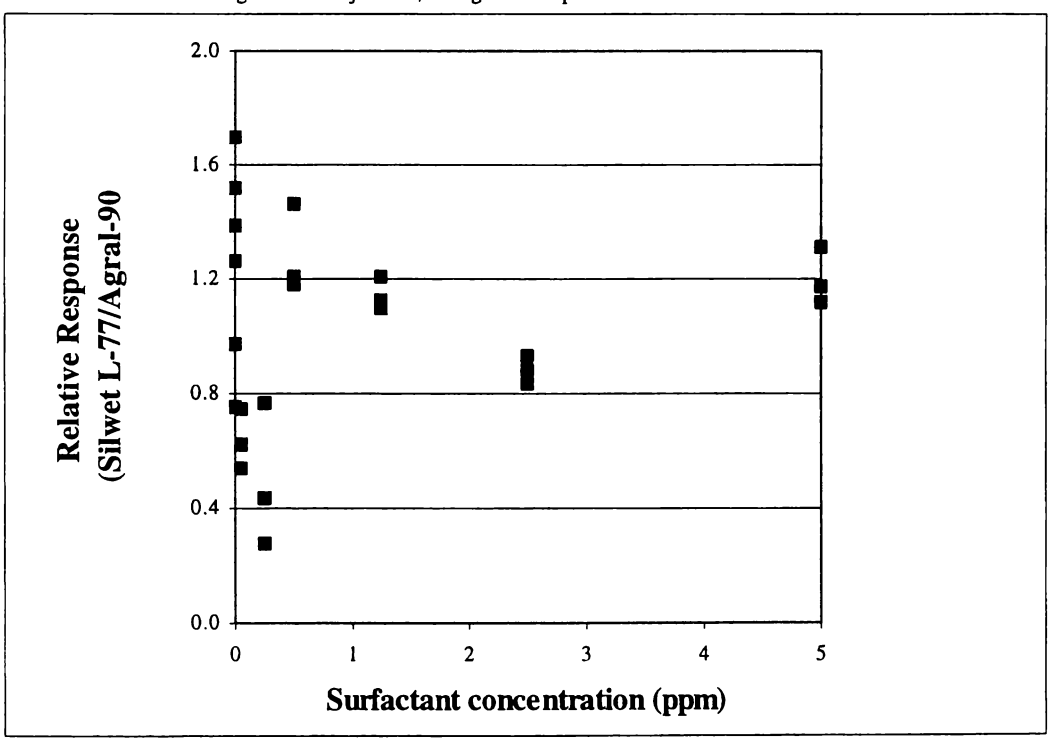

Figure 4.15. Relative response of Silwet L-77 with Agral-90 as the internal standard, over a range of concentrations (Silwet L-77: Agral-90 concentration ratio constant)

A response curve for separate solutions of the surfactants, Silwet L-77 and Agral-90 (using the response from the single $(EO)_6$ oligomers) under APcI/MS is shown in Figure 4.16. Although the responses are not linear over the entire concentration range, both curvilinear fits gave $R^2 > 0.99$. At the two lowest concentrations, the response of Agral-90 exceeds that of Silwet L-77, in contrast to the trend observed at higher concentrations, which indicates that linearity may not be achieved over a wide concentration range.

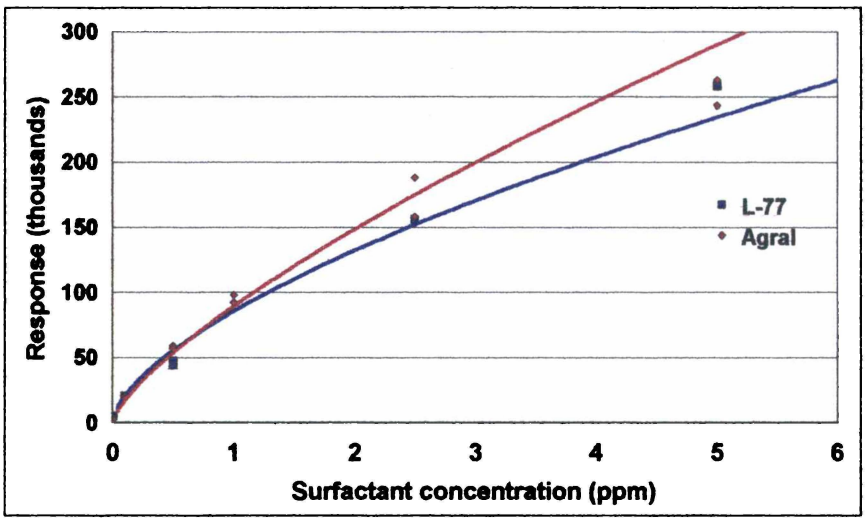

Figure 4.16. Absolute response of separate solutions of Agral-90 and Silwet L-77 [$(EO)_6$ oligomers]

In this (n = 7) and the previous study (Section 4.3.2.1.1, n = 6) only the response of a single Silwet L-77 oligomer was monitored. However in these results, the response observed for the washoffs was higher than that for the standards corresponding to ≥100% recovery. This is initially counterintuitive, as, due to a potentially higher background matrix in washoffs, a lower than actual response, if anything, would be expected as a result of ionisation competition effects. The observed result implies that either (i) the other unquantified ions in the mixture (i.e. other surfactant oligomers) are of lower concentration than in the standard solution (i.e. the initial commercial blend), or (ii) the analyte response is being enhanced by the matrix. The former (i) explanation would be possible only if the other oligomers were more readily taken up into plants. However, this is not expected on the basis of results obtained from subsequent single oligomer studies. As described in Chapter 5, the percentage uptake for the n = 6 oligomer into *C. album* was one of the highest for the oligomers investigated. Response

enhancement (ii) may be possible due to an increased concentration of cations in the matrix of the washoffs, causing an increase in the concentration of adducts with the nonionic analyte.

According to the quantitative methods proposed by Kebarle et.al.[1] and Guilhaus et.al.[2] all ions in the reaction mixture should be monitored. In the quantitation of complex mixtures such as those analysed here this is not a practical option as data analysis times would become excessive. The method adopted here, and in the previous section, selected a single oligomer from within the surfactant formulation and assumed the uptake of this oligomer was representative of the entire mixture. Popenoe et.al. proposed a model that determines total surfactant concentration from measured data from selected components only, according to known surfactant distribution.[19] Both these methods assume the distribution of oligomers is unchanged from the original blends, and thus must be used with caution when analysing extracts from the environment/plants. Variations in uptake for different oligomers into plants is well documented (discussed further in Chapter 5) and sorption properties also vary with polarity. If however, the distribution of oligomers is unchanged from the original blends, then this model may be especially useful in the analysis of surfactants by the flow injection method. This model takes into account all compounds present and thus may compensate for ionisation suppression experienced by analytes in API/MS mixtures.

The trisiloxane surfactants are renowned for their ability to lower surface tension of solutions to very low levels.[20] Their ability to wet surfaces beyond levels implied by their surface tension indicates that adsorption/migration to the phase interfaces is also considerably higher than for conventional surfactants. Analysis of a 0.25 μL droplet of Silwet L-77 showed a decrease in the bulk solution concentration of more than 50% as a result of surfactant adsorption at the interfaces.[20] These properties may have a large bearing on analysis of mixtures containing these compounds by API/MS, due to the competitive nature of the ionisation process. If Silwet L-77 is preferentially locating to the outside of the charged droplet, then inconsistent response of other compounds present, i.e. the internal standard, with varying Silwet L-77 concentrations can be envisaged. Inaccurate quantitative data will thus result. It has also been reported however, that the organosilicone surfactants are often ineffective at altering surface tensions

or spread areas when mixed with most conventional surfactants (i.e. Triton X-45, Agral-90).[20] This would imply that quantitation may be possible.

From these results, it is clear that many issues complicate quantitation by flow injection API/MS methods. Data can not be considered reliable without fully characterising or controlling the contribution of these factors. The complicated nature of the ionisation of surfactant molecules, and their complex oligomeric composition indicate that online separation methods may be essential in order to obtain accurate quantitative data by API/MS methods.

4.3.6.3 *Chenopodium album* study by HPLC/APcI/MS

Methods for quantitation of surfactant mixtures by HPLC/API/MS are well established, and in fact all quantitative studies reported to date utilise an online HPLC system.

Silwet L-77 was applied to *C. album* plants and the washoff solutions analysed by standard HPLC and HPLC/APcI/MS. A comparison of the two sets of results obtained are shown in Table 4.25.

Table 4.25. Comparison of %Uptake of Silwet L-77 into *C. album* as determined by HPLC and HPLC/APcI/MS

Time (minutes)	HPLC %Uptake (SD)*	HPLC/APcI/MS %Uptake (SD)
5	34 (9)	35 (6)
30	47 (14)	44 (4)
120	72 (7)	75 (5)
240	82 (9)	83 (5)
Regression	linear	linear
R^2	0.971	0.983

* SD = standard deviation

The APcI/MS and HPLC data were within replicate standard deviation for all of the solutions analysed. Furthermore the HPLC/APcI/MS data showed lower standard deviation for the samples and a higher regression coefficient for the standard solutions. These results demonstrate the improved accuracy offered by HPLC/APcI/MS methods over conventional HPLC methods.

Conditions such that all the Silwet L-77 oligomers coeluted were selected. This simplified the quantitation, enhanced the detection levels, and reduced analysis time. Analysis was conducted in the total ion mode and thus accounted

for all the oligomers in the mixture, and furthermore removed the need to control adduct formation.

The development of the HPLC/API/MS analytical method enabled improvements in the applicability and consistency of results obtained from the API/MS methods investigated. Furthermore the HPLC/APcI/MS analytical method potentially offers the opportunity to study not only surfactant and herbicide uptake, but also individual oligomers and the presence of any metabolites or degradation products that may be produced over time. This method was used throughout the analyses presented in Chapter 5, and consistently reproducible and accurate results were obtained.

4.4 CONCLUSION

Consistently reproducible quantitative results were only obtained with the HPLC/APcI/MS method. A number of models have been proposed for the quantitation of mixtures by flow injection API/MS, as described in Chapter 1. However none of the models have been applied to the analysis of non-laboratory prepared samples, and the highly complex nature of the matrix in such cases may preclude the application of these methods. The matrix of environmental samples will often differ significantly from the matrix of the standards, and may either enhance or suppress analyte response. Quantitative data susceptible to interference should be thus be interpreted with caution, and avoided where possible. Methods that incorporate online HPLC separation are consequently a much more practical solution for the analysis of environmental samples as chromatographic purification will improve consistency between and therefore comparability of the sample and standard matrices. HPLC/APcI/MS is thus considered a superior method over any mathematical manipulations of data obtained by the flow injection method. In practice, time taken for the two methods may well be comparable.

In these investigations it was found that ionisation competition and variations in detector response are two factors which preclude accurate quantitation. The HPLC/APcI/MS method accounts for these sources of error by (i) enabling the use of an internal standard to account for detector fluctuations and yet (ii) separating the analyte and internal standard prior to detection such that suppression/enhancement of response is avoided.

4.5 REFERENCES

[1] P. Kebarle, L. Tang, *Anal. Chem.*, 1993, **65**, 972A-987A

[2] D.S. Selby, M. Guilhaus, J. Murby, R.J. Wells, *J. Mass Spectrom.*, 1998, **33**, 1232-1236

[3] D.S. Selby, personal correspondence, 5/5/00

[4] T. Covey, *Biochemical and Biotechnological Applications of Electrospray Ionisation Mass Spectrometry*, Ed. A.P. Snyder, ACS Symposium series 619, ACS, Washington DC, 1996, 21-59

[5] H. Ozaki, N. Itou, S. Terabe, Y. Takada, M. Sakairi, H. Koizumi, *J. Chromatogr. A.*, 1995, **716**, 69-79

[6] H. Ozaki, S. Terabe, *J. Chromatogr. A.*, 1998, **794**, 317-325

[7] L. Yang, A.K. Harrata, C.S. Lee, *Anal. Chem.*, 1997, **69**, 1820-1826

[8] K.L. Rundlett, D.W. Armstrong, *Anal. Chem.*, 1996, **68**, 3493-3497

[9] J. Varghese, R.B. Cole, *J. Chromatogr. A.*, 1993, **652**, 369-376

[10] K. Tang, A. Gomez, *Phys. Fluids*, 1994, **6**, 2317-2332

[11] *a.* C. Crescenzi, A. Di Corcia, R. Samperi, A. Marcomini, *Anal. Chem.*, 1995, **67**, 1797-1804; *b.* A. Di Corcia, *J. Chromatogr. A.*, 1998, **794**, 165-185; *c.* D.Y. Shang, M.G. Ikonomou, R.W. Macdonald, *J. Chromatogr. A.*, 1999, **849**, 467-482; *d.* D.D. Popenoe, S.J. Morris, III, P.S. Horn, K.T. Norwood, *Anal. Chem.*, 1994, **66**, 1620-1629; *e.* K.A. Evans, S.T. Dubey, L. Kravetz, S.W. Evetts, I. Dzidic, C.C. Dooyema, *J. Amer. Oil Chem. Soc.*, 1997, **74**, 765-773; *f.* M. Castillo, C.M. Alonso, J. Riu, D. Barcelo, *Environ. Sci. Tech.*, 1999, **33**, 1300-1306; *g.* S.D. Scullion, M.R. Clench, M. Cooke, A.E. Ashcroft, *J. Chromatogr. A.*, 1996, **733**, 207-216

[12] P. Kebarle, personal correspondence, 6/5/00

[13] W.A. Forster, K.D. Steele, J.A. Zabkiewicz, NZ FRI Bulletin No. 193, *Proc. 4th Int. Symp. on Adjuvants for Agrochemicals*, ed. R.E. Gaskin, Melbourne, 1995, 267-271

[14] C. Crescenzi, A. Di Corcia, R. Samperi, A. Marcomini, *Anal. Chem.*, 1995, **67**, 1797-1804

[15] D.Y. Shang, M.G. Ikonomou, R.W. Macdonald, *J. Chromatogr. A.*, 1999, **849**, 467-482

[16] K.A. Evans, S.T. Dubey, L. Kravetz, S.W. Evetts, I. Dzidic, C.C. Dooyema, *J. Amer. Oil Chem. Soc.*, 1997, **74**, 765-773

[17] P. Kebarle, L. Tang, *Anal. Chem.*, 1993, **65**, 3654-3668

[18] A. Di Corcia, *J. Chromatogr. A.*, 1998, **794**, 165-185

[19] D.D. Popenoe, S.J. Morris, III, P.S. Horn, K.T. Norwood, Anal. Chem., 1994, **66**, 1620-1629

[20] M. Knoche, *Weed. Res.*, 1994, **34**, 221-239

CHAPTER 5

Uptake of M_2D-C_3-O-$(EO)_n$-Me Surfactants and Herbicides into *Chenopodium album*

5.1 INTRODUCTION

Agrochemical active ingredients are classified as systemic or non-systemic depending whether they act within or on the surface of the plant, respectively. Non-systemic active ingredients often require complete and uniform foliage coverage for maximum effectiveness. In such cases, surfactant adjuvants can be added as spray modifiers to improve wetting/spreading properties of the formulations. Fungicides and insecticides commonly fall into this category.

Herbicidal active ingredients are often systemic and as such, can effect a number of vital metabolic processes in the plant. These include transpiration, respiration, uptake and translocation processes, photosynthesis, growth differentiation, mitosis, meiosis, and amino acid, protein, lipid, pigment and nucleic acid synthesis. Surfactants which aid foliar absorption and/or biological activity of systemic active ingredients are classified as activator adjuvants.

5.1.1 Activator adjuvants

The addition of surfactants to agrochemical formulations generally greatly enhances the uptake of systemic active ingredients into plant foliage.[1a-c] The uptake mechanisms of agrochemical formulations, and the role that surfactants play in this process, however are not well understood. The delivery of active ingredients to the target site depends on a number of factors, such as retention on the leaf surface and penetration through/into the cuticular wax, cuticle and leaf tissues.[2] There are many physical properties that can be influenced by surfactants to affect this process, including droplet spreading, drying times, hygroscopicity and permeability of the cuticle and cell membrane.[3]

Foliar penetration is a complex process involving a large number of variables, and as such, a number of different mechanisms may apply. The surfactant may enhance uptake at the leaf surface or at sites within the leaf. There are six potential mechanisms that can be envisaged for action on the leaf surface. These are (i) an increase in effective contact area, (ii) disruption of the epicuticular waxes, (iii) solubilisation of the active, (iv) prevention or delay of crystallisation

of the active, (v) a humectant-type action, and (vi) promotion of stomatal infiltration. Within the leaf and cuticle, the possible mechanisms of action include enhancement of solubility, partition and diffusion processes, activation of aqueous and/or lipid 'pathways', increased permeabilities of membranes, and copenetration.[1b] In this study, factors pertaining to uptake at the leaf surface are mainly addressed.

There are two distinct types of surfactant-induced uptake, non-interactive and interactive. In non-interactive activation, the rate of the surfactant penetration is relatively unchanged by the presence of the active. In interactive activation, the absorption of the surfactant is also affected, and this can be either by an increase or a decrease. Interactive facilitation tends to be dependent on surfactant concentration, and is often interpreted as co-penetration.[1b]

5.1.2 Modelling of foliar uptake

The enhancement of active uptake by surfactants is generally specific to the plant, surfactant and the agrochemical, and as such there is no one unifying mechanism. As a consequence, the development of agrochemical formulations is still largely empirical. The application of models to predict and optimise performance therefore offers tremendous potential economic and environmental benefits.

Uptake enhancement can be via stomatal infiltration or cuticular penetration. Stomatal infiltration is a mass flow process and is thus independent of the physico-chemical properties and concentration of the active.[4] Foliar penetration has been described as a partition/diffusion process,[1c] and as such fundamental physico-chemical principles can be applied to prognostic models for the process. There are indications that there are two pathways for cuticular entry, a 'lipophilic pathway' through the epicuticular wax and a hydrophilic pathway, known as the 'aqueous pathway'. Models based on octanol-water (log P_{ow}) and alkane-water (log P_{alk}) partition coefficients have been proposed to predict which of these pathways will predominate.[5] The validity of these values has however been challenged on the basis that they are solvent-solvent partition coefficients being used to describe the situation of foliar applied chemicals. Wax-water coefficients have also been used to model the process, however the applicability of this coefficient is also questionable, as agricultural sprays are, more accurately, hydrated formulations rather than aqueous systems.[2]

Increased experimental data has since become available which has enabled the development of more realistic models.[2,6a,b] Studies of penetration of surfactant formulations through isolated cuticles yielded partition coefficients (K_{Cfr}) which characterise the differential solubility between the cuticle and the formulation residue. This coefficient is currently considered more appropriate for modelling cuticle permeance. The aforementioned constants may however still be applicable to other stages in the uptake process, i.e. to predict diffusion rates from the cuticle into aqueous parts of the leaf, etc.[2]

5.1.3 Surfactant structure and the influence of EO content

Nonionic polyoxyethylene condensates are commonly used activator adjuvants. Examples of the hydrophobes used include alkylphenols, medium chain-length alcohols and tallow-amines, and more recently trisiloxanes and quaternary ammonium salts.[1a,5] Mean molar EO contents of such adjuvants range from *ca* 5 to 20, and the importance of surfactant EO content on enhancement of active uptake is well documented.[1a,7] In general, a correlation between EO content of the surfactant and polarity of the active has been observed for maximal enhancement of cuticular penetration.[5] The uptake of lipophilic actives tends to be enhanced with low EO oligomers,[8,9] whilst hydrophilic active uptake is most typically improved with adjuvants of higher EO content.[1b,10a-f] Less dependence on surfactant EO content is observed for herbicides of intermediate lipophilicity.[2,9,10d,e]

Mechanistic information has been obtained from experiments comparing the uptake of two surfactants differing in EO content, $C_{12}(EO)_{16}$ and $C_{13}(EO)_6$, and various actives into a range of plants.[7] All enhanced uptake with $C_{13}(EO)_6$ was interactive and concentration dependent, and thus it was concluded that parallel uptake of $C_{13}(EO)_6$ (copenetration) was imperative to the uptake mechanism. However significant penetration of the high EO surfactant was not always required for active uptake. Significant enhancement of methylglucose into wheat and bean was observed in the presence of $C_{12}(EO)_{16}$, despite very slow surfactant uptake. This non-interactive mechanism led authors to the conclusion that $C_{12}(EO)_{16}$ acts at the leaf surface, or at the initial stage of partitioning into the cuticle. Interactive mechanisms for other plants and actives with $C_{12}(EO)_{16}$, were also observed however indicating that $C_{12}(EO)_{16}$ uptake is also required for some

uptake processes. In general, little interaction between polar compounds and $C_{13}(EO)_6$, or apolar compounds and $C_{12}(EO)_{16}$ was observed. The mobility of $C_{13}(EO)_6$ into and through the leaf surface was generally faster than $C_{12}(EO)_{16}$. The results led authors to the conclusion that higher ethoxylates penetrate more slowly, but are more likely to be retained within the plant cuticle than lower ethoxylates. It was also proposed that higher ethoxylates assist the penetration of water-soluble compounds, possibly by hydration of the cuticle, whilst lower ethoxylates appear to depend on continued flow through the cuticle for effective action. Elsewhere it was also reported that only those surfactants with long hydrophilic or hydrophobic chains are likely to be retained in the cuticle or epidermis for any significant length of time.[1b] The effect of EO content on active uptake may thus depend on the nature of the surfactant-active interactions, i.e. interactive or non-interactive.

5.1.4 Chapter objectives

Fundamental studies of surfactant and agrochemical uptake into plant foliage have been frustrated by a lack of suitable radio-labelled surfactants or sufficiently sensitive analytical techniques. Previous methods utilising chromatographic techniques[11,12] have established that it is possible to quantify surfactant uptake without the need for radio-labelled chemicals, but the methods require relatively large numbers of replications, tedious extraction and separation methods, and the agrochemical to be analysed in parallel, using radio-tracer methodology. The application of API/MS to such analyses offers large improvements due to the simplicity of the sample preparation and the high sensitivity, enabling analysis of solutions at concentrations down to parts-per-billion. It should also be possible to analyse both the active ingredient and the adjuvant from the same sample, obviating the need for parallel radio-tracer or chromatographic trials.

The objective of the research described in this chapter was to obtain mechanistic information regarding the uptake of Silwet L-77 into plant foliage. The uptake of Silwet L-77 and $M_2D\text{-}C_3\text{-}O\text{-}(EO)_n\text{-}Me$ oligomers thereof into *Chenopodium album* foliage under several conditions was investigated. *C. album* (common lambsquarters) was selected as the plant species for the experiments as it is a widely distributed weed species occurring commonly in commercially

important crops. The stomata of the leaf are very small resulting in limited stomatal uptake and furthermore the contact angle of the leaf surface is described as 'complete repulsion'.[13] This renders it difficult to achieve good retention on the leaf surface and therefore uptake of agrochemicals into the plant. The parameters defining stomatal infiltration are well defined, as discussed in later sections, and therefore it was of interest to investigate the cuticular penetration uptake process.

A quantitative comparison was made between the API/MS and established high performance liquid chromatography (HPLC) methods. Uptake in the presence of the herbicidal active ingredients glyphosate (**17**) and bentazone (**18**), was also investigated, with the active uptake determined using established radio-tracer methods.

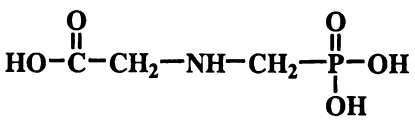

17

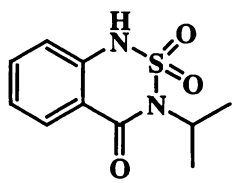

18

Efficacy and rainfastness of bentazone and glyphosate formulations on *C. album*,[14] and enhanced uptake of bentazone into *Abutilon theophrasti* (velvetleaf),[15a,b] with silicone adjuvants has been reported. The latter uptake was concluded to be non-stomatal and interactive.[15b,16] The research reported in this chapter was conducted in order to understand the mechanisms of M_2D-C_3-O-$(EO)_n$-Me uptake into plants, and their effect on the uptake of other compounds.

It was proposed that analysis of formulations with single surfactants may give further insight into the mechanisms involved in uptake processes. Purified samples of M_2D-C_3-O-$(EO)_n$-Me surfactants and individual M_2D-C_3-O-$(EO)_n$-Me oligomers were thus used to investigate the mechanism of uptake of surfactant and active ingredients. By variation of the EO composition a range of physical properties can be achieved which should provide useful information regarding this process. Furthermore the differences in polarity of the two actives investigated should be informative.

Preliminary investigations compared the uptake of different concentrations of Silwet L-77 in the presence of glyphosate, and the corresponding glyphosate

uptake (Section 5.3.4).[17] The API/MS analysis of these samples was by the flow injection method. Subsequent investigations (Section 5.3.5) compared the uptake of Silwet L-77 with that of pure components (purified M_2D-C_3-O-$(EO)_n$-Me [n = 3 - 16] and pure M_2D-C_3-O-$(EO)_n$-Me [n = 3, 5, 6, 7, 9, 11, 13+14] oligomers). In this and subsequent experiments, an online HPLC/APcI/MS method was adopted for the analysis of the surfactant content in the samples. In Section 5.3.6, the uptake of glyphosate in the presence of pure M_2D-C_3-O-$(EO)_n$-Me oligomers (n = 3, 6, 13+14) is presented and in Section 5.3.7, the effect of changing glyphosate concentration is shown. The influence of pure M_2D-C_3-O-$(EO)_n$-Me oligomers (n = 3, 6, 9) on the uptake of bentazone was also investigated (Section 5.3.8). Spread areas, drying times and surface tensions of the solutions were determined to aid interpretation of the results obtained.

5.2 MATERIALS AND METHODS

The numbering system used in this Chapter has been designed such that the 'Materials and Methods' number is as for that of the corresponding 'Results and Discussion' section. For example the materials and methods used to generate the results described in Section 5.3.1 are listed in Section 5.2.1.

Chemicals

The M_2D-C_3-O-$(EO)_n$-Me surfactants were obtained by the chromatographic separation and synthetic procedures described in Chapter 2. Triton X-45, $C_6(EO)_3$ and Agral-90 were used as the internal standards. Glyphosate was prepared as the isopropylamine (IPA) salt, with IPA added at a 1.2 molar equivalent of the acid. Bentazone was obtained as the sodium salt. Solutions for radiolabel determinations were prepared by adding the [^{14}C]-labelled active to unlabelled active at less than 0.2% (w/v) of total active concentration. Blankophor-P, Uvitex NFW, Uvitex CF and Erio Acid Red XB were used as the fluorescing agents in spread area determinations.

API/MS conditions

The APcI/MS was operated in positive ion mode for surfactant analysis with the previously established optimal instrument settings (Chapter 4, Appendix II). Cone voltage for each analysis was as specified.

Plants

Chenopodium album plants were grown from seed in a controlled environment (temperature: 25 °C/ 15 °C day/ night; RH: 70%; illumination: 350 μmol m^{-2} s^{-1}, 14 h per day). Plants at the stage of fully expanded second leaves (c. 30-40 days after sowing) were used for uptake and spread area studies.

Solution applications

Droplets (0.24 μL/1 μL) of the formulations were applied to leaf and glass surfaces using a Hamitonian micro-syringe. The syringe was calibrated using radiolabelled solutions to ensure accuracy of the volumes dispensed.

Active uptake

Uptake of active was determined with the use of [^{14}C]-radiolabelled active formulations, by previously established methods.[16] Uptake of [^{14}C]-active was calculated from the difference in radioactivity recovered in the leaf washes and the amount originally applied to the leaves. The data are presented as a percentage of active applied.

Control treatments

A control treatment for surfactant recovery was provided by application of Silwet L-77 (2 g L^{-1}) to glass slides (5 replicates). Recoveries from the slides were determined by quantitation of the residue at 10 minutes and 24 hours with 1:1 MeOH/H_2O as the wash-off solvent (determined as ideal).[12] Control recoveries of herbicide were determined by placing droplets without surfactant on *C. album* leaves (5 replicates) and washing-off immediately after visual drying of the droplet and after 4 hours. Recovery efficiencies for the active treatments were also determined by combusting whole field bean plants 24 hours after treatment with radiolabelled glyphosate.[16]

5.2.1 Spread areas of M_2D-C_3-O-$(EO)_n$-Me solutions

Spread areas of M_2D-C_3-O-$(EO)_n$-Me solutions were determined by image analysis of the dried deposits (A.II.7). The application solutions, prepared with 1% Blankophor-P (w/v), were applied (0.24 μL droplets) to recently excised *C. album* leaves and visualised under UV light. Multiple droplets (2-6) were applied to each leaf replicate ensuring that droplet overlap did not occur. A minimum of 6 leaves, all from different plants, were used.

At higher concentrations of glyphosate (>5% [w/v]), the solutions containing Blankophor-P were found to be unstable. Solutions containing the fluorescing agents Uvitex CF, Uvitex NFW and Erio were thus also investigated. However no improvement to the stability was achieved. The spread areas for the solutions with varying concentrations of glyphosate (Section 5.3.7, Table 5.13) were thus determined by manually outlining the droplet area (determined visually) and analysing with a conventional light source.

5.2.2 Surface Tension of M_2D-C_3-O-$(EO)_n$-Me solutions

Equilibrium surface tension values were obtained by the Wilhelmy plate method (A.II.9) using surfactant solutions at 3.2×10^{-3} mol L^{-1} (~ 2 g L^{-1}). Values reported are the average of triplicate measurements.

5.2.3 Drying times of formulations

The drying times of M_2D-C_3-O-$(EO)_n$-Me and [M_2D-C_3-O-$(EO)_n$-Me + active] solutions were determined by monitoring the evaporative weight loss of the solutions with respect to time. Ten droplets (1 μL) were applied to glass slides on an electronic balance, with the number of slides adjusted accordingly to prevent droplet overlap.* The data (mass change over time) were electronically collected (A.II.8). Results are the means of 6 replicate measurements, except for the (M_2D-C_3-O-$(EO)_6$-Me + active) solutions for which only 2 replicates were obtained.

5.2.4 Glyphosate and Silwet L-77 uptake with varying Silwet L-77 concentration

Treatments and extractions

Solutions at concentrations of 1, 2 and 5 g L^{-1} Silwet L-77 with 10 g L^{-1} glyphosate were prepared in water. Droplets (0.24 μL) of each formulation (20, 14 and 10 droplets/leaf, respectively) were applied onto the upper surface of the second pair of true leaves of the *C. album* using a micro-syringe. The dose of the surfactant on each leaf was 4.8, 6.7, and 12 μg, for each of the concentrations. Each treatment contained 5 replicates (2 leaves/replicate). All plants were kept under constant growing conditions for the uptake period. At intervals of 10, 30 and 240 minutes after application, the treated leaves were excised and the residue collected by washing off with H_2O/MeOH (1:1 v/v; 2 x 2 mL). Agral 90 (10 μg, 100 μL) was added to the washoff and the solution made up to 10 mL with methanol (to provide a 1 ppm internal standard solution). Method validation was achieved by control applications of surfactant to glass slides (5 replicates).[12] Aliquots (2 mL) were taken for radio-chemical (active) and MS (surfactant) analysis, with the remaining sample used for analysis by HPLC (surfactant).

---

* Number of slides used: M_2D-C_3-O-$(EO)_3$-Me, 1 slide; M_2D-C_3-O-$(EO)_6$-Me, M_2D-C_3-O-$(EO)_9$-Me, 0.1% Silwet L-77, 0.2% Silwet L-77, [M_2D-C_3-O-$(EO)_6$-Me + active], 2 slides; 0.287% Silwet L-77, 0.5% Silwet L-77, 3 slides.

Preparation of the standard solutions

Solutions of Silwet L-77 (0.25 – 2 ng μL^{-1}) containing the Agral-90 internal standard (1 ng μL^{-1}) were used to generate relative response ratio curves (0.25 – 2 ppm equivalent). The solutions were prepared by serial dilution of a 0.1 g L^{-1} stock solution of Silwet L-77 with a 1 ng μL^{-1} internal standard solution.

HPLC determinations of Silwet L-77

An elution solvent of H_2O/MeOH/MeCN at a ratio of 12:68:20 respectively, was used at a constant flow of 0.9 mL min^{-1}. The column used was a Phenomenex 4.6 x 150 mm RP C_{18} (3 μm) column. Peak area data for sample and internal standard was transferred to a spreadsheet for calculation of amounts of surfactant recovered and therefore the percentage uptake of the surfactant applied to the leaves. Results (percentage uptake of applied) were the means of ten analyses (5 replicates in duplicate).

Mass spectrometric analyses of Silwet L-77

Detection was by the flow injectionAPcI/MS method using a 10 μL injection aliquot of the sample solution, a multiplier setting of 650 and a cone voltage of 60V. The elution solvent used was 60% MeOH/H_2O at a flow rate of 1 mL min^{-1}. Analysis was conducted in selected ion mode (SIR) with settings of: dwell time, 0.15 s; inter-channel delay, 0.07 s; and span, 0.5 a.m.u., adopted. The ions representing the Na^+ adducts of M_2D-C_3-O-$(EO)_6$-Me (*m/z* 581) and the $(EO)_6$ nonylphenol ethoxylate oligomer (*m/z* 507) were selected and the peak area responses integrated for quantitation.* The Na^+ adducts were dominant for all spectra (>80% total pseudo-parent ions). Results are the means of 25 analyses (five replicates analysed five times). All other conditions were as previously specified.

5.2.5 M_2D-C_3-O-$(EO)_n$-Me surfactant uptake in the absence of active

Treatments and extractions

All surfactant solutions were prepared in water at a concentration of 3.2 x 10^{-3} mol L^{-1}. This equates to 2 g L^{-1} for the purified M_2D-C_3-O-$(EO)_n$-Me (Ave n ≈

* A smaller number of ions were selected to reduce the time required for data analysis

7.5) solution* and 2.86 g L^{-1} for Silwet L-77 (70% M_2D-C_3-O-$(EO)_n$-Me).† Solutions of the synthesised n = 3 (1.37 g L^{-1}), n = 6 (1.79 g L^{-1}) and n = 9 (2.21 g L^{-1}) M_2D-C_3-O-$(EO)_n$-Me oligomers‡ were also prepared at a concentration of 3.2 x 10^{-3} mol L^{-1}. A solution of Triton X-45 (0.05 g L^{-1}, 50 ppm) prepared with 40: 60 H_2O/MeOH was used as the internal standard stock solution.

Droplets of each formulation (0.24 µL; 14 droplets/leaf) were applied to give a dose of 1.08 x 10^{-8} moles of surfactant/leaf. Each treatment contained 5 replicates (2 leaves/replicate). At intervals of 5, 30, 120 and 240 minutes after application, the treated leaves were excised and washed with 1:1 H_2O/MeOH (1 x 4 mL). Triton X-45 (5 µg in 100 µL) was added and the solution made up to 10 mL with methanol (providing a 0.5 ppm internal standard solution).

A second trial was conducted following the above procedure, but with sampling only at 120 minutes after application. In this trial, preparations of the single oligomers n = 3 (1.37 g L^{-1}),** n = 5 (1.65 g L^{-1}),§ n = 6 (1.79 g L^{-1}),** n = 7 (1.93 g L^{-1}),†† n = 11 (2.49 g L^{-1})†† and n = 13+14 (2.85 g L^{-1})†† were used, also at a concentration of 3.2 x10^{-3} mol L^{-1}.

Preparation of the standard solutions

Solutions of surfactants (0.32 – 8.97 x 10^{-8} moles µL $^{-1}$) containing the internal standard (0.5 ng µL^{-1}) were used to generate standard response ratio curves (0.05 – 1.3 ppm equivalent for the purified surfactant preparation). The solutions (equivalent to 4 – 100 % recoveries) were prepared by dispensing 1, 3, 5, 7, 10, 14, 20 and 28 droplets (0.24 µL) of the 3.2 x 10^{-3} mol L^{-1} stock solutions. Aliquots of the internal standard (5 µg in 100 µL) were added and the resulting solutions made up to 10 mL.

HPLC determinations of Silwet L-77

An elution solvent of 10:72:18 H_2O/MeOH/MeCN at a constant flow of 1 mL min^{-1} was used. The column used was a Waters Nova-Pak RP C_{18}, 100 x 8 mm (4 µm) Radial-Pak column equipped with a guard column assembly. The light scattering mass detector operating conditions were: gas flow, 1.3 L min^{-1};

---

* Obtained by purification of the commercial Silwet L-77 formulation (Section 2.2.1.1).
† Calculated as a molar equivalent based on chromatographic determinations (Section 2.2.1.3)
‡ Obtained by the synthetic procedures described in Section 2.2.2.
§ Obtained by separation of the commercial Silwet L-77 formulation (Section 2.2.1.2).

evaporator tube temperature, 85°C; and attenuation, 1/32. Samples were analysed in duplicate, or in triplicate when the values obtained showed large variation. Linear regressions were used for all of the standard response curves. All other equipment and methods were as for the previous section.

HPLC/APcI/MS analyses.

The elution solvent, H_2O/MeOH/MeCN at a ratio of 8:76:16 respectively, was delivered to the online HPLC column at a constant flow of 1 mL min^{-1}. The column was that used in the HPLC analyses above. Sample solutions were injected manually every 7 minutes. Total run time was 9 minutes with only the final 5 minutes being recorded to reduce file size. The Triton X-45 and Silwet L-77 peaks eluted at 5.4 and 7.6 minutes respectively. Injector loops of varying volumes were used depending on the M_2D-C_3-O-$(EO)_n$-Me oligomer,* in order to obtain linear responses for the standard curves.† A cone voltage setting of 60V was used in all analyses, excluding the second analysis of M_2D-C_3-O-$(EO)_3$-Me, for which a setting of 20V was adopted in order to enhance sensitivity. Analysis was performed in total ion mode (TIC) over a range of *m/z* 300 – 1000, with a scan time of 4 seconds and inter-scan time of 0.1 seconds. Results are the means of 10 analyses (five replicates analysed twice). Peak areas obtained were transferred to a spreadsheet for calculations using linear or power (M_2D-C_3-O-$(EO)_6$-Me) regressions of the standard response curves.

5.2.6 Glyphosate uptake with varying surfactant EO content

Treatments and extractions

All surfactant solutions were prepared in water at a concentration of 6.4 x 10^{-3} mol L^{-1} (~0.4 % [w/v] equivalent relative to n = 7.5 M_2D-C_3-O-$(EO)_n$-Me). Solutions of the synthesised n = 3 (2.74 g L^{-1}) and n = 6 (3.58 g L^{-1}), and the isolated n = 13+14 (5.70 g L^{-1}) M_2D-C_3-O-$(EO)_n$-Me oligomers were prepared. The glyphosate solution was prepared in water at a concentration of 1.2 x 10^{-1} mol L^{-1}, equating to a 2% (w/v) solution (20 g L^{-1}). Solutions of the (surfactant + active) at 1:1 (v/v) were prepared to give application concentrations of ~0.2%

* n = 3: 500 (2nd trial) and 100 µL (1st trial) loops; n = 5: 50 µL loop; n = 6, 7, 7.5 (Silwet L-77), 11, 13+14: 10 µL loop; n = 7.5 (purified), 9: 5 µL loop.

† Ionisation efficiencies increased for increasing EO content and thus smaller volumes were required for linearity with larger oligomers

surfactant and ~1% active. Plant treatments were as for Section 5.2.4, although only one leaf was used per replicate, and only the uptake of the active was determined (radiolabel determination). Intervals of 5, 30, 120 and 240 minutes and 24 hours were adopted for analysis.

5.2.7 Surfactant and glyphosate uptake with varying glyphosate concentration

Treatments and extractions

M_2D-C_3-O-$(EO)_6$-Me was prepared in water at a concentration of 6.4 x 10^{-3} mol L^{-1} (3.58 g L^{-1}, 0.36% [w/v]), the molar equivalent of a 0.4% (w/v) M_2D-C_3-O-$(EO)_{7.5}$-Me solution. Three solutions of glyphosate IPA were prepared in water at a concentrations of 0.12 mol L^{-1} (20 g L^{-1} active, 2% [w/v]), 0.6 mol L^{-1} (100 g L^{-1} active, 10% [w/v]) and 1.2 mol L^{-1} (200 g L^{-1} active, 20% [w/v]). Solutions of the (surfactant + active) at 1:1 (v/v) were prepared to give application concentrations of ~0.2% surfactant (3.2 x 10^{-3} mol L^{-1}) and 1% (w/v, 10 g L^{-1}), 5% (w/v, 50 g L^{-1}) and 10% (w/v, 100 g L^{-1}) active. Treatments and glyphosate determinations were as for Section 5.2.4.

A parallel trial for analysis by HPLC/APcI/MS was conducted, following the above procedure, but without the radiolabelled active, and with sampling only at 120 minutes after application. For comparison, uptake of the M_2D-C_3-O-$(EO)_6$-Me alone (i.e. in the absence of active) was also investigated. Triton X-45, prepared at a concentration of 0.025 g L^{-1} (25 ppm), was added to each washoff sample as the internal standard solution (100 μL, 2.5 μg) and the solutions diluted to 10 mL.

Preparation of the standard solutions for HPLC/APcI/MS.

Relative response ratios of solutions of the surfactants (0.32 – 4.49 x 10^{-8} moles μL^{-1}) containing internal standard (0.25 ng μL^{-1}) were used to generate standard curves (0.04 – 0.6 ppm). The solutions (equivalent to 7 – 100 % recoveries) were prepared by dispensing 1, 3, 7, 11 and 14 droplets (0.24 μL) of the 3.2 x 10^{-3} mol L^{-1} stock solution. Aliquots of the internal standard (5 μg in 100 μL) were added and the resulting solutions made up to 10 mL.

HPLC/APcI/MS analyses of the surfactant uptake.

The HPLC/APcI/MS conditions were as for Section 5.2.5, but with an injector loop of 20 μL loop used for all samples. The regressions yielding the highest R^2 were used for the standard response curves, such that linear regressions were used for the M_2D-C_3-O-$(EO)_6$-Me surfactant alone and 5% glyphosate applications, and power regressions for the 1% and 10% glyphosate applications.

5.2.8 Bentazone uptake with varying surfactant EO content

The methodology described in Section 5.2.6 was used. All additional solutions were prepared at equivalent molar concentrations (bentazone [sodium salt], 1.2 x 10^{-1} mol L^{-1} [31 g L^{-1}]; M_2D-C_3-O-$(EO)_9$-Me*, 6.4 x 10^{-3} mol L^{-1} [4.42 g L^{-1}]).

* Obtained by the synthetic procedures described in Section 2.2.2.

5.3.1 Spread areas of M_2D-C_3-O-$(EO)_n$-Me solutions

Organosilicone surfactants have been shown to be very effective wetting agents, with Silwet L-77 solutions exhibiting spreading over nine times higher than water.[22] The degree of agrochemical uptake in the presence of trisiloxane surfactants is reported to be closely related to the spreading performance of the solutions, and in general this is associated with promotion of stomatal infiltration.[18]

In this section the spread areas for the various M_2D-C_3-O-$(EO)_n$-Me solutions were thus determined and the results are discussed with respect to the EO content. The average spread areas for the surfactant solutions (0.24 μL droplets), and dosage calculations are shown in Table 5.1.

Table 5.1. Spread areas for M_2D-C_3-O-$(EO)_n$-Me oligomers[a] on *Chenopodium album* foliage

n (M_2D-C_3-O-$(EO)_n$-Me)	3	5	6	6	≈7.5[b]	≈7.5[c]	9	11	13+14
Average spread area (mm^2)[d]	1.8	18	43	50	59	56	50	9	1.7
SD	0.2	3	3	5	6	7	4	5	0.4
CV	11%	14%	7%	10%	10%	13%	8%	59%	22%
Dosage/ 0.24 μL droplet (10^{-9} moles mm^{-2})	43	4.3	1.8	1.5	1.3	1.4	1.5	8.6	45

[a] 3.2 x10^{-3} mol L^{-1} solutions; [b] Silwet L-77 (70% M_2D-C_3-O-$(EO)_n$-Me, n = 3 – 16); [c] Purified Silwet L-77 (100% M_2D-C_3-O-$(EO)_n$-Me, n = 3 – 16); per 0.24 μL droplet

The plot of the average spread area against EO content for the M_2D-C_3-O-$(EO)_n$-Me oligomers, Figure 5.1, shows a Poisson-type distribution, with the maximum value observed for the Silwet L-77 solution (Ave. n ≈ 7.5). Both high and low oligomers (n = 3 and 13+14) showed very little spreading.

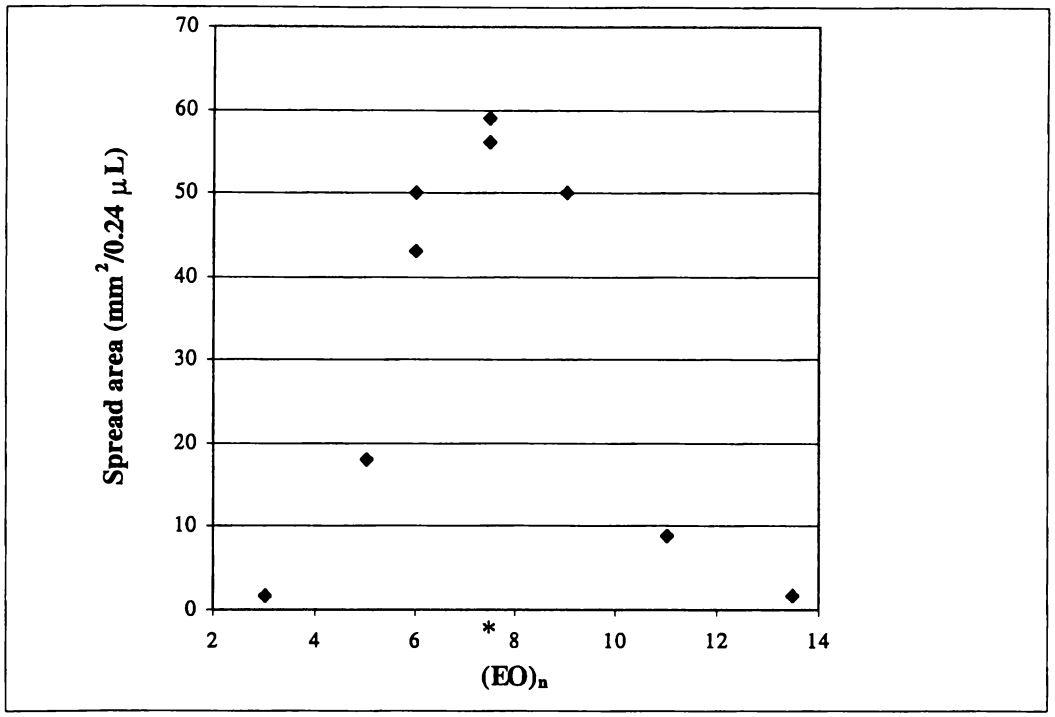

Figure 5.1. Average spread areas of Silwet L-77* and M_2D-C_3-O-$(EO)_n$-Me oligomers on *Chenopodium album* foliage

This result suggests that the properties of Silwet L-77 are consistent with those of the average oligomer (M_2D-C_3-O-$(EO)_{7.5}$-Me). Other authors have also reported that the spreading behaviour of binary and ternary mixtures of M_2D-C_3-O-$(EO)_n$-Me oligomers mimics that of the equivalent single oligomer (average EO content).[19] In other investigations into the spreading behaviour of M_2D-C_3-O-$(EO)_n$-Me oligomers (n = 3 – 9) on hydrophobic silicon wafers, the best spreading performance (largest spreading area and highest spreading velocity) was observed with the $(EO)_6$ oligomer, followed closely by the Silwet L-77 formulation.[20] Consistent with these results, no spreading was observed for the $(EO)_3$ oligomer. Spreading of M_2D-C_3-O-$(EO)_n$-H on low-energy surfaces was also described, for which similar trends to those observed here were seen. Of the oligomers investigated (n = 4, 8, 12), the oligomer of intermediate EO content (n = 8) showed the highest spreading velocity. The n = 7 oligomers of M_2D-C_3-O-$(EO)_n$-R (R = H, CH_3, $COCH_3$) have been reported to exhibit higher spreading velocities than the n = 4 and 12 oligomers on hydrophobic surfaces, and spreading for the n = 12 and 18 surfactants was only observed on less hydrophobic surfaces.[36]

* Silwet L-77 and Purified Silwet L-77 data (M_2D-C_3-O-$(EO)_n$-Me, Ave. n ≈ 7.5).

The plot of the relative dosages per droplet (moles applied/spread area) with respect to the EO content is shown graphically in Figure 5.2. The trends of the dosage values can only loosely be applied to the uptake trials in the following sections however, as droplet overlap on the leaf surface occurred for the solutions with high spread area values. The low spread areas of the n = 3 and n = 13+14 solutions prevented droplet overlap so the dosage values are relevant for these two solutions.

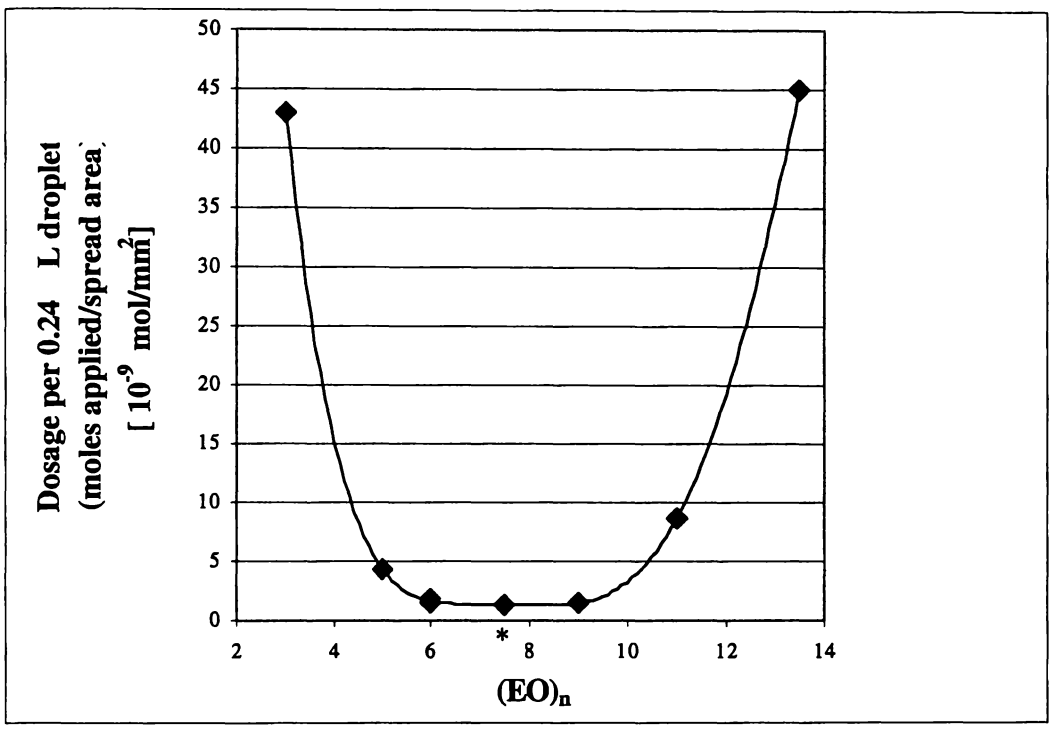

Figure 5.2. Dosage of Silwet L-77* and M_2D-C_3-O-$(EO)_n$-Me oligomers on *Chenopodium album* foliage

In general, higher spreading is associated with improved efficacy of agrochemical formulations, as more of the active is brought into intimate contact with the target.[22] This is especially so for cuticular penetration and for uptake of lipophilic xenobiotics,[8] due to the nature of the uptake mechanisms. However, under some circumstances, especially those involving water-soluble actives, high spreading is thought to be responsible for inhibition of active uptake.[3,38] Uptake of water-soluble actives is often thought to be by diffusion/partition processes, and as such is driven by high concentrations. This concentration gradient is lost with very high spreading. Other studies have reported that increased herbicide

* Silwet L-77 and Purified Silwet L-77 data (M_2D-C_3-O-$(EO)_{7.5}$-Me, Ave. n ≈ 7.5).

uptake or biological activity did not appear to be related to the spreading properties of the solutions.[10a,b] Experiments with a range of silicone adjuvants have also indicated that efficacy was not solely based on the reduction in surface tension or enhanced wetting.[14] The effect of formulation spread area on the uptake of M_2D-C_3-O-$(EO)_n$-Me and herbicidal active ingredients will be addressed in subsequent sections.

5.3.2 Surface Tension of M_2D-C_3-O-$(EO)_n$-Me solutions

Correlations between surface tension and activity of herbicidal sprays have been observed.[21] Furthermore, in many applications the extremely low surface tension of Silwet L-77 has been implicated in their ability to be absorbed and to enhance the absorption of other xenobiotics.[4,21,22] The surface tensions of the various M_2D-C_3-O-$(EO)_n$-Me solutions were thus investigated, the results of which will be discussed further in the subsequent plant uptake experiments.

The surface tension values observed (Table 5.2, Figure 5.3) showed the inverse trend to that obtained for spread area. The lowest surface tension was observed for the Silwet L-77 and purified Silwet L-77 solutions. The $(EO)_6$ oligomer gave the next lowest value, followed by the $(EO)_9$ solution, with the $(EO)_3$ solution exhibiting a significantly higher value. The Silwet L-77 solutions follow the trend of the other oligomers, exhibiting a surface tension value as expected for an oligomer of average $(EO)_n$ content of $n \approx 7.5$.

Table 5.2. Static surface tension of solutions of M_2D-C_3-O-$(EO)_n$-Me with varying EO content

$(EO)_n$	Average (dynes cm^{-1})	SD	CV
3	27.70	0.11	0.4%
6	21.62	0.08	0.4%
7.5*	21.35	0.03	0.1%
7.5**	21.47	0.17	0.8%
9	22.73	0.08	0.3%

* Silwet L-77; ** Purified Silwet L-77

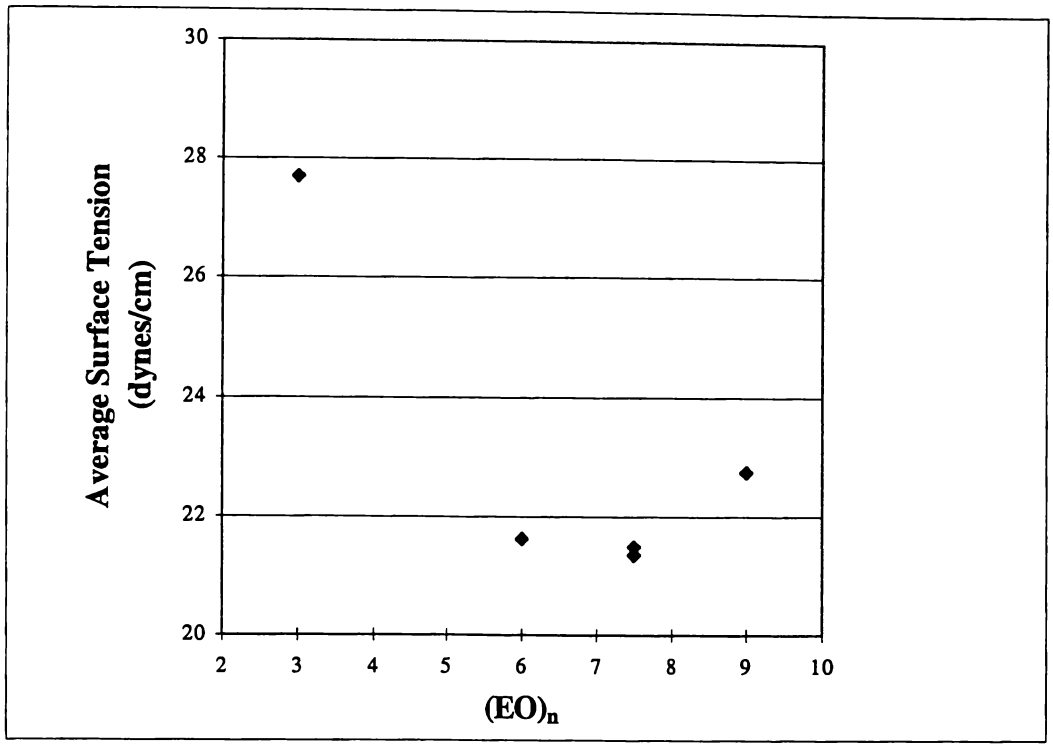

Figure 5.3. Static surface tension of solutions of M_2D-C_3-O-$(EO)_n$-Me as a function of EO content

Low aqueous solution surface tension is necessary for spreading, and is a notable characteristic of many organosilicone surfactants. The inverse however does not apply, with low surface tension not necessarily equating to efficient spreading. Other surfactants exhibiting lower surface tension than the organosilicone surfactants show reduced spreading ability.[4] Structural interactions and bulk solution properties of the trisiloxane surfactants are thought to be the cause of the different behaviour, and in particular the compact hydrophobic moiety has been implicated.[35] It has been shown that surfactants capable of reducing surface tension below 30 dynes cm^{-1} can cause stomatal flooding of plants, considered a major mechanism of uptake enhancement by Silwet L-77.[22]

5.3.3 Control recoveries

Control recoveries for Silwet L-77 (2 g L^{-1}) from glass slides were 96% (±11) and 93% (±7) after 10 minutes and 24 hours, respectively.[12] Control recoveries of glyphosate from *C. album* foliage with washing-off immediately following visual drying of the droplet and after 4 hours provided 98% and 97% recoveries,

respectively. Recovery efficiencies for radiolabelled glyphosate after 24 hours was >97% as determined by combustion of whole field bean plants.[16]

5.3.4 Glyphosate and Silwet L-77 uptake with varying Silwet L-77 concentration

Silwet L-77 is known to enhance the uptake and/or efficacy of glyphosate under certain conditions.[4,21] In some cases however, the uptake is known to be unaffected,[4] and even inhibited.[4,7,23,24a,b,29] These various effects of Silwet L-77 have been associated with a number of factors including leaf morphology,[16,26] concentration,[23,38] droplet spread[1b,38] and moisture content.[1b] The enhancement of glyphosate uptake by Silwet L-77 through stomatal infiltration, has been well documented.[25] Investigations of glyphosate uptake in the presence of Silwet L-77 into perennial ryegrass, showed significantly higher uptake into the stomatal upper leaf surface, as compared with the astomatous lower leaf surface.[26] Active uptake into other non-stomatous adaxial leaf surfaces (*Eucalyptus botryoides*, *Citrus nobilis*) in the presence of Silwet L-77 was also limited, as compared with other organosilicone surfactants said to enhance cuticular penetration.[4] Other reports have also described inhibition of cuticular penetration with increased Silwet L-77 concentration.[11,24] This was associated with the low dosage at later application times resulting from extensive initial stomatal infiltration.

The uptake of Silwet L-77 over time into *C. album* leaves, at varying concentrations was determined by HPLC and APcI/MS methods. Uptake was in the presence of glyphosate, and the active uptake was also measured. The percentage uptake results of Silwet L-77 are presented in Table 5.3 and graphically in Figure 5.4.

Table 5.3. Percentage uptake of glyphosate and Silwet L-77 into *Chenopodium album*

[Silwet L-77] ($g\ L^{-1}$)	Time (minutes)	Silwet L-77 [APcI/MS]*	Glyphosate [^{14}C]	Glyphosate (dosage corrected)
		% Uptake (SD) [a]		
1	10	64 (9)	13 (2)	13 (2)
	30	72 (10)	12 (6)	12 (6)
	240	80 (4)	10 (2)	10 (2)
2	10	70 (5)	19 (5)	34 (9)
	30	70 (5)	14 (5)	25 (9)
	240	84 (4)	15 (4)	27 (7)
5	10	49 (9)	5 (4)	20 (16)
	30	65 (11)	9 (4)	38 (17)
	240	85 (3)	9 (4)	38 (17)

[a] SD = Standard deviation

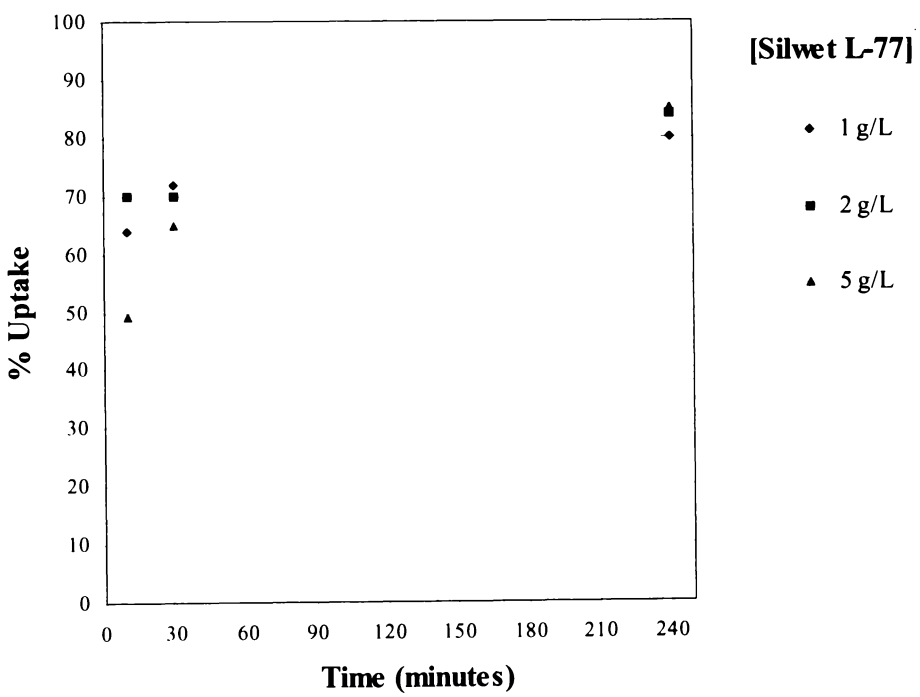

Figure 5.4. Percentage uptake of Silwet L-77 into *Chenopodium album* over time (APcI/MS)

The results show that Silwet L-77 is rapidly absorbed into *C. album* foliage, and that relatively little additional uptake occurs after 30 minutes. For all concentrations of Silwet L-77 applied, the fastest rate of uptake was observed

* The HPLC and APcI/MS results were in agreement (See Table 4.24). The MS method generally gave lower and more consistent SD values at all time periods and surfactant concentrations.

within the first 10 minutes of exposure to the leaf surface. This is consistent with results from other studies investigating fundamental cuticle diffusion, which suggested that the major interactions between organosilicone surfactants and the cuticle occur within 10 minutes.[27,28]

No increase in percentage uptake with increasing surfactant concentration is observed at the 10 minute uptake interval, indicating a lack of stomatal infiltration through the upper leaf surface in this species. Stomatal infiltration is a concentration dependent process and consequently an increase in uptake is expected with an increase in surfactant concentration at this time interval.[21] These results demonstrate that the uptake mechanism of Silwet L-77 into *C. album* foliage is by cuticular penetration and confirm observations reported elsewhere that the trisiloxane surfactants can be rapidly absorbed into leaves, through the cuticle as well as by stomatal infiltration.[14*b*,15,29]

The percentage uptake values at 30 and 240 minutes were within experimental error for all concentrations of surfactant investigated, indicating that application concentration does not influence final percentage uptake. This has been observed elsewhere for uptake by cuticular penetration,[6*a*,29,30] and also for stomatal infiltration.[4]

The percentage uptake of glyphosate in the presence of varying concentrations of Silwet L-77 is also presented in Table 5.3. The results show little increase in uptake with increasing surfactant concentration and application time. Unlike the surfactant, glyphosate is poorly taken up into *C. album* foliage under these conditions, with less than 20% uptake for all concentrations and time intervals.

The highest uptake was observed with the 2 g L^{-1} surfactant solution, with a significant decrease in uptake observed with the 5 g L^{-1} surfactant solution. This trend is consistent with that observed for the surfactant uptake at the early time interval (10 minutes). This suggests that the enhancement of glyphosate uptake by Silwet L-77 occurs early in the uptake process, and that it may be directly related to the relative uptake of the surfactant, i.e. that the uptake is an interactive process, possibly involving copenetration. Results reported elsewhere also described an enhancement of glyphosate uptake in the first hour, in the presence of Silwet formulations.[24*a*]

In order to rationalise these results, spread areas and drying times for the solutions were investigated. The spread areas for the three solutions are shown in Table 5.4.*

Table 5.4. Spread areas of solutions of glyphosate (10 g L^{-1}) [a] with varying concentrations of Silwet L-77

[Silwet L-77] (g L^{-1})	1 [b]	2 [c]	5 [d]
Average area (mm^2) [e]	14	26	61
SD	3	4	6
CV	21%	16%	10%
Silwet L-77 dosage (10^{-9} moles/mm^2)	0.019 (0.004)	0.020 (0.003)	0.021 (0.002)
Glyphosate dosage (10^{-9} moles/mm^2)	1.03 (0.2)	0.55 (0.09)	0.24 (0.02)

[a] 6 x 10^{-2} mol L^{-1}, 14.4 x 10^{-9} moles per 0.24 µL droplet; [b] 1.1 x 10^{-3} mol L^{-1}, 0.26 x 10^{-9} moles per 0.24 µL droplet; [c] 2.2 x 10^{-3} mol L^{-1}, 0.53 x 10^{-9} moles per 0.24 µL droplet; [d] 5.6 x 10^{-3} mol L^{-1}, 1.3 x 10^{-9} moles per 0.24 µL droplet; [e] per 0.24 µL droplet

The spread areas increased proportionally with increased Silwet L-77 concentration. This is not consistent with the observed uptake trends and thus demonstrates that the uptake is not proportional to spread area under these conditions. Due to the increased spread area with increasing Silwet L-77 concentration, the dosage of the Silwet L-77 is effectively unchanged, whilst the glyphosate dosage is reduced, as shown in Table 5.4. It has previously been observed that uptake is dosage, i.e. concentration, dependent.[29,18] The inhibition of glyphosate absorption in the presence of Silwet L-77 has been directly related to surfactant concentration and inversely related to glyphosate concentration elsewhere,[24,29,31] consistent with the results observed here for the two higher Silwet L-77 concentrations. The glyphosate uptake data corrected for the reduced dosages is thus also presented in Table 5.3 for comparison. The percentage uptake was within experimental error for the two higher concentrations when the reduced dosage was taken into account. The effect of glyphosate dosage on uptake will be investigated further in Section 5.3.7.

* Control spread areas of the glyphosate solution in the absence of Silwet L-77 could not be determined as 0.24 µL droplets could not be dispensed due to the high surface tension

Results from other investigations have indicated that glyphosate uptake is much faster during droplet drying than from dry deposits.[1a,3,32] Due to enhanced spreading of the droplets with higher concentration, it was proposed that drying times might be affected. The drying times of the Silwet L-77 solutions were thus investigated (Table 5.5).

Table 5.5. Drying times of solutions of Silwet L-77 as a function of concentration

[Silwet L-77] ($g\ L^{-1}$)	Average (minutes)	SD.	CV
1	7	1	14%
2	9	2	21%
3	8	1	16%
5	7	1	20%

The drying time values for the different concentrations of Silwet L-77 all show complete drying within the first 10 minute time interval. The highest rates of glyphosate uptake were observed in this time period, indicating that solvation of the compounds is an important factor in the initial uptake mechanism. At the actual application rates (0.24 μL cf. 1 μL droplets) drying would be even faster. Although not indicated by these results, *in vivo* drying times can be expected to be shorter with higher spread (concentration),[21] which may account for the observed uptake trends. The use of glass slides, rather than surfaces more closely resembling the leaf surface, may have contributed to this anomaly.

Another possible cause of the lower glyphosate uptake at higher surfactant concentration may be due to immobilisation of the active by the surfactant on the leaf surface. This was not investigated further here however such phenomena, described as K-depression, have been described for surfactant formulations.[33] In general this is more commonly observed for lipophilic compounds, as a result of higher solubilities in the surfactant micelle than in water.[2,34] However, by this same logic it could also be perceived that water-soluble actives could be retarded on the leaf surface if the active was more soluble in the neat surfactant than in the epicuticular wax. The low solubility of glyphosate in epicuticular wax, which precludes its uptake via the lipophilic pathway, has been described.[5] In support of this theory, the same trend in the glyphosate uptake is observed for Silwet L-77 at the crucial early time interval (over the different surfactant concentrations). The

comparatively high uptake of Silwet L-77 and the change in the trends at later time intervals may not however lend favourably to this postulate.

In the presence of glyphosate, a discrimination in the uptake of M_2D-C_3-O-$(EO)_n$-Me oligomers has been observed, with lower oligomers being preferentially absorbed.[11] Two explanations can be offered to rationalise this, firstly that the short chain oligomers were preferentially absorbing into the cuticular waxes due to their lower polarities and/or secondly, retardation of the long chain oligomers by the hydrophilic glyphosate was occurring. The preferential absorption of short chain oligomers is well known, as described previously.[7] The second postulate would be in support of the K-depression theory, although it is important to note that this is not a theory which is generally accepted.

Initial uptake rates were not higher with increased surfactant concentration demonstrating uptake is cuticular rather than stomatal. The results indicate that the uptake of the active is inversely proportional to the spread area and/or that solvation and solubilisation of the active by the aqueous formulation and the surfactant respectively, may also influence uptake.

5.3.5 M_2D-C_3-O-$(EO)_n$-Me surfactant uptake in the absence of active

The results in the preceding section showed that uptake into *C. album* is by cuticular penetration rather than stomatal infiltration. As discussed previously, cuticular penetration is a partition/diffusion process, and is thus determined by a number of factors including physico-chemical properties of the solutions applied. In this section, the uptake of M_2D-C_3-O-$(EO)_n$-Me oligomers of varying EO content were investigated in order to determine the influence of different physico-chemical properties on organosilicone surfactant uptake into *C. album* leaves.

The percentage uptake of Silwet L-77* (Ave. n ≈ 7.5), purified M_2D-C_3-O-$(EO)_n$-Me (Ave. n ≈ 7.5) and individual oligomers thereof (n = 3, 6 and 9), at intervals of 5, 30, 120 and 240 minutes, are presented in Table 5.6. A concentration of 0.2 % (w/v) for the purified M_2D-C_3-O-$(EO)_n$-Me was used, and other formulations were prepared as molar equivalents thereof (3.2×10^{-3} mol L^{-1}). Analysis was by HPLC and HPLC/APcI/MS.

* 70% M_2D-C_3-O-$(EO)_n$-Me

Table 5.6. Comparison of percentage uptake of Silwet L-77 and pure M_2D-C_3-O-$(EO)_n$-Me oligomers into *Chenopodium album* as determined by HPLC and HPLC/APcI/MS

Surfactant solution	Time (minutes)	HPLC %Uptake (SD)	HPLC/APcI/MS %Uptake (SD)	%Uptake per unit area [a] (SD) [b]
M_2D-C_3-O-$(EO)_3$-Me*	6	ND [c]	22 (14)	12 (9)
	30	ND	33 (21)	18 (13)
	120	ND	56 (20)	31 (14)
	240	ND	61 (16)	33 (12)
M_2D-C_3-O-$(EO)_6$-Me†	5	37 (11)	34 (5)	0.7 (0.2)
	30	60 (21)	59 (10)	1.3 (0.4)
	120	87 (1)	89 (1)	1.9 (0.2)
	240	85 (6)	88 (7)	1.9 (0.3)
M_2D-C_3-O-$(EO)_9$-Me‡	5	37 (11)	43 (2)	0.9 (0.1)
	30	53 (9)	54 (3)	1.1 (0.1)
	120	74 (6)	71 (6)	1.4 (0.2)
	240	77 (6)	76 (5)	1.5 (0.2)
Silwet L-77§	5	34 (9)	35 (6)	0.6 (0.2)
(Ave. n ≈ 7.5)	30	47 (14)	44 (4)	0.7 (0.1)
	120	72 (7)	75 (5)	1.3 (0.2)
	240	82 (9)	83 (5)	1.4 (0.2)
Purified	5	29 (4)	31 (8)	0.6 (0.2)
M_2D-C_3-O-$(EO)_n$-Me**	30	56 (7)	55 (6)	1.0 (0.2)
(Ave. n ≈ 7.5)	120	75 (3)	72 (4)	1.3 (0.2)
	240	86 (6)	85 (3)	1.5 (0.2)

[a] %Uptake/spread area (mm^2)/0.24 µL droplet; [b] HPLC/APcI/MS data used; [c] ND = not detectable

Both forms of detection were in agreement within experimental error for all results obtained, with the MS method generally giving lower SD values. Regression fits for the standard curves obtained by the APcI/MS method were equal to or better than those obtained by HPLC in all cases, demonstrating the improved accuracy possible with this analytical method.

The APcI/MS uptake data are presented graphically in Figure 5.5 as a function of time. As observed previously, the results show that the Silwet L-77 surfactant and components thereof are rapidly absorbed into *C. album* foliage. Greater than

* R^2 (Regression for the standard curve used): HPLC, n/a; HPLC/APcI/MS, 0.963 (linear)
† R^2: HPLC, 0.974 (linear); HPLC/APcI/MS, 0.991 (power)
‡ R^2: HPLC, 0.972 (linear); HPLC/APcI/MS, 0.997 (linear)
§ R^2: HPLC, 0.971 (linear); HPLC/APcI/MS, 0.983 (linear)
** R^2: HPLC, 0.981 (linear); HPLC/APcI/MS, 0.981 (linear)

50% uptake was achieved for all solutions within 2 hours of application. Relatively little additional uptake over the 120 to 240 minute treatment period was observed for all analytes.

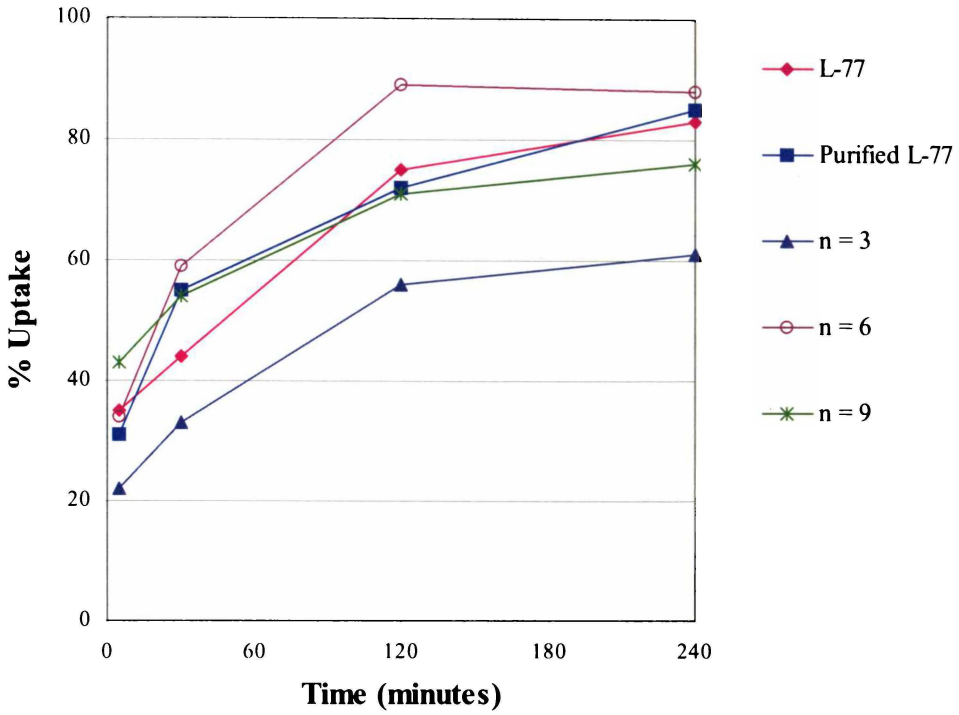

Figure 5.5. Percentage uptake of Silwet L-77 and pure M_2D-C_3-O-$(EO)_n$-Me components into *Chenopodium album* over time as determined by HPLC/APcI/MS

The results obtained show lowest uptake for the n = 3 M_2D-C_3-O-$(EO)_n$-Me oligomer at all time intervals. The uptake trend for the other formulations varied with application time. The highest initial uptake was observed for the n = 9 oligomer, whilst the n = 6 oligomer exhibited the highest overall uptake. Silwet L-77 and purified M_2D-C_3-O-$(EO)_n$-Me showed intermediate uptake rates. The uptake of Silwet L-77 and purified M_2D-C_3-O-$(EO)_n$-Me (Ave. n $\approx$ 7.5) was intermediate to that of the n = 6 and n = 9 analogues. This result suggests that the uptake of oligomeric mixtures resembles that of the average oligomer. This has also been described for spreading behaviour of M_2D-C_3-O-$(EO)_n$-Me mixtures (Section 5.3.1).

The uptake values obtained for Silwet L-77 and purified M_2D-C_3-O-$(EO)_n$-Me were within experimental error at all time intervals. This indicates that the presence of synthetic impurities does not affect surfactant uptake at equivalent dosages. Although not investigated here, it may be possible that the presence of

synthetic impurities in the Silwet L-77 formulation may however influence the active uptake. This might be especially relevant in the case of polar actives such as glyphosate, as the impurities in the Silwet L-77 commercial blend are more hydrophilic in nature. The Silwet L-77 formulation has been shown to contain ~ 25% polar impurities, including PEG derivatives.* PEG compounds are often used as humectants,[1b] and in studies of isolated cuticles, HO-$(EO)_n$-H (n ≈ 8) was found to be a good solvent for polar and non-polar solutes.[2] It has been reported that the inhibition of glyphosate uptake observed in the presence of Silwet L-77, can be partially overcome by humectants such as PEG.[4] An increase in the initial rate of glyphosate absorption into grasses with the addition of humectants has been described, although overall uptake was still decreased.[4] M_2D-C_3-O-$(EO)_n$-H compounds constitute ~ 5 % of the Silwet L-77 formulation, and may also influence uptake. Uptake of glyphosate into velvetleaf was unchanged for M_2D-C_3-O-$(EO)_n$-Me and M_2D-C_3-O-$(EO)_n$-H,[35] however M_2D-C_3-O-$(EO)_n$-H was better for glyphosate uptake into giant foxtail.[36] Improved uptake of acifluorofen into velvetleaf has been observed with M_2D-C_3-O-$(EO)_n$-Me over M_2D-C_3-O-$(EO)_n$-H.

At all time intervals investigated the n = 3 oligomer exhibited the lowest uptake. This is consistent with the very low droplet spread area (1.8 ± 0.2 mm^2) and high surface tension (27.7 dynes cm^{-1}) relative to the other surfactant solutions. The low uptake is not however, consistent with the high relative dosage indicating that spread area and surface tension may be of greater importance than dosage in the uptake mechanism of M_2D-C_3-O-$(EO)_n$-Me surfactants. The n = 3 oligomer gave the highest uptake per unit area (Table 5.6) but not the highest percentage uptake indicating that spread is important for overall uptake, but that dosage is important for unit area uptake. The droplet spread areas and dosages for the n = 6, 7.5 and 9 solutions were all within experimental error (Table 5.1). The differences in spread area and dosage observed did not conform with the variation in the percentage uptake indicating other factors must contribute to the uptake mechanism. The highest uptake results obtained were also not for the solutions showing lowest surface tension (Silwet L-77, Table 5.2). This indicates that whilst important, these properties are not necessarily the sole contributing factors in the uptake process. Results from determinations of bentazone and glyphosate

* Section 2.3.1.3

formulations on *C. album* with a range of silicone adjuvants, also demonstrated that efficacy was not solely based on surface tension.[14] In other reports, the uptake of actives in the presence of the surfactant, M_2D-C_3-O-$(EO)_n$-$COCH_3$, was not correlated to spread area.[15a]

The surfactant uptake data for the different application times as a function of EO content is presented graphically in Figure 5.6.

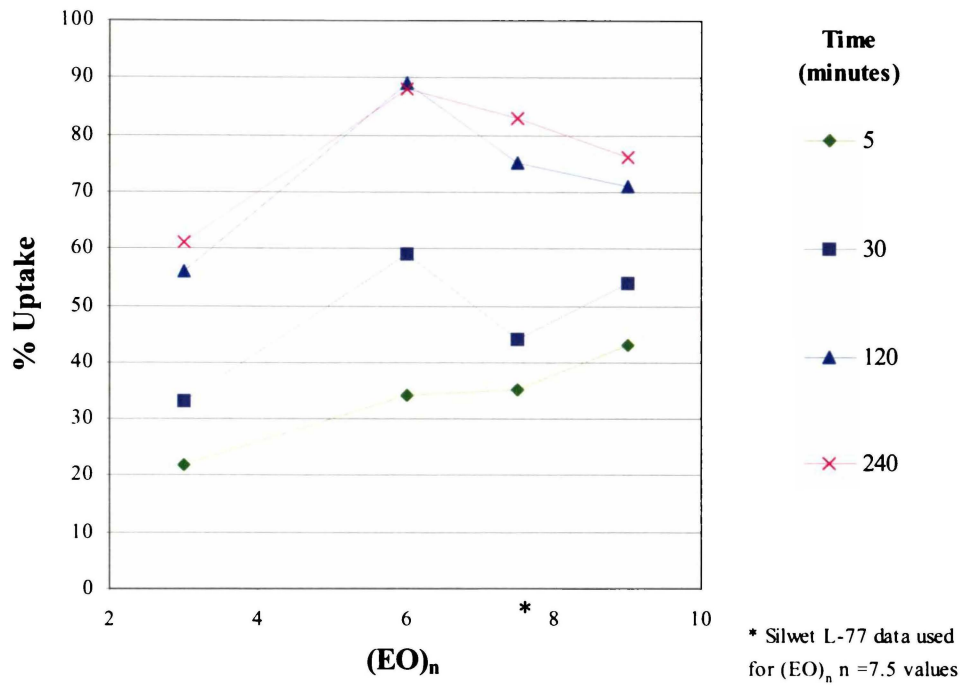

Figure 5.6. Percentage uptake of M_2D-C_3-O-$(EO)_n$-Me into *Chenopodium album* as a function of varying EO content, at varying time intervals (HPLC/APcI/MS)

At the 5 minute time interval, the percentage uptake of M_2D-C_3-O-$(EO)_n$-Me oligomers was higher with higher EO content, whilst at the 30, 120 and 240 minute time intervals the n = 6 oligomer showed the highest percentage uptake. These results indicate that there are two phases of uptake.

Although the relevance to these studies has not been determined it is interesting to note that sorption into epicuticular waxes has also been reported to be a biphasic process, with a rapid initial phase followed by a prolonged phase.[2] This could imply that the uptake of M_2D-C_3-O-$(EO)_n$-Me compounds under these conditions is controlled by wax sorption processes.

The results from the preceding section have indicated that stomatal infiltration is not a contributing pathway to the uptake of M_2D-C_3-O-$(EO)_n$-Me into *C. album*. The early phase of rapid uptake must therefore be attributable to some other mechanism.

At the 5 minute time interval, the proportion of time that the compounds are in the aqueous phase on the leaf surface would be significantly higher. This suggests that solvation of the compounds may be an important factor in the initial uptake mechanism. The drying times for the various solutions were thus determined and are shown in Table 5.7.

Table 5.7. Drying times of solutions of M_2D-C_3-O-$(EO)_n$-Me with varying EO content

$(EO)_n$	Average (minutes)	SD	CV
3	17	3	18%
6	10	2	18%
7.5*	8	1	16%
9	9	1	10%

* Silwet L-77

A significantly longer interval was required for drying of the $(EO)_3$ solution, whilst values for all other solutions (n = 6, 7.5, 9) were comparable. These results are consistent with the observed spread areas for the solutions. From the values obtained it can be assumed that at the 5 minute time interval the applied chemicals were still in the aqueous phase. This indicates that the uptake values obtained at this time interval provide information pertaining to the uptake of aqueous solutions, which is thought to be a crucial period for uptake.[1a,32]

The relative rates of uptake at this time interval showed a dependence on EO content, such that increased uptake was observed for increased hydrophilicity. These results may indicate that solvation and solubility of the surfactant in the aqueous formulation is important in the initial uptake of M_2D-C_3-O-$(EO)_n$-Me into *C. album*. The importance of compound solubilisation to uptake is well documented. [1b,37] The results obtained in Section 5.3.4 for the uptake of Silwet L-77 and glyphosate also indicated that solvation plays an important part in the uptake process.

At the 30, 120 and 240 minute time intervals the uptake is generally consistent with the trends observed for the spread area and surface tension values. The 30

minute time interval exhibited a profile intermediary to the 5 minute and 120 minute profiles indicating that both the initial and later uptake mechanisms are showing some influence. Uptake between the 120 and 240 minute time intervals showed very little variation for all formulations investigated. This indicates that the most significant uptake occurs in the first 2 hours following application, as discussed in the previous section.

Further trials, aimed at expanding the data range to include oligomers of higher EO content were subsequently conducted (time interval of 120 minutes). Comparison of the uptake with n = 5, 7, 11 and 13+14 M_2D-C_3-O-$(EO)_n$-Me oligomers showed a skewed Poisson-like trend with the n = 6 oligomer exhibiting the maximum uptake (Table 5.8, Figure 5.7).

Table 5.8. Percentage uptake of M_2D-C_3-O-$(EO)_n$-Me oligomers into *Chenopodium album* at 120 minutes (HPLC/APcI/MS)

M_2D-C_3-O-$(EO)_n$-Me n	%Uptake (SD)[a]
3 [b]	56 (20)
3	61 (5)
5	82 (6)
6 [b]	89 (1)
6	83 (10)
7	75 (5)
9 [b]	71 (6)
11	66 (14)
13+14	47 (13)
Silwet L-77 [b]	75 (5)
Purified L-77 [b]	72 (4)

[a] SD = Standard deviation; [b] Data from Table 5.6

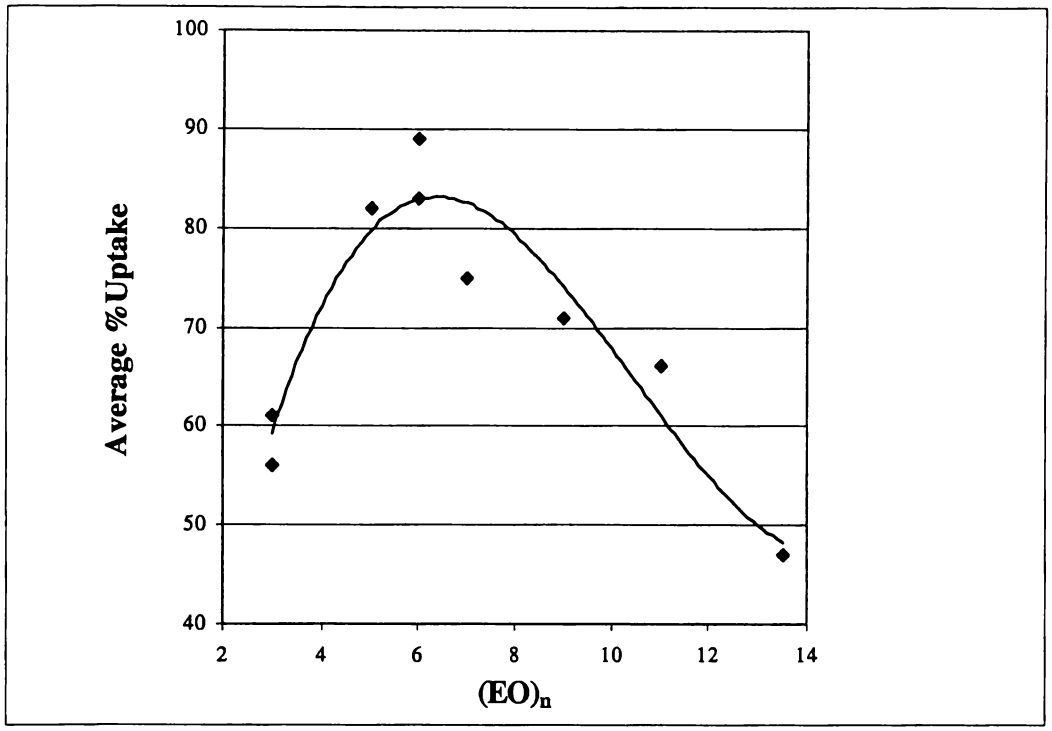

Figure 5.7. Average percentage uptake of M_2D-C_3-O-$(EO)_n$-Me single oligomers into *Chenopodium album* at 120 minutes (HPLC/APcI/MS)

The uptake trend for the oligomers at 120 minutes is generally consistent with that observed for the spread area results (Table 5.1, Figure 5.1). The uptake is also inversely proportional to the surface tension of the solutions (Figure 5.3). Once again, the corresponding percentage uptake of Silwet L-77 (75%, Table 5.2), falls around the expected value for M_2D-C_3-O-$(EO)_{7.5}$-Me in the above data series.

These results are also consistent with those obtained with $C_{13}(EO)_6$ and $C_{12}(EO)_{16}$ adjuvants, for which the $(EO)_6$ compound was taken up at a faster rate.[10b] Studies on a class of surfactants with a range of EO lengths also exhibited more rapid uptake with n = 6 and 7 oligomers over longer chains.[11]

5.3.6 Glyphosate uptake with varying surfactant EO content

The results of Sections 5.3.3 and 5.3.4 indicated that solvation and solubility are important in the uptake mechanisms of M_2D-C_3-O-$(EO)_n$-Me into *C. album*. This is consistent with results from numerous other studies, which have shown surfactant hydrophilicity to be important in the uptake of water-soluble xenobiotics.[4] Several investigations into the uptake of glyphosate have demonstrated enhanced uptake with surfactants of higher EO content.[1b,7,10a,c,f,24b,38]

The corresponding lower droplet spread has also been implicated as being influential.[38,1b] In this section, the effect of varying EO content on the uptake of glyphosate was thus investigated. The uptake of glyphosate in the presence of M_2D-C_3-O-$(EO)_n$-Me oligomers (n = 3, 6 and 13+14), as determined by radiolabel determinations, is presented in Table 5.9, and in Figures 5.8 and 5.9.

Table 5.9. Percentage uptake of glyphosate[a] into *Chenopodium album* over time in the presence of different oligomers of M_2D-C_3-O-$(EO)_n$-Me[b*]

M_2D-C_3-O-$(EO)_n$-Me	n = 3	n = 6	n = 13+14
Time (hours)		%Uptake (SD)	
0.08	0 (3)	6 (3)	1 (2)
0.5	2 (2)	15 (11)	4 (1)
2	6 (5)	14 (11)	5 (2)
4	3 (2)	13 (7)	6 (3)
24	6 (3)	17 (7)	18 (12)

[a] [glyphosate] = 10 g L-1; [b] n[M_2D-C_3-O-$(EO)_n$-Me] = 3.2 x 10^{-3} mol L^{-1}

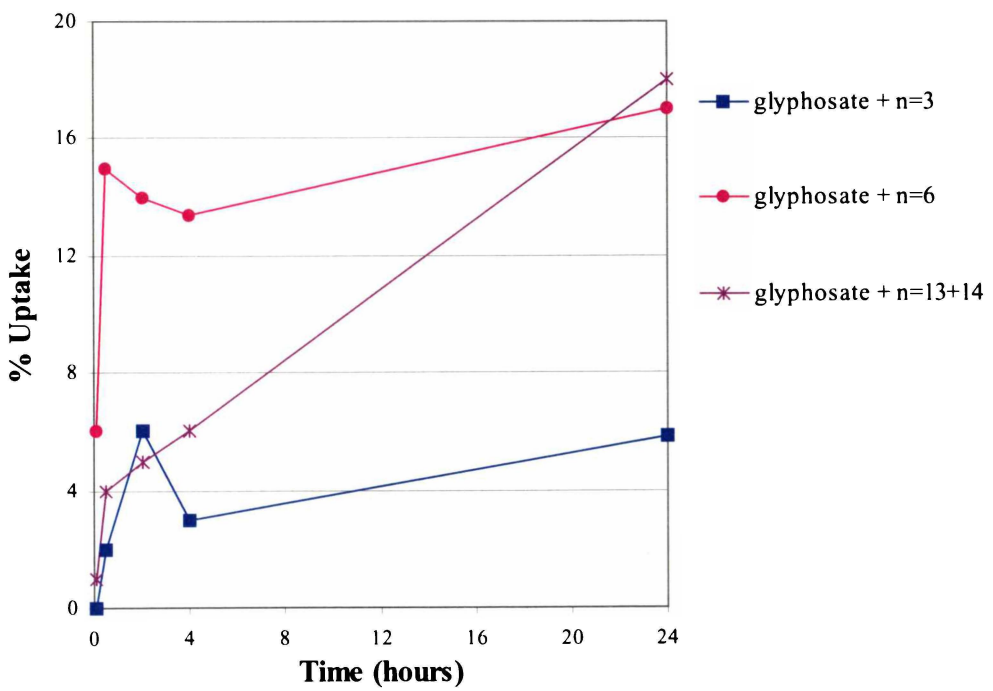

Figure 5.8. Percentage uptake of glyphosate into *Chenopodium album* over time in the presence of various M_2D-C_3-O-$(EO)_n$-Me oligomers

* The uptake of glyphosate in the absence of Silwet L-77 was less than 3% over 4 hours (Section 5.3.3). The results however are not directly comparable as equivalent droplet volumes (0.24 µL) could not be delivered due to the high surface tension of the solution in the absence of surfactant.

The uptake of glyphosate was low with all M_2D-C_3-O-$(EO)_n$-Me oligomers investigated. These results are consistent with those observed in Section 5.3.4 for Silwet L-77, where the percentage uptake of glyphosate did not exceed 20%, for all surfactant concentrations investigated. In general it has been observed that surfactants of low EO contents tend not to enhance cuticular penetration of glyphosate. Under all conditions investigated, cuticular penetration of glyphosate did not exceed 10% with Silwet L-77 present, rather was higher for the control (12%), despite the cuticular penetration of Silwet L-77 itself.[11]

The formulations showed quite different uptake profiles, although all exhibited higher initial relative rates of uptake. The M_2D-C_3-O-$(EO)_6$-Me showed higher rates of uptake overall, although the average percentage uptake was comparable with the M_2D-C_3-O-$(EO)_n$-Me of higher EO content (n = 13+14) at the 24 hour time interval. The initial uptake with the M_2D-C_3-O-$(EO)_6$-Me formulation was very rapid (0 - 30 minutes), followed by very little subsequent uptake. Reports of the uptake of glyphosate in the presence of Silwet L-77 also describe an enhanced initial uptake with no improvement after 4 hours.[24b] The uptake in the presence of the higher EO content oligomer appears to be more linear with respect to time, when compared with the other oligomers investigated. The uptake for glyphosate in the presence of M_2D-C_3-O-$(EO)_3$-Me was very low at all time intervals analysed.

The higher uptake observed with the n = 6 oligomer implies that like-polarity of the surfactant and active ingredient, considered significant,[5] is not the sole determining factor in M_2D-C_3-O-$(EO)_n$-Me enhancement of active uptake. If this was an important contributing factor then higher glyphosate uptake would have been expected with the more hydrophilic n = 13+14 M_2D-C_3-O-$(EO)_n$-Me formulation. However, for the less efficiently absorbed oligomers (n = 3 and 13+14) the uptake is generally higher for the oligomer of higher EO content indicating that like-polarity may exhibit some influence. This is investigated further in Section 5.3.8, where uptake of a less polar active with varying M_2D-C_3-O-$(EO)_n$-Me oligomers is compared.

The uptake in the presence of the longer chain oligomer improved relative to the other oligomers with time. This result is in support of the theory that activation of uptake may be a result of hydration of the cuticle, as previously suggested.[2,7]

The results also demonstrate that uptake is not significantly influenced by spread area or dosage, as these values were equivalent for the n = 3 and the n = 13+14 M_2D-C_3-O-$(EO)_n$-Me solutions (Table 5.1), whilst uptake was quite different. The dosage of the n = 6 oligomer was also much less, confirming that this property is not important for this adjuvant system.

The herbicide uptake data over the 0 – 4 hour period are presented in Figure 5.9 along with surfactant uptake data obtained in Section 5.3.4. The surfactant data were obtained in the absence of active, and thus can be used for general comparisons only.

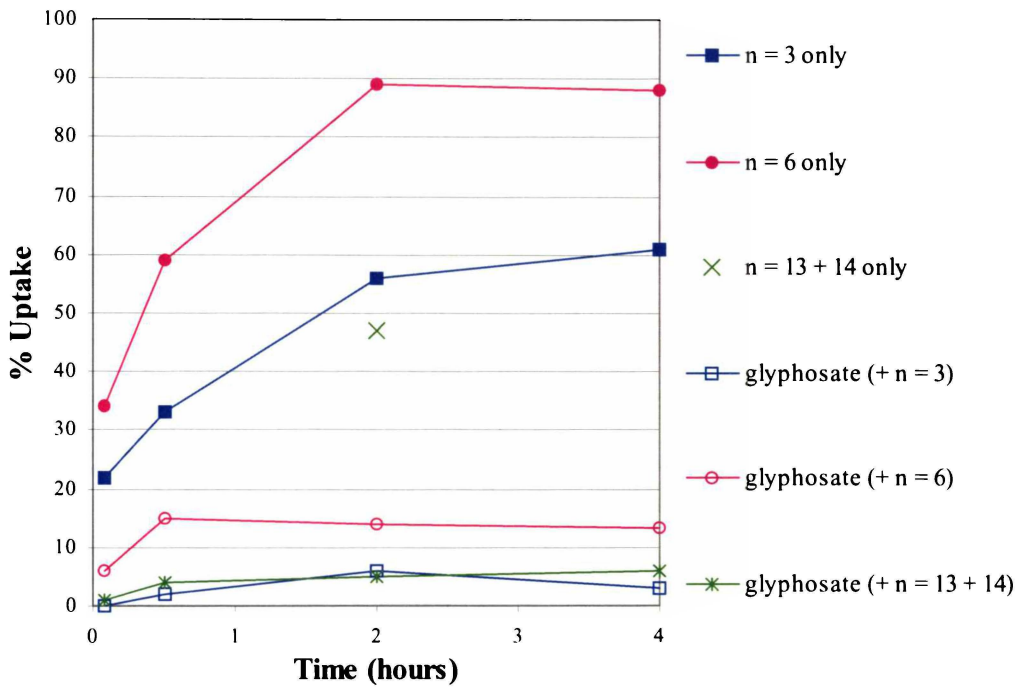

Figure 5.9. Percentage uptake of glyphosate and M_2D-C_3-O-$(EO)_n$-Me surfactants into *Chenopodium album* over 4 hours*

The uptake of glyphosate in the presence of the M_2D-C_3-O-$(EO)_n$-Me oligomers follows the same trends as that of the surfactant uptake. Related uptakes for active and surfactant were also observed for the non-stomatal uptake of bentazone and acifluorofen with Sylgard L-309 into velvetleaf,[14a,b,15] and for glyphosate with $C_{12}(EO)_{16}$ on wheat.[7]

The highest uptake was observed for the M_2D-C_3-O-$(EO)_6$-Me oligomer both with and without active present. This may indicate that the uptake mechanism

* Uptake of glyphosate < 3% over 4 hours in the absence of Silwet L-77 (Section 5.3.3)

involves copenetration of the surfactant and active. The experiments described in Sections 5.3.6 and 5.3.7 investigate this concept further.

The n = 6 oligomer exhibits higher spread area and lower surface tension values than the other formulations investigated, indicating that these properties may be significant to the uptake mechanism. Furthermore the influence on the uptake was within the first 30 minutes, confirming observations that organosilicone enhancement occurs early in the uptake process (Section 5.3.4). It was possible however, that the plateau in uptake after this initial time period may be attributed to the subsequent low dosage due to the large spread area. The effect of different dosages of active on uptake is thus investigated in the following section by varying concentrations of the active.

Surfactants of higher EO content (15-20) which have poor spreading properties have been described as the best activators for water-soluble compounds.[1b] Investigations of glyphosate uptake into wheat with AE adjuvants showed higher absorption with higher EO content and lower droplet spread,[38] properties which were synonymous. The results obtained here indicate that it is the EO content rather than droplet spread that is important.

It has been suggested that the rapid absorption of Silwet L-77 into the cuticle may contribute to the observed inhibition of glyphosate absorption.[11,24] The results obtained here suggest that this is not a contributing factor, as a higher uptake would thus be expected for the oligomers with less rapid uptake. The proposal that hydration of the cuticle leads to the enhancement of hydrophilic compound penetration,[2] appears to be the more valid mechanism according to the results obtained here.

The results in this section have indicated that the hydration of the cuticle may be an important factor in the activation of active uptake by $M_2D\text{-}C_3\text{-}O\text{-}(EO)_n\text{-}Me$. In general, highest uptake of the active was observed with the surfactant oligomer showing highest uptake indicating that the uptake mechanism may be by copenetration.

5.3.7 Surfactant and glyphosate uptake with varying glyphosate concentration

The reduction of glyphosate absorption in the presence of Silwet L-77 has been described as inversely related to glyphosate concentration,[24,29] and the results

obtained in Section 5.3.4 with varying Silwet L-77 concentration, were consistent with this postulate. A plateau in uptake after 30 minutes was observed in Section 5.3.6, and low glyphosate dosage (due to large spread areas) was implicated as a possible cause. Furthermore, penetration of low doses of glyphosate are known to be inhibited by low EO surfactants.[7] In Section 5.3.6, it was also postulated that the mechanism for Silwet L-77 enhancement of glyphosate uptake may require copenetration of the surfactant and active. The effect of increased glyphosate concentration on resulting uptake in the presence of M_2D-C_3-O-$(EO)_n$-Me was thus investigated in this section. The percentage uptake results for glyphosate at varying concentrations in the presence of M_2D-C_3-O-$(EO)_6$-Me are shown in Table 5.10 and Figure 5.10.

Table 5.10. Percentage uptake of glyphosate into *Chenopodium album* over time[a] in the presence of M_2D-C_3-O-$(EO)_6$-Me[b]

[Glyphosate]	1%[c]	1%	5%	10%
Time(hours)		%Uptake (SD)		
0.08	6 (3)		7 (5)	1.9 (0.8)
0.5	15 (11)	7 (3)	4 (2)	3.2 (0.6)
2	14 (11)		8.0 (0.9)	5 (3)
24	17 (7)		13 (7)	7 (4)

[a] Uptake of glyphosate < 3% over 4 hours in the absence of surfactant (Section 5.3.3); [b] n[M_2D-C_3-O-$(EO)_6$-Me] = 3.2×10^{-3} mol L^{-1}; [c] Duplicate data from Section 5.3.6, Table 5.9

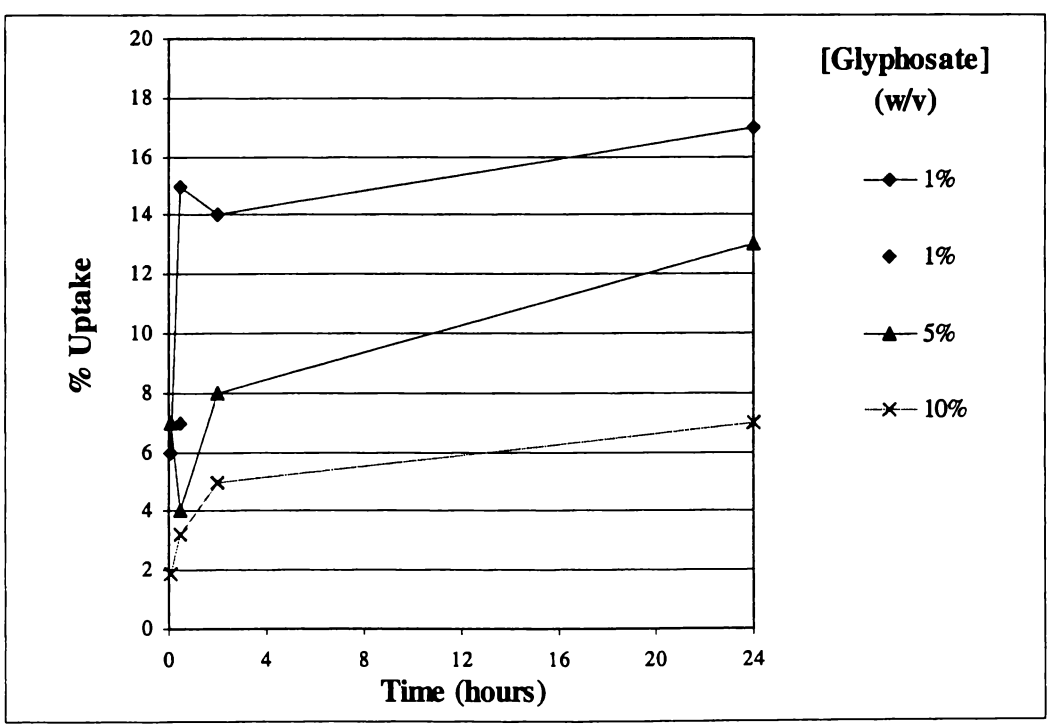

Figure 5.10. Percentage uptake of glyphosate into *Chenopodium album* over time in the presence of M_2D-C_3-O-$(EO)_6$-Me

The highest percentage uptake values were obtained for the 1% glyphosate formulation, the lowest concentration investigated here, and also the concentration used in the preceding investigations. The result obtained for the repeat of the 1% glyphosate solution (30 minutes) falls within the standard deviation of the corresponding data of the previous investigation. Use of this value in the preceding series would also give rise to a more gradual uptake profile as compared to the rapid initial uptake profile observed (Figure 5.8).

The molar values for the glyphosate uptake are shown in Table 5.11. Higher uptake is observed with higher glyphosate concentration confirming that dosage is important for glyphosate uptake.

Table 5.11. Molar uptake of glyphosate into *Chenopodium album* over time[a] in the presence of M_2D-C_3-O-$(EO)_6$-Me[b]

[Glyphosate]	1%[c]	1%	5%	10%
Moles of glyphosate applied/plant	4.0×10^{-7}	4.0×10^{-7}	20.2×10^{-7}	40.4×10^{-7}
Time(hours)		Molar Uptake		
0.08	0.24		1.4	0.8
0.5	0.60	0.28	0.8	1.3
2	0.56		1.6	2.0
24	0.56		2.6	2.8

[a] Uptake of glyphosate < 3% over 4 hours in the absence of surfactant (Section 5.3.3); [b] n[M_2D-C_3-O-$(EO)_6$-Me] = 3.2×10^{-3} mol L^{-1}; [c] Duplicate data from Section 5.3.6, Table 5.9

Table 5.12 shows the corresponding percentage uptake results for M_2D-C_3-O-$(EO)_6$-Me in the presence of glyphosate at varying concentrations.

Table 5.12. Percentage uptake of M_2D-C_3-O-$(EO)_6$-Me into *Chenopodium album* at 2 hours in the presence of glyphosate of varying concentration

[Glyphosate]	0	1%	5%	10%
%Uptake (SD)	65 (10)	54 (6)	34 (5)	39 (14)
CV	15%	11%	15%	36%

The highest percentage uptake for the surfactant was observed with the 1% glyphosate formulation. This was also the concentration for which the highest percentage uptake for glyphosate was observed. These results further indicate that uptake of the active is directly related to the uptake of the surfactant, as proposed

in Section 5.3.6. These results may also support the possibility of a K-depression type effect, described in Section 5.3.4, with uptake of the active and surfactant retarded by mutual solubilisation at the leaf surface in preference to in the cuticle.

In the preceding section it was postulated that spread area and surface tension are also important for this adjuvant system. The spread areas for the solutions were thus determined, and are presented in Table 5.13.

Table 5.13. Spread areas of solutions of M_2D-C_3-O-$(EO)_6$-Me with varying concentrations of glyphosate

	[Glyphosate]			
	0*	1%	5%	10%
Average area**(SD)	35 (4)	42 (5)	32 (7)	26 (7)
CV	11%	12%	20%	27%

* i.e. surfactant alone; ** Area (mm^2) per 0.24 µL droplet;

A significant reduction in the spread areas of the solutions was observed with increasing glyphosate concentration. The glyphosate percentage uptake values are consistent with the trends observed for the spread area data, supporting the hypothesis that high spread area is important for M_2D-C_3-O-$(EO)_n$-Me enhancement of glyphosate uptake.

It was noted that the integrity of the solutions was compromised at high glyphosate concentrations, with a rapid reduction in spread area observed with time. The instability of Silwet L-77 solutions under acidic conditions is well documented,[18,39] and is discussed further in Chapter 6. The spread areas listed in Table 5.13 above were obtained prior to detectable changes in the solution properties. The uptake data observed here should however be interpreted with caution as the stability of the solutions over the time trial was not established.

5.3.8 Bentazone uptake with varying surfactant EO content

The results obtained in Section 5.3.6 indicated that like-polarity of active and surfactant may exhibit some influence. This is investigated further in this section by determining the uptake of a less polar active with varying M_2D-C_3-O-$(EO)_n$-Me oligomers. The results obtained will also provide a means of further investigating the postulate that the mechanism for Silwet L-77 enhancement of uptake is by copenetration of the surfactant and active.

The uptake of bentazone in the presence of M_2D-C_3-O-$(EO)_n$-Me oligomers (n = 3, 6 and 9) is presented in Table 5.14 and Figures 5.11 – 5.12.

Table 5.14. Percentage uptake of bentazone into *Chenopodium album* over time in the presence of different oligomers of M_2D-C_3-O-$(EO)_n$-Me

M_2D-C_3-O-$(EO)_n$-Me	n = 3	n = 6	n = 9
Time (hours)		%Uptake (SD)	
0.08	1.8 (0.8)	9 (6)	5 (4)
0.5	2 (3)	10 (2)	7 (3)
2	9 (8)	23 (18)	10 (3)
4	23 (9)	39 (23)	16 (8)
24	68 (15)	78 (16)	82 (5)

The observed uptake of bentazone into *C. album* foliage is relatively high and constant over time, following a standard pattern of diffusion.

The n = 6 and 9 oligomers gave comparable uptake values at the 24 hour time interval, but showed quite different uptake profiles. The uptake with the M_2D-C_3-O-$(EO)_6$-Me formulation was more rapid over the 0 to 4 hour period whilst the uptake in the presence of M_2D-C_3-O-$(EO)_9$-Me was more gradual over time. The uptake for bentazone in the presence of M_2D-C_3-O-$(EO)_3$-Me was lower than for the other formulations at all time intervals analysed.

The herbicide uptake data, along with surfactant uptake data obtained in Section 5.3.5, are presented in Figure 5.11. The surfactant data were obtained in the absence of active, and thus can be used for general comparisons only.

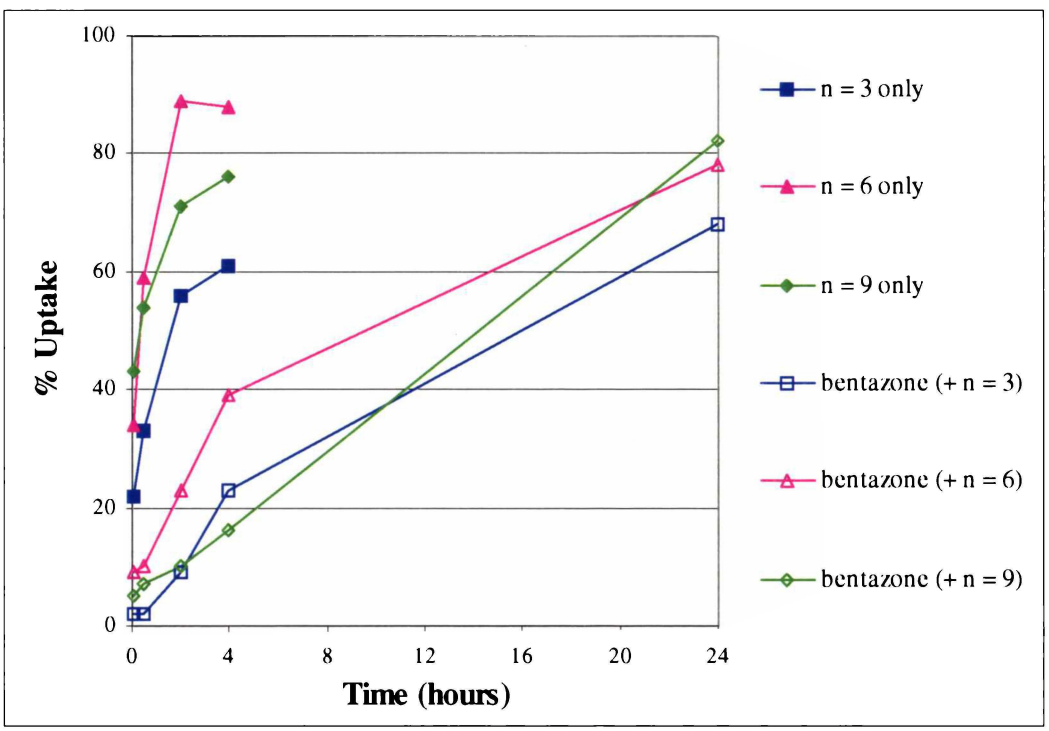

Figure 5.11. Percentage uptake of bentazone and M_2D-C_3-O-$(EO)_n$-Me surfactants into *Chenopodium album*

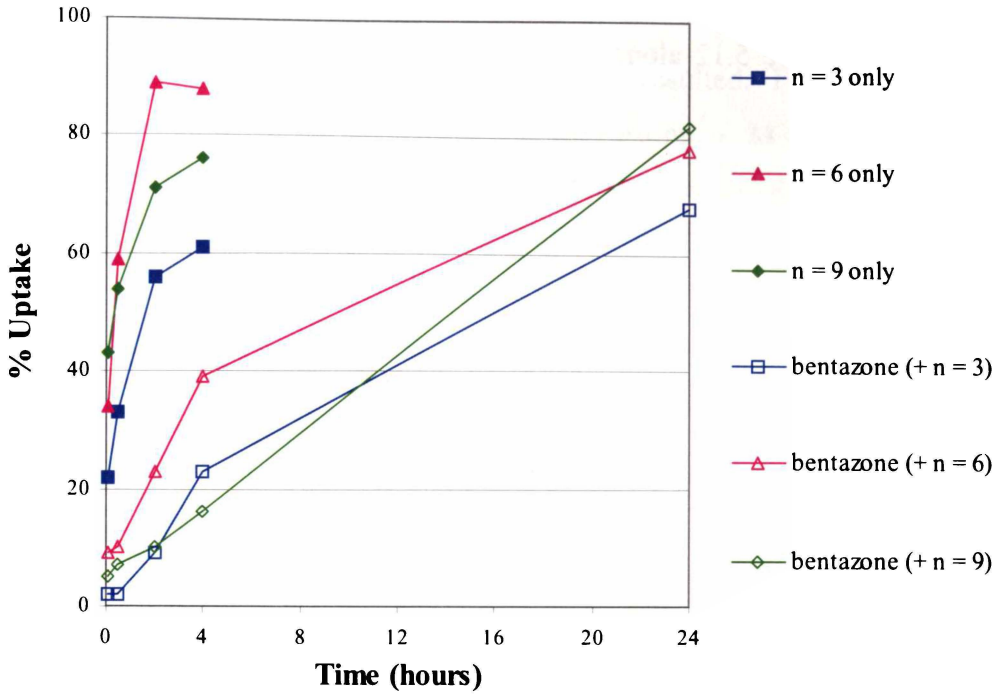

Figure 5.11. Percentage uptake of bentazone and M_2D-C_3-O-$(EO)_n$-Me surfactants into *Chenopodium album*

The highest uptake was observed for the M_2D-C_3-O-$(EO)_6$-Me oligomer both with and without active present, as observed for the uptake of glyphosate (Section 5.3.6). This supports the hypothesis that the uptake of active is directly related to that of the surfactant. The results indicate that copenetration may be important for the uptake mechanism, however the uptake of both compounds independently and in mixtures will need to be determined to confirm this.

Results from Sections 5.3.5 and 5.3.6 also indicated that spread area has an important influence on uptake. The spread area data for the bentazone formulations are thus presented in Table 5.15.

Table 5.15. Spread areas of solutions of bentazone[a] with M_2D-C_3-O-$(EO)_n$-Me oligomers

M_2D-C_3-O-$(EO)_n$-Me	n = 3	n = 6	n = 9
Average area [b] (mm^2)	7	39	27
SD	2	5	6
CV	30%	13%	23%

[a] 1.5% w/v; [b] per 0.24 µL droplet

The highest spread area observed was for the $(EO)_6$ oligomer, consistent with the highest uptake. The uptake also follows the trend predicted by the surface tensions of the M_2D-C_3-O-$(EO)_n$-Me solutions (Section 5.3.2).

To aid comparison and interpretation, the results of the bentazone uptake are presented in Figure 5.12 along with the glyphosate uptake results from Section 5.3.6.

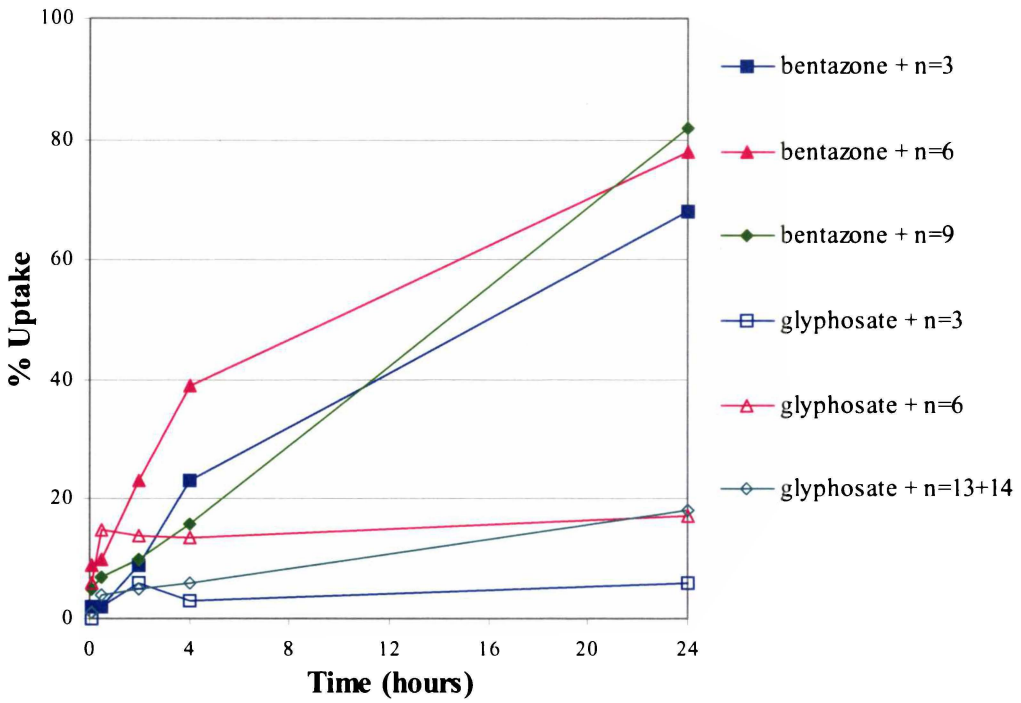

Figure 5.12. Percentage uptake of herbicides into *Chenopodium album* over time in the presence of various M_2D-C_3-O-$(EO)_n$-Me oligomers

The overall uptake of bentazone is much higher than that of glyphosate for all formulations investigated. These differences are not discussed further here, rather only the differences specific to the postulates raised in the preceding sections are addressed.

The highest uptake was observed with the M_2D-C_3-O-$(EO)_6$-Me oligomer for both actives. This result confirms that like-polarity of the surfactant and active ingredient is not a vital factor for enhancement of active uptake by M_2D-C_3-O-$(EO)_n$-Me surfactants. In such circumstances, higher bentazone uptake would have been expected with the more lipophilic M_2D-C_3-O-$(EO)_3$-Me formulation.

The physico-chemical properties of the [bentazone + M_2D-C_3-O-$(EO)_3$-Me] solution were however quite different to that of the other formulations. The surface tension was significantly higher than that observed for formulations containing the other oligomers, and for the glyphosate solutions.* The high

* The stability of the M_2D-C_3-O-$(EO)_3$-Me component in the bentazone solution was thus investigated to confirm degradation was not induced. Qualitative ESI/MS results showed the

surface tension inhibited the dispensing of the 0.24 μL droplets, and larger application droplets, of inconsistent volumes, thus resulted. Phytotoxicity on the leaf surface was also observed with the [bentazone + M_2D-C_3-O-$(EO)_3$-Me] solution at the 24 hour time interval. Phytotoxicity was not observed with any of the other M_2D-C_3-O-$(EO)_n$-Me formulations. These results are consistent with other reports which link the absence of phytotoxicity for Silwet L-77 to a dilution effect due to the high spreading.[4]

Of the two least effective adjuvants in each trial, the oligomer of higher EO content showed higher uptake over the early time intervals for both herbicides. This result supports the postulate raised in Section 5.3.4 that solvation and solubility of the aqueous formulation is also important in the uptake mechanism of these adjuvants.

At the shorter time intervals (≤2 hours) the uptake of glyphosate and bentazone with the equivalent M_2D-C_3-O-$(EO)_n$-Me oligomers (n = 3 and 6) are comparable. The 4 and 24 hour uptake values for the two herbicides however are vastly different. At the 24 hour time interval the percentage uptake for both herbicides was higher with M_2D-C_3-O-$(EO)_n$-Me of higher EO content, although the differences were within experimental error of the M_2D-C_3-O-$(EO)_6$-Me results. The uptake of both the herbicides in the presence of higher EO content M_2D-C_3-O-$(EO)_n$-Me oligomers appears to be more linear with respect to time, when compared with the other oligomers investigated.

5.4 CONCLUSION

The uptake of Silwet L-77, and M_2D-C_3-O-$(EO)_n$-Me components thereof, into *C. album* foliage is rapid and efficient. The uptake of the M_2D-C_3-O-$(EO)_n$-Me oligomers shows a Poisson-like distribution and in general is highest for the n = 6 oligomer and lowest for the n = 3 and 13+14 formulations.

The uptake of glyphosate was low with all M_2D-C_3-O-$(EO)_n$-Me formulations investigated (≤ 20% after 24 hours). The observed rate of bentazone uptake was relatively high and constant over time (≥ 68%), and followed a standard pattern of

---

M_2D-C_3-O-$(EO)_3$-Me was still present as an intact molecule after 24 hours exposure to the bentazone solution and the relative response was essentially unchanged. No other peaks were observed in the GC/MS chromatogram over the 24 hour time period of the trial confirming stability of the surfactant.

diffusion. Stomatal infiltration did not contribute to the uptake mechanism in this species.

Silwet L-77 appears to reduce glyphosate uptake when the mode of uptake is by cuticular penetration. No significant increase in glyphosate percentage uptake was observed with increases in Silwet L-77 concentration, and inhibition of the uptake was observed at high surfactant concentrations. Increased molar uptake for glyphosate with increasing glyphosate concentration was observed, indicating that inhibition of glyphosate uptake by Silwet L-77 may be a dosage-related phenomenon.

There is a possibility that the glyphosate may be retarded on the leaf surface due to a higher solubility in the neat surfactant than in the epicuticular wax. Retardation of surfactant uptake is also observed in the presence of glyphosate.

The uptake of the herbicides (bentazone and glyphosate) in the presence of M_2D-C_3-O-$(EO)_n$-Me oligomers follows the same general trends observed for formulations of the surfactant alone. The uptake of the active appeared to be directly related to the uptake of the surfactant, and the uptake mechanism may thus be by copenetration.

The results suggest that two there are two phases in the uptake mechanism. The initial rapid uptake showed a dependence on EO content, such that increased uptake was observed for increased hydrophilicity. These results may indicate that solvation and solubility is important in the uptake mechanisms of M_2D-C_3-O-$(EO)_n$-Me into *C. album.*

Over the first 4 hours, formulations containing the n = 6 oligomer exhibited the maximum uptake for both herbicides at all time intervals. For the other, less efficiently absorbed oligomers investigated, the higher EO oligomer shows higher uptake. At the 24 hour time interval the percentage uptake for both herbicides was higher with higher EO content, although the values were comparable with those obtained for the M_2D-C_3-O-$(EO)_6$-Me formulations. The uptake of the herbicides in the presence of the larger M_2D-C_3-O-$(EO)_n$-Me oligomers appears to be more linear with respect to time when compared with the other formulations investigated. These results indicate that like-polarity of the surfactant and active ingredient is not a vital factor for surfactant enhanced active uptake and that hydration of the cuticle may be a contributing mechanism.

5.5 REFERENCES

[1] *a.* R.C. Kirkwood, *Pestic. Sci.*, 1993, **38**, 93-102; *b.* D. Stock, P.J. Holloway, *Pestic. Sci.*, 1993, **38**, 165-177; *c.* P.J. Holloway, D. Stock, *Industrial Applications of Surfactants II*, Ed. D.R. Karsa, Special Publication No. 77, Royal Soc., Cambridge, 1990, 303-337

[2] R.C. Kirkwood, *Pestic. Sci.*, 1999, **55**, 69-77

[3] H. de Reuiter, E. Meinen, M.A.M. Verbeck, *Adjuvants for Agrichemicals*, Ed. C.L. Foy, CRC Press, 1992, Chapter 8, 109-116

[4] M. Knoche, *Weed. Res.*, 1994, **34**, 221-239

[5] P.J. Holloway, *Proc. 4th Int. Symp. on Adjuvants for Agrochemicals*, NZ FRI Bulletin No. 193, Ed. R.E. Gaskin, 1995, 167-175

[6] *a.* J. Schönherr, P. Baur, *Pestic. Sci.*, 1994, **42**, 185-208; *b.* P. Baur, J. Schönherr, B.T. Grayson, *Pestic. Sci.*, 1999, **55**, 831-842

[7] D. Stock, B.M. Edgerton, R.E. Gaskin, P.J. Holloway, *Pestic. Sci.*, 1992, **34**, 233-242

[8] P. Leroy, A.R. Chamel, S. Santier, J. Coret, *Proc. 4th Int. Symp. on Adjuvants for Agrochemicals*, NZ FRI Bulletin No. 193, Ed. R.E. Gaskin, Melbourne, 1995, 285 - 290

[9] R.F. van Toor, A.L. Hayes, P.J. Holloway, *Proc. 4th Int. Symp. on Adjuvants for Agrochemicals*, NZ FRI Bulletin No. 193, Ed. R.E. Gaskin, Melbourne, 1995, 279 - 284

[10] *a.* R.F. van Toor, A.L. Hayes, B.K. Cooke, P.J. Holloway, *Crop Prot.*, 1994, **13**, 260-270; *b.* P.J. Holloway, W.W.C. Wong, H.J. Partridge, D. Seaman, R.B. Perry, *Pestic. Sci.*, 1992, **34**, 109-118; *c.* J. Coret, A. Chamel, *Proc. 4th Int. Symp. on Adjuvants for Agrochemicals*, NZ FRI Bulletin No. 193, Ed. R.E. Gaskin, Melbourne, 1995, 272; *d.* D. Stock, P.J. Holloway, P. Whitehouse, B.T. Grayson, *Adjuvants for Agrichemicals*, Ed. C.L. Foy, CRC Press, 1992, Chapter 13, 159-167; *e.* R.C. Kirkwood, H. Knight, I. McKay, J.P.N.R. Chandrasena, *Adjuvants for Agrichemicals*, Ed. C.L. Foy, CRC Press, 1992, Chapter 9, 117-126; *f.* R.E. Gaskin, P.J. Stevens, *Pestic. Sci.*, 1993, **38**, 193-200

[11] J.A. Zabkiewicz, P.J.G. Stevens, W.A. Forster, K.D. Steele, *Pestic. Sci.*, 1993, **38**, 135-143

[12] W.A. Forster, K.D. Steele, J.A. Zabkiewicz, *NZ FRI Bulletin No. 193, Proc. 4th Int. Symp. on Adjuvants for Agrochemicals*, NZ FRI Bulletin No. 193, Ed. R.E. Gaskin, Melbourne, 1995, 267-271

[13] J. Harr, R. Guggenheim, G. Schulke, R.H. Falk, *The Leaf Surface of Major Weeds*, Fricker Ltd, Witterswil, Switzerland, 1991

[14] F.C. Roggenbuck, L. Rowe, D. Penner, L. Petroff, R. Burow, *Weed Technol.*, 1990, **4**, 576-580

[15] *a.* F.C. Roggenbuck, D. Penner, R.F. Burow, B. Thomas, *Pestic. Sci.*, 1993, **37**, 121-125; *b.* F.C. Roggenbuck, R.F. Burow, D. Penner, *Weed Technol.*, 1994, **8**, 582-585

[16] R.E. Gaskin, *Proc. 4th Int. Symp. on Adjuvants for Agrochemicals*, NZ FRI Bulletin No. 193, Ed. R.E. Gaskin, Melbourne, 1995, 243-248

[17] J.A. Zabkiewicz, L.S. Bonnington, W.A. Forster, W. Henderson, *Proc. 5th Int. Symp. on Adjuvants for Agrochemicals*, Memphis, USA, Ed. P.M. McMullan, Chem. Prod. Coop., 1998, 85-92

[18] G.A. Policello, P.J. Stevens, W.A. Forster, G.J. Murphy, *Pesticide Formulations and Application Systems*, Eds. F.R. Hall, P.D. Berger, H.M. Collins, ASTM publishers, 1995, Vol. 14, 313-317

[19] R. Wagner, Y. Wu, H.v. Berlepsch, F. Rexin, T. Rexin, L. Perepelittchenko, *Appl. Organometal. Chem.*, 1999, **13**, 621-630

[20] R. Wagner, Y. Wu, G. Czichocki, H.v. Berlepsch, B. Weiland, F. Rexin, L. Perepelittchenko, *Appl. Organometal. Chem.*, 1999, **13**, 611-620

[21] P.J.G. Stevens, *Pestic. Sci.*, 1993, **38**, 103-122

[22] D.S. Murphy, G.A. Policello, E.D. Goddard, P.J. Stevens, *Pesticide Formulations and Application Systems*, Eds. B.N. Devisetty, D.G. Chasin, P.D. Berger, ASTM publishers, 1993, Vol. 12, 45 - 56

[23] Z.Q. Liu, J.A. Zabkiewicz, *Proc. 5th Int. Symp. on Adjuvants for Agrochemicals*, Memphis, USA, Ed. P.M. McMullan, Chem. Prod. Coop., 1998

[24] *a.* R.E. Gaskin, P.J.G. Stevens, *Pestic. Sci.*, 1993, **38**, 185-192; *b.* R.E. Gaskin, P.J.G. Stevens, *Pestic. Sci.*, 1993, **38**, 193-200

[25] P.J.G. Stevens, R.E. Gaskin, S-O. Hong, J.A. Zabkiewicz, *Pestic. Sci.*, 1991, **33**, 371-382

[26] R.J. Field, N.G. Bishop, *Pestic. Sci.*, 1988, **24**, 55-62

[27] J. Schönherr, *Pestic. Sci.*, 1993, **38**, 155-164

[28] J. Coret, B. Gambonnet, F. Brabet, A.R. Chamel, *Pestic. Sci.*, 1993, **38**, 201-210

[29] J.A. Zabkiewicz, W.A. Forster, K.D. Steele, Z.Q. Liu, *Proc. 4th Int. Symp. on Adjuvants for Agrochemicals* , NZ FRI Bulletin No. 193, Ed. R.E. Gaskin, 1995, 219-224

[30] R.D. Buich, R.J. Field, A.B. Robson, G.D. Buchan, *Adjuvants for Agrichemicals*, Ed. C.L. Foy, CRC Press, 1992, Chapter 6, 87-99

[31] Z.Q. Liu, J.A. Zabkiewicz, *Proc 50th New Zealand Plant Protection Conf.*, Ed. M. O'Callaghan, 1997, 129-133

[32] P.J.G. Stevens, E.A. Baker, N.H. Anderson, *Pestic. Sci.*, 1988, **24**, 31-53

[33] P. Baur, J. Schönherr, B.T. Grayson, *Pestic. Sci.*, 1999, **55**, 831-842

[34] J. Schönherr, H. Bauer, *Adjuvants for Agrichemicals*, Ed. C.L. Foy, CRC Press, 1992, Chapter 2, 18-35

[35] J. Sun, C.L. Foy, *Proc. 4th Int. Symp. on Adjuvants for Agrochemicals*, NZ FRI Bulletin No. 193, Ed. R.E. Gaskin, Melbourne, 1995, 225-230

[36] R.F. Burow, D. Penner, F.C. Roggenbuck,, R.M. Hill, *Proc. 4th Int. Symp. on Adjuvants for Agrochemicals*, NZ FRI Bulletin No. 193, Ed. R.E. Gaskin, Melbourne, 1995, 54-59

[37] P.J.G. Stevens, M.J. Bukovac, *Pestic. Sci.*, 1987, **20**, 37-52

[38] J.D.Nalewaja, R. Matysiak, , *Proc. 4th Int. Symp. on Adjuvants for Agrochemicals*, NZ FRI Bulletin No. 193, Ed. R.E. Gaskin, Melbourne, 1995, 291-296

[39] M. Knoche, H. Tamura, M.J. Bukovac, *J. Agric. Food Chem.*, 1991, **39**, 202-206

CHAPTER 6

A Study of the Degradation of Silwet L-77

6.1 INTRODUCTION

The use of organosilicone surfactants, such as Silwet L-77, in agrochemical formulations has become increasingly widespread. It is thus of interest to study the degradation of these compounds in order to determine their possible environmental impact. The apparently low environmental toxicity[1,2] of the Silwet products combined with the rapid degradation under even very mild conditions[3,4] lends favourably to its use in the natural environment. The objective of this study was to provide more detailed information on the degradation process using controlled laboratory conditions.

6.1.1 Siloxane degradation

The initial degradation of siloxane surfactants is thought to occur predominantly at the siloxane moiety and the stability of silane surfactants to conditions of extreme pH,[5] as compared with siloxane surfactants confirms this. Siloxane degradation has been the subject of extensive research, especially that of polydimethylsiloxane (PDMS) polymers. Much of the information on the degradation products and mechanisms of PDMS polymers has been obtained by thermal degradation in inert atmospheres. PDMS polymers are very stable towards heat and radiation and only under very extreme conditions is degradation observed. The term degradation is used to describe cleavage of all bonds within the molecule whilst depolymerisation refers to the cleavage of the Si-O bond. The Si-O bond is the most easily cleaved bond within the polymer, although in inert atmospheres it is still found to be stable up to 300°C for PDMS polymers with silanol terminal groups (PDMS-OH) and to 400°C for PDMS polymers with TMS terminal groups (PDMS-OTMS). Stability to depolymerisation has been shown to be higher with increasing molecular weight.[6] The addition of a catalyst (NaOH) lowered the polymer decomposition temperature maximum significantly (by 300°C), although it was noted that the product ratios obtained were not affected.[7] Variation in the thermal conditions also showed little effect on the final product distribution.[8]

In the thermal degradation of PDMS-OH polymers a chain lengthening is initially observed, due to condensation reactions (Equation 6.1).

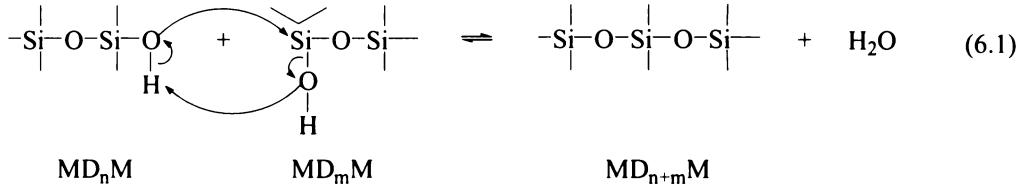

MD_nM MD_mM $MD_{n+m}M$ (6.1)

This is followed by formation of small chain cyclic siloxanes by intra-molecular depolymerisation (Equation 6.2). This occurs via four-centre cyclic transition states, which are stabilised by the vacant 3d orbitals on the Si.

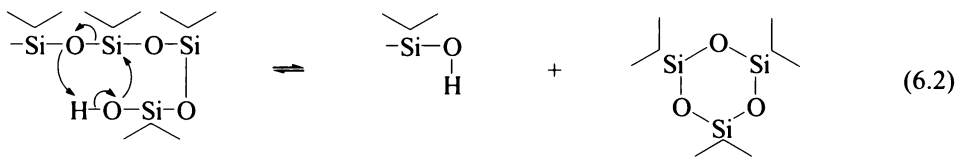

MD_nM $MD_{n-3}M$ D_3 (6.2)

Similar processes are observed for PDMS-OTMS degradation, with MM and MDM products also formed (Equation 6.3). The main products are low molecular weight cyclic siloxanes, with D_3 dominant .

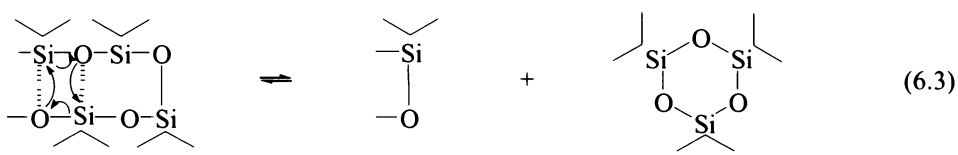

MD_nM $MD_{n-3}M$ D_3 (6.3)

This mechanism also applies to intermolecular reactions, as found by heating blends of siloxane polymers, thus generating higher molecular weight starting materials and low molecular weight volatile cyclics (Equation 6.4).[6]

$$MD_nM + MD_mM \rightarrow MD_{(n-x)+(m-y)}M + D_3 + MD_{(x-1)+(y-2)}M \quad (6.4)$$

6.1.2 Siloxane hydrolysis

The siloxanes are considered to be stable towards water in the absence of a catalyst. The reaction of siloxanes with water is accelerated in the presence of acids with high dissociation constants ($\geq 10^{-2}$), and under the influence of acids or bases the hydrolysis of siloxane bonds proceeds easily (Equation 6.5).[9] The reaction is thought to proceed via a six-membered activated intermediate complex involving the siloxane and two molecules of water. One of the water molecules is protonated to H_3O^+ in the catalytic step and thus the reaction has been shown to be 1st order in the siloxane and H^+, and 2nd order in H_2O.

$$(TMS)_2O + 2H_2O \xrightarrow{H^+} 2TMS\text{-}OH + H_3O^+ \qquad (6.5)$$

Trialkylsilanols undergo homocondensation with comparative ease to give the corresponding disiloxanes. The hydroxyl group in trialkylsilanols is more reactive towards acidic and basic reagents than the tertiary alcohol equivalents. The stability of trialkylsilanols to condensation increases with increase in the chain length of the alkyl substituent.

The silicon atom is capable of carrying more than one hydroxy group and as such numerous $R_2Si(OH)_2$ and even some $RSi(OH)_3$ compounds are known. The stability is determined by the nature of the substituents on the silicon atom, with silane diols, $R_2Si(OH)_2$, where R=H unknown. Siloxane diols are also increasingly stable with increasing siloxane chain length.[9]

Increasing siloxane chain length also infers increased stability to cyclic siloxanes, with the siloxane bond in cyclotetrasiloxanes found to be significantly more stable to acid and base catalysts than the cyclotrisiloxane analogues.[6]

6.1.3 Silwet L-77 degradation

Whilst it has been established elsewhere that the degradation of Silwet L-77 is by hydrolysis,[2] very little is understood about the mechanisms and products of this process. The instability of Silwet L-77 to extremes of pH is well documented, as discussed in Chapter 2.[3,10] The degradation in acidic and alkaline media has been followed, but only using the change in surface tension and loss of parent compound (by GC) as the index.[3] Complete primary degradation was observed in 12 hours at pH 3, as determined by the absence of Silwet L-77 parent peaks in the

GC chromatogram. Stability at ambient pH values was demonstrated, with no increase in surface tension observed even after 40 days at pH 6 – 8.[3] At high concentrations with buffering to pH 7, stability, as determined by spreading, was maintained over 2 years of solution storage.[10] The use of surface tension as an indicator of degradation is however, only of use when the surfactant concentration is below the CMC (critical micelle concentration). Surface tension is constant above this value and thus variations in concentration will not be detected. It was also noted that the final surface tension values obtained were dependent on the Silwet L-77 starting concentration. This was interpreted as a result of variation in distribution of the products formed. The final products of the degradation process were not characterised, although due to the increased solution clarity observed, an increase in the water solubility of the products was inferred.

The degradation products of Silwet L-77 show increased water solubility over the parent surfactant.[3] The potential sites of cleavage for Silwet L-77 are illustrated in Scheme 6.1, all of which would generate more polar products. The Si–O bond (*c.*) is a likely site of cleavage, according to the chemistry of siloxanes and the relative instability of this bond to hydrolysis.

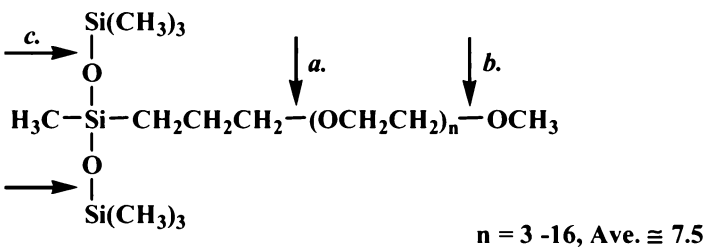

Scheme 6.1. Proposed sites of cleavage (→) in the degradation of Silwet L-77

Cleavage between the hydrophobic head group and the hydrophilic tail group (*a.*) would generate the products, **19** and **20**, whilst cleavage at the terminal methyl group (*b.*) would give rise to M_2D-C_3-O-$(EO)_n$-H type products. A combination of hydrolysis at (*a.*) and (*b.*) would also yield HO-$(EO)_n$-H type products. If hydrolysis at (*b.*) did occur then shorter chain analogues of M_2D-C_3-O-$(EO)_n$-H, HO-$(EO)_n$-H and HO-$(EO)_n$-CH_3 would also be expected due to the comparable nature of the bonds being cleaved.

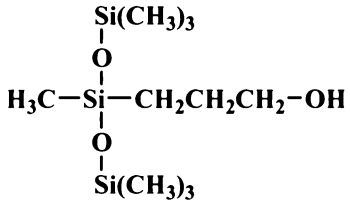

19

20

Hydrolysis of the Si–O bond (*c.*) will lead to the silanol intermediates, **21** and**22**, with the concomitant generation of TMS-OH. The stability of these silanol compounds will be dependent on the substituents and conditions. The subsequent condensation of two molecules of TMS–OH to yield $(TMS)_2$–O is expected to be rapid.

As discussed in Section 6.1, increasing alkyl chain lengths infers increased stability to silanols.[9] Consequently, this would indicate that, in the degradation of Silwet L-77, condensation products will dominate for the lower EO content products and the silanol-type products will be more prevalent for higher EO content products.

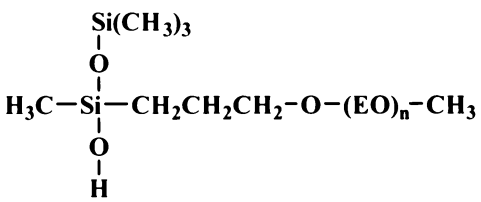

21

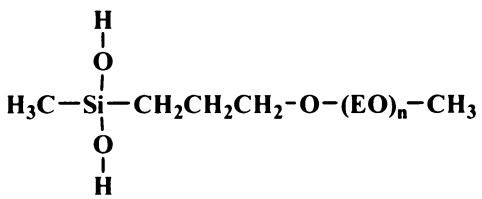

22

Condensation of the silanols **21** and **22** will result in the formation of a number of linear products of the general structure, **23**.

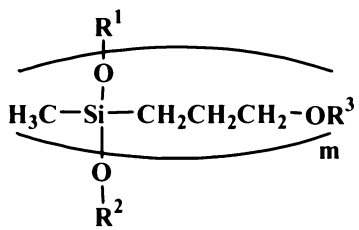

R^1, R^2 = H, $Si(CH_3)_3$; R^3 = H, $(EO)_n$–CH_3

23

Structures of type **23** for m = 2, 3 and 4 etc are described as linear dimers (**24**), trimers (**25**), and tetramers etc, respectively.

Silanols possessing longer chain siloxane backbones also show increased stability.[9] Thus linear polymers (**23**) where the *m* value is large with long EO chains may not be commonly observed products of Silwet L-77.

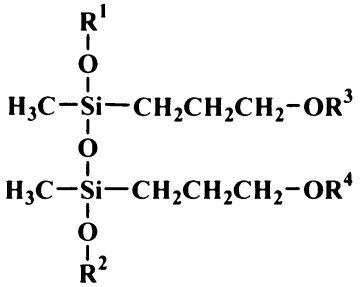

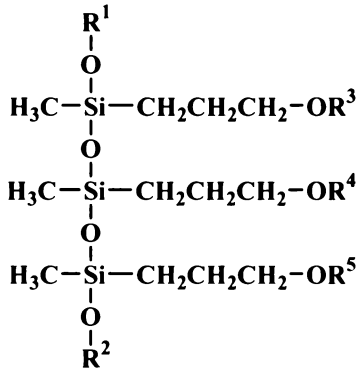

R, R^2 = H, $Si(CH_3)_3$; R^3, R^4, R^5 = H, $(EO)_n$–CH_3

24 **25**

Cyclisation of the linear products will yield products of the generic structure, **26**. The m = 3 and m = 4 variants of **26** are referred to as the cyclic trimer (**27**) and tetramers (**28**) respectively.

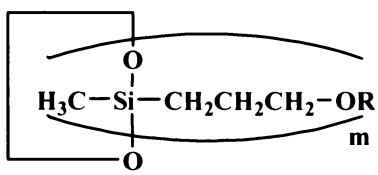

$m \geq 3$, R = H, $(EO)_n$–CH_3

26

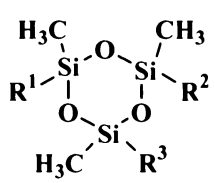

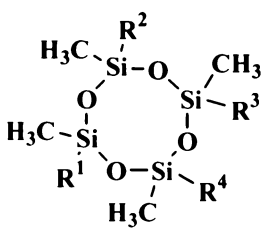

R = $(CH_2)_3$–OH, $(CH_2)_3$–O–$(EO)_n$–CH_3

27 **28**

As discussed in the introduction, increased stability is inferred with increased ring size. The formation of larger cyclics of **26** ($m \geq 5$) for Silwet L-77 may be an essentially irreversible process under the "mild" conditions used here.

The siloxane nomenclature (M, D, T and Q) introduced in Chapter 2, can also be applied to these structures and are listed in Table 6.1.

Table 6.1. Siloxane nomenclature of proposed degradation products

Compound	Abbreviation*	Compound	Abbreviation*
19	M_2D^R	**25**	$M^x(D^R)_3M^y$
21	$MD^R(OH)$	**26**	$(D^R)_m$
22	$D^R(OH)_2$	**27**	$(D^R)_3$
23	$M^x(D^R)_mM^y$	**28**	$(D^R)_4$
24	$M^x(D^R)_2M^y$		

* $M = R_3SiO_{0.5}$; $D = R_2SiO_{(0.5)2}$; R = $-CH_2CH_2CH_2-OH$, $-CH_2CH_2CH_2-O-(EO)_n-CH_3$; x, y = –OH, –OTMS

As can be seen, taking into account the ability of siloxanes to rearrange into a variety of lengths and structures, and compounded by the variation in EO content in components of Silwet L-77, the potential products of Silwet L-77 degradation are numerous. The calculated molecular weights and adduct masses of the above described compounds are listed in Appendix A.III.

6.1.5 Chapter objectives

The objective of the research described in this chapter was to identify the products and mechanisms of the abiotic degradation of Silwet L-77 under hydrolytic conditions. The effect of pH on the relative rates of this degradation was also investigated. API/MS (ESI/MS, APcI/MS and FTICR/MS), HPLC, NMR and GC/MS methods were employed.

The degradation of PEG reference compounds, as determined by ESI/MS, is described in Section 6.3.1. In Section 6.3.2, the results of a preliminary survey of the products of Silwet L-77 degradation as determined by API/MS methods, are presented. In some cases up to eight structures could be envisaged for a particular *m/z* value observed according to the hydrolysis chemistry of siloxane structures. At the level of accuracy offered by the ESI/MS technique used these could not be distinguished. In Section 6.3.3, results from analysis by online HPLC/ESI/MS are described, where separation of the mixture was hoped to clarify assignment. The

FTICR/MS technique was also applied to the samples to provide more information on the structures (Section 6.3.4). The high resolution data obtained allowed the possible structures to be ranked in order of likelihood, and thus unlikely structures could be determined and discarded. Where possible, commercially available products were analysed and comparison of the exact masses of the commercial products [i.e. $CH_3O(EO)_nH$] was made with those observed in the degraded Silwet L-77. The isotope patterns for the products were also addressed as a possible method for structural elucidation.

The degradation of less complex samples was also investigated in order to simplify assignment. The degradation of purified $M_2D\text{-}C_3\text{-}O\text{-}(EO)_n\text{-}CH_3$ samples (6.3.5), and single oligomers of $M_2D\text{-}C_3\text{-}O\text{-}(EO)_n\text{-}CH_3$ (6.3.6), as determined by ESI/MS and HPLC/ESI/MS methods, is described.

In Section 6.3.7, results from FTICR/MS studies on $M_2D\text{-}C_3\text{-}O\text{-}(EO)_n\text{-}CH_3$ degradation are presented. In-source degradation in the gas phase using concentrated acetic acid was also investigated. Results from GC/MS and NMR studies on Silwet L-77 degradation are discussed in Sections 6.3.8 and 6.3.9, respectively. Sections 6.3.10 and 6.3.11 cover quantitative studies on Silwet L-77 degradation by API/MS and HPLC methods, respectively.

6.2 MATERIALS AND METHODS

6.2.1 Acid degradation of PEG reference compounds

Degradation of $CH_3O(EO)_nH$ (Ave. n ≈ 7.5), $HO(EO)_nH$ (Ave. n ≈ 8), and $CH_3O(EO)_3H$, was investigated. Samples of the PEG derivatives (0.2 g) were allowed to react with 2M HCl (5 mL) over 4 days at room temperature. The resulting reaction mixtures were analysed by ESI/MS.

6.2.2 Analysis of Silwet L-77 degradation by API/MS

6.2.2.1 Degradation (40 000 ppm) with varying HCl concentration

Three 0.2 g/ 5mL solutions of Silwet L-77, prepared in 2 M, 0.2 M and 0.02 M HCl, respectively, were allowed to react at room temperature for 4 days. A water/heptane (25 mL: 30 mL) solvent extraction was performed on the product mixtures and the resulting solutions concentrated by rotary evaporation and vacuum. The mass recoveries of the water-soluble fractions were 63%, 77% and 79%, respectively. The heptane-soluble fractions comprised 1% of the mass recoveries for all concentrations investigated. Overall mass recoveries of 64%, 78% and 80% were thus obtained.

Solutions of all fractions prepared in MeOH (100 ppm), were characterised by ESI/MS and APcI/MS using an elution solvent of 1:1 MeOH/H_2O. The heptane-soluble fractions were also analysed by ESI/MS using CH_2Cl_2 as the preparation solvent and CH_3CN as the elution solvent.

6.2.2.2 Acid degradation with varying Silwet L-77 concentration (200, 2000 and 20 000 ppm)

Three solutions of Silwet L-77 (0.1, 0.01, 0.001 g) were prepared in 5 mL of 0.2 M HCl and allowed to react at room temperature for 4 days. A water/heptane (10 mL: 20 mL) solvent extraction was performed and the resulting solutions concentrated by rotary evaporation and vacuum methods. The mass recoveries of the water-soluble fractions for the 0.1, 0.01 and 0.001 g degraded samples respectively, were 77%, 88% and 100%. The heptane-soluble fractions gave mass recoveries of <1% in all cases.

Solutions of the H_2O-soluble fractions were prepared in MeOH and characterised by ESI/MS with 1:1 MeOH/H_2O as the elution solvent. The

heptane-soluble fractions were prepared in CH_2Cl_2 and analysed with CH_3CN as the ESI/MS elution solvent.

6.2.2.3 Base degradation of Silwet L-77 (40 000 ppm)

A solution of Silwet L-77 (0.2 g) in 0.2 M NaOH (5 mL) was allowed to react at room temperature for 2 days. A water/heptane (10 mL: 30 mL) solvent extraction was performed and the resulting solutions concentrated by rotary evaporation and vacuum. The heptane-soluble fractions gave a mass recovery of 0.2%. The water-soluble fraction was applied to a RP C_{18} Sep-pak column and the NaOH removed by elution with 100% H_2O. The sample was eluted with 100% MeOH and concentrated by rotary evaporation. The mass recovery of the MeOH-soluble fraction was 52%. ESI/MS spectra of the H_2O- and MeOH- eluted Sep-pak fractions, and the heptane-soluble solvent partition fraction, were obtained.

6.2.2.4 Bulk Silwet L-77 acid degradation

6.2.2.4.1 Degradation at high concentration (500 000 ppm)

A solution of Silwet L-77 (10 g) in 2.0 M HCl (10 mL) was allowed to react at room temperature for 30 hours. An ESI/MS spectrum was acquired to determine complete degradation of the Silwet L-77. The resulting mixture was then transferred to a 100 mL separating funnel with 30 mL of H_2O and 50 mL of n-heptane. The H_2O layer was removed and the heptane layer then washed twice with 5 mL of H_2O. The solvent fractions were evaporated to dryness by rotary evaporation and vacuum. An overall mass recovery of 94% was obtained, with the heptane- and water- soluble fractions giving mass recoveries of 2% (0.172 g) and 92% (9.199 g) of the starting mass, respectively.

6.2.2.4.2 Degradation at intermediate concentration (40 000 ppm)

A 5 g / 125 mL solution of Silwet L-77 in 2.0 M HCl was stirred at room temperature for 3 days. Solvent extraction was then performed following addition of 20 mL H_2O and 100 mL of n-heptane. The heptane layer was washed three times with 5 mL of H_2O then evaporated to dryness by rotary evaporation and vacuum. The H_2O-soluble fraction was evaporated to dryness by vacuum and freeze drying methods. The heptane- and water- soluble fractions gave mass

recoveries of 0.4% (0.0217 g) and 75% (3.7528 g) of the starting mass, respectively, to give an overall mass recovery of 75%.

6.2.3 Analysis of Silwet L-77 degradation by HPLC

6.2.3.1 Analysis of the water-soluble products by RP C_{18} HPLC/ESI/MS

The water-soluble fraction of a degraded Silwet L-77 sample (Section 6.2.2.1.*b*) was analysed by RP C_{18} HPLC/ESI/MS using a H_2O/MeOH solvent gradient (elution profile: 0 –20 minutes, 85:15; 20 – 60 minutes, 70:30; 60-120 50:50). The MS conditions were as described previously.

6.2.3.2 Analysis of the heptane-soluble products by SiO_2 HPLC/ESI/MS

A normal phase open column separation of the heptane-soluble fraction of degraded Silwet L-77 (Section 6.2.2.4) was performed using a gradient of 100% hexane to 50:50 hexane:EtOAc to 100% EtOAc to 100% EtOH. The sample (160 mg) was applied to a SiO_2 column (30 g, 60-120 mesh) and eluted with 50 mL volumes of each solvent composition. The column was further washed with 100% EtOH (125 mL total) until no further products were eluted.

Fractions were analysed by ESI/MS and SiO_2-HPLC/ESI/MS. It was found that post column addition of a salt solution was required to enable detection of the analytes by SiO_2-HPLC/ESI/MS. The equipment used is shown schematically below.

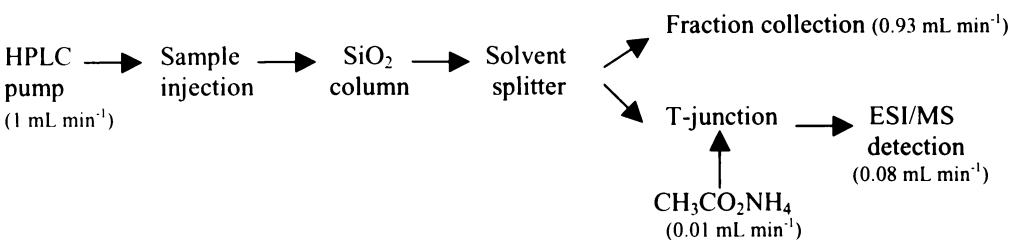

ESI/MS detection was conducted in TIC mode with a *m/z* range of 200-1100 and a scan time of 2.15 seconds. The source temperature was set at 40°C and gas flow rates at 200 and 12.5 L h^{-1}. An elution solvent of 1:1 EtOAc/CH_2Cl_2 and 10 mM $CH_3CO_2NH_4$ solutions were used.

6.2.3.3 Analysis of the heptane-soluble products by RP C_{18} HPLC/ESI/MS

The heptane-soluble fraction of a degraded Silwet L-77 sample (Section 6.2.2.4.1, 0.02 mg, 10 μL) was analysed by RP C_{18} HPLC/ESI/MS using an elution solvent of 3:1 CH_2Cl_2/CH_3CN (0.05 mL min^{-1}). The instrument settings were as established previously for standard ESI/MS (Table 3.12), with analysis in TIC mode using a scan range of *m/z* 100-1600 and scan time of 5 seconds.

6.2.4 Analysis of Silwet L-77 degradation by FTICR/MS

Solutions of the water- and heptane- soluble fractions of acid degraded Silwet L-77 (6.2.2.4.2) were prepared in CH_3CN (0.2 mg mL^{-1}) for analysis by FTICR/MS. NaI (0.1 mg mL^{-1}) was added to both prior to analysis to aid ionisation. The heptane-soluble fraction was analysed by APcI/MS, whilst ESI/MS was used for the H_2O-soluble fraction, to maximise ionisation as discussed in Section 1.2.4. For comparison the FTICR/MS spectrum of $CH_3O(EO)_nH$ (Ave. n ≈ 7.5) was also acquired.

6.2.5 Degradation of M_2D-C_3-O-$(EO)_n$-Me purified from Silwet L-77

6.2.5.1 Degradation of M_2D-C_3-O-$(EO)_n$-Me

A solution of M_2D-C_3-O-$(EO)_n$-Me* was left to stand for ten days at room temperature in 25:75 H_2O/MeOH, and the resulting solution separated by preparative HPLC. The early eluting polar fractions were collected and analysed by ESI/MS, HPLC/ESI/MS and FTICR/MS.

6.2.5.2 Acid degradation of M_2D-C_3-O-$(EO)_n$-Me

A solution of M_2D-C_3-O-$(EO)_n$-Me† in 2 M HCl (1.4:1 H_2O/CH_3CN) was allowed to stand at 8°C and analysis by ESI/MS performed at selected intervals up to 2 months.

6.2.6 Degradation of pure M_2D-C_3-O-$(EO)_n$-R oligomers

All single oligomers used for the following degradation studies were obtained by chromatographic methods,‡ excluding M_2D-C_3-O-$(EO)_3$-Me* and M_2D-C_3-O-EO-H.†

---

* Purified by RP C_{18} column chromatography, Section 2.2.1.2
† Purified by preparative RP C_{18} HPLC, Section 2.2.1.1
‡ Purified by RP C_{18} HPLC, Section 2.2.1.2

6.2.6.1 Acid degradation of M_2D-C_3-O-$(EO)_3$-Me

6.2.6.1.1 Degradation at low concentration (1 000 ppm)

A solution of M_2D-C_3-O-$(EO)_3$-Me (1 mg mL^{-1}) was prepared in 5% HCO_2H (75:25 MeOH/H_2O) and monitored directly by ESI/MS (20V and 60V) at selected time intervals. MeOH was used to aid miscibility. Analysis was performed at t = 0, 15, 30 and 60 minutes, 2, 4, 6, and 24 hours and 2, 3 and 15 days. Salt solutions were used to aid assignment of peaks where necessary.

6.2.6.1.2 Degradation at high concentration (500 000 ppm)

A 0.3 g sample of M_2D-C_3-O-$(EO)_3$-Me was allowed to react with 0.3 mL of 0.44 M HCl (prepared by 1:8 dilution of 4 M HCl with THF) at room temperature with stirring. THF was required to facilitate miscibility. At selected time intervals aliquots were taken, diluted with MeOH and characterised by ESI/MS. Analysis was performed at t = 6, 24, 80 and 120 hours.

6.2.6.2 Acid and base degradation of M_2D-C_3-O-$(EO)_6$-Me (1000 ppm)

Solutions of M_2D-C_3-O-$(EO)_6$-Me (1 mg mL^{-1}) were prepared in 0.1 M HCl and NaOH respectively, and allowed to react at room temperature for 54 hours. A water/heptane (10 mL: 12 mL) solvent extraction was performed and the resulting solutions concentrated by rotary evaporation and vacuum. The water-soluble fraction of the base degraded sample was applied to a RP C_{18} Sep-pak column and fractions eluted with 100% H_2O and 100% MeOH.

Solutions for ESI/MS characterisation were prepared in MeOH and eluted with 2:1 MeOH/H_2O. The heptane-soluble fractions were also analysed following preparation in CH_2Cl_2 using CH_3CN as the elution solvent.

6.2.6.3 Acid degradation of M_2D-C_3-O-$(EO)_9$-Me

A solution (1 mg mL^{-1}) of M_2D-C_3-O-$(EO)_9$-Me was prepared in 5% HCO_2H (1:1 MeOH/H_2O). At selected time intervals aliquots were taken, diluted with MeOH/H_2O and characterised by ESI/MS. Analysis was performed at t = 0, 15, 30, 45, 60, 75, 90 and 105 minutes, 2, 3, 14, 47, 122 and 194 hours. Salt solutions were used to aid assignment of peaks where necessary. For the final time

---

* Synthesised by the procedure described in Section 2.2.2.1

† Obtained from Witco Corporation, Organosilicones Group, Tarrytown, NY.

measurement, a water/heptane solvent extraction was also performed prior to ESI/MS analysis.

6.2.6.4 Acid degradation of M_2D-C_3-O-$(EO)_n$-Me, n = (7+8+9)

A solution (1 mg mL^{-1}) of the oligomeric mixture was prepared in 10% HCO_2H. At selected time intervals aliquots were taken, diluted with MeOH/H_2O and characterised by ESI/MS. Analysis was performed at t = 0, 10, 30, 45, 60, 75, 90 and 105 minutes, 2, 2.5, 3, 3.5, 4, 15 and 48 hours. Salt solutions were used to aid assignment of peaks where necessary. For the final time measurement a water/heptane solvent extraction was also performed prior to ESI/MS analysis.

6.2.6.5 Acid degradation of M_2D-C_3-O-$(EO)_n$-Me, n = 6, n = (8+9) and n = (12+13)

Samples of the M_2D-C_3-O-$(EO)_n$-Me oligomeric mixtures were allowed to react at room temperature with 2 M HCl (1 mg mL^{-1}) for 24 hours. The resulting solution from the n = 6 oligomer degradation was concentrated under a stream of compressed air with gentle heating. The n = (8+9) and n = (12+13) degradation solutions were concentrated under a stream of nitrogen gas with gentle heating with the latter also further dried by vacuum. The samples were then diluted to a 100 ppm concentration with 1:1 MeOH/H_2O and characterised by ESI/MS. Salt solutions were added to confirm the adduct ions and therefore parent molecular weight.

6.2.6.6 Acid degradation of M_2D-C_3-O-EO-H

6.2.6.6.1 Qualitative study of M_2D-C_3-O-EO-H degradation (40 000 ppm)

A sample of M_2D-C_3-O-EO-H (1 g) was allowed to react with aqueous 2 M HCl (25 mL) over four weeks at room temperature with stirring. At selected time intervals aliquots were taken, extracted between water and heptane, and both fractions characterised by ESI/MS. Analysis was performed at t = 2, 3, 7 and 12 days and 4 weeks. Salt solutions were used to aid assignment of peaks where necessary. Because the M_2D-C_3-O-EO-H was insoluble in water, the experiment was repeated in 1:1 and 3:1 THF/H_2O to aid miscibility.

6.2.6.6.2 Quantitative study of M_2D-C_3-O-EO-H degradation (500 ppm)

Solutions of M_2D-C_3-O-EO-H (25 mg, 50 mL) were prepared in 100% H_2O and in 5% HCO_2H (3:1 THF/H_2O). At selected time intervals, 30 μL aliquots were mixed [1:1 (v/v)] with the internal standard, $C_6(EO)_3$ (1000 ppm), and characterised by ESI/MS. Analysis was performed at t = 0, 1, 2, 3, 8, 24, 48 and 72 hours. A value was obtained for the response of the internal standard at each time interval relative to that at t = 0. Each ion response is reported as a function of this ratio in order to minimise the effects of instrument variation.

6.2.7 FTICR/MS studies on M_2D-C_3-O-$(EO)_n$-R degradation

6.2.7.1 Acid degradation of M_2D-C_3-O-$(EO)_6$-Me

A 1 mg solution of M_2D-C_3-O-$(EO)_6$-Me* in 1 mL of 2M HCl was allowed to react over 26 hours at room temperature. The resulting solution was evaporated to dryness at 40°C under a stream of compressed air. For MS analysis a 0.1 mg mL^{-1} solution was prepared in MeOH, 0.1 mg mL^{-1} of NaI added [1:1 (v/v)], and the sample spiked with untreated M_2D-C_3-O-$(EO)_6$-Me.

6.2.7.2 Gas-phase acid degradation of M_2D-C_3-O-$(EO)_{10}$-Me

The ion at *m/z* 757 [Na^+ adduct of M_2D-C_3-O-$(EO)_{10}$-Me] was isolated and activated by sustained offline resonance irradiation (SORI) of a sample of Silwet L-77. Gaseous CH_3CO_2H was then introduced into the ionisation chamber via the vacuum leak valve.

6.2.8 GC/MS studies on Silwet L-77 degradation

6.2.8.1 Acid degradation of M_2D^H (100 000 ppm)

A solution of M_2D^H (5 g) in 2.0 M HCl (5 mL) was allowed to react at room temperature with stirring in a sealed vessel. THF (40 mL) was added to aid miscibility. An aliquot of the product mixture was taken and analysed by GC/MS (EI) after 30 hours.

6.2.8.2 Acid degradation of Silwet L-77

GC/MS analysis was conducted on the heptane-soluble fraction of acid degraded Silwet L-77 (Section 6.2.2.4.1).

---

* Purified by RP C_{18} HPLC, Section 2.2.1.2

6.2.8.3 Head space analysis of acid degraded Silwet L-77 (500 000 ppm)

A solution of Silwet L-77 (50 g) in 2 M HCl (50 mL) was allowed to react at room temperature in a sealed vessel. A sample of the gas phase above the solution was removed by syringe after 48 hours, and analysed by GC coupled with EI/MS detection.

6.2.9 NMR studies on Silwet L-77 degradation

6.2.9.1 ^{1}H NMR of M_2D-C_3-O-$(EO)_n$-Me polar degradation products

The polar fraction obtained by separation of degraded M_2D-C_3-O-$(EO)_n$-R (Section 6.2.5.1) was concentrated by rotary evaporation and vacuum and analysed by ^{1}H NMR methods.

6.2.9.2 ^{1}H and ^{13}C NMR of Silwet L-77 degradation under acidic conditions

The water- and heptane- soluble fractions of acid degraded Silwet L-77 (Section 6.2.2.1) were analysed by ^{1}H and ^{13}C NMR.

6.2.9.3 ^{29}Si NMR studies of Silwet L-77 degradation under acidic conditions

A 50% solution of Silwet L-77 prepared in THF, was mixed with 2M HCl (4:1) and analysed by ^{29}Si NMR at 20 minutes, 1 hour, 1 week and 2 years. For comparison, the ^{29}Si NMR spectrum of a 50% solution of Silwet L-77 prepared in THF was also analysed.

6.2.10 Quantitative API/MS studies on Silwet L-77 degradation

The flow injection APcI/MS method was used to monitor the response of Silwet L-77 relative to the internal standard, $C_6(EO)_3$. The MS conditions were as described previously (Table 3.14), with analysis conducted in the TIC mode (*m/z* range: 200 – 1100; scan time: 2.15 seconds).

The ions corresponding to the Na^+ and K^+ adducts of the M_2D-C_3-O-$(EO)_6$-CH_3 oligomer (*m/z* 581 and 597) and the Na^+ adduct of the $C_6(EO)_3$ (*m/z* 257), were used for quantitation. The chromatograms of these ions were extracted from the total ion current chromatogram.

Standard solutions of Silwet L-77 and $C_6(EO)_3$ were prepared as in Chapter 4. The solutions were analysed at the beginning, middle and end of every MS session (3 to 5 replicate injections per solution), storing under refrigeration when

not in use. A linear response from standard solutions was ensured before sample analysis. Standard curves were run before, during and after each set of measurements. Recoveries were obtained by extrapolation from the appropriate standard curve using least-squares fit linear regressions.

6.2.10.1 Bulk solution analysis (10 ppm)

Two solutions of Silwet L-77 (10 ppm) were prepared with 100% Milli-Q H_2O (pH 6.0) and 0.01% HCO_2H (pH 3.2) respectively, and left to stand at room temperature. At selected time intervals (t = 0, 2, 4, 6, 12 and 48 hours, 7, 16, 28, 42 and 56 days) aliquots were taken, mixed 1:1 (v/v) with $C_6(EO)_3$ (10 ppm) and analysed by APcI/MS.

6.2.10.2 Multiple sample analysis (1000 ppm)

Individual samples (20) of 1000 ppm Silwet L-77 (1 mL) were prepared (100% Milli-Q H_2O) and left to stand at room temperature. At selected time intervals (t = 0, 6, 12, 24 and 48 hours, 4, 7, 14, 21 and 28 days) two samples were taken and worked up for MS analysis. The samples were diluted with MeOH (1 mL), a 100 µL aliquot was taken and this aliquot further diluted to 5 mL with 50% MeOH. The solutions were freezer stored until the end of the 28 day experiment period, when all samples were analysed. Immediately prior to analysis the samples were mixed with an equivalent volume (250 µL) of internal standard (10 ppm). Each solution was analysed five times. The experiment was repeated 3 times and results are presented as compared with those obtained by HPLC methods (6.2.11.2).

6.2.11 Quantitative HPLC studies on Silwet L-77 degradation

The degradation of Silwet L-77 in organic (6.2.11.1) and aqueous (6.2.11.2) solvents was investigated by HPLC (light scattering mass detection) using 90:10 MeOH/H_2O as the elution solvent. An external standard method was adopted for quantitation, where the responses of the sample solutions were compared with those obtained for Silwet L-77 solutions of known concentrations to determine recoveries (i.e. no internal standard was added to the sample solutions).

6.2.11.1 Degradation in 90:10 MeOH/H_2O

Four samples of Silwet L-77 were prepared in 90:10 MeOH/H_2O (1 g L^{-1}) with varying quantities of formic acid (0%, 0.1%, 1%, 10%). Aliquots were taken at selected time intervals over a 40 day time period. Percentage recoveries were determined by comparison with the responses obtained for a series of standard solutions. The Silwet L-77 standard solutions were prepared by serial dilution of a 0.1 g L^{-1} (100% recovery) Silwet L-77 solution (90:10 MeOH/H_2O) to give concentrations equating to 90, 80, 70, 60, 40, 20 and 10% recoveries.

6.2.11.2 Degradation in 100% H_2O

Four samples of Silwet L-77 in 100% Milli-Q H_2O (2 g L^{-1}), with varying quantities of formic acid (0%, 0.01%, 0.1%, 1%), were analysed over a 5 day time period. Aliquots (200 µL) were taken at selected time intervals, mixed with MeOH (200 µL) and analysed by HPLC. Percentage recoveries were determined by comparison with the responses of standard solutions as for 6.2.11.1.

6.3 RESULTS AND DISCUSSION

In the following discussions, the term M is used to describe the parent molecules, M_2D-C_3-O-$(EO)_n$-R. Products are formed by hydrolysis, therefore in reactions involving the loss of TMS groups a water molecule is incorporated, and in condensations a water molecule is released. For simplicity, the water loss/incorporation has not been included, rather is assumed in the product descriptions used. For example, the term M-TMS is used to define the parent molecule with one terminal TMS group cleaved through hydrolysis (M–TMS+H). Similarly, the M-2TMS description refers to the parent molecule with both terminal TMS groups hydrolytically removed (M–2TMS+2H).

In descriptions of products containing more than one EO chain, the total number of EO units within the molecule is denoted by n_{TOTAL}. The $n_{EO/chain\#}$ term is used to define the number of EO units per chain assuming all chain lengths are equivalent. In reality EO chains of differing length will occur within a compound and the $n_{EO/chain\#}$ value is only the average of the sum of these units. The actual EO chain lengths will be whole integers. For example, a linear dimer described as having a n_{TOTAL} of 5 and $n_{EO/chain\#}$ of 2.5, has two EO chains of average EO content of 2.5, within the molecule. In reality, the structure will consist of one $(EO)_2$ and one $(EO)_3$ chain, the only possible EO distribution in this case. The synthetic conditions of Silwet L-77 are such that most of the n = 1 and n = 2 M_2D-C_3-O-$(EO)_n$-CH_3 oligomers should be removed.[11] In order for a proposed structure to be valid the $n_{EO/chain\#}$ value must therefore exceed 2.

The term *ion series* is used to refer to a succession of ions varying by 44 a.m.u. (the molecular weight of an EO unit).

In Section 6.3.2, the results of a preliminary survey of the products of Silwet L-77 degradation are presented. The products were partitioned by an organic/aqueous solvent extraction to simplify assignment, and to provide information pertaining to the polarity of the products (Scheme 6.2).

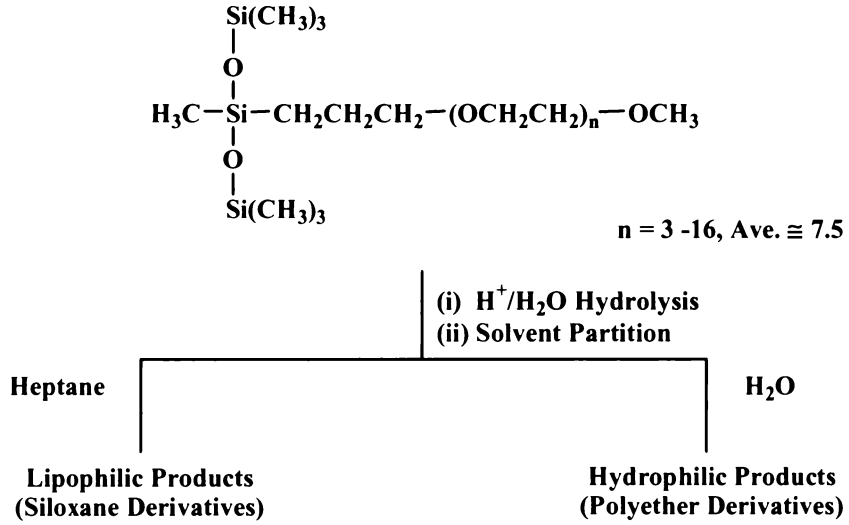

Scheme 6.2. Degradation and solvent extraction of Silwet L-77

A number of other properties can be used to aid in the tentative assignment of structures. All products containing the $(EO)_n$-CH_3 moiety formed, should be of molecular weights corresponding to $n \geq 2$, the lowest EO chain length possible, as defined by the starting materials used. The EO distribution of the starting materials ($n = 3 - 16$, ave. $n \approx 7.5$) can also be used to predict likely structures and the expected polarity of products can be used to infer likelihood of structures with respect to their partitioning following solvent extraction. It may also be possible to use adduct formation patterns to determine likelihood of structures according to EO chain length (i.e. using cation chelating properties as discussed in Chapter 3).

The stability inferred to silanol products by different siloxane backbone and EO chain lengths may also provide potential grounds for structural discrimination. The presence of precursors may also provide support for certain structures. Variation in the isotope patterns for the products are also discussed as a possible method for structural elucidation.

6.3.1 Acid degradation of PEG reference compounds

The acid catalysed degradation of PEG derivatives was investigated in order to determine the likelihood of hydrolysis of the EO chain and the terminal CH_3 group of M_2D-C_3-O-$(EO)_n$-Me [i.e. *b.*-type cleavage (Scheme 6.1)]. This would provide information regarding the probability of shorter chain $CH_3O(EO)_nH$ oligomers, $HO(EO)_nH$ and M_2D-C_3-O-$(EO)_n$-H structures as possible degradation products of Silwet L-77.

The spectra of $CH_3O(EO)_nH$ (Ave. n ≈ 7.5), $HO(EO)_nH$ (Ave. n ≈ 8) and $CH_3O(EO)_3H$ following exposure to acid were essentially unchanged. The parent molecules dominated the spectra in all cases, with only the adduct distribution affected. In the absence of acid, the Na^+ adducts were dominant, whilst with the addition of acid the major ions were the H^+ adducts.

6.3.2 Analysis of Silwet L-77 degradation by API/MS

6.3.2.1 Degradation (40 000 ppm) with varying HCl concentration

Solutions of Silwet L-77 were degraded in 2 M, 0.2 M and 0.02 M HCl, solvent extracted, and analysed by ESI/MS. The spectra obtained for all fractions were very complex and yielded many ions, especially in the high molecular mass range, complicating assignment. A major series of ions in the spectra of the water-soluble fractions was observed at *m/z* 187, 231, 275, 319, 363, 407, 451, 495, 539, 583, 627, 671 and 715 (Δ*m/z* 44). These ions dominated the spectra of the 2 M and 0.2 M HCl degraded samples (Figure 6.1, *a.* and *b.*) and correspond to the cleaved monomethyl-ethoxylate chains, $CH_3O(EO)_nH$ (**20**, n = 3 - 15, Na^+ adducts).

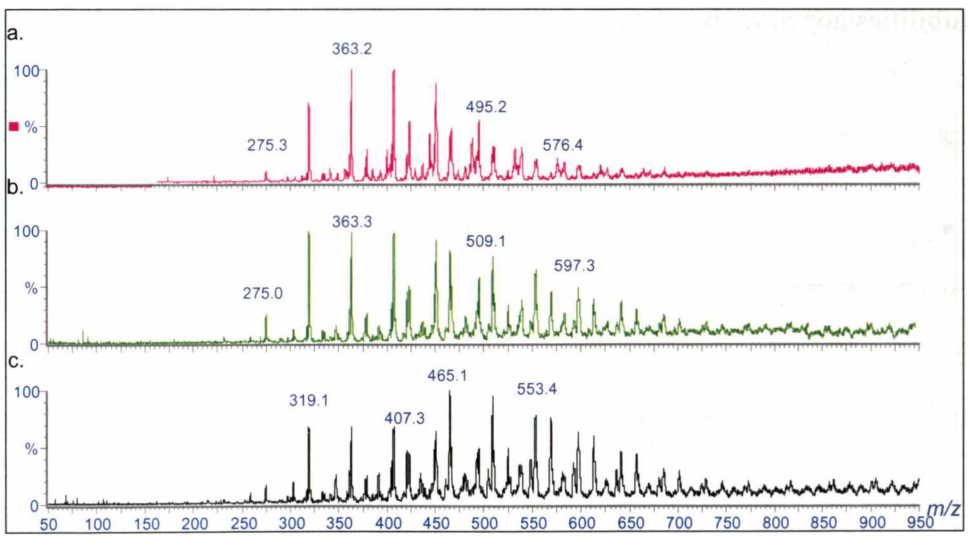

Figure 6.1. ESI/MS spectra of H_2O-soluble fractions of Silwet L-77 degraded with: *a.* 2 M; *b.* 0.2 M; and *c.* 0.02 M HCl

A series at *m/z* 377, 421, 465, 509, 553, 597, 641, 685, 729, 773, 817 and 861 was observed in the spectra of the 0.2 M and 0.02 M HCl degraded samples, and was the major series in the spectrum of the latter (Figure 6.1.*c*). These ions correspond to the parent molecules less one TMS group, i.e. **21** (n = 3 - 14, Na^+

adducts), and to the synthetic by-product $(M^{OH})_2D\text{-}O\text{-}(EO)_n\text{-}CH_2CH{=}CH_2$, **11** (n = 5 – 16), proposed in Chapter 2. Higher molecular weight ions of this series (NH_4^+ adducts) were also observed (*m/z* 812, 856, 900, 944), for which the M-TMS structure (**21**, n = 13 – 16) is feasible. The EO content for the **11** structure (n = 15 – 18) however is not valid for these ions. The two distinct *ion series* for the same $\Delta m/z$ 44 series indicates the ions are attributable to two different molecular products. The adduct formation of these ions also supports this, as in general, for the same molecular series preference for the sodium cation over the ammonium cation would be expected for higher molecules, and the reverse of this is observed here.

Four other possible structures exist for the higher molecular weight series, including the linear dimer **24** [R^1 = H; R^2 = TMS; R^3, R^4 = $(EO)_n\text{-}CH_3$; n_{TOTAL} = 10 – 13; $n_{EO/chain\#}$ = 5 – 6.5] and the linear trimer **25** [R^1, R^2 = TMS; R^3 = $(EO)_n\text{-}CH_3$; n = 6 – 9; R^4, R^5 = H]. The cyclic tetramer **28** [R^1 = $(CH_2)_3\text{-}O\text{-}(EO)_n\text{-}CH_3$; n = 7 - 10; R^2, R^3, R^4 = $(CH_2)_3$-OH] also matches, as does the linear trimer **25** [R^1 = H; R^2 = TMS; R^3, R^4, R^5 = $(EO)_n\text{-}CH_3$; n_{TOTAL} = 7 – 10; $n_{EO/chain\#}$ = 2.3 – 3.3].

In terms of polarity, the latter can probably be discarded as such a structure would be expected to partition into the organic phase. The three former possibilities appear to be of sufficient polarity to be found in the aqueous phase.

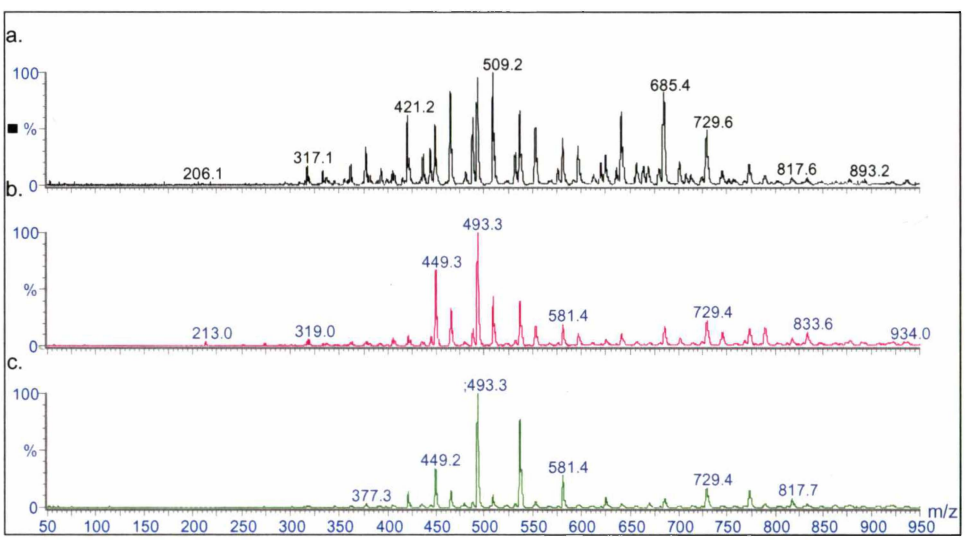

Figure 6.2. ESI/MS spectra of Heptane-soluble fractions of Silwet L-77 degraded with: *a.* 2 M; *b.* 0.2 M; and *c.* 0.02 M HCl

The same *ion series* were observed in the heptane-soluble fractions for the three different concentrations, however the relative distributions were varied.

Comparable spectra were obtained for the 0.2 and 0.02 M HCl degraded samples, in contrast to the 2 M HCl degraded sample (Figure 6.2).

A major series of ions, and the dominant series for the 0.2 and 0.02 M HCl samples, was observed at *m/z* 317, 361, 405, 449, 493, 537, 581 and 625. (Na^+ adducts). This series corresponds to the synthetic by-product $MD(M^{OH})$-O-$(EO)_n$-$CH_2CH{=}CH_2$, (**10**, n = 2 – 9), proposed in Chapter 2.

The next major series was observed at *m/z* 553, 597, 641, 685, 729, 773 and 817 (Na^+ adducts) and was also observed in the water-soluble fraction. According to required EO content, only the M-TMS structure (**21**, n = 7 – 13), $(M^{OH})_2$D-O-$(EO)_n$-$CH_2CH{=}CH_2$ (**11**, 9 – 15) and the linear dimer **24** [R = H; R^2 = TMS; R^3, R^4 = $(EO)_n$-CH_3; n_{TOTAL} = 4 - 10; $n_{EO/chain\#}$ = 2 – 5] correspond, however the linear dimer **24** is probably more likely due to the polarity of the fraction. Lower ions of this series (*m/z* 333, 377, 421, 465, 509) are observed in the 2M HCl spectrum which can only be assigned to M-TMS (**21**, n = 2 - 6). A distinct bimodal distribution is observed indicating the ions, despite belonging to the same $\Delta m/z$ 44 series, are for two distinct products (Figure 6.2.*a*). This is consistent with required EO content and expected oligomeric distribution with respect to polarity.

A third series is observed at *m/z* 740, 784, 828, 872, 916 and 960. Several structures match the molecular masses although these can be limited to three plausible structures (NH_4^+ adducts). The linear siloxanes with both TMS groups cleaved but all EO chains intact, i.e. **23** for all values of *m* correspond, but in terms of the EO content only the m = 2 (n_{TOTAL} = 10 – 15; $n_{EO/chain\#}$ = 5 – 7.5). and m = 3 analogues (n_{TOTAL} = 7 - 12; $n_{EO/chain\#}$ = 2.3 – 4) are feasible. The linear trimer **25** [R^1 = H; R^2 = TMS; R^3 = $(EO)_n$-CH_3; n = 6 – 11; R^4, R^5 = H] also corresponds, as does the M-2TMS structure (**21**, n = 13 - 17). The M-2TMS structure can however be discarded as the EO content at these molecular weights is not feasible in terms of both the starting material and the polarity of the fraction.

Three plausible structures can be assigned to the series at *m/z* 893, 937, 981 and 1025 (Na^+ adducts). The molecular weight matches the linear trimer **25** [R^1, R^2 = H; R^3 = $(EO)_n$-CH_3; n = 11 – 14; R^4, R^5 = H] and also the linear tetramer [**23**; m = 4; R^1, R^2 = H; R^3, R^4 = $(EO)_n$-CH_3; n_{TOTAL} = 8 – 11; $n_{EO/chain\#}$ = 4 – 5.5; R^5, R^6 = H]. The linear pentamer [**23**; m = 5; R^1 = H; R^2 = TMS; R^3 = $(EO)_n$-CH_3; n = 4 – 7; R^4, R^5, R^6, R^7 = H] also corresponds.

Further series were observed at *m/z* 1259, 1303, 1347, 1391, 1435; *m/z* 1023, 1067, 1111, 1155, 1199, 1243, 1287, 1331, 1375, 1419, 1463; *m/z* 1169, 1213; and *m/z* 1185, 1229, all of which appear to be NH_4^+ adducts, although no structures could be assigned

6.3.2.2 Acid degradation with varying Silwet L-77 concentration (200, 2000 and 20 000 ppm)

The spectra obtained were very similar for all three concentrations of Silwet L-77 investigated (0.1 g, 0.01 g and 0.001 g; 0.2 M HCl), indicating that surfactant concentration has only a minor effect on the types of products formed. In further support of this, the spectra observed for the 0.2 M HCl degraded sample in Section 6.3.2.1 (*b*, 0.2 g) were very comparable. The higher molecular weight range (*m/z* > 600) was a highly complex broad peak in all cases (Figure 6.3) and was unassigned.

The major series of ions in the water-soluble fractions correspond to **20** as for Section 6.3.2.1 (*b*, 0.2 M HCl). However in contrast to the previous results obtained for 0.2 M HCl (6.3.2.1.*b*), but consistent with the results obtained for 2 M HCl (6.3.2.1.*c*), no ions corresponding to M-TMS (**21**) were observed. The previous results indicated that acid concentration has a significant influence on the products formed. The acid concentration relative to Silwet L-77 in these experiments will be much higher due to the lower masses of Silwet L-77 used and thus, such results can be expected.

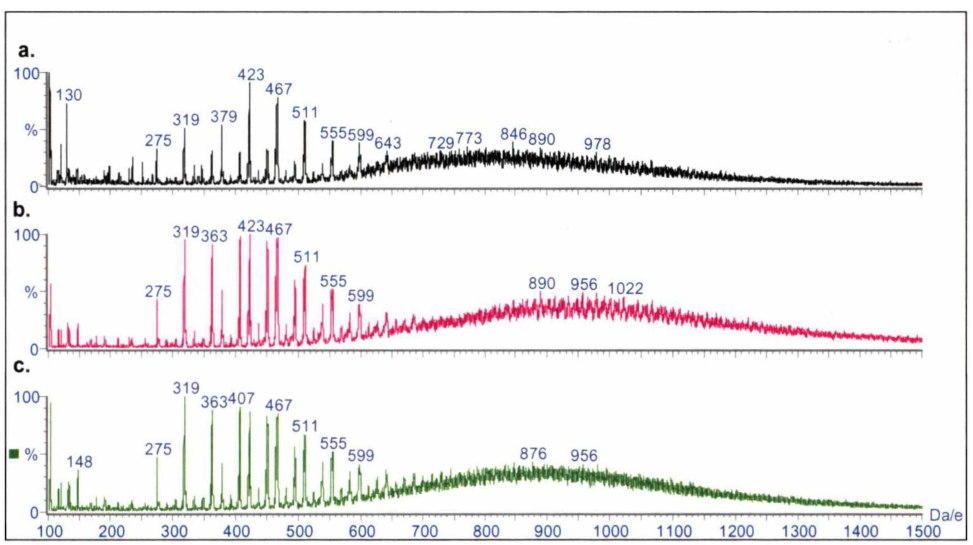

Figure 6.3. ESI/MS spectra of the H_2O-soluble fractions of: *a.* 0.1 g; *b.* 0.01 g; and *c.* 0.001 g Silwet L-77 degraded with 0.2 M HCl (5 mL) after 98 hours

The spectra of the heptane-soluble fraction for the 0.1 g/5 mL sample (Figure 6.4) gave the same results as from the previous 0.2 g/5 mL degradation experiment (Section 6.3.2.1).* The heptane-soluble fractions of the two lower concentration preparations (0.01 g and 0.001 g) were of too low a concentration to detect any ions conclusively above the background noise.

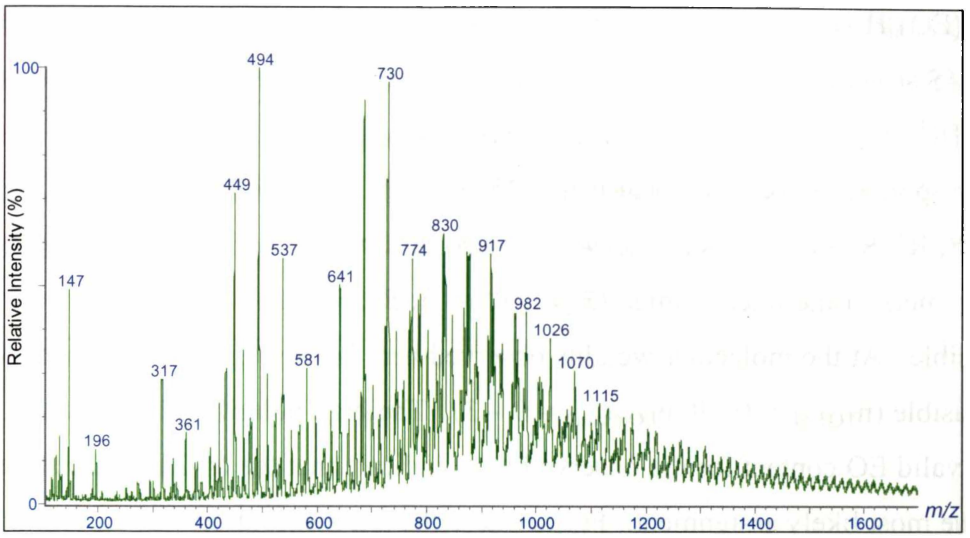

Figure 6.4. ESI/MS spectrum of the heptane-soluble fraction of Silwet L-77 degraded with 0.2 M HCl (0.01 g, 5 mL) after 98 hours

6.3.2.3 Base Degradation of Silwet L-77 (40 000 ppm)

A sample of Silwet L-77, degraded with NaOH, was partitioned between water and heptane, and the water-soluble fraction further separated via a RP C_{18} Sep-pak column eluting with 100% H_2O and 100% MeOH.

---

* The major series of ions corresponded to the synthetic by-product $MD(M^{OH})$-O-$(EO)_n$-$CH_2CH{=}CH_2$, (**10**, n = 2 – 9). The next major series shows a bimodal distribution, the lower ions of which are assigned to M-TMS (**21**, n = 2 - 6) and the higher ions best corresponding to the linear dimer **24** [R = H; R^2 = TMS; R^3, R^4 = $(EO)_n$-CH_3; n_{TOTAL} = 4 - 10; $n_{EO/chain\#}$ = 2 – 5] due to the polarity of the fraction. Three plausible structures match the molecular masses of the third series - the linear siloxanes, **23** with both TMS groups cleaved but all EO chains intact (m = 2, n_{TOTAL} = 10 – 15, $n_{EO/chain\#}$ = 5 – 7.5; and m = 3, n_{TOTAL} = 7 – 12, $n_{EO/chain\#}$ = 2.3 – 4) and the linear trimer **25** [R^1 = H; R^2 = TMS; R^3 = $(EO)_n$-CH_3; n = 6 – 11; R^4, R^5 = H]. Three plausible structures can also be assigned to the next series - namely the linear trimer **25** [R^1, R^2 = H; R^3 = $(EO)_n$-CH_3; n = 11 – 14; R^4, R^5 = H], the linear tetramer [**23**; m = 4; R^1, R^2 = H; R^3, R^4 = $(EO)_n$-CH_3; n_{TOTAL} = 8 – 11; $n_{EO/chain\#}$ = 4 – 5.5; R^5, R^6 = H] and the linear pentamer [**23**; m = 5; R^1 = H; R^2 = TMS; R^3 = $(EO)_n$-CH_3; n = 4 – 7; R^4, R^5, R^6, R^7 = H].

ESI/MS spectra of the H_2O-eluted Sep-pak fraction revealed some highly polar products had eluted with this solvent. The major series of ions observed in the spectrum of the water-soluble fraction was observed at *m/z* 305, 349, 393, 437, 481, 525, 569, 613, 657, 701, 745, 789, 833 and is assignable to four possible structures. The M-2TMS structure (**22**, n = 3 – 15, Na^+ adducts) is valid for all the ions observed, whilst the earlier ions of the series can also be assigned to $HO(EO)_nH$ (n = 6 – 19). Two other possible structures in addition to the M-2TMS structure, also exist for the higher molecular weight ions. The linear dimer **24** [R^1, R^2 = H; R^3, R^4 = $(EO)_n$-CH_3; n_{TOTAL} = 0 - 12; $n_{EO/chain\#}$ = 0 – 6] corresponds, as does the linear trimer **25** [R^1 = H; R^2 = TMS; R^3 = $(EO)_n$-CH_3; n = 0 - 8; R^4, R^5 =H]. This *ion series* was also observed in Section 6.3.2.1 for which oligomers of the linear trimer **25** [R^1, R^2 = H; R^3, R^4, R^5 = $(EO)_n$-CH_3] were also feasible. At the molecular weights observed here however, this assignment is not plausible (n_{TOTAL} = 0 - 9; $n_{EO/chain\#}$ = 0 – 3). The high polarity of the fraction, and the valid EO content for the observed ions, indicate that the M-2TMS **22** structure is the most likely assignment. Furthermore the ion distribution was representative of a single product series, rather than a bimodal distribution as would be required for the other structures to be valid.

Ions (*m/z* 187, 275, 319, 363, 407, 451, 495, 539, 583, 627, 671, 715, Na^+ adducts) corresponding to **20**, the cleaved monomethyl-ethoxy chains $CH_3O(EO)_nH$ (n = 3 – 15), were also significant.

The spectrum of the MeOH-soluble fraction (Figure 6.5.*b*) also contained the $CH_3O(EO)_nH$ (**20**) series and a series (Na^+ adducts) at *m/z* 377, 421, 465, 509, 553, 597, 641, 685, 729, 773, 817 and 861. All the ions of this series are assignable to the M-1TMS (**21**, n = 3 - 14) and $(M^{OH})_2D$-O-$(EO)_n$-$CH_2CH{=}CH_2$, (**11**, n = 5 – 16) structures, whilst several other structures can also be assigned to the larger molecules. The linear dimer [**24**; R^1 = H; R^2 = TMS; R^3, R^4 = $(EO)_n$-CH_3; n_{TOTAL} = 0 - 11; $n_{EO/chain\#}$ = 0 – 5.5], the linear trimer [**25**; R^1, R^2 = TMS; R^3 = $(EO)_n$-CH_3; n = 0 - 7; R^4, R^5 = H] and the cyclic tetramer [**28**; R^1 = $(CH_2)_3$-O-$(EO)_n$-CH_3; n = 0 - 8; R^2, R^3, R^4 = $(CH_2)_3$-OH] also correspond. The linear trimer [**25**; R^1 = H; R^2 = TMS; R^3, R^4, R^5 = $(EO)_n$-CH_3] is not likely based on the EO content (n_{TOTAL} = 0 - 8; $n_{EO/chain\#}$ = 0 – 2.7).

A series at *m/z* 523, 567, 611, 655, 699, 743, 787, 831, 875, 919, 963 and 1007 was observed which could be assigned to the linear dimer **24** [R^1, R^2 = TMS; R^3 = $(EO)_n$-CH_3; n = 2 - 13; R^4 = H] and the cyclic trimer **27** [R^1 = $(CH_2)_3$-O-$(EO)_n$-CH_3; n = 3 - 14; R^2, R^3, R^4 = $(CH_2)_3$-OH]. The higher *m/z* oligomers of this series can also be assigned to the linear trimer [**25**; R^1, R^2 = TMS; R^3, R^4 = $(EO)_n$-CH_3; n_{TOTAL} = 0 - 10; $n_{EO/chain\#}$ = 0 – 5; R^5 = H] and the cyclic tetramer [**28**; R^1, R^2 = $(CH_2)_3$-O-$(EO)_n$-CH_3; n_{TOTAL} = 0 - 11; $n_{EO/chain\#}$ = 0 – 5.5; R^3, R^4 = $(CH_2)_3$-OH]. On the basis of EO content, the cyclic trimer **27** assignment is the most feasible.

The spectrum of the MeOH-soluble fraction was much more complex over the higher mass range (*m/z* > 700) as compared with the water-soluble fraction, and thus was largely unassigned.

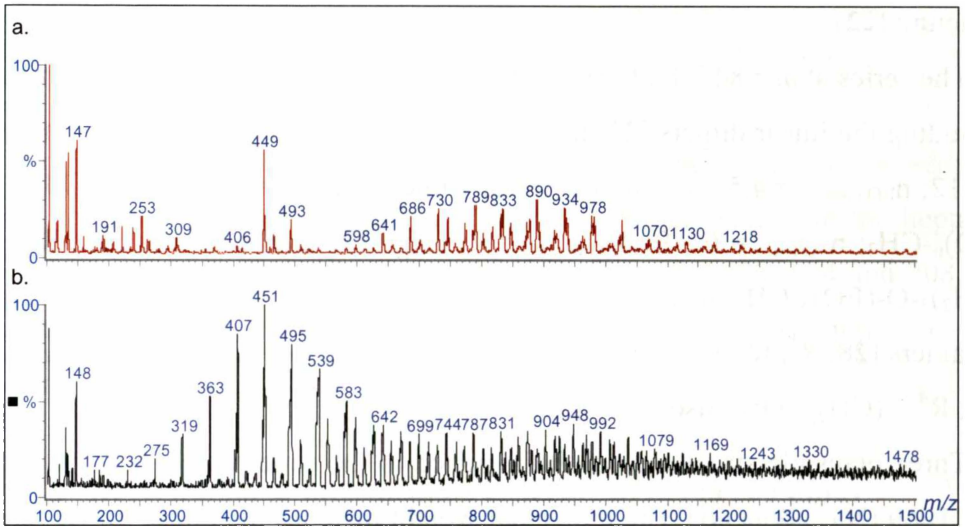

Figure 6.5. ESI/MS spectra of the: *a.* heptane; and *b.* MeOH-soluble fractions of NaOH-degraded Silwet L-77

The spectrum of the heptane-soluble fraction (Figure 6.5.*a*) showed a low molecular weight series at *m/z* 405, 449, 493, consistent with MD(M^{OH})-O-$(EO)_n$-$CH_2CH{=}CH_2$, **10** (n = 4 – 6).

Ions observed at *m/z* 597, 641, 685, 729, 773, 817 and 861 were also observed in the MeOH fraction, although lower oligomers of the series were seen in the more polar fraction. This is counter-intuitive as the lower oligomers would be expected to be more prevalent in the less polar fraction. This indicates that the two series, for which 5 possible assignments exist, are not the same. The possible assignments are listed here again to enable comparisons of the EO contents. [M-TMS, **21**, n = 8 – 14; $(M^{OH})_2$D-O-$(EO)_n$-$CH_2CH{=}CH_2$, **11**, n = 10 – 16; linear

dimer, **24**, R^1 = H, R^2 = TMS, R^3 = R^4 = $(EO)_n$-CH_3, n_{TOTAL} = 5 - 11; $n_{EO/chain\#}$ = 2.5 – 5.5; linear trimer, **25**, R^1 = R^2 = TMS, R^3 = $(EO)_n$-CH_3, n = 1 - 7; R^4, R^5 = H; cyclic tetramer, **28**, R^1 = $(CH_2)_3$-O-$(EO)_n$-CH_3; n = 2 – 8, R^2 = R^3 = R^4 = $(CH_2)_3$-OH; linear trimer, **25**, R^1 = H, R^2 = TMS, R^3 = R^4 = R^5 = $(EO)_n$-CH_3, n_{TOTAL} = 2 – 8, $n_{EO/chain\#}$ = 0 – 2.7].

Three possible structures can be assigned to the series observed at *m/z* 701, 745, 789, 833, 877, 921 and 965. The linear dimer (**23**; m = 2; n_{TOTAL} = 9 - 15; $n_{EO/chain\#}$ = 4.5 – 7.5) and linear trimer (**23**; m = 3; n_{TOTAL} = 6 – 12; $n_{EO/chain\#}$ = 2 – 4) with both TMS groups cleaved but all EO chains intact [i.e. R^1, R^2 = H; R^3 = $(EO)_n$-CH_3] both correspond, as does the linear trimer [**25**; R^1 = H; R^2 = TMS; R^3 = $(EO)_n$-CH_3; n = 5 –11; R^4, R^5 = H]. The high EO content required (n = 12 - 18), is not feasible in terms of either polarity or starting materials for the M-2TMS structure (**22**).

The series at *m/z* 845, 889, 933 and 977 can also be assigned to four structures, including the linear dimers [**23**; m = 2; R^1, R^2 = TMS; R^3 = $(EO)_n$-CH_3; n_{TOTAL} = 9 - 12; $n_{EO/chain\#}$ = 4.5 – 6] and the linear trimers [**23**; m = 3; R^1, R^2 = TMS; R^3 = $(EO)_n$-CH_3; n_{TOTAL} = 6 - 9; $n_{EO/chain\#}$ = 2 – 3]. The cyclic trimers [**27**; R^1, R^2 = $(CH_2)_3$-O-$(EO)_n$-CH_3; n_{TOTAL} = 10 – 13; $n_{EO/chain\#}$ = 5 – 6.5; R^3 = $(CH_2)_3$-OH] and tetramers [**28**, R^1, R^2, R^3 = $(CH_2)_3$-O-$(EO)_n$-CH_3; n_{TOTAL} = 7 - 10; $n_{EO/chain\#}$ = 2.3 – 3.3; R^4 = $(CH_2)_3$-OH] also correspond.

Three plausible structures can be assigned to the series at *m/z* 937, 981, 1025 and 1069 (Na^+ adducts). The molecular weight matches the linear trimer [**25**; R^1, R^2 = H; R^3 = $(EO)_n$-CH_3; n = 12 – 15; R^4, R^5 = H] and also the linear tetramer [**23**; m = 4; R^1, R^2 = H; R^3, R^4 = $(EO)_n$-CH_3; n_{TOTAL} = 9 – 12; $n_{EO/chain\#}$ = 4.5 – 6; R^5, R^6 = H]. The linear pentamers **23** [m = 5; R^1 = H; R^2 = TMS; R^3 = $(EO)_n$-CH_3; n = 5 – 8; R^4, R^5, R^6, R^7 = H] and **23** [m = 5; R^1, R^2 = H; R^3, R^4, R^5 = $(EO)_n$-CH_3; n_{TOTAL} = 6 – 9; $n_{EO/chain\#}$ = 2 – 3; R^6, R^7 = H] also correspond.

6.3.2.4 Bulk Silwet L-77 acid degradation

6.3.2.4.1 Degradation at high concentration (500 000 ppm)

The complex ESI/MS spectrum obtained for Silwet L-77 reacted in 2.0 M HCl (10 g, 10 mL) for 30 hours is shown in Figure 6.6.

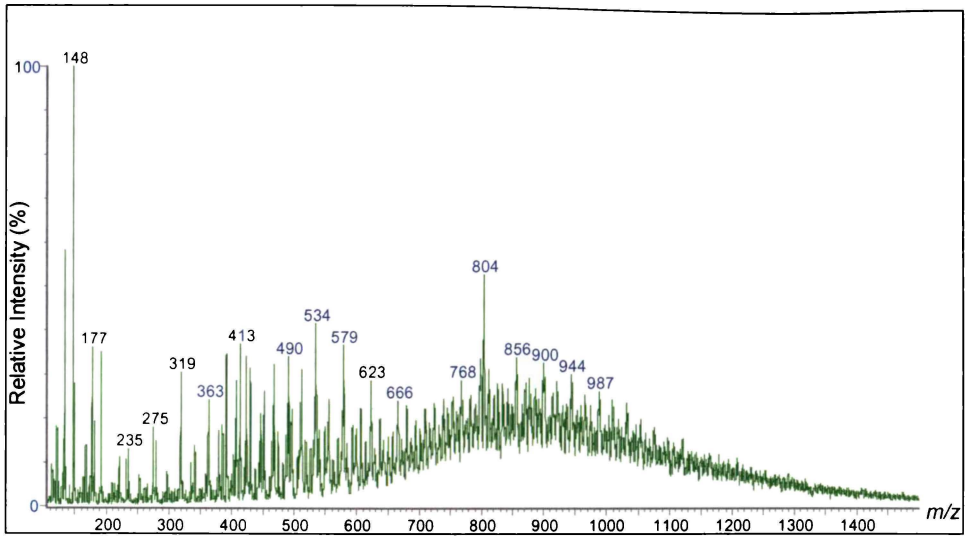

Figure 6.6. ESI/MS spectrum of the product mixture of Silwet L-77 after 30 hours in 2 M HCl (10g, 10 mL)

The water-soluble fraction gave a complex spectrum similar to that shown above. Only the $CH_3O(EO)_nH$ series (**20**) at *m/z* 335, 379, 423, 467, 511, 555, 599 and 643 (n = 6 – 13) could be unequivocally assigned, aided by the addition of KCl to simplify adduct formation. The major series of ions in the heptane-soluble fraction was observed at *m/z* 444, 488, 532, 576, 620, 664 and 708, for which the synthetic by-product $MD(M^{OH})$-O-$(EO)_n$-$CH_2CH{=}CH_2$, **10** (n = 5 – 11) structure corresponds.

6.3.2.4.2 Degradation at intermediate concentration (40 000 ppm)

A solution of Silwet L-77 (5 g) in 2.0 M HCl (125 mL) was extracted between H_2O and heptane following 3 days stirring at room temperature.

The ESI/MS spectrum of the water-soluble fraction (Figure 6.7) showed an *ion series* ($\Delta m/z$ 44) at *m/z* 121, 165, 209, 253, 297, 341, 385, 429, 473, 517, 561, 605 and 649 assignable to the H^+ adducts of the $CH_3O(EO)_nH$ series (**20**, n = 2 - 14). The K^+ adducts of the $CH_3O(EO)_nH$ series (**20**, n = 6 - 15, major n = 9) at *m/z* 335, 379, 423, 467, 511, 555, 599, 643, 687 and 731 could also be assigned with the addition of KCl, and the Na^+ adducts (n = 6 – 15) were evident in the APcI/MS spectrum.

The *ion series* observed at *m/z* 327, 371, 415, 459, 503, 547 and 591 (H^+ adducts) is assignable to the M-2TMS structure (**22**, n = 4 – 10) and to the $HO(EO)_nH$ series (n = 7 – 13). Higher oligomers of the same series were observed with addition of KCl (*m/z* 409, 453, 497, 541, 585, 629, 673, 761, 805,

849, 893, 937, 981, 1025, 1069). According to the $(EO)_n$ values, the earlier ions of the series can only be assigned to the M-2TMS (**22**, n = 5 – 20) and $HO(EO)_nH$ (n = 8 – 23) structures, but the larger ions of these series are not feasible in terms of the starting materials used. The higher molecular weight ions can be assigned to the linear trimer **25** [R^1 = H; R^2 = TMS; R^3 = $(EO)_n$-CH_3; n = 0 – 13; R^4, R^5 = H] and also to the linear siloxanes **23**, with both TMS groups cleaved but all EO chains intact [R^1, R^2 = H; R^3 = $(EO)_n$-CH_3]. The linear siloxanes **23** for m = 2 (n_{TOTAL} = 0 - 17; $n_{EO/chain\#}$ = 0 – 8.5) and m = 3; n_{TOTAL} = 0 – 14; $n_{/EO\ chain\#}$ = 0 – 4.7) show viable EO chain lengths. The Na^+ adducts of this series were also observed in the APcI/MS spectrum.

An *ion series* at *m/z* 397, 441, 485, 529, 573, 617, 661, 705, 749, 793, 837, 881, 925, 969, 1014 and 1058 was observed, the higher molecular weight ions of which correspond to the H^+ adducts of the cyclic trimer [**26**; R = $(EO)_n$-CH_3; n_{TOTAL} = 0 - 15; $n_{EO/chain\#}$ = 0 – 5]. The lower weight ions however do not have a feasible EO chain length for this structural assignment, and the *ion series* also could not be confirmed by KCl addition. No other plausible structures could be found to match these ions.

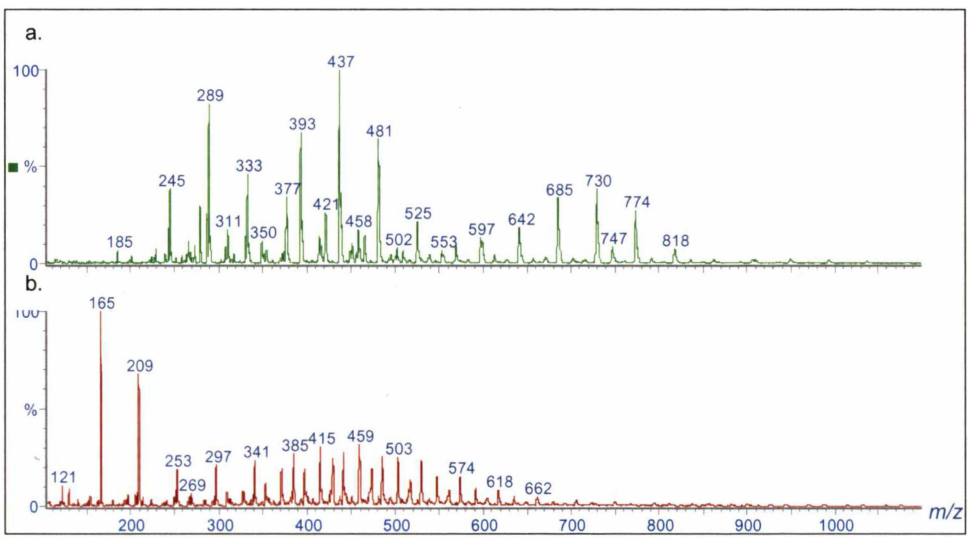

Figure 6.7. ESI/MS spectra of *a.* Heptane and *b.* water-soluble fractions of Silwet L-77 after 3 days in 2M HCl (5g, 125 mL)

The ESI/MS spectrum of the heptane-soluble fraction showed two series of ions at *m/z* 333, 377, 421, 465, 509, 553 and *m/z* 553, 597, 641, 685, 729, 773, 817, 861 belonging to the same $\Delta m/z$ 44 *ion series*. The bimodal distribution of these ions indicates they are due to two different structures (Figure 6.7.*a*). The

former series of ions corresponds to the M-TMS (**21**, n = 2 – 7) and $(M^{OH})_2$D-O-$(EO)_n$-$CH_2CH{=}CH_2$ (**11**, n = 4 – 9) structures. Compound **21** (n = 7 – 14) and **11** (n = 9 – 16) contain valid EO contents for the later series, however are unlikely due to the polarity of the sample. Four other structures show valid molecular weights for this series. The linear dimer **24** [R^1 = H; R^2 = TMS; R^3, R^4 = $(EO)_n$-CH_3; n_{TOTAL} = 4 – 11; $n_{EO/chain\#}$ = 2 – 5.5] corresponds as does the cyclic tetramer [**28;** R^1 = $(CH_2)_3$-O-$(EO)_n$-CH_3; n = 1 - 8; R^2, R^3, R^4 = $(CH_2)_3$-OH]. The linear trimer **25** [R^1, R^2 = TMS; R^3 = $(EO)_n$-CH_3; n = 0 - 7; R^4, R^5 = H] and linear trimer **25** [R^1 = H; R^2 = TMS; R^3, R^4, R^5 = $(EO)_n$-CH_3; n_{TOTAL} = 1 – 8; $n_{EO/chain\#}$ = 0.3 – 2.7] also match. The linear dimer is the most likely in terms of EO content.

The series of ions observed at *m/z* 349, 393, 437, 481, 525, 569 and 613 can be assigned to M-2TMS (**22**; n = 4 - 10) and $HO(EO)_nH$ (n = 7 – 13) structures. The linear siloxane structures matching this molecular series* do not show feasible EO chain lengths.

Another significant series was observed at *m/z* 444, 488, 532, 576, 620, 664, 708, 752 and 796 (NH_4^+ adducts), the Na^+ adducts of which were also observed in the APcI/MS spectrum (*m/z* 405, 449, 493, 537, 581, 625, 669, 713, 757, 801, 845 and 889). The $MD(M^{OH})$-O-$(EO)_n$-$CH_2CH{=}CH_2$, **10** (n = 4 – 15) structure is consistent with these values.

The higher mass range was highly complicated under expansion, by either API/MS methods, and as such the *ion series* could not be identified with confidence.

6.3.2.5 Summary of analysis by ESI/MS

The results from the preceding ESI/MS analyses show that the ions observed can be classified into 6 major series. These are abbreviated to Series A, B, C, D, E, F as summarised in Table 6.2.

* linear trimer **25** [R^1 = H; R^2 = TMS; R^3 = EO_n-CH_3; n = 0 – 3; R^4, R^5 = H]; linear siloxane **23** [m = 2; R^1, R^2 = H; R^3 = EO_n-CH_3; n_{TOTAL} = 1 - 7; $n_{EO\ chain\#}$ = 0 – 3.5]; and linear siloxane **23** [m = 3; R^1, R^2 = H; R^3 = EO_n-CH_3; n_{TOTAL} = 0 – 4; $n_{EO\ chain\#}$ = 0 – 1.3]

Table 6.2. Possible structures for ions observed in degraded Silwet L-77 product mixtures

Series	Molecular mass [a] ($\Delta m/z$ = 44)	Possible structures
A	120 --- 780 [b]	• $HO(EO)_nCH_3$, **20**
B	310 --- 1234 [c]	• $(M^{OH})_2D\text{-}O\text{-}(EO)_n\text{-}CH_2CH{=}CH_2$, **11** • M-TMS, **21** • Linear siloxanes, **23** R^1 = H; R^2 = TMS; $R^3 = (EO)_n\text{-}CH_3$ • Linear siloxanes, **23** R^1, R^2 = TMS; m-2[$R^3 = (EO)_n\text{-}CH_3$]; 2[R^3 = H] • Cyclic tetramer, **28** $R^1 = (CH_2)_3\text{-}O\text{-}(EO)_n\text{-}CH_3$; R^2, R^3, $R^4 = (CH_2)_3\text{-}OH$
C	282 --- 1030 [d]	• M-2TMS, **22** • Linear siloxanes, **23** R^1, R^2 = H; $R^3 = (EO)_n\text{-}CH_3$ • Linear trimer, **25** R^1 = H; R^2 = TMS; $R^3 = (EO)_n\text{-}CH_3$; R^4, R^5 = H • $HO(EO)_nH$
D	870 --- 1047 [e]	• Linear trimer, **23**, m = 3 R^1, R^2 = H; $R^3 = (EO)_n\text{-}CH_3$; R^4, R^5 = H • Linear tetramer, **23**, m = 4 R^1, R^2 = H; R^3, $R^4 = (EO)_n\text{-}CH_3$; R^5, R^6 = H • Linear pentamer, **23**, m = 5 R^1, R^2 = H; R^3, R^4, $R^5 = (EO)_n\text{-}CH_3$; R^6, R^7 = H • Linear pentamer, **23**, m = 5 R^1 = H; R^2 = TMS; $R^3 = (EO)_n\text{-}CH_3$; R^4, R^5, R^6, R^7 = H
E	456 --- 984 [f]	• Linear dimer, **24** R^1, R^2 = TMS; $R^3 = (EO)_n\text{-}CH_3$; R^4 = H • Linear trimer, **25** R^1, R^2 = TMS; R^3, $R^4 = (EO)_n\text{-}CH_3$; R^5 = H • Cyclic trimer, **27** $R^1 = (CH_2)_3\text{-}O\text{-}(EO)_n\text{-}CH_3$; R^2, R^3 =$(CH_2)_3$-OH • Cyclic tetramer, **28**, R^1, $R^2 = (CH_2)_3\text{-}O\text{-}(EO)_n\text{-}CH_3$; R^3, R^4 $(CH_2)_3$-OH
F	294--- 954 [g]	• $MD(M^{OH})\text{-}O\text{-}(EO)_n\text{-}CH_2CH{=}CH_2$, **10** • Linear siloxanes, **23** R^1, R^2 = TMS; $R^3 = (EO)_n\text{-}CH_3$ • Cyclic trimer, **27** R^1, $R^2 = (CH_2)_3\text{-}O\text{-}(EO)_n\text{-}CH_3$; $R^3 = (CH_2)_3\text{-}OH$ • Cyclic tetramer, **28** R^1, R^2, $R^3 = (CH_2)_3\text{-}O\text{-}(EO)_n\text{-}CH_3$; $R^4 = (CH_2)_3\text{-}OH$

[a] Molecular and adduct masses listed in Appendix A.IV.3; [b] 120, 164, 208, 252, 296, 340, 384, 428, 472, 516, 560, 604, 648, 692, 736, 780 a.m.u.; [c] 310, 354, 398, 442, 486, 530, 574, 618, 662, 706, 750, 794, 838, 882, 926, 970, 1014, 1058, 1102, 1146, 1190, 1234 a.m.u.; [d] 282, 326, 370, 414, 458, 502, 546, 590, 634, 678, 722, 766, 810, 854, 898, 942, 986, 1030 a.m.u.; [e] 870, 914, 958, 1002, 1047 a.m.u.; [f] 456, 500, 544, 588, 632, 676, 720, 764, 808, 852, 896, 940, 984 a.m.u.; [g] 294, 338, 382, 426, 470, 514, 558, 602, 646, 690, 734, 778, 822, 866, 910, 954 a.m.u.

It is important to note that these *ion series* are only those observed, and may not be representative of all the products present, nor the quantities thereof. The nature of the ESI/MS process is such that competition between analytes for

ionisation occurs, and as such compounds with higher surface activity and EO content can be expected to dominate in resulting spectra. Suppression effects may thus preclude observation rather than confirm absence. As a consequence, the use of additional techniques (HPLC, GC/MS, NMR) to provide complementary data is described in later sections. Isotope patterns were also investigated here as a potential method for distinguishing between the possible assignments, however the expected patterns did not vary sufficiently between the possible structures to enable assignment via this method.

The observed series in the different experiments conducted are summarised in Table 6.3. The high number of possible structures for each *ion series* observed, rendered it difficult to assign structures with confidence. Consequently, in the following sections, results from HPLC (6.3.3) and high resolution FTICR/MS (6.3.4) are used to further aid in the assignments.

Table 6.3. *Ion series* observed for the different degradation methods for Silwet L-77

Section No.	6.3.2.1	6.3.2.2	6.3.2.3	6.3.2.4.1	6.3.2.4.2
H_2O-soluble fraction	A, B	A	A, C	A	A, C
Heptane-soluble fraction	B, C, D, F	B, C, D, F	B, C, D, F	F	B, C, F
MeOH-soluble fraction			A, B, E, F		

6.3.2.6 Mass recoveries

The mass recoveries for the different degradation conditions experiments described in this section are summarised in Table 6.4.

Table 6.4. Conditions and mass recoveries for Silwet L-77 degradation experiments

Section No.	6.3.2.1			6.3.2.2			6.3.2.3	6.3.2.4.1	6.3.2.4.2
	a	*b*	*c*	*a*	*b*	*c*			
Acid/Base	HCl			HCl			NaOH	HCl	HCl
Conc. of Acid/Base (M)	2	0.2	0.02	0.2	0.2	0.2	0.2	2	2
Reaction time (days)	4			4			2	1	3
Mass (Silwet L-77) (g)	0.2	0.2	0.2	0.1	0.01	0.001	0.2	10	5
[Silwet L-77] (ppm)	40 000	40 000	40 000	20 000	2 000	200	40 000	500 000	40 000
Organic fraction % Recovery	1	1	1	-	-	-	0.2	2	0.4
Aqueous fraction % Recovery	63	77	79	77	88*	100*	52**	92	75
Overall Recovery (%)	64	77	80	77	88*	100*	-***	94	75

* %Error will be high due to low starting mass; ** mass of fraction eluted from Sep-pak with MeOH; *** An accurate mass recovery for the base degradation experiment was not obtained due residual NaOH in the H_2O-soluble fraction.

The mass recoveries of the water-soluble fractions were significantly higher than that of the heptane-soluble fractions, for all conditions investigated. In general, mass recoveries were reduced with respect the starting material used. In theory, mass recoveries should increase with hydrolysis due to addition of H_2O to the molecule. The work-up procedure involved a solvent extraction only and therefore recovery losses can be assumed to be minimal. The mass loss upon degradation is thus assumed to be due to the production of volatile species. The formation of volatile siloxane compounds in the degradation of siloxane compounds has been documented in the literature. Cyclic (D_3, D_4, D_5),[12a,b] linear (TMS-endblocked oligomers, MD_nM), i.e. TMS-O-TMS,[12b] and monomeric $[(Me)_2Si(OH)_2]$[13a-c] products have been reported. $(Me)_2Si(OH)_2$ can not be formed from Silwet L-77, however it is possible that the monomeric $^{(OH)_2}M^{CH_2CH_2CH_2OH}$ equivalent may be volatile. TMS-O-TMS would be generated by the condensation of two TMS-OH molecules formed in Silwet L-77 silanol, i.e. **21** and **22**, formation, the volatility of which is well established. Cyclic compounds (**27**) with short chain substituents may also be possible volatile products of Silwet L-77 degradation. In order to investigate this, the head space above degraded samples of Silwet L-77 was analysed, the results of which are discussed in Section 6.3.8.3.

The masses of the H_2O-soluble fractions of the degradation products were significantly higher than the organic fractions. The solubility properties of a compound and its degradation products are significant with respect to their ultimate impact on the environment. Water solubility enables dispersal and dilution and also exposure to conditions appropriate for further degradation. Accumulation is more likely for hydrophobic compounds[13c,14] and thus such compounds may be more likely to impart negative effects on natural systems.

For comparison, a H_2O/heptane solvent extraction of Silwet L-77 (40 000 ppm) was performed.* Silwet L-77 partitioned preferentially into the H_2O fraction (80%), whilst 17% of the mass was recovered in the heptane-soluble fraction. An unaccounted mass loss of 3% was incurred. The oligomeric distribution for both fractions was comparable, with the n = 3 – 16 oligomers [major $(EO)_n$ oligomer, n

* Silwet L-77 (0.8 g) was partitioned between H_2O (120 mL) and n-heptane (120 mL) following gentle shaking. The fractions were analysed by ESI/MS using CH_3CN as the preparation and elution solvent. The heptane-soluble fraction was concentrated by rotary evaporation and vacuum methods and the H_2O-soluble fraction by freeze drying, for mass determinations.

= 7.5] and n = 4 – 16 oligomers [major $(EO)_n$ oligomer, n = 8] observed in the heptane- and H_2O-soluble fractions respectively. A larger proportion Silwet L-77 was recovered in the heptane-soluble fraction as compared with degraded samples. This indicates that hydrophobic siloxane components are being lost from the degradation products and/or that products more hydrophilic than Silwet L-77 are being formed. Both postulates are likely and result from the same process. Initial hydrolysis of Silwet L-77 will yield TMS-OH and PEG-containing silanols (**21** and **22**). The TMS-OH molecules will be lost by volatilisation following dimerisation, and condensation of the PEG-containing silanols will give rise to products containing increased numbers of PEG chains, which will exhibit increased water solubility. The hydrophilic portion (EO chain) of the M_2D-C_3-O-$(EO)_n$-Me molecule (Ave. n $\approx$ 7.5) comprises 58% of mass whilst the proportion of hydrophilic components in the degradation mixture was higher than this in all cases. This indicates that some siloxane moieties will be contained within products partitioning to the H_2O fraction.

The results from Section 6.3.2.1 showed decreased mass recovery with increasing acid concentration (Table 6.4). This would indicate that a larger proportion of volatile products are formed with higher acid concentrations. As acid acts as a catalyst for the degradation process this trend is logical, as increased hydrolysis will occur at higher acid concentrations.

In Section 6.3.2.2, a reduction in mass recovery was observed with increasing Silwet L-77 concentration. However large errors will be associated with these values due to the low initial values used. On this basis, the results from Sections 6.3.2.1.*b* and 6.3.2.2.*a* may provide a more accurate comparison for the effects of surfactant concentration on recovery. Identical values were obtained for these two preparations (two-fold concentration difference). In support of this the spectra obtained for Sections 6.3.2.1.*b* and 6.3.2.2.*a-c* were very comparable, as discussed in Section 6.3.2.2.

Comparison of the 2 M HCl degradation experiments (6.3.2.4.1, 6.3.2.4.2, 6.3.2.1.*a*) show decreased mass recovery with increased time exposed to the acidic conditions (1 day, 94%; 3 days 75%; 4 days, 63%, respectively).

6.3.3 Analysis of Silwet L-77 degradation by HPLC

A number of chromatographic methods (RP C_{18}, SiO_2) were used in an attempt to separate the products of degraded Silwet L-77. Separation and characterisation of pure components was found to be extremely difficult due to the highly complex nature of the product mixture.

6.3.3.1 Analysis of the water-soluble products by RP C_{18} HPLC/ESI/MS

The water-soluble fraction of a degraded Silwet L-77 sample (Section 6.3.2.1.*b*) was analysed by RP C_{18} HPLC/ESI/MS. Four series of peaks were observed in the chromatogram, the results of which are summarised in Table 6.5. The ions belonging to the same molecular series eluted in order of consecutive addition of 44 a.m.u. for each of the series.

Table 6.5. Retention times and corresponding ions observed for the RP C_{18} HPLC/ESI/MS[a] chromatogram of degraded Silwet L-77[b]

Time (min)	*Ion Series*[c]	Possible Assignment	*Ion Series*	Possible Assignments		*Ion Series*	Possible Assignments		*Ion Series*	Possible Assignment
	A *(m/z)*	**20**	*C* *(m/z)*	**22**	**PEG**	*B* *(m/z)*	**21**	**11**	*F* *(m/z)*	**10**
45	226	n = 4								
55	270	n = 5								
65	319	n = 6								
73	358	n = 7								
82	402	n = 8								
85	446	n = 9								
87	490	n = 10								
89	534	n = 11								
90	578	n = 12								
92	622	n = 13								
93	666	n = 14	520	n = 8	n = 11	504	n = 6	n = 8		
94	710	n = 15	564	n = 9	n = 12	548	n = 7	n = 9		
96	754	n = 16	608	n = 10	n = 13	592	n = 8	n = 10		
98	798	n = 17	652	n = 11	n = 14	636	n = 9	n = 11		
100	842	n = 18	696	n = 12	n = 15	680	n = 10	n = 12		
102			740	n = 13	n = 16	724	n = 11	n = 13		
104			784	n = 14	n = 17	768	n = 12	n = 14	356	n = 3
106						812	n = 13	n = 15	400	n = 4
109						856	n = 14	n = 16	444	n = 5
112									493	n = 6
116									532	n = 7

[a] H_2O/MeOH solvent gradient elution profile: 0 –20 minutes, 85:15; 20 – 60 minutes, 70:30; 60-120 50:50; [b] Water-soluble fraction; [c] Refer to Table 6.2 and Appendix A.IV.3

The spectra of the first series eluted showed ions corresponding to $CH_3O(EO)_nH$ (**20**, n = 4 – 18, *Series A*). The assignment was confirmed by comparison of the RP C_{18} HPLC/ESI/MS chromatogram with that of the

commercially available $CH_3O(EO)_nH$, for which identical retention times and spectra were obtained.

The second series is due to ions belonging to *Series C*, for which M-2TMS (**22**, n = 8 – 14) and $HO(EO)_nH$ (n = 11 – 17) are valid structures. The $HO(EO)_nH$ assignment can be eliminated as $HO(EO)_nH$ structures should elute prior to $CH_3O(EO)_nH$ by reversed phase chromatography. This was confirmed by analysis of the RP C_{18} HPLC/ESI/MS chromatogram of $CH_3O(EO)_nH$, which contains $HO(EO)_nH$ as synthetic by-products. The retention times for the $CH_3O(EO)_nH$ oligomers were longer than the $HO(EO)_nH$ oligomers, as shown in Table 6.6.

Table 6.6. Retention times and corresponding ions observed for the RP C_{18} HPLC/ESI/MS chromatogram of $CH_3O(EO)_nH$ [a]

Time (min)	Ions (*m/z*) [b]	$HO(EO)_nH$	Ions (*m/z*) [b]	$CH_3O(EO)_nH$
9.0	129	n = 2		
9.3	173	n = 3		
9.7	217	n = 4		
10	261	n = 5		
10.5	305	n = 6	143	n = 2
11.1	349	n = 7	187	n = 3
119	393	n = 8	231	n = 4
12.9	437	n = 9	275	n = 5
13.8	481	n = 10	319	n = 6
15.2	525	n = 11	363	n = 7
17.1	569	n = 12	407	n = 8

[a] 60:40 H_2O/MeOH isocratic solvent elution; [b] Na^+ adducts

The afore-described *Series C* ions assigned to M-2TMS (**22**, n = 8 – 14) coelute with a third series, corresponding to ions from *Series B* (refer to Table 6.5). Two possible structures, M-TMS (**21**, n = 6 – 14) and $(M^{OH})_2D\text{-}O\text{-}(EO)_n\text{-}CH_2CH{=}CH_2$, (**11**, n = 8 – 16) can be assigned. In terms of polarity, it is difficult to predict which structure is more likely. The $(M^{OH})_2D\text{-}O\text{-}(EO)_n\text{-}CH_2CH{=}CH_2$ structure has the same EO and silanol content for coeluting oligomers of M-2TMS $[(M^{OH})_2D\text{-}C_3\text{-}O\text{-}(EO)_n\text{-}CH_3]$. However longer retention times might be expected for this structure due to the decreased polarity of the terminal group ($CH_2CH{=}CH_2$ vs CH_3). Longer retention times for the monosilanol (**21**) structure over analogous oligomers of the disilanol (**22**) are observed, however this would be expected due to the decreased polarity inferred by the additional TMS group. On this basis, the *Series B* ions cannot be assigned to either of the M-TMS (**21**) or $(M^{OH})_2D\text{-}O\text{-}(EO)_n\text{-}CH_2CH{=}CH_2$ (**11**) structures with confidence.

The fourth series corresponds to ions of *Series F*. Only the $MD(M^{OH})\text{-}O\text{-}(EO)_n\text{-}CH_2CH{=}CH_2$ (**10**, n = 3 – 7) structure has feasible molecular weights for

the ions observed. The retention time of this series compared to *Series A*, *B* and *C* is also logical for the **10** assignment. The longer retention time demonstrates the lower polarity of these structures as compared with $CH_3O(EO)_nH$ (**20**), M-2TMS (**22**), M-1TMS (**21**) and $(M^{OH})_2D\text{-}O\text{-}(EO)_n\text{-}CH_2CH{=}CH_2$ (**11**) type structures. Compound **10** $[MD(M^{OH})\text{-}O\text{-}(EO)_n\text{-}CH_2CH{=}CH_2]$ can be described as an alkylated or silylated version of **20**, **21**, **22**, and **11**, and thus would be expected to exhibit longer retention times than any of these compounds. As a result, the retention time of **10** cannot be used to aid in the tentative assignment of the *Series B* ions.

6.3.3.2 Analysis of Silwet L-77 degradation by SiO_2 HPLC/ESI/MS

The heptane-soluble fraction of a degraded Silwet L-77 sample (6.3.1.4) was purified by SiO_2 column chromatography, and the 50:50 heptane/EtOAc eluted fraction was analysed by normal phase HPLC/ESI/MS with post column addition of $CH_3CO_2NH_4$ (Figure 6.8). Significant peak overlap was observed such that structural determination could not be conducted with confidence. Improvement in the peak separation was not achieved with changes to the HPLC elution solvent composition.

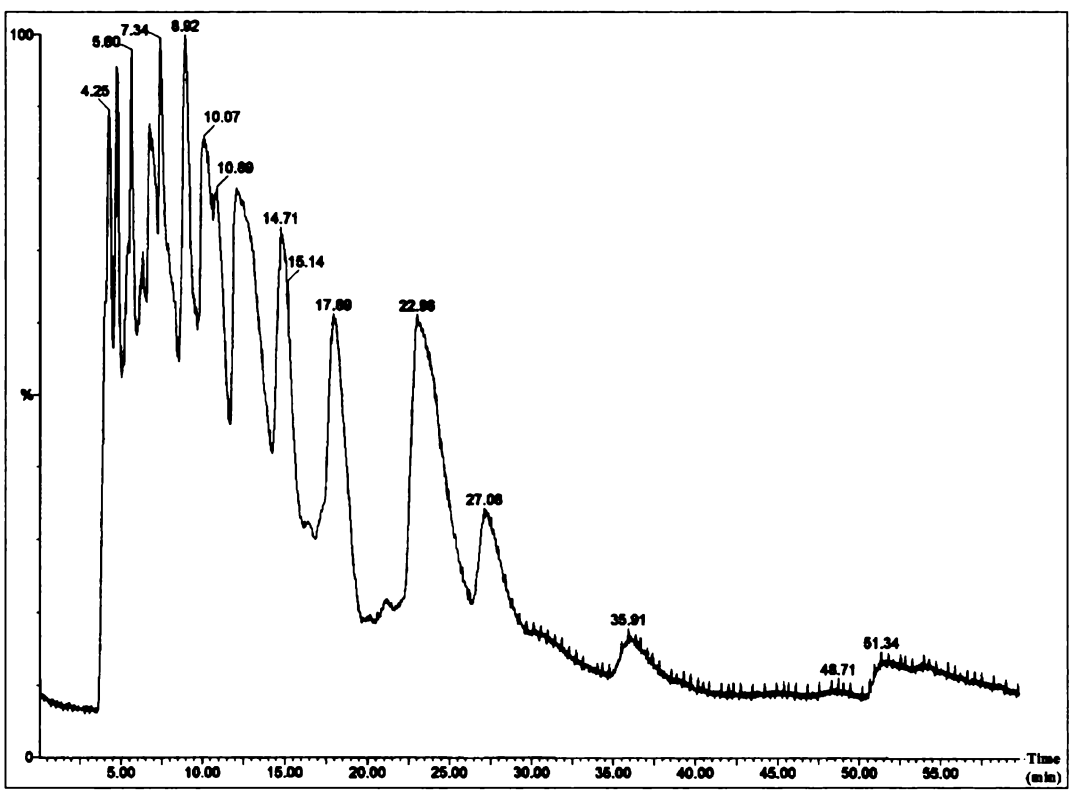

Figure 6.8. SiO_2 HPLC/ESI/MS chromatogram of the heptane-soluble fraction of acid degraded Silwet L-77

6.3.3.3 Analysis of the heptane-soluble products by RP C_{18} HPLC/ESI/MS

The RP C_{18} HPLC/ESI/MS chromatograms were also highly complicated, and did not provide information to aid structural assignment.

It was however noted that the spectra of each peak in the chromatogram showed ions varying by 148 a.m.u., to which ions from *Series F, B, C, D* could be matched to the consecutively increasing mass ions. It thus followed that similar structural series within the possible assignments for these *ion series* should be investigated. Amongst the possible assignments for *Series F, B* and *C*, linear siloxanes with 2, 1 and no TMS groups attached respectively, exist. For a net gain in mass of 148 a.m.u. to occur in conjunction with hydrolytic loss of TMS (-72 a.m.u.), a unit of 220 a.m.u. must be adding into the structure consecutively. Increments of a D^R unit, where R = C_3-O-$(EO)_2$-Me, into a D_n or M_2D_n type polymer correspond to this molecular weight. Such condensation products are consistent with expected structures for short-chain silanol compounds, as discussed previously. The *D* series however also shows an increase in 148 a.m.u., but does not fit into this sequence as no further TMS groups are available for cleavage.

6.3.4 Analysis of Silwet L-77 degradation by FTICR/MS

Acid degraded Silwet L-77 samples (Section 6.2.2.4) were analysed by FTICR/MS and the high resolution mass data obtained compared with calculated values. Due to the number of possible assignments for many of the observed ions, high resolution FTICR/MS was used to discriminate between some of the proposed structures. It was found that variation of certain parameters (i.e. offset setting) exhibited a large influence on the ions observed and therefore, in order to accurately determine all of the products present, a number of spectra for each sample were acquired.

The FTICR/MS spectra of the H_2O-soluble fractions showed four assignable ($\Delta m/z$ = 44) *ion series* at: *m/z* 319, 363, 407, 451, 495, 539, 583, 627, 671, 715, 759, 803 (*Series A*); *m/z* 729, 773, 817, 861, 905, 949, 993 (*Series B*); *m/z* 1475, 1519, 1563, 1607, 1651, 1739, 1783, 1827, 1871, 1915; and *m/z* 1594, 1638, 1682, 1726, 1770, 1814, 1858, 1902 (*Series F*). The calculated masses of the $CH_3O(EO)_nH$ (**20**), M-TMS (**21**), cyclic tetramer [**28**; R^1, R^2, R^3, R^4 = $(CH_2)_3$-O-

$(EO)_n$-CH_3] and linear dimer [**24**; R^1, R^2 = TMS; R^3, R^4 = $(EO)_n$-CH_3] structures respectively, are in highest agreement with the observed high resolution mass data. (Table 6.7).

Table 6.7. FTICR/MS analysis of the H_2O-soluble fractions – classified by molecular weight

MW (observed)	*Ion Series*[a]	Possible structures[b]	Molecular Formula	MW (calculated)	Δm/M[c] (ppm)
495.2761	A[d]	• $HO(EO)_{10}CH_3$, **20**	$C_{21}H_{44}O_{11}Na$	495.2776	3
729.4162	B[e,f]	• M-TMS, **21**, n = 11	$Si_2C_{30}H_{66}O_{14}Na$	729.3882	38
		• Linear dimer, **24** R^1 = H; R^2 = TMS; R^3, R^4 = EO_4-CH_3	$Si_3C_{29}H_{66}O_{13}Na$	729.3702	63
		• Linear trimer, **25** R^1, R^2 = TMS; R^3 = $(EO)_4$-CH_3; R^4, R^5 = H	$Si_5C_{27}H_{66}O_{11}Na$	729.3540	85
		• Cyclic tetramer, **28** R^1 = $(CH_2)_3$-O-$(EO)_5$-CH_3 R^2, R^3, R^4 = $(CH_2)_3$-OH	$Si_4C_{27}H_{62}O_{13}Na$	729.3404	104
		• $(M^{OH})_2$D-O-$(EO)_{13}$-$CH_2CH{=}CH_2$, **11**	$SiC_{30}H_{62}O_{16}Na$	729.3705	63
1607.8162	G[g,h]	• Cyclic tetramer, **28** R^1,R^2,R^3,R^4 = $(CH_2)_3$-O-$(EO)_6$-CH_3	$Si_4C_{68}H_{144}O_{32}Na$	1607.8609	28
		• Cyclic trimer, **27** R^1, R^2, R^3 = $(CH_2)_3$-O-$(EO)_9$-CH_3	$Si_3C_{69}H_{144}O_{33}Na$	1607.8789	39
1594.0147	F[i]	• Linear siloxane, **23**, m = 2 R^1, R^2 = TMS; R^3 = $(EO)_{12}$-CH_3	$Si_4C_{68}H_{146}O_{30}Na$	1593.8823	83
		• Linear siloxane, **23**, m = 3 R^1, R^2 = TMS; R^3 = $(EO)_{7.6}$-CH_3	$Si_5C_{67}H_{146}O_{30}Na$	1593.8643	94
		• Linear siloxane, **23**, m = 4 R^1, R^2 = TMS; R^3 = $(EO)_5$-CH_3	$Si_6C_{66}H_{146}O_{29}Na$	1593.8463	106
		• Linear siloxane, **23**, m = 5 R^1, R^2 = TMS; R^3 = $(EO)_{3.4}$-CH_3	$Si_7C_{65}H_{146}O_{28}Na$	1593.8283	117
		• Cyclic trimer, **27** R^1, R^2 = $(CH_2)_3$-O-$(EO)_{13.5}$-CH_3 R^3 =$(CH_2)_3$-OH	$Si_3C_{68}H_{142}O_{33}Na$	1593.8639	95
		• Cyclic tetramer, **28** R^1, R^2, R^3 = $(CH_2)_3$-O-$(EO)_8$-CH_3; R^4 =$(CH_2)_3$-OH	$Si_4C_{67}H_{142}O_{32}Na$	1593.8459	106

[a] Refer to Table 6.2 and Appendix A.IV.3; [b] Na^+ adducts; [c] Difference in observed and calculated masses)/Calculated mass; [d] *m/z* 319, 363, 407, 451, 495, 539, 583, 627, 671, 715, 759, 803; [e] *m/z* 729, 773, 817, 861, 905, 949, 993; [f] linear trimer **25** [R^1 = H; R^2 = TMS; R^3, R^4, R^5 = $(EO)_n$-CH_3] not included as EO content not feasible; [g] *m/z* 1475, 1519, 1563, 1607, 1651, 1739, 1783, 1827, 1871, 1915; [h] Not identified in ESI/MS analyses; [i] *m/z* 1594, 1638, 1682,1726, 1770, 1814, 1858, 1902

For comparison the spectrum of commercially available $CH_3O(EO)_nH$ (Ave. n $\approx$ 7.5) was obtained, in which the Na^+ adducts of $CH_3O(EO)_nH$ and $HO(EO)_nH$ were observed. The ion corresponding to $[CH_3O(EO)_7H + Na]^+$ in the commercial product sample was observed at *m/z* 363.1957. The corresponding ion in the H_2O-soluble fraction of the degraded Silwet L-77 was observed at *m/z* 363.1955. The mass difference for these values is 0.5 ppm, well within acceptable variation for equivalent structures. This unequivocably confirmed the $CH_3O(EO)_nH$ (**20**) assignment.

Eight FTICR/MS spectra were acquired for the heptane-soluble fraction, from which 20 different assignable *ion series* in total were obtained. A further six molecular series could not be assigned. Table 6.8 below lists the products by molecular weight, from which the likelihood of different structures of the same molecular weight can be compared. Table 6.9 lists the same information classified by structural type. Data classification in this manner enables the likelihood of the structures to be assessed as the presence of related series provides support for the proposed structures.

The structures described correspond to $[M + H]^+$, $[M + NH_4]^+$, $[M + Na]^+$ and $[M + K]^+$ adduct ions. It is important to note here however, that only $[M + Na]^+$ adducts were observed in the FTICR/MS spectra of Silwet L-77, $CH_3O(EO)_nH$ and $HO(EO)_nH$. The ions assigned to other adducts in the following tables may thus not be likely structures on this basis. FTICR/MS analysis of M_2D-C_3-O-EO-H and 2-deoxy-D-glucose did however yield ions corresponding to the $[M + H]^+$, $[M + NH_4]^+$, $[M + Na]^+$ and $[M + K]^+$ adducts, indicating that adduct formation may be dependent on the molecular structure.

Table 6.8. FTICR/MS of the heptane-soluble fractions – classified by molecular weight

Ion Series[*]	Possible structures	Adduct	Molecular Formula	MW (calculated)	MW (observed)	Δm/M (ppm)
A[a]	• $HO(EO)_6CH_3$,**20**	H^+	$C_{13}H_{29}O_7$	297.190777	297.192485	6
H[b]	-				307.140163	
B[c]	• M-TMS, **21**, n = 2	H^+	$Si_2C_{12}H_{31}O_5$	311.171006	311.171476	2
	• $(M^{OH})_2$D-O-$(EO)_4$-$CH_2CH{=}CH_2$, **11**	H^+	$SiC_{12}H_{27}O_7$	311.152607		61
A[d]	• $HO(EO)_6CH_3$, **20**	NH_4^+	$C_{13}H_{32}O_7N$	314.181401	314.218820	119
F[e]	• $MD(M^{OH})$-O-$(EO)_4$-$CH_2CH{=}CH_2$, **10**	NH_4^+	$Si_2C_{15}H_{38}O_7N$	400.218685	400.238553	50
I[f]	• $CH_3O(EO)_8\ CH_2CH{=}CH_2$	H^+	$C_{20}H_{41}O_9$	425.275058	425.240096	82
J[g]	-				441.199239	
C[h]	• M-2TMS, **22**, n = 6	K^+	$SiC_{17}H_{38}O_9K$	453.192219	453.262594	155
	• $HO(EO)_9H$	K^+	$C_{18}H_{38}O_{10}K$	453.210205		115
E[i]	• Cyclic trimer, **27**, $R^1 = (EO)_2$-CH_3; $R^2, R^3 = H$	Na^+	$Si_3C_{17}H_{40}O_8Na$	479.192873	479.278786	179
C[j]	• M-2TMS, **22**, n = 7-10	H^+	$SiC_{21}H_{47}O_{11}$	503.288175	503.235537	105
	• $HO(EO)_nH$, n = 10 - 13	H^+	$C_{22}H_{47}O_{12}$	503.306184		140
	• Linear dimer, **24**, $R^1, R^2 = H$; $R^3, R^4 = (EO)_{2.5}$-CH_3	H^+	$Si_2C_{20}H_{47}O_{10}$	503.270170		69
B[k]	• $(M^{OH})_2$D-O-$(EO)_{13}$-$CH_9CH{=}CH_2$, **11**	NH_4^+	$SiC_{22}H_{50}O_{12}N$	548.310230	548.275693	63
	• M-TMS, **21**, n = 7 - 12	NH_4^+	$Si_2C_{22}H_{54}O_{10}N$	548.328629		97
	• Linear dimer, **24**, $R^1 = H$; $R^2 = TMS$; $R^3, R^4 = (EO)_2$-CH_3	NH_4^+	$Si_3C_{21}H_{54}O_9N$	548.310643		64
C[l]	• M-2TMS, **22**, n = 7	K^+	$SiC_{25}H_{54}O_{13}K$	629.296515	629.323069	42
	• $HO(EO)_{10}H$	K^+	$C_{26}H_{54}O_{14}K$	629.314511		14
	• Linear dimer, **24**, $R^1, R^2 = H$; $R^3, R^4 = (EO)_{3.5}$-CH_3	K^+	$Si_2C_{24}H_{54}O_{12}K$	629.278515		71
	• Linear trimer, **25**, $R^1, R^2 = H$; $R^3 = (EO)_5$-CH_3; $R^4, R^5 = H$	Na^+	$Si_3C_{23}H_{54}O_{12}Na$	629.281526		66
	• Linear trimer, **25**, $R^1 = H$; $R^2 = TMS$; $R^3 = (EO)_3$-CH_3; $R^4, R^5 = H$	K^+	$Si_4C_{22}H_{54}O_{10}K$	629.242515		128

Table 6.8 (continued). FTICR/MS of the heptane-soluble fractions – by molecular weight

Ion series[*]	Possible structures	Adduct	Molecular Formula	MW (calculated)	MW (observed)	Δm/M (ppm)
K [m]	-				634.313155	
B [k]	• Linear trimer, **25** R^1, R^2 = TMS; R^3 = $(EO)_2$-CH_3; R^4, R^5 = H	NH_4^+	$Si_5C_{23}H_{62}O_9N$	636.326510	636.329874	5
	• Cyclic tetramer, **28** R^1=$(EO)_3$-CH_3; R^2 - R^4 =H	NH_4^+	$Si_4C_{23}H_{58}O_{11}N$	636.308135		34
F [n]	• Cyclic trimer, **27**, R^1, R^2 = $(EO)_3$-CH_3; R^3 = H	H^+	$Si_3C_{26}H_{59}O_{12}$	647.331438	647.328711	4
	• $MD(M^{OH})$-O-$(EO)_{10}$-$CH_2CH{=}CH_2$, **10**	H^+	$Si_2C_{27}H_{58}O_{13}$	647.349424		32
E [o]	• Linear dimer, **24**, R^1, R^2 = TMS; R^3 = $(EO)_6$-CH_3; R^4 = H	H^+	$Si_4C_{27}H_{65}O_{11}$	677.360402	677.288732	111
	• Cyclic trimer, **27**, R^1 = $(EO)_7$-CH_3; R^2, R^3 = H	H^+	$Si_3C_{27}H_{61}O_{13}$	677.342002		79
E [o]	• Linear trimer, **25** R^1, R^2 = TMS; R^3, R^4 = $(EO)_2$-CH_3; R^5 = H	H^+	$Si_5C_{28}H_{69}O_{11}$	721.368029	721.315968	72
	• Cyclic tetramer, **28** R^1, R^2 = $(EO)_{2.5}$-CH_3; R^3, R^4 = H	H^+	$Si_4C_{28}H_{61}O_{13}$	721.349650		47
L [p]	• Linear dimer, **24**, R^1 = H; R^2 = TMS; R^3 =$(EO)_{12}$-CH_3; R^4 = H	H^+	$Si_3C_{36}H_{81}O_{17}$	869.478162	869.352488	144
	• Linear trimer, **25**, R^1 = H; R^2 = TMS; R^3, R^4 = $(EO)_{4.5}$-CH_3; R^5 = H	H^+	$Si_4C_{35}H_{81}O_{16}$	869.460175		124
M [q]	-				989.371510	
G [r]	• Cyclic trimer, **27**, R^1, R^2, R^3 = $(EO)_{5.3}$-CH_3	H^+	$Si_3C_{47}H_{101}O_{22}$	1101.608628	1101.582875	23
	• Cyclic tetramer, **28**, R^1 – R^4 = $(EO)_{3.3}$-CH_3	H^+	$Si_4C_{46}H_{101}O_{21}$	1101.590636		7

[a] *m/z* 297, 341, 386; [h] *m/z* 307, 351; [i] *m/z* 311, 355, 399, 443; [d] *m/z* 314, 358; [e] *m/z* 400, 444, 488, 532, 576; [f] *m/z* 425, 469, 513, 557, 601; [g] *m/z* 441, 485, 529, 573, 617, 661, 705; [h] *m/z* 453, 497, 541, 585, 629, 673, 717; [i] *m/z* 479, 523; [j] *m/z* 459, 503, 547, 591; [k] *m/z* 548, 592, 636, 680, 724, 768; [l] *m/z* 585, 629, 673, 717; [m] *m/z* 634, 678, 722; [n] *m/z* 647, 691, 735; [o] *m/z* 633, 677, 721, 765, 809; [p] *m/z* 825, 869, 913, 957; [q] *m/z* 901, 945, 989, 1033, 1077; [r] *m/z* 793, 837, 881, 925, 969, 1013, 1057, 1101, 1145, 1189, 1233, 1277; [*] Refer to Table 6.2 and Appendix A.IV.3

Table 6.9. FTICR/MS analysis of the heptane-soluble fractions – classified by structural type

Ion series[*]	Possible structures	Adduct	Molecular Formula	MW (calculated)	MW (observed)	Δm/M (ppm)
	M-TMS, 21					
B[c]	• n = 2 - 5	H^+	$Si_2C_{12}H_{31}O_5$	311.171006	311.171476	1.5
B[k]	• n = 7 - 12	NH_4^+	$Si_2C_{22}H_{54}O_{10}N$	548.328629	548.275693	97
	M-2TMS, 22					
C[j]	• n = 7 - 10	H^+	$SiC_{21}H_{47}O_{11}$	503.288175	503.235537	105
C[l]	• n = 6 - 12	K^+	$SiC_{25}H_{54}O_{13}K$	629.296515	629.323069	42
	$HO(EO)_nCH_3$, 20					
A[a]	• n = 6 - 8	H^+	$C_{13}H_{29}O_7$	297.190777	297.192485	5.7
A[d]	• n = 6 - 7	NH_4^+	$C_{13}H_{32}O_7N$	314.181401	314.218820	119
	$HO(EO)_nH$					
[j]	• n = 10 - 13	H^+	$C_{22}H_{47}O_{12}$	503.306184	503.235537	140
[l]	• n = 9 - 15	K^+	$C_{26}H_{54}O_{14}K$	629.314511	629.323069	14
	$CH_3O(EO)_8CH_2$-CH=CH_2					
I[f]	• n = 8 - 12	H^+	$C_{20}H_{41}O_9$	425.275058	425.240096	82
	MD(M^{OH})-O-$(EO)_n$-CH_2-CH=CH_2, 10					
F[e]	• n = 4 - 8	NH_4^+	$Si_2C_{15}H_{38}O_7N$	400.218685	400.238553	50
	Linear dimers, 24					
	R^1, R^2 = TMS					
E[o]	• $R^3 = (EO)_n$-CH_3; n = 5 - 9; R^4 = H	H^+	$Si_4C_{27}H_{65}O_{11}$	677.360402	677.288732	111
	R^1 = H; R^2 = TMS					
B[k]	• R^3, $R^4 = (EO)_2$-CH_3	NH_4^+	$Si_3C_{21}H_{54}O_9N$	548.310643	548.275693	64
L[p]	• $R^3 = (EO)_{12}$-CH_3; R^4 = H	H^+	$Si_3C_{36}H_{81}O_{17}$	869.478162	869.352488	144
	R^1, R^2 = H; **R^3, $R^4 = (EO)_n$-CH_3**					
C[j]	• n_{TOTAL} = 5; $n_{/EO\ chain\#}$ = 2.5	H^+	$Si_2C_{20}H_{47}O_{10}$	503.270170	503.235537	69
C[l]	• n_{TOTAL} = 7; $n_{/EO\ chain\#}$ = 3.5	K^+	$Si_2C_{24}H_{54}O_{12}K$	629.278515	629.323069	71

Table 6.9 (continued). FTICR/MS of the heptane-soluble fractions – by structural type

Ion series[*]	Possible structures	Adduct	Molecular Formula	MW (calculated)	MW (observed)	Δm/M (ppm)
	Linear trimers, 25					
	R^1, R^2 = TMS					
B [k]	• $R^3 = (EO)_2$-CH_3; R^4, R^5 = H	NH_4^+	$Si_5C_{23}H_{62}O_9N$	636.326510	636.329874	5
E [o]	• R^3, $R^4 = (EO)_2$-CH_3; R^5 = H	H^+	$Si_5C_{28}H_{69}O_{11}$	721.368029	721.315968	72
	R^1 = H; R^2 = TMS					
C [l]	• $R^3 = (EO)_3$-CH_3; R^4, R^5 = H	K^+	$Si_4C_{22}H_{54}O_{10}K$	629.242515	629.323069	128
L [p]	• R^3, $R^4 = (EO)_{4.5}$-CH_3; R^5=H	H^+	$Si_4C_{35}H_{81}O_{16}$	869.460175	869.352488	124
	R^1, R^2 = H					
C [l]	• $R^3 = (EO)_5$-CH_3; R^4, R^5 = H	Na^+	$Si_3C_{23}H_{54}O_{12}Na$	629.281526	629.323069	66
	Cyclic trimers, 27					
G [r]	• R^1, R^2, $R^3 = (EO)_{5.3}$-CH_3	H^+	$Si_3C_{47}H_{101}O_{22}$	1101.608628	1101.582875	23
F [n]	• R^1, R^2 =$(EO)_3$-CH_3; R^3 =H	H^+	$Si_3C_{26}H_{59}O_{12}$	647.331438	647.328711	4
E [i]	• R^1=$(EO)_2$-CH_3; R^2, R^3 =H	Na^+	$Si_3C_{17}H_{40}O_8Na$	479.192873	479.278786	179
E [o]	• R^1=$(EO)_7$-CH_3; R^2, R^3 =H	H^+	$Si_3C_{27}H_{61}O_{13}$	677.342002	677.288732	79
	Cyclic tetramer, 28					
G [r]	• R^1 - R^4 =$(EO)_{3.3}$-CH_3	H^+	$Si_4C_{46}H_{101}O_{21}$	1101.590636	1101.582875	7
E [o]	• R^1, $R^2 = (EO)_{2.5}$-CH_3; R^3, R^4 = H	H^+	$Si_4C_{28}H_{61}O_{13}$	721.349650	721.315968	47
B [k]	• R^1=$(EO)_3$-CH_3; R^2 - R^4 =H	NH_4^+	$Si_4C_{23}H_{58}O_{11}N$	636.308135	636.329874	34
H [h]	-				307.140163	
J [g]	-				441.199239	
K [m]	-				634.313155	
M [q]	-				989.371510	

For keys to superscripts refer to Table 6.8.

Variation in the isotope patterns under high resolution was also investigated as a potential method for distinguishing the possible assignments, however the structures could not be confirmed by this method due to the limited variation observed.

6.3.5 Degradation of M_2D-C_3-O-$(EO)_n$-Me purified from Silwet L-77

M_2D-C_3-O-$(EO)_n$-Me structures comprise only 70% of the commercial Silwet L-77 formulation (Section 2.2.1.3). Polyethoxylate starting materials and siloxane derivatives are also present in the commercial blend. Because these compounds are also possible degradation products it was thus necessary to investigate the degradation of purified M_2D-C_3-O-$(EO)_n$-Me, in order to distinguish between degradation products and synthetic impurities.

In particular, these experiments were conducted in order to establish the source of the structures $CH_3O(EO)_nH$ (**20**), $HO(EO)_nH$, HO-$(EO)_n$-$CH_2CH{=}CH_2$, CH_3O-$(EO)_n$-$CH_2CH{=}CH_2$, M_2D-C_3-O-$(EO)_n$-H (**2**) and $(M^R)_2D$-O-$(EO)_n$-$CH_2CH{=}CH_2$ (**9**, **10**, **11**; R = H or CH_3), as either by-products of the synthetic procedure, excess starting materials or degradation products. It was also hoped that, by removal of the excess starting materials, further confirmation of structures could be assigned to *ion series* sharing the same molecular weight.

For simplicity, the *ion series* observed will be referred to using the '*Series*' classifications described in Table 6.2. Only the structures displaying feasible EO content will be discussed here.

6.3.5.1 Degradation of M_2D-C_3-O-$(EO)_n$-Me

The polar components of M_2D-C_3-O-$(EO)_n$-Me* degradation (25:75 H_2O/MeOH, 10 days, room temperature) were collected by preparative HPLC, and analysed by ESI/MS, HPLC/ESI/MS and FTICR/MS. The ESI/MS spectrum is shown in Figure 6.9.a, as compared with the polar synthetic impurities of Silwet L-77 (Figure 6.9.*b*). Two dominant series are observed, the first corresponding to *Series C* ions (*m/z* 520, 564, 608, 652, 696, 740, 784, 828 and 872, NH_4^+ adducts). The EO content of the M-2TMS (**22**, n = 8 - 16) structures is compatible with the ions observed as is the linear dimer **24** [R^1, R^2 = H; R^3, R^4 = $(EO)_n$-CH_3; n_{TOTAL} = 4 – 12; $n_{EO/chain\#}$ = 2 – 6], however the former (**22**) is more likely in terms of the polarity of the fraction. The linear dimer product would be a condensate of shorter $(EO)_n$ chain length Silwet L-77 monomers ($n_{EO/chain\#}$ = 2 – 6) and as such can be considered an unlikely assignment due to the high polarity of the fraction. The $HO(EO)_nH$ (n = 11 –19) assignment for the ions observed is not feasible in terms of the EO content of the starting materials used.

---

* Purified by RP C_{18} column chromatography, Section 2.2.1.2

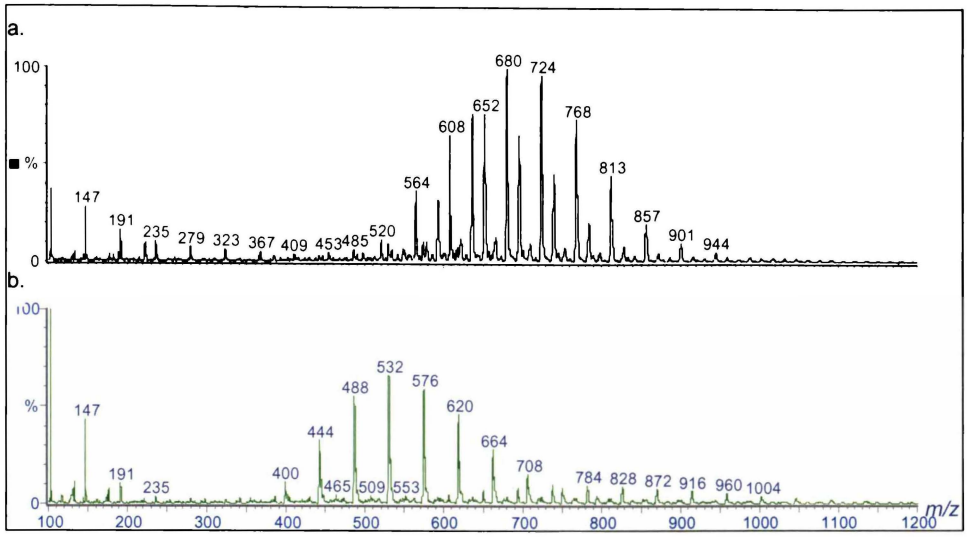

Figure 6.9. ESI/MS spectra of: *a.* Polar degradation products of M_2D-C_3-O-$(EO)_n$-Me; and *b.* polar fractions within the Silwet L-77 formulation.

Analysis of the polar degradation products by online RP C_{18} HPLC/ESI/MS (70:30 H_2O/CH_3CN) revealed lower oligomers (*m/z* 305, 349, 393, 437 and 481) of the series (Figure 6.10). This eliminates the linear dimer as a possible structure, due to required EO content, and thus confirms the M-2TMS (**22**, EO n_{TOTAL} = 3 - 16) assignment. Differences in the retention time (HPLC/ESI/MS) of this *ion series* as compared with those observed for a $HO(EO)_nH$ standard provided further confirmation of the M-2TMS (**22**) structure.

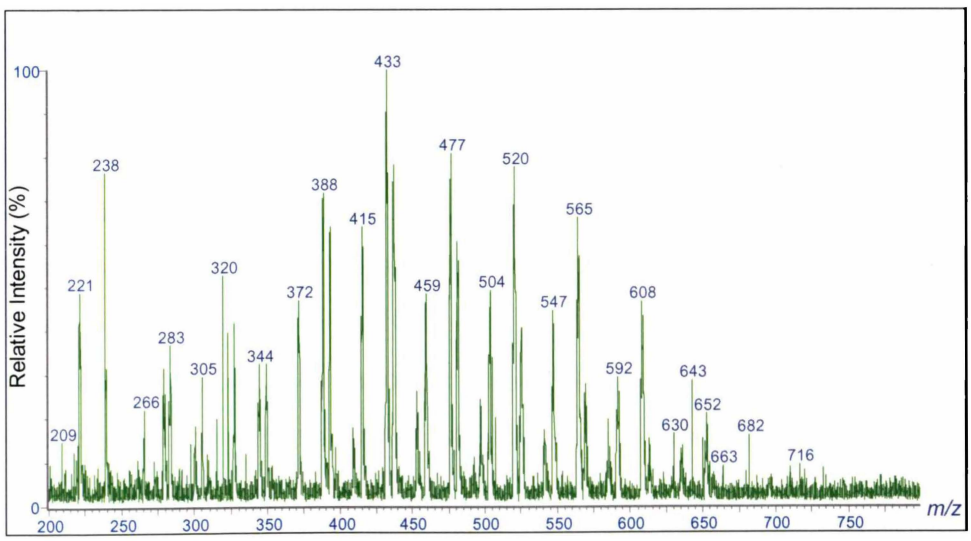

Figure 6.10. ESI/MS spectrum of the polar products of M_2D-C_3-O-$(EO)_n$-Me degradation (RP C_{18} HPLC/ESI/MS, retention time = 5 minutes)

The second series observed in Figure 6.9.a (*m/z* 548, 592, 636, 680, 724, 768, 813, 857, 901 and 944) corresponds to the NH_4^+ adducts of *Series B*. Both the M-TMS (**21**, $(EO)_n$ n = 7 - 16) structure and the linear dimer [**24**; R^1 = TMS; R^2 = H; R^3, R^4 = $(EO)_n$-CH_3; n_{TOTAL} = 4 – 13] have plausible EO content, however the polarity of the fraction supports the former (**21**) assignment. The EO content for the $(M^{OH})_2$D-O-$(EO)_n$-$CH_2CH{=}CH_2$ (**11**, n = 9 – 18) assignment is not feasible for the ions observed.

The spectrum obtained by HPLC/ESI/MS (Figure 6.10) also revealed lower oligomers of the series (*m/z* 328, 372, 416, 460, 504) ruling out the linear dimer assignment. Further support for the M-TMS (**21**) structure was obtained from the high resolution FTICR/MS data (Table 6.10).

A higher molecular weight series corresponding to *Series B* ions (*m/z* 1081, 1125, 1169, 1213 and 1257) was also observed by FTICR/MS. Several possible structures can be assigned, although the high resolution data shows that the linear dimer [**24**, R^1 = TMS; R^2 = H; R^3, R^4 =$(EO)_n$-CH_3, n_{TOTAL} = 16 - 20; $n_{EO/chain\#}$ = 8 – 10] assignment is in highest agreement with the observed mass. This assignment is also consistent with the high polarity of the series.

Table 6.10. FTICR/MS analysis of the polar degradation products of Silwet L-77

*Ion Series**	Possible structures[a]	Molecular Formula	MW (calculated)	MW (observed)	Δm/M (ppm)
B[b]	• M-TMS, **21**, n = 10	$Si_2C_{28}H_{62}O_{13}Na$	685.3627	685.3704	11
	• Linear dimer, **24** R^1 = TMS; R^2 = H; R^3, R^4 =$(EO)_{3.5}$-CH_3	$Si_3C_{27}H_{62}O_{12}Na$	685.3447		37
	• $(M^{OH})_2D$-O-$(EO)_{12}$-$CH_2CH{=}CH_2$, **11**	$SiC_{28}H_{58}O_{15}Na$	685.3442		38
B[c]	• Linear dimer, **24** R^1 = TMS; R^2 = H; R^3, R^4 =$(EO)_8$-CH_3	$Si_3C_{45}H_{98}O_{21}Na$	1081.5806	1081.6030	21
	• Linear trimer, **25** R^1 = TMS; R^2 = H; R^3, R^4, R^5 = $(EO)_{4.3}$-CH_3	$Si_4C_{44}H_{98}O_{20}Na$	1081.5626		37
	• Linear tetramer, **23** R^1 = TMS; R^2 = H; m = 4, R^3 = $(EO)_{2.5}$-CH_3	$Si_5C_{43}H_{98}O_{19}Na$	1081.5446		54
	• Linear trimer, **25** R^1, R^2 = TMS; R^3 = $(EO)_{12}$-CH_3; R^4, R^5 = H	$Si_5C_{43}H_{66}O_{19}Na$	1081.5446		54
	• Linear tetramer, **23** R^1, R^2 = TMS; m = 4 R^3, R^4 = $(EO)_{4.5}$-CH_3; R^5, R^6 = H	$Si_6C_{42}H_{66}O_{18}Na$	1081.5266		71
	• Linear pentamer, **23** R^1, R^2 = TMS; m = 5 R^3, R^4, R^5 = $(EO)_2$-CH_3; R^6, R^7 = H	$Si_7C_{41}H_{66}O_{17}Na$	1081.5087		87
	• Cyclic tetramer, **28** R^1 = $(CH_2)_3$-O-$(EO)_{13}$-CH_3 R^2, R^3, R^4 = $(CH_2)_3$-OH	$Si_4C_{43}H_{94}O_{21}Na$	1081.5262		71

* Refer to Table 6.2 and Appendix A.IV.3; [a] Na^+ adducts; [b] *m/z* 553, 597, 641, 685, 729, 773, 818, 862, 906, 949; [c] *m/z* 1081, 1125, 1169, 1213, 1257

The online RP C_{18} HPLC/ESI/MS chromatogram of the polar degradation products using an elution solvent with a higher water content (60:40 H_2O/MeOH) is shown in Figure 6.11.*b*. A peak at the solvent front (4 minutes), followed by a series of peaks at 7.6, 8.3, 9.2, 10.5, 12.0, 13.7, 15.7, 18.1, 21.3 and 25 minutes can be observed. The spectrum of the peak eluting at 4 minutes shows two $\Delta m/z$ = 44 series corresponding to the M-TMS (**21**) and M-2TMS (**22**) structures.

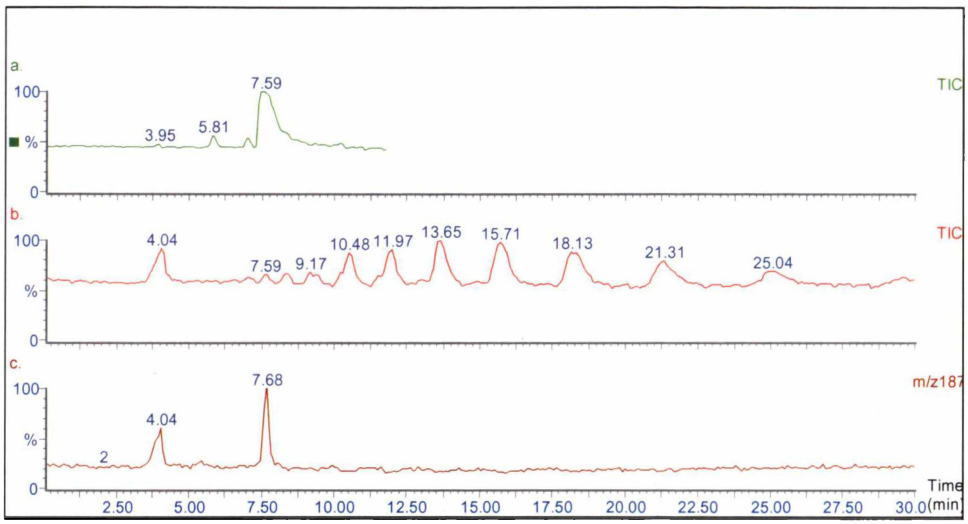

Figure 6.11. RP C_{18} HPLC/ESI/MS chromatograms of: *a.* $CH_3O(EO)_3H$; *b.* polar degradation products of M_2D-C_3-O-$(EO)_n$-Me; and *c.* the extracted chromatogram of $CH_3O(EO)_3H$ (m/z 187) from trace *b.*

The later resolved peaks correspond to the $CH_3O(EO)_nH$ (**20**, n = 3 - 12) series. Comparison with the chromatogram of commercially available $CH_3O(EO)_3H$ showed identical retention times and spectra confirming the $CH_3O(EO)_nH$ assignment (Figure 6.11), and confirming **20** as a degradation product of M_2D-C_3-O-$(EO)_n$-Me.

6.3.5.2 Acid degradation of M_2D-C_3-O-$(EO)_n$-Me

A solution of M_2D-C_3-O-$(EO)_n$-Me* in HCl (15:85 H_2O/CH_3CN) was left to stand at 8 °C, and analysed by ESI/MS at selected intervals up to 2 months. Analysis of the reaction mixture after 2 days exposure to 2 M HCl showed no parent ions remained (Figure 6.12.*a*). The major *ion series* was observed at *m/z* 349, 393, 437, 481, 525, 569, 613, 657, 701 and 745, corresponding to *Series C* (Na^+ adducts). Only the M-2TMS (**22**, n = 4 - 10) and $HO(EO)_nH$ (n = 7 –16) assignments are in accord with required EO content. The $HO(EO)_nH$ assignment can be eliminated on the grounds that this was not a product of acid degradation of $CH_3O(EO)_nH$ (Section 6.3.3). The ion distribution for the M-2TMS assignment (major ion equating to the n = 7 oligomer) is also in agreement with that expected for the starting material used.

Another significant series was observed at *m/z* 221, 265, 309, 397, 441, 485, 529, 573, 617, 661, 705, 749, 793 and 837 (major ion *m/z* 529) although no

* Purified by preparative RP C_{18} HPLC, Section 2.2.1.1

plausible structures could be assigned. With the addition of Na^+ and K^+ salt solutions, a series of ions (*m/z* 231, 275, 319, 363, 407, 451, 495, 539, 583, 627, 671, 715, 759 and 803, Na^+ adducts) assignable to $CH_3O(EO)_nH$ (**20**, n = 4 - 17, major ion n = 9) was observed.

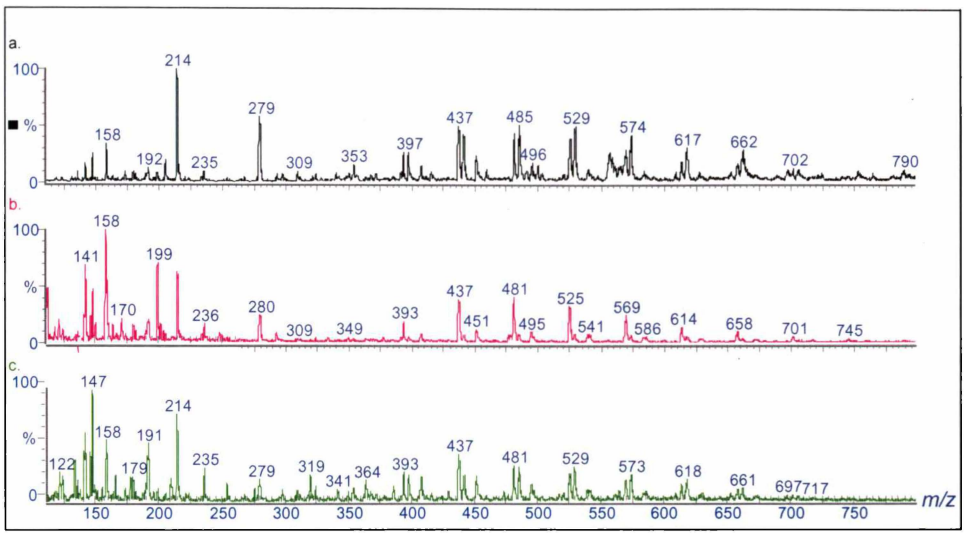

Figure 6.12. ESI/MS spectra of M_2D-C_3-O-$(EO)_n$-Me after: *a.* 2 days; *b.* 1 month; and *c.* 6 weeks exposure to 2 M HCl (8 °C)

Similar spectra were obtained after 1 month and 6 weeks under the acidic conditions (Figure 6.12, *b.* and *c.*), with ions corresponding to $CH_3O(EO)_nH$ (**20**, *m/z* 275, 319, 363) more significant in the 6 week spectrum.

The HPLC/ESI/MS chromatogram (60:40 H_2O/MeOH) after 2 months in acid (Figure 6.13.*c*) showed a pattern similar to that described in Section 6.3.5.1 (non-acidified conditions, Figure 6.11.*b*), although the relative ion intensities were significantly different.

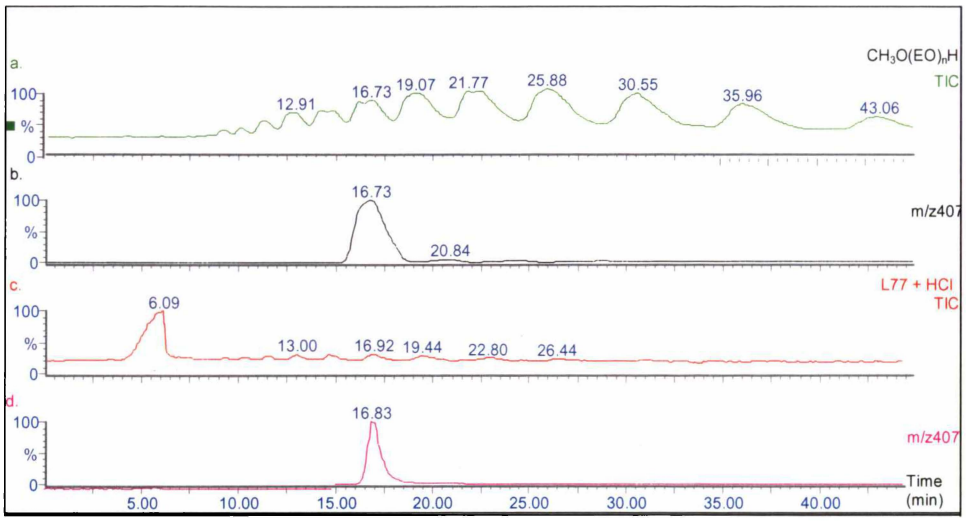

Figure 6.13. RP C_{18} HPLC/ESI/MS chromatograms of: *a.* $CH_3O(EO)_nH$; *b.* the extracted chromatogram of $CH_3O(EO)_8H$ (m/z 407) from a; *c.* HCl degraded M_2D-C_3-O-$(EO)_n$-Me; and *d.* the extracted chromatogram of $CH_3O(EO)_8H$ (m/z 407) from the M_2D-C_3-O-$(EO)_n$-Me *c.* trace.

The combined spectrum of the most polar peak eluted (6 minutes) is much more complicated in the lower mass region (Figure 6.14), as compared with the corresponding spectrum from the non-acidified conditions (Figure 6.10). The previously described ions corresponding to M-2TMS (**22**, n = 4 - 12, *m/z* 349, 393, 437, 481, 525, 569, 613, 657, 701) and M-1TMS type structures (**21**) were also evident, although at much lower intensity.

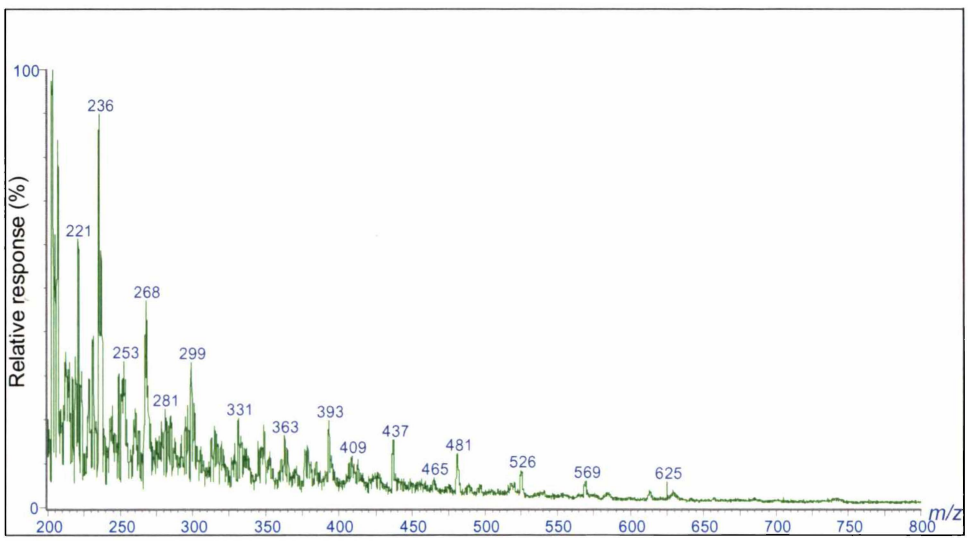

Figure 6.14. The spectrum of the 6 minute peak in the RP C_{18} HPLC/ESI/MS chromatogram of 2 M HCl degraded M_2D-C_3-O-$(EO)_n$-Me (after 2 months).

The spectra of the low intensity peaks eluted over the 7.5 – 30 minute time period in Figure 6.13.*c* correspond with $CH_3O(EO)_nH$ (**20**) structures. Comparison of the retention times and spectra with commercially available $CH_3O(EO)_nH$ (Figure 6.13.*a*) confirmed the $CH_3O(EO)_nH$ series to be products of Silwet L-77 degradation as demonstrated by the analogous extracted ion chromatograms (Figure 6.13, *b* and *d*).

Minor amounts of the uncapped polyethylene-glycols were also observed in the degradation product mixture, as determined by ESI/MS and confirmed by comparison of the HPLC/ESI/MS with that of commercially available PEG-400 (not shown). It was important to ascertain whether these were real degradation products or artifacts due to residual M_2D-C_3-O-$(EO)_n$-H in the starting material. In order to determine the source of these compounds, the purity of the starting material and the HCl degradation of PEG reference compounds (6.3.3) was investigated.

The chromatogram of the purified M_2D-C_3-O-$(EO)_n$-Me used in the degradation studies is shown in Figure 6.15, and can be compared with the chromatogram of the commercial Silwet L-77 formulation (Figure 2.3).

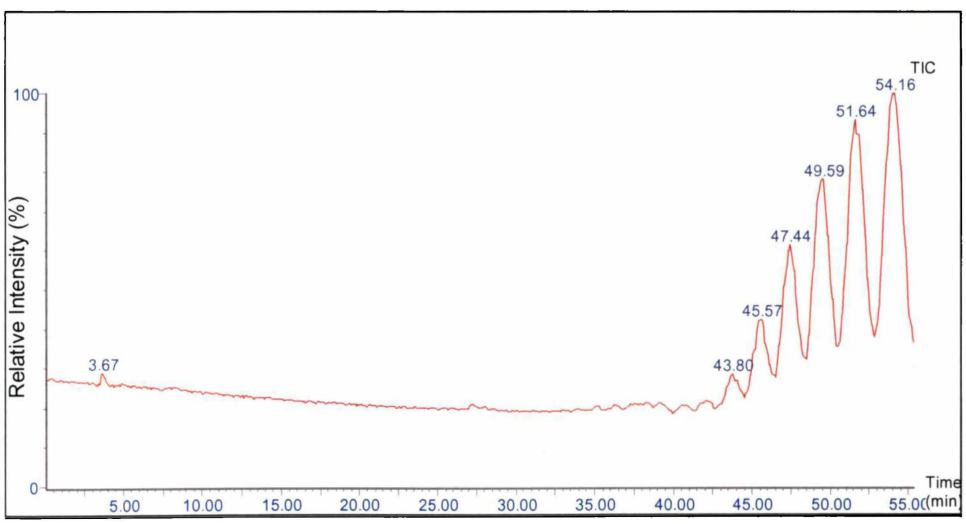

Figure 6.15. RP C_{18} HPLC/ESI/MS chromatogram of the M_2D-C_3-O-$(EO)_n$-Me used in degradation studies

The combined spectrum of the chromatogram over 33.5 - 42.5 minutes is shown below (Figure 6.16). Ions at *m/z* 279 and 242 (not shown) were the major ions in the spectrum, and although not of significant intensity, ions corresponding

to n = 3 - 9 M_2D-C_3-O-$(EO)_n$-H (*m/z* 435, 479, 523, 567, 611, 655, 699) can be observed. $HO(EO)_nH$ would be a degradation product of these structures.

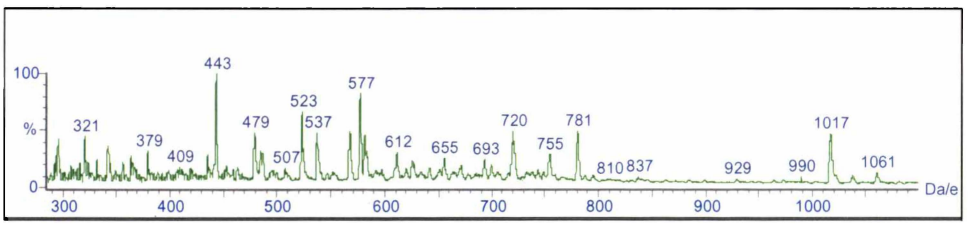

Figure 6.16. Combined spectrum from HPLC/ESI/MS chromatogram (33.5 – 42.5 minutes) of purified M_2D-C_3-O-$(EO)_n$-Me sample used

6.3.6 Degradation of pure M_2D-C_3-O-$(EO)_n$-R oligomers

The degradation of single oligomers and less complex mixtures of M_2D-C_3-O-$(EO)_n$-R oligomers was investigated in order to confirm the proposed products, and to aid structural determination in situations where a large number of possible assignments existed.

6.3.6.1 Acid degradation of M_2D-C_3-O-$(EO)_3$-Me

In the following description the ion values reported are the Na^+ ion adducts of the described species.

6.3.6.1.1 Degradation at low concentration (1 000 ppm)

A solution of M_2D-C_3-O-$(EO)_3$-Me in 5% HCO_2H ($MeOH/H_2O$) was monitored by ESI/MS at selected time intervals (0, 15, 30 and 60 minutes, 2, 4, 6, and 24 hours and 2, 3 and 15 days).

At t = 0 minutes, ions at *m/z* 449 and 377, which can be assigned to M and M-TMS (**21**) respectively, were observed. At t = 30 minutes, ions at *m/z* 731 and 803 are observed. These correspond to the linear tetramers [**23**; m = 4; R^3 = H, H, H, $(EO)_3$-CH_3] possessing one (R^1 = H, R^2 = TMS) and two TMS (R^1, R^2 = TMS) groups respectively. These structures can only be assigned tentatively however, as the required precursors (i.e. the corresponding dimers [**23**; m = 2] and trimers [**23**; m = 3]) were not observed.

An ion assignable to M-2TMS (**22**, *m/z* 305) appeared at t = 60 minutes, as did an ion at *m/z* 165 (H^+ adduct of $CH_3O(EO)_3H$, **20**). At 4 hours, an ion at *m/z* 659 was observed, which corresponded to the linear tetramer with all TMS groups cleaved [**23**; m = 4; R^3 = OH, OH, OH, O-$(EO)_3$-CH_3; R^1, R^2 = H]. This

assignment is also tentative as the linear dimer and trimer intermediates were not observed, although the structure could be formed by loss of a TMS group from the afore-mentioned linear tetramer intermediate (*m/z* 731).

At 6 hours, ions at *m/z* 569, 641 and 713, corresponding to the linear dimers [**24**, R^3, R^4 = -$(EO)_3$-CH_3] with both (R^1, R^2 = H), one (R^1 = H, R^2 = TMS) and no (R^1, R^2 = TMS) TMS groups cleaved respectively were detected. The presence of the three structural analogues supports the assignment as does the presence of the necessary precursors (i.e. the monomers M-TMS, **21** and M-2TMS, **22**). An ion of *m/z* 641 can, however also be assigned to the cyclic tetramer [**28**; R^1, R^2, R^3 = $(CH_2)_3$-OH; R^4 = $(CH_2)_3$-O-$(EO)_3$-CH_3]. This product can be formed by cyclisation, with concurrent loss of H_2O, of the afore-mentioned tentatively assigned linear tetramer intermediate (**23**, m = 4, *m/z* 659). At 24 hours, the parent ion intensity was very small (i.e. < 5%).

At 48 hours an ion at *m/z* 833 was observed which was assigned to the linear trimer **25** [R^1, R^2 = H; R^3, R^4, R^5 = $(EO)_3$-CH_3]. This would form from the condensation of a M-2TMS (**22**, *m/z* 305) molecule (monomer) with the *m/z* 569 linear dimer [**24**; R^3, R^4 = $(EO)_3$-CH_3], both of which are observed.

In general, no significant changes were observed in the subsequent spectra, although at 3 weeks ions at *m/z* 1079 and *m/z* 905 were observed. The former can be assigned to the cyclic tetramer **28** [R^1, R^2, R^3, R^4 = $(CH_2)_3$-O-$(EO)_3$-CH_3], and the later, low intensity ion to the linear trimer **25** [R^1 = H; R^2 = TMS; R^3, R^4, R^5 = $(EO)_3$-CH_3].

Methylated products of the silanol intermediates were also observed in the reaction mixture concurrent with the respective silanol (*m/z* 319 [*m/z* 305+14], M-2TMS+H+CH_3; *m/z* 333 [*m/z* 305+14+14], M-2TMS+2CH_3; *m/z* 391 [*m/z* 377+14], M-TMS+CH_3; *m/z* 583 [*m/z* 569+14]; *m/z* 655 [*m/z* 641+14]; *m/z* 673 [*m/z* 659+14]; *m/z* 687 [*m/z* 659+14+14]; *m/z* 847 [*m/z* 833+14]; *m/z* 919 [*m/z* 905+14]). These can be formed by reaction with the MeOH solvent to give the + 14 a.m.u. products.

Condensation of silanols to give products of the type $RSiOCH_3$, as shown in Equation 6.6, is well documented.[9]

$$R_3SiOH + CH_3OH \leftrightarrow R_3SiOCH_3 + H_2O \qquad (6.6)$$

The reaction is reversible, however it is possible and likely that the $RSiOCH_3$ species is not as reactive as the corresponding RSiOH species. This may provide a possible explanation of why few of the potential products are observed in this experiment.

Analogous reactions with higher alcohols are also known,[15] and thus it followed that products resulting from the condensation of silanols with PEG components in the reaction mixture may be formed. No evidence of such products were observed in these experiments. Reactions with PEG would be expected to be much slower than with methanol, and these results demonstrate that the condensation does not occur within the time frame monitored here, if at all.

Parallel reactions of siloxanes with alcohols are also well known (Equation 6.7) and the reactions proceed to the thermodynamically more stable mixture.

$$RSiOSiR' + R''OH \leftrightarrow RSiOH + R''OSiR' \qquad (6.7)$$

The conversion of cyclotrisiloxanes to higher cyclosiloxanes in the presence of MeOH has also been reported.[9]

The organic solvent was used in order to provide miscibility for the starting material, as it was proposed that solubility would have a large influence on the products formed and also on recovery. The degradation of the single oligomers of $M_2D\text{-}C_3\text{-}O\text{-}(EO)_n\text{-}Me$ was conducted in order to provide models for the degradation of Silwet L-77. Because Silwet L-77 is soluble in water, conditions such that the $M_2D\text{-}C_3\text{-}O\text{-}(EO)_3\text{-}Me$ was soluble were selected to duplicate this process as closely as possible. As described above, however the presence of MeOH can significantly influence the degradation products obtained. Consequently the solvent was altered to the inert organic solvent THF in the following experiments.

6.3.6.1.2 Degradation at high concentration (500 000 ppm)

The results obtained from the higher concentration degradation in THF were very different to those from the preceding low concentration degradation conducted in MeOH (6.3.6.1.1).

After 6 hours of exposure to the acid solution assignable ions were observed at *m/z* 377, 449, 641, 713, 815, 905, 977, 1023, 1079, 1095, 1169, 1241, 1433, 1505, 1697, 1769 and 2033. The ions at *m/z* 500, 551, 632, 764 and 875 are as yet unassigned.

The ions observed at *m/z* 449 and 377 are assigned to M and M-TMS (**21**), respectively. The ions at *m/z* 641 and 713 correspond to the linear dimers [**24**; R^3, R^4 = $(EO)_3$-CH_3] with one (R^1 = H, R^2 = TMS) and two TMS groups (R^1, R^2 = TMS) attached respectively. The simultaneous observation of the species at *m/z* 377, 641 and 713 fit the hydrolysis mechanism of condensation of two M-TMS (**21**) monomers (*m/z* 377) to give the linear dimer containing two TMS groups (*m/z* 713), followed by a loss of one TMS (*m/z* 641). At t = 6 hours in the previous experiment, ions corresponding to the analogous linear dimers with no and one TMS groups attached respectively were observed (**24**, *m/z* 569 and 641), in further support of this assignment.

The small ion at *m/z* 815 can be assigned to the cyclic trimer [**26**; m = 3; R = $(EO)_3$-CH_3]. Ions corresponding to the linear trimers [**25**, R^3, R^4, R^5 = $(EO)_3$-CH_3] are observed at *m/z* 905 (R^1 = H, R^2 = TMS) and *m/z* 977 (R^1, R^2 = TMS). The ion at *m/z* 933 corresponds to the cyclic tetramer **28** [R^1 = $(CH_2)_3$-OH; R^2, R^3, R^4 = $(CH_2)_3$-O-$(EO)_3$-CH_3], whilst *m/z* 1079 can be assigned to the cyclic tetramer [**28**; R^1, R^2, R^3, R^4 = $(CH_2)_3$-O-$(EO)_3$-CH_3].

The ions at *m/z* 1023 and 1095 correspond to the linear tetramers [**23**; m = 4; R^3 = H, $(EO)_3$-CH_3, $(EO)_3$-CH_3, $(EO)_3$-CH_3] with one (R^1 = H, R^2 = TMS) and both TMS groups (R^1, R^2 = TMS) attached respectively. The linear tetramers [**23**; m = 4; R^3 = $(EO)_3$-CH_3] and pentamers [**23**, m = 5; R^3 = $(EO)_3$-CH_3], with both (R^1, R^2 = TMS) and one TMS groups (R^1 = H, R^2 = TMS) intact, are assigned to the ions at *m/z* 1169, 1241 and 1433 and 1505, respectively. The linear hexamers [**23**; m = 6; R^3 = $(EO)_3$-CH_3] with both (R^1, R^2 = TMS) and one TMS groups (R^1 = H, R^2 = TMS) intact, are assigned to the ions at *m/z* 1769 and 1697. The linear heptamer [**23**; m = 7; R^1, R^2 = TMS; R^3 = $(EO)_3$-CH_3] is observed at low intensity at *m/z* 2033.

At 24, 80 and 120 hours essentially the same spectra to that after 6 hours were obtained, with varying ion intensities. The parent ion was also still present at a significant intensity at these times. The addition of salts was found to enhance the

response of the smaller ions (higher MW) and the use of smaller acquisition ranges and higher resolution was also used to confirm these products. Consequently at 80 hours low intensity ions at *m/z* 819 and 847 (K^+ adducts), corresponding to the linear tetramer [**23**; m = 4; R^1, R^2 = TMS; R^3 = H, H, H, $(EO)_3$-CH_3] and the linear trimer [**25**; R^1, R^2 = TMS; R^3, R^4 = $(EO)_3$-CH_3; R^5 = H] respectively, were observed. An ion (*m/z* 849, K^+ adduct) corresponding to the linear trimer [**25**; R^1, R^2 = H; R^3, R^4, R^5 = $(EO)_3$-CH_3] was also observed at very low intensity.

Note that in the higher concentration experiment the silanol products with both terminal TMS groups cleaved (M-2TMS etc) were rarely observed, and products with one TMS were also of very low intensity. These products are of considerable reactivity, and thus are expected to condense with other silanols present. At high concentrations the interactions will be increased leading to more extensive condensation.

6.3.6.2 Acid and base degradation of M_2D-C_3-O-$(EO)_6$-Me

Solutions of M_2D-C_3-O-$(EO)_6$-Me (1 mg) were reacted with 0.1 M HCl (1 mL) and NaOH. Spectra of the fractions obtained by subsequent solvent extraction and RP C_{18} sep-pak purification were very complicated and yielded many ions that were difficult to assign. The addition of salts also failed to change the adduct pattern in many cases making it difficult to determine the parent ion molecular weight. The samples were re-analysed on three different occasions, but no improvement was found. Overall the results from these experiments were not overly informative. The extremely low initial concentration of the analyte, such that contamination by background ions was significant, was considered to be the main source of the difficulties encountered. This is further compounded by the large number of potential products.

6.3.6.2.1 Acid degradation

The major ion observed in the spectrum of the water-soluble fraction was at *m/z* 977. This corresponds to the Na^+ adduct of the linear dimer (**24**) with both terminal TMS groups and $(EO)_6$ chains intact. Another significant ion is observed at *m/z* 1229, corresponding to the Na^+ adduct of the linear trimer (**25**) with all

three $(EO)_6$ chains intact but both terminal TMS groups cleaved. A very faint ion at *m/z* 319 can be attributed to the Na^+ adduct of the cleaved monomethyl-ethoxy chain, $CH_3O(EO)_6H$, **20**.

The major ion observed in the spectrum of the heptane-soluble fraction was at *m/z* 402. A dominant ion at *m/z* 440 in subsequent spectra indicates a compound of molecular weight 401 (the *m/z* 402 and 440 ions being the H^+ and K^+ adducts, respectively), although no structure can be assigned. The next largest ion was at *m/z* 372 which corresponds to the NH_4^+ adduct of the cyclic trimer (**27**) with all ethoxylate chains cleaved. To confirm this assignment it is necessary to confirm whether the proposed structure would be detectable by ESI/MS despite the absence of any ethoxylate chains. An ion at *m/z* 365 with addition of KCl indicates a linear dimer (**24**) structure with one terminal TMS group and both $(EO)_6$ chains cleaved. In the spectra with additional NaCl present ions at *m/z* 669 and 739 are observed. These can be assigned to the NH_4^+ adducts of the linear trimer (**25**) with two EO chains cleaved and both and one TMS groups cleaved respectively. In the same spectra, an ion at *m/z* 977 is observed corresponding to the Na^+ adduct of the linear dimer (**24**) with both terminal TMS groups and $(EO)_6$ chains intact. This ion was also observed in the spectrum of the water-soluble fraction.

6.3.6.2.2 Base degradation

The spectrum of the water-soluble fraction was extremely complicated and thus structures could not be assigned with confidence. The major ion observed in the spectrum of the heptane-soluble fraction was at *m/z* 349. An ion at *m/z* 365 with addition of KCl indicates a linear dimer structure (**24**) with one terminal TMS group and both $(EO)_6$ chains cleaved. This ion was also observed in the spectrum of the heptane-soluble fraction of the acid catalysed degradation. An ion was observed at *m/z* 674 is consistent with a linear trimer (**25**) with both TMS groups cleaved, and one $(EO)_6$ chain intact. Ions at *m/z* 413, 625 and 739 could not be assigned, although salt addition indicated these to be Na^+ adducts.

The inability to distinguish the adduct formation unequivocally in these spectra sheds doubt on the assignments. The use of higher concentrations is required to clarify assignment of the products.

6.3.6.3 Acid degradation of M_2D-C_3-O-$(EO)_9$-Me

Degradation of a solution of M_2D-C_3-O-$(EO)_9$-Me in 5% HCO_2H (1 mg, 1 mL, 1:1 $MeOH/H_2O$) was monitored by ESI/MS at selected time intervals (0, 15, 30, 45, 60, 75, 90 and 105 minutes, 2, 3, 14, 47, 122 and 194 hours).

At 1.5 hours an ion assignable to M-TMS (**21**, *m/z* 641) was detected, whilst the ion assignable to M-2TMS (**22**, *m/z* 569) was observed after 2 hours. At 14 hours the responses of these degradation products exceeded that of the starting material. The response of the M-TMS (**21**) ion dominated the spectra until 14 hours, with the M-2TMS (**22**) ion dominating thereafter. At 8 days (194 hours) the starting material was no longer detectable (Figure 6.17). Few other ions of significant intensity were observed.

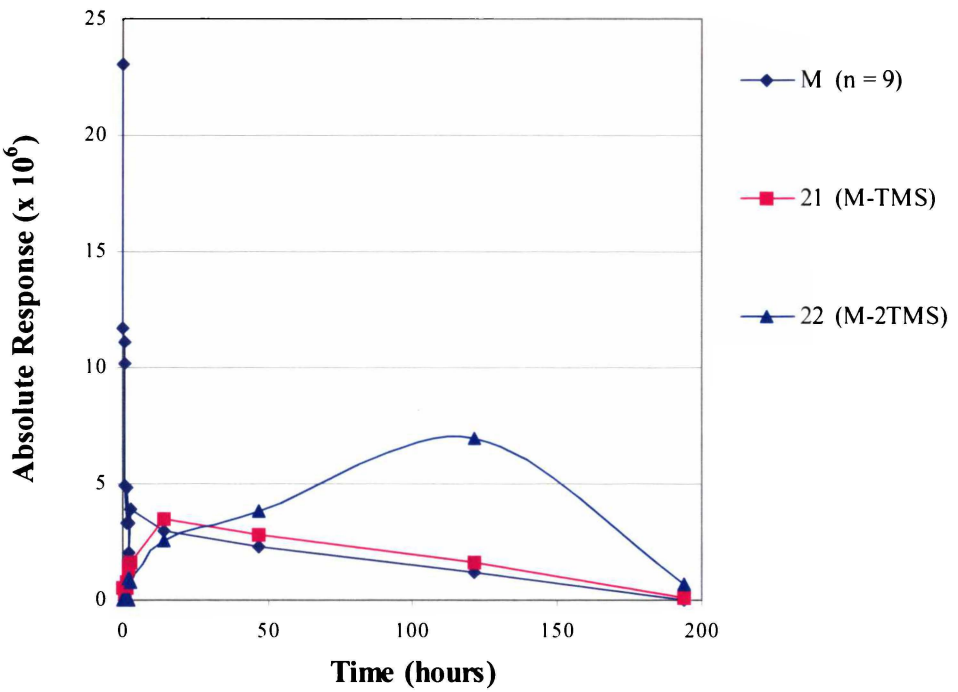

Figure 6.17. Absolute response of M_2D-C_3-O-$(EO)_9$-Me and degradation products over time (0 - 194 hours) under acidic conditions as determined by ESI/MS

6.3.6.4 Acid degradation of M_2D-C_3-O-$(EO)_n$-Me, n = (7+8+9)

Degradation of the oligomeric mixture in 10% HCO_2H (1 mg, 1 mL) was monitored by ESI/MS at 0, 10, 30, 45, 60, 75, 90 and 105 minutes, 2, 2.5, 3, 3.5, 4, 15 and 48 hours.

At t = 10 minutes, ions which could be assigned to M-TMS (**21**) were observed. Expansion of the spectrum at 3.5 hours showed ions assignable to M -

2TMS (**22**). Few other significant ions were observed with the spectra becoming very complicated, especially between *m/z* 600 – 1100.

6.3.6.5 Acid degradation of M_2D-C_3-O-$(EO)_n$-Me, n = 6, n = (8+9) and n = (12+13)

Solutions of the M_2D-C_3-O-$(EO)_n$-Me oligomers (1 mg) were reacted with 2 M HCl (1 mL) for 24 hours. The major product observed by ESI/MS for all samples was the cleaved monomethyl-ethoxylate chain, i.e. adducts of the corresponding $CH_3O(EO)_nH$ (**20**). Few other ions were observed, as to be expected when cleavage of the ethoxylate chain occurs. As discussed previously, in order for these nonionic compounds to be detected by ESI/MS, the cation-chelating ethoxylate moiety is required.

At this concentration of sample and strength of acid, the conditions appear to be too extreme to see a variety of silanol-type products.

6.3.6.6 Acid degradation of M_2D-C_3-O-EO-H

6.3.6.6.1 Qualitative study of M_2D-C_3-O-EO-H degradation

A solution of M_2D-C_3-O-EO-H in 2 M HCl (1 g, 25 mL, 40 000 ppm) was analysed by ESI/MS after 2, 3, 7 and 12 days, and 4 weeks. To simplify the spectra and aid assignment the product mixture was solvent partitioned between heptane and water. After 2 days of exposure to the acid solution, the spectrum of M_2D-C_3-O-EO-H revealed several new ions. Minimal changes to the spectra with further exposure to the acid solution was observed. In order to determine the effect of solubility on product formation analogous experiments were conducted in THF/H_2O solvent mixtures. Results in the organic solvents were very similar to those obtained here (100% H_2O) and are omitted for brevity.

The water-soluble fraction showed assignable ions at *m/z* 203, 365, 437, 495, 527, 613, 657, 671, 689, 833 and 851, although ions at *m/z* 307, 451, 469, 569, 649, 793, 811 and 1013 could not be unassigned. The ion (*m/z* 203), assignable to M-2TMS (**29**; m = 1; R^1, R^2 = H), was detected at 2 days, although was much more significant at t = 3 days. No ions assignable to the M-1TMS structure (**29**, m = 1, R^1 = H, R^2 = TMS) were detected in any of the spectra, in contrast to previous investigations.

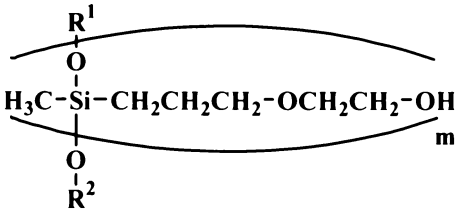

29

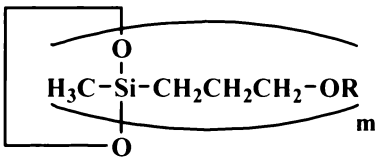

m ≥ 3, R = H, EO-H

30

At t = 2 days, the most intense ion was the unassigned *m/z* 307 ion, whilst the second most intense ion was at *m/z* 365, which corresponds to the linear dimer (**29**; m = 2; R^1, R^2 = H). The linear dimer (**29**; R^1 = H, R^2 = TMS) at *m/z* 437 was also observed, but at a much lower intensity.

Ions at *m/z* 527, 689 and 851 can be assigned to the linear trimer, tetramer and pentamers (**29**; m = 3, 4, 5; R^1, R^2 = H), respectively. The ion at *m/z* 671 corresponds to the linear trimer (**29**; m = 3; R^1, R^2 = TMS) and also to the cyclic tetramer (**30**, m = 4; R^1 – R^4 = EO-H). The silylated linear trimer structure may be the less likely assignment due to the high polarity of the fraction. Furthermore, in this fraction only the linear siloxanes with both TMS groups cleaved were observed for the more polar m = 4 and 5 derivatives.

An ion at *m/z* 495 corresponding to the cyclic tetramer (**30**; m = 4; R^1 - R^4 = H) was observed. Cyclic pentamer structures (**30**; m = 5) can be assigned to the ions at *m/z* 613 (R^1 - R^5 = H), *m/z* 657 (R^1 - R^4 = H; R^5 = EO-H), and *m/z* 833 (R^1 - R^5 = EO-H).

The spectrum of the heptane-soluble fraction at t = 2 days revealed the major ion at *m/z* 509, corresponding to both the linear dimer (**29**; m = 2; R^1, R^2 = TMS) and also to the cyclic trimer (**30**; m = 3; R^1 – R^3 = EO-H). In terms of polarity both structures can be justified. Consistent with the polarities of the fractions, the linear dimer analogue with both TMS groups cleaved was observed at high intensity in the water-soluble fraction. Both the (R^1, R^2 = H) and (R^1 = H, R^2 = TMS) linear dimer analogues were only observed at low intensity in the heptane-soluble fraction (*m/z* 365 and 437). The observation of all three ions of the structural series may support this assignment, however the cyclic trimer assignment can not be excluded as higher cyclic structures were also observed. The larger analogues of the cyclic series (**30**; m = 4, 5) were identified in the water-soluble fraction, consistent with the increased EO content.

The responses of the ions at *m/z* 495 (**30**; m = 4; R^1 - R^4 = H) and 657 (**30**; m = 5; R^1 - R^4 = H; R^5 = EO-H) are much higher in this fraction than for the water-

soluble fraction, the *m/z* 495 response becoming the most intense ion in the spectrum at 7 days. At 4 weeks, the afore-mentioned *m/z* 671 ion (**29**; m = 3; R^1, R^2 = TMS/ **30**, m = 4; R^1 – R^4 = EO-H) also became significant in this fraction. Again, the observation of structural analogues of both series complicates assignment. In terms of fraction polarity, the silylated linear trimer may be the more feasible structure for this fraction, whilst in the water-soluble fraction the cyclic tetramer may be more likely.

Consistent with previously described silanol stabilities, no ions corresponding to linear siloxanes with cleaved EO chains were observed. These are more likely to condense/cyclise and such cyclic products were observed (Section 6.1). The absence of such ions in the ESI/MS spectra does not however preclude their existence as such structures will be of low ionisation capacity by this method (Section 1.2.4).

6.3.6.6.2 Quantitative study of M_2D-C_3-O-EO-H degradation

The ESI/MS response of solutions of M_2D-C_3-O-EO-H (500 ppm) in aqueous and acidic media were monitored over time. The response of the M_2D-C_3-O-EO-H (M) and the mono and disilanol degradation products thereof, under both conditions are presented graphically in Figure 6.18.

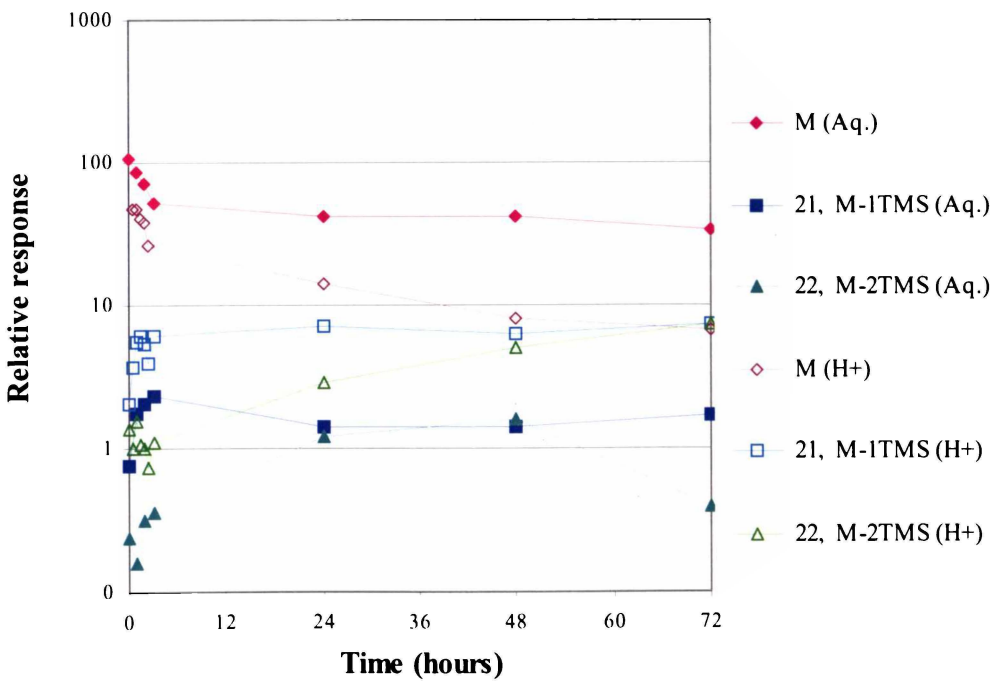

Figure 6.18. Relative response (ESI/MS) of M_2D-C_3-O-EO-H and degradation products over time (0 - 144 hours) under aqueous conditions [neutral (Aq.) and acidic (H^+)]

The response of the M_2D-C_3-O-EO-H was reduced much more quickly under the acidic conditions than in the aqueous system. Both mono- and di- silanol products were produced to a higher level in the acidic medium. The monosilanol response was generally higher and the levels more constant with respect to time for both systems as compared with the disilanol. The disilanol response showed a steady increase in the acidic medium, but a reduction at the later interval was observed for the aqueous system.

6.3.7 FTICR/MS studies on M_2D-C_3-O-$(EO)_n$-Me degradation

6.3.7.1 Acid degradation of M_2D-C_3-O-$(EO)_6$-Me

The FTICR/MS spectrum of M_2D-C_3-O-$(EO)_6$-Me* reacted with 2M HCl (1 mg, 1 mL, 26 hours) showed the Na^+ adduct of the starting material (spike) at *m/z* 581. Ions at *m/z* 301, 465, 815 and 861, in addition to some higher molecular weight products, were also observed, none of which could be assigned.

6.3.7.2 Gas-phase acid degradation of M_2D-C_3-O-$(EO)_{10}$-Me

No fragment ions were observed in the spectra acquired with gas-phase introduction of acetic acid to the MS isolated M_2D-C_3-O-$(EO)_{10}$-Me ion (*m/z* 757, Na^+ adduct). Introduction of the acetic acid prior and post activation was attempted, with neither methods yielding structurally informative ions.

Because degradation has been observed in the presence of acid in aqueous systems previously, the absence of degradation products may indicate H_2O is also required for the acid degradation of Silwet L-77. However this could not be confirmed as introduction of H_2O to the source was not possible. Its low volatility would complicate removal from the system following the experiment and compromise results obtained thereafter.

Fragmentation experiments on Silwet L-77 alone (Section 3.3.4) were also unsuccessful, demonstrating that CID and gas-phase reactions are not informative methods for analysis of Silwet L-77.

---

* Purified by RP C_{18} column chromatography, Section 2.2.1.2

6.3.8 GC/MS studies on Silwet L-77 degradation

6.3.8.1 Acid degradation of M_2D^H

The acid catalysed degradation of M_2D^H was investigated as a reference compound for Silwet L-77 degradation. The GC/MS chromatogram revealed 7 peaks which, according to the EI/MS spectra, belonged to two molecular series (Figure 6.19.*a*). The first series showed increases of 60 mass units with increasing retention time, corresponding to the D^H unit. The second series showed increases corresponding to D^H and D units (60 and 74 mass units).

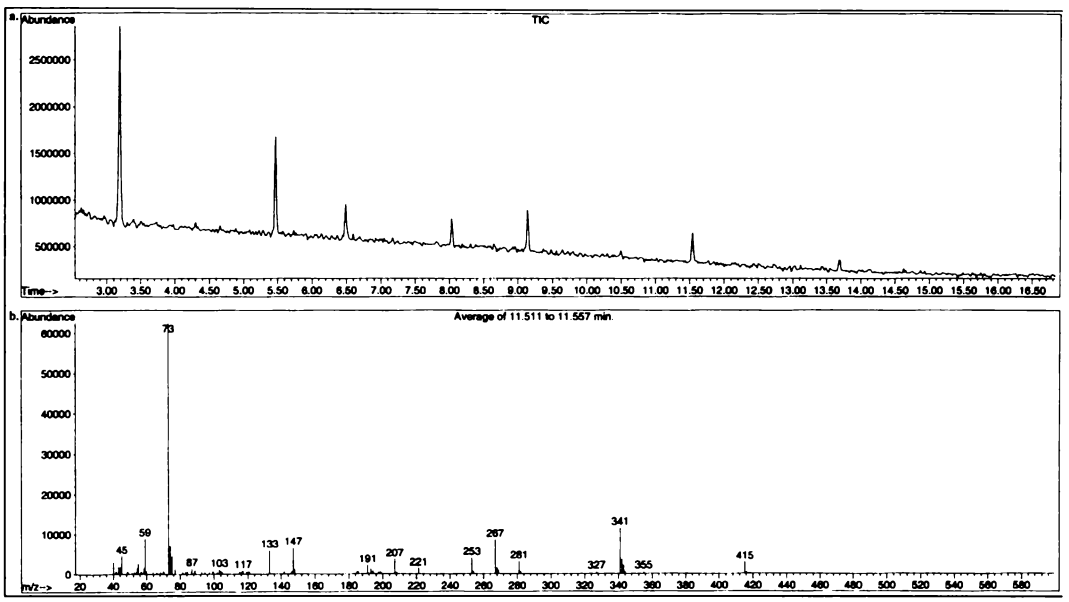

Figure 6.19. ***a.*** **GC/MS chromatogram of acid degraded M_2D^H and** ***b.*** **spectrum of peak at 11.5 minutes**

The peaks of the first series were eluted at 3.2, 5.5 and 8.0 minutes. The first peak showed an EI/MS spectrum consistent with that of M_2D^H. Ions at *m/z* 73, 133, 207 and 221 were observed, corresponding to $[SiCH_3]^+$, $[M_2D^H - OTMS]^+$, $[M_2D^H - CH_3]^+$ and $[M_2D^H - H]^+$, respectively. The largest ion in the spectrum of the second peak was observed at *m/z* 267, corresponding to the dimeric condensation product, $[M_2(D^H)_2 - CH_3]^+$. The expected fragment ions (*m/z* 73, $[SiCH_3]^+$; *m/z* 133, $[M_2(D^H)_2 - MD^H]^+$; *m/z* 193, $[M_2(D^H)_2 - OTMS]^+$) were also observed. The third peak in the series (8 minutes) showed an ion at *m/z* 327 in the EI/MS spectrum. This corresponds to the trimeric condensation product, $[M_2(D^H)_3 - CH_3]^+$. The expected fragment ions showing loss of M and D^H units were also observed (*m/z* 73, $[SiCH_3]^+$; *m/z* 133, $[M_2(D^H)_3 - M(D^H)_2]^+$; *m/z* 193, $[M_2(D^H)_3 - MD^H]^+$; *m/z* 253, $[M_2(D^H)_3 - OTMS]^+$).

The peaks of the second series were eluted at 6.5, 9.1, 11.5 and 13.5 minutes. The spectrum of the 6.5 minute peak showed a fragmentation pattern matching that expected for M_2D^HD. The observed ions at *m/z* 295 and 207 correspond to $[M_2D^HD - H]^+$ and $[M_2D^HD - OTMS]^+$, respectively. The M_2D^HD structure requires a dimethyl substituted D unit in the molecular backbone. Analysis of the M_2D^H starting material (Section 2.3.2.4) indicated the presence of M^HDM, which is a plausible source for this compound. The peak eluting at 9.1 minutes showed a fragmentation pattern indicative of the structure $M_2D^HD_2$. Fragment ions assignable to $[M_2D^HD_2 - CH_3]^+$, $[M_2D^HD_2 - OTMS]^+$, $[M_2D^HD_2 - DM]^+$, $[M_2D^HD_2 - D^HDM]^+$ and $[M_2D^HD_2 - D_2M]^+$ were observed (*m/z* 355, 281, 207, 147, 133). The spectrum of the 11.5 minute peak showed a further increase of 60 mass units for the largest ion (*m/z* 415) corresponding to the structure, $M_2(D^H)_2D_2$ (Figure 6.19.*b*). The fragmentation pattern supports this assignment, with ions observed at *m/z* 415, 341, 267, 207, 147, and 133. These correspond to $[M_2(D^H)_2D_2 - CH_3]^+$, $[M_2(D^H)_2D_2 - OTMS]^+$, $[M_2(D^H)_2D_2 - DM]^+$, $[M_2(D^H)_2D_2 - D^HDM]^+$, $[M_2(D^H)_2D_2 - (D^H)_2DM]^+$, $[M_2(D^H)_2D_2 - D^HD_2M]^+$, respectively. The molecular mass of the final peak observed (13.5 minutes) could not be determined according to the $[parent - CH_3]^+$ ion, due to extensive fragmentation. Ions at *m/z* 341, 327, 253, 207, 147 and 73 were observed, which can be assigned to the fragments $[M(D^H)_2D_2]^+$, $[M(D^H)_3D]^+$, $[MD^HD]^+$, $[MD]^+$, and M^+. The assigned fragment ion structures and structures of the previous compounds eluted in the chromatogram indicate a possible molecular structure of $M_2(D^H)_3D_2$ for the 13.5 minute peak.

The results of this investigation indicate the linear siloxanes are the major products of the acid catalysed degradation of M_2D^H and M^HDM. No cyclic products were observed. The observed products were assigned to M_2D^H, $M_2(D^H)_2$, $M_2(D^H)_3$, M_2D^HD, $M_2D^HD_2$, $M_2(D^H)_2D_2$ and $M_2(D^H)_3D_2$.

6.3.8.2 Acid degradation of Silwet L-77

The strongest peak in the GC/MS chromatogram of the heptane-soluble fraction of acid-degraded Silwet L-77 (Section 6.2.2.4.1) eluted at 6.5 minutes. The highest molecular weight ion in the corresponding EI/MS spectrum was observed at *m/z* 295. This corresponds to the fragment ion structure $[M - (CH_2)_3\text{-}OH]^+$ expected for the cyclic trimer, **27** [R^1, R^2, R^3 = $-(CH_2)_3$-OH]. Other ions in

the spectrum were observed at *m/z* 279, 265, 247, 207, 247, 207, 191, 177, 163, 147, 133, 119, 103, 87, 73, 59 and 45, but were not easily assigned.

Bulky groups tend to promote ring formation, and the observation of the cyclic product in the acid catalysed degradation of Silwet L-77, whilst only linear siloxanes were detected for M_2D^H and M^HDM, is consistent with this general trend.

Further peaks of much lower intensity were observed in the GC/MS chromatogram at 8.6, 11.5, 15.5, 15.6, 18.3, 18.7, 20.7, 21.1, 22.9 and 23.1 minutes, all showing spectra characteristic of siloxane compounds. Due to the limited information obtained from EI/MS spectra, in particular that pertaining to parent molecule structure, no further analysis of the data was conducted.

6.3.8.3 Head space analysis of acid degraded Silwet L-77

In preceding experiments investigating the degradation of Silwet L-77 significantly reduced mass recoveries were observed (Section 6.3.2.6). This was attributed to the formation of volatile compounds. Analysis of the head space over a degrading sample in sealed conditions, was thus conducted in order to confirm the volatilisation of siloxane derivatives.

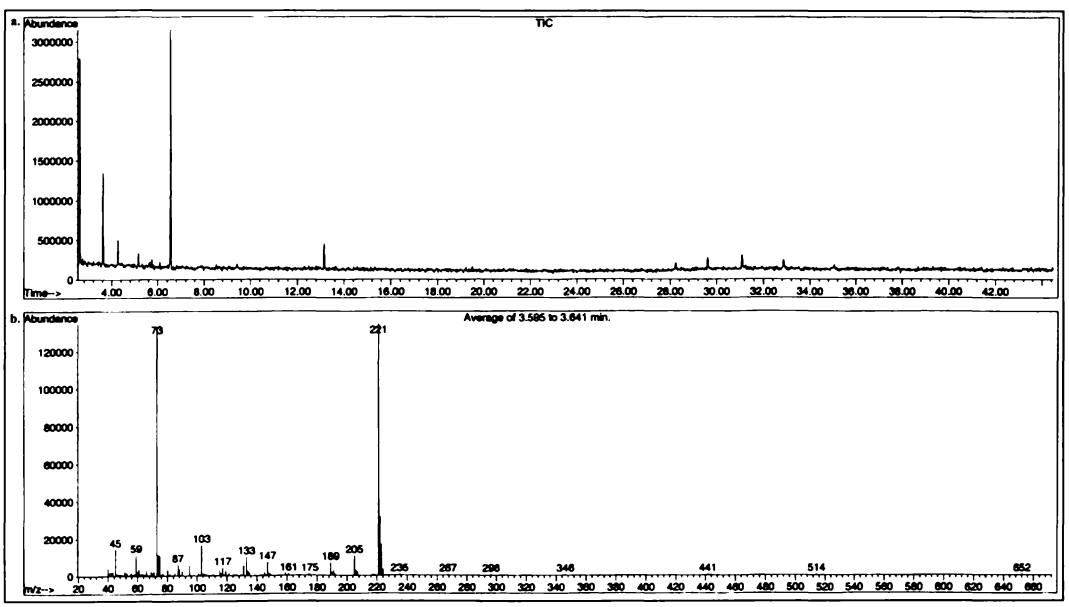

Figure 6.20. ***a.*** **GC/MS chromatogram of head space over acid degrading Silwet L-77 and** ***b.*** **spectrum of peak at 3.6 minutes**

Peaks in the GC/MS chromatogram were observed at 3.6, 5.2, 6.6, 28.2, 29.6, 21.1, 32.9 and 35.0 minutes (Figure 6.20.*a*). The largest ion in the spectrum of

the first peak (3.6 minutes) was at *m/z* 221 (Figure 6.20.*b*). This can be assigned to the fragment $[M_2D^R - R]^+$. This structure is as expected for EI/MS fragmentation, as in general, the larger R substituents on the Si atom are cleaved preferentially.[16] The observation of the $[M_2D^R - R]^+$ fragment ion indicates M_2D^R type volatile compounds are produced in the degradation of Silwet L-77, although little information can be obtained pertaining to the structure of the parent molecule. No further structural information could be deduced from the fragment ions observed (*m/z* 73, 103, 133, 189, 203, 221). The peak at 5.2 minutes showed ions at *m/z* 235, 221, 191, 133, 96 and 73, but no assignments were made. The 6.5 minute spectrum showed fragment ions expected for the structure, M_2DD^H (*m/z* 295, $[M_2DD^H - H]^+$; *m/z* 207, $[M_2DD^H - M]^+$), although this is not a plausible degradation product of Silwet L-77. The spectra of the peaks eluting over 28.2 to 35.0 minutes were characteristic of siloxane compounds, although parent ion structures could not be determined. The fragmentation patterns showed several losses of 60 and 74 mass units, corresponding to D^H and D units, neither of which are contained within the Silwet L-77 structure.

No further interpretation of the data was conducted, due to limited information regarding parent molecule structure. The results did however confirm the formation of volatile siloxane products in the degradation of Silwet L-77, and provided a source for the observed mass loss.

6.3.9 NMR studies on Silwet L-77 degradation

6.3.9.1 ^{1}H NMR of M_2D-C_3-O-$(EO)_n$- Me polar degradation products

The ^{1}H NMR spectrum* of the polar degradation products of purified M_2D-C_3-O-$(EO)_n$-CH_3† showed a reduction in the relative proportions of the Si-methyl resonances in comparison to that observed for Silwet L-77.‡ Integration of the spectrum shows the number of Si-methyl groups to propylene groups is 2:1. Inferences to structure can not be made however as API/MS analysis demonstrated this fraction consisted of several structural series.

---

* ^{1}H spectrum of polar degradation products of purified M_2D-C_3-EO_n-CH_3 ($CDCl_3$): $SiCH_3$, 0.09 ppm (m, 6H); $SiCH_2$, 0.5 ppm (m, 2H); $SiCH_2CH_2$, 1.6 ppm (m, 2H); OCH_3, 3.3 ppm (s, 3H); $SiCH_2CH_2CH_2$, 3.5 ppm (m, 2H); OCH_2CH_2, 3.6 ppm (m, 45H).

† Purified by preparative RP C_{18} HPLC, Section 2.2.1.1

‡ ^{1}H spectrum of Silwet L-77 ($CDCl_3$): $SiCH_3$, 0.1 ppm (br.s, 21H); $SiCH_2$, 0.8 ppm (d.d, 2H); $SiCH_2CH_2$, 1.5 ppm (t.t, 2H); OCH_3, 3.3 ppm (s, 19H); $SiCH_2CH_2CH_2$, 3.5 ppm (t, 2H); OCH_2CH_2, 3.6 ppm (m, 160H).

The EO proton: terminal OCH_3 group ratio indicates an average chain length of n = 10. This is consistent with the ESI/MS results obtained for the fraction (Figure 6.9). *Ion series* assigned to the M-TMS (**21**) and M-2TMS (**22**) structures both showed maximum peak intensities for the n = 10 oligomer (*m/z* 680 and 652, respectively). Other structures identified in the fraction also displayed relatively high EO contents.

6.3.9.2 ^{1}H and ^{13}C NMR of acid degraded Silwet L-77

Acid degraded samples of Silwet L-77 (Section 6.2.2.1) were analysed by ^{1}H and ^{13}C NMR following solvent extraction. The ^{1}H spectra obtained were significantly changed from that of the parent compound. In particular the distribution of the EO content was significantly affected. Integration of the peaks in the Silwet L-77 spectrum showed a ratio of 1:8 TMS: EO protons. In the spectrum of the heptane-soluble fraction, a ratio of 1:0.67 was observed, demonstrating a significant loss in EO chain content for the compounds comprising this fraction. The corresponding H_2O-soluble fraction showed a ratio of 1:16, indicating a significant increase in EO content. The relative integration also showed a decrease in the number of $SiCH_3$ groups relative to the propyl substituents, indicating a loss/reduction in terminal TMS groups through cleavage and/or condensation.

The heptane-soluble fractions gave ^{1}H spectra that matched that expected for a cyclic trimer with all the EO chains cleaved. Signals were observed at δ_H 0.1 (3), 0.8 (2), 1.26 (3), 1.5 (2) and 3.6 (2) ppm, which can be assigned to $SiC\mathbf{H_3}$, $SiC\mathbf{H_2}$, $\mathbf{OH}$, $SiCH_2C\mathbf{H_2}$, and $SiCH_2CH_2C\mathbf{H_2}$, respectively, for the tentative cyclic trimer assignment.

Only four signals (1.9, 23.2, 29.7, 70.6 ppm) were observed in the ^{13}C spectrum of the heptane-soluble fractions in contrast to that of the parent compound.* These were assignable to Si-substituted methyl and propyl groups. These results indicate the major constituent of this fraction is the cyclic trimer with all EO chains cleaved, consistent with the ^{1}H NMR data. The methyl carbon resonance (δ_C 1.9) is lower field than expected for a D Si-substituted methyl, actually showing a resonance more in the vicinity expected for a M Si-substituted

* ^{13}C spectrum of Silwet L-77 ($CDCl_3$): D^{Me}, 0.1 ppm; M^{Me}, 2.3 ppm; $SiCH_2$, 14.1 ppm; $SiCH_2CH_2$, 23.9 ppm; OCH_3, 58.9 ppm; $SiCH_2CH_2CH_2$, OCH_2CH_2, 70.7, 70.9, 71.1, 72.5, 73.9 ppm; $ROCH_2CH_2OH$, 61.7 ppm; $ROCH_2CH_2OH$, 73.4 ppm.

atom. This is consistent with literature observations, where a shift to lower field for the D-substituted methyl groups was reported for the cyclic trimer D_3 as compared to those of the linear M_2D_3 analogue.[17]

The H_2O-soluble fractions showed a similar ^1H spectrum to that of Silwet L-77, with one new signal observed at 4.66 ppm (s, 4H). This is tentatively assigned to the OH functionality. Signals for the methyl capped EO chain were observed at 3.3 ppm (δ_H C**H**$_3$O, s, 4H) and 3.6 ppm (δ_H C**H**$_2$C**H**$_2$O, m, 44H), respectively. The Si-substituted CH_3 and $CH_2CH_2CH_2OR$ groups, were also evident (SiC**H**$_3$: 0.1 ppm, s, 3H; SiC**H**$_2$: 0.5 ppm, d.d, 2H; SiCH$_2$C**H**$_2$: 1.6 ppm, t.t, 2H; SiCH$_2$CH$_2$C**H**$_2$OR: 3.4 ppm (d.d, 2H). The relative integrations show a ratio of one Si-substituted CH_3 to each propyl group. This indicates a loss of terminal TMS groups. The product/s may be present as the silanols, or as condensation products thereof. The new signal observed at 4.66 ppm is thus tentatively assigned to the Si-OH proton, and the structure therefore to M-2TMS, **22**.

The ^{13}C spectrum of the H_2O-soluble fraction showed no peaks corresponding to M^{Me} type carbons, with multiple signals observed around δ_C –0.6 ppm characteristic of D^{Me} resonances. Resonances assignable to the α and β methylene carbons of a propyl group adjacent to an Si atom were observed (Si**C**H$_2$: δ_C 12.8, 13.1; SiCH$_2$**C**H$_2$: δ_C 22.7, 22.9), and the number of peaks observed suggests more than one chain type is present. More than one signal for the terminal methoxy carbon was also observed (δ_C 58.4 and 60.7). The differences in the propyl group resonances as compared with the heptane-soluble fraction suggest that the cleaved chain, –$CH_2CH_2CH_2OH$, is not a significant substituent of the products of this fraction. Multiple resonances (δ_C 69.6, 69.8, 69.9, 70.0, 70.6, 71.4, 72.1, 73.5, 73.7) of relatively high intensity were observed for carbons assignable to the EO carbons and SiCH$_2$CH$_2$**C**H$_2$OR resonances.

6.3.9.3 ^{29}Si NMR studies of acid degraded Silwet L-77

The spectrum of a solution of Silwet L-77* was compared with a sample exposed to acidic conditions (4:1 THF/H_2O, 0.4 M HCl). The acid degraded sample was analysed at 20 minutes, 1 hour, 1 week and 2 years.

---

* ^{29}Si spectrum of Silwet L-77 (THF): M, δ_{Si} 10.39 ppm, 2Si; D, δ_{Si} –17.81 ppm, 1Si; δ_{Si} –90 - – 120 ppm.

The ^{29}Si spectrum of Silwet L-77 after 20 minutes in the acidic conditions was essentially unchanged from that taken in the absence of acid. Two strong signals were observed at δ_{Si} 10.37 and –17.85, assigned to the M and D silicon atoms respectively, The assignment was consistent with the observed ratio of 2:1 and with the expected chemical shifts as defined by the number of neighbouring oxygen atoms. The broad peak at –90 - –130 ppm, assignable to the Si of the glass NMR tube, had doubled in intensity relative to the Silwet L-77 spectrum.

At 1 hour, in addition to the δ_{Si} 10.36 ppm (M^R) and –17.88 (D^R) resonances, several new signals were observed. Signals assignable to M^R Si atoms at δ_{Si} 15.15, 10.49 and 9.94, and a signal at δ_{Si} –10.83, assignable to either M^{OH} or D^R were observed. A signal at δ_{Si} –18.58 assignable to D^R was also observed, and a further increase in the relative intensity of the broad glass Si-OH peak was also observed.

After 1 week, a large number of peaks were observed between –10 and –20 ppm. The signals at δ_{Si} –10.88, –11.78 and –14.91 are assignable to either M^{OH} or D^R resonances. The chemical shifts of -16.02, -17.90, -18.61 and -19.13 are attributable to new D^R Si signals. Strong signals at δ_{Si} 10.46 and 10.33, and a smaller signal at 15.03 ppm can be assigned to M^R Si resonances. The broad glass peak at –80 - –130 ppm had increased further in relative intensity.

After 2 years, the intensity of the peaks was much reduced relative to the glass peak (–90 - –140 ppm, br). No signals assignable to M^R silicon atoms were observed with most of the signals observed at D^R resonances (δ_{Si} –16.53, –19.46, –20.46, –22.21, –24.68, –27.18). Signals at –62.15 and –63.16 ppm were observed, and are resonances characteristic of D^{OH} structures. These results show significant proportions of the terminal M^R groups have been cleaved from the parent molecules and that extensive condensation has occurred. The D^{OH} resonances indicate that linear silanols are contained in the mixture, but the results can not be used to distinguish with confidence between cyclic and linear resonances.

6.3.10 Quantitative API/MS studies on Silwet L-77 degradation

The flow injection API/MS method was used to monitor the degradation of Silwet L-77 over time at pH 5.6 and pH 2.3. The ratio of the Silwet L-77 (M_2D-C_3-O-$(EO)_6$-H) ion relative to the internal standard [$C_6(EO)_3$] ion was monitored

and quantified by comparison with a standard curve. Two variations on the sample preparation method were adopted, the first using a single bulk solution (10 ppm) from which aliquots were removed throughout for analysis (6.2.10.1). In the second method (6.2.10.2), a large number of identical samples were prepared (1000 ppm), and two worked up individually at each analysis interval. Results from parallel HPLC determinations are also presented in Section 6.3.10.2.

6.3.10.1 Bulk solution analysis

The degradation of a bulk solution of Silwet L-77 (10 ppm) under acidic (0.01% HCO_2H, pH 3.2) and aqueous conditions (pH 5.8) is shown in Figure 6.23.

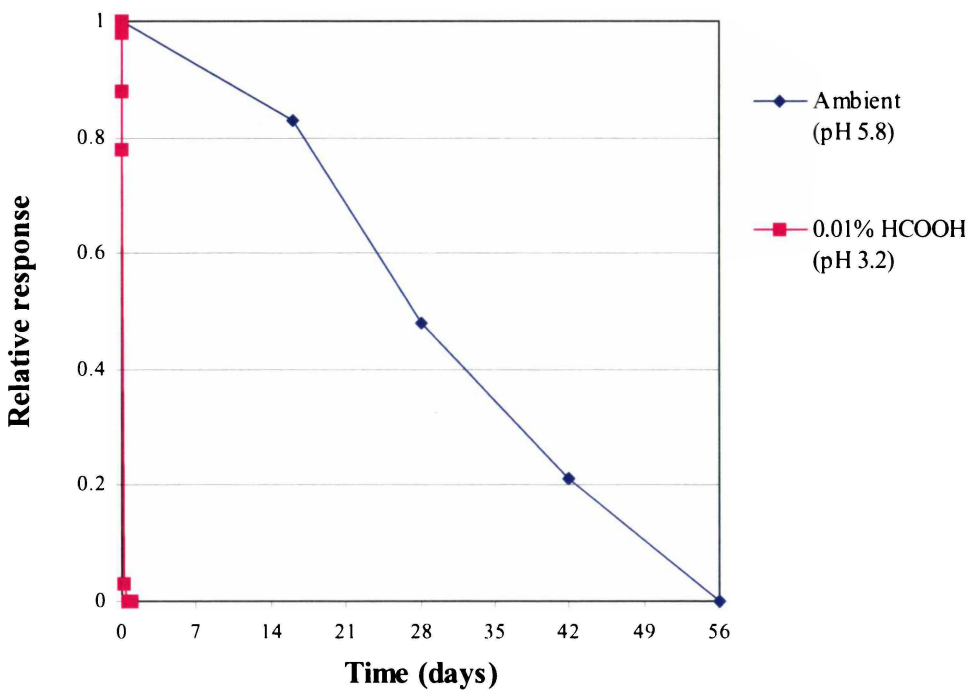

Figure 6.21. Relative response of Silwet L-77 (10 ppm) over time under aqueous and acidic conditions (APcI/MS)

Under the acidic conditions, the Silwet L-77 was completely degraded in 12 hours, with a half-life of ~3 hours. Complete degradation of Silwet L-77 under the aqueous conditions was observed after 56 days at this concentration, such that a half-life of ~28 days was obtained. The rate of degradation was relatively constant over the analysis time period.

6.3.10.2 Multiple sample analysis

The degradation of individual samples of Silwet L-77 (1000 ppm) in aqueous conditions over 28 days, as determined by flow injection APcI/MS and HPLC methods is shown in Figure 6.22.

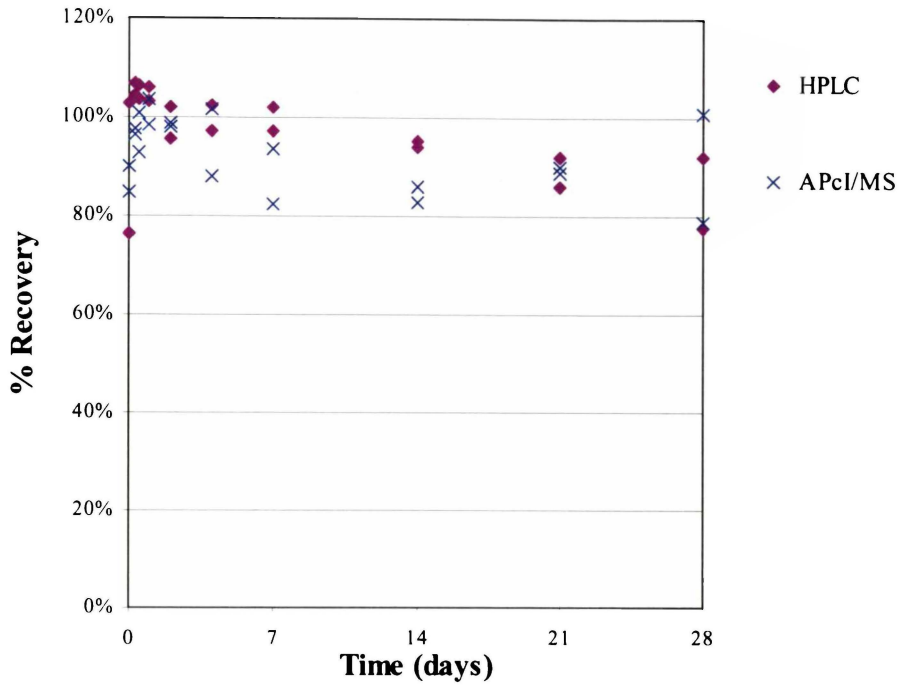

Figure 6.22. Response of Silwet L-77 (1000 ppm) over time in aqueous conditions (APcI/MS and HPLC/LSD)

The recovery of Silwet L-77 (1000 ppm) was greater than 75% over the 28 day analysis period by both methods. In the previous section (6.3.10.1), 28 days was the half-life obtained for Silwet L-77 at 10 ppm, indicating that degradation is more rapid at lower concentrations. By extrapolation, a half-life of ~66 days was obtained, although the margin of error was high due to high variability in the data obtained.

6.3.11 Quantitative HPLC-LSD studies on Silwet L-77 degradation

The degradation of Silwet L-77 over time in aqueous and organic solvents at varying pH values was investigated. The degradation in 90:10 MeOH/H_2O (6.2.9.1) and 100% H_2O (6.2.9.2) was investigated.

6.3.11.1 Degradation in 90:10 MeOH/H_2O

The percentage recoveries of Silwet L-77 solutions (1000 ppm, 90:10 MeOH/H_2O) with varying quantities of formic acid (0%, 0.1%, 1%, 10%) over a 40 day time period are presented in Figure 6.23.

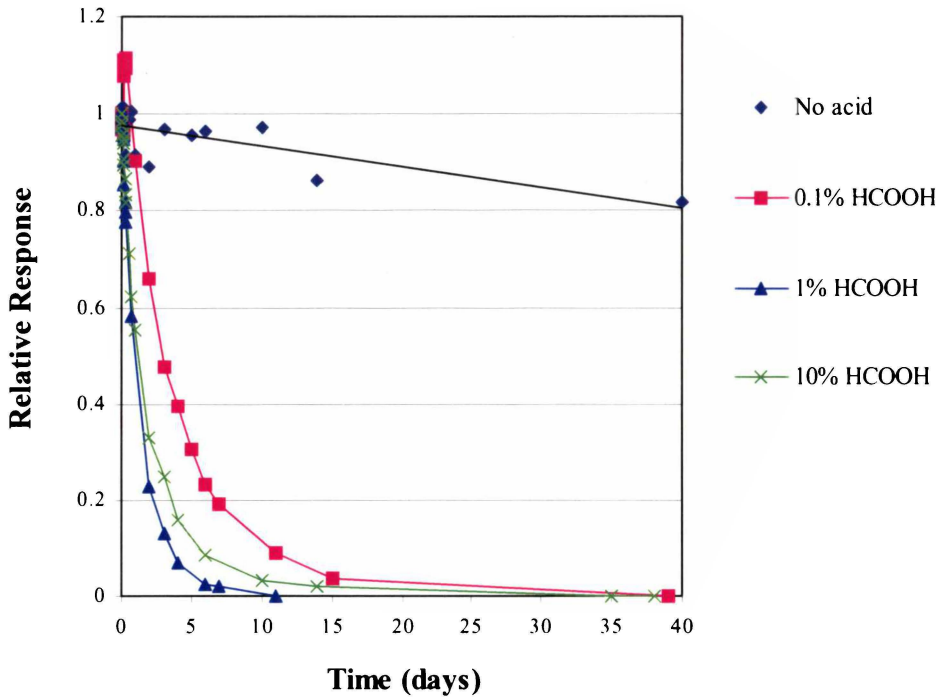

Figure 6.23. Response of Silwet L-77 (1000 ppm) over time (0 – 40 days) in 90% MeOH with varying acid concentrations (HPLC-LSD)*

The sample was relatively stable in the non-acidified organic solvent with >80% recovery at 40 days. A half-life of 110 days was obtained by extrapolation of the least squares fit trendline. The half-life values obtained under the acidic conditions were 3 days for the 0.1% HCO_2H solution, and 1 day for the 1 and 10% acid solutions.

6.3.11.2 Degradation in 100% H_2O

The recoveries of Silwet L-77 solutions (2000 ppm, 100% Milli-Q H_2O) over a 5 day time period in the presence of varying quantities of formic acid (0%, 0.01%, 0.1%, 1%) are presented in Figure 6.24. The degradation in the aqueous system was much more rapid than that observed in the organic/aqueous solvent mixture (6.2.11.1). The half-life value for the non-acidified aqueous conditions was 19

* Quantified by comparison with Silwet L-77 external standard solutions.

days as obtained by extrapolation. The acidic conditions gave half-life values of 2, <1 and <0.5 hours for the 0.01%, 0.1% and 1% HCO_2H solutions, respectively.

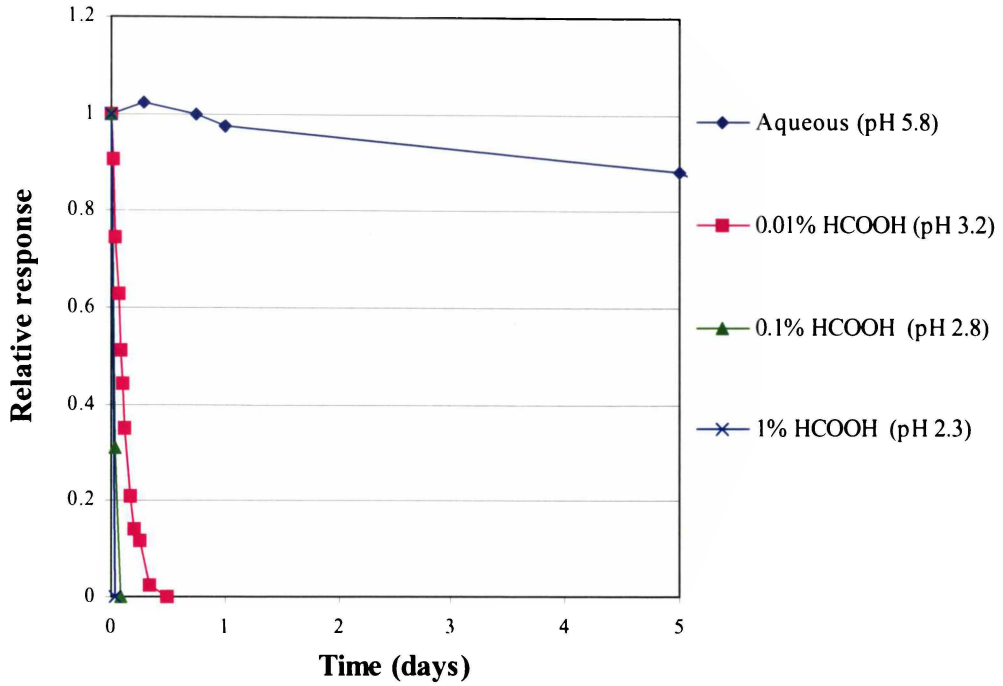

Figure 6.24. Response of Silwet L-77 (2000 ppm) over time (0 – 5 days) under aqueous and acidic conditions (HPLC-LSD)

The differences in the degradation rates for the two solvent systems are demonstrated more clearly in Figure 6.25.

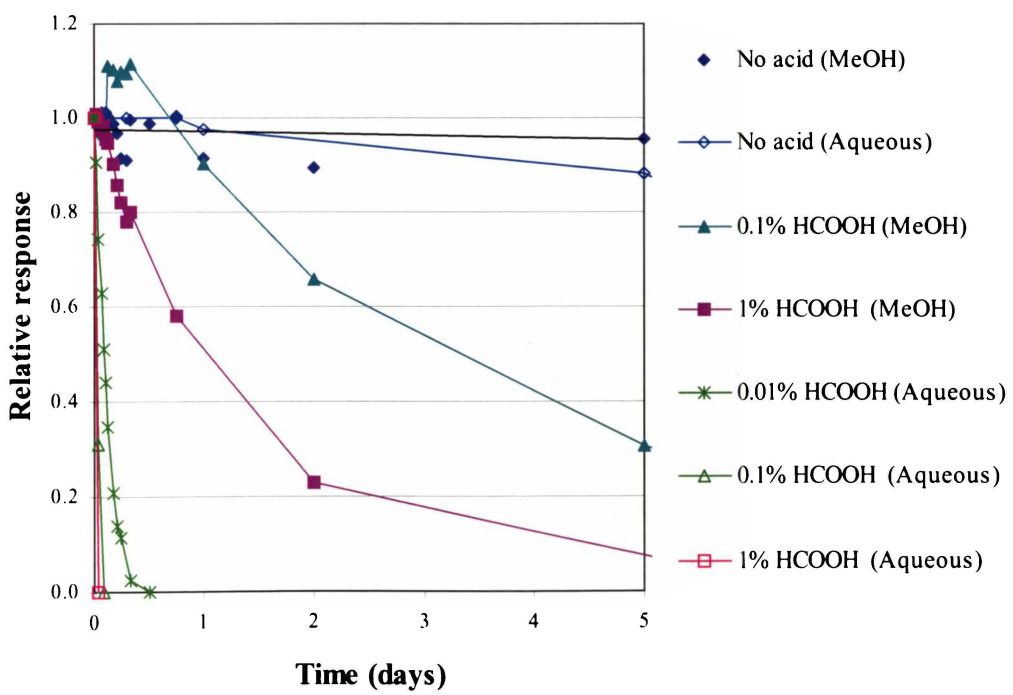

Figure 6.25. Response of Silwet L-77 (2000 ppm) over time (0 – 5 days) in aqueous and organic/aqueous media with varying acid concentrations (HPLC-LSD)

The reduced rate of degradation in the organic solvent is attributed to adverse side reactions with the MeOH solvent. As discussed in Section 6.3.6.1.1, both siloxanes and silanols are capable of reacting with alcohols.[9] Reaction of the siloxane $R_3SiOSiR_3$ with MeOH will yield a silanol (R_3SiOH) and a methylated siloxane (CH_3OSiR_3). Further reaction of the silanol R_3SiOH with MeOH can also occur to yield the methylated siloxane R_3SiOCH_3 and a molecule of H_2O.

The results obtained in Section 6.3.6.1.1 showed that in the presence of MeOH few of the potential degradation products were produced. It was suggested that the R_3SiOCH_3 species may not be as reactive as the corresponding R_3SiOH species, thus inhibiting further reactions. This would account for the results obtained here, as the non-specific HPLC method used would be unable to discriminate between Silwet L-77 and the R_3SiOCH_3 under the conditions adopted.

6.4 CONCLUSION

The range of products formed in the degradation of Silwet L-77 were numerous as a result of the ability of the siloxane moiety to rearrange into a variety of lengths and structures, and compounded by the large number of components comprising the Silwet L-77 product. Unequivocal assignment of degradation product structure was thus complicated. Several commonly occurring *ion series* were observed in preliminary investigations (Section 6.3.2) using a variety of degradation conditions. The possible assignments for these *ion series* were described (Table 6.2). Mass recovery was reduced in all experiments indicating the loss of volatile siloxane compounds (6.3.2.6), as confirmed by a headspace analysis (6.3.8.3). An increase in overall water-solubility was also observed. Rates and products appeared to be dependent on the conditions used, especially pH and time.

The use of FTICR/MS high resolution data enabled the tentative assignment of four major *ion series* in the water-soluble fraction (Table 6.7). These were $CH_3O(EO)_nH$ (**20**), M-TMS (**21**), cyclic tetramer [**28**; R^1, R^2, R^3, $R^4 = (CH_2)_3$-O-$(EO)_n$-CH_3] and linear dimer [**24**; R^1, R^2 = TMS; R^3, R^4 = $(EO)_n$-CH_3]. Assignment of the heptane-soluble fraction was significantly more complicated with 20 assignable *ion series* obtained (Table 6.8 and 6.9).

Analysis of the degradation of purified $M_2D\text{-}C_3\text{-}O\text{-}(EO)_n\text{-}Me$ (ave. n ~ 7.5) samples (6.3.5) by ESI/MS, FTICR/MS and HPLC/ESI/MS indicated $CH_3O(EO)_nH$ (**20**), M-TMS (**21**) and M-2TMS (**22**) as common degradation products. The linear dimer **24**, [R^1 = H, R^2 = TMS; R^3, R^4 = $(EO)_n\text{-}CH_3$] was also indicated. The results also demonstrated that the $HO(EO)_nH$, $M_2D\text{-}C_3\text{-}O\text{-}(EO)_n\text{-}H$ (**2**) and $(M^R)_2D\text{-}O\text{-}(EO)_n\text{-}CH_2CH{=}CH_2$ (**9**, **10**, **11**; R = H or CH_3) compounds observed in the Silwet L-77 degradation mixture were synthetic by-products rather that real degradation products.

The degradation of single $M_2D\text{-}C_3\text{-}O\text{-}(EO)_n\text{-}R$ oligomers (6.3.6) confirmed the $CH_3O(EO)_nH$ (**20**), M-TMS (**21**) and M-2TMS (**22**) assignments, and also indicated a range of linear and cyclic products both with and without the EO chains and terminal TMS groups intact. In general, the more silylated analogues of a structural series partitioned preferentially into the heptane-soluble fraction, and higher EO content derivatives were more commonly observed in the water-soluble fraction. Typically the products formed followed that for expected silanol stabilities, with longer EO chain products more stable as low condensation polymers and silanols, and short EO chains more commonly observed in cyclic products.

GC/MS analysis of the degradation of M_2D^H and M^HDM showed linear siloxane products equating to linear dimers, trimers, tetramers and pentamers (i.e. $M_2(D^R)_n$, n = 2, 3, 4, 5), had been formed. The GC/MS analysis of the heptane-soluble fraction of acid-degraded Silwet L-77 enabled the tentative assignment of the cyclic trimer, **27** [R^1, R^2, R^3 = $-(CH_2)_3\text{-}OH$] product. ^1H and ^{13}C NMR data also indicated this structure. ^1H NMR of the water-soluble fraction showed proton integration values indicative of the M-2TMS (**22**) structure. After 2 years, the terminal M^R groups were no longer detectable and extensive condensation had occurred, as determined by ^{29}Si NMR.

Quantitative studies gave variable results, with half-life values of 19, 28 and 66 days obtained for the aqueous system, depending on the conditions employed. Degradation in acidic media was significantly higher and half-life values was decreased to a matter of hours.

The results of this study demonstrate the rapid degradation of Silwet L-77 and derivatives thereof under extremes of pH. The results demonstrate the highly complex nature of the products formed, although several of the products have

been identified and assigned. API/MS was a valid and informative method for the study of the products formed, especially the high resolution FTICR/MS technique. The use of additional techniques such as HPLC/API/MS, GC/MS and NMR all provided useful confirmatory and complementary information.

6.5 REFERENCES

[1] D. Coupland, J.A. Zabkiewicz, F.J. Ede, *Ann. Appl. Biol.*, 1989, **115**, 147-156

[2] P.J.G. Stevens, *NZ FRI Bulletin No. 193, Proc. 4th Int. Symp. on Adjuvants for Agrochemicals*, Ed. R.E. Gaskin, Melbourne, 1995, 345-349

[3] M. Knoche, H. Tamura, M.J. Bukovac, *J. Agric. Food Chem.*, 1991, **39**, 202-206

[4] M. Knoche, *Weed Res.*, 1994, **34**, 221-39

[5] K.D. Klein, S. Wilkowski, J. Selby, *Proc. 4th Int. Symp. Adj. for Agrochem.*, 1995, FRI Bulletin No. 193, 27-31

[6] T.C. Kendrick, B. Parbhoo, J.W. White, *The Silicon – Heteroatom Bond*, Eds. S. Patai, Z. Rappoport, John Wiley and Sons Ltd, 1991, Chapter 3, 67-150

[7] A. Ballistreri, D. Garozzo, G. Montaudo, *Macromol.*, 1984, **17**, 1312-1315

[8] J.C. Kleinert, C.J. Weschler, *Anal. Chem.*, 1980, **52**, 1245-1248

[9] M. G. Voronkov, V. P. Mileshkevich, and Yu. A. Yuzhelevskii, *The Siloxane Bond – Physical Properties and Chemical Transformations*, Consultants Bureau, New York, 1978

[10] G.A. Policello, P.J. Stevens, W.A. Forster, G.J. Murphy, *Pesticide Formulations and Application Systems*, Eds. F.R. Hall, P.D. Berger, H.M. Collins, ASTM publishers, 1995, Vol. 14, p 313-317

[11] Personal correspondence, George Policello, 8/11/99, Witco Corporation, Organosilicones Group, Tarrytown, NY

[12] *a.* S. Xu, *Environ. Sci. Technol.*, 1998, **32**, 3162-3168; *b.* R.R. Buch, D.N. Ingebrigtson, *Environ. Sci. Technol.*, 1979, **13**, 676-679

[13] *a.* R. G. Lehmann, J. R. Miller, *Environ. Toxicol. Chem.*, 1996, **15**, 1455-1460; *b.* R. G. Lehmann, S. Varaprath, C.L. Frye, *Environ. Toxicol. Chem.*, 1994, **13**, 1753-1759; *c.* C. Stevens, *J. Inorg. Biochem.*, 1998, **69**, 203-207

[14] R.G. Lehmann, J.R. Miller, S. Xu, U.B. Singh, C.F. Reece, *Environ. Sci. Technol.*, 1998, **32**, 1260-1264

[15] I. Kohlheim, D. Lange, H. Kelling, *Organosilicon Chemistry II: From Molecules to Materials*, Eds. N. Auner, J. Weis, VCH, 1996, 215-218

[16] J.A. Moore, *The Analytical Chemistry of Silicones*, Ed. A. Lee Smith, John Wiley and Sons Ltd, 1991, Chapter 12, 421-470

[17] G. Engelhardt, H. Jancke, M. Magi, T. Pehk, E. Lippmaa, *J. Organometal. Chem.*, 1971, **28**, 293-300

CHAPTER 7

Environmental Aspects of Silwet L-77 Degradation

7.1 INTRODUCTION

7.1.1 Surfactants in the environment

Various investigations have been conducted on the interaction of surfactants with soils,[1a-h] soil components,[2] clays,[3] and sediments,[4a-d] and on their behaviour in aqueous environments.[5a-i] The biodegradation of surfactants has also been the subject of extensive research, and is discussed in a comprehensive review by Swisher.[6] API/MS methods have been successfully applied to the qualitative and quantitative analysis of surfactants in the environment, both on sediments[7,8] and in aqueous samples.[9a-h] ESI/MS has also been used to investigate photocatalytic degradation of secondary alcohol ethoxylates[10,11] and biodegradation mechanisms of secondary alcohol[12] and nonylphenol ethoxylate surfactants.[13]

The effect of surfactants on the degradation of other compounds has also been investigated. Surfactants are often used in bioremediation systems to enhance the bioavailability and microbial degradation of contaminants. However both enhancements and inhibitions of the biodegradation of organic compounds in the presence of surfactants have been reported. Surfactants can act by enhancing adsorption of compounds and microorganisms to substrates, or by aiding solubilisation of sorbed contaminants. These contrasting properties can be interpreted as positive or negative, depending upon the conditions in which they are applied/observed.

Solubilisation of sorbed contaminants is a useful property in instances where the degradation of contaminants is limited by their exposure to degrading conditions. The degradation of agrochemicals in the presence of surfactants has been investigated, where the enhancement was a result of increased solubilisation of the contaminant.[14a-c] This technique can also potentially be applied to restoration of contaminated soils through leaching in controlled environments. A potentially negative aspect of surfactants in the environment may arise from the ability of surfactants to mobilise toxic compounds adsorbed to the soil.[5f,15]

Enhancing adsorption of compounds to substrates may also increase degradation[16] and also provides a potential method for clean up and recovery of contaminants in leachates. Passing wastewater through filters containing

surfactants has been shown to be a highly efficient method for separation and recovery of hydrophilic degradation-resistant polymeric substances, e.g. humic acid removal.[17]

7.1.2 Environmental toxicology of surfactants

Until recently, surfactants have been considered relatively environmentally benign and as result, have not been subjected to the restrictions and regulations imposed on other environmental xenobiotics such as pesticides and herbicides. The revelation that surfactants induce ecotoxicological effects on a wide range of aquatic and terrestrial organisms[18] indicates that a change to the current procedures is required.

The widely used alkylphenol surfactants are now well known to exhibit detrimental effects in the environment including acute toxicity to aquatic organisms and bioaccumulation.[19] Alkylphenol ethoxylates and related compounds exhibit estrogenic properties* and furthermore the toxicity of the degradation products is known to be higher than that of the parent compounds. Toxicity to aquatic organisms has also been described for alcohol ethoxylate surfactants.[20] It has thus become clear that a better understanding of the products and rates of surfactant degradation in the environment is required.

A significant amount of research has addressed the behaviour and toxicological effects of surfactants in the aquatic environment, stemming from the widespread occurrence in domestic and commercial wastewaters.[5] Surfactants also often reach the terrestrial environment through application of agrochemical formulations and sewage sludge-amended soil.[1,4] The behaviour and fate of surfactants in soil has also been reviewed comprehensively by Kuhnt.[15]

Most organic surfactants exhibit poor anaerobic degradability and furthermore their biodegradability can be inhibited by sorption, where their relatively high sorption affinities can lead to considerable accumulation in the environment. In general, the most significant effect of surfactants on soil systems is the influence on surface activity. The amphoteric nature of surfactant molecules results in alterations to soil physics, chemistry and biology,[15] and thus rapid primary degradation of surfactants is highly desirable. Primary degradation of surfactants is defined as structural modification that results in the loss of the surface

* Mimic the effects of estradiol both *in vitro* and *in vivo*

activity.[19] The resulting degradation products may however also exhibit ecotoxicity, as in the case of the alkylphenol ethoxylates, and thus ultimate degradation is ideal for any chemical contaminant. Ultimate degradability is the conversion of the primary degradation products to compounds ubiquitous to the environment, such as CO_2 and H_2O.[19]

The presence of surfactants in soil water lowers surface tension thereby enhancing water mobility. This changes the distribution of water and air between and within soil pores and can thus lead to difficulties in reaeration of the soil and a lowering of the redox potential for longer periods. Surfactants can lead to reduced percolation or accelerated drying, depending on the soil composition and nature of the surfactant. This can lead to higher run-off rates and accelerated soil erosion.[15]

The surface character of the soil, i.e. sorption capacity, can also change due to surfactant sorption. A change in sorption capacity can effect the mobility of toxins, agrochemical active ingredients and nutrients. Increased mobility of toxins can lead to higher rates of leaching, plant uptake and volatilisation, or can stimulate their biodegradation. Surfactants alter the permeability of membranes and thus can adversely affect many *in vivo* processes in soil/aquatic micro- and macro- organisms. Both positive and negative effects on plant growth and soil productivity have been described. The fate and toxicity of surfactants in soil has been especially attributed to the effect on sorption processes. Degradation of surfactants can be enhanced or inhibited by sorption, although strong adsorption has been observed to inhibit microbial degradation.[15]

7.1.3 Trisiloxane surfactants in the environment

In Chapter 6, the rapid degradation of Silwet L-77 under abiotic hydrolytic conditions was demonstrated. As discussed in Section 7.1.2, many of the adverse effects of surfactants are a result of the surface-active nature of the molecules. The high instability of the Silwet L-77 molecule would thus be favourable in terms of environmental impact, as the rapid loss of the surface activity would reduce any subsequent ecotoxicological effects.

The amount of information available on the behaviour of trisiloxane surfactants in environmental media is limited, with the only reports to date using surface tension, spreading ability and ^{14}C-labelling methods to monitor their fate.[21*a-c*] However the non-specificity of these methods limits the quality of the information

obtained regarding the fate of surfactants in these environments. Changes in surface tension and spreading ability may not be an appropriate test for the determination of surfactant degradation, as these methods do not account for the influence of the degradation products on these properties. The ^{14}C-labelling method is also non-specific and fails to discriminate between the parent molecule and degradation products thereof.

An investigation into the behaviour of the trisiloxane surfactant, M_2D-C_3-EO_7-$COCH_3$ (Sylgard 309) on five soil substrates showed low mobility of the surfactant, as determined by radiolabelling methods in conjunction with adsorption/desorption isotherms and TLC methods.[21b] The results indicated both clay and organic matter content influence adsorptive behaviour. This work was further extended to soil columns, where ^{14}C-labelled compounds was used to determine the distribution of the surfactant in the gas, liquid and solid phases of the system.[21c] Over the time period investigated (>10 weeks), more than 50% of the radiolabel was recovered in the leachate. This was interpreted as indicating a relatively high mobility of the surfactant, in contrast to the results obtained previously. Due to the differences in the time scales, it is suggested here that it is not appropriate to compare the results of the two experiments in terms of parent molecule mobility. Although not interpreted in this manner by the authors, it seems logical that the initial experiments (24 hour duration) were a closer determination of the behaviour of the parent molecule. The experiments conducted on the soil columns over the longer time period, probably more accurately reflect the behaviour of the degradation products. Indeed, the authors noted that the mass recovery of THF-soluble fractions from the aqueous leachates was significantly less than that obtainable for the parent molecule, indicating the formation of more polar water-soluble molecules. This is consistent with the properties of Silwet L-77 degradation products – observed to be more water-soluble than the surfactant parent molecule (Section 6.3.1.6).

The behaviour of Silwet L-77 on a silt loam and silty clay loam soil has been investigated, with surface tension and spreading ability used as the indicators of degradation/recovery.[21a] The results obtained showed that the 'inactivation' of Silwet L-77 under these soil conditions far exceeded any likely input by agricultural practices. Increased degradation was observed at more extreme pH values – both on substrates and in aqueous media. Adsorption to the soil

particulate was considered to have contributed significantly to the effective removal of Silwet L-77 from solution in both slurry and soil column determinations.

The results presented in Chapter 6 demonstrated that cleavage of the siloxane head group and PEG chain is a common and rapid degradation mechanism of Silwet L-77. In general the negative aspects of surfactants in the environment have been attributed to their ability to affect soil physics, chemistry and biology especially through alterations to sorption processes.[15] The rapid degradation of Silwet L-77 to constituents not possessing surface activity indicates - assuming the constituents themselves are not toxic - that Silwet L-77 will be relatively environmentally benign as compared with other surfactants.

It follows that the environmental fate of Silwet L-77 may thus be as for the siloxane and PEG constituents. Studies have been made on the environmental occurrence of siloxanes,[22,23] and in particular on their degradation on soils[24a-i] and clay minerals.[25,26] The acceleration of siloxane hydrolysis in the presence of acid clays has been reported.[27] The low water solubility of PDMS fluids means that conventional methods for determining biodegradability do not apply. In aqueous conditions degradation is limited, and as a result PDMS may be perceived as not biodegradable.[23] However, the use of ^{14}C-methyl PDMS to qualitatively and quantitatively follow the environmental degradation of these compounds has been reported. Abiotic reaction on contact with solid substrates initiates the depolymerisation, the major product of which is thought to be the monomeric diol (DMSD).[22,23,24a,f,g,26] This product is then thought to be oxidised by photolytic demethylation in water, microbially in soil, and by sunlight-induced hydroxyl radicals in the atmosphere (following volatilisation). The results indicate that the ultimate degradation products are $CO_{2(g)}$ and $Si(OH)_4$. Both are inherent to the natural environment, the latter of which should precipitate to form soil minerals. The degradation is inversely dependent on water content, i.e. is inhibited by high moisture levels, and soil type and composition also plays an important role.[24b,c,25,26]

The biodegradation of PEG compounds has been extensively investigated.[28a-d] The ability of PEG compounds to non-covalently bind to a range of substrates, including mica,[29] silica,[30] montmorillonite[31] and sediments,[32] is also well known. Complexes involving covalently bound PEGs have also been the subject of some

research,[33] with both covalent and non-covalent complexes of potential use in catalytic applications.

Some toxicological data for Silwet L-77 have been reported, with tests for the toxicity to earthworms yielding a LC_{50} of >4700 mg/kg and a zero mortality level of 2800 mg/kg.[21a] Toxicity toward *Daphnia*.sp has also been reported for an undisclosed silicone polyether, although no further details were given.[34]

There have been some reports in the literature pertaining to Silwet L-77 phytotoxicity. The results of three methods comparing the toxicity of several surfactants, including Silwet L-77 have been presented.[35] For all methods used, a higher phytotoxicity was observed for the less water-soluble surfactants within each structural type (Silwet L-7607 < Silwet L-77, Agral-90 < Triton X-45). Potential phytotoxicity was investigated using the *in vitro* betacyanin pigment efflux method.* The ranking obtained in order of increasing toxicity was: Silwet L-7607 < Silwet L-77 < Agral-90 < Triton X-45 < Hyspray (tallow amine ethoxylate surfactant). The evolution of ethylene gas, an *in vivo* measure of plant stress, also demonstrated this trend.

The leakage of ions from excised leaves immersed in surfactant solutions has also been used as a measure of phytotoxicity. In general, more ion leakage was observed in the presence of the organosilicones as compared with the conventional surfactants. The validity of the ion efflux method has been questioned however, as leakage is likely to be a function of infiltration – predicted to be higher for the lower surface tension surfactants, such as Silwet L-77 – and may not be an accurate representation of the situation in foliar-applied systems.[36,37] Indeed, leaf necrosis is rarely reported for Silwet L-77 formulations, and this is attributed to the high spreading which acts as a dilution factor.

7.1.4 Chapter objectives

The mechanisms and products of Silwet L-77 degradation under aqueous, acidic, and alkaline conditions have been described in the preceding chapter. The objective of the research described in this chapter was to examine the degradation in a number of other chemical environments. Recovery in the presence of various substrates inherently present in natural systems was investigated. This was hoped to provide information pertaining to the behaviour of Silwet L-77 in the

* Measures the leakage of pigment from beetroot tissue immersed in surfactant solutions

environment. API/MS, HPLC-LSD and HPLC/MS methods were employed to aid in these determinations. Recovery of Silwet L-77 in the presence of clay minerals was investigated to determine the effect of high surface-areas, surface charges and sorptive properties. The effect of TiO_2 on Silwet L-77 recovery was also investigated as TiO_2 is often used in photocatalytic degradation of surfactants.[38a-j] In these experiments the effect of the substrate was investigated in the absence of irradiation with light.

Preliminary studies involved monitoring the response of Silwet L-77 and its degradation products over time in the presence of several substrates by APcI/MS (Section 7.3.2.1). The substrates investigated include sand, pumice, FeO(OH) (goethite),* Fe_2O_3 (hematite),† halloysite,‡ TiO_2 (anatase),§ $Al(OH)_3$, talc**, and $CaCO_3$ (calcite).†† Further APcI/MS studies investigated the recovery of Silwet L-77 in the presence of halloysite, kaolinite,‡‡ and illite clays (Section 7.3.2.2).§§ HPLC-LSD and HPLC/APcI/MS were also used to determine recoveries from sand, halloysite, kaolinite, montmorillonite*** and Te Kowhai soil (Section

---

* Goethite, α-FeO(OH), is the most common iron oxide mineral,[40] and has an hcp structure.[41]

† Hematite, α-Fe_2O_3, is slightly less common than goethite and is also of hcp structure. Hematite and goethite usually occur together in the environment and are stable in normal soil conditions. Both are stable in an oxidising environment, but unstable under reducing conditions.[40]

‡ Halloysite, $Al_2Si_2O_5(OH)_4.2H_2O$, is a 1:1 layer clay where the 1:1 layers are separated by a layer of H_2O molecules, with a c-spacing of 10.1 Å. It forms early in the weathering process and is usually found in soils formed from volcanic deposits, particularly volcanic ash and glass. Halloysite often occurs as tubular or spheroidal particles whereas most clay silicates (including the structural analogue kaolinite) occur as thin plates.[40]

§ Anatase is the less common polymorph of TiO_2, and is generally considered a secondary mineral. Four edges of the octahedra are shared with adjacent octahedra (c.f. 2 and 3 in rutile and brookite polymorphs), causing a variation in the Ti-O bond lengths. It is a ccp form of TiO_2 and is poorly crystalline.[41]

** Talc, $(Mg_3(OH)_2Si_4O_{10})$, occurs rarely in soils. It is formed from low-grade metamorphic rocks and consists of stacked 2:1 dioctahedral layers.[40] It has no structural charge.[41]

†† Calcite is one of the most common $CaCO_3$ mineral forms and occurs in a wide variety of soils.[40]

‡‡ Kaolinite, $Al_2Si_2O_5(OH)_4$, is a 1:1 dioctahedral layer aluminium-silicate, and differs from halloysite only in the absence of the inter-layer water molecules. There is no overall structural charge, the layers being held together by hydrogen-bonding between OH^- and O^{2-} ions of adjacent layers.[39] Non-specific van der Waals interactions also contribute to the strong interlayer attraction and consequently the clay does not swell in water.[48] Under certain conditions, i.e. with the use of a highly polar proton-accepting liquid either in conjuction with or to pre-expand the clay, some intercalation of organic compounds has been observed. It has a c-axis spacing of 7 Å, low specific surface area (80-150 m^2/g) and low cation exchange capacity (10-40 cmoles/kg).[39]

§§ Illite, $Si_{3.34}Al_{1.95}Fe_{0.6}Mg_{0.18}Ti_{0.04}O_{10}(OH)_2.K_{0.61}Na_{0.02}Ca_{0.01}$, is a clay sized hydrous mica, with less K^+ and more structural water molecules than other mica. It is a 2:1 layered clay with an overall negative charge compensated by interlayer cations.[47] The interlayer cations (K^+) are fixed between the layers preventing swelling. It has a c-axis spacing of 10 Å, low specific surface area (5-20 m^2/g) and low cation exchange capacity (1-15 cmoles/kg).[39]

*** Montmorillonite is a 2:1 layer dioctahedral smectite clay, of the formula $Si_4Al_{1.5}Mg_{0.5}O_{10}(OH)_2Ca_{0.25}$.[39] It is an expanding mineral with an overall negative charge.[47] It has a large surface area (760 m^2/g), c-axis spacing of 9.5 Å (swelling up to 22.5 Å) and high cation exchange capacity (7-15 me/kg).

7.3.2.3).* The recovery of Silwet L-77 in the presence of talc, silica, alumina and sand was also investigated (HPLC-LSD, Section 7.3.2.4).

In the presence of a solid substrate a change in response of an analyte can be attributed to either recovery losses or actual degradation. It is possible that recovery losses in the presence of clay minerals may be more pronounced due to the high surface-areas inherent to the layered structures of clay minerals. The stability of analytes may also be affected by surface charges often carried by clay minerals, a result of isomorphous replacement (usually during formation) of ions in the clay sheets.[39,40,41]

In this chapter, rates for recovery loss of Silwet L-77 in a range of conditions were evaluated (Section 7.3.4), and are discussed with respect to observed pH values for the media investigated (Section 7.3.1). The effect of varying equilibration and extraction conditions, moisture content and concentration was also investigated (Section 7.3.3). Information regarding the products formed following exposure of Silwet L-77 to substrates is presented for both the substrate and supernatant (Section 7.3.5). The results of toxicity tests for Silwet L-77 and degradation products thereof on a range of organisms are also presented (Section 7.3.6.1). Phytotoxicity of Silwet L-77 and the degradation products thereof was not extensively investigated in this work, however the effect of M_2D-C_3-EO_n-CH_3 formulations *in vivo* on foliar systems was visibly determined, and dosage effects with respect to potential phytotoxicity are briefly discussed (Section 7.3.6.2).

7.2 MATERIALS AND METHODS

Materials

C_6EO_3 and Triton X-45 were used as the internal standard solutions (10 ppm) for flow injection APcI/MS and HPLC/APcI/MS, respectively. The same solution was used throughout each experiment, and stored at - 15°C when not in use.

The kaolinite* and illite† samples used were clay mineral standards obtained from Ward's Natural Science Est. Inc. NY. The montmorillonite was XRD

* Weighted average mineral content of Te Kowhai soil control sections: *a.* Sand: Quartz, 5%; Feldspar, 12%; Volcanic Glass, 72%; Cristobalite, 10%; Total heavy minerals, 0.9%; *b.* Heavy Minerals: Total heavy minerals, 0.9%; Mica, 5%; Hornblende, 28%; Augite, 5%; Hypersthene, 25%; Total opaque minerals (i.e. magnetite + ilemite), 32%; *c.* Clay: Halloysite, 47%; Volcanic Glass, 49%; Cristobalite, 3%; *d.* Soil solution Si 17.8 g m^{-3}.[49]; Total Organic Content: low (2 - 4%)

standard Wyoming sodium montmorillonite and the halloysite used was obtained from NZ China Clay.[‡] The Fe_2O_3 was a laboratory chemical obtained from AJAX Chemicals[§] and the TiO_2 was obtained from Merck.[**] The $Al(OH)_3$[††], $CaCO_3$[‡‡] and talc[§§] used were obtained from BDH Chemicals Ltd and the acid-washed sand from M&B Chemicals. The goethite used was a synthesised sample.[42***]

X-ray diffraction was used to determine the morphology of the substrates used where necessary. The Fe_2O_3 was determined to be α-Fe_2O_3 (hematite), the TiO_2 anatase, the $Al(OH)_3$ synthetic aluminium hydroxide, and the $CaCO_3$ calcite.

Substrate preparation

The inorganic substrates (50 g), excluding the montmorillonite, illite and kaolinite samples, were washed with three volumes of H_2O and MeOH (50 mL each). Gravity filtration was sufficient for washing of the coarser sand, pumice, silica, alumina, $Al(OH)_3$, and $CaCO_3$. However the fine powdered Fe_2O_3, goethite, TiO_2, talc, and halloysite required centrifuging, with decantation of the supernatant of each wash. The substrates were then allowed to dry overnight at 60 °C, and (excluding the sand, pumice, silica, alumina and $Al(OH)_3$) were reground by pestle and mortar once dry. The kaolinite and illite samples were grated through a 0.75 micron mesh sieve prior to use, and the Te Kowhai soil particle size was < 2 mm. The montmorillonite was used as obtained.

Treatments and extractions

The inorganic substrates were weighed out as 100 mg sub-samples in glass vials. At t_{zero} 1 mL of freshly prepared Silwet L-77 at a concentration of 1000 ppm was added to each 100 mg sample (1000 $\mu g\ mL^{-1}$, 10 000 $\mu g\ g^{-1}$). All samples were left standing at room temperature for the analysis period. At the selected time intervals, 1 mL of MeOH was added to the treated sample to yield a

---

* Collected from No.5, Lamar Pit, Bath, South Carolina
† Collected from No. 35, Fithian, Illinois
‡ Standard product A, 05/07/93, Batch EP 112693
§ ~81% Fe_2O_3, Batch No. 61068409
** LR grade, Art. 808, 828K03703708
†† LR grade, Dry, 62-67%
‡‡ LR grade, for chromatographic adsorption, Prod. No. 15008, Batch No. 1407990
§§ Fine powder purified by acids, Prod. No. 33124, Batch No. 1771050
*** 8/3/94 synthesised, $N_{2(g)}$ stored

500 ppm solution (1:1 H_2O:MeOH)[43*] which was centrifuged twice to remove all solid substrate. A 100 µL aliquot of the supernatant was taken and diluted with 4.9 mL of 1:1 H_2O:MeOH (1 in 50 dilution) to give a final concentration of 10 ppm for 100% recovery. Where possible these solutions were analysed immediately, or were stored in a freezer (-15 °C) until analysis. The surfactant solution was mixed (1:1 v/v) with the internal standard solution immediately prior to APcI/MS analysis.

Standardisation

Standard solutions of Silwet L-77 were prepared by dilution of a 1000 ppm (0.1 g/ 0.1 L) stock solution (1:1 H_2O:MeOH). Concentrations of 1.0, 2.5, 5.0, 7.5, 10.0, 15.0 and 20.0 ppm were prepared. These were mixed with an equivalent volume of internal standard solution, and analysed every MS session, storing under refrigeration when not in use.

Flow injection APcI/MS

The samples and standards were analysed by flow injection APcI/MS using 2:1 MeOH/H_2O as the eluant. A solvent flow rate of 1 mL min^{-1} and injection aliquots of 10 µL were used. Analysis was conducted in total ion current mode (TIC), over the *m/z* range of 200 – 1100 a.m.u. Continuum mode was used adopting the minimum possible scan time of 2.15 seconds and an inter-scan time of 0.1 seconds. Ion chromatograms corresponding to the n = 6 M_2D-C_3-EO_n-CH_3 oligomer (Na^+ adduct, *m/z* 581) and the C_6EO_3 Na^+ adduct (*m/z* 257) were extracted from the total ion current chromatogram for quantitation. Peak areas obtained were transferred to a spreadsheet for calculations using linear (unless stated otherwise) regressions of the standard response curves to determine Silwet L-77 concentration and therefore percentage recoveries. All values were calculated relative to the internal standard and sample recoveries were reported as ratio of the recovery obtained at t_{zero} for each treatment. Each result is the average of 1 replicate analysed 6 times by flow injection APcI/MS.

* With a solvent composition of 1:1 MeOH/H_2O complete recovery of Silwet L-77 from glassware etc is achieved

HPLC/APcI/MS

The HPLC/APcI/MS conditions were those used in Chapter 5, with a 500 μL injection volume used for all samples.

HPLC-LSD

The HPLC-LSD conditions were as described in Appendix II, with an elution solvent of 90:10 MeOH/H_2O.

7.2.1 pH Determinations

Suspensions of the substrates (1 g) were prepared in Milli-Q H_2O (10 mL) and left to stand at room temperature. At 0, 0.25, 0.5, 1, 2, 4, 7, 14, 21 and 28 days the pH of the supernatant was measured following decantation. The supernatant was returned to the vessel holding the substrate following measurement. The montmorillonite was highly absorbent, leaving no supernatant, and therefore pH was determined by immersion of the electrode directly into the resulting slurry. The experiment was performed twice* and repeated a third time† when the duplicate results were not within acceptable experimental error.

7.2.2 Control Experiments

Solutions of Silwet L-77 (1000 μg mL^{-1}) in the absence of any substrate were treated identically to the samples containing substrates and the percentage recovery determined. Samples were stored for 10 days (-15°C) and then re-analysed to determine the affects of storage on recoveries obtained. Control recoveries of Silwet L-77 in the presence of substrate were obtained by extraction of the surfactant immediately following application to the substrate. All samples were treated such that a 100% recovery would equate to a concentration of 10 ppm.

7.2.2.1 Control recoveries in the absence of substrate

Solutions of Silwet L-77 (1000 μg mL^{-1}) were diluted with MeOH (1 mL), centrifuged twice and a 100 μL aliquot diluted to 5 mL with 1:1 MeOH/H_2O. The

* Eutech cybernetics waterproof pH Scan WP meter
† EDT Instruments BA350 pH meter, Series 3

solutions were analysed fresh by flow injection APcI/MS* and after lengthy storage (1 year, -15°C) by HPLC/APcI/MS.†

7.2.2.2 Control recoveries in the presence of substrate

Solutions of Silwet L-77 (1000 μg mL^{-1}) were applied to the substrates (10 000 μg g^{-1}) and extracted immediately. The solutions were analysed fresh by flow injection APcI/MS‡ and after lengthy storage (1 year, -15°C) by HPLC/APcI/MS.§

7.2.2.3 Variation between replicates

The percentage recovery of Silwet L-77 from halloysite (1000 μg mL^{-1}, 10 000 μg g^{-1}) was determined with three replicates per time interval (0, 12 and 24 hours).

7.2.2.4 Variation in extraction solvent composition

Four replicates of Silwet L-77 (1000 μg mL^{-1}) on halloysite clay (100 mg) were prepared. After 24 hours, MeOH/H_2O (9 mL) was added to the mixtures such that compositions of 25%, 50%, 75% and 90% MeOH were obtained (25 %MeOH: 6.5 mL H_2O, 2.5 mL MeOH; 50 %MeOH: 4 mL H_2O, 5 mL MeOH; 75 %MeOH: 1.5 mL H_2O, 7.5 mL MeOH; 90 %MeOH: 9 mL MeOH). The solutions were centrifuged twice and a 100 μL aliquot diluted with 900 μL of 1:1 MeOH/H_2O.

7.2.3 Percentage Recovery Determinations

7.2.3.1 Recoveries of Silwet L-77 from various substrates (APcI/MS)

Percentage recoveries of Silwet L-77 (1000 μg mL^{-1}) over time in the presence of sand, pumice, Fe_2O_3, halloysite, TiO_2, $Al(OH)_3$, talc, $CaCO_3$, and goethite (10 000 μg g^{-1}) were investigated. At time intervals of 0.5, 1, 1.5, 2, 4, 6, 12, 24 and 48 hours and 1, 2, 3, and 4 weeks after application the supernatant was extracted and the solution analysed by flow injection APcI/MS. Each treatment contained 1 replicate. Immediately prior to APcI/MS analysis, the surfactant solution was mixed (1:1 v/v) with the internal standard solution (250 μL each), and six replicate injections of the solution were analysed.

---

* 2 replicates, 6 analyses/replicate
† 5 replicates, 1 analysis/replicate
‡ 2 replicates, 6 analyses/replicate
§ 3 replicates, 1 analysis/replicate

7.2.3.2 Recoveries of Silwet L-77 from selected clays (APcI/MS)

Percentage recoveries of Silwet L-77 (1000 μg mL^{-1}) over time in the presence of kaolinite, halloysite and illite (10 000 μg g^{-1}) were investigated. Each treatment contained 2 replicates. At time intervals of 0, 3, 6, 12, 24 and 48 hours after application the supernatant was extracted and analysed by flow injection APcI/MS as described previously.

7.2.3.3 Recoveries of Silwet L-77 from various substrates (HPLC-LSD and HPLC/APcI/MS)

Percentage recoveries of Silwet L-77 (1000 μg mL^{-1}) over time in the presence of sand, kaolinite, halloysite, montmorillonite and Te Kowhai soil (10 000 μg g^{-1}) were investigated. Each treatment contained 2 replicates. At time intervals of 0, 6, 12, 24 and 48 hours and 1, 2, 3, and 4 weeks after application the supernatant was extracted as described previously. This extraction method however was not appropriate for montmorillonite as the substrate was highly absorbent, leaving no supernatant. The sample was thus extracted by dilution of the substrate mixture with 9 mL of 5:4 MeOH/H_2O. The solutions were centrifuged and filtered, and a 500 μL aliquot then diluted with 4.5 mL of 1:1 MeOH/H_2O. The solutions were analysed by HPLC-LSD within 4 weeks of sampling. HPLC/APcI/MS analyses were conducted after lengthy storage (~ 1 yr, - 15°C).

Immediately prior to HPLC/APcI/MS analysis, the surfactant solution was mixed (1:1 v/v) with the internal standard solution. Percentage recoveries reported were calculated using the relative response curve of standard solutions. The solutions were analysed by HPLC-LSD in the absence of internal standard, and recoveries were determined using an absolute response curve of Silwet L-77 standard solutions. The results reported are the average of 2 and 1 injections per replicate for the HPLC-LSD and HPLC/APcI/MS determinations, respectively.

7.2.3.4 Recoveries of Silwet L-77 from various substrates (HPLC-LSD)

Silwet L-77 (1000 μg mL^{-1}, H_2O) was added to 100 mg samples of silica (20 000 μg g^{-1}), alumina (10 000 μg g^{-1}) and sand (10 000 μg g^{-1}) in glass vials at volumes of 2 mL, 1 mL and 1 mL, respectively. At time intervals of 0, 1, 2, 4, 7, 18 and 24 hours, 2, 5, 6, 9 and 10 days, an equivalent volume of MeOH was

added to the treated substrate, to give a 500 ppm solution in 1:1 H_2O: MeOH, and the solutions analysed by HPLC-LSD.

7.2.4 Sorption vs Degradation

7.2.4.1 Variation in extraction method

Four replicates of Silwet L-77 (1000 ppm, 1 mL, H_2O) on halloysite (100 mg) were allowed to stand for 24 hours. MeOH (1 mL) was added and the resulting solutions mixed by orbital shaker for 0, 5, 15 and 30 minutes, respectively. The solutions were centrifuged twice and a 100 µL aliquot diluted with 4.9 mL of 1:1 MeOH/H_2O.

7.2.4.2 Variation in the concentration of Silwet L-77 applied

Six concentrations (50, 100, 500, 1000, 5000, 10 000 ppm) of Silwet L-77 (1 mL, H_2O) were applied to 100 mg samples of the substrate. After 24 hours 1 mL of MeOH was added, the solutions centrifuged twice and aliquots diluted accordingly with MeOH/H_2O to give a 10 ppm equivalent solution.*

7.2.4.3 Variation in the volume of Silwet L-77 applied

Varying volumes (0.2, 0.5, 1, 2 mL) of Silwet L-77 (1000 ppm, H_2O) were applied to four samples of halloysite (100 mg), and left to stand for 24 hours. An equivalent volume of MeOH (0.2, 0.5, 1, 2 mL, respectively) was added, the solutions centrifuged twice and 100 µL aliquots diluted with 4.9 mL of 1:1 MeOH/H_2O.

7.2.4.4 Variation in the equilibration method

Two samples of Silwet L-77 (1000 ppm, 1 mL, H_2O) on halloysite (100 mg) were prepared and allowed to react, one with continuous mixing (orbital shaker) and one with standing. After 24 hours MeOH (1 mL) was added, the resulting solutions centrifuged twice and a 100 µL aliquot diluted with 4.9 mL of 1:1 MeOH/H_2O.

---

* 50 ppm: 2 in 5 dilution; 100 ppm: 1 in 5 dilution; 500 ppm: 1 in 25 dilution; 1000 ppm: 1 in 50 dilution; 5000 ppm: 1 in 250 dilution; 10 000 ppm: 1 in 500 dilution

7.2.5 Degradation Product Formation

A solution of Silwet L-77 (0.97 g, 10 000 ppm) in water (90 mL) was applied to halloysite clay (1.00 g) and left to stand for 24 hours.* MeOH (100 mL) was added to the suspension and the solid and supernatant separated by decantation following centrifuging. The solid was washed by this process a further three times with 1:1 MeOH/H_2O as the solvent. The solid fraction was then dried under vacuum to give 0.99 g (99% mass recovery). The supernatant solutions were combined and concentrated by rotary evaporation and vacuum methods, yielding 0.90 g of product (92% mass recovery). An overall mass recovery of 96% was obtained for the procedure. A control procedure where halloysite was washed by the same methods in the absence of Silwet L-77 gave a 98% mass recovery for the substrate, and no mass recovery for the supernatant fraction, validating the method used.

Carbon and hydrogen percentage compositions were determined for the substrate fractions (Section 7.3.5.2).† The supernatant fraction was analysed by ESI/MS and HPLC/APcI/MS‡ (Section 7.3.5.3). APcI/MS was used for the product identification determinations (Section 7.3.5.4) using samples from Section 7.2.4.1.

7.2.6 Toxicity

7.2.6.1 Biotoxicity

The effect of the heptane-soluble and water-soluble fractions of acid degraded Silwet L-77 (Section 6.2.1.4.2) and Silwet L-77 on the growth of nematode (*Panagrellus*), fungi (*Botrytis*, *Diplodia*, *Colletotrichum*), maggot (*Lucilia*), brine shrimp (*Artemia*) and caterpillar (*Epiphyas*) was investigated.§

Solutions (1000 ppm) of Silwet L-77 and the water-soluble fraction were prepared in water (1 mg/mL) and compared with a water control. A dilution series of 10% (100 ppm), 1% (10 ppm) and 0.1% (1 ppm) were also analysed. The heptane-soluble fraction was prepared in petroluem ether (1 mg/mL) and compared with a petroleum ether control.

---

* Solution pH 4.5 (prior to addition of Silwet L-77)
† Elemental analysis – determined by combustion
‡ RP C_{18}, 8:76:16 H_2O: MeOH: MeCN, *m/z* 300 - 1100
§ Tests conducted by Biodiscovery, Auckland, NZ

7.2.6.2 Phytotoxicity

Various formulations containing Silwet L-77 and single M_2D-C_3-EO_n-CH_3 oligomers (n = 3, 5, 6, 7, 7.5, 9, 11, 13.5, 16) were applied to *C. album* foliage as described in Chapter 5. Leaves were visibly examined for leaf necrosis at various time intervals (0 – 24 hours).

7.3 RESULTS AND DISCUSSION

7.3.1 pH Determinations

The pH of supernatants in the presence of the various substrates investigated was monitored (in the absence of surfactant) at selected intervals over 4 weeks (Figure 7.1). The ratio of solvent (Milli-Q H_2O) to substrate was proportional to that used in the percentage recovery experiments.

The substrate supernatants listed in order of decreasing pH were as follows, where the pH values shown (in parentheses) are those observed at 4 weeks. Montmorillonite (8.5) > Fe_2O_3 (7.8) ≈ goethite (7.8) ≈ $CaCO_3$ (7.8) > talc (7.7) > TiO_2 (7.0) > $Al(OH)_3$ (6.7) ≈ pumice (6.6) > aqueous (Milli-Q H_2O, 5.8) ≈ kaolinite (5.8) > Te Kowhai soil (5.5) > distilled water (5.2) > sand (4.8) > halloysite (3.5).

The pH values of illite (4 days, pH 5.8,), silica (10 days, pH 5.1) and alumina (10 days, pH 7.4) were determined over the duration of the respective percentage recovery experiments. A variation in pH for the different batches of Milli-Q H_2O used was observed (pH 5.8 – 6.5),* and therefore repeat determinations for each experiment were required.

* Solution pH is lowered due to dissolved $CO_{2(g)}$: $H_2O + CO_2 \leftrightarrow$ "H_2CO_3" $\leftrightarrow HCO_3^- + H^+$

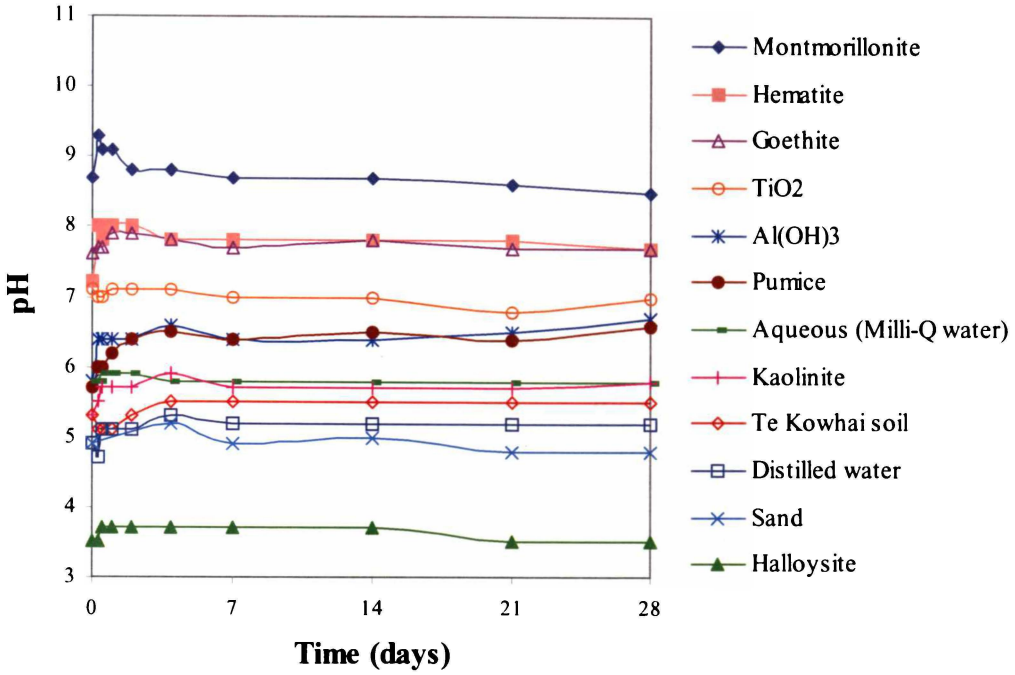

Figure 7.1. pH of supernatants of various substrates over time

7.3.2 Control Experiments

7.3.2.1 Control recoveries in the absence of substrate

The percentage recovery for the Silwet L-77 solutions as determined by flow injection APcI/MS and HPLC/APcI/MS was 92 ± 25% and 103 ± 12%, respectively. Analysis of the same solutions after 10 days at –15°C by flow injection APcI/MS gave 98% of the original response indicating that variation with storage between sample work-up and analysis was sufficiently small to be ignored. The high recovery obtained (HPLC/APcI/MS results) after 1 year of storage (103%), confirmed the stability of the solutions under these conditions.

7.3.2.2 Control recoveries in the presence of substrate

The results obtained for extraction of the Silwet L-77 solutions immediately following application to the substrates (t = 0 minutes) are presented in Table 7.1.

Table 7.1. Percentage recovery of Silwet L-77 from substrates at t_{zero}

	% Recovery (SD)		
Substrate	HPLC-LSD	APcI/MS	HPLC/APcI/MS
None	96 (1)	92 (25)	103 (12)
Sand	100 (2)	88 (7)	85 (7)
Pumice	109 (10)		90 (3)
Goethite	104 (1)		104 (14)
Fe_2O_3	98 (1)		88 (8)
Halloysite	90 (2)	94 (9)	97 (4)
Kaolinite	96 (6)	91 (2)	94 (7)
Illite	78 (5)		77 (9)
Montmorillonite	77 (6)	74 (11)	
Te Kowhai soil	101 (8)	86 (8)	85 (15)
TiO_2	111 (8)		104 (2)
Al_2O_3	103 (-)[a]		94 (4)
$Al(OH)_3$	103 (3)		91 (0.1)

a. one replicate only

Because the solutions were washed off immediately following application, degradation can be assumed to be negligible, and any reduced recovery can be attributed to sorption phenomenon. This was confirmed by qualitative analysis of the spectra obtained. Silwet L-77 integrity was maintained for all substrates investigated as demonstrated in Figure 7.2.

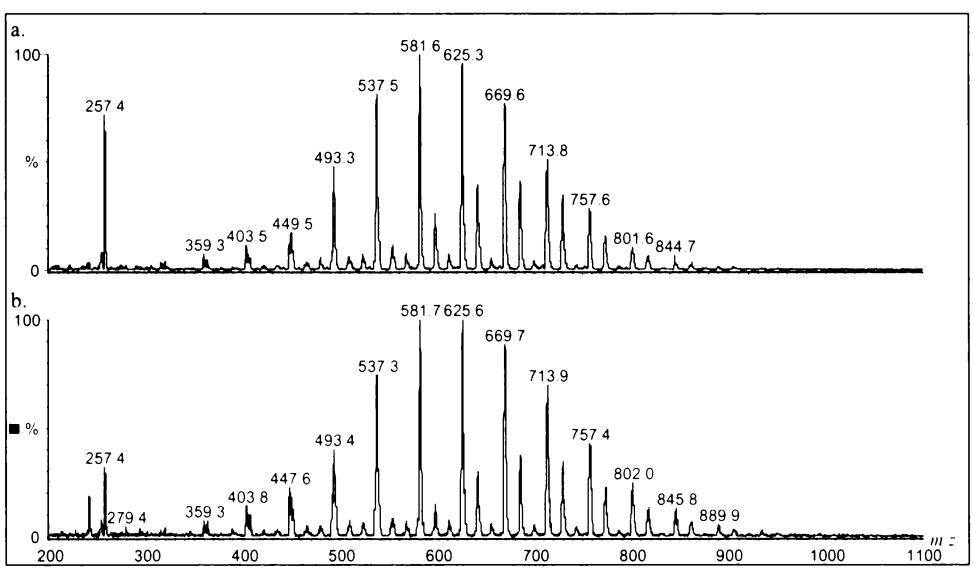

Figure 7.2. APcI/MS spectra for the t_{zero} washoffs of Silwet L-77 from a. montmorillonite and b. illite.

The results from the three methods show recoveries to be within experimental error of 100% recovery for all substrates other than illite and montmorillonite. The montmorillonite swelled extensively upon application of the surfactant solution, indicating that the reduced recovery was a result of trapping of the surfactant in between the clay layers. The absorption of organic compounds into the interlayer space of montmorillonite due to its expanding lattice structure and high cation exchange capacity is well known.[44] Sorption of a range of PEG oligomers (Ave. MW 200, 3000, 400, 600, 1500 and 20 000) by montmorillonite has been reported, and furthermore higher affinity was observed with increased molecular weight.[45] Results from surfactant-substrate studies obtained elsewhere also indicated extensive surfactant-montmorillonite interactions, in contrast to non-swelling sand, illite and kaolinite substrates.[2] Additional investigations have demonstrated stronger interactions for surfactants with montmorillonite and illite substrates as compared with sand and kaolinite.[1g] Results of studies on pesticides with kaolinite and montmorillonite substrates also showed stronger interactions with montmorillonite.[44,46]

The interlayer spacing of illite has been shown to be unchanged when treated with ethylene glycol,[47] as expected for a non-swelling clay. Interactions between illite and PEG-300 have been demonstrated, although the sorption was less than for montmorillonite and was shown to be limited to external surfaces.[45] This indicates that the reduced recovery observed in the results obtained here is due to adsorption rather than intercalation. This is probable in the case of illite as the clay carries an overall negative charge, a result of isomorphous replacement of some Si and Al ions in the clay sheets with Fe, Mg and Ti ions, and adsorption to the sides of the clay can thus be expected.

Complete recovery of the applied Silwet L-77 from halloysite was obtained, however the ability of halloysite to intercalate a range of organic liquids including mono-, di- and tri- ethylene glycols has been described.[48] Halloysite has a basal spacing of 1.01 nm and is capable of intercalating a single layer of ethylene glycol, thereby swelling to 1.08 nm. Montmorillonite intercalates two layers of ethylene glycol and swells up to 2.25 nm. This difference however, is possibly due to the difference in nature of the surface charges of the clays rather than swelling capability. Halloysite is amphoteric – one side of the clay is a network of negatively charged O ions, whilst the other side consists of positively charged

α-hydroxide ions. The interlayer space is thus only capable of accepting one layer of a non-ionic species in terms of ion-dipole attractions. Montmorillonite being negatively charged accepts two layers.

Molecular modelling* was thus used to determine if the interlayer space of halloysite was large enough to accommodate the Silwet L-77 molecule. Preliminary investigations indicated that the maximum thickness of the siloxane head group is 0.92 nm (fully extended structure), whilst the thickness of an ethylene glycol chain is 0.21 nm. The basal spacing of swelled halloysite (1.1 nm) and montmorillonite (2.2 nm) are thus both theoretically large enough to accommodate this structure, although the dimensions may be too close to allow it to occur in reality for halloysite. The results obtained here show that absorption into halloysite does not occur immediately, however it is possible that it may occur with more time for diffusion. Infusion of the bulk solution into the clay structure will not be immediate, as the scale is molecular.

Sorption tends to show a logarithmic profile with respect to time, with a rapid initial rate gradually plateauing toward a maximum value. This known as the equilibrium i.e. is the time whereafter no further increase in the percent adsorbed is observed. The results here are thus only a reflection of the initial rate of adsorption.

The experiments described in Section 7.3.4 investigate the sorption closer to equilibrium (24 hours).

7.3.2.3 Variation between replicates

The results obtained (Table 7.2) show that the variation between sample replicates is within the standard deviation for the analytical method. The standard deviations are very high as has been associated with the analytical method employed (flow injection APcI/MS). The initial determinations were conducted using this method (Sections 7.3.3.1 and 7.3.3.2), but where possible the refined HPLC/APcI/MS method developed in Chapter 4 was applied (Section 7.3.3.3).

* Spartan Version 5.0, running on a Silicon Graphics I02 computer

Table 7.2. Percentage recovery of Silwet L-77 from halloysite clay over time with three replicates

Time (hours)	Replicate	% Recovery	SD	CV (%)
0	1	90	47	52
	2	104	26	25
	3	131	36	28
12	1	24	6	25
	2	24	7	28
	3	35	8	23
24	1	7	4	58
	2	6	4	67
	3	4	2	63

7.3.2.4 Variation in extraction solvent composition

In all recovery experiments conducted an extraction solvent of 50% MeOH was used. The recovery of Silwet L-77 after 24 hours on halloysite clay, using varying compositions of MeOH in the extraction solvent is presented in Table 7.3.

Table 7.3. Percentage recovery of Silwet L-77 from halloysite clay with varying extraction solvents

% MeOH	% Recovery	SD	CV (%)
25%	26	4	17
50%	40	8	20
75%	43	8	19
90%	45	5	12

If the reduced recovery of Silwet L-77 was due to weak electrostatic interactions, a higher percentage recovery could be expected with solvents of higher organic composition. A significant increase in recovery was observed with an increase in MeOH composition from 25% to 50%, but recovery was comparable within experimental error with solvents of higher methanol content. These results validate the use of 50% MeOH as the extraction solvent.

7.3.3 Percentage Recovery Determinations

7.3.3.1 Recoveries of Silwet L-77 from various substrates (APcI/MS)

The percentage recovery data obtained for Silwet L-77 (1000 µg mL^{-1}) on various substrates (10 000 µg g^{-1}) as determined by flow injection APcI/MS on single replicates is presented in Figure 7.3.

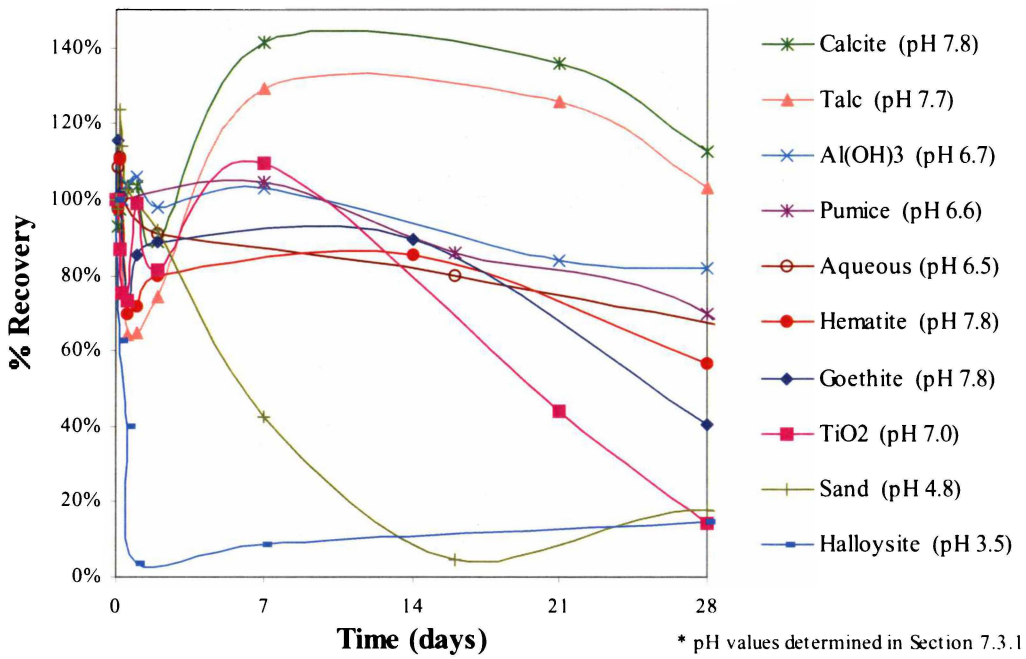

Figure 7.3. Percentage recovery of Silwet L-77 over time from various substrates (APcI/MS)

The results indicate a dependence of recovery on supernatant pH. In general, lower recovery was observed on the substrates showing more extreme pH values (halloysite, sand). The pH instability of Silwet L-77 under aqueous conditions has been described, and half-life of the surfactant at pH 3 was demonstrated to be only a matter of hours (Chapter 6).

Information pertaining to small variations in percentage recovery could not be determined from these results due to the large margin of error for the values obtained. This is demonstrated by the calcite and talc data for which "recoveries" of up to 140% were observed. As discussed previously (Chapter 4), high variability is observed with the flow injection APcI/MS method, and these results can thus only be interpreted loosely to gain an idea of general recovery trends. In particular, the rapid loss in the presence of halloysite indicated that recovery on clay substrates should be analysed in more detail. Recovery rates on three clay

substrates, using an increased number of replicates to improve the reliability of the data obtained were thus investigated in the following section (7.3.3.2).

7.3.3.2 Recoveries of Silwet L-77 from selected clays (APcI/MS)

The percentage recovery data obtained for Silwet L-77 (1000 μg mL^{-1}) on various clay substrates (10 000 μg g^{-1}) as determined by flow injection APcI/MS on duplicate samples is presented in Figure 7.4.

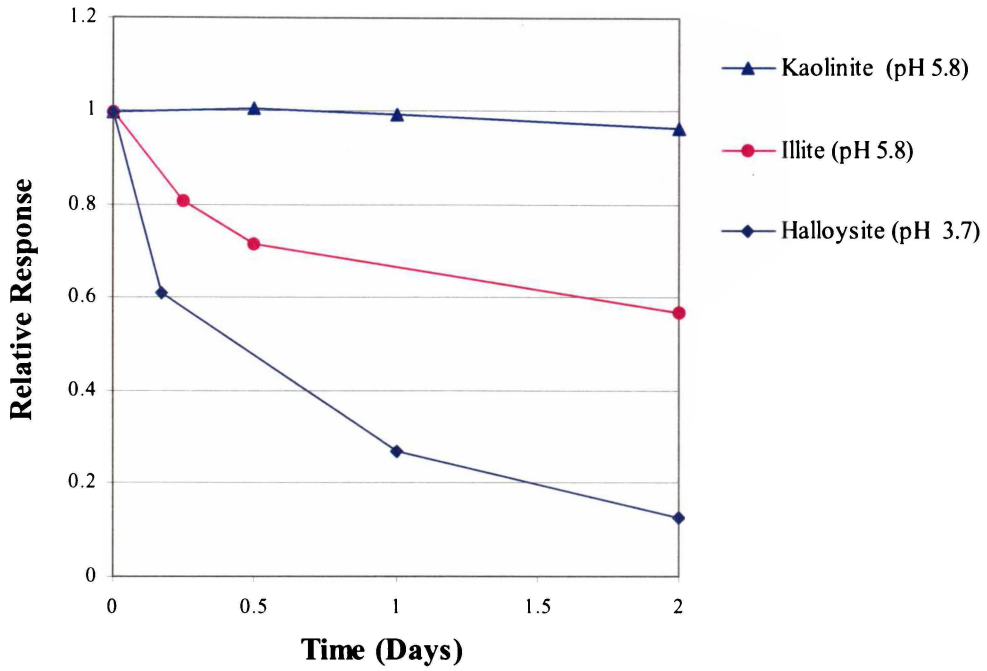

Figure 7.4. Recovery of Silwet L-77 over time from various clay substrates (APcI/MS)

The lowest recoveries were observed in the presence of halloysite. Again, these could be due to either sorption or degradation, or a combination of the two mechanisms. In this case degradation is considered to be the most significant pathway, because this is known to be pH dependent and halloysite exhibited the most acidic supernatant of the clays investigated.

The reduction in recovery in the presence of illite was more rapid than for kaolinite despite comparable acidities for the two media, indicating that factors other than supernatant pH also influence Silwet L-77 recovery on clay substrates. Both clays are non-swelling and thus intercalation is not a likely cause of the difference observed. Adsorption phenomena/surface interactions are thus most likely responsible for the observed behaviour of Silwet L-77 on illite. Illite carries

an overall negative charge whereas kaolinite is a neutral-type lattice. The results obtained in the t_{zero} control experiments (Section 7.3.2.2) also showed reduced recovery in the presence of illite.

The preliminary results obtained for talc (Section 7.3.3.1) support that supernatant pH, intercalation and surface charges are important factors in the sorption/degradation process. High recovery over a 4 week period was observed on this clay, which is non-swelling, non-charged and exhibits a relatively neutral supernatant pH.

7.3.3.3 Recoveries of Silwet L-77 from various substrates (HPLC-LSD and HPLC/APcI/MS)

Percentage recoveries of Silwet L-77 (1000 μg mL^{-1}) over time in the presence of sand, kaolinite, halloysite, montmorillonite and Te Kowhai soil (10 000 μg g^{-1}) were investigated by HPLC-LSD and HPLC/APcI/MS methods. The flow injection APcI/MS method was not used as comparisons (Chapter 4) demonstrated the method to be less reliable than that incorporating online-HPLC separation.

The results obtained by the HPLC-LSD and HPLC/APcI/MS methods were comparable and are presented in Figures 7.5 and 7.6, respectively.

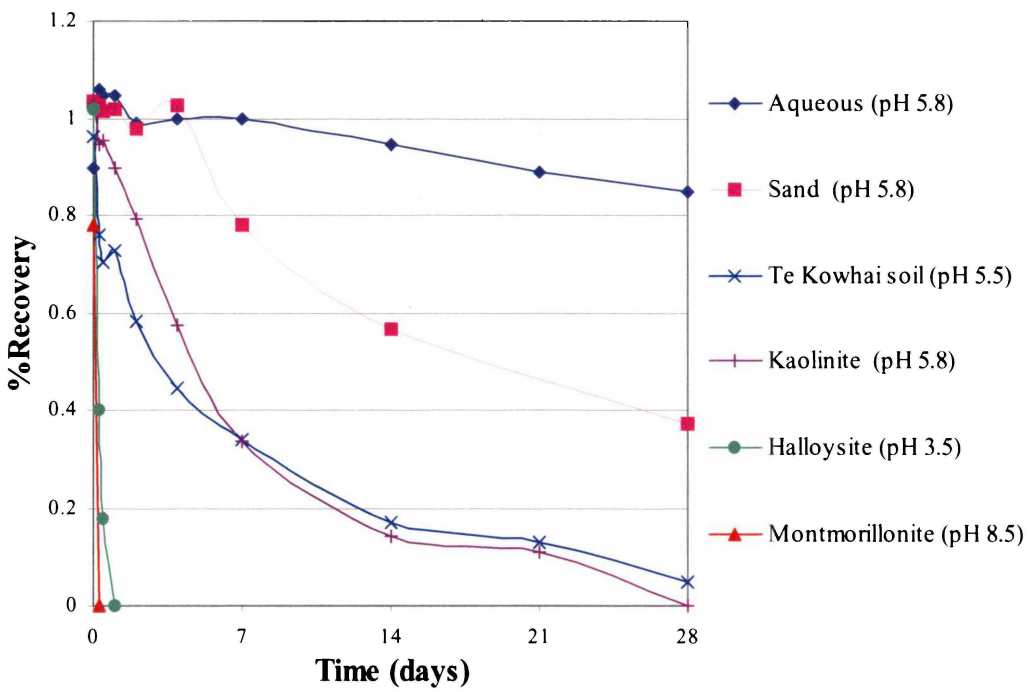

Figure 7.5. Percentage recovery of Silwet L-77 over time from various substrates (HPLC-LSD)

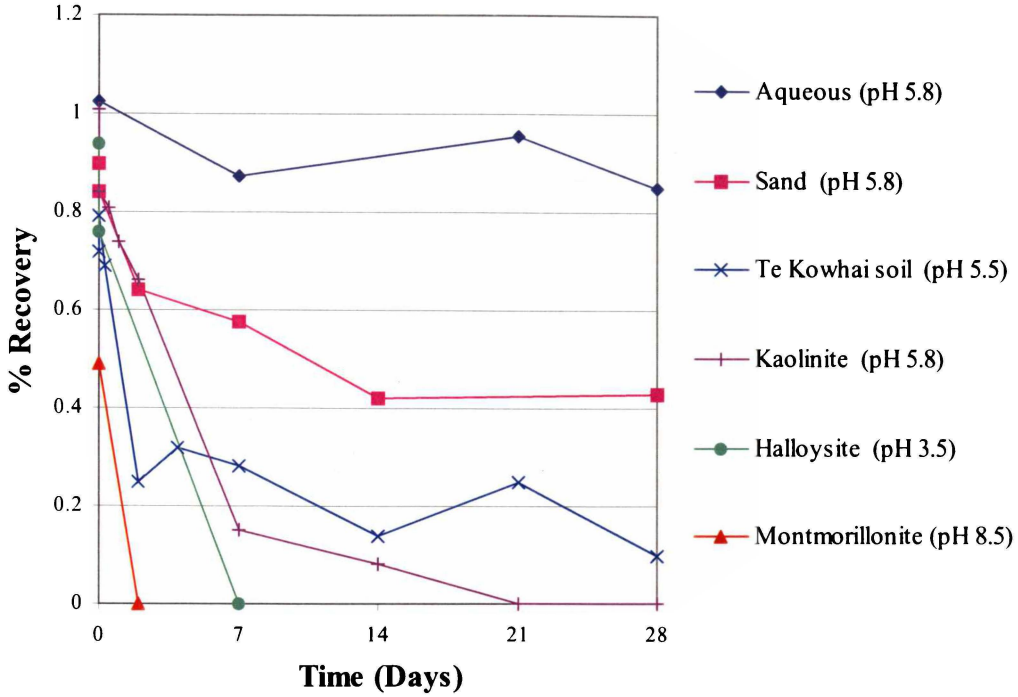

Figure 7.6. Percentage recovery of Silwet L-77 over time from various substrates (HPLC/APcI/MS)

The rates in order of increasing recovery, as determined by both methods were aqueous (108)* > sand (17) > kaolinite (4) > Te Kowhai soil (3) > halloysite (1) > montmorillonite (0.1). The values shown in parentheses are the surfactant half-life in days.† The reduction in recovery was most rapid for the substrates exhibiting extreme pH values (halloysite, montmorillonite), and greatest for the absorbant, negatively-charged montmorillonite. The variation in the rates for the other media investigated, all of which showed comparable acidities, indicate that factors other than supernatant pH also influence Silwet L-77 recovery on substrates, as discussed in Section 7.3.3.2.

The higher recovery on sand compared to the other substrates indicates that the high surface charges and surface area inherent to clays exhibit a considerable influence on substrate recovery. The recovery from Te Kowhai soil is intermediate to that of sand and halloysite consistent with the described clay compositions (49% volcanic glass, 47% halloysite).[49]

* Obtained by extrapolation
† Average of two results

7.3.3.4 Recoveries of Silwet L-77 from various substrates (HPLC-LSD)

Percentage recoveries of Silwet L-77 (1000 μg mL^{-1}) over time in the presence of alumina (10 000 μg g^{-1}), sand (10 000 μg g^{-1}) and silica (20 000 μg g^{-1}), as determined by HPLC-LSD, are presented in Figure 7.7. Degradation under aqueous and acidic conditions is included for comparison (data from Section 6.3.9.2).

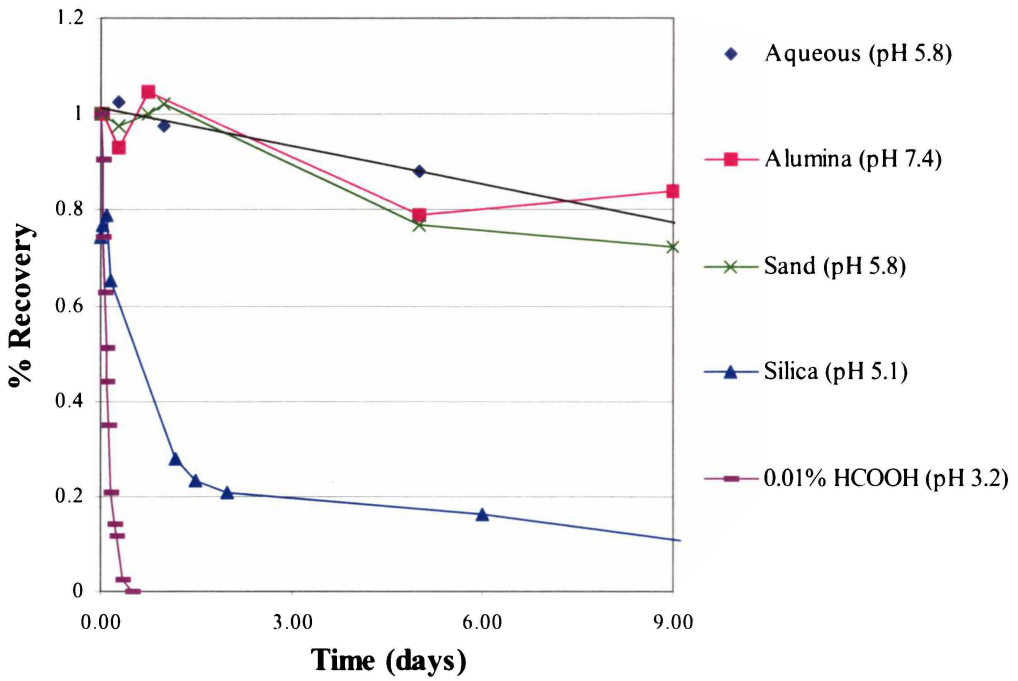

Figure 7.7. Percentage recovery of Silwet L-77 over time from various substrates (HPLC-LSD)

The recovery rates in decreasing order were: alumina (22)* > aqueous (19)* > sand (14)* > silica (0.6) > 0.01% HCO_2H (0.1), where the values shown in parentheses are the surfactant half-lives (days). The reduction in recovery was most rapid for the conditions showing more extreme supernatant pH values.

* Obtained by extrapolation

7.3.3.5 Summary of recoveries from various substrates

The time to 50% loss in recovery for Silwet L-77 in the presence of all substrates investigated was reduced in comparison to the aqueous system (Table 7.4).

Table 7.4. Half-life of Silwet L-77 in the presence of various substrates

Substrate (pH)	$t_{1/2}$ (days)
None (6.5)	66[f]
Pumice (6.6)	32[a]
Hematite (7.8)	32[ag]
Goethite (7.8)	25[a]
Alumina (7.2)	22[eg]
TiO_2 (7.0)	20[a]
Sand (5.8)	6[a]
Kaolinite (5.8)	4[cd]
Te Kowhai Soil (5.5)	3[cd]
Illite (5.9)	2.5[bg]
Silica (4.9)	0.6[e]
Halloysite (3.5)	0.4[ab]
Montmorillonite (8.5)	0.1[cd]
0.01% HCO_2H (3.2)	0.1[e]
Calcite (7.8)	ND[h]
Talc (7.7)	ND[h]
$Al(OH)_3$ (6.7)	ND[h]

[a] Section 7.3.3.1; [b] Section 7.3.3.2; [c] Section 7.3.3.3-HPLC-LSD data; [d] Section 7.3.3.3- HPLC/APcI/MS data; [e] Section 7.3.3.4; [f] Average; [g] Obtained by extrapolation; [h] Not determined (>28 days)

These results indicate that there is little chance of Silwet L-77 persistence in typical soil and aqueous environments. In general the rates of loss observed show a dependence on supernatant pH, with lower recoveries in acidic and alkaline pH media. The recoveries from the clay minerals were also reduced.

7.3.4 Sorption vs Degradation

It is of interest to ascertain whether any reduction in Silwet L-77 recovery is a reflection of losses through sorption or actual degradation. Qualitatively, degradation can be readily determined by analysis of the API/MS spectrum. This is demonstrated by the ESI/MS spectrum obtained for Silwet L-77 after 24 hours equilibration on halloysite (Figure 7.8).

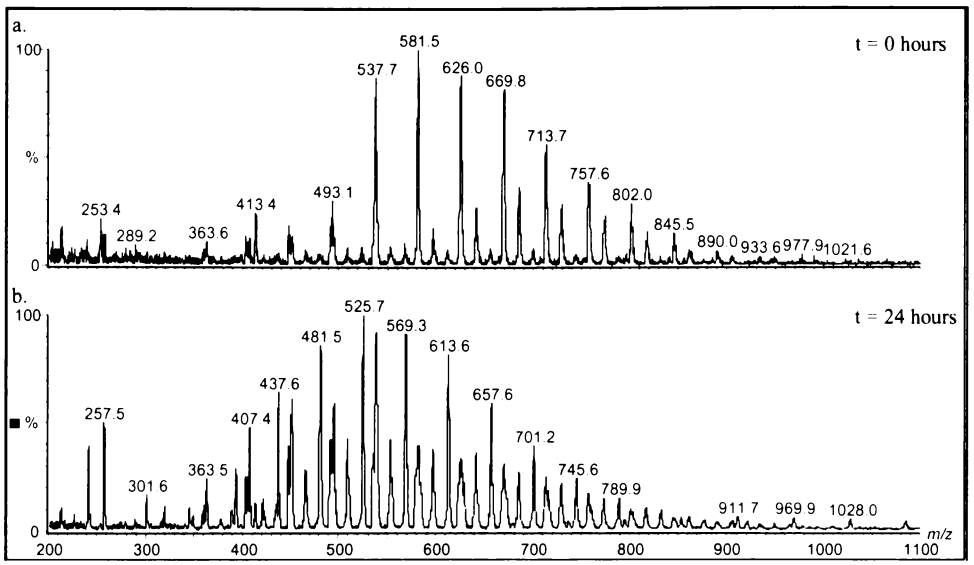

Figure 7.8. APcI/MS spectra of Silwet L-77 after *a.* 0 hours and *b.* 24 hours in the presence of halloysite

However in reality, it is difficult to quantify the degradation due to the unknown extent of the sorption processes. Sorbed material can fall into two fractions: (i) weakly adsorbed (i.e. by electrostatic attraction, and (ii) strongly adsorbed (i.e. by covalent bonding). The proportion of the latter tends to increase with exposure time and thus adsorption can become progressively less reversible. Covalent bonding requires degradation of the siloxane to a silanol so in effect "irreversible sorption" can actually be considered a measure of Silwet L-77 degradation. Furthermore irreversible sorption is, in any case, an inactivation of the compound on the substrate, which by most environmental standards is classified as being removed from the system. Elsewhere extraction of bound silanols has been described, however highly acidic conditions were used.[24e-g,i] This method would not be appropriate for the extraction of Silwet L-77 as its degradation would be catalysed in the process.

In this section, the contribution of weak adsorption processes to the recoveries obtained for Silwet L-77 on halloysite clay samples was investigated. This was attempted by determining the effect of variations in the (i) extraction methods, (ii) concentration of Silwet L-77 applied, (iii) volume of Silwet L-77 applied, and (iv) equilibration methods. A 24 hour equilibration period was adopted. It may be possible that the effects of weak adsorption will be more pronounced at shorter equilibration times, and that at the time interval used little influence will be

observed. Furthermore, the effect of the extreme pH exhibited by the halloysite clay may mask the influence of other factors that would otherwise contribute to Silwet L-77 sorption/degradation on substrates.

7.3.4.1 Variation in extraction method

Samples of Silwet L-77 (1000 μg mL^{-1}) on halloysite clay (10 000 μg g^{-1}) for 24 hours were extracted using an orbital shaker for varying lengths of time. Enhanced mixing of the organic solvent through the substrate did not alter the recovery of Silwet L-77, as shown in Table 7.5.

Table 7.5. Percentage recovery of Silwet L-77 from halloysite clay with varying extraction (mixing) time

Extraction time (minutes)	% Recovery	SD	CV (%)
0	27	5	17
5	28	5	19
15	26	4	17
30	28	4	15

Sorption to clay substrates, as a result of the high surface area and layered structure is well known. The control experiments conducted in Section 7.3.2.2 indicated that Silwet L-77 is not adsorbed immediately by halloysite. The results obtained here, using a longer equilibration time to allow diffusion to occur, indicate that the reduced recovery is not due to weak sorption processes or trapping within the layers. In such cases a higher percentage recovery would be expected with longer extraction times. Intercalation of mono-, di- and tri-ethylene glycol by halloysite has been reported,[48] however release of intercalated compounds from clays has been shown to be diffusion dependent[45] and thus increased recovery would be expected with enhanced mixing of the extraction solvent through the substrate.

7.3.4.2 Variation in the concentration of Silwet L-77 applied

The percentage recovery of Silwet L-77 applied to halloysite clay and allowed to react for 24 hours, was in general not affected by changes in the Silwet L-77 application concentration (Table 7.6).

Table 7.6. Percentage recovery of Silwet L-77 from halloysite clay with varying Silwet L-77 concentration

[Silwet L-77] ($\mu g\ mL^{-1}$)	m(Silwet L-77)/m(clay) ($\mu g\ g^{-1}$)	% Recovery	SD	CV (%)
50	500	68	23	34
100	1 000	41	12	29
500	5 000	33	7	21
1 000	10 000	32	9	29
5 000	50 000	41	9	22
10 000	100 000	45	10	22

The highest recovery was observed for the lowest application concentration, however the largest standard deviation was also observed for this concentration, and thus this anomaly is not considered to be a real variation. The trend was not maintained throughout the series, further indicating the value to be an outlier.

If loss was by weak adsorption, a higher percentage recovery might be expected for higher application concentrations through saturation of adsorption sites. This was not observed indicating that under these conditions, weak adsorption processes are not contributing factors to the change in Silwet L-77 recovery.

Results obtained from alterations to the surfactant to clay ratio may also be informative in regards to clay surface interactions. If clay surface interactions were a significant influence in the reduction in recovery, higher losses would be expected for lower concentrations. These results thus indicate that the high surface area of the clay is not a controlling factor in the recovery obtained for this system.

7.3.4.3 Variation in the volume of Silwet L-77 applied

An small increase in percentage recovery of Silwet L-77 (1000 $\mu g\ mL^{-1}$) from halloysite clay after 24 hours, was obtained with increasing application volume, although the values were not significantly varied beyond the experimental error (Table 7.7).

Table 7.7. Recovery of Silwet L-77 from halloysite clay with varying Silwet L-77[a] volume

v(Silwet L-77) (mL)	m(Silwet L-77)/m(clay) (μg g^{-1})	% Recovery	SD	CV (%)
0.2	2 000	22	4	20
0.5	5 000	26	4	15
1	10 000	27	5	17
2	20 000	32	5	16

[a] 1000 ppm solution

This may be attributable to sorption processes as higher recoveries might be expected for higher loadings if adsorption was a contributing factor to recovery losses. Other factors may also be responsible for this trend, such as the effect of moisture content on degradation processes. A trend of lower recoveries with smaller volumes is observed. This is consistent with the affect of high moisture levels on the rate of hydrolysis of PDMS on soils[24b,i] and clays.[26] However in contrast to this, increased degradation is reported for surfactants on soils and peat with increased soil moisture content.[1b]

7.3.4.4 Variation in the equilibration method

Utilisation of an orbital shaker throughout Silwet L-77 (1000 μg mL^{-1}) exposure to the substrate (10 000 μg g^{-1}) investigated the effect of varying solution diffusion rates. The variation in recovery was within experimental error for samples equilibrated by standing or with constant mixing (Table 7.8).

Table 7.8. Percentage recovery of Silwet L-77 from halloysite clay with varying equilibration methods

Equilibration method	% Recovery	SD	CV (%)
Stationary	27	5	17
Shaken	30	6	18

Lower recoveries might be expected for the well-mixed sample if contact with the clay surface contributed significantly to the surfactant recovery under these conditions. This did not influence the recovery indicating that other factors (i.e. supernatant pH) exhibit a greater effect in the case of halloysite. The limited influence of surface effects may be a reflection of the neutral nature of the clay. However, it is possible that equilibrium has been reached at this point (24 hours)

and thus that the influence of diffusion rates is not observed. Effects may be more pronounced at shorter equilibration times.

7.3.5 Degradation Product Formation

7.3.5.1 Mass Recovery

Irreversible binding of halloysite clay to the glass vessel used was observed after 24 hours exposure to a Silwet L-77 solution (10 000 μg mL^{-1}, 10 000 μg g^{-1}). The release required strongly acidic conditions. A reduced mass recovery was obtained for the surfactant solution (92%), whereas the halloysite clay was quantitatively recovered (within experimental error). The covalent bonding of the clay to the glass can only be rationalised by incorporation of some portion of the Silwet L-77 molecule as a linking agent, as this was not observed for halloysite on glass in the absence of Silwet L-77. Similar observations, such as the condensation of triorganosilanols with the Si-OH group of silicate substrates (e.g. muscovite [a common mica], chrysotile, asbestos and talc),[27] and the covalent binding of silanols to soils[24e-g,i] have been reported elsewhere. In the latter reports, the release of the bound silanol required hydrolysis with 0.1 M HCl.

7.3.5.2 Elemental Analysis

An increase in the C (0.18%) and H (0.06%) percentage compositions was observed for the halloysite clay exposed to Silwet L-77 (Table 7.9). The increase in organic content demonstrates that Silwet L-77 has been irreversibly bound and therefore retained by halloysite.

Table 7.9. Effect of Silwet L-77 on the C and H percentage compositions of halloysite clay

	%C [d]	%H [c]
Control (clay only) [a]	0.15 ± 0.02	1.67 ± 0.06
Control (clay only) [b]	0.14 ± 0.01	1.51 ± 0.02
Clay [c] + Silwet L-77	0.32 ± 0.00	1.57 ± 0.02

[a] Clay as obtained from source; [b] MeOH washed; [c] MeOH washed (before and after exposure to Silwet L-77 solution; [d] Error associated with replicate chemical analysis determinations

In land applications, the covalent bonding of Silwet L-77 derivatives could result in aggregation of silicate minerals, inhibiting drainage and/or affect the sorption capacity of the soil. An increase in sorption capacity may have positive or detrimental effects. Potentially toxic compounds could be immobilised and

therefore inactivated, whilst degradation of other degradable compounds may be inhibited by the sorption.

7.3.5.3 Supernatant analysis

The supernatant of the solution of Silwet L-77 reacted with halloysite clay over 24 hours was analysed by API/MS methods. Two molecular series were observed in the ESI/MS spectrum of the supernatant, corresponding to $M_2D\text{-}C_3\text{-}EO_n\text{-}CH_3$[*] and $CH_3O(EO)_nH$ (**20**, n = 4 - 15)[†]. The observation of ions corresponding to $M_2D\text{-}C_3\text{-}EO_n\text{-}CH_3$ of n < 2 indicated that the assignment may not be correct and therefore the sample was analysed by HPLC/APcI/MS, to compare retention times with those of a Silwet L-77 standard solution.

Qualitative HPLC/APcI/MS analysis of the supernatant showed a similar profile to that of a Silwet L-77 standard, although more peaks were observed in the early eluting polar region. Oligomers of $M_2D\text{-}C_3\text{-}EO_n\text{-}CH_3$ (n = 3 – 15) and $M_2D\text{-}C_3\text{-}EO_n\text{-}H$ (n = 4 – 13) were observed for both solutions (7.5 and 6.4 minutes, respectively) showing that complete degradation had not occurred. The smaller ions of the former series[‡] (observed in the previously described ESI/MS spectrum) eluted at a much shorter retention time (3.0 minutes) and correspond to the *Ion Series F*, described in Table 6.3. Ions corresponding to *Ion Series B* were also observed at two retention times (3.3[§] and 3.7 minutes[**]). The 3.3 minute peak of *Series B* ion was also observed in the standard solution.[††] A peak eluting at 2.8 minutes was observed in both the supernatant and standard, the spectra of which revealed two series. The first corresponded to *Ion Series B* ($CH_3O(EO)_nH$),[‡‡] whilst the later[§§] was unassigned.

The higher recovery of undegraded Silwet L-77 obtained in this section (pH 4.5) as compared with the previous halloysite treatments (pH 3.5) confirms that solution pH contributes significantly to the recovery of Silwet L-77 from halloysite.

---

[*] *m/z* 273, 317, 361, 405, 449, 493, 537, 581, 625, 669, 713, 757, 801, 845, 889, 933, 977 (Na^+ adducts)
[†] *m/z* 231, 275, 319, 363, 407, 451, 495, 539, 583, 627, 671, 715 (Na^+ adducts)
[‡] *m/z* 312, 356, 400, 444, 488, 532, 576, 620, 664, 708, 752, 796, 840 (NH_4^+ adducts)
[§] *m/z* 416, 460, 504, 548, 592, 636, 680, 724, 768, 812, 856, 900 (NH_4^+ adducts)
[**] *m/z* 856, 900, 944, 988, 1032, 1076 (NH_4^+ adducts)
[††] *m/z* 504, 548, 592, 636, 680 (NH_4^+ adducts)
[‡‡] *m/z* 319, 363, 407, 451, 495, 539, 583, 627, 671, 715, 759
[§§] *m/z* 379, 423, 467, 511, 555, 599, 643, 687, 731, 775, 819, 863, 907, 951

7.3.5.4 Product Quantitation

Figure 7.9 shows the spectrum of Silwet L-77 following exposure to halloysite clay after 2 weeks as compared with the initial spectrum.

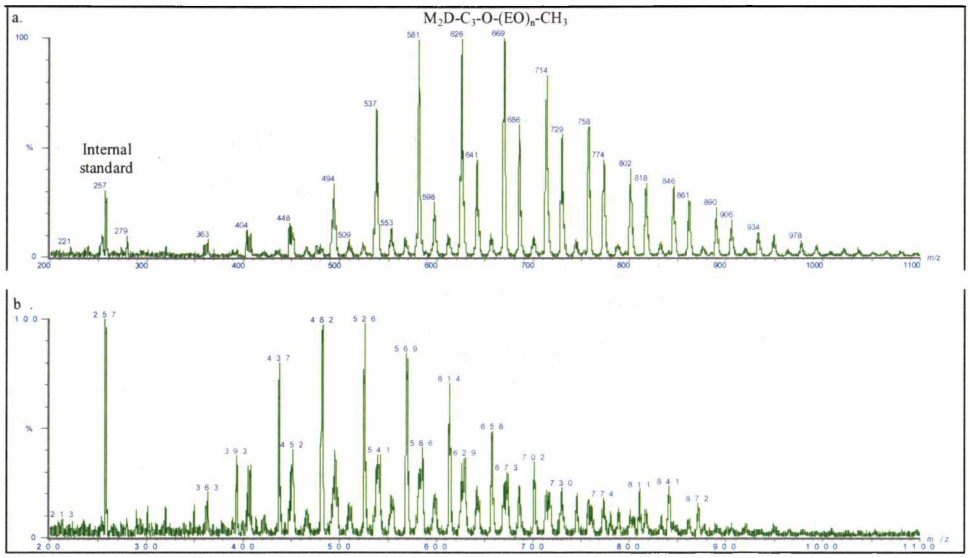

Figure 7.9. ESI/MS spectra of Silwet L-77 extracted from halloysite clay after *a.* 0 minutes and *b.* 2 weeks equilibration in aqueous suspension

The significant change in the spectrum demonstrates that degradation rather than adsorption is a significant source of the reduced Silwet L-77 recovery observed. The major products observed after 2 weeks in the presence of halloysite correspond to ions from Series C (Table 6.2), most likely to be the parent less both TMS groups (i.e. **22**). This result is consistent with the observed crosslinking of the clay to the glass support (Section 7.3.6.1), for which silanol precursors are required.

The rates of formation of selected degradation products of Silwet L-77 over 2 days in the presence of halloysite are presented in Figure 7.10 along with the parent molecule recovery.

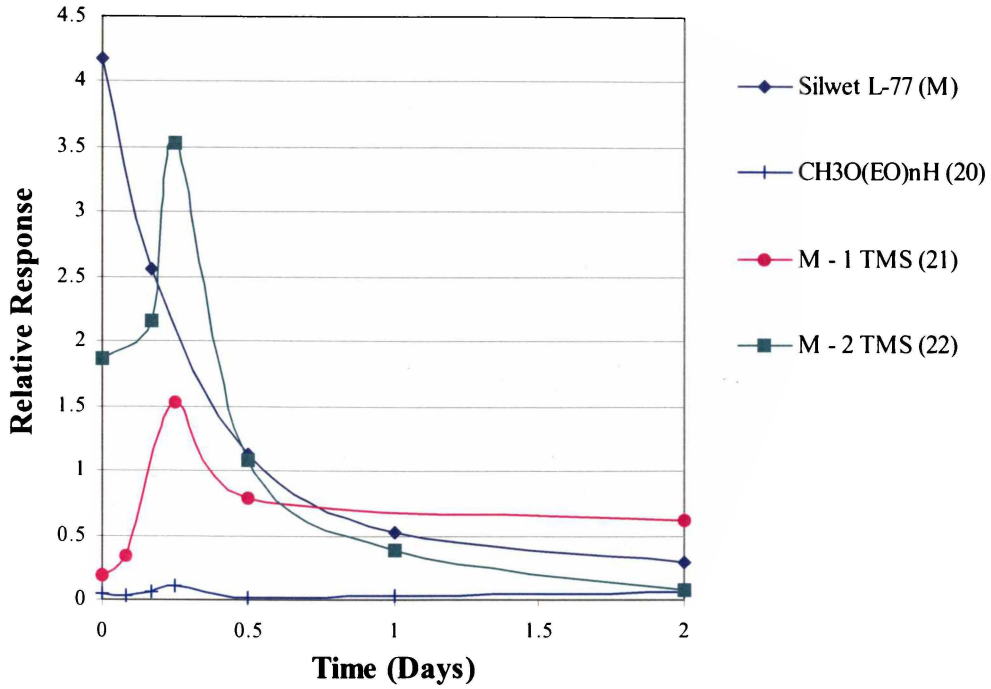

Figure 7.10. Behaviour of Silwet L-77 and selected degradation products thereof on halloysite clay over two days in aqueous suspension

The reduced recovery of Silwet L-77 in the presence of halloysite is rapid and is paralleled by the concomitant production of silanol monomer products thereof (**21** and **22**). This further demonstrates that the reduced recovery of Silwet L-77 is the result of degradation rather than inactivation (sorption) processes.

7.3.6 Toxicity

7.3.6.1 Biotoxicity

The effect of Silwet L-77 and the degradation products thereof on the growth of various organisms was investigated. No effect on the growth of the nematode or fungi was observed. The effect on maggot growth was minimal with moderate inhibition being observed only at high concentration (1000 ppm) for the Silwet L-77 and heptane-soluble fraction at 24 hours. No inhibition was observed at 48 hours.

Silwet L-77 was moderately toxic to caterpillar larvae at 1000 ppm (50% mortality) and 100 ppm (25% mortality) concentrations, and also affected feeding at these dosages. A high mortality rate was also observed for the heptane-soluble fraction at 1000 ppm (75%), and feeding was also affected. The water-soluble fraction exhibited no effects.

Brine shrimp growth was affected by Silwet L-77 at all concentrations (1000, 100, 10, 1 ppm) investigated, and also by the heptane-soluble fraction (1000 ppm). Growth in the presence of the water-soluble fraction was as for the control.

The concentrations required for biotoxicity for Silwet L-77 and degradation products thereof are in large excess of any likely input by agricultural practices. This is especially so for the heptane-soluble products, which occur as a very minor proportion of the products formed. In general, organosilicones and PEG derivatives are considered relatively environmentally benign. It is worth noting however that the ability of organosilicones, and in particular $(TMS\text{-}O)_2$ –Si, to methylate inorganic mercury(II) has been demonstrated under laboratory conditions,[50] and may be a potential hazard of these compounds. The sample preparation methods used here were such that all volatile components were removed, and therefore the potential effect of these compounds was not addressed.

7.3.6.2 Phytotoxicity

Distinct localised symptoms of phytotoxicity were observed only for the n = 3 and n = 16 $M_2D\text{-}C_3\text{-}EO_n\text{-}CH_3$ oligomers. These solutions exhibited minimal spreading as compared with other $M_2D\text{-}C_3\text{-}EO_n\text{-}CH_3$ and Silwet L-77 formulations. These results confirm Silwet L-77 formulations exhibit low phytotoxicity, probably as a result of dilution due to high spreading, and indicate that the ion efflux method is not an appropriate phytotoxicity test for foliar-applied chemicals, as discussed in the introduction.

7.4 CONCLUSION

The results indicate that there is little chance of surfactant persistence on typical soil substrates in aqueous environments. Reduced recovery was considered to be a result of degradation and/or strong sorption processes. Losses were most significant on substrates exhibiting extreme supernatant pH values (montmorillonite, halloysite). Reduced recoveries were also higher with higher clay content. Studies on clays indicated that supernatant pH, potential for intercalation and surface charges are important factors in the process. In the case of the montmorillonite and illite clays, recoveries may be more significantly affected by sorption, as strong surfactant-substrate interactions were observed immediately following application.

The results obtained support previous observations that Silwet L-77 is relatively benign in the natural environment. Primary degradation is rapid and ultimate degradation to naturally occurring compounds i.e. CO_2, H_2O and $Si(OH)_4$, can be predicted according to the structures of the observed intermediates. However covalent bonding of degradation products to substrates was observed which would result in some environmental accumulation. In land applications this could cause aggregation of silicate minerals and/or affect the sorption capacity of the soil. An increase in sorption capacity could have positive or detrimental effects.

The concentrations required for biotoxicity for Silwet L-77 and degradation products thereof are in large excess of any likely input by agricultural practices. Phytotoxicity is also low and this appears to be a result of the dilution effects caused by high spreading.

7.5 REFERENCES

[1] *a.* W. W. Miller, N. Valoras, J. Letey, *Soil Sci. Soc. Amer. Proc.*, 1975, **39**, 11-16; *b.* N. Valoras, J. Letey, J. P. Martin, J. Osborn, *Soil Sci. Soc. Amer. J.*, 1976, **40**, 60-63; *c.* Haigh, S. D., *Sci. Total Environ.*, 1996, **185**, 161-170; *d.* W. W. Miller, J. Letey, *Soil Sci. Soc. Amer. Proc.*, 1975, **39**, 17-22; *e.* W. de Wolf, T. Feijtel, *Chemosphere,* 1998, **36**, 1319-1343; *f.* M.A.Mustafa, J. Letey, *Soil Sci.*, 1969, **107**, 343-347; *g.* D. B. Knaebel, T. W. Federle, D. C. McAvoy, J. R. Vestal, *Appl. Environ. Microbiol.,* 1994, **60**, 4500-4508; *h.* D.M. Di Toro, L.J. Dodge, V.C. Hand, *Environ. Sci. Technol.*, 1990, **24**, 1013-1020

[2] D. B. Knaebel, T. W. Federle, D. C. McAvoy, J. R. Vestal, *Environ. Toxicol. Chem.,* 1996, **15**, 1865-1875

[3] J. Wang, B. Han, M. Dai, H. Yan, Z. Li, R. K. Thomas, *J. Colloid Interface Sci.*, 1999, **213**, 596-601

[4] *a* M. L. Cano, P. B. Dorn, *Environ. Toxicol. Chem.,* 1996, **15**, 684-690; *b.* M. L. Cano, P. B. Dorn, *Chemosphere,* 1996, **33**, 981-994; *c.* A. Kreisselmeier, H. W. Dürbeck, *J. Chromatogr. A,* 1997, **775**, 187-196; *a.* V.C. Hand, R.A. Rapaport, R.H. Wendt, *Environ. Toxicol. Chem.,* 1990, **9**, 467-471

[5] *a.* K. Fytianos, S. Pegiadou, N Raikkos, I. Eleftheruadis, H. Tsoukali, *Chemosphere*, 1997, **35**, 1423-1429; *b.* L. G. Mackay, M. Y. Croft, D. S. Selby, R. J. Wells, *J. AOAC Int.*, 1997, **80**, 401-407; *c.* M. Ahel, F. E. Scully, J. Hoigné, W. Giger, *Chemosphere*, 1994, **28**, 1361-1368; *d.* K. A. Evans, S. T. Dubey, L. Kravetz, I. Dzidic, J. Gumulka, R. Mueller, J. R. Stork, *Anal. Chem.*, 1994, **66**, 699-705; *e.* E. Mattijs, G. Debaere, N. Itrich, P. Masscheleyn, A. Rotters, M. Stalmans, T. Federle, *Water Sci. Tech.*, 1995, 31, 321-328; *f.* H. Fr. Schröder, *J. Chromatogr. A,* 1993, **647**, 219-234; *g.* E. Gonzalez-Mazo, A. Gomez-Parra, *Trends Anal. Chem.*, 1996, **15**, 375-380; *h.* E. Kubeck, C.G. Naylor, *JAOCS*, 1990, **67**, 400-405; *i.* A. Marcomini, G. Pojana, *Analusis*, 1997, **25**, M35-M37

[6] R.D. Swisher, *Surfactant Biodegradation*, 2nd Ed., 1987, Marcel Dekker Inc. Publishers, New York

[7] D. Y. Shang, R. W. MacDonald, M. G. Ikonomou, *Environ. Sci. Technol.*, 1999, **33**, 1366-1372

[8] D.Y. Shang, M.G. Ikonomou, R.W. Macdonald, *J. Chromatogr. A.*, 1999, **849**, 467-482

[9] *a.* C. Crescenzi, A. Di Corcia, R. Samperi, A. Marcomini, *Anal. Chem.*, 1995, **67**, 1797-1804; *b.* D.D. Popenoe, S.J. Morris, III, P.S. Horn, K.T. Norwood, *Anal. Chem.*, 1994, **66**, 1620-1629; *c.* S. Pattanaargsorn, P. Sangvanich, A. Petsom, S. Roeengsumran, *Analyst*, 1995, **120**, 1573-1576; *d.* M. Castillo, D. Barcelo, *Anal. Chem.*, 1999, **71**, 3769-3776; *e.* K.A. Evans, S.T. Dubey, L. Kravetz, S.W. Evetts, I. Dzidic, C.C. Dooyema, *J. Amer. Oil Chem. Soc.*, 1997, **74**, 765-773; *f.* M. Castillo, C.M. Alonso, J. Riu, D. Barcelo, *Environ. Sci. Tech.*, 1999, **33**, 1300-1306; *g.* S.D. Scullion, M.R. Clench, M. Cooke, A.E. Ashcroft, *J. Chromatogr. A.*, 1996, **733**, 207-216; *h.* H. Fr. Schröder, *J. Chromatogr. A,* 1997, **777**, 127-139

[10] K.B. Sherrard, P.J. Marriott, R.G. Amiet, R. Colton, M.J. McCormick, G.C. Smith, *Environ. Sci. Technol.*, 1995, **29**, 2235-2242

[11] K.B. Sherrard, P.J. Marriott, M.J. McCormick, R. Colton, G. Smith, *Anal. Chem.*, 1994, **66**, 3394-3399

[12] A. Di Corcia, C. Crescenzi, A. Marcomini, R. Samperi, *Environ. Sci. Technol.*, 1998, **32**, 711-718

[13] A. Di Corcia, A. Costantino, C. Crescenzi, E. Marinoni, R. Samperi, *Environ. Sci. Technol.*, 1998, **32**, 2401-2409

[14] *a.* G. You, G. D. Sayles, M. J. Kupferle, I. S. Kim, P. L. Bishop, *Chemosphere*, 1996, **32**, 2269-2284; *b.* M. Sanchez-Cmazano, E. Iglesias-Jimenez, M. J. Sanchez-Martin, *Chemosphere*, 1997, **35**, 3003-3012; *c.* F. S. Tanaka, R. G. Wien, E. R. Mansager, *J. Agric. Food Chem.*, 1981, **29**, 227-230

[15] G. Kuhnt, *Environ. Toxicol. Chem.*, 1993, **12**, 1813-1820

[16] G.F. White, *Wat. Sci. Tech.*, 1995, **31**, 61-70

[17] S. Matsui, Y. Sakamoto, T. Hirane, *Japanese Patent*, 1998, JP 10094703

[18] P.Y. Caux, P. Weinberger, A. Szabo, *Can. J. Bot.*, 1991, **71**, 1291-1297

[19] A.C. Nimrod, W.H. Benson, *Crit. Rev. Toxicol.*, 1996, **26**, 335-364

[20] T. Madsen, G. Petersen, C. Seiero, J. Torslov, *JAOCS*, 1996, **73**, 929-933

[21] *a.* P.J.G. Stevens, *NZ FRI Bulletin No. 193, Proc. 4th Int. Symp. on Adjuvants for Agrochemicals*, Ed. R.E. Gaskin, Melbourne, 1995, 345-349; *b.* E. F. C. Griessbach, A. Copin, R. Deleu, P. Dreze, *Sci. Total Environ.*, 1997, **201**, 89-98; *c.* E. F. C. Griessbach, A. Copin, R. Deleu, P. Dreze, *Sci. Total Environ.*, 1998, **221**, 159-169

[22] N. J. Fendinger, D. C. McAvoy, W. S. Eckhoff, B. B. Price, *Environ. Sci. Technol.*, 1997, **31**, 1555-1563

[23] C. Stevens, *J. Inorg. Biochem.*, 1998, **69**, 203-207

[24] *a.* J. C. Carpenter, J. A. Cella, S. B. Dorn, *Environ. Sci. Technol.*, 1995, **29**, 864-868; *b.* R. G. Lehmann, J. R. Miller, S. Xu, U. B. Singh, C. F. Reece, *Environ. Sci. Technol.*, 1998, **32**, 1260-1264; *c.* R. R. Buch, D. N. Ingebrigtson, *Environ. Sci. Technol.*, 1979, **13**, 676-679; *d.* S. Varaprath, R. G. Lehmann, *J. Environ. Polym. Degrad.*, 1997, **5**, 17-31; *e.* R. G. Lehmann, S. Varaprath, R. B. Annelin. J. L. Arndt, *Environ. Toxicol. Chem.*, 1995, **14**, 1299-1305; *f.* R. G. Lehmann, S. Varaprath, C.L. Frye, *Environ. Toxicol. Chem.*, 1994, **13**, 1753-1759; *g.* R. G. Lehmann, J. R. Miller, *Environ. Toxicol. Chem.*, 1996, **15**, 1455-1460; *h.* R. G. Lehmann, *Environ. Toxicol. Chem.*, 1993, **12**, 1851-1853; *i.* R. G. Lehmann, S. Varaprath, C.L. Frye, *Environ. Toxicol. Chem.*, 1994, **13**, 1061-1064

[25] S. Xu, R. G. Lehmann, J. R. Miller, G. Chandra, *Environ. Sci. Technol.*, 1998, **32**, 1199-1206

[26] S. Xu, *Environ. Sci. Technol.*, 1998, **32**, 3162-3168

[27] M. G. Voronkov, V. P. Mileshkevich, and Yu. A. Yuzhelevskii, *The Siloxane Bond – Physical Properties and Chemical Transformations*, Consultants Bureau, New York, 1978

[28] *a.* G.F. White, N.J. Russell, E.C. Tidswell, *Microbiol. Rev.*, 1996, **60**, 216-232; *b.* D.P. Cox, *Adv. Appl. Microbiol.*, 1978, **23**, 173-194; *c.* N. Jones, G.K. Watson, Biochem. Soc. Trans., 1976, 564th meeting, 891-892; *d.* J.R. Haines, M. Alexander, *Appl. Microbiol.*, 1975, **29**, 621-625

[29] P. M. Claesson, C. Gölander, *J. Colloid Interface Sci.*, 1987, **117**, 366-374

[30] L. Hong, E. Ruckenstein, *J. Chem. Soc., Chem. Commun.*, 1993, 1486-1487

[31] P. Aranda, E. Ruiz-Hitzky, *Chem. Mater.*, 1992, **4**, 1395-1403

[32] R. T. Podoll, K. C. Irwin, S. Brendlinger, *Environ. Sci. Technol.*, 1987, **21**, 562-568

[33] C. G. Gölander, J. N. Herron, K. Lim, P. Claesson, P. Steinius, J. D. Andrade, *Poly(Ethylene Glycol) Chem.*, Ed. J. M. Harris, Plenum Publishers, New York, 1992, 221-245

[34] E. F. C. Griessbach, A. Copin, R. Deleu, P. Dreze, *Sci. Total Environ.*, 1997, **201**, 89-98

[35] D. Coupland, J. A. Zabkiewicz, F. J. Ede, *Ann. Appl. Biol.*, 1989, **115**, 147-156

[36] P.J.G. Stevens, *Pestic. Sci*, 1993, **38**, 103-122

[37] M. Knoche, *Weed Res.*, 1994, **34**, 221-39

[38] *a.* K.B. Sherrard, P.J. Marriott, R.G. Amiet, R. Colton, M.J. McCormick, G.C. Smith, *Environ. Sci. Tech.*, 1995, **29**, 2235-2242; *b.* S. Tanaka, T. Ichikawa, *Wat. Sci. Tech.*, 1993, **28**, 103-110; *c.* K.B. Sherrard, P.J. Marriott, R.G. Amiet, M.J. McCormick, R. Colton, K. Millington, *Chemosphere*, 1996, **33**, 1921-1940; *d.* N. Nageswara Rao, S. Dube, *J. Mol. Catal. A: Chem.*, 1996, **104**, L197-L199; *e.* H. Hidaka, J. Zhao, Y. Satoh, K. Nohara, E. Pelizzetti, N. Serpone, *J. Mol. Catal.*, 1994, **88**, 239-248; *f.* J. Zhao, H. Hidaka, A. Takamura, E. Pelizzetti, N. Serpone, *Langmuir*, 1993, **9**, 1646-1650; *g.* S. Dube, N. Nageswara Rao, *J. Photochem. Photobiol. A: Chem.*, 1996, **93**, 71-77; *h.* H. Hidaka, K. Nohara, J. Zhao, E. Pelizzetti, N. Serpone, *J. Photochem. Photobiol. A: Chem.*, 1995, **91**, 145-152; *i.* E. Pelizzetti, C. Minero, V. Maurino, A. Sciafani, H. Hidaka, N. Serpone, *Environ. Sci. Technol.*, 1989, **23**, 1380-1385; *j.* H. Hidaka, Y. Asai, J. Zhao, K. Nohara, E. Pelizzetti, N. Serpone, *J. Phys. Chem.*, 1995, **99**, 8244-8248

[39] M.B. McBride, *Environmental chemistry of soils*, Oxford University Press, New York, 1994;

[40] D.G. Schulze, *Minerals in soil environments*, 2nd Edition, Eds. J. B. Dixon, S. B. Weed, Soil Science Society of America, Wisconsin, 1989, 1-34

[41] R.M. Taylor, *Chemistry of Clays and Clay Minerals*, Ed. A.C.D. Newman, Longman Scientific and Technical, 1987, 129-201

[42] M. Raksasataya, *Aspects of the Chemistry of Lead in Multiphase Soil Model Systems and the Environment*, Ph.D. Thesis, University of Waikato, 1998

[43] W.A. Forster, K.D. Steele, J.A. Zabkiewicz, *NZ FRI Bulletin No. 193, Proc. 4th Int. Symp. on Adjuvants for Agrochemicals*, NZ FRI Bulletin No. 193, Ed. R.E. Gaskin, Melbourne, 1995, 267-271

[44] J.B. Weber, H.D. Coble, *J. Agr. Food Chem.*, 1968, **16**, 475-478

[45] B.K.G. Theng, *Developments in Soil Science –Formation and Properties of Clay-Polymer Complexes*, Elsevier, NY, Vol. 9, 1979

[46] A. Torrents, S. Jayasundera, *Chemosphere*, 1997, **35**, 1549-1565

[47] B. Velde, *Developments in Sedimentology - Clay Minerals*, Elsevier, NY, Vol. 40, 1985

[48] B.K.G. Theng, *The Chemistry of Clay-Organic Reactions*, Adam Hilger Ltd, London, 1974

[49] P. L. Singleton, *DSIR Land Resources Scientific Report No. 5*, 1991

[50] H. Nagase, Y. Ose, T. Sato, *Sci. Total Environ.*, 1988, **73**, 29-38

APPENDICES

A.I MATERIALS

A.I.1 Chemicals

$CH_3O(EO)_3H$ (Lot No. 06009KQ), $CH_3O(EO)_nH$ (Ave Mol. Wt. 350, Lot No. 116HO940), $(ClCH_2CH_2OCH_2)_2$ and DOG (2-deoxy-D-glucose, a.k.a. 2-Deoxy-D-arabinohexose) were obtained from Sigma Aldrich. $HO(EO)_3H$ (anhydrous) from Fluka AG was used. $H_2PtCl_6.xH_2O$, $ClCH_2CH{=}CH_2$, $HOCH_2CH{=}CH_2$, HCl, $SOCl_2$, pyridine, isopropylamine (IPA), triethylamine (Et_3N) and Al_2O_3 (neutral, Brockman activity II) were obtained from BDH and SiO_2 (Silica gel 60, 0.063 – 0.200 mm) from Merck. NaOH (pellets) were from Scientific Supplies Ltd and NaH was obtained from Koch-Light Laboratories Ltd in pure powder form. $CH_3CO_2NH_4$ (AR grade) from Ajax and HCO_2H (AR reagent grade) from M&B Chemicals were used. Blankophor-P was obtained from Bayer, and Uvitex NFW, Uvitex CF and Erio Acid Red XB from Ciba-Geigy.

$ClCH_2CH{=}CH_2$ was distilled prior to the first use (Section 2.2.2.1 synthesis) but was not purified thereafter for subsequent syntheses. $HOCH_2CH{=}CH_2$ was freshly distilled before use (Section 2.2.2.4).

A.I.1.1 Organosilicones

Silwet L-77® (**1**, Batch No. 0642HA062590), Silwet L-408® (**2**, Batch No. 19555FO82194), $[Si(CH_3)_3\text{-}O\text{-}]_2\text{-}SiH(CH_3)$ (**3**, Y-12899, Lot No. 121311096) and $[Si(CH_3)_3\text{-}O\text{-}]_2\text{-}Si(CH_3)\text{-}CH_2CH_2CH_2\text{-}OCH_2CH_2\text{-}OH$ were obtained from Witco Corporation, Organosilicones Group, Tarrytown, NY.

A.I.1.2 Internal Standards

Triton X-45®, an octylphenol ethoxylate with mean molar EO = 5, was obtained from Rohm and Haas, Philadelphia, USA. Agral-90, a nonylphenol ethoxylate with mean molar EO = 9 containing ~ 10% isopropyalcohol, was purchased from ICI Chemicals, UK. Agral-100 was prepared by concentration under vacuum of the commercial Agral-90 product. PEG-400, a polyethylene glycol $(HO\text{-}[CH_2CH_2O]_n\text{-}H)$ of average molecular weight ~ 400, was obtained from Merck and PPG-425, a

polypropylene glycol (HO-$[CH_2CH_2CH_2O]_n$-H) of average molecular weight ~ 425 was from Aldrich Chemical Co. Triethylene glycol monohexyl ether (CH_3-$[CH_2]_5$-$O[CH_2CH_2O]_3$-H) was obtained from Sigma Aldrich (T-3644, Lot No. 36F0301). Jeffamine M-600 (R-$[CH_2CHR'O]_n$-$CH_2CH[CH_3]NH_2$; R, R' = PO/EO, 9:1) a polyoxyalkylene monoamine of average molecular weight ~ 600 was obtained from Texaco Chemical Company.

A.I.1.3 Active ingredients

Glyphosate (**17**, N-(phosphonomethyl)glycine) was obtained as a 98% pure solid from Monsanto and the [^{14}C]-glyphosate (2.0 GBq $mmol^{-1}$) was obtained from Amersham. Bentazone (**18**) was obtained as the sodium salt from BASF Germany, also the source of the [^{14}C]-bentazone.

A.I.2 Solvents

All H_2O used was distilled deionised Milli-Q H_2O and the MeOH, THF, petroleum spirits, isopropylalcohol, ether and EtOAc used were distilled drum grade, unless otherwise stated. AR grade (Analar) ethanol and acetonitrile were obtained from BDH, and AR grade (Univar) n-heptane from AJAX chemicals. HPLC grade acetonitrile (Hipersolv, BDH) and AR grade MeOH (Scharlau) were used for API/MS and HPLC analyses.

A.II INSTRUMENTATION AND GENERAL PROCEDURES

A.II.1 API/MS conditions

Analysis was performed with a VG Platform II mass spectrometer (Fisons/Micromass), equipped with multiple API interfaces (ESI and APcI). Ion separation and detection were by quadrupole mass filter and photomultipler, respectively. The instrument control and data processing was performed with the MassLynx 2.0 software. Sample injection was performed manually, as single pulse injections, via a Rheodyne Model 7125 injector. A Spectra System P1000 isocratic pump (Spectra-Physics Analytical) was used to deliver the eluant to the API interface. An elution solvent of 2:1 MeOH/H_2O and a 10 µL injector loop were used unless otherwise stated. For standard ESI/MS determinations, a fused silica capillary (Polysil, 75 µm id) was used to connect the injector and API interface, whilst for the higher flow rate methods PEEK tubing (200 µm id) was used.

Prior to all determinations the instrument was cleaned (counter electrode and sample cone) and then allowed to stabilise for a considerable length of time (at least 12 hours). The instrument was run with all operating conditions set for at least one hour preceding all measurements and therefore stability of the instrument and parameters is assumed.

The instrument conditions adopted were those established in Chapter 3 (Tables 3.3, 3.13 and 3.14) unless otherwise stated.

For qualitative determinations, NaCl (1 g L^{-1}), KCl (1 g L^{-1}) and NH_4CO_2H (5 g L^{-1}) salt solutions were added to sample preparations (~1:1) to aid assignment of peaks where necessary.

A.II.2 Quantitative HPLC conditions - detection by mass scattering light detection

A Biorad Model AS-100 automatic sampler and Rheodyne valve (sample loop volume 0.5 mL) was used for injection of samples. The pump was a Hewlett Packard Model 1050, operated isocratically. Detection was with a Varex ELSD Mk III light scattering mass detector, operating conditions typically: gas flow (air) 1.4 L min^{-1};

evaporator tube temperature, 90°C; time, 1 second (constant); and attenuation 1/32 or 1/16. A Hewlett Packard 3396A integrator was used to measure peak areas.

A.II.3 GC/MS conditions

A HP5890 GC coupled to a 5970 series mass selective detector was used for the GC/MS measurements. A HP-1 (crosslinked methyl siloxane) column of dimensions 25 m x 0.2 mm x 0.3 μm was used. Head pressure was set at 15 psi and total flow at ~ 100 mL min^{-1}. A temperature profile of 50 °C for 1 minute, followed by increments of 10 °C min^{-1} up to 280 °C, then 10 minutes at 280 °C was adopted. For some of the larger, less volatile analytes the GC was held at 280 °C for up to 30 minutes. Samples for analysis were prepared in CH_2Cl_2 (1 ppm).

A.II.4 FTICR/MS

Mass spectra were obtained using a Spectrospin CM-47 FTICR instrument,[‡] equipped with a cylindrical ICR cell (radius 30 x 60 mm) within a 4.7 T superconducting magnet. Samples were directly infused via a syringe pump operating at a flow rate of 1 μL min^{-1}. The instrument settings were as follows: UHV vacuum gauge, 10^{-10} - 10^{-11} mBar; SRC vacuum gauge, 10^{-7} - 10^{-6} mBar; drying gas, 10 L h^{-1}; heater 250-300°C. For ESI measurements settings of: Capillary, 1 kV; Skimmer, 0.7 kV; skimmer lens offset ,+/- 1 V; extraction voltage, 0 V; and Trp, 10 were adopted. Instrument settings of: drying gas, 5 L h^{-1}, 200°C; needle sheath gas, 60L h^{-1}; APcI heater, 200-350 °C; solvent flow-rate, 0.2-1 mL min^{-1}; cylinder, 1300-1400 V; end plate, 2500 V; and capillary, 2800 V were used for APcI measurements.

The instrument setting for SORI CID were as follows: JSB, 10 000; Vacuum gauge controller, V_1 and V_2 ~ 10^{-1} - 10^{-2} mBar; P(26), 5000-10 000 μsec; Ion Activation parameters: P(8), 250 000 μsec; PL(8), 40 dB; Ploff(0), -500 Hz; reaction delay, 2-3 sec.

All samples were prepared at 0.1 mg mL^{-1} concentrations in MeOH with 0.1 mg mL^{-1} of NaI added to facilitate ionisation.

[‡] School of Chemistry, University of New South Wales, Sydney, Australia

It was found that the oligomer distribution in the spectra obtained was affected by the offset setting, so it was important to acquire a number of spectra for each sample to determine all of the compounds actually present.

The nature of the acquisition is such that better resolution is achieved for lower molecular masses. For the scan range selected, half of the data points fall between the starting mass and two times the starting mass, a quarter of the data points fall between two and four times the starting mass, and so forth. Consequently highest accuracy is found for peaks falling between one and two times the starting mass and thus acquisition ranges were adjusted accordingly to allow maximum number of data points at the peak of interest.

A.II.5 NMR

^{1}H and ^{13}C NMR spectra were acquired on a Bruker DRX400 instrument, using the observation frequencies of 400.13 and 100.62 MHz respectively. Samples were prepared in $CDCl_3$ and referenced to $CHCl_3$ at 7.26 and 77.06 ppm, respectively. ^{29}Si NMR spectra were acquired on a Bruker AC300 instrument using an observation frequency of 59.63 MHz. Samples were prepared in $CDCl_3$ or measured neat, and were externally referenced to TMS at 0 ppm.

A.II.6 Powder X-ray diffraction (XRD)

XRD spectra were acquired using a Philips PW 1729 X-ray generator equipped with a PW 1840 diffractometer control and PM 8203A online recorder. Voltage and current were set at 22.5 kV and 20mA, respectively.

A.II.7 Spread area measurements

Spread areas of the solutions were determined by image analysis. The leaves were analysed under UV light using a calibrated JVC TK-1270 colour video camera (Canon FD 50 mm 1:3.5 lens) at 500 % magnification. The images were processed with V^{++} Precision Digital Imaging System (IMASCAN) software (Version 4) installed on a Compac Deskpro Pentium PC running on Windows 95.

A.II.8 Drying time measurements

The drying times were determined by monitoring the evaporative weight loss of the solutions with respect to time. A Precision 40SM-200A electronic balance and Balance-logger software installed on a Compac Concerto laptop computer were used.

A.II.9 Surface Tension measurements

Equilibrium surface tension values were obtained by the Wilhelmy plate method, using a Dynamic Contact Angle Analyzer (DCA Series 300, Cahn Instruments Inc.). Instrument control and data processing was performed with the Cahn software installed on a PC Direct 486 with Windows 3.1. The surface tension is determined by the measuring the force exerted on a perpendicular glass slide (due to the wetting of plate) as it is gradually immersed into the solution using a calibrated balance.

A.II.10 Concentration methods

All rotary evaporation was conducted in a water bath set to 40°C with suction via a water pump (25 mm Hg). Vacuum concentration was conducted at 2 mm Hg.

A.III CALCULATED MASSES OF COMPOUNDS (molecular and adduct)*

A.III.1 Silwet L-77 (1) and Silwet L-408 (2)

$(EO)_n$	1	H^+	NH_4^+	Na^+	K^+	2	H^+	NH_4^+	Na^+	K^+
0	294.5	295.5	312.5	317.5	333.5	280.5	281.5	298.5	303.5	319.4
1	338.5	339.5	356.6	361.5	377.5	324.5	325.5	342.5	347.5	363.5
2	382.5	383.6	400.6	405.5	421.5	368.5	369.5	386.6	391.5	407.5
3	426.6	427.6	444.6	449.6	465.5	412.6	413.6	430.6	435.5	451.5
4	470.6	471.6	488.6	493.6	509.6	456.6	457.6	474.6	479.6	495.5
5	514.6	515.6	532.7	537.6	553.6	500.6	501.6	518.6	523.6	539.6
6	558.6	559.7	576.7	581.6	597.6	544.6	545.6	562.7	567.6	583.6
7	602.7	603.7	620.7	625.7	641.6	588.7	589.7	606.7	611.6	627.6
8	646.7	647.7	664.7	669.7	685.7	632.7	633.7	650.7	655.7	671.6
9	690.7	691.7	708.8	713.7	729.7	676.7	677.7	694.7	699.7	715.7
10	734.8	735.8	752.8	757.7	773.7	720.7	721.7	738.8	743.7	759.7
11	778.8	779.8	796.8	801.8	817.7	764.8	765.8	782.8	787.8	803.7
12	822.8	823.8	840.8	845.8	861.8	808.8	809.8	826.8	831.8	847.8
13	866.8	867.8	884.9	889.8	905.8	852.8	853.8	870.8	875.8	891.8
14	910.9	911.9	928.9	933.8	949.8	896.8	897.8	914.9	919.8	935.8
15	954.9	955.9	972.9	977.9	993.8	940.9	941.9	958.9	963.9	979.8
16	998.9	999.9	1016.9	1021.9	1037.9	984.9	985.9	1002.9	1007.9	1023.9

A.III.2 PEG derivatives

$(EO)_n$	20	H^+	NH_4^+	Na^+	K^+	$HO(EO)_nH$	H^+	NH_4^+	Na^+	K^+
0	32	33	50	55	71	18	19	36	41	57
1	76	77	94	99	115	62	63	80	85	101
2	120	121	138	143	159	106	107	124	129	145
3	164	165	182	187	203	150	151	168	173	189
4	208	209	226	231	247	194	195	212	217	233
5	252	253	270	275	291	238	239	256	261	277
6	296	297	314	319	335	282	283	300	305	321
7	340	341	358	363	379	326	327	344	349	365
8	384	385	402	407	423	370	371	388	393	409
9	428	429	446	451	467	414	415	432	437	453
10	472	473	490	495	511	458	459	476	481	497
11	516	517	534	539	555	502	503	520	525	541
12	560	561	578	583	599	546	547	564	569	585
13	604	605	622	627	643	590	591	608	613	629
14	648	649	666	671	687	634	635	652	657	673
15	692	693	710	715	731	678	679	696	701	717
16	736	737	754	759	775	722	723	740	745	761

* The exact masses of the most abundant isotopes (Table 2.1) were used to calculate the listed masses

A.III.3 Allyl ethoxylates [$CH_2CH{=}CH_2O(EO)_nR$]

$(EO)_n$	R = CH_3	H^+	NH_4^+	Na^+	K^+	R = H	H^+	NH_4^+	Na^+	K^+
0	72	73	90	95	111	58	59	76	81	97
1	116	117	134	139	155	102	103	120	125	141
2	160	161	178	183	199	146	147	164	169	185
3	204	205	222	227	243	190	191	208	213	229
4	248	249	266	271	287	234	235	252	257	273
5	292	293	310	315	331	278	279	296	301	317
6	336	337	354	359	375	322	323	340	345	361
7	380	381	398	403	419	366	367	384	389	405
8	424	425	442	447	463	410	411	428	433	449
9	468	469	486	491	507	454	455	472	477	493
10	512	513	530	535	551	498	499	516	521	537
11	556	557	574	579	595	542	543	560	565	581
12	600	601	618	623	639	586	587	604	609	625
13	644	645	662	667	683	630	631	648	653	669
14	688	689	706	711	727	674	675	692	697	713
15	732	733	750	755	771	718	719	736	741	757
16	776	777	794	799	815	762	763	780	785	801

A.III.4 Compounds 9, 10 and 11

$(EO)_n$	9	H^+	NH_4^+	Na^+	K^+	10	H^+	NH_4^+	Na^+	K^+	11	H^+	NH_4^+	Na^+	K^+
0	278	279	296	301	317	206	207	224	229	245	134	135	152	157	173
1	322	323	340	345	361	250	251	268	273	289	178	179	196	201	217
2	366	367	384	389	405	294	295	312	317	333	222	223	240	245	261
3	410	411	428	433	449	338	339	356	361	377	266	267	284	289	305
4	454	455	472	477	493	382	383	400	405	421	310	311	328	333	349
5	498	499	516	521	537	426	427	444	449	465	354	355	372	377	393
6	542	543	560	565	581	470	471	488	493	509	398	399	416	421	437
7	586	587	604	609	625	514	515	532	537	553	442	443	460	465	481
8	630	631	648	653	669	558	559	576	581	597	486	487	504	509	525
9	674	675	692	697	713	602	603	620	625	641	530	531	548	553	569
10	718	719	736	741	757	646	647	664	669	685	574	575	592	597	613
11	762	763	780	785	801	690	691	708	713	729	618	619	636	641	657
12	806	807	824	829	845	734	735	752	757	773	662	663	680	685	701
13	850	851	868	873	889	778	779	796	801	817	706	707	724	729	745
14	894	895	912	917	933	822	823	841	845	861	750	751	768	773	789
15	938	939	956	961	977	867	868	885	889	905	794	795	812	817	833
16	982	983	1000	1005	1021	911	912	929	934	950	838	839	856	861	877

A.III.5 Internal standards

A.III.5.1 Alkylphenol ethoxylates [$C_mH_{2m+1}C_6H_4O(EO)_nH$]

$(EO)_n$	**Agral-90** (m = 9)	H^+	NH_4^+	Na^+	K^+	**Triton X-45** (m = 8)	H^+	NH_4^+	Na^+	K^+
0	220.2	221.2	238.2	243.2	259.1	206.2	207.2	224.2	229.2	245.1
1	264.2	265.2	282.2	287.2	303.2	250.2	251.2	268.2	273.2	289.2
2	308.2	309.2	326.3	331.2	347.2	294.2	295.2	312.3	317.2	333.2
3	352.3	353.3	370.3	375.3	391.2	338.2	339.3	356.3	361.2	377.2
4	396.3	397.3	414.3	419.3	435.3	382.3	383.3	400.3	405.3	421.2
5	440.3	441.3	458.3	463.3	479.3	426.3	427.3	444.3	449.3	465.3
6	484.3	485.3	502.4	507.3	523.3	470.3	471.3	488.4	493.3	509.3
7	528.4	529.4	546.4	551.4	567.3	514.3	515.4	532.4	537.3	553.3
8	572.4	573.4	590.4	595.4	611.4	558.4	559.4	576.4	581.4	597.3
9	616.4	617.4	634.5	639.4	655.4	602.4	603.4	620.4	625.4	641.4
10	660.4	661.5	678.5	683.4	699.4	646.4	647.4	664.5	669.4	685.4
11	704.5	705.5	722.5	727.5	743.4	690.5	691.5	708.5	713.4	729.4
12	748.5	749.5	766.5	771.5	787.5	734.5	735.5	752.5	757.5	773.4
13	792.5	793.5	810.6	815.5	831.5	778.5	779.5	796.5	801.5	817.5
14	836.5	837.6	854.6	859.5	875.5	822.5	823.5	840.6	845.5	861.5
15	880.6	881.6	898.6	903.6	919.5	866.6	867.6	884.6	889.5	905.5
16	924.6	925.6	942.6	947.6	963.6	910.6	911.6	928.6	933.6	949.5

A.III.5.2 Polyether derivatives

$(EO)_n$	PEG-400	H^+	NH_4^+	Na^+	K^+	PPG-425	H^+	NH_4^+	Na^+	K^+
0	18.0	19.0	36.0	41.0	57.0	18.0	19.0	36.0	41.0	57.0
1	62.0	63.0	80.1	85.0	101.0	76.1	77.1	94.1	99.0	115.0
2	106.1	107.1	124.1	129.1	145.0	134.1	135.1	152.1	157.1	173.1
3	150.1	151.1	168.1	173.1	189.1	192.1	193.1	210.2	215.1	231.1
4	194.1	195.1	212.1	217.1	233.1	250.2	251.2	268.2	273.2	289.1
5	238.1	239.1	256.2	261.1	277.1	308.2	309.2	326.3	331.2	347.2
6	282.2	283.2	300.2	305.2	321.2	366.3	367.3	384.3	389.3	405.2
7	326.2	327.2	344.2	349.2	365.2	424.3	425.3	442.3	447.3	463.3
8	370.2	371.2	388.3	393.2	409.2	482.3	483.4	500.4	505.3	521.3
9	414.2	415.3	432.3	437.2	453.3	540.4	541.4	558.4	563.4	579.4
10	458.3	459.3	476.3	481.3	497.3	598.4	599.4	616.5	621.4	637.4
11	502.3	503.3	520.3	525.3	541.3	656.5	657.5	674.5	679.5	695.4
12	546.3	547.3	564.4	569.3	585.3	714.5	715.5	732.5	737.5	753.5
13	590.3	591.4	608.4	613.3	629.4	772.6	773.6	790.6	795.5	811.5
14	634.4	635.4	652.4	657.4	673.4	830.6	831.6	848.6	853.6	869.6
15	678.4	679.4	696.4	701.4	717.4	888.6	889.6	906.7	911.6	927.6
16	722.4	723.4	740.5	745.4	761.5	946.7	947.7	964.7	969.7	985.6

A.III.6 Degradation Products of Silwet L-77

A.III.6.1 Linear monomers

$(EO)_n$	21	H^+	NH_4^+	Na^+	K^+	22	H^+	NH_4^+	Na^+	K^+
0	222	223	240	245	261	150	151	168	173	189
1	266	267	284	289	305	194	195	212	217	233
2	310	311	328	333	349	238	239	256	261	277
3	354	355	372	377	393	282	283	300	305	321
4	398	399	416	421	437	326	327	344	349	365
5	442	443	460	465	481	370	371	388	393	409
6	486	487	504	509	525	414	415	432	437	453
7	530	531	548	553	569	458	459	476	481	497
8	574	575	592	597	613	502	503	520	525	541
9	618	619	636	641	657	546	547	564	569	585
10	662	663	680	685	701	590	591	608	613	629
11	706	707	724	729	745	634	635	652	657	673
12	750	751	768	773	789	678	679	696	701	717
13	794	795	812	817	833	722	723	740	745	761
14	838	839	856	861	877	766	767	784	789	805
15	882	883	900	905	921	810	811	828	833	849
16	926	927	944	949	965	854	855	872	877	893

A.III.6.2 Linear dimers (24)

A.III.6.2.1 R^1, R^2 = H

	R^3, R^4 = H					R^3 = H, R^4 = $(EO)_nCH_3$					R^3, R^4 = $(EO)_nCH_3$				
$(EO)_n$		H^+	NH_4^+	Na^+	K^+		H^+	NH_4^+	Na^+	K^+		H^+	NH_4^+	Na^+	K^+
0	254	255	272	277	293	268	269	286	291	307	282	283	300	305	321
1	298	299	316	321	337	312	313	330	335	351	326	327	344	349	365
2	342	343	360	365	381	356	357	374	379	395	370	371	388	393	409
3	386	387	404	409	425	400	401	418	423	439	414	415	432	437	453
4	430	431	448	453	469	444	445	462	467	483	458	459	476	481	497
5	474	475	492	497	513	488	489	506	511	527	502	503	520	525	541
6	518	519	536	541	557	532	533	550	555	571	546	547	564	569	585
7	562	563	580	585	601	576	577	594	599	615	590	591	608	613	629
8	606	607	624	629	645	620	621	638	643	659	634	635	652	657	673
9	650	651	668	673	689	664	665	682	687	703	678	679	696	701	717
10	694	695	712	717	733	708	709	726	731	747	722	723	740	745	761
11	738	739	756	761	777	752	753	770	775	791	766	767	784	789	805
12	782	783	800	805	821	796	797	814	819	835	810	811	828	833	849
13	826	827	844	849	865	840	841	858	863	879	854	855	873	877	893
14	870	871	889	893	909	884	885	903	907	923	898	900	917	921	937
15	914	916	933	937	953	929	930	947	951	967	943	944	961	966	981
16	959	960	977	982	997	973	974	991	996	1011	987	988	1005	1010	1026
17	1003	1004	1021	1026	1042	1017	1018	1035	1040	1056	1031	1032	1049	1054	1070
18	1047	1048	1065	1070	1086	1061	1062	1079	1084	1100	1075	1076	1093	1098	1114
19	1091	1092	1109	1114	1130	1105	1106	1123	1128	1144	1119	1120	1137	1142	1158
20	1135	1136	1153	1158	1174	1149	1150	1167	1172	1188	1163	1164	1181	1186	1202
21	1179	1180	1197	1202	1218	1193	1194	1211	1216	1232	1207	1208	1225	1230	1246
22	1223	1224	1241	1246	1262	1237	1238	1255	1260	1276	1251	1252	1269	1274	1290
23	1267	1268	1285	1290	1306	1281	1282	1299	1304	1320	1295	1296	1313	1318	1334
24	1311	1312	1329	1334	1350	1325	1326	1343	1348	1364	1339	1340	1357	1362	1378
25	1355	1356	1373	1378	1394	1369	1370	1387	1392	1408	1383	1384	1401	1406	1422
26	1399	1400	1417	1422	1438	1413	1414	1431	1436	1452	1427	1428	1445	1450	1466
27	1443	1444	1461	1466	1482	1457	1458	1475	1480	1496	1471	1472	1489	1494	1510
28	1487	1488	1505	1510	1526	1501	1502	1519	1524	1540	1515	1516	1533	1538	1554
29	1531	1532	1549	1554	1570	1545	1546	1563	1568	1584	1559	1560	1577	1582	1598
30	1575	1576	1593	1598	1614	1589	1590	1607	1612	1628	1603	1604	1621	1626	1642
31	1619	1620	1637	1642	1658	1633	1634	1651	1656	1672	1647	1648	1665	1670	1686
32	1663	1664	1681	1686	1702	1677	1678	1695	1700	1716	1691	1692	1709	1714	1730

A.III.6.2.2 R^1 = H, R^2 = TMS

	R^3, R^4 = H					R^3 = H, R^4 = $(EO)_nCH_3$					R^3, R^4 = $(EO)_nCH_3$				
$(EO)_n$		H^+	NH_4^+	Na^+	K^+		H^+	NH_4^+	Na^+	K^+		H^+	NH_4^+	Na^+	K^+
0	326	327	344	349	365	340	341	358	363	379	354	355	372	377	393
1	370	371	388	393	409	384	385	402	407	423	398	399	416	421	437
2	414	415	432	437	453	428	429	446	451	467	442	443	460	465	481
3	458	459	476	481	497	472	473	490	495	511	486	487	504	509	525
4	502	503	520	525	541	516	517	534	539	555	530	531	548	553	569
5	546	547	564	569	585	560	561	578	583	599	574	575	592	597	613
6	590	591	608	613	629	604	605	622	627	643	618	619	636	641	657
7	634	635	652	657	673	648	649	666	671	687	662	663	680	685	701
8	678	679	696	701	717	692	693	710	715	731	706	707	724	729	745
9	722	723	740	745	761	736	737	754	759	775	750	751	768	773	789
10	766	767	784	789	805	780	781	798	803	819	794	795	812	817	833
11	810	811	828	833	849	824	825	842	847	863	838	839	856	861	877
12	854	855	872	877	893	868	869	887	891	907	882	883	901	905	921
13	898	899	917	921	937	912	914	931	935	951	927	928	945	950	965
14	943	944	961	965	981	957	958	975	980	995	971	972	989	994	1010
15	987	988	1005	1010	1025	1001	1002	1019	1024	1040	1015	1016	1033	1038	1054
16	1031	1032	1049	1054	1070	1045	1046	1063	1068	1084	1059	1060	1077	1082	1098
17	1075	1076	1093	1098	1114	1089	1090	1107	1112	1128	1103	1104	1121	1126	1142
18	1119	1120	1137	1142	1158	1133	1134	1151	1156	1172	1147	1148	1165	1170	1186
19	1163	1164	1181	1186	1202	1177	1178	1195	1200	1216	1191	1192	1209	1214	1230
20	1207	1208	1225	1230	1246	1221	1222	1239	1244	1260	1235	1236	1253	1258	1274
21	1251	1252	1269	1274	1290	1265	1266	1283	1288	1304	1279	1280	1297	1302	1318
22	1295	1296	1313	1318	1334	1309	1310	1327	1332	1348	1323	1324	1341	1346	1362
23	1339	1340	1357	1362	1378	1353	1354	1371	1376	1392	1367	1368	1385	1390	1406
24	1383	1384	1401	1406	1422	1397	1398	1415	1420	1436	1411	1412	1429	1434	1450
25	1427	1428	1445	1450	1466	1441	1442	1459	1464	1480	1455	1456	1473	1478	1494
26	1471	1472	1489	1494	1510	1485	1486	1503	1508	1524	1499	1500	1517	1522	1538
27	1515	1516	1533	1538	1554	1529	1530	1547	1552	1568	1543	1544	1561	1566	1582
28	1559	1560	1577	1582	1598	1573	1574	1591	1596	1612	1587	1588	1605	1610	1626
29	1603	1604	1621	1626	1642	1617	1618	1635	1640	1656	1631	1632	1649	1654	1670
30	1647	1648	1665	1670	1686	1661	1662	1679	1684	1700	1675	1676	1693	1698	1714
31	1691	1692	1709	1714	1730	1705	1706	1723	1728	1744	1719	1720	1737	1742	1758
32	1735	1736	1753	1758	1774	1749	1750	1767	1772	1788	1763	1764	1781	1786	1802

A.III.6.2.3 R^1, R^2 = TMS

	R^3, R^4 = H					R^3 = H, R^4 = $(EO)_nCH_3$					R^3, R^4 = $(EO)_nCH_3$				
$(EO)_n$		H^+	NH_4^+	Na^+	K^+		H^+	NH_4^+	Na^+	K^+		H^+	NH_4^+	Na^+	K^+
0	398	399	416	421	437	412	413	430	435	451	426	427	444	449	465
1	442	443	460	465	481	456	457	474	479	495	470	471	488	493	509
2	486	487	504	509	525	500	501	518	523	539	514	515	532	537	553
3	530	531	548	553	569	544	545	562	567	583	558	559	576	581	597
4	574	575	592	597	613	588	589	606	611	627	602	603	620	625	641
5	618	619	636	641	657	632	633	650	655	671	646	647	664	669	685
6	662	663	680	685	701	676	677	694	699	715	690	691	708	713	729
7	706	707	724	729	745	720	721	738	743	759	734	735	752	757	773
8	750	751	768	773	789	764	765	782	787	803	778	779	796	801	817
9	794	795	812	817	833	808	809	826	831	847	822	823	840	845	861
10	838	839	856	861	877	852	853	870	875	891	866	867	885	889	905
11	882	883	901	905	921	896	897	915	919	935	910	912	929	933	949
12	926	928	945	949	965	941	942	959	963	979	955	956	973	978	993
13	971	972	989	994	1009	985	986	1003	1008	1023	999	1000	1017	1022	1038
14	1015	1016	1033	1038	1054	1029	1030	1047	1052	1068	1043	1044	1061	1066	1082
15	1059	1060	1077	1082	1098	1073	1074	1091	1096	1112	1087	1088	1105	1110	1126
16	1103	1104	1121	1126	1142	1117	1118	1135	1140	1156	1131	1132	1149	1154	1170
17	1147	1148	1165	1170	1186	1161	1162	1179	1184	1200	1175	1176	1193	1198	1214
18	1191	1192	1209	1214	1230	1205	1206	1223	1228	1244	1219	1220	1237	1242	1258
19	1235	1236	1253	1258	1274	1249	1250	1267	1272	1288	1263	1264	1281	1286	1302
20	1279	1280	1297	1302	1318	1293	1294	1311	1316	1332	1307	1308	1325	1330	1346
21	1323	1324	1341	1346	1362	1337	1338	1355	1360	1376	1351	1352	1369	1374	1390
22	1367	1368	1385	1390	1406	1381	1382	1399	1404	1420	1395	1396	1413	1418	1434
23	1411	1412	1429	1434	1450	1425	1426	1443	1448	1464	1439	1440	1457	1462	1478
24	1455	1456	1473	1478	1494	1469	1470	1487	1492	1508	1483	1484	1501	1506	1522
25	1499	1500	1517	1522	1538	1513	1514	1531	1536	1552	1527	1528	1545	1550	1566
26	1543	1544	1561	1566	1582	1557	1558	1575	1580	1596	1571	1572	1589	1594	1610
27	1587	1588	1605	1610	1626	1601	1602	1619	1624	1640	1615	1616	1633	1638	1654
28	1631	1632	1649	1654	1670	1645	1646	1663	1668	1684	1659	1660	1677	1682	1698
29	1675	1676	1693	1698	1714	1689	1690	1707	1712	1728	1703	1704	1721	1726	1742
30	1719	1720	1737	1742	1758	1733	1734	1751	1756	1772	1747	1748	1765	1770	1786
31	1763	1764	1781	1786	1802	1777	1778	1795	1800	1816	1791	1792	1809	1814	1830
32	1807	1808	1825	1830	1846	1821	1822	1839	1844	1860	1835	1836	1853	1858	1874

A.III.6.3 Linear trimers (24)

A.III.6.3.1 R^1, R^2 = H

	R^3, R^4, R^5 = H					R^3, R^4 = H; R^5 = $(EO)_nCH_3$					R^3 = H; R^4, R^5 = $(EO)_nCH_3$					R^3, R^4, R^5 = $(EO)_nCH_3$				
$(EO)_n$		H^+	NH_4^+	Na^+	K^+		H^+	NH_4^+	Na^+	K^+		H^+	NH_4^+	Na^+	K^+		H^+	NH_4^+	Na^+	K^+
0	372	373	390	395	411	386	387	404	409	425	400	401	418	423	439	414	415	432	437	453
1	416	417	434	439	455	430	431	448	453	469	444	445	462	467	483	458	459	476	481	497
2	460	461	478	483	499	474	475	492	497	513	488	489	506	511	527	502	503	520	525	541
3	504	505	522	527	543	518	519	536	541	557	532	533	550	555	571	546	547	564	569	585
4	548	549	566	571	587	562	563	580	585	601	576	577	594	599	615	590	591	608	613	629
5	592	593	610	615	631	606	607	624	629	645	620	621	638	643	659	634	635	652	657	673
6	636	637	654	659	675	650	651	668	673	689	664	665	682	687	703	678	679	696	701	717
7	680	681	698	703	719	694	695	712	717	733	708	709	726	731	747	722	723	740	745	761
8	724	725	742	747	763	738	739	756	761	777	752	753	770	775	791	766	767	784	789	805
9	768	769	786	791	807	782	783	800	805	821	796	797	814	819	835	810	811	829	833	849
10	812	813	830	835	851	826	827	845	849	865	840	841	859	863	879	855	856	873	877	893
11	856	857	875	879	895	871	872	889	893	909	885	886	903	908	923	899	900	917	922	937
12	901	902	919	924	939	915	916	933	938	953	929	930	947	952	968	943	944	961	966	982
13	945	946	963	968	984	959	960	977	982	998	973	974	991	996	1012	987	988	1005	1010	1026
14	989	990	1007	1012	1028	1003	1004	1021	1026	1042	1017	1018	1035	1040	1056	1031	1032	1049	1054	1070
15	1033	1034	1051	1056	1072	1047	1048	1065	1070	1086	1061	1062	1079	1084	1100	1075	1076	1093	1098	1114
16	1077	1078	1095	1100	1116	1091	1092	1109	1114	1130	1105	1106	1123	1128	1144	1119	1120	1137	1142	1158
17	1121	1122	1139	1144	1160	1135	1136	1153	1158	1174	1149	1150	1167	1172	1188	1163	1164	1181	1186	1202
18	1165	1166	1183	1188	1204	1179	1180	1197	1202	1218	1193	1194	1211	1216	1232	1207	1208	1225	1230	1246
19	1209	1210	1227	1232	1248	1223	1224	1241	1246	1262	1237	1238	1255	1260	1276	1251	1252	1269	1274	1290
20	1253	1254	1271	1276	1292	1267	1268	1285	1290	1306	1281	1282	1299	1304	1320	1295	1296	1313	1318	1334
21	1297	1298	1315	1320	1336	1311	1312	1329	1334	1350	1325	1326	1343	1348	1364	1339	1340	1357	1362	1378
22	1341	1342	1359	1364	1380	1355	1356	1373	1378	1394	1369	1370	1387	1392	1408	1383	1384	1401	1406	1422
23	1385	1386	1403	1408	1424	1399	1400	1417	1422	1438	1413	1414	1431	1436	1452	1427	1428	1445	1450	1466
24	1429	1430	1447	1452	1468	1443	1444	1461	1466	1482	1457	1458	1475	1480	1496	1471	1472	1489	1494	1510
25	1473	1474	1491	1496	1512	1487	1488	1505	1510	1526	1501	1502	1519	1524	1540	1515	1516	1533	1538	1554
26	1517	1518	1535	1540	1556	1531	1532	1549	1554	1570	1545	1546	1563	1568	1584	1559	1560	1577	1582	1598
27	1561	1562	1579	1584	1600	1575	1576	1593	1598	1614	1589	1590	1607	1612	1628	1603	1604	1621	1626	1642

A.III.6.3.2 R^1 = H, R^2 = TMS

	R^3, R^4, R^5 = H					R^3, R^4 = H; R^5 = $(EO)_nCH_3$					R^3 = H; R^4, R^5 = $(EO)_nCH_3$					R^3, R^4, R^5 = $(EO)_nCH_3$				
$(EO)_n$		H^+	NH_4^+	Na^+	K^+		H^+	NH_4^+	Na^+	K^+		H^+	NH_4^+	Na^+	K^+		H^+	NH_4^+	Na^+	K^+
0	444	445	462	467	483	458	459	476	481	497	472	473	490	495	511	486	487	504	509	525
1	488	489	506	511	527	502	503	520	525	541	516	517	534	539	555	530	531	548	553	569
2	532	533	550	555	571	546	547	564	569	585	560	561	578	583	599	574	575	592	597	613
3	576	577	594	599	615	590	591	608	613	629	604	605	622	627	643	618	619	636	641	657
4	620	621	638	643	659	634	635	652	657	673	648	649	666	671	687	662	663	680	685	701
5	664	665	682	687	703	678	679	696	701	717	692	693	710	715	731	706	707	724	729	745
6	708	709	726	731	747	722	723	740	745	761	736	737	754	759	775	750	751	768	773	789
7	752	753	770	775	791	766	767	784	789	805	780	781	798	803	819	794	795	812	817	833
8	796	797	814	819	835	810	811	828	833	849	824	825	842	847	863	838	839	857	861	877
9	840	841	858	863	879	854	855	873	877	893	868	870	887	891	907	883	884	901	906	921
10	884	886	903	907	923	899	900	917	922	937	913	914	931	936	951	927	928	945	950	966
11	929	930	947	952	967	943	944	961	966	982	957	958	975	980	996	971	972	989	994	1010
12	973	974	991	996	1012	987	988	1005	1010	1026	1001	1002	1019	1024	1040	1015	1016	1033	1038	1054
13	1017	1018	1035	1040	1056	1031	1032	1049	1054	1070	1045	1046	1063	1068	1084	1059	1060	1077	1082	1098
14	1061	1062	1079	1084	1100	1075	1076	1093	1098	1114	1089	1090	1107	1112	1128	1103	1104	1121	1126	1142
15	1105	1106	1123	1128	1144	1119	1120	1137	1142	1158	1133	1134	1151	1156	1172	1147	1148	1165	1170	1186
16	1149	1150	1167	1172	1188	1163	1164	1181	1186	1202	1177	1178	1195	1200	1216	1191	1192	1209	1214	1230
17	1193	1194	1211	1216	1232	1207	1208	1225	1230	1246	1221	1222	1239	1244	1260	1235	1236	1253	1258	1274
18	1237	1238	1255	1260	1276	1251	1252	1269	1274	1290	1265	1266	1283	1288	1304	1279	1280	1297	1302	1318
19	1281	1282	1299	1304	1320	1295	1296	1313	1318	1334	1309	1310	1327	1332	1348	1323	1324	1341	1346	1362
20	1325	1326	1343	1348	1364	1339	1340	1357	1362	1378	1353	1354	1371	1376	1392	1367	1368	1385	1390	1406
21	1369	1370	1387	1392	1408	1383	1384	1401	1406	1422	1397	1398	1415	1420	1436	1411	1412	1429	1434	1450
22	1413	1414	1431	1436	1452	1427	1428	1445	1450	1466	1441	1442	1459	1464	1480	1455	1456	1473	1478	1494
23	1457	1458	1475	1480	1496	1471	1472	1489	1494	1510	1485	1486	1503	1508	1524	1499	1500	1517	1522	1538
24	1501	1502	1519	1524	1540	1515	1516	1533	1538	1554	1529	1530	1547	1552	1568	1543	1544	1561	1566	1582
25	1545	1546	1563	1568	1584	1559	1560	1577	1582	1598	1573	1574	1591	1596	1612	1587	1588	1605	1610	1626
26	1589	1590	1607	1612	1628	1603	1604	1621	1626	1642	1617	1618	1635	1640	1656	1631	1632	1649	1654	1670
27	1633	1634	1651	1656	1672	1647	1648	1665	1670	1686	1661	1662	1679	1684	1700	1675	1676	1693	1698	1714

A.III.6.3.3 R^1 , R^2 = TMS

	R^3, R^4, R^5 = H					R^3, R^4 = H; R^5 = $(EO)_nCH_3$					R^3 = H; R^4, R^5 = $(EO)_nCH_3$					R^3, R^4, R^5 = $(EO)_nCH_3$				
$(EO)_n$		H^+	NH_4^+	Na^+	K^+		H^+	NH_4^+	Na^+	K^+		H^+	NH_4^+	Na^+	K^+		H^+	NH_4^+	Na^+	K^+
0	516	517	534	539	555	530	531	548	553	569	544	545	562	567	583	558	559	576	581	597
1	560	561	578	583	599	574	575	592	597	613	588	589	606	611	627	602	603	620	625	641
2	604	605	622	627	643	618	619	636	641	657	632	633	650	655	671	646	647	664	669	685
3	648	649	666	671	687	662	663	680	685	701	676	677	694	699	715	690	691	708	713	729
4	692	693	710	715	731	706	707	724	729	745	720	721	738	743	759	734	735	752	757	773
5	736	737	754	759	775	750	751	768	773	789	764	765	782	787	803	778	779	796	801	817
6	780	781	798	803	819	794	795	812	817	833	808	809	826	831	847	822	823	840	845	861
7	824	825	842	847	863	838	839	856	861	877	852	853	871	875	891	866	867	885	889	905
8	868	869	887	891	907	882	883	901	905	921	897	898	915	919	935	911	912	929	934	949
9	913	914	931	935	951	927	928	945	950	965	941	942	959	964	979	955	956	973	978	994
10	957	958	975	980	995	971	972	989	994	1010	985	986	1003	1008	1024	999	1000	1017	1022	1038
11	1001	1002	1019	1024	1040	1015	1016	1033	1038	1054	1029	1030	1047	1052	1068	1043	1044	1061	1066	1082
12	1045	1046	1063	1068	1084	1059	1060	1077	1082	1098	1073	1074	1091	1096	1112	1087	1088	1105	1110	1126
13	1089	1090	1107	1112	1128	1103	1104	1121	1126	1142	1117	1118	1135	1140	1156	1131	1132	1149	1154	1170
14	1133	1134	1151	1156	1172	1147	1148	1165	1170	1186	1161	1162	1179	1184	1200	1175	1176	1193	1198	1214
15	1177	1178	1195	1200	1216	1191	1192	1209	1214	1230	1205	1206	1223	1228	1244	1219	1220	1237	1242	1258
16	1221	1222	1239	1244	1260	1235	1236	1253	1258	1274	1249	1250	1267	1272	1288	1263	1264	1281	1286	1302
17	1265	1266	1283	1288	1304	1279	1280	1297	1302	1318	1293	1294	1311	1316	1332	1307	1308	1325	1330	1346
18	1309	1310	1327	1332	1348	1323	1324	1341	1346	1362	1337	1338	1355	1360	1376	1351	1352	1369	1374	1390
19	1353	1354	1371	1376	1392	1367	1368	1385	1390	1406	1381	1382	1399	1404	1420	1395	1396	1413	1418	1434
20	1397	1398	1415	1420	1436	1411	1412	1429	1434	1450	1425	1426	1443	1448	1464	1439	1440	1457	1462	1478
21	1441	1442	1459	1464	1480	1455	1456	1473	1478	1494	1469	1470	1487	1492	1508	1483	1484	1501	1506	1522
22	1485	1486	1503	1508	1524	1499	1500	1517	1522	1538	1513	1514	1531	1536	1552	1527	1528	1545	1550	1566
23	1529	1530	1547	1552	1568	1543	1544	1561	1566	1582	1557	1558	1575	1580	1596	1571	1572	1589	1594	1610
24	1573	1574	1591	1596	1612	1587	1588	1605	1610	1626	1601	1602	1619	1624	1640	1615	1616	1633	1638	1654
25	1617	1618	1635	1640	1656	1631	1632	1649	1654	1670	1645	1646	1663	1668	1684	1659	1660	1677	1682	1698
26	1661	1662	1679	1684	1700	1675	1676	1693	1698	1714	1689	1690	1707	1712	1728	1703	1704	1721	1726	1742
27	1705	1706	1723	1728	1744	1719	1720	1737	1742	1758	1733	1734	1751	1756	1772	1747	1748	1765	1770	1786

A.III.6.4 Linear tetramers (23, m = 4)

A.III.6.4.1 R^1, R^2 = H

	$R^3 - R^6$ = H					$R^3 - R^5$ = H; $R^6 = (EO)_nCH_3$					R^3, R^4 = H; R^5, $R^6 = (EO)_nCH_3$					R^3 = H; $R^4 - R^6 = (EO)_nCH_3$					$R^3 - R^6 = (EO)_nCH_3$				
$(EO)_n$		H^+	NH_4^+	Na^+	K^+		H^+	NH_4^+	Na^+	K^+		H^+	NH_4^+	Na^+	K^+		H^+	NH_4^+	Na^+	K^+		H^+	NH_4^+	Na^+	K^+
0	490	491	508	513	529	504	505	522	527	543	518	519	536	541	557	532	533	550	555	571	546	547	564	569	585
1	534	535	552	557	573	548	549	566	571	587	562	563	580	585	601	576	577	594	599	615	590	591	608	613	629
2	578	579	596	601	617	592	593	610	615	631	606	607	624	629	645	620	621	638	643	659	634	635	652	657	673
3	622	623	640	645	661	636	637	654	659	675	650	651	668	673	689	664	665	682	687	703	678	679	696	701	717
4	666	667	684	689	705	680	681	698	703	719	694	695	712	717	733	708	709	726	731	747	722	723	740	745	761
5	710	711	728	733	749	724	725	742	747	763	738	739	756	761	777	752	753	770	775	791	766	767	784	789	805
6	754	755	772	777	793	768	769	786	791	807	782	783	800	805	821	796	797	814	819	835	810	811	828	833	849
7	798	799	816	821	837	812	813	830	835	851	826	827	844	849	865	840	841	858	863	879	854	855	873	877	893
8	842	843	860	865	881	856	857	874	879	895	870	871	889	893	909	884	885	903	907	923	899	900	917	922	937
9	886	887	905	909	925	900	901	919	923	939	915	916	933	937	953	929	930	947	952	967	943	944	961	966	982
10	931	932	949	953	969	945	946	963	968	983	959	960	977	982	997	973	974	991	996	1012	987	988	1005	1010	1026
11	975	976	993	998	1013	989	990	1007	1012	1028	1003	1004	1021	1026	1042	1017	1018	1035	1040	1056	1031	1032	1049	1054	1070
12	1019	1020	1037	1042	1058	1033	1034	1051	1056	1072	1047	1048	1065	1070	1086	1061	1062	1079	1084	1100	1075	1076	1093	1098	1114
13	1063	1064	1081	1086	1102	1077	1078	1095	1100	1116	1091	1092	1109	1114	1130	1105	1106	1123	1128	1144	1119	1120	1137	1142	1158
14	1107	1108	1125	1130	1146	1121	1122	1139	1144	1160	1135	1136	1153	1158	1174	1149	1150	1167	1172	1188	1163	1164	1181	1186	1202
15	1151	1152	1169	1174	1190	1165	1166	1183	1188	1204	1179	1180	1197	1202	1218	1193	1194	1211	1216	1232	1207	1208	1225	1230	1246
16	1195	1196	1213	1218	1234	1209	1210	1227	1232	1248	1223	1224	1241	1246	1262	1237	1238	1255	1260	1276	1251	1252	1269	1274	1290
17	1239	1240	1257	1262	1278	1253	1254	1271	1276	1292	1267	1268	1285	1290	1306	1281	1282	1299	1304	1320	1295	1296	1313	1318	1334
18	1283	1284	1301	1306	1322	1297	1298	1315	1320	1336	1311	1312	1329	1334	1350	1325	1326	1343	1348	1364	1339	1340	1357	1362	1378
19	1327	1328	1345	1350	1366	1341	1342	1359	1364	1380	1355	1356	1373	1378	1394	1369	1370	1387	1392	1408	1383	1384	1401	1406	1422
20	1371	1372	1389	1394	1410	1385	1386	1403	1408	1424	1399	1400	1417	1422	1438	1413	1414	1431	1436	1452	1427	1428	1445	1450	1466
21	1415	1416	1433	1438	1454	1429	1430	1447	1452	1468	1443	1444	1461	1466	1482	1457	1458	1475	1480	1496	1471	1472	1489	1494	1510
22	1459	1460	1477	1482	1498	1473	1474	1491	1496	1512	1487	1488	1505	1510	1526	1501	1502	1519	1524	1540	1515	1516	1533	1538	1554
23	1503	1504	1521	1526	1542	1517	1518	1535	1540	1556	1531	1532	1549	1554	1570	1545	1546	1563	1568	1584	1559	1560	1577	1582	1598
24	1547	1548	1565	1570	1586	1561	1562	1579	1584	1600	1575	1576	1593	1598	1614	1589	1590	1607	1612	1628	1603	1604	1621	1626	1642
25	1591	1592	1609	1614	1630	1605	1606	1623	1628	1644	1619	1620	1637	1642	1658	1633	1634	1651	1656	1672	1647	1648	1665	1670	1686
26	1635	1636	1653	1658	1674	1649	1650	1667	1672	1688	1663	1664	1681	1686	1702	1677	1678	1695	1700	1716	1691	1692	1709	1714	1730

A.III.6.4.2 R^1 = H, R^2 = TMS

	$R^3 - R^6$ = H					$R^3 - R^5$ = H; $R^6 = (EO)_nCH_3$					R^3, R^4 = H; R^5, $R^6 = (EO)_nCH_3$					R^3 = H; $R^4 - R^6 = (EO)_nCH_3$					$R^3 - R^6 = (EO)_nCH_3$				
$(EO)_n$		H^+	NH_4^+	Na^+	K^+		H^+	NH_4^+	Na^+	K^+		H^+	NH_4^+	Na^+	K^+		H^+	NH_4^+	Na^+	K^+		H^+	NH_4^+	Na^+	K^+
0	562	563	580	585	601	576	577	594	599	615	590	591	608	613	629	604	605	622	627	643	618	619	636	641	657
1	606	607	624	629	645	620	621	638	643	659	634	635	652	657	673	648	649	666	671	687	662	663	680	685	701
2	650	651	668	673	689	664	665	682	687	703	678	679	696	701	717	692	693	710	715	731	706	707	724	729	745
3	694	695	712	717	733	708	709	726	731	747	722	723	740	745	761	736	737	754	759	775	750	751	768	773	789
4	738	739	756	761	777	752	753	770	775	791	766	767	784	789	805	780	781	798	803	819	794	795	812	817	833
5	782	783	800	805	821	796	797	814	819	835	810	811	828	833	849	824	825	842	847	863	838	839	857	861	877
6	826	827	844	849	865	840	841	858	863	879	854	855	872	877	893	868	869	886	891	907	882	884	901	905	921
7	870	871	888	893	909	884	885	902	907	923	898	899	917	921	937	912	914	931	935	951	927	928	945	950	965
8	914	915	933	937	953	928	930	947	951	967	943	944	961	965	981	957	958	975	980	995	971	972	989	994	1010
9	959	960	977	981	997	973	974	991	996	1011	987	988	1005	1010	1026	1001	1002	1019	1024	1040	1015	1016	1033	1038	1054
10	1003	1004	1021	1026	1042	1017	1018	1035	1040	1056	1031	1032	1049	1054	1070	1045	1046	1063	1068	1084	1059	1060	1077	1082	1098
11	1047	1048	1065	1070	1086	1061	1062	1079	1084	1100	1075	1076	1093	1098	1114	1089	1090	1107	1112	1128	1103	1104	1121	1126	1142
12	1091	1092	1109	1114	1130	1105	1106	1123	1128	1144	1119	1120	1137	1142	1158	1133	1134	1151	1156	1172	1147	1148	1165	1170	1186
13	1135	1136	1153	1158	1174	1149	1150	1167	1172	1188	1163	1164	1181	1186	1202	1177	1178	1195	1200	1216	1191	1192	1209	1214	1230
14	1179	1180	1197	1202	1218	1193	1194	1211	1216	1232	1207	1208	1225	1230	1246	1221	1222	1239	1244	1260	1235	1236	1253	1258	1274
15	1223	1224	1241	1246	1262	1237	1238	1255	1260	1276	1251	1252	1269	1274	1290	1265	1266	1283	1288	1304	1279	1280	1297	1302	1318
16	1267	1268	1285	1290	1306	1281	1282	1299	1304	1320	1295	1296	1313	1318	1334	1309	1310	1327	1332	1348	1323	1324	1341	1346	1362
17	1311	1312	1329	1334	1350	1325	1326	1343	1348	1364	1339	1340	1357	1362	1378	1353	1354	1371	1376	1392	1367	1368	1385	1390	1406
18	1355	1356	1373	1378	1394	1369	1370	1387	1392	1408	1383	1384	1401	1406	1422	1397	1398	1415	1420	1436	1411	1412	1429	1434	1450
19	1399	1400	1417	1422	1438	1413	1414	1431	1436	1452	1427	1428	1445	1450	1466	1441	1442	1459	1464	1480	1455	1456	1473	1478	1494
20	1443	1444	1461	1466	1482	1457	1458	1475	1480	1496	1471	1472	1489	1494	1510	1485	1486	1503	1508	1524	1499	1500	1517	1522	1538
21	1487	1488	1505	1510	1526	1501	1502	1519	1524	1540	1515	1516	1533	1538	1554	1529	1530	1547	1552	1568	1543	1544	1561	1566	1582
22	1531	1532	1549	1554	1570	1545	1546	1563	1568	1584	1559	1560	1577	1582	1598	1573	1574	1591	1596	1612	1587	1588	1605	1610	1626
23	1575	1576	1593	1598	1614	1589	1590	1607	1612	1628	1603	1604	1621	1626	1642	1617	1618	1635	1640	1656	1631	1632	1649	1654	1670
24	1619	1620	1637	1642	1658	1633	1634	1651	1656	1672	1647	1648	1665	1670	1686	1661	1662	1679	1684	1700	1675	1676	1693	1698	1714
25	1663	1664	1681	1686	1702	1677	1678	1695	1700	1716	1691	1692	1709	1714	1730	1705	1706	1723	1728	1744	1719	1720	1737	1742	1758
26	1707	1708	1725	1730	1746	1721	1722	1739	1744	1760	1735	1736	1753	1758	1774	1749	1750	1767	1772	1788	1763	1764	1781	1786	1802

A.III.6.4.3 R^1, R^2 = TMS

	$R^3 - R^6 = H$					$R^3 - R^5 = H$; $R^6 = (EO)_nCH_3$					R^3, $R^4 = H$; R^5, $R^6 = (EO)_nCH_3$					$R^3 = H$; $R^4 - R^6 = (EO)_nCH_3$					$R^3 - R^6 = (EO)_nCH_3$				
$(EO)_n$		H^+	NH_4^+	Na^+	K^+		H^+	NH_4^+	Na^+	K^+		H^+	NH_4^+	Na^+	K^+		H^+	NH_4^+	Na^+	K^+		H^+	NH_4^+	Na^+	K^+
0	634	635	652	657	673	648	649	666	671	687	662	663	680	685	701	676	677	694	699	715	690	691	708	713	729
1	678	679	696	701	717	692	693	710	715	731	706	707	724	729	745	720	721	738	743	759	734	735	752	757	773
2	722	723	740	745	761	736	737	754	759	775	750	751	768	773	789	764	765	782	787	803	778	779	796	801	817
3	766	767	784	789	805	780	781	798	803	819	794	795	812	817	833	808	809	826	831	847	822	823	840	845	861
4	810	811	828	833	849	824	825	842	847	863	838	839	856	861	877	852	853	870	875	891	866	867	885	889	905
5	854	855	872	877	893	868	869	886	891	907	882	883	900	905	921	896	897	915	919	935	911	912	929	933	949
6	898	899	916	921	937	912	913	931	935	951	926	927	945	949	965	941	942	959	963	979	955	956	973	978	994
7	942	943	961	965	981	957	958	975	979	995	971	972	989	994	1009	985	986	1003	1008	1023	999	1000	1017	1022	1038
8	987	988	1005	1010	1025	1001	1002	1019	1024	1039	1015	1016	1033	1038	1054	1029	1030	1047	1052	1068	1043	1044	1061	1066	1082
9	1031	1032	1049	1054	1070	1045	1046	1063	1068	1084	1059	1060	1077	1082	1098	1073	1074	1091	1096	1112	1087	1088	1105	1110	1126
10	1075	1076	1093	1098	1114	1089	1090	1107	1112	1128	1103	1104	1121	1126	1142	1117	1118	1135	1140	1156	1131	1132	1149	1154	1170
11	1119	1120	1137	1142	1158	1133	1134	1151	1156	1172	1147	1148	1165	1170	1186	1161	1162	1179	1184	1200	1175	1176	1193	1198	1214
12	1163	1164	1181	1186	1202	1177	1178	1195	1200	1216	1191	1192	1209	1214	1230	1205	1206	1223	1228	1244	1219	1220	1237	1242	1258
13	1207	1208	1225	1230	1246	1221	1222	1239	1244	1260	1235	1236	1253	1258	1274	1249	1250	1267	1272	1288	1263	1264	1281	1286	1302
14	1251	1252	1269	1274	1290	1265	1266	1283	1288	1304	1279	1280	1297	1302	1318	1293	1294	1311	1316	1332	1307	1308	1325	1330	1346
15	1295	1296	1313	1318	1334	1309	1310	1327	1332	1348	1323	1324	1341	1346	1362	1337	1338	1355	1360	1376	1351	1352	1369	1374	1390
16	1339	1340	1357	1362	1378	1353	1354	1371	1376	1392	1367	1368	1385	1390	1406	1381	1382	1399	1404	1420	1395	1396	1413	1418	1434
17	1383	1384	1401	1406	1422	1397	1398	1415	1420	1436	1411	1412	1429	1434	1450	1425	1426	1443	1448	1464	1439	1440	1457	1462	1478
18	1427	1428	1445	1450	1466	1441	1442	1459	1464	1480	1455	1456	1473	1478	1494	1469	1470	1487	1492	1508	1483	1484	1501	1506	1522
19	1471	1472	1489	1494	1510	1485	1486	1503	1508	1524	1499	1500	1517	1522	1538	1513	1514	1531	1536	1552	1527	1528	1545	1550	1566
20	1515	1516	1533	1538	1554	1529	1530	1547	1552	1568	1543	1544	1561	1566	1582	1557	1558	1575	1580	1596	1571	1572	1589	1594	1610
21	1559	1560	1577	1582	1598	1573	1574	1591	1596	1612	1587	1588	1605	1610	1626	1601	1602	1619	1624	1640	1615	1616	1633	1638	1654
22	1603	1604	1621	1626	1642	1617	1618	1635	1640	1656	1631	1632	1649	1654	1670	1645	1646	1663	1668	1684	1659	1660	1677	1682	1698
23	1647	1648	1665	1670	1686	1661	1662	1679	1684	1700	1675	1676	1693	1698	1714	1689	1690	1707	1712	1728	1703	1704	1721	1726	1742
24	1691	1692	1709	1714	1730	1705	1706	1723	1728	1744	1719	1720	1737	1742	1758	1733	1734	1751	1756	1772	1747	1748	1765	1770	1786
25	1735	1736	1753	1758	1774	1749	1750	1767	1772	1788	1763	1764	1781	1786	1802	1777	1778	1795	1800	1816	1791	1792	1809	1814	1830
26	1779	1780	1797	1802	1818	1793	1794	1811	1816	1832	1807	1808	1825	1830	1846	1821	1822	1839	1844	1860	1835	1836	1853	1858	1874

A.III.6.5 Linear pentamers (23, m = 5)

A.III.6.5.1 R^1, R^2 = H

	$R^3 - R^7$ = H					$R^3 - R^6$ = H; $R^7 = (EO)_nCH_3$					$R^3 - R^5$ = H; R^6, $R^7 = (EO)_nCH_3$				
$(EO)_n$		H^+	NH_4^+	Na^+	K^+		H^+	NH_4^+	Na^+	K^+		H^+	NH_4^+	Na^+	K^+
0	608	609	626	631	647	622	623	640	645	661	636	637	654	659	675
1	652	653	670	675	691	666	667	684	689	705	680	681	698	703	719
2	696	697	714	719	735	710	711	728	733	749	724	725	742	747	763
3	740	741	758	763	779	754	755	772	777	793	768	769	786	791	807
4	784	785	802	807	823	798	799	816	821	837	812	813	830	835	851
5	828	829	846	851	867	842	843	860	865	881	856	857	874	879	895
6	872	873	890	895	911	886	887	904	909	925	900	901	918	923	939
7	916	917	934	939	955	930	931	949	953	969	944	945	963	967	983
8	960	961	979	983	999	974	976	993	997	1013	989	990	1007	1012	1027
9	1005	1006	1023	1028	1043	1019	1020	1037	1042	1057	1033	1034	1051	1056	1072
10	1049	1050	1067	1072	1088	1063	1064	1081	1086	1102	1077	1078	1095	1100	1116
11	1093	1094	1111	1116	1132	1107	1108	1125	1130	1146	1121	1122	1139	1144	1160
12	1137	1138	1155	1160	1176	1151	1152	1169	1174	1190	1165	1166	1183	1188	1204
13	1181	1182	1199	1204	1220	1195	1196	1213	1218	1234	1209	1210	1227	1232	1248
14	1225	1226	1243	1248	1264	1239	1240	1257	1262	1278	1253	1254	1271	1276	1292
15	1269	1270	1287	1292	1308	1283	1284	1301	1306	1322	1297	1298	1315	1320	1336
16	1313	1314	1331	1336	1352	1327	1328	1345	1350	1366	1341	1342	1359	1364	1380
17	1357	1358	1375	1380	1396	1371	1372	1389	1394	1410	1385	1386	1403	1408	1424
18	1401	1402	1419	1424	1440	1415	1416	1433	1438	1454	1429	1430	1447	1452	1468
19	1445	1446	1463	1468	1484	1459	1460	1477	1482	1498	1473	1474	1491	1496	1512
20	1489	1490	1507	1512	1528	1503	1504	1521	1526	1542	1517	1518	1535	1540	1556
21	1533	1534	1551	1556	1572	1547	1548	1565	1570	1586	1561	1562	1579	1584	1600
22	1577	1578	1595	1600	1616	1591	1592	1609	1614	1630	1605	1606	1623	1628	1644
23	1621	1622	1639	1644	1660	1635	1636	1653	1658	1674	1649	1650	1667	1672	1688
24	1665	1666	1683	1688	1704	1679	1680	1697	1702	1718	1693	1694	1711	1716	1732
25	1709	1710	1727	1732	1748	1723	1724	1741	1746	1762	1737	1738	1755	1760	1776
26	1753	1754	1771	1776	1792	1767	1768	1785	1790	1806	1781	1782	1799	1804	1820
27	1797	1798	1815	1820	1836	1811	1812	1829	1834	1850	1825	1826	1843	1848	1864
28	1841	1842	1859	1864	1880	1855	1856	1873	1878	1894	1869	1870	1887	1892	1908
29	1885	1886	1903	1908	1924	1899	1900	1917	1922	1938	1913	1914	1931	1936	1952
30	1929	1930	1947	1952	1968	1943	1944	1961	1966	1982	1957	1958	1975	1980	1996
31	1973	1974	1991	1996	2012	1987	1988	2005	2010	2026	2001	2002	2019	2024	2040
32	2017	2018	2035	2040	2056	2031	2032	2049	2054	2070	2045	2046	2063	2068	2084
33	2061	2062	2079	2084	2100	2075	2076	2093	2098	2114	2089	2090	2107	2112	2128
34	2105	2106	2123	2128	2144	2119	2120	2137	2142	2158	2133	2134	2151	2156	2172
35	2149	2150	2167	2172	2188	2163	2164	2181	2186	2202	2177	2178	2195	2200	2216
36	2193	2194	2211	2216	2232	2207	2208	2225	2230	2246	2221	2222	2239	2244	2260
37	2237	2238	2255	2260	2276	2251	2252	2269	2274	2290	2265	2266	2283	2288	2304
38	2281	2282	2299	2304	2320	2295	2296	2313	2318	2334	2309	2310	2327	2332	2348
39	2325	2326	2343	2348	2364	2339	2340	2357	2362	2378	2353	2354	2372	2376	2392
40	2369	2370	2388	2392	2408	2383	2384	2402	2406	2422	2398	2399	2416	2420	2436
41	2414	2415	2432	2436	2452	2428	2429	2446	2451	2466	2442	2443	2460	2465	2481
42	2458	2459	2476	2481	2497	2472	2473	2490	2495	2511	2486	2487	2504	2509	2525
43	2502	2503	2520	2525	2541	2516	2517	2534	2539	2555	2530	2531	2548	2553	2569

A.III.6.5.1 (continued) $R^1, R^2 = H$

	$R^3, R^4 = H;$ $R^5 - R^7 = (EO)_nCH_3$					$R^3 = H;$ $R^4 - R^7 = (EO)_nCH_3$					$R^3 - R^7 = (EO)_nCH_3$				
$(EO)_n$		H^+	NH_4^+	Na^+	K^+		H^+	NH_4^+	Na^+	K^+		H^+	NH_4^+	Na^+	K^+
0	650	651	668	673	689	664	665	682	687	703	678	679	696	701	717
1	694	695	712	717	733	708	709	726	731	747	722	723	740	745	761
2	738	739	756	761	777	752	753	770	775	791	766	767	784	789	805
3	782	783	800	805	821	796	797	814	819	835	810	811	828	833	849
4	826	827	844	849	865	840	841	858	863	879	854	855	872	877	893
5	870	871	888	893	909	884	885	902	907	923	898	899	917	921	937
6	914	915	933	937	953	928	929	947	951	967	942	944	961	965	981
7	958	960	977	981	997	973	974	991	996	1011	987	988	1005	1010	1025
8	1003	1004	1021	1026	1041	1017	1018	1035	1040	1056	1031	1032	1049	1054	1070
9	1047	1048	1065	1070	1086	1061	1062	1079	1084	1100	1075	1076	1093	1098	1114
10	1091	1092	1109	1114	1130	1105	1106	1123	1128	1144	1119	1120	1137	1142	1158
11	1135	1136	1153	1158	1174	1149	1150	1167	1172	1188	1163	1164	1181	1186	1202
12	1179	1180	1197	1202	1218	1193	1194	1211	1216	1232	1207	1208	1225	1230	1246
13	1223	1224	1241	1246	1262	1237	1238	1255	1260	1276	1251	1252	1269	1274	1290
14	1267	1268	1285	1290	1306	1281	1282	1299	1304	1320	1295	1296	1313	1318	1334
15	1311	1312	1329	1334	1350	1325	1326	1343	1348	1364	1339	1340	1357	1362	1378
16	1355	1356	1373	1378	1394	1369	1370	1387	1392	1408	1383	1384	1401	1406	1422
17	1399	1400	1417	1422	1438	1413	1414	1431	1436	1452	1427	1428	1445	1450	1466
18	1443	1444	1461	1466	1482	1457	1458	1475	1480	1496	1471	1472	1489	1494	1510
19	1487	1488	1505	1510	1526	1501	1502	1519	1524	1540	1515	1516	1533	1538	1554
20	1531	1532	1549	1554	1570	1545	1546	1563	1568	1584	1559	1560	1577	1582	1598
21	1575	1576	1593	1598	1614	1589	1590	1607	1612	1628	1603	1604	1621	1626	1642
22	1619	1620	1637	1642	1658	1633	1634	1651	1656	1672	1647	1648	1665	1670	1686
23	1663	1664	1681	1686	1702	1677	1678	1695	1700	1716	1691	1692	1709	1714	1730
24	1707	1708	1725	1730	1746	1721	1722	1739	1744	1760	1735	1736	1753	1758	1774
25	1751	1752	1769	1774	1790	1765	1766	1783	1788	1804	1779	1780	1797	1802	1818
26	1795	1796	1813	1818	1834	1809	1810	1827	1832	1848	1823	1824	1841	1846	1862
27	1839	1840	1857	1862	1878	1853	1854	1871	1876	1892	1867	1868	1885	1890	1906
28	1883	1884	1901	1906	1922	1897	1898	1915	1920	1936	1911	1912	1929	1934	1950
29	1927	1928	1945	1950	1966	1941	1942	1959	1964	1980	1955	1956	1973	1978	1994
30	1971	1972	1989	1994	2010	1985	1986	2003	2008	2024	1999	2000	2017	2022	2038
31	2015	2016	2033	2038	2054	2029	2030	2047	2052	2068	2043	2044	2061	2066	2082
32	2059	2060	2077	2082	2098	2073	2074	2091	2096	2112	2087	2088	2105	2110	2126
33	2103	2104	2121	2126	2142	2117	2118	2135	2140	2156	2131	2132	2149	2154	2170
34	2147	2148	2165	2170	2186	2161	2162	2179	2184	2200	2175	2176	2193	2198	2214
35	2191	2192	2209	2214	2230	2205	2206	2223	2228	2244	2219	2220	2237	2242	2258
36	2235	2236	2253	2258	2274	2249	2250	2267	2272	2288	2263	2264	2281	2286	2302
37	2279	2280	2297	2302	2318	2293	2294	2311	2316	2332	2307	2308	2325	2330	2346
38	2323	2324	2341	2346	2362	2337	2338	2356	2360	2376	2351	2352	2370	2374	2390
39	2367	2368	2386	2390	2406	2382	2383	2400	2404	2420	2396	2397	2414	2419	2434
40	2412	2413	2430	2435	2450	2426	2427	2444	2449	2465	2440	2441	2458	2463	2479
41	2456	2457	2474	2479	2495	2470	2471	2488	2493	2509	2484	2485	2502	2507	2523
42	2500	2501	2518	2523	2539	2514	2515	2532	2537	2553	2528	2529	2546	2551	2567
43	2544	2545	2562	2567	2583	2558	2559	2576	2581	2597	2572	2573	2590	2595	2611

A.III.6.5.2 $R^1 = H$, $R^2 = TMS$

	$R^3 - R^7 = H$					$R^3 - R^6 = H$; $R^7 = (EO)_nCH_3$					$R^3 - R^5 = H$; $R^6, R^7 = (EO)_nCH_3$				
$(EO)_n$		H^+	NH_4^+	Na^+	K^+		H^+	NH_4^+	Na^+	K^+		H^+	NH_4^+	Na^+	K^+
0	680	681	698	703	719	694	695	712	717	733	708	709	726	731	747
1	724	725	742	747	763	738	739	756	761	777	752	753	770	775	791
2	768	769	786	791	807	782	783	800	805	821	796	797	814	819	835
3	812	813	830	835	851	826	827	844	849	865	840	841	858	863	879
4	856	857	874	879	895	870	871	888	893	909	884	885	902	907	923
5	900	901	918	923	939	914	915	932	937	953	928	929	946	951	967
6	944	945	962	967	983	958	959	977	981	997	972	974	991	995	1011
7	988	989	1007	1011	1027	1003	1004	1021	1025	1041	1017	1018	1035	1040	1055
8	1033	1034	1051	1056	1071	1047	1048	1065	1070	1086	1061	1062	1079	1084	1100
9	1077	1078	1095	1100	1116	1091	1092	1109	1114	1130	1105	1106	1123	1128	1144
10	1121	1122	1139	1144	1160	1135	1136	1153	1158	1174	1149	1150	1167	1172	1188
11	1165	1166	1183	1188	1204	1179	1180	1197	1202	1218	1193	1194	1211	1216	1232
12	1209	1210	1227	1232	1248	1223	1224	1241	1246	1262	1237	1238	1255	1260	1276
13	1253	1254	1271	1276	1292	1267	1268	1285	1290	1306	1281	1282	1299	1304	1320
14	1297	1298	1315	1320	1336	1311	1312	1329	1334	1350	1325	1326	1343	1348	1364
15	1341	1342	1359	1364	1380	1355	1356	1373	1378	1394	1369	1370	1387	1392	1408
16	1385	1386	1403	1408	1424	1399	1400	1417	1422	1438	1413	1414	1431	1436	1452
17	1429	1430	1447	1452	1468	1443	1444	1461	1466	1482	1457	1458	1475	1480	1496
18	1473	1474	1491	1496	1512	1487	1488	1505	1510	1526	1501	1502	1519	1524	1540
19	1517	1518	1535	1540	1556	1531	1532	1549	1554	1570	1545	1546	1563	1568	1584
20	1561	1562	1579	1584	1600	1575	1576	1593	1598	1614	1589	1590	1607	1612	1628
21	1605	1606	1623	1628	1644	1619	1620	1637	1642	1658	1633	1634	1651	1656	1672
22	1649	1650	1667	1672	1688	1663	1664	1681	1686	1702	1677	1678	1695	1700	1716
23	1693	1694	1711	1716	1732	1707	1708	1725	1730	1746	1721	1722	1739	1744	1760
24	1737	1738	1755	1760	1776	1751	1752	1769	1774	1790	1765	1766	1783	1788	1804
25	1781	1782	1799	1804	1820	1795	1796	1813	1818	1834	1809	1810	1827	1832	1848
26	1825	1826	1843	1848	1864	1839	1840	1857	1862	1878	1853	1854	1871	1876	1892
27	1869	1870	1887	1892	1908	1883	1884	1901	1906	1922	1897	1898	1915	1920	1936
28	1913	1914	1931	1936	1952	1927	1928	1945	1950	1966	1941	1942	1959	1964	1980
29	1957	1958	1975	1980	1996	1971	1972	1989	1994	2010	1985	1986	2003	2008	2024
30	2001	2002	2019	2024	2040	2015	2016	2033	2038	2054	2029	2030	2047	2052	2068
31	2045	2046	2063	2068	2084	2059	2060	2077	2082	2098	2073	2074	2091	2096	2112
32	2089	2090	2107	2112	2128	2103	2104	2121	2126	2142	2117	2118	2135	2140	2156
33	2133	2134	2151	2156	2172	2147	2148	2165	2170	2186	2161	2162	2179	2184	2200
34	2177	2178	2195	2200	2216	2191	2192	2209	2214	2230	2205	2206	2223	2228	2244
35	2221	2222	2239	2244	2260	2235	2236	2253	2258	2274	2249	2250	2267	2272	2288
36	2265	2266	2283	2288	2304	2279	2280	2297	2302	2318	2293	2294	2311	2316	2332
37	2309	2310	2327	2332	2348	2323	2324	2341	2346	2362	2337	2338	2355	2360	2376
38	2353	2354	2371	2376	2392	2367	2368	2386	2390	2406	2381	2382	2400	2404	2420
39	2397	2398	2416	2420	2436	2411	2413	2430	2434	2450	2426	2427	2444	2449	2464
40	2442	2443	2460	2465	2480	2456	2457	2474	2479	2494	2470	2471	2488	2493	2509
41	2486	2487	2504	2509	2525	2500	2501	2518	2523	2539	2514	2515	2532	2537	2553
42	2530	2531	2548	2553	2569	2544	2545	2562	2567	2583	2558	2559	2576	2581	2597
43	2574	2575	2592	2597	2613	2588	2589	2606	2611	2627	2602	2603	2620	2625	2641

A.III.6.5.2 (continued) $R^1 = H, R^2 = TMS$

	$R^3, R^4 = H;$ $R^5 - R^7 = (EO)_nCH_3$					$R^3 = H;$ $R^4 - R^7 = (EO)_nCH_3$					$R^3 - R^7 = (EO)_nCH_3$				
$(EO)_n$		H^+	NH_4^+	Na^+	K^+		H^+	NH_4^+	Na^+	K^+		H^+	NH_4^+	Na^+	K^+
0	722	723	740	745	761	736	737	754	759	775	750	751	768	773	789
1	766	767	784	789	805	780	781	798	803	819	794	795	812	817	833
2	810	811	828	833	849	824	825	842	847	863	838	839	856	861	877
3	854	855	872	877	893	868	869	886	891	907	882	883	900	905	921
4	898	899	916	921	937	912	913	930	935	951	926	927	945	949	965
5	942	943	961	965	981	956	958	975	979	995	971	972	989	993	1009
6	987	988	1005	1009	1025	1001	1002	1019	1024	1039	1015	1016	1033	1038	1054
7	1031	1032	1049	1054	1070	1045	1046	1063	1068	1084	1059	1060	1077	1082	1098
8	1075	1076	1093	1098	1114	1089	1090	1107	1112	1128	1103	1104	1121	1126	1142
9	1119	1120	1137	1142	1158	1133	1134	1151	1156	1172	1147	1148	1165	1170	1186
10	1163	1164	1181	1186	1202	1177	1178	1195	1200	1216	1191	1192	1209	1214	1230
11	1207	1208	1225	1230	1246	1221	1222	1239	1244	1260	1235	1236	1253	1258	1274
12	1251	1252	1269	1274	1290	1265	1266	1283	1288	1304	1279	1280	1297	1302	1318
13	1295	1296	1313	1318	1334	1309	1310	1327	1332	1348	1323	1324	1341	1346	1362
14	1339	1340	1357	1362	1378	1353	1354	1371	1376	1392	1367	1368	1385	1390	1406
15	1383	1384	1401	1406	1422	1397	1398	1415	1420	1436	1411	1412	1429	1434	1450
16	1427	1428	1445	1450	1466	1441	1442	1459	1464	1480	1455	1456	1473	1478	1494
17	1471	1472	1489	1494	1510	1485	1486	1503	1508	1524	1499	1500	1517	1522	1538
18	1515	1516	1533	1538	1554	1529	1530	1547	1552	1568	1543	1544	1561	1566	1582
19	1559	1560	1577	1582	1598	1573	1574	1591	1596	1612	1587	1588	1605	1610	1626
20	1603	1604	1621	1626	1642	1617	1618	1635	1640	1656	1631	1632	1649	1654	1670
21	1647	1648	1665	1670	1686	1661	1662	1679	1684	1700	1675	1676	1693	1698	1714
22	1691	1692	1709	1714	1730	1705	1706	1723	1728	1744	1719	1720	1737	1742	1758
23	1735	1736	1753	1758	1774	1749	1750	1767	1772	1788	1763	1764	1781	1786	1802
24	1779	1780	1797	1802	1818	1793	1794	1811	1816	1832	1807	1808	1825	1830	1846
25	1823	1824	1841	1846	1862	1837	1838	1855	1860	1876	1851	1852	1869	1874	1890
26	1867	1868	1885	1890	1906	1881	1882	1899	1904	1920	1895	1896	1913	1918	1934
27	1911	1912	1929	1934	1950	1925	1926	1943	1948	1964	1939	1940	1957	1962	1978
28	1955	1956	1973	1978	1994	1969	1970	1987	1992	2008	1983	1984	2001	2006	2022
29	1999	2000	2017	2022	2038	2013	2014	2031	2036	2052	2027	2028	2045	2050	2066
30	2043	2044	2061	2066	2082	2057	2058	2075	2080	2096	2071	2072	2089	2094	2110
31	2087	2088	2105	2110	2126	2101	2102	2119	2124	2140	2115	2116	2133	2138	2154
32	2131	2132	2149	2154	2170	2145	2146	2163	2168	2184	2159	2160	2177	2182	2198
33	2175	2176	2193	2198	2214	2189	2190	2207	2212	2228	2203	2204	2221	2226	2242
34	2219	2220	2237	2242	2258	2233	2234	2251	2256	2272	2247	2248	2265	2270	2286
35	2263	2264	2281	2286	2302	2277	2278	2295	2300	2316	2291	2292	2309	2314	2330
36	2307	2308	2325	2330	2346	2321	2322	2339	2344	2360	2335	2336	2354	2358	2374
37	2351	2352	2370	2374	2390	2365	2366	2384	2388	2404	2380	2381	2398	2402	2418
38	2396	2397	2414	2418	2434	2410	2411	2428	2433	2448	2424	2425	2442	2447	2462
39	2440	2441	2458	2463	2478	2454	2455	2472	2477	2493	2468	2469	2486	2491	2507
40	2484	2485	2502	2507	2523	2498	2499	2516	2521	2537	2512	2513	2530	2535	2551
41	2528	2529	2546	2551	2567	2542	2543	2560	2565	2581	2556	2557	2574	2579	2595
42	2572	2573	2590	2595	2611	2586	2587	2604	2609	2625	2600	2601	2618	2623	2639
43	2616	2617	2634	2639	2655	2630	2631	2648	2653	2669	2644	2645	2662	2667	2683

A.III.6.5.3 R^1, R^2 = TMS

	$R^3 - R^7 = H$					$R^3 - R^6 = H$; $R^7 = (EO)_nCH_3$					$R^3 - R^5 = H$; R^6, $R^7 = (EO)_nCH_3$				
$(EO)_n$		H^+	NH_4^+	Na^+	K^+		H^+	NH_4^+	Na^+	K^+		H^+	NH_4^+	Na^+	K^+
0	752	753	770	775	791	766	767	784	789	805	780	781	798	803	819
1	796	797	814	819	835	810	811	828	833	849	824	825	842	847	863
2	840	841	858	863	879	854	855	872	877	893	868	869	886	891	907
3	884	885	902	907	923	898	899	916	921	937	912	913	930	935	951
4	928	929	946	951	967	942	943	960	965	981	956	957	975	979	995
5	972	973	991	995	1011	986	987	1005	1009	1025	1001	1002	1019	1023	1039
6	1017	1018	1035	1039	1055	1031	1032	1049	1054	1069	1045	1046	1063	1068	1083
7	1061	1062	1079	1084	1099	1075	1076	1093	1098	1114	1089	1090	1107	1112	1128
8	1105	1106	1123	1128	1144	1119	1120	1137	1142	1158	1133	1134	1151	1156	1172
9	1149	1150	1167	1172	1188	1163	1164	1181	1186	1202	1177	1178	1195	1200	1216
10	1193	1194	1211	1216	1232	1207	1208	1225	1230	1246	1221	1222	1239	1244	1260
11	1237	1238	1255	1260	1276	1251	1252	1269	1274	1290	1265	1266	1283	1288	1304
12	1281	1282	1299	1304	1320	1295	1296	1313	1318	1334	1309	1310	1327	1332	1348
13	1325	1326	1343	1348	1364	1339	1340	1357	1362	1378	1353	1354	1371	1376	1392
14	1369	1370	1387	1392	1408	1383	1384	1401	1406	1422	1397	1398	1415	1420	1436
15	1413	1414	1431	1436	1452	1427	1428	1445	1450	1466	1441	1442	1459	1464	1480
16	1457	1458	1475	1480	1496	1471	1472	1489	1494	1510	1485	1486	1503	1508	1524
17	1501	1502	1519	1524	1540	1515	1516	1533	1538	1554	1529	1530	1547	1552	1568
18	1545	1546	1563	1568	1584	1559	1560	1577	1582	1598	1573	1574	1591	1596	1612
19	1589	1590	1607	1612	1628	1603	1604	1621	1626	1642	1617	1618	1635	1640	1656
20	1633	1634	1651	1656	1672	1647	1648	1665	1670	1686	1661	1662	1679	1684	1700
21	1677	1678	1695	1700	1716	1691	1692	1709	1714	1730	1705	1706	1723	1728	1744
22	1721	1722	1739	1744	1760	1735	1736	1753	1758	1774	1749	1750	1767	1772	1788
23	1765	1766	1783	1788	1804	1779	1780	1797	1802	1818	1793	1794	1811	1816	1832
24	1809	1810	1827	1832	1848	1823	1824	1841	1846	1862	1837	1838	1855	1860	1876
25	1853	1854	1871	1876	1892	1867	1868	1885	1890	1906	1881	1882	1899	1904	1920
26	1897	1898	1915	1920	1936	1911	1912	1929	1934	1950	1925	1926	1943	1948	1964
27	1941	1942	1959	1964	1980	1955	1956	1973	1978	1994	1969	1970	1987	1992	2008
28	1985	1986	2003	2008	2024	1999	2000	2017	2022	2038	2013	2014	2031	2036	2052
29	2029	2030	2047	2052	2068	2043	2044	2061	2066	2082	2057	2058	2075	2080	2096
30	2073	2074	2091	2096	2112	2087	2088	2105	2110	2126	2101	2102	2119	2124	2140
31	2117	2118	2135	2140	2156	2131	2132	2149	2154	2170	2145	2146	2163	2168	2184
32	2161	2162	2179	2184	2200	2175	2176	2193	2198	2214	2189	2190	2207	2212	2228
33	2205	2206	2223	2228	2244	2219	2220	2237	2242	2258	2233	2234	2251	2256	2272
34	2249	2250	2267	2272	2288	2263	2264	2281	2286	2302	2277	2278	2295	2300	2316
35	2293	2294	2311	2316	2332	2307	2308	2325	2330	2346	2321	2322	2339	2344	2360
36	2337	2338	2355	2360	2376	2351	2352	2369	2374	2390	2365	2366	2383	2388	2404
37	2381	2382	2399	2404	2420	2395	2396	2414	2418	2434	2409	2411	2428	2432	2448
38	2425	2427	2444	2448	2464	2440	2441	2458	2462	2478	2454	2455	2472	2477	2492
39	2470	2471	2488	2493	2508	2484	2485	2502	2507	2523	2498	2499	2516	2521	2537
40	2514	2515	2532	2537	2553	2528	2529	2546	2551	2567	2542	2543	2560	2565	2581
41	2558	2559	2576	2581	2597	2572	2573	2590	2595	2611	2586	2587	2604	2609	2625
42	2602	2603	2620	2625	2641	2616	2617	2634	2639	2655	2630	2631	2648	2653	2669
43	2646	2647	2664	2669	2685	2660	2661	2678	2683	2699	2674	2675	2692	2697	2713

A.III.6.5.3 (continued) R^1, R^2 = TMS

	R^3, R^4 = H; $R^5 - R^7 = (EO)_nCH_3$					R^3 = H; $R^4 - R^7 = (EO)_nCH_3$					$R^3 - R^7 = (EO)_nCH_3$				
$(EO)_n$		H^+	NH_4^+	Na^+	K^+		H^+	NH_4^+	Na^+	K^+		H^+	NH_4^+	Na^+	K^+
0	794	795	812	817	833	808	809	826	831	847	822	823	840	845	861
1	838	839	856	861	877	852	853	870	875	891	866	867	884	889	905
2	882	883	900	905	921	896	897	914	919	935	910	911	928	933	949
3	926	927	944	949	965	940	941	959	963	979	954	955	973	977	993
4	970	971	989	993	1009	985	986	1003	1007	1023	999	1000	1017	1022	1037
5	1015	1016	1033	1038	1053	1029	1030	1047	1052	1067	1043	1044	1061	1066	1082
6	1059	1060	1077	1082	1098	1073	1074	1091	1096	1112	1087	1088	1105	1110	1126
7	1103	1104	1121	1126	1142	1117	1118	1135	1140	1156	1131	1132	1149	1154	1170
8	1147	1148	1165	1170	1186	1161	1162	1179	1184	1200	1175	1176	1193	1198	1214
9	1191	1192	1209	1214	1230	1205	1206	1223	1228	1244	1219	1220	1237	1242	1258
10	1235	1236	1253	1258	1274	1249	1250	1267	1272	1288	1263	1264	1281	1286	1302
11	1279	1280	1297	1302	1318	1293	1294	1311	1316	1332	1307	1308	1325	1330	1346
12	1323	1324	1341	1346	1362	1337	1338	1355	1360	1376	1351	1352	1369	1374	1390
13	1367	1368	1385	1390	1406	1381	1382	1399	1404	1420	1395	1396	1413	1418	1434
14	1411	1412	1429	1434	1450	1425	1426	1443	1448	1464	1439	1440	1457	1462	1478
15	1455	1456	1473	1478	1494	1469	1470	1487	1492	1508	1483	1484	1501	1506	1522
16	1499	1500	1517	1522	1538	1513	1514	1531	1536	1552	1527	1528	1545	1550	1566
17	1543	1544	1561	1566	1582	1557	1558	1575	1580	1596	1571	1572	1589	1594	1610
18	1587	1588	1605	1610	1626	1601	1602	1619	1624	1640	1615	1616	1633	1638	1654
19	1631	1632	1649	1654	1670	1645	1646	1663	1668	1684	1659	1660	1677	1682	1698
20	1675	1676	1693	1698	1714	1689	1690	1707	1712	1728	1703	1704	1721	1726	1742
21	1719	1720	1737	1742	1758	1733	1734	1751	1756	1772	1747	1748	1765	1770	1786
22	1763	1764	1781	1786	1802	1777	1778	1795	1800	1816	1791	1792	1809	1814	1830
23	1807	1808	1825	1830	1846	1821	1822	1839	1844	1860	1835	1836	1853	1858	1874
24	1851	1852	1869	1874	1890	1865	1866	1883	1888	1904	1879	1880	1897	1902	1918
25	1895	1896	1913	1918	1934	1909	1910	1927	1932	1948	1923	1924	1941	1946	1962
26	1939	1940	1957	1962	1978	1953	1954	1971	1976	1992	1967	1968	1985	1990	2006
27	1983	1984	2001	2006	2022	1997	1998	2015	2020	2036	2011	2012	2029	2034	2050
28	2027	2028	2045	2050	2066	2041	2042	2059	2064	2080	2055	2056	2073	2078	2094
29	2071	2072	2089	2094	2110	2085	2086	2103	2108	2124	2099	2100	2117	2122	2138
30	2115	2116	2133	2138	2154	2129	2130	2147	2152	2168	2143	2144	2161	2166	2182
31	2159	2160	2177	2182	2198	2173	2174	2191	2196	2212	2187	2188	2205	2210	2226
32	2203	2204	2221	2226	2242	2217	2218	2235	2240	2256	2231	2232	2249	2254	2270
33	2247	2248	2265	2270	2286	2261	2262	2279	2284	2300	2275	2276	2293	2298	2314
34	2291	2292	2309	2314	2330	2305	2306	2323	2328	2344	2319	2320	2337	2342	2358
35	2335	2336	2353	2358	2374	2349	2350	2367	2372	2388	2363	2364	2382	2386	2402
36	2379	2380	2398	2402	2418	2393	2395	2412	2416	2432	2408	2409	2426	2430	2446
37	2424	2425	2442	2446	2462	2438	2439	2456	2461	2476	2452	2453	2470	2475	2491
38	2468	2469	2486	2491	2507	2482	2483	2500	2505	2521	2496	2497	2514	2519	2535
39	2512	2513	2530	2535	2551	2526	2527	2544	2549	2565	2540	2541	2558	2563	2579
40	2556	2557	2574	2579	2595	2570	2571	2588	2593	2609	2584	2585	2602	2607	2623
41	2600	2601	2618	2623	2639	2614	2615	2632	2637	2653	2628	2629	2646	2651	2667
42	2644	2645	2662	2667	2683	2658	2659	2676	2681	2697	2672	2673	2690	2695	2711
43	2688	2689	2706	2711	2727	2702	2703	2720	2725	2741	2716	2717	2734	2739	2755

A.III.6.6 Cyclic trimers (27)

	$R^1, R^2, R^3 = (CH_2)_3$-OH					$R^1, R^2 = (CH_2)_3$-OH; $R^3 = (CH_2)_3$-O-$(EO)_n$-CH_3					$R^1 = (CH_2)_3$-OH; $R^2, R^3 = (CH_2)_3$-O-$(EO)_n$-CH_3					$R^1, R^2, R^3 = (CH_2)_3$-O-$(EO)_n$-CH_3				
$(EO)_n$		H^+	NH_4^+	Na^+	K^+		H^+	NH_4^+	Na^+	K^+		H^+	NH_4^+	Na^+	K^+		H^+	NH_4^+	Na^+	K^+
0	354	355	372	377	393	368	369	386	391	407	382	383	400	405	421	396	397	414	419	435
1	398	399	416	421	437	412	413	430	435	451	426	427	444	449	465	440	441	458	463	479
2	442	443	460	465	481	456	457	474	479	495	470	471	488	493	509	484	485	502	507	523
3	486	487	504	509	525	500	501	518	523	539	514	515	532	537	553	528	529	546	551	567
4	530	531	548	553	569	544	545	562	567	583	558	559	576	581	597	572	573	590	595	611
5	574	575	592	597	613	588	589	606	611	627	602	603	620	625	641	616	617	634	639	655
6	618	619	636	641	657	632	633	650	655	671	646	647	664	669	685	660	661	678	683	699
7	662	663	680	685	701	676	677	694	699	715	690	691	708	713	729	704	705	722	727	743
8	706	707	724	729	745	720	721	738	743	759	734	735	752	757	773	748	749	766	771	787
9	750	751	768	773	789	764	765	782	787	803	778	779	796	801	817	792	793	810	815	831
10	794	795	812	817	833	808	809	826	831	847	822	823	841	845	861	836	837	855	859	875
11	838	839	857	861	877	852	853	871	875	891	867	868	885	889	905	881	882	899	904	919
12	883	884	901	905	921	897	898	915	920	935	911	912	929	934	950	925	926	943	948	964
13	927	928	945	950	966	941	942	959	964	980	955	956	973	978	994	969	970	987	992	1008
14	971	972	989	994	1010	985	986	1003	1008	1024	999	1000	1017	1022	1038	1013	1014	1031	1036	1052
15	1015	1016	1033	1038	1054	1029	1030	1047	1052	1068	1043	1044	1061	1066	1082	1057	1058	1075	1080	1096
16	1059	1060	1077	1082	1098	1073	1074	1091	1096	1112	1087	1088	1105	1110	1126	1101	1102	1119	1124	1140
17	1103	1104	1121	1126	1142	1117	1118	1135	1140	1156	1131	1132	1149	1154	1170	1145	1146	1163	1168	1184
18	1147	1148	1165	1170	1186	1161	1162	1179	1184	1200	1175	1176	1193	1198	1214	1189	1190	1207	1212	1228
19	1191	1192	1209	1214	1230	1205	1206	1223	1228	1244	1219	1220	1237	1242	1258	1233	1234	1251	1256	1272
20	1235	1236	1253	1258	1274	1249	1250	1267	1272	1288	1263	1264	1281	1286	1302	1277	1278	1295	1300	1316
21	1279	1280	1297	1302	1318	1293	1294	1311	1316	1332	1307	1308	1325	1330	1346	1321	1322	1339	1344	1360
22	1323	1324	1341	1346	1362	1337	1338	1355	1360	1376	1351	1352	1369	1374	1390	1365	1366	1383	1388	1404
23	1367	1368	1385	1390	1406	1381	1382	1399	1404	1420	1395	1396	1413	1418	1434	1409	1410	1427	1432	1448
24	1411	1412	1429	1434	1450	1425	1426	1443	1448	1464	1439	1440	1457	1462	1478	1453	1454	1471	1476	1492
25	1455	1456	1473	1478	1494	1469	1470	1487	1492	1508	1483	1484	1501	1506	1522	1497	1498	1515	1520	1536
26	1499	1500	1517	1522	1538	1513	1514	1531	1536	1552	1527	1528	1545	1550	1566	1541	1542	1559	1564	1580
27	1543	1544	1561	1566	1582	1557	1558	1575	1580	1596	1571	1572	1589	1594	1610	1585	1586	1603	1608	1624

A.III.6.7 Cyclic tetramers (28)

	$R^1 - R^4 = (CH_2)_3\text{-OH}$					$R^1 - R^3 = (CH_2)_3\text{-OH}$; $R^4 = (CH_2)_3\text{-O-(EO)}_n\text{-CH}_3$					$R^1, R^2 = (CH_2)_3\text{-OH}$; $R^3, R^4 = (CH_2)_3\text{-O-(EO)}_n\text{-CH}_3$					$R^1 = H$; $R^2 - R^4 = (CH_2)_3\text{-O-(EO)}_n\text{-CH}_3$					$R^1 - R^4 = (CH_2)_3\text{-O-(EO)}_n\text{-CH}_3$				
$(EO)_n$		H^+	NH_4^+	Na^+	K^+		H^+	NH_4^+	Na^+	K^+		H^+	NH_4^+	Na^+	K^+		H^+	NH_4^+	Na^+	K^+		H^+	NH_4^+	Na^+	K^+
0	472	473	490	495	511	486	487	504	509	525	500	501	518	523	539	514	515	532	537	553	528	529	546	551	567
1	516	517	534	539	555	530	531	548	553	569	544	545	562	567	583	558	559	576	581	597	572	573	590	595	611
2	560	561	578	583	599	574	575	592	597	613	588	589	606	611	627	602	603	620	625	641	616	617	634	639	655
3	604	605	622	627	643	618	619	636	641	657	632	633	650	655	671	646	647	664	669	685	660	661	678	683	699
4	648	649	666	671	687	662	663	680	685	701	676	677	694	699	715	690	691	708	713	729	704	705	722	727	743
5	692	693	710	715	731	706	707	724	729	745	720	721	738	743	759	734	735	752	757	773	748	749	766	771	787
6	736	737	754	759	775	750	751	768	773	789	764	765	782	787	803	778	779	796	801	817	792	793	810	815	831
7	780	781	798	803	819	794	795	812	817	833	808	809	826	831	847	822	823	840	845	861	836	837	854	859	875
8	824	825	842	847	863	838	839	856	861	877	852	853	870	875	891	866	867	885	889	905	880	881	899	903	919
9	868	869	886	891	907	882	883	901	905	921	896	897	915	919	935	911	912	929	933	949	925	926	943	948	963
10	912	913	931	935	951	927	928	945	949	965	941	942	959	964	979	955	956	973	978	994	969	970	987	992	1008
11	957	958	975	980	995	971	972	989	994	1010	985	986	1003	1008	1024	999	1000	1017	1022	1038	1013	1014	1031	1036	1052
12	1001	1002	1019	1024	1040	1015	1016	1033	1038	1054	1029	1030	1047	1052	1068	1043	1044	1061	1066	1082	1057	1058	1075	1080	1096
13	1045	1046	1063	1068	1084	1059	1060	1077	1082	1098	1073	1074	1091	1096	1112	1087	1088	1105	1110	1126	1101	1102	1119	1124	1140
14	1089	1090	1107	1112	1128	1103	1104	1121	1126	1142	1117	1118	1135	1140	1156	1131	1132	1149	1154	1170	1145	1146	1163	1168	1184
15	1133	1134	1151	1156	1172	1147	1148	1165	1170	1186	1161	1162	1179	1184	1200	1175	1176	1193	1198	1214	1189	1190	1207	1212	1228
16	1177	1178	1195	1200	1216	1191	1192	1209	1214	1230	1205	1206	1223	1228	1244	1219	1220	1237	1242	1258	1233	1234	1251	1256	1272
17	1221	1222	1239	1244	1260	1235	1236	1253	1258	1274	1249	1250	1267	1272	1288	1263	1264	1281	1286	1302	1277	1278	1295	1300	1316
18	1265	1266	1283	1288	1304	1279	1280	1297	1302	1318	1293	1294	1311	1316	1332	1307	1308	1325	1330	1346	1321	1322	1339	1344	1360
19	1309	1310	1327	1332	1348	1323	1324	1341	1346	1362	1337	1338	1355	1360	1376	1351	1352	1369	1374	1390	1365	1366	1383	1388	1404
20	1353	1354	1371	1376	1392	1367	1368	1385	1390	1406	1381	1382	1399	1404	1420	1395	1396	1413	1418	1434	1409	1410	1427	1432	1448
21	1397	1398	1415	1420	1436	1411	1412	1429	1434	1450	1425	1426	1443	1448	1464	1439	1440	1457	1462	1478	1453	1454	1471	1476	1492
22	1441	1442	1459	1464	1480	1455	1456	1473	1478	1494	1469	1470	1487	1492	1508	1483	1484	1501	1506	1522	1497	1498	1515	1520	1536
23	1485	1486	1503	1508	1524	1499	1500	1517	1522	1538	1513	1514	1531	1536	1552	1527	1528	1545	1550	1566	1541	1542	1559	1564	1580
24	1529	1530	1547	1552	1568	1543	1544	1561	1566	1582	1557	1558	1575	1580	1596	1571	1572	1589	1594	1610	1585	1586	1603	1608	1624
25	1573	1574	1591	1596	1612	1587	1588	1605	1610	1626	1601	1602	1619	1624	1640	1615	1616	1633	1638	1654	1629	1630	1647	1652	1668
26	1617	1618	1635	1640	1656	1631	1632	1649	1654	1670	1645	1646	1663	1668	1684	1659	1660	1677	1682	1698	1673	1674	1691	1696	1712
27	1661	1662	1679	1684	1700	1675	1676	1693	1698	1714	1689	1690	1707	1712	1728	1703	1704	1721	1726	1742	1717	1718	1735	1740	1756
28	1705	1706	1723	1728	1744	1719	1720	1737	1742	1758	1733	1734	1751	1756	1772	1747	1748	1765	1770	1786	1761	1762	1779	1784	1800

A.IV DATA

A.IV.1 Comparison of HPLC responses of standard solutions of commercial Silwet L-77 (2.87 gL^{-1}) and a purified M_2D-C_3-O-$(EO)_n$-Me sample (2.00 gL^{-1})

[M_2D-C_3-O-$(EO)_n$-Me] ($molL^{-1}$)	Purified L-77/ Commercial L-77	Purified (L-77/TX-45)/ Commercial (L-77/TX-45)
2.31×10^7	0.8554	1.0608
3.85×10^7	1.6149	0.7821
	0.6482	1.5435
	0.5455	1.8551
5.38×10^7	1.2047	0.8456
	0.9623	0.8583
	1.0168	0.9575
7.69×10^7	1.0047	1.1604
	0.7367	1.4375
	0.8740	1.0612
1.08×10^6	1.2766	0.8070
	1.0657	0.8292
	0.9056	1.0574
1.54×10^6	1.0364	0.9317
	1.0713	0.8861
	0.9246	1.0668
2.15×10^6	1.2938	0.8638
	1.3108	0.9455
	0.9371	1.0032
Average	1.0	1.0
Std.Dev.	0.2	0.3

A.IV.2 Comparison of percentage uptake of Silwet L-77 into Citrus leaves as determined by HPLC and APcI/MS methods

	Time (minutes)	Silwet L-77 [HPLC] [b] (SD)[b]	Silwet L-77 [APcI/MS] [c] (SD)
Least squares fit[a]		y = 0.6533x – 0.1809	y = 1.1418x + 0.0567
R^2		0.9691	0.9867
With cuticular stripping	2.5	13 (14)	-16 (9)
	10	14 (7)	-34 (33)
	30	12 (7)	-23 (16)
	240	18 (9)	5 (7)
Without cuticular stripping	2.5	-24 (23)	-257 (105)
	10	5 (9)	-18 (9)
	30	8 (16)	-75 (85)
	240	22 (10)	5 (11)

[a] y = relative response(Silwet L-77/Agral-90), x = [Silwet L-77]/[Agral-90]; [b] A higher regression coefficient was obtained with a power leas-squares fit (0.9774), however subsequent sample data gave more recoveries exceeding 100% (negative uptake) using this standard curve; [c] All regressions and API/MS methods used (APcI/MS, ESI/MS; +/- internal standard) gave sample recoveries exceeding 100%

A.IV.3 ***Ion series*** [a] **observed in degraded Silwet L-77 product mixtures** [b]

Series	Adduct				*Series*	Adduct				*Series*	Adduct				*Series*	Adduct				*Series*	Adduct				*Series*	Adduct			
A	H^+	NH_4^+	Na^+	K^+	B	H^+	NH_4^+	Na^+	K^+	C	H^+	NH_4^+	Na^+	K^+	D	H^+	NH_4^+	Na^+	K^+	E	H^+	NH_4^+	Na^+	K^+	F[c]	H^+	NH_4^+	Na^+	K^+
32	33	50	55	71	46	47	64	69	85	18	19	36	41	57	34	35	52	57	73	16	17	34	39	55	30	31	48	53	69
76	77	94	99	115	90	91	108	113	129	62	63	80	85	101	78	79	96	101	117	60	61	78	83	99	74	75	92	97	113
120	**121**	138	143	159	134	135	152	157	173	106	107	124	129	145	122	123	140	145	161	104	105	122	127	143	118	119	136	141	157
164	**165**	182	**187**	203	178	179	196	201	217	150	151	168	173	189	166	167	184	189	205	148	149	166	171	187	162	163	180	185	201
208	**209**	226	**231**	247	222	223	240	245	261	194	195	212	217	233	210	211	228	233	249	192	193	210	215	231	206	207	224	229	245
252	**253**	270	**275**	291	266	267	284	289	305	238	239	256	261	277	254	255	272	277	293	236	237	254	259	275	250	251	268	273	289
296	**297**	**314**	**319**	**335**	310	**311**	**328**	**333**	349	282	283	300	**305**	321	298	299	316	321	337	280	281	298	303	319	294	295	312	**317**	333
340	**341**	**358**	**363**	**379**	354	**355**	**372**	**377**	393	326	**327**	344	**349**	365	342	343	360	365	381	324	325	342	347	363	338	339	356	**361**	377
384	**385**	402	**407**	**423**	398	**399**	**416**	**421**	437	370	**371**	388	**393**	**409**	386	387	404	409	425	368	369	386	391	407	382	383	**400**	**405**	421
428	**429**	446	**451**	**467**	442	**443**	**460**	**465**	481	414	**415**	432	**437**	**453**	430	431	448	453	469	412	413	430	435	451	426	427	**444**	**449**	465
472	**473**	490	**495**	**511**	486	487	**504**	**509**	525	458	**459**	476	**481**	**497**	474	475	492	497	513	456	457	474	**479**	495	470	471	**488**	**493**	509
516	**517**	534	**539**	**555**	530	531	**548**	**553**	569	502	**503**	**520**	**525**	**541**	518	519	536	541	557	500	501	518	**523**	539	514	515	**532**	**537**	553
560	**561**	578	**583**	**599**	574	575	**592**	**597**	613	546	**547**	**564**	**569**	**585**	562	563	580	585	601	544	545	562	**567**	583	558	559	**576**	**581**	597
604	**605**	622	**627**	**643**	618	619	**636**	**641**	657	590	**591**	**608**	**613**	**629**	606	607	624	629	645	588	589	606	**611**	627	602	603	**620**	**625**	641
648	**649**	666	**671**	**687**	662	663	**680**	**685**	701	634	635	**652**	**657**	**673**	650	651	668	673	689	632	**633**	650	**655**	671	646	**647**	**664**	**669**	685
692	693	710	**715**	**731**	706	707	**724**	**729**	745	678	679	**696**	**701**	**717**	694	695	712	717	733	676	**677**	694	**699**	715	690	**691**	**708**	**713**	729
736	737	754	**759**	775	750	751	**768**	**773**	789	722	723	**740**	**745**	**761**	738	739	756	761	777	720	**721**	738	**743**	759	734	**735**	**752**	**757**	773
780	781	799	**803**	819	794	795	**812**	**817**	833	766	767	**784**	**789**	**805**	782	783	800	805	821	764	**765**	782	**787**	803	778	779	**796**	**801**	817
824	826	843	847	863	838	839	**856**	**861**	877	810	811	**828**	**833**	**849**	826	827	845	849	865	808	**809**	826	**831**	847	822	**823**	840	**845**	861
869	870	887	892	907	882	883	**900**	**905**	921	854	855	**872**	**877**	**893**	870	871	888	**893**	909	852	853	871	**875**	891	866	**867**	884	**889**	905
913	914	931	936	952	926	927	**944**	**949**	965	898	899	**916**	**921**	**937**	914	915	932	**937**	953	896	899	914	**919**	935	910	**911**	928	**933**	949
957	958	975	980	996	970	971	988	**993**	1009	942	943	**960**	**965**	**981**	958	959	976	**981**	997	940	941	958	**963**	979	954	**955**	972	**977**	993
1001	1002	1019	1024	1040	1014	1015	1032	**1037**	1053	986	987	1004	1009	**1025**	1002	1003	1020	**1025**	1041	984	985	1002	**1007**	1023	999	1000	1017	1022	1038
1045	1046	1063	1068	1084	1058	1059	1076	**1081**	1097	1030	1031	1048	1053	**1069**	1047	1048	1065	**1070**	1086	1029	1030	1047	1052	1068	1043	1044	1061	1066	1082
1089	1090	1107	1112	1128	1102	1103	1120	**1125**	1141	1074	1075	1092	1097	1113	1091	1092	1109	1114	1130	1073	1074	1091	1096	1112	1087	1088	1105	1110	1126
1133	1134	1151	1156	1172	1146	1147	1164	**1169**	1185	1118	1119	1136	1141	1157	1135	1136	1153	1158	1174	1117	1118	1135	1140	1156	1131	1132	1149	1154	1170
1177	1178	1195	1200	1216	1190	1191	1208	**1213**	1229	1162	1163	1180	1185	1201	1179	1180	1197	1202	1218	1161	1162	1179	1184	1200	1175	1176	1193	1198	1214
1221	1222	1239	1244	1260	1234	1235	1252	**1257**	1273	1206	1207	1224	1229	1245	1223	1224	1241	1246	1262	1205	1206	1223	1228	1244	1219	1220	1237	1242	1258

[a] Δ *m/z* = 44 a.m.u.; [b] Bolded values are actual ions observed; [c] Ion series at *m/z* 1594, 1638, 1682,1726, 1770, 1814, 1858, 1902 also observed

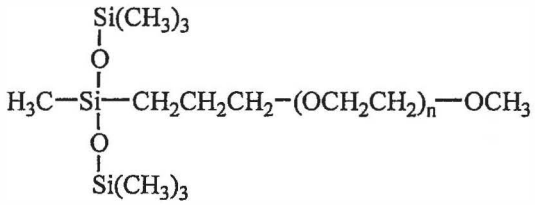

n = 3 - 16, Average n ~ 7.5

1 (Silwet L-77)

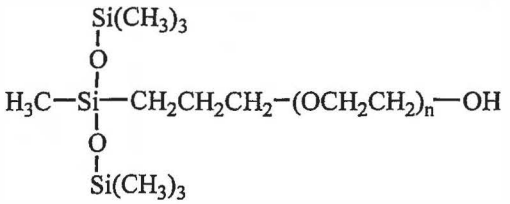

n = 3 - 16, Average n ~ 7.5

2 (Silwet L-408)

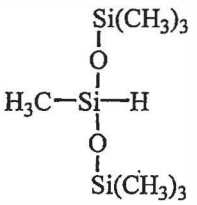

3 (M_2D^H)

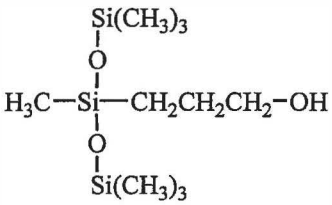

5

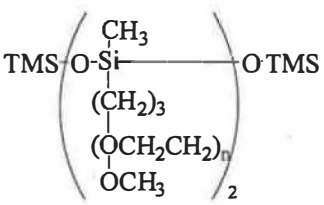

6

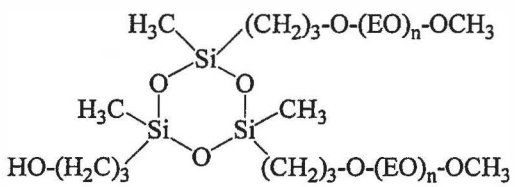

7

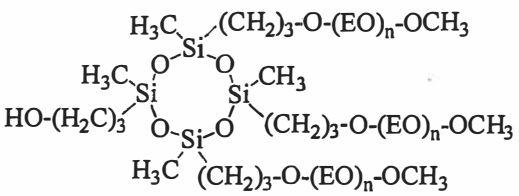

8

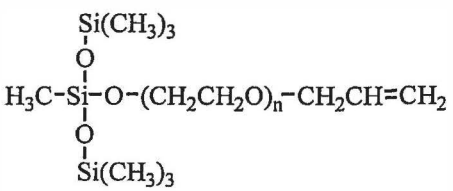

9

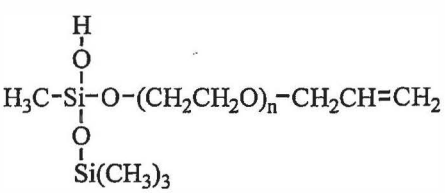

10

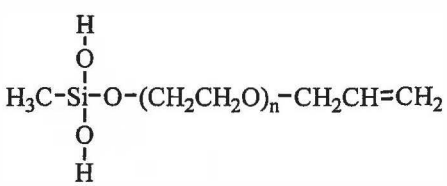

11

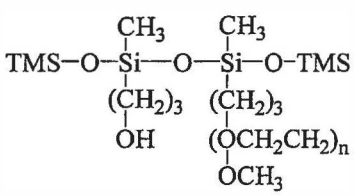

12

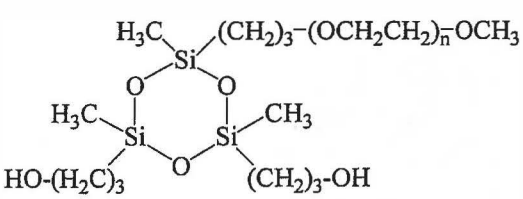

13

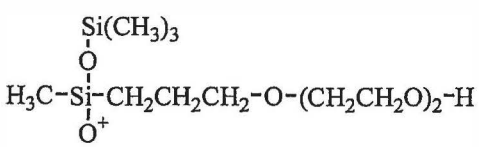

14

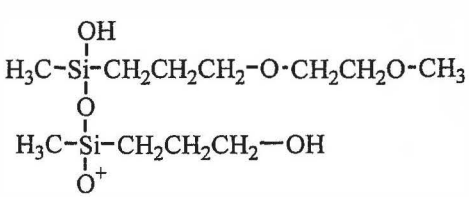

15

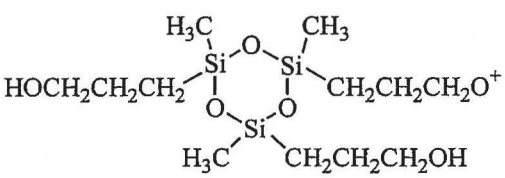

16

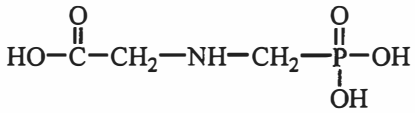

17

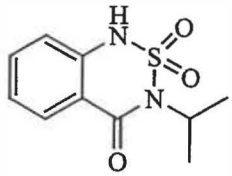

18

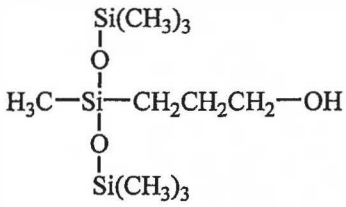

19

20

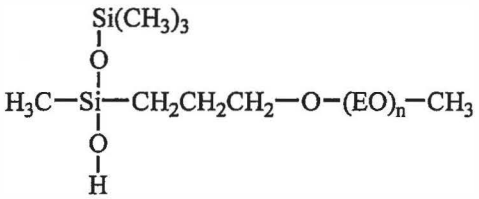

21

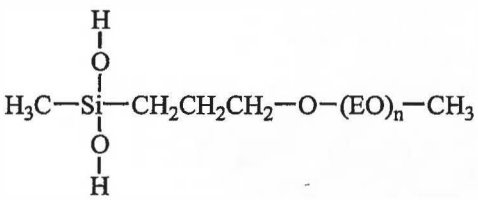

22

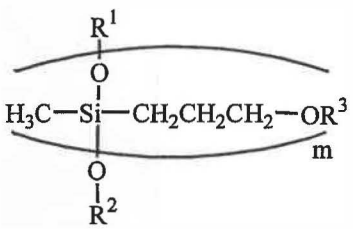

23

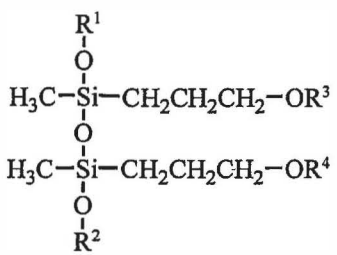

24

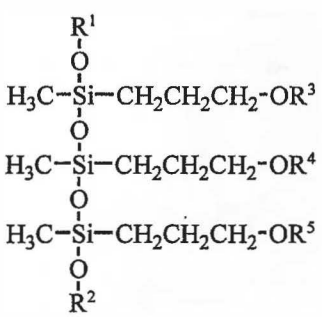

25

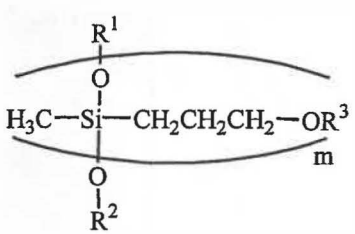

26

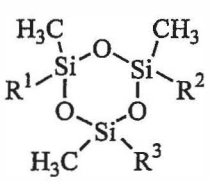

27

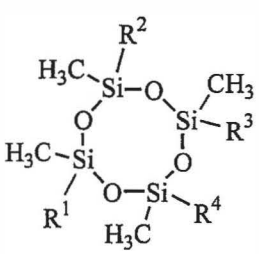

28

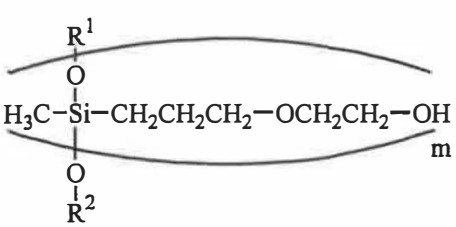

29

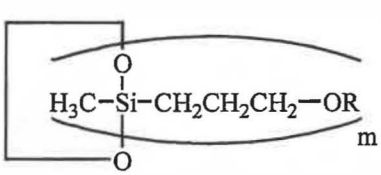

30